

# CONTENTS

CONTRIBUTORS . . . . .	vii
PREFACE . . . . .	ix

## Clinical Studies of Camptothecin and Derivatives

OTTO SOEPENBERG, ALEX SPARREBOOM, AND JAAP VERWEIJ

I. Introduction . . . . .	1
II. Mechanisms of Action . . . . .	3
III. Mutagenicity and Resistance Mechanisms . . . . .	7
IV. Irinotecan . . . . .	9
V. Topotecan . . . . .	19
VI. Considerations of Route of Administration . . . . .	27
VII. Investigational Derivatives . . . . .	29
VIII. Conclusions . . . . .	33
References . . . . .	35

## Tremorgenic and Nontremorgenic 2,3-Fused Indole Diterpenoids

HEATHER SINGS AND SHEO SINGH

I. Introduction . . . . .	51
II. Isolation . . . . .	53
III. Synthesis . . . . .	125
IV. Biosynthesis . . . . .	144
V. Structure and Tremorgenicity . . . . .	155
References . . . . .	158

## The *Daphniphyllum* Alkaloids

JUN'ICHI KOBAYASHI AND HIROSHI MORITA

I. Introduction . . . . .	165
II. Structures of Representative Alkaloids . . . . .	170
III. Biosynthesis and Biogenesis . . . . .	184
IV. Synthesis . . . . .	193
V. Conclusions . . . . .	202
References . . . . .	203

## The Manzamine Alkaloids

JIN-FENG HU, MARK T. HAMANN, RUSSELL HILL,  
AND MICHELLE KELLY

I. Introduction. . . . .	207
II. Isolation and Structure Elucidation from Marine Sponges . . . . .	214
III. Biogenesis and Biosynthesis . . . . .	223
IV. Synthesis . . . . .	264
V. Pharmacology. . . . .	270
VI. Conclusions . . . . .	277
References. . . . .	278

## Sesquiterpene Pyridine Alkaloids

LUCIANO M. LIÃO

I. Introduction. . . . .	287
II. Evoninate Sesquiterpene Pyridine Alkaloids and Derivatives . . . . .	289
III. Wilfordate Sesquiterpene Pyridine Alkaloids and Derivatives . . . . .	307
IV. Edulinate Sesquiterpene Pyridine Alkaloids . . . . .	315
V. Cassinate Sesquiterpene Pyridine Alkaloids . . . . .	317
VI. Lower Molecular Weight Sesquiterpene Pyridine Alkaloids. . . . .	317
VII. Non-Celastraceous Sesquiterpene Pyridine Alkaloids . . . . .	318
VIII. Biosynthesis and Biogenesis . . . . .	322
IX. Biological Activity . . . . .	330
X. Taxonomic Considerations. . . . .	334
XI. Synthesis . . . . .	334
References. . . . .	339

## Chemical and Biological Aspects of Melanin

D.P. CHAKRABORTY AND SHYAMALI ROY

I. Introduction. . . . .	345
II. Biogenesis of Melanin . . . . .	347
III. Natural Melanins. . . . .	354
IV. Investigations of Melanins by Physical Methods. . . . .	373
V. Synthetic Melanins . . . . .	376
VI. Physicochemical Properties and Biological Functions of Melanins . . . . .	379
References. . . . .	384
Index . . . . .	393

## CONTRIBUTORS

*Numbers in parentheses indicate the pages on which the authors' contributions begin.*

D.P. CHAKRABORTY (345), Institute of Natural Products, Calcutta 700 036, India

MARK T. HAMANN (207), Department of Pharmacognosy and National Center for the Development of Natural Products (NCNPR), School Pharmacy, The University of Mississippi, University, Mississippi, USA

RUSSELL HILL (207), The Center of Marine Biotechnology (COMB), University of Maryland Biotechnology Institute, Columbus Center, Baltimore, MD, USA

JIN-FENG HU (207), Department of Pharmacognosy and National Center for the Development of Natural Products (NCNPR), School Pharmacy, The University of Mississippi, University, Mississippi, USA

MICHELLE KELLY (207), National Center for Aquatic Biodiversity and Biosecurity, National Institute of Water and Atmospheric Research (NIWA) Ltd., Newmarket, Auckland, New Zealand

JUN'ICHI KOBAYASHI (165), Graduate School of Pharmaceutical Sciences, Hokkaido University, Sapporo 060, Japan

LUCIANO M. LIÃO (287), Instituto de Quimica, Universidade Federal de Goiás, Goiânia, GO, 74001-970, Brazil

HIROSHI MORITA (165), Graduate School of Pharmaceutical Sciences, Hokkaido University, Sapporo 060, Japan

SHYAMALI ROY (345), Institute of Natural Products, Calcutta 700 036, India

SHEO SINGH (51), Merck Research Laboratories, Rahway, NJ 07065, USA

HEATHER SINGS (51), Merck Research Laboratories, Rahway, NJ 07065, USA

OTTO SOEPENBERG (1), Department of Medical Oncology, Erasmus MC – Daniel den Hoed Cancer Center, Rotterdam, The Netherlands

ALEX SPARREBOOM (1), Department of Medical Oncology, Erasmus MC – Daniel den Hoed Cancer Center, Rotterdam, The Netherlands

JAAP VERWEIJ (1), Department of Medical Oncology, Erasmus MC – Daniel den Hoed Cancer Center, Rotterdam, The Netherlands

## PREFACE

This volume marks the 60th in this series, which began publication in 1950 under the editorship of the late Professor R.H.F. Manske. Through the successive editorships of Professor Russell Rodrigo and Dr. Arnold Brossi, the series evolved in scope in an effort to try to keep up with the burgeoning field of "alkaloids." As Editor, I have tried to continue this evolutionary process, blending together diverse chapters on the discovery, biological evaluation, and clinical applications of alkaloids. In this volume, the six chapters reflect areas of alkaloid research which are new to the series and others which require updating because of the recent progress.

In Chapter 1, Soepenbergh, Sparreboom, and Verweij present a detailed discussion of the clinical aspects of camptothecin, one of the most important alkaloids to be studied in the past 40 years. In Chapter 2, Sings and Singh describe the various 2,3-fused indole diterpenoid derivatives and their powerful biological effects. A much needed update on the *Daphniphyllum* alkaloids is offered by Kobayashi and Morita in Chapter 3.

A significant group of marine alkaloids, the manzamines, which have attracted a lot of interest in the past few years, is reviewed by Hamann and colleagues in Chapter 4, and Lião summarizes in Chapter 5 the advances that have been made in the sesquiterpene alkaloids, a group not reviewed previously in the series. Finally, following the untimely death of Professor D.P. Chakraborty, Dr. Shyamali Roy agreed to complete the work of updating the field of melanin chemistry and biology.

Geoffrey A. Cordell  
*University of Illinois at Chicago*

# CLINICAL STUDIES OF CAMPTOTHECIN AND DERIVATIVES

OTTO SOEPENBERG, ALEX SPARREBOOM, AND JAAP VERWEIJ

*Department of Medical Oncology, Erasmus MC – Daniel den Hoed Cancer  
Center, Rotterdam, The Netherlands*

- I. Introduction
  - II. Mechanisms of Action
  - III. Mutagenicity and Resistance Mechanisms
  - IV. Irinotecan
  - V. Topotecan
  - VI. Considerations of Route of Administration
  - VII. Investigational Derivatives
  - VIII. Conclusions
- References

## I. Introduction

About a half century ago, thousands of natural products were chemically screened in a program initiated by the National Cancer Institute to search for steroidal saponin precursors which would be cortisone precursors. This program led to the discovery of the plant alkaloids, the camptothecins (CPTs) – isolated from the stem wood of the Chinese tree Xi Shu or *Camptotheca acuminata* (Decaisne, Nyssaceae) (1–5). Initial *in vitro* and *in vivo* studies using the chloroform extract of the aqueous ethanolic residue of *C. acuminata* suggested widespread antitumor activity (2,3). Camptothecins are related to the monoterpenoid indole alkaloids, and the parent alkaloid was shown to be a high-melting substance [molecular weight (MW) 348.111] comprising a unique and highly unsaturated pentacyclic-ring structure (1,3). The structures of CPT and selected analogs are shown in Fig. 1.

The six-membered quinoline B-ring and the five-membered C-ring are formed by a ring expansion and contraction sequence of reactions. The E-ring presents a  $\alpha$ -hydroxylactone system which can undergo a pH-dependent reversible

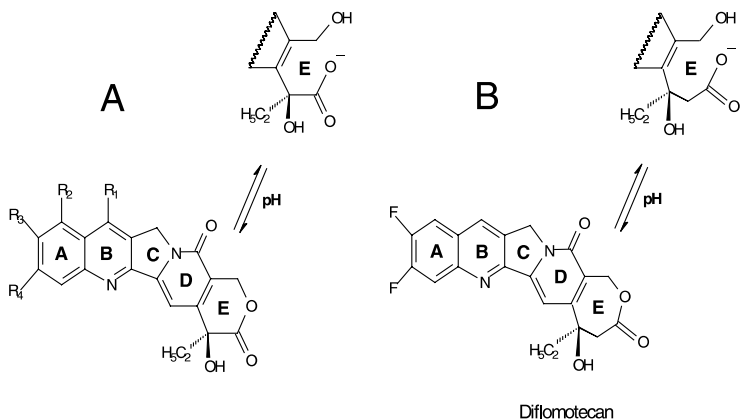


FIGURE A	R <sub>1</sub>	R <sub>2</sub>	R <sub>3</sub>	R <sub>4</sub>
Camptothecin	H	H	H	H
9-Nitrocamptothecin	H	NO <sub>2</sub>	H	H
9-Aminocamptothecin	H	NH <sub>2</sub>	H	H
Topotecan	H		H	H
Irinotecan (CPT-11)	CH <sub>2</sub> CH <sub>3</sub>	H		H
SN-38	CH <sub>2</sub> CH <sub>3</sub>	H	OH	H
Lurtotecan		H		H
DX-8951		H	CH <sub>3</sub>	F

Figure 1. Lactone–carboxylate interconversion and chemical structures of six- and seven-membered E-ring camptothecin analogs.

hydrolysis. Camptothecin forms the sodium salt of a hydroxy acid after adding alkali and is lactonized on acidification. Both the E-ring and the D-ring, which has a conjugated pyridone moiety, are essential structural features for the antitumor activity of CPT (3).

Triggered by the preclinical antitumor activity, early Phase I clinical trials were performed in the early 1970s using CPT as a water-soluble sodium salt formulation, because of its ease of use as an intravenous (i.v.) formulation (6). Although in the first Phase I study five, short-lasting partial remissions were reported in 18 patients with primarily gastrointestinal cancers, these results could not be confirmed in subsequent Phase I and II studies in the USA (7–9). In contrast, a large program in the People's Republic of China involving up to 1000 patients treated with the sodium salt formulation of CPT reported favorable results, but for a variety of reasons these had to be interpreted with caution (3). However, unpredictable severe adverse events, i.e., life-threatening diarrhea, considerable hemorrhagic cystitis, and myelosuppression, likely related to the poor aqueous solubility of the parent compound, led to the suspension of the further development of this antineoplastic agent during the next two decades. The recognition that the nuclear enzyme DNA topoisomerase I was the prime target in the mechanism of action of the CPTs, and the possibility to develop numerous semisynthetic CPT analogs with improved aqueous solubility, and, in consequence, a more predictable toxicity profile, resulted in renewed interest in these cytotoxic agents.

Currently, two CPT derivatives, irinotecan and topotecan, are registered for use in oncologic practice. Irinotecan is registered for use in metastatic colorectal cancer. Topotecan is approved for the treatment of patients with cisplatin-refractory ovarian cancer and for small-cell lung cancer (SCLC) after the failure of first-line chemotherapy. During the last 10 years, knowledge of the pharmacokinetic and pharmacodynamic properties of the semisynthetic CPT analogs has significantly increased. The next challenge in their development will be to maximize efficacy and to minimize side effects in the treatment by biomodulation of the pharmacokinetic and pharmacodynamic properties. For instance, the pharmacological profile of irinotecan is extremely complex and the various processes involved in drug elimination, either through metabolic breakdown or excretion, likely impact substantially on interindividual variability in drug handling. Strategies to individualize irinotecan administration schedules based on patient profiles in enzyme and protein expression or by co-administration of specific agents modulating side effects are under investigation (10). Once the results of pharmacogenetics can be more crystallized, this may ultimately lead to more selective or “tailor-made” dose scheduling for patients to adjust the “fine-tuning” administration of these agents.

In this review, we will focus on the clinically important aspects of the CPT alkaloids with an emphasis on their mechanisms of action and resistance, their pharmacokinetic and pharmacodynamic behavior, and their routes of administration.

## II. Mechanisms of Action

The cytotoxic CPTs belong to the class of topoisomerase I inhibitors. DNA topoisomerases are essential enzymes found in all nucleated cells. These enzymes



are involved in the regulation of DNA topology and are necessary for the preservation of the integrity of the genetic material during DNA metabolism, e.g., RNA transcription, DNA replication, recombination, chromatin remodeling, chromatin condensation, and repair during cell division (11,12). Based on their different reaction mechanism and cellular function, there are two types of DNA topoisomerases (type I and type II). Their characteristics are summarized in Table I.

Human topoisomerase I is a monomeric  $\sim 91$ -kDa polypeptide of 765 amino acids encoded by an active-copy gene located on chromosome 20q12–13.2 and two pseudogenes on chromosomes 1q23–24 and 22q11.2–13.1 (13–15). The coding sequence of the gene is split into 21 exons spread over at least 85 kilobase pairs of human genomic DNA (16). The human topoisomerase I gene promoter is influenced by positively and negatively acting transcription factors, which are described in more detail elsewhere (16,17).

This protein is comprised of four major domains: a highly charged NH<sub>2</sub>-terminal domain (MW 24 kDa), a conserved core domain (MW 56 kDa), a

TABLE I.  
Differentiation of Human DNA Topoisomerases Type I and II.

---

Type I topoisomerase
– Monomeric protein, molecular weight $\sim 91$ kDa
– Single-copy gene located on chromosome 20q12–13.2
– Transiently breaks one strand of duplex DNA and forms a 3'-phosphotyrosine covalent intermediate
– Single-step changes in the linking number of circular DNAs
– Its expression is continuous during the cell cycle and in quiescent cells
– Mainly involved in relaxation of supercoiled DNA during RNA transcription
– ATP independent
Type II topoisomerase
– Homodimeric protein, molecular weight 170 kDa (isoenzyme II $\alpha$ ) and 180 kDa (isoenzyme II $\beta$ )
– Single-copy gene located on chromosome 17q21–22 (isoenzyme II $\alpha$ ) and chromosome 3p24 (isoenzyme II $\beta$ )
– Breaks both strands of duplex DNA and forms a pair of 5'-phosphotyrosine covalent intermediates
– Generates a gate through which another region of DNA can be passed
– Double-step changes in the linking number of circular DNAs
– Its expression increases during S-phase of the cell cycle (especially isoenzyme II $\alpha$ ) and almost absent in quiescent cells (primarily expression of isoenzyme II $\beta$ )
– Involved in DNA replication, recombination, RNA transcription, and repair
– ATP dependent

---

positively charged linker domain (MW 7 kDa), and a highly conserved COOH-terminal domain (MW 6 kDa) containing the active-site tyrosine, i.e., the nucleophilic Tyr<sup>723</sup> amino acid residue (15,18). Human topoisomerase promotes the relaxation of both positively and negatively torsionally strained (supercoiled) duplex DNA with equal efficiency so that transcription and replication can proceed (15). Hereby, a transesterification reaction takes place by which topoisomerase I cleaves one strand of the double-helix structure of DNA using the C<sub>4</sub>-oxygen atom of the active-site tyrosine (Tyr<sup>723</sup>) residue and constitutes a transient, covalent phosphotyrosyl intermediate with the 3' end of the nicked DNA strand, the so-called cleavable complex. This way it changes the linking number in single steps (15,19). Later, the energy of this covalent attachment is recycled for the reverse transesterification reaction that reseals the DNA strands (religation) and liberates the enzyme. Consequently, for these intertwining processes neither energy cofactors nor metal cations are required by human topoisomerase I (20).

Recent studies have revealed more detailed insights in the three-dimensional structure of human topoisomerase I and its interactive function with the DNA molecule (21,22). In Table II, the principal structural characteristics of human topoisomerase I are summarized.

The mechanism of DNA relaxation after formation of the covalent complex and before religation is still not completely elucidated (21). So far, two mechanisms are supposed, viz. the strand-passage model and the free-rotation model. Both models represent the two extremes of a continuum in the conceptual framework for how topoisomerase I might effect changes in linking number (21,22). In the strand-passage (or enzyme-bridging) model, it is hypothesized that the intact DNA strand is passed through an enzyme-bridged gate, which is made by the covalent linkage of the 3' end and by noncovalent binding to the 5' end of the broken strand. On the other hand, in the free-rotation model, relaxation of torsionally strained duplex DNA is possible due to releasing of the 5' end of the broken strand from the active site and as a result is allowed to rotate freely about the complementary unbroken strand (15,22). X-Ray crystallographic studies with complexes of human topoisomerase I and DNA lead to the proposal that the relaxation of supercoiled DNA elapsed by a controlled rotation mechanism (21,22).

In the controlled rotation model, the DNA structure is allowed to rotate completely free at 30° intervals downstream of the cleavage site round the intact DNA strand modulated by the interaction of the nose-cone helices of subdomains I and II in a positively charged cavity formed by the cap of the enzyme and the linker domain (15). *In vitro* studies with reconstituted human topoisomerase I have revealed the more precise function of the linker region. During the normal relaxation of supercoiled DNA it acts to slow the religation (18). From these studies, it is also hypothesized that the inhibition of DNA relaxation caused by CPT – by stabilizing the cleavable complex – depends on a direct effect of the cytotoxic agent on DNA rotation which is mediated by electrostatic interactions between the linker domain and DNA (18).

TABLE II.  
Structural Characteristics of Human DNA Topoisomerase Type I.

---

*Two domains with essential functions for catalytic activity and relaxation function*

I. Core domain (MW 56 kDa)

- Amino acid residues 215–635 (Ile<sup>215</sup>–Arg<sup>635</sup>)
- Subdomain I
  - Amino acid residues 215–232 and 320–433
  - Two  $\alpha$  helices and nine  $\beta$  strands
- Subdomain II
  - Amino acid residues 233–319
  - Five  $\alpha$  helices and two  $\beta$  strands
- Subdomain III
  - Amino acid residues 434–635
  - Ten  $\alpha$  helices and five  $\beta$  strands
  - Contains all active-site residues except the Tyr<sup>723</sup>
  - Extends from the top half of the molecule downward through two long  $\alpha$  helices that functions like a hinge that opens and closes the enzyme around the DNA
- Subdomains I and II are folded tightly together and form the “cap” (top-lobe) region of the enzyme
- Subdomains I and II have two long “nose-cone” helices ( $\alpha 5$  and  $\beta 6$ ) that make an  $\sim 90^\circ$  angle with each other and come together in a “V”-figure at a point 25 Å away from the body of the molecule, and enclose a triangular-shaped empty space between them
- Subdomain III forms the bottom lobe of the enzyme
- Subdomains I and III interact via two short “lips” opposite from the long-hinge helices

II. COOH-terminal domain (MW 6 kDa)

- Amino acid residues 713–765 (Gln<sup>713</sup>–Phe<sup>765</sup>)
- Contains the active-site (catalytic) thymosine Tyr<sup>723</sup>

*Two domains without essential functions for catalytic activity and relaxation function*

III. NH<sub>2</sub>-terminal domain (MW 24 kDa)

- Amino acid residues 1–214 (Met<sup>1</sup>–Gly<sup>214</sup>)
- Highly charged, very few hydrophobic amino acids, is largely disordered, and contains several nuclear-targeting signals
- Involved in nucleolar localization through interactions with nucleolin

IV. Linker domain (MW 7 kDa)

- Amino acid residues 636–712 (Pro<sup>636</sup>–Lys<sup>712</sup>)
  - Coiled-coil structure that is positively charged
  - Reaches 50 Å away from the body of the enzyme
-

When the attachment of CPT is modeled in the three-dimensional structure of human topoisomerase I, it is believed that the DNA duplex is extended in such a way that carbon positions 7 and 9 of the CPT structure are facing out into open space. These carbon positions are very accessible to chemical modifications. Consequently, this gives the opportunity to expand the potency of modified CPT analogs by auspicious interactions of these derivatives with distant proteins or DNA atoms at the binding site (22).

Stabilization of the cleavable complex by CPTs is not sufficient in itself for the induction of cell death because the complex can reverse spontaneously in a short time. The lethal effects of these drugs are caused by the interaction between a moving replication fork (or transcription process) and the drug-stabilized cleavable complex, resulting in irreversible arrest of DNA replication and the formation of a double-strand break located at the fork. This so-called fork-collision model leads to the arrest of the cell cycle in the S/G<sub>2</sub>-phase, and finally to apoptosis (23). As cells in the S-phase division are up to 1000-fold more sensitive to topoisomerase I inhibitors than cells in G<sub>1</sub>- or G<sub>2</sub>/M-phases after exposure, the cytotoxicity of these agents is considered S-phase specific (24–27).

The time of persistence of the drug-stabilized cleavable complex depends on the production and/or repair of replication or transcription lesions. In general, transcription lesions require longer persistence, i.e., greater stability of the cleavable complex, than do replication lesions (28). Unfortunately, the fraction of replicating cells in tumor tissues is underrepresented. This means that cell kill results predominantly from the transcription lesion mechanism. For this reason, the potency of different CPT analogs to stabilize the cleavable complex is of paramount importance for efficacious therapeutic use (28). Of relevance for all topoisomerase I inhibitors are the data from *in vitro* experiments which revealed that the cytotoxicity increases with the duration of exposure. Short-time exposures to high concentrations are less effective than long-term exposures to low concentrations (29,30).

### III. Mutagenicity and Resistance Mechanisms

Owing to their mechanism of action, topoisomerase I inhibitors are a double-edged sword, because besides their cytotoxic properties, these agents are potential mutagens, although their mutagenicity and oncogenicity still remain to be elucidated (31–33). This is stressed by the fact that mutations may lead to drug resistance, limiting further treatment, or to the development of secondary malignancies. If mutations arise in germ cells, this could eventually be transmitted to subsequent generations. Furthermore, the tendency to administer topoisomerase I inhibitors in protracted schedules or prolonged exposure regimens could hypothetically lead to an increased risk of mutagenicity (34,35).

The stabilization of the cleavable complexes by topoisomerase I inhibitors disrupts the DNA integrity and interferes with the normal processes of

DNA topology, including replication, transcription, DNA repair, chromosome condensation, and chromosome separation (31). The formation of these drug-induced cleavable complexes is essential, but is not sufficient in itself to cause cytotoxicity. This implies that cells need to undergo DNA synthesis to yield maximum toxicity (31,36–38). Experimental studies showed that in the presence of topoisomerase II inhibitors chromosomal aberrations arise during replication which seems a more important cause of cytotoxicity (31,36,39). Furthermore, it was postulated that recombination processes must be initiated to bypass the replication block created by topoisomerase II inhibitor-stabilized complexes, and that some of these events cause aberrant, illegitimate, or nonhomologous recombination, which may lead to cytotoxicity and/or mutations. Nonhomologous recombination that causes deletions of an essential gene, partially or completely, resulted in the loss of gene products and finally to cell death. In contrast, aberrant recombination or rearrangement causing deletion of a suppressor gene, or activation of a proto-oncogene, stimulated cell growth with the potential to induce secondary cancers (31).

Similar data exist for topoisomerase II inhibitors (31), one use of which has been related to the occurrence of acute myeloid leukemia (40–51). These secondary leukemias are characterized by a short induction period and present as myelomonocytic or monocytic leukemia, rather than myelodysplasia (52). The rearrangements are usually distinguished by balanced chromosomal translocations involving either the MLL (ALL-1, HRX) gene at 11q23 or the AML1 gene 21q22 (53,54).

In principle, topoisomerase I inhibitors can produce similar molecular alterations as those caused by topoisomerase II inhibitors. Consequently, they may have similar clinical consequences (31). Direct comparative *in vitro* studies have shown that, on a molar basis, the topoisomerase I inhibitors were more mutagenic than the topoisomerase II-inhibitor etoposide (31). Topotecan was found to be less mutagenic than the parent compound CPT.

So far, the clinical use of topoisomerase I inhibitors has not been linked to secondary malignancies. However, the relative survival time of patients treated with irinotecan or topotecan as compared with those treated with epipodophyllotoxins (e.g., testicular cancer or hematological malignancies) possibly results in a less clinically apparent mutagenic risk of topoisomerase I inhibitors.

As with decreased levels of topoisomerase I, various point mutations of topoisomerase I in different CPT-resistant cell lines have been associated with CPT resistance (55–63). The different point mutations in human topoisomerase I in several CPT-resistant cell lines are summarized in Table III. These point mutations cause alterations to the topoisomerase I enzyme, resulting in decreased topoisomerase I catalytic activity or impaired binding of CPT to topoisomerase I (55,64). In some models, single amino acid changes resulted in partial resistance, while double mutation induced a synergistic resistance (55).

TABLE III.  
Different Point Mutations of Human Topoisomerase I.

CPT-resistant cell line	Point mutation	Reference
CPT <sup>R</sup> -2000 cell line	Gly <sup>717</sup> to Val, and Thr <sup>729</sup> to Ile	(55)
CPT-K5 cell line	Asp <sup>533</sup> to Gly*, and Asp <sup>583</sup> to Gly	(58)
PC-7/CPT cell line	Asp <sup>583</sup> to Gly	
PC-7/CPT cell line	Thr <sup>729</sup> to Ala	(59)
By <i>in vitro</i> mutagenesis	Gly <sup>363</sup> to Cys	(60)
Chinese hamster DC3F/C-10	Gly <sup>505</sup> to Ser	(62)
U-937/CR cell line	Phe <sup>361</sup> to Ser	(63)

\*Only Asp<sup>533</sup> to Gly is responsible for resistance.

In a small clinical study involving eight non-small cell lung cancer (NSCLC) patients treated with irinotecan, two-point mutations were identified that were located near a site in topoisomerase I that was previously identified as a position of a mutation in the CPT-resistant human lung cancer cell line PC7/CPT (64). Although this is the first prospective clinical study which demonstrates that point mutations in topoisomerase I occur after chemotherapy with irinotecan, further clinical studies will be needed to verify if the occurrence of topoisomerase I gene mutations relates to the occurrence of clinical resistance to topoisomerase I inhibitors (64).

#### IV. Irinotecan

##### A. CLINICAL PHARMACOLOGY

Irinotecan (CPT-11; 7-ethyl-10-{4-[1-piperidino]-1-piperidino}-carbonyloxy-camptothecin) is a semisynthetic, water-soluble prodrug that requires hydrolysis or de-esterification by carboxylesterases to form its active-metabolite SN-38 (7-ethyl-10-hydroxycamptothecin), which is 100–1000-fold more cytotoxic *in vitro* than the parent compound (65). Irinotecan contains a dibasic, bispiperidine substituent, linked through a carbonyl group to the hydroxyl at C-10, crucial for water solubility.

Irinotecan pharmacology is extremely complex and still the subject of research (65). It is known to be dependent on various enzyme and protein systems for metabolic transformation and active transport, all regulating intestinal absorption and hepatobiliary secretion mechanisms. Both irinotecan and SN-38 exist in an active lactone form and an inactive carboxylate form, through an equilibrium that depends on the pH and the presence of binding proteins (65). SN-38 is detoxified in the liver by the polymorphic enzyme uridine-diphosphate glucuronosyltransferase 1A1 (UGT1A1) to SN-38 glucuronide (SN-38G) (66). This isoenzyme is also responsible for bilirubin glucuronidation (67). Because of this,

patients with hereditary UGT enzyme polymorphism – e.g., familial hyperbilirubinemia conditions (Crigler–Najjar syndrome types I and II or Gilbert’s disease) – are at increased risk for irinotecan-induced diarrhea due to decreased glucuronidation of SN-38 (68).

Irinotecan showed a linear pharmacokinetic behavior (69–73). Both the lactone form and the carboxylate form of irinotecan and SN-38 are detectable in plasma shortly after i.v. administration (74). The AUC of SN-38 is only approximately 4% of the AUC of irinotecan, which means that only a small fraction of the dose is converted to the active form. After administration of irinotecan as a short-time i.v. infusion over 30–90 min, there is a three-exponential decline of the plasma concentration of the drug (75). The biological half-life of the lactone form of SN-38 is 11.5 h. This is much longer than for other CPTs, for instance topotecan (70,74). The clearance of irinotecan lactone (53.5 l/h/m<sup>2</sup>) is approximately two times larger than that of topotecan. At steady state, the mean volume of distribution of the total drug is 142 l/m<sup>2</sup>, representing approximately four times the total body weight (74). When irinotecan is administered as a protracted i.v. infusion over 7–21 days, the plasma levels of irinotecan, SN-38, and SN-38G are comparable on days 7, 14, or 21 during the infusion. The AUC ratio of SN-38 to irinotecan was 16% and was constant over the tested dose range (76). This metabolic ratio was higher compared with the ratios found after short-time infusion, namely 3–9%. This partly explains the relatively low maximum-tolerated doses (MTDs) achieved with the continuous infusion regimens, which are thus due to the greater conversion of irinotecan to the cytotoxic-metabolite SN-38.

Recently, Xie *et al.* reported a population analysis in 70 cancer patients on the clinical pharmacokinetics of irinotecan and four of its metabolites (77). These authors found that the interconversion between the lactone and carboxylate forms of irinotecan was relatively rapid, with an equilibration half-life of 14 min in the central compartment and hydrolysis occurring at a rate five times faster than lactonization. Also, the same interconversion took place in the peripheral compartments. The irinotecan lactone form had extensive tissue distribution ( $V_{ss}$ , 445 l) in comparison with the carboxylate form ( $V_{ss}$ , 78 l, excluding peripherally formed irinotecan carboxylate) (77). The clearance of the lactone form (74.3 l/h) was higher than the carboxylate form (12.3 l/h). These models revealed that there was a preference of SN-38 and NPC to be formed out of the lactone form of irinotecan, whereas APC could be modeled best by presuming formation from irinotecan carboxylate (77). The interconversion between SN-38 lactone and carboxylate was slower than that of irinotecan. SN-38 lactone is more tightly bound to serum albumin than the carboxylate form, and for this reason the dynamic equilibrium is preferential toward the lactone form. Although the clearances for SN-38 lactone and carboxylate were similar, the lactone form had more extensive tissue distribution (77).

Diarrhea originates from intestinal epithelium cell damaged by SN-38. This reversible reaction can be modulated by changing the intestinal flora using

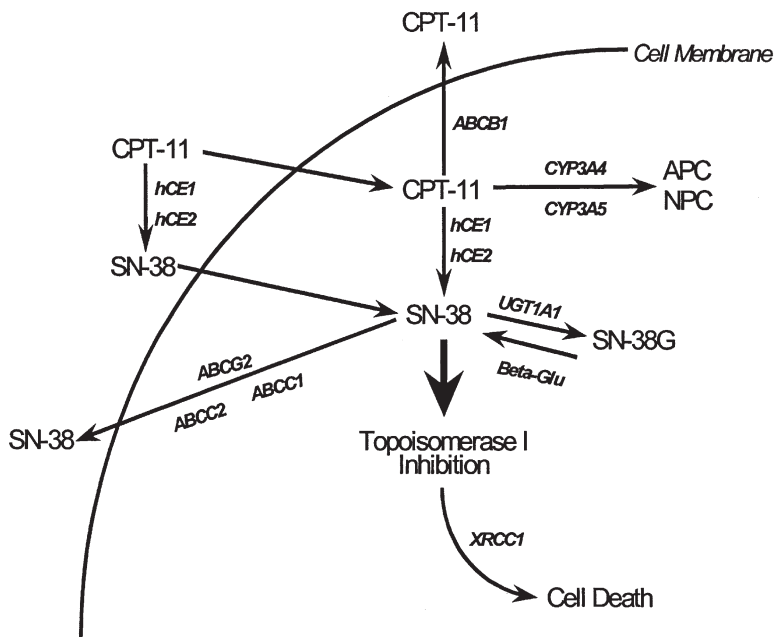


Figure 2. Summary of irinotecan-elimination (CPT-11) routes, showing esterase- (hCE1 and hCE2) mediated conversion to the active-metabolite SN-38, its further conjugation into the glucuronic-acid derivative SN-38G by UGT1A1, the reversible deconjugation by bacterial beta-glucuronidase (Beta-Glu), CYP3A-mediated conversion to the oxidized derivatives APC and NPC, P-glycoprotein- (ABCB1) mediated cellular efflux of irinotecan, and MDR1- (ABCC1), cMOAT- (ABCC2), and BCRP- (ABCG2) mediated transport of SN-38.

antibiotics, e.g., neomycin or other beta-glucuronidase inhibitors, such as cyclosporin A, which inhibits the cMOAT-mediated biliary excretion of SN-38 (78,79). Furthermore, cytochrome P-450 3A4 (CYP3A4) metabolizes irinotecan into several oxidized derivatives, including APC (7-ethyl-10-[4-*N*-5-aminopentanoic acid)-1-piperidino]-carbonyloxycamptothecin) and NPC (7-ethyl-10-[4-*N*-(1-piperidino)-1-amino]-carbonyloxycamptothecin) (71,80–83). The various genes with a putative role in irinotecan disposition are shown in Fig. 2. Both metabolites are also poor inhibitors of topoisomerase I and only the minor-metabolite NPC can be further converted to SN-38 (74,83,84). Because CYP3A4 is involved in the biotransformation of many other drugs, there is a potential risk of clinically relevant drug interactions. A Phase I study of irinotecan in malignant glioma patients revealed that the clearance of irinotecan was significantly faster in patients who required cotreatment with anticonvulsants and glucocorticoids – inducers of the CYP3A4 enzyme – as compared with patients who did not



receive such concomitant treatment (85). A recent investigation indicates that a significant interaction occurs between irinotecan and the herbal product St. John's wort because of CYP3A4 induction, resulting in 42% decreased circulating concentrations of SN-38 (86). In contrast, inhibition of CYP3A4 activity, for example by ketoconazole, leads to substantially increased exposure (~two-fold) to SN-38 (87). It has also been shown that the sequence of treatment with irinotecan and infusional 5-FU affects the tolerability of this combination, with the SN-38 area under the concentration versus time curve (AUC) being 40% lower ( $P < 0.05$ ) when irinotecan preceded 5-FU. This suggests that well-defined 5-FU/irinotecan regimens are needed because the administration sequence or the interval between the agents might affect treatment tolerance and perhaps also activity (88).

Elimination of irinotecan occurs primarily in the feces via hepatobiliary and intestinal secretion and secondarily in the urine (89). Approximately, 50% of the total administered dose of irinotecan is recovered in urine (28%) and feces (25%) as unchanged parent compound or its inactive metabolites (81). The hepatobiliary elimination route is dependent on the presence of drug-transporting proteins, notably P-glycoprotein and canalicular multispecific organic anion transporter (cMOAT), present on the bile canalicular membrane (10). Because of the close connection of irinotecan with liver biotransformation and elimination, the drug should not be administered in case of increased bilirubin concentrations or elevated transaminases (68,90).

The cytotoxic activity of SN-38 is performed by producing intermediate forms of drug-stabilized covalent DNA/topoisomerase I complexes, also referred earlier as the cleavable complexes, as outlined previously. SN-38 exerts this cytotoxic function by trapping cleavable complexes instead of inhibiting topoisomerase I enzyme function. Antitumor activity of CPT analogs can be predicted *in vitro* based upon gene-copy number, mRNA content, and protein expression of topoisomerase I (90). The fact that in human tumor samples from colon cancer, there was increased topoisomerase I expression and activity as compared to normal mucosa, could partly explain the activity of irinotecan in this disease (90–93).

## B. DOSE-FINDING TRIALS

Phase I studies were performed first in Japan, later in the USA and Europe. The recommended regimen of irinotecan in the USA is 125 mg/m<sup>2</sup> administered as a 90-min i.v. infusion once weekly for 4 or 6 weeks (70). In Europe, the approved administration schedule of irinotecan is 350 mg/m<sup>2</sup> given as an i.v. infusion over 60–90 min once every 3 weeks (94), while a recent reevaluation indicated a maximum-tolerable dose of 320 mg/m<sup>2</sup>, or 290 mg/m<sup>2</sup> in patients with prior abdominal/pelvic radiation therapy (95). Finally in Japan, the administration schedule of irinotecan was developed as 100 mg/m<sup>2</sup> every week or 150 mg/m<sup>2</sup> every other week (96). Remarkably, the dose intensity (DI) of all applied dosage

regimens of irinotecan is approximately  $100 \text{ mg/m}^2/\text{week}$ , which suggested a schedule independency. This phenomenon can be explained by the long half-life of SN-38, which is achieved after a single dosage of irinotecan. Although the half-life of SN-38 does not fully support this approach, in an effort to further explore the possible therapeutic advantage of prolonged exposure to CPTs, protracted or repeated dosing regimens of irinotecan have been studied. Irinotecan was administered as a short infusion repeated on 5 consecutive days, as a 4-day i.v. continuous infusion weekly for 2 weeks every 3 weeks, and as a 14-day continuous i.v. infusion every 3 weeks (97). Since protracted i.v. infusion is inconvenient for patients, an oral formulation of irinotecan is also under study (71).

In the transatlantic Phase I clinical trials, the maximum DI of irinotecan was achieved with short-time i.v. infusion once every 2 or 3 weeks (mean DI  $125 \text{ mg/m}^2/\text{week}$ ; range,  $80\text{--}167 \text{ mg/m}^2/\text{week}$ ), whereas the lowest DI was achieved with continuous i.v. infusion (DI 27 and  $47 \text{ mg/m}^2/\text{week}$ ). In the weekly  $\times 4$  schedule and the daily i.v. infusion over 3 or 5 consecutive days, the mean calculated DI was  $83 \text{ mg/m}^2/\text{week}$  (range,  $73\text{--}100 \text{ mg/m}^2/\text{week}$ ). Thus, the maximum DI achieved with prolonged exposure schedules of irinotecan is 2–3 times lower than that achieved with short-infusion administration. But, as indicated previously, irinotecan is more effectively converted to SN-38 during protracted i.v. infusion. The SN-38 to irinotecan AUC ratios ranged from 16% to 24% (97). After oral administration of irinotecan, the absolute bioavailability of the drug based on lactone measurements is relatively low (74). However, the SN-38 to irinotecan AUC ratio, expressed on a molar basis, is three times greater after oral administration than after i.v. infusion. Possibly, the first-pass conversion of irinotecan to SN-38 in the intestine and liver could explain this observation (74).

The principal dose-limiting toxicity (DLT) for all schedules used was delayed diarrhea, with or without neutropenia (70,94,96). The frequency of severe diarrhea (grade 3 or 4) was reported as 35% in the Phase I studies. The incidence of this toxicity can be reduced by more than 50% if an intensive treatment with loperamide is used as described in the safety guidelines in Table IV (98).

Neutropenia was dose related, generally of brief duration and noncumulative, and occurred in 14–47% of patients treated once every 3 weeks and less frequently using the weekly schedule (12–19%) (98–102). In approximately 3% of patients, the neutropenia was associated with fever. In one Phase I study, where irinotecan was given as a 96-h continuous infusion for 2 weeks every 3 weeks, thrombocytopenia was also dose limiting (103). Due to inhibition of acetylcholinesterase activity by irinotecan within the first 24 h after dosing of the drug, an acute cholinergic reaction can be observed. The symptomatology of this syndrome, as well as the other nonhematological toxicities of irinotecan, is summarized in Table V.

TABLE IV.  
Safety Guidelines for the Use of Irinotecan.

- 
- Proper patient selection according to known risk factors:
    - For severe neutropenia: Performance status; serum bilirubin level
    - For severe diarrhea: Performance status; prior abdominopelvic radiation therapy, hyperleucocytosis
  - Proper training of the treating medical oncologist and his staff, and extensive information to the patient:
    - Including patient's information leaflet about management of toxicities
  - Early use of high-dose loperamide as soon as the first loose stool occurs.
    - Recommendation:
      - 4 mg Loperamide for the first intake and then 2 mg every 2 h at least 12 h After the last loose stool for a maximum of 48 h
  - Early use of oral broad-spectrum antibiotics (e.g., fluoroquinolone) in case of:
    - Any grade 4<sup>a</sup> diarrhea
    - Febrile diarrhea
    - Diarrhea with concomitant grade 3<sup>a</sup> or 4 neutropenia
    - Failure of a 48-h high-dose loperamide therapy
  - Dose reduction in case of:
    - Grade 4 neutropenia (even asymptomatic)
    - Grade 3 neutropenia concomitant with fever and/or infection
    - Severe diarrhea
  - Contraindication for use in patients with:
    - WHO<sup>b</sup> performance status > 2
    - Predictable poor compliance
    - Baseline serum bilirubin > 1.5 × UNL<sup>c</sup>
  - Treatment only with caution and close survey between cycles in patients with:
    - WHO performance status = 2
    - Baseline serum bilirubin between 1 and 1.5 × UNL
    - Prior abdominopelvic radiation therapy
    - Baseline hyperleucocytosis
- 

<sup>a</sup>Grade 3 and 4 according to NCI common toxicity criteria (version 2.0).

<sup>b</sup>WHO, World Health Organization.

<sup>c</sup>UNL, upper normal limit.

### C. ANTITUMOR EFFICACY

Phase II studies consistently revealed response rates of 10–35% to single-agent irinotecan in advanced or metastatic colorectal cancer (89,90,104,105), independent of the applied schedules. There was no apparent difference between the applied schedules with respect to the median remission duration and median survival time, respectively 6–8 months and 8–13 months (90).

TABLE V.  
Main Toxicities of Irinotecan.

---

*Hematological*

- Grade 3<sup>a</sup> and 4<sup>a</sup> neutropenia
  - Dose and schedule dependent
  - Lowest frequencies in protracted dose regimens
  - Reversible, noncumulative, and of short duration
  - Febrile neutropenia occurred in about 3% of patients

*Nonhematological*

- Acute cholinergic-like syndrome ( $\pm 9\%$  of patients)
    - Caused by rapid and reversible inhibition of acetylcholinesterase by lactone form of irinotecan and can be induced by co-administration of oxaliplatin
    - Symptoms may occur shortly or within several hours after drug administration, and are short lasting, never life threatening
    - Symptoms: diarrhea, gastrointestinal cramps, nausea, vomiting, anorexia, asthenia, diaphoresis, chills, malaise, dizziness, visual-accommodation disturbances, salivation, lacrimation, and asymptomatic bradycardia
    - Responsive to and preventable by subcutaneous administration of 0.25–1.0 mg atropine
  - Delayed-onset diarrhea
    - Could be severe and unpredictable at all dose levels with increased intensity and frequency at higher dose levels ( $\pm 34\%$  of patients grade 3 or 4 after use of loperamide) and occurred later than 24 h after drug administration with peak incidence at day 5 or 6
  - Nausea and vomiting ( $\pm 86\%$  of patients, but  $\pm 19\%$  grade  $\geq 3$ )
    - Manageable with 5-HT<sub>3</sub> antagonists
  - Other common toxicities
    - Fatigue ( $\pm 17\%$ ), mucositis ( $\pm 12\%$ ), skin toxicity ( $\pm 5\%$ ), asthenia, alopecia, and elevated liver transaminases
  - Less common toxicities
    - Pulmototoxicity (pneumonitis), cardiotoxicity (bradycardia), microscopic hematuria, cystitis, dysarthria, and immune thrombocytopenia
- 

<sup>a</sup>Grade 3 and 4 according to NCI common toxicity criteria (version 2.0).

In a randomized Phase III study, comparing treatment with irinotecan given as a 300–350 mg/m<sup>2</sup> i.v. infusion every 3 weeks to best-supportive care in patients refractory to previous treatment with 5-FU based chemotherapy, the one-year survival rate was significantly greater for the irinotecan-treated group than for the control group, 36% and 14% ( $P < 0.01$ ), respectively (99). Another randomized Phase III study, comparing treatment with irinotecan to three different continuous i.v.-infusion schedules of 5-FU in patients with previously treated advanced colorectal cancer, revealed a survival advantage for the irinotecan-treated group in comparison to the 5-FU-treated group (100). The one-year survival rates were 45% and 32%, respectively ( $P < 0.05$ ).

TABLE VI.  
Phase II Studies of Single-Agent Irinotecan.

Tumor type	Dose level and schedule	Overall response rate (%)
SCLC <sup>a</sup>	100 mg/m <sup>2</sup> /wk <sup>c</sup>	47
NSCLC <sup>b</sup>	100 mg/m <sup>2</sup> /wk	32
Gastric cancer	100–150 mg/m <sup>2</sup> /1–2 wk	23
Pancreatic cancer	100–150 mg/m <sup>2</sup> /1–2 wk	10
	350 mg/m <sup>2</sup> /3 wk	9
Breast cancer	100–150 mg/m <sup>2</sup> /1–2 wk	14–20
	200 mg/m <sup>2</sup> /3–4 wk	
	350 mg/m <sup>2</sup> /3 wk	8
Cervical cancer	350 mg/m <sup>2</sup> /3 wk	15–23
	125 mg/m <sup>2</sup> /wk × 4 q <sup>d</sup> .6 wk	0–23
Ovarian cancer	100–150 mg/m <sup>2</sup> /1–2 wk	24
Head and neck cancer	75–125 mg/m <sup>2</sup> /wk × 4 q.6 wk	21
Leukemia/lymphoma	40 mg/m <sup>2</sup> /d <sup>e</sup> × 5 q.3–4 wk	17–24
	40 mg/m <sup>2</sup> /d × 3 q.wk	38

<sup>a</sup>SCLC, small-cell lung cancer.

<sup>b</sup>NSCLC, non-small cell lung cancer.

<sup>c</sup>wk, week(s).

<sup>d</sup>q, every.

<sup>e</sup>d, day(s).

Apart from colorectal cancer antitumor activity, single-agent irinotecan was also active in Phase II studies in several other solid tumors summarized in Table VI (65,74,106,107).

Based on the activity data in colorectal cancer derived from Phase I/II studies on the combination of irinotecan with 5-FU/leucovorin, two randomized Phase III studies were performed comparing this combination to single-agent 5-FU/leucovorin in the first-line treatment of metastatic colorectal cancer (108,109). Saltz *et al.* randomized 683 patients to receive either a weekly × 4 regimen of a 90-min i.v. infusion of irinotecan at a dose of 125 mg/m<sup>2</sup> and leucovorin at a dose of 20 mg/m<sup>2</sup> as a 15-min i.v. infusion, followed by 5-FU i.v. bolus at a dose of 500 mg/m<sup>2</sup> (arm A, *n* = 231), or conventional low-dose 5-FU/leucovorin (arm B, *n* = 226), or irinotecan at a dose of 125 mg/m<sup>2</sup> for 4 consecutive weeks every 6 weeks (arm C, *n* = 226) (108). An intention-to-treat analysis showed that the combination of irinotecan and 5-FU/leucovorin (arm A) yielded a significantly higher remission rate (*P* < 0.001), significantly longer progression-free survival (*P* = 0.004), and significantly longer median survival (*P* = 0.04) in comparison to single-agent 5-FU/leucovorin (arm B). There was no difference between single-agent irinotecan (arm C) and 5-FU/leucovorin (arm B) in terms of overall response rate, median time to disease progression, and median overall survival time (108).

Severe diarrhea (grade 3 or 4) (arm A 23%; arm B 13%; and arm C 31%) and neutropenia (grade 4) (arm A 42%; arm B 24%; and arm C 12%) were the most prominent toxicities in this study, but these side effects did not preclude the administration of approximately 75% of the prescribed doses of irinotecan and 5-FU (108). The reverse side of the study was the bias of unreported toxic deaths in the combination treatment arm (arm A).

Douillard *et al.* randomized 385 patients to (arm A,  $n=169$ ) the combination of irinotecan and an infusional schedule of 5-FU. The regimens were: once weekly, irinotecan 80 mg/m<sup>2</sup> with 5-FU 2300 mg/m<sup>2</sup> by 24 h infusion, and leucovorin 500 mg/m<sup>2</sup> (arm A1); or every 2 weeks, irinotecan 180 mg/m<sup>2</sup> on day 1 with 5-FU 400 mg/m<sup>2</sup> bolus and 600 mg/m<sup>2</sup> by 22 h infusion, and leucovorin 200 mg/m<sup>2</sup> on days 1 and 2 (arm A2) (109). For the control arm (arm B,  $n=169$ ), the regimens were: once weekly, 5-FU 2600 mg/m<sup>2</sup> by 24 h infusion and leucovorin 500 mg/m<sup>2</sup> (arm B1); or every 2 weeks, 5-FU and leucovorin at the same doses and administration as in arm A2 (109). Although there was a good balance between both treatment arms for known risk factors, the number of primary rectal cancers in arm A was slightly higher. Compared with the study by Saltz *et al.*, in this study proportionally more patients had received prior adjuvant 5-FU-based chemotherapy 10% versus 25%, respectively (90). An objective response rate of 41% was reported in treatment arm A (combination irinotecan with 5-FU and leucovorin) compared with 23% in the schedule of 5-FU and leucovorin alone (arm B) ( $P<0.001$ ) (109). Also, the median time to disease progression ( $P<0.001$ ) and median survival time ( $P<0.028$ ) were statistically significant in favor of the combination treatment arm (arm A) compared to the control arm (arm B).

The overall response rate of treatment arm A1 was 51% and for arm A2 38%. For the weekly single-agent 5-FU and leucovorin (arm B1) and biweekly 5-FU/leucovorin (arm B2), the overall response rates were 29% and 21%, respectively (109). More severe neutropenia (29% vs. 21%,  $P<0.01$ ) and severe diarrhea (24% vs. 11%) were seen in the combination arm (arm A) compared with the control arm (arm B). The neutropenia was not significantly associated with fever or infection.

In a multiregression Cox model analysis, the influence of baseline characteristics of patients on the efficacy of the cytotoxic therapy in terms of time to progression and survival were determined. This analysis revealed that excellent performance status (WHO 0 vs. 1 or more), extension of organ involvement (1 vs. 2 or more sites), and normal values for lactate dehydrogenase (LDH), bilirubin, and leucocytes were the major prognostic factors for longer overall survival (90). A significant prolongation of time to progression adjusted for normal values of LDH and disease extension (only one organ site) ( $P=0.0001$ ) was established for the combination irinotecan and 5FU/leucovorin compared to single-agent 5-FU/leucovorin, in both studies (90).

Combined analysis of both studies confirmed that the addition of irinotecan to 5-FU/leucovorin significantly increases response rate, median time to disease progression, and median time to survival, especially for patients with excellent prognostic characteristics will have a survival benefit of this combination therapy (90). The abovementioned treatment schedules of both studies are approved by the FDA as first-line chemotherapy for patients with metastatic colorectal cancer (90). Yet, randomized trials to evaluate the merits of this combination in the adjuvant setting are ongoing (74). Furthermore, clinical trials evaluating the antitumor efficacy of irinotecan in combination with an oral fluoropyrimidine (capecitabine), which may replace infusional 5-FU, are currently in progress (74).

#### D. OTHER COMBINATION CHEMOTHERAPY TRIALS

The combination of irinotecan and raltitrexed was evaluated in two Phase I studies, whereby asthenia was found as the DLT in both studies. The recommended doses were irinotecan 350 mg/m<sup>2</sup> and raltitrexed 3 mg/m<sup>2</sup> once every 3 weeks (110,111).

*In vitro* and *in vivo* studies have revealed synergism or additivity between irinotecan and cisplatin in numerous tumor cell lines and human tumor xenografts (112–120). The mechanism of interaction between both agents involves a delay by the topoisomerase I inhibitor in the reversal of cisplatin-induced DNA interstrand cross-links (ISCs) without modifying the formation of ISCs (120,121). No alteration in cleavable complexes formation or reversion was observed.

All Phase I studies on the combination of irinotecan and cisplatin, except for one, focused on fractionated dose schedules for both agents (120,122–128). Neutropenia (grade 4 in 35% of the patients) and diarrhea were the dose-limiting toxicities. In only 4% of all patients neutropenia was complicated by fever. A 33% and 65% increase in DI of irinotecan could be achieved by adding G-CSF to schedules with neutropenia as the DLT (126,127). Only one Phase I study involved the 3-weekly administration and studied the relevance of sequence of drug administration (128). Patients were randomized to receive irinotecan, immediately followed by cisplatin in the first course, and the reversed sequence in the second course or vice versa. Significant differences in toxicity between the treatment schedules were not observed. Neither could a pharmacokinetic interaction be discerned. In addition, irinotecan had no influence on the platinum DNA-adduct formation in peripheral leukocytes in either sequence (128). Apparently there is no administration sequence that should clearly be favored for this particular topoisomerase I inhibitor.

Phase II studies of this combination indicate high levels of activity in various tumors, but none of these studies were randomized, so their interpretation is difficult (74). A Phase III study using this combination as first-line chemotherapy for patients with extensive disease of SCLC showed a significant improvement

in the one-year survival rate (60%) in comparison with conventional treatment with etoposide and cisplatin (40%) ( $P=0.005$ ) (129).

The combination of irinotecan and oxaliplatin was evaluated in Phase I studies using a once every 2 weeks and once every 3 weeks schedule with neutropenia, and a combination of diarrhea and neutropenia as dose-limiting side effects in the different schedules, respectively (130–132). Remarkably, the interaction of both drugs showed acute cholinergic toxicities, whose severity is potentiated by oxaliplatin (133–135). The recommended dose of oxaliplatin is 85 mg/m<sup>2</sup> for both schedules. The recommended dose of irinotecan is 175 mg/m<sup>2</sup> for the once every 2 weeks and is 200 mg/m<sup>2</sup> for the once every 3 weeks. In a Phase II study in patients with advanced colorectal cancer, this combination was compared with raltitrexed as first-line treatment, which showed an acceptable toxicity profile after dose reduction of irinotecan to 150 mg/m<sup>2</sup> once every 3 weeks (136).

In Phase I and/or II studies, irinotecan is also combined with other cytotoxic agents, including etoposide (137–142), carboplatin (143–145), docetaxel (146,147), paclitaxel (148,149), mitomycin-C (150,151), and also the triplet combination with carboplatin and docetaxel (152,153). This topic about combination treatment is reviewed in more detail by De Jonge *et al.* (120). The combination of irinotecan and etoposide seems to be hepatotoxic (154).

## V. Topotecan

### A. CLINICAL PHARMACOLOGY

Topotecan (TPT; 9-dimethylaminomethyl-10-hydroxycamptothecin) is a semisynthetic, water-soluble CPT derivative, synthesized by modification of 10-hydroxycamptothecin (155). It undergoes CYP3A-catalyzed metabolism to *N*-desmethyl topotecan. *N*-Desmethyl topotecan is a less-active metabolite of which only low plasma levels were found, suggesting minimal CYP3A-related conversion. Nonetheless, clinical trials have shown significantly altered clearance of topotecan in patients on CYP3A-inducing anticonvulsants, similar to that observed with irinotecan (65). Both topotecan and *N*-desmethyl topotecan exist in an active lactone and inactive carboxylate form in a similar equilibrium (156). Only a very small amount of total topotecan is present in the lactone form at equilibrium. At physiological pH, most topotecan is in the inactive carboxylate form, whereas in an acidic environment the ratio is opposite (157). These circumstances have practical consequences because, on reconstitution in normal saline, a large amount of topotecan is converted to the carboxylate form, whereas at lower pH of 5% dextrose for injection, the maximum extent of conversion is 10% with equilibrium being achieved within half an hour (74,158). For this reason, a new parenteral formulation has been produced that contains tartaric acid in the infusion diluent to provide a sufficiently low pH to maintain the agent in the essential lactone form (159).



Both the carboxylate form and the lactone form of topotecan may undergo further metabolism into an UGT-mediated glucuronide product (i.e., topotecan-*O*-glucuronide and *N*-desmethyl topotecan-*O*-glucuronide) (160). This is a reversible transformation because beta-glucuronidase is able to reform topotecan and *N*-desmethyl topotecan. Because topotecan is metabolized in the liver only to a minor extent, it is not surprising that the pharmacokinetics in patients with impaired liver function did not significantly differ from those in patients with normal hepatic function (161). In contrast, patients with moderately impaired renal function had significantly reduced plasma clearance (162). As a clinical practical consequence, dose modifications are recommended for patients with impaired renal function and are not required for patients with liver dysfunction (161,162).

Topotecan is most commonly administered as a 30-min i.v. infusion (74). Within 5–10 min after the end of the infusion plasma concentrations of the carboxylate form exceed those of the lactone form. Under the abovementioned circumstances, the AUC ratio of the lactone to total drug ranges from 30% to 40%. The same AUC ratio of both compounds in plasma is achieved when topotecan is administered as a prolonged infusion once steady-state concentration is reached (163–172). After i.v. infusion of topotecan, the plasma levels of the lactone form and total drug descend in a biexponential way with similar terminal half-lives of 2.4–4.3 h. Compared with most other CPT derivatives, the biological half-life of topotecan is short. Consequently, no drug accumulation will occur when five daily doses of topotecan are administered by a 30-min i.v. infusion at an interval of 24 h, which is the recommended dosing regimen for topotecan (74).

Over the range of tested doses of 0.4–22.5 mg/m<sup>2</sup>, topotecan showed linear pharmacokinetic behavior for both the total drug and intact lactone species. This pharmacokinetic behavior did not change significantly when topotecan was given daily (74). The total body clearance of topotecan on the average is 27.4 l/h/m<sup>2</sup> for the lactone form and 13.4 l/h/m<sup>2</sup> for the total drug (164–171). Owing to its hydrophilic properties, topotecan showed a moderate, steady-state apparent volume of distribution, being only approximately two times the body weight for the lactone species and total drug. In comparison with other CPT analogs, the fraction of topotecan bound to plasma proteins is much lower. Possibly, this property accounts for the more efficacious penetration of topotecan in cerebrospinal fluid (173–175) and pleural fluid and ascites (176) as compared to other CPT derivatives.

Furthermore, the plasma pharmacokinetics of topotecan did not change due to the presence of third spaces, i.e., ascites and/or pleural effusion (176). The ratio between the exposure to topotecan in the third space and in the plasma compartment was 55%. Consequently, topotecan can be safely administered to patients with malignant ascites and pleural effusion, and it might contribute to local tumor effects due to its substantial penetration in the third space (176).

A Phase I study on the intraperitoneal (i.p.) administration of topotecan revealed that the MTD was 20 mg/m<sup>2</sup> once every 3 weeks delivered by the i.p.

route, achieving cytotoxic plasma levels of topotecan, with acceptable toxicity and avoiding myelotoxicity (177). Peritoneal total topotecan was cleared from the peritoneal cavity at  $0.4 \pm 0.3$  L/h·m<sup>2</sup> with a half-life of  $2.7 \pm 1.7$  h. The mean peritoneal to plasma AUC ratio for total topotecan was  $54 \pm 34\%$  (177). These data were in good agreement with those from a Phase I study using a topotecan 24-h continuous i.p. infusion (178). The terminal half-life for peritoneal topotecan and for plasma total topotecan was similar for both studies (177,178). These data suggest that it would be possible to combine the i.p. administration of topotecan with other active chemotherapeutic agents.

In a randomized trial on topotecan administered either orally or intravenously, Herben *et al.* found that the urinary and fecal excretion of unchanged drug were the major routes of elimination (179). The principal route of excretion was via the kidneys, accounting for approximately 49% of the intravenously administered dose and 20% of the oral dose (179). Furthermore, approximately 18% and 33% of the i.v. and oral dose of topotecan, respectively, was excreted unchanged in the feces. Elimination through other routes was approximately 28% of the i.v. dose and 43% of the oral dose.

As mentioned earlier, in patients with impaired renal function the clearance of total topotecan is reduced, i.e., a 33% decrease in patients with a creatinine clearance (CrCl) ranging from 40 to 59 ml/min and a 75% decrease in patients with CrCl between 20 and 39 ml/min, compared to patients with normal renal function (i.e., CrCl  $\geq 60$  ml/min) (162). In patients with reduced renal clearance of topotecan, a second plasma peak was seen after the end of infusion due to increased bile excretion which, in turn, leads to enterohepatic recycling (162,179). Nevertheless, this is likely not of clinical relevance.

The oral bioavailability of topotecan is influenced by different factors. Firstly, the relatively high pH in the intestines leads to conversion to the carboxylate form, which is poorly absorbed by the intestinal walls (180). Secondly, the bioavailability is reduced by protein-mediated drug transport of topotecan. The breast cancer-resistance protein (BRCP), a protein of the adenosine triphosphate (ATP)-binding cassette family of transmembrane transporters, is highly expressed in the small intestine and mediates the apically directed drug transport of topotecan (179,181). Thirdly, the bioavailability is partly influenced by the binding of topotecan to food, proteins, and intestinal fluids, or by decomposition in the gastrointestinal fluid. Furthermore, the metabolism to *N*-desmethyl topotecan was demonstrated as a minor mechanism for elimination (179).

Population pharmacokinetic studies in patients treated with intravenously administered topotecan revealed that patient characteristics (i.e., gender, height, weight) and laboratory values (i.e., serum creatinine concentration) give a moderate ability to predict the clearance of topotecan in an individual patient (182). Although a significant correlation between the clearance of topotecan and patient age was not established, pharmacokinetic results of a greater number

of patients are warranted in order to make more definite conclusions on this specific issue.

## B. DOSE-FINDING TRIALS

Numerous Phase I clinical trials with topotecan in different schedules of drug administration have been performed (183). Based on the *in vitro* data on long-term exposure and the fact that efficacy of the drug has been demonstrated to be dependent on the schedules of administration, two schedules were selected for Phase II studies. Firstly, there is a 30-min i.v. infusion daily for 5 consecutive days every 3 weeks, at a dose of 1.5 mg/m<sup>2</sup>/day. In this schedule, the DLT is short lasting, noncumulative myelosuppression (184–186). Nonhematological toxicities are usually mild and reversible and include nausea, vomiting, fatigue, alopecia, and sometimes diarrhea. Phase II studies with the drug administered in this schedule revealed response rates ranging from 9.5 to 25% in pretreated patients with ovarian cancer, and response rates of 10–39% in patients with SCLC (187–190). In addition, a comparative randomized, multicenter trial in which patients with recurrent ovarian cancer were treated, showed that topotecan was at least as effective as paclitaxel in terms of response rate (20% vs. 13%), median duration of response, and median time to progression (191–197). In other tumor types, topotecan was much less active (198–217). A summary of the safety profiles and clinically observed toxicities is provided in Tables VII and VIII, respectively (218,219).

Secondly, various schedules focusing on the continuous infusion of topotecan have been studied, including a 24-h infusion weekly, and every 3 weeks, a 72-h infusion administered weekly, every 14 days and every 21 days, a 120-h infusion every 3–4 weeks, and 21-day low-dose continuous infusion every 4 weeks (27). In addition to the DLT of leucocytopenia, the longest infusion schedules also induce thrombocytopenia.

With the continuous i.v. administration for 21 days every 28 days, the MTD was 0.53 mg/m<sup>2</sup>/day (220). The steady-state concentration of lactone topotecan was only approximately 4 ng/ml. No consistent relationship between drug level and hematological toxicity was found. Of interest, the Phase I study showed several partial tumor responses in tumor types which were initially chemotherapy resistant (220). In a Phase II study with this regimen in patients with progressive and platinum-refractory ovarian cancer, the response rate was 37% (221).

Since 21-day continuous infusion is inconvenient, an oral formulation of topotecan was also investigated (166). The oral bioavailability of topotecan is approximately 30–35% with acceptable interpatient variation and independent of the formulation used. In view of this, the oral route of administration may provide a more convenient approach to clinical-prolonged exposure (166,222,223). After oral administration, topotecan is rapidly absorbed with peak plasma

TABLE VII.  
Safety Guidelines for the Use of Topotecan.

- 
- Proper patient selection according to known risk factors:
    - For severe neutropenia: Renal impairment, prior myelosuppressive chemotherapy (both platinum analogs and alkylating agents), prior bone marrow transplantation, prior wide-field radiotherapy
    - For severe thrombocytopenia: Renal impairment, prior myelosuppressive chemotherapy (especially carboplatin)
  - Proper training of the treating medical oncologist and his staff, and extensive information to the patient:
    - Including a patient information leaflet about the management of toxicities
  - Dose reduction in case of:
    - Grade 4<sup>a</sup> neutropenia > 2 weeks (with G-CSF<sup>b</sup>)
    - Grade 3<sup>a</sup> neutropenia concomitant with fever and/or infection
    - Complicated grade 3 or 4 thrombocytopenia
    - Renal impairment; creatinine clearance < 60 ml/min and extensive prior therapy; creatinine clearance < 40 ml/min and minimal prior therapy
    - Treatment delay > 2 weeks
    - Elevated bilirubin in combination with poor performance status and comorbidities
  - Contraindication for use in patients with:
    - WHO<sup>c</sup> performance status > 2
    - Predictable poor compliance
    - Creatinine clearance < 20 ml/min
    - Baseline serum bilirubin > 1.5 × UNL<sup>d</sup>
  - Treatment only with caution and close survey between cycles in patients with:
    - WHO performance status = 2
    - Creatinine clearance < 60 ml/min
    - Prior myelosuppressive chemotherapy (carboplatin)
    - Prior abdominopelvic radiation therapy
- 

<sup>a</sup>Grade 3 and 4 according to NCI common toxicity criteria (version 2.0).

<sup>b</sup>G-CSF, granulocyte colony-stimulating factor.

<sup>c</sup>WHO, World Health Organization.

<sup>d</sup>UNL, upper normal limit.

concentrations reached at 0.6–0.78 h after intake (157). Lactone to carboxylate ratios was comparable after oral and i.v. administration (166,223). No relationship was found between bioavailability and age, gender, performance status, and the presence of liver metastases. Currently, topotecan is supplied in gelatin capsules and is administered at least 10 min before a meal, although combination with high-fat meal only led to a small decrease in the rate of absorption, not in the extent of absorption (224).

TABLE VIII.  
Main Toxicities of Topotecan.

---

*Hematological*

- Grade 4<sup>a</sup> neutropenia (81% of patients)
  - Dose related, reversible, noncumulative
  - (Extensive) prior treatment dependent
  - Median onset occurred on day 9
  - Median duration of 6 days (in 12% of patients duration longer than 7 days)
  - Febrile neutropenia or infections occurred in 26% of patients
- Grade 4 thrombocytopenia (26% of patients)
  - Dose related, reversible, noncumulative
  - (Extensive) prior treatment dependent
  - Platelet transfusions necessary in 13% of patients
- Grade 4 anemia (40% of patients)
  - Dose related, reversible, noncumulative
  - Blood transfusions necessary in 56% of patients

*Non-hematological*

- Other common toxicities
    - Alopecia, nausea, vomiting, fatigue, stomatitis, constipation, diarrhea, abdominal pain, asthenia
- 

<sup>a</sup>Grade 4 according to NCI common toxicity criteria (version 2.0).

In order to mimic a prolonged exposure regimen and based on the relatively short half-life of the drug (average 2.4 h), a twice daily oral administration schedule for 21 days every 28 weeks was studied (222). The dose-limiting side effect was diarrhea, at a dose of 0.6 mg/m<sup>2</sup> twice daily. It occurred in 55% of patients with a median day of onset on day 15 (range, 12–20) and resolved after a median of 8 days (range, 7–16). Administration of high-dose loperamide did not limit the diarrhea (222). The hematological toxicity was mild and comprised mainly of neutropenia (35%).

Because of this diarrhea occurring beyond day 15, and in view of the emerging insights that topoisomerase I inhibition might be no longer optimal after 14 days of continuous drug administration, a shorter schedule was investigated (224,225). Patients were treated once daily or twice daily for 10 days every 21 days (224). In the once-daily regimen, dose-limiting thrombocytopenia and diarrhea was seen at a dose of 1.6 mg/m<sup>2</sup>/day. The DLTs were similar occurring at a dose of 0.8 mg/m<sup>2</sup> b.i.d. (157,224).

Because of the persistence of diarrhea as a side effect in the 10-day schedule, finally a 5-day schedule was studied (226). The DLT was neutropenia similar to the i.v. drug use, with a nadir between days 8 and 15 and median duration of

6 days (range, 2–12). Nonhematological toxicities were mild to moderate. Moderate to severe diarrhea ( $\geq$  CTC grade 2) was observed in 21% of the patients and this event was self-limiting. The recommended dose was 2.3 mg/m<sup>2</sup>/day. Assuming an average body surface area in patients of 1.75 m<sup>2</sup>, the recommended dose of 2.3 mg/m<sup>2</sup>/day equals a fixed dose of 4 mg/day. Pharmacokinetics and toxicity were studied at this fixed dose in order to ascertain whether dosing based on per square milligram offered any advantage over flat dosing. Such an advantage was not found (226).

In summary, hematological toxicity is more pronounced with the shorter oral regimens, but is still mostly mild and noncumulative, whereas diarrhea is a severe and intractable side effect of more prolonged daily administration (157). An analysis of the pharmacokinetic/pharmacodynamic relationships revealed that the total AUC per course did not differ between the various regimens, and in an analysis of the time over the threshold concentration of 1 ng/ml, it appeared that the daily-times-five schedule provided the best systemic exposure and toxicity profile (227).

In acute leukemia, the maximum-tolerable dose of a daily 30-min i.v. infusion for 5 consecutive days every 3 weeks was 4.5 mg/m<sup>2</sup>/day (228). Dose-limiting toxicity at higher dose levels were a complex of symptoms, comprising high fever, rigors, precipitous anemia, and hyperbilirubinemia. Although the precise etiology of these adverse effects was not known, it was believed that high doses of topotecan had induced an acute hemolytic reaction (228).

### C. ANTITUMOR EFFICACY

The dosage regimen of topotecan approved for clinical use is 1.5 mg/m<sup>2</sup>/day given as a 30-min i.v. infusion daily for 5 days every 3 weeks. Dose-related, reversible, and noncumulative myelosuppression is the most important side effect of topotecan (229). Neutropenia – the nadir is usually approximately 9 days after the start of the treatment and the median duration is approximately 7–10 days – occurred more frequently and is often more severe than thrombocytopenia. Also, neutropenia was more severe in heavily pretreated patients compared with minimally pretreated patients (229). Besides myelosuppression, stomatitis (24–28% of patients) and late-onset diarrhea (40%) were noted at higher doses (65,229). Other nonhematological toxicities reported included alopecia (76–82% of patients), nausea (75–78%), vomiting (53–64%), fatigue (30–41%), and asthenia (21–22%) (229).

Antitumor activity of topotecan, given as a single agent in various schedules of administration, was established in a variety of Phase II studies, including ovarian cancer [overall response rate (OR), 14–38%], SCLC (OR, ~39%), NSCLC (OR, ~13%), breast cancer (OR, ~10%), myelodysplastic syndrome (MDS) [complete response rate (CR), ~37%], and chronic myelomonocytic leukemia (CMML) (CR, ~27%) (65). Marginal activity was seen in head and neck cancer

(202,230), prostate cancer (231), pancreatic cancer (210,215,217), gastric cancer (211,212), esophageal carcinoma (204), hepatocellular carcinoma (213), and recurrent malignant glioma (216).

In a Phase III study, the daily-times-five i.v. topotecan regimen was compared with paclitaxel (3-h infusion of 175 mg/m<sup>2</sup>/day every 3 weeks) in ovarian cancer. In this disease, topotecan and paclitaxel were equally effective with regard to response rates, progression-free survival, and overall survival (191). The median duration of response was 26 weeks (range, 7–84 weeks) for topotecan and 22 weeks (range, 9–67 weeks) for paclitaxel. The respective median times to progression were 19 weeks (range, <1–93 weeks) and 15 weeks (range, <1–77 weeks), while the median survival was 63 weeks (range, <1–122 weeks) versus 53 weeks (range, <1–130 weeks) (232).

In an open-label, multicenter study comparing the activity and tolerability of oral versus i.v. topotecan, 266 patients with relapsed epithelial ovarian cancer after failure of one platinum-based regimen, which could have included a taxane, were randomized to the two arms (233). Oral versus i.v. doses of topotecan were administered as 2.3 and 1.5 mg/m<sup>2</sup>/day, respectively, for 5 consecutive days every 3 weeks. The principal toxicity was noncumulative myelosuppression, although moderate to severe neutropenia was less frequently seen in patients treated with oral topotecan. Furthermore, grade 3 and 4 gastrointestinal toxicities were seen slightly higher in the oral treatment arm. No difference in response rates between the treatment arms was reported. Although a small, statistically significant difference in survival favored the i.v. formulation (58 weeks) versus the oral formulation (51 weeks) ( $P=0.033$ ), in the context of second-line palliative treatment for ovarian cancer, this outcome has only limited clinical significance (233). For this reason, oral topotecan could be an alternative treatment modality in this setting because of its convenience and good tolerability. Its definite place has to be clarified in further studies.

A Phase III study compared single-agent topotecan with combination chemotherapy, comprising cyclophosphamide, doxorubicin, and vincristine (CAV), in 211 patients with SCLC relapsing after first-line chemotherapy (234). Although response rate, time to disease progression, and overall survival were similar, palliative efficacy of disease-related symptoms was better with topotecan (234). In a randomized Phase III trial performed by the Eastern Cooperative Oncology Group (ECOG), topotecan was compared with best support of care in patients with extensive SCLC. In this trial, topotecan was administered as a consolidation therapy after response induction with cisplatin and etoposide (235). Although topotecan induced a moderate increase in the time to disease progression, it did not improve survival (235). Finally, similar to the study in ovarian cancer, oral topotecan was compared to i.v. administration of topotecan in patients with relapsed and chemosensitive SCLC. The oral formulation was found to be similar in efficacy with less severe neutropenia and greater convenience of drug administration (236). Based on these data, topotecan

has been approved by the FDA for the treatment of recurrent SCLC in the USA (74).

Although topotecan has shown some activity against hematological malignancies, its use for this specific indication has still to be further explored in research (237). As indicated, the complete remission rate is interesting in MDSs (37%) and in CMML (27%) (238,239). Of note, the presence of a mutation of the *ras*-oncogene seems to predict insensitivity to topotecan treatment in CMML. In relapsed or resistant multiple myeloma, the overall response rate was 16% (95% CI, 7–31%). Responses have lasted 70 to 477+ days, with a median progression-free survival of 13 months and a median survival time of 28 months (240,241).

## VI. Considerations of Route of Administration

As mentioned earlier, cytotoxicity of topoisomerase I inhibitors increases with the duration of exposure. *In vitro* studies showed that short-term exposures to high concentrations are less effective than long-term exposure to low concentrations (29,30). Low-dose, prolonged exposure *in vivo* studies in animal models also resulted in less toxicity (242–246). On the other hand, *in vitro* and animal models have shown to be poor predictors of clinical efficacy and toxicity for several reasons, including species differences in drug disposition, tolerability, and intrinsic differences in tumor sensitivity, and the ascertainment that animal models are relatively resistant to the myelosuppressive effects of the CPT analogs (157). As a consequence, various Phase I and II studies have been performed to focus on low-dose prolonged exposure to or continuous infusion of CPT derivatives in the treatment of cancer patients (76,170,171,209,220,242,247,248). In addition, the results of studies in animal models showing that the intragastric administration of CPTs was effective, added to the fact that the low gastric pH would favor the active lactone-ring configuration of the CPTs; these data would favor oral drug application (157).

From a clinical point of view, as long as equivalent safety and efficacy can be ensured, the majority of patients prefer oral instead of i.v. administration of chemotherapy, predominantly due to the convenience of administration outside a clinical setting and avoidance of vascular complications, related to i.v. access, including catheter-associated infections or potential thrombosis (249,250).

From a pharmacological point of view, the oral route of drug administration has some disadvantages. Absorption of an oral drug from the gastrointestinal (GI) tract is a prerequisite for its activity, but this process can be influenced by several factors. Delays or losses of the drug during absorption may contribute to variability in drug response or may even result in failure of the treatment (250). Both anatomical and physiological factors affect the overall rate and extent of absorption from the GI tract and they influence the precise quantitative prediction. Ideally, a cytostatic drug should have little interpatient



variability in absorption and AUC, and even more important, little inpatient variability with successive doses (251). As an inverse relationship is demonstrated between decreasing absolute bioavailability of drugs and the interindividual variation in bioavailability, it is recommended that caution must be taken in prescribing oral drugs with low oral bioavailability as the therapeutic index is narrow and thus, either toxic or subtherapeutic dosing may easily occur (250). For instance, given the relatively low bioavailability of orally administered topotecan, ranging from 30% to 40%, and the relatively high variability in the AUC both between patients (CV, 40–73%) and within the same patient (CV, 25–96%), this issue of a narrow therapeutic index is clearly demonstrated for the oral administration of topotecan at its maximum-tolerable dose (166,252).

The variability of pharmacokinetics of orally administered anticancer drugs can among other things be explained by the affinity for drug-transporting proteins expressed in the intestinal epithelium and directed toward the gut lumen (250). Currently, three major classes of drug pumps, including P-glycoprotein (ABCB1), multidrug resistance-associated protein (MRP1 or ABCC1) and its homolog MRP2 (also known as cMOAT or ABCC2), and BRCP (synonymous for MXR, ABCP1, or ABCG2), have been characterized, that may play a role in mediating transmembrane transport of anticancer agents, including irinotecan and topotecan (250). The abovementioned proteins belong to the large superfamily of ATP-binding cassette transporters that are found in almost all prokaryotic and eukaryotic cells. The characteristic tissue distribution of these drug transporters strengthens the indication that they play an important role in detoxification and protection against xenobiotic substances (250). *In vivo* studies with genetic knockout of murine P-glycoprotein genes revealed that the intestinal absorption of various anticancer drugs, including paclitaxel and topotecan, was increased (181,250). These experimental studies led to the development of clinical trials of anticancer drugs modulated by co-administration of inhibitors of P-glycoprotein and BCRP. Recently, a proof-of-concept study in 16 patients with solid tumors was reported in which topotecan was administered in the presence and absence of GF120918, a potent inhibitor of BCRP and P-glycoprotein (253). This study showed that the co-administration of the inhibitor of the drug transporters significantly increased the systemic exposure of oral topotecan, with the mean AUC of total topotecan increasing from  $32.4 \pm 9.6 \mu\text{g h/l}$  without co-administration of GF120918 to  $78.7 \pm 20.6 \mu\text{g h/l}$  with co-administration of GF120918 ( $P=0.008$ ). Furthermore, the apparent oral bioavailability increased significantly from 40% to 97.1% ( $P=0.008$ ) (253). Interpatient variability of the apparent bioavailability was 17% without versus 11% with co-administration of the inhibitor.

There is no doubt that, in order to approach the conceptual starting point of prolonged exposure to a minimum concentration of the drug for optimizing therapeutic efficacy, daily oral dosing would be preferable to continuous i.v. infusion. But, up till now Phase I and II studies did not show superior efficacy after prolonged exposure of topotecan (172,220,222,253,254).

Actually, the assumptions about the importance of prolonged exposure are being reconsidered (254).

## VII. Investigational Derivatives

### A. 9-SUBSTITUTED CAMPTOTHECINS

9-Aminocamptothecin (9-AC) is a semisynthetic CPT derivative which showed outstanding preclinical activity against a wide spectrum of tumor types, including those of breast, colon, lung, prostate, and melanoma (255). In clinical trials, the drug has been very extensively studied using two different formulations based on the use of dimethylacetamide/polyethylene glycol 400 or a colloidal dispersion preparation, which enhances solubility and stability. Clinical Phase I investigations have been conducted using a variety of i.v. administration schedules, including a 30-min infusion given daily for 5 days every 3 weeks (256), and more prolonged infusion schedules using 24-h (257), 72-h (258–261), 120-h (262), or 7-day continuous dosing repeated every 4 weeks (263). In addition, trials have evaluated the usefulness of delivering the agent intraperitoneally (264) or orally (265–267).

All of the studies report neutropenia as the DLT, while thrombocytopenia is also frequent and sometimes severe. Gastrointestinal toxicity is the second most reported, though not dose limiting. Other toxicities are considered mild to moderate. Numerous multi-institutional Phase II studies have been conducted in several disease types, and overall, 9-AC shows only very modest single-agent activity with the prolonged (72- or 120-h infusion) regimens. These include trials in breast cancer (268), colorectal cancer (269–272), glioblastoma (273), head and neck cancer (274), lymphoma (275,276), and NSCLC (277,278). Therefore, its further evaluation does not seem to be indicated. It has been suggested that the lack of clinically relevant antitumor efficacy relates to substantial inactivation of the agent due to the unfavorable lactone/carboxylate ratio in patients (279,280). In addition, using preclinical studies it has been shown that solid-tumor xenografts were highly sensitive to 9-AC therapy, but the systemic exposure required for antitumor effects was in excess of that achievable clinically in patients (281).

Because of the poor aqueous solubility and poor antitumor activity of 9-AC clinically, some major efforts have been put into the design and synthesis of more derivatives that could be alternatives to the parent drug, including an *N*-(2-hydroxypropyl)methacrylamide copolymer conjugate (282). Some of the synthesized compounds have shown only marginal improvements in solubility or are too unstable to allow administration in a clinical setting. In addition to solving solubility issues, linkage of specific carriers to 9-AC offers the possibility of targeted drug delivery that may enhance the therapeutic index. The potential targeting of 9-AC to tumor cells has been investigated with the use of enzyme-activatable prodrugs, which include a 9-AC-glucuronide (283) and a 20-carbonate-linked

derivative (284) designed for activation by tumor-associated beta-glucuronidase and plasmins, respectively.

To date, only one approach in prodrug design has yielded an agent that has progressed to clinical evaluation, i.e., the 9-nitro derivative of CPT [i.e., 9-nitrocamptothecin (9-NC; RFS 2000; rubitecan)], which acts as a partial prodrug of 9-AC (285,286). 9-NC has a nitro group in the C-9 position and is highly insoluble in water, and was initially identified as a precursor in the semisynthetic production of 9-AC. Since nearly all human cells are able to convert 9-NC to 9-AC, including tumor cells, it has been proven difficult to identify whether 9-NC-mediated antitumor activity is directly associated with the parent drug alone or with 9-AC alone, or the combination of both (287).

Phase I clinical evaluation of 9-NC has been focused on oral administration in a daily-times-five per week regimen, either given alone (288,289) or in combination with cisplatin (290). More recently, attempts have been made to administer the drug as an aerosolized liposomal preparation (290,291). Preliminary evidence generated in Phase II clinical trials with the oral formulation suggests that 9-NC has moderate activity in the treatment of advanced pancreatic cancer (292,293) and refractory ovarian cancer (294). An extensive Phase II clinical program is currently being conducted in Europe to test the efficacy of this agent against various malignant diseases. Thus far, oral 9-NC has been shown to be inactive against metastatic colorectal cancer (295), advanced glioblastoma multiform (296), and cutaneous or uveal melanoma (297).

## B. EXATECAN MESYLATE (DX-8951f)

The hexacyclic camptothecin analog exatecan mesylate (DX-8951f) ([1*S*,9*S*]-1-amino-9-ethyl-5-fluoro-1,2,3,9,12,15-hexahydro-9-hydroxy-4-methyl-10*H*,13*H*-benzo[*de*]-pyrano[3',4':6,7]-indolizino[1,2-*b*]quinoline-10,13-dione monomethane sulfonate [salt], dihydrate) is a synthetic derivative with an amino group at C-1 and a fluorine atom at C-5. The compound has increased aqueous solubility in comparison with other CPT analogs. As exatecan does not require enzymatic activation, interindividual variability in efficacy and side effects might be reduced as compared to some prodrug analogs (298). The anhydrous free-base form of the drug is referred to as DX-8951. The lactone form of DX-8951 is hydrolyzed into an open-ring hydroxy-acid form, comparable with most other CPTs. Similarly, the lactone and hydroxy-acid form coexist in solution according to a reversible pH-dependent equilibrium, i.e., DX-8951 is presented by its lactone form at acidic pH and by its hydroxy-acid form in neutral and basic pH (299,300).

Exatecan showed superior and a broader spectrum of antitumor activity *in vitro* and *in vivo* in comparison with some other CPT analogs tested (298,301–306). Comparable with other CPT derivatives, exatecan is metabolized by CYP3A4 and CYP1A2, resulting in the formation of at least two hydroxylated metabolites

referred to as UM-1 and UM-2. The antitumor activity of these metabolites is much less potent than the parent compound itself (299,307,308).

Phase I clinical studies included DX-8951f administered as a 30-min i.v. infusion once every 3 weeks, as a 30-min i.v. infusion daily for 5 days every 3 weeks, as a 24-h continuous i.v. infusion every 3 weeks, and as a weekly 24-h i.v. infusion 3 of every 4 weeks (309–314).

Reversible, noncumulative, and dose-related neutropenia was the DLT in all five schedules (309–313). With a 24-h continuous infusion every 3 weeks, thrombocytopenia was an added DLT in heavily pretreated patients (310). Neutrophil and platelet count nadirs occurred between days 10 and 15, with recovery by day 22. Nonhematological toxicities included mild to moderate gastrointestinal toxicity (nausea, vomiting, stomatitis, diarrhea), fatigue, asthenia, and alopecia (309–313). Transient and reversible liver dysfunction was also observed, and in a Japanese study this event was dose limiting at the dose of 6.65 mg/m<sup>2</sup> (309,312).

In advanced leukemia, stomatitis was dose limiting (314). Remarkably, the MTD in leukemia (at 0.9 mg/m<sup>2</sup>/daily for 5 days) is almost double the one in solid tumors (314).

For Phase II clinical trials, the 30-min infusion regimen with daily administration for 5 consecutive days every 3 weeks was selected because this schedule in Phase I studies showed mostly antitumor activity.

Exatecan was already tested in a Phase II study program in a variety of malignancies, including NSCLC, pancreatic cancer, ovarian cancer, and colorectal cancer, and Phase III studies are currently ongoing. Only preliminary results of these Phase II studies are available, and the Phase III studies have yet not been reported (242,315).

### C. DIFLOMOTECAN (BN80915)

Diflomotecan (BN80915) (5-ethyl-9,10-difluoro-4,5-dihydroxy-5-hydroxy-1*H*-oxepino[3',4':6,7]indolazino[1,2-*b*]quinolone-3,15[13*H*]dione) belongs to the class of fluorinated homocamptothecins. Homocamptothecins are synthetic, water-insoluble CPT analogs with a stabilized lactone ring due to modification of the naturally occurring six-membered  $\alpha$ -hydroxylactone ring into a seven-membered  $\beta$ -hydroxylactone ring by insertion of a methylene spacer between the alcohol and the carboxyl moieties (242). Lactones are cyclic carboxylic esters and are rather unstable molecules (316). The inductive effect from the electronegative oxygen of the adjacent hydroxyl group causes higher reactivity of the carboxyl group of CPTs. By inserting a methylene spacer between the carboxylic and alcoholic functions of the E-ring, it was believed that the electronic influence of the hydroxyl group was removed (316). The alcohol moiety was seen as an important

structure for stabilizing the cleavable complex, because neither dehydroxycamptothecin nor the non-natural enantiomer of CPT is biologically active (316). Since a one-carbon ring expansion is chemically termed a homologation, these new lactone- or E-ring modified compounds were named homocamptothecins (317).

In comparison with most other CPTs, which show rapid hydrolysis of the lactone moiety until a pH- and protein-dependent equilibrium has been reached, homocamptothecins display a slow and irreversible hydrolytic lactone-ring opening (318). This key feature of irreversibility of E-ring opening may lead to reduced toxicity (316). After 3 h incubation of camptothecin and homocamptothecin in human whole blood at 37 °C, the fraction present in the lactone form was 6% in the case of camptothecin and 80% in the case of homocamptothecin. Besides the slower ring opening of homocamptothecin, this difference is also due to a higher affinity of homocamptothecin for red-blood cells (316). Indeed, the homocamptothecins were shown to be more stable than camptothecin, were a highly potent inhibitor of cell growth with superior topoisomerase I-inhibitory activity as compared to camptothecin, and changed the sequence specificity of the drug-induced DNA cleavage by topoisomerase I (319–321). *In vitro* studies revealed that the fluorinated homocamptothecins showed the best antiproliferative activity in the A427 human lung carcinoma cell line in comparison with other homocamptothecin compounds (316).

Diflomotecan, one of the fluorinated homocamptothecin derivatives, has entered Phase I clinical testing. Oral diflomotecan administered once daily for 5 days every 3 weeks was limited by dose-dependent myelosuppression (317). Other toxicities observed were gastrointestinal (i.e., mild nausea and vomiting), alopecia, and fatigue. The recommended dose for Phase II studies is 0.27 mg once daily for 5 days every 3 weeks. The i.v. studies have yet not been published.

Oral diflomotecan exerts a linear, dose-independent, pharmacokinetic profile over the higher dose-range studied with high inter- and inpatient variability. It was also reported that flat dosing of oral diflomotecan resulted in the same variation in AUC as dosing per square meter would have done, as already established for many other cytotoxic agents (322). In the future, population pharmacokinetic studies might enable to reduce the interpatient variability. But, as long as these models are not available, the more convenient flat dosing of diflomotecan is as accurate as the more complex dosing per body surface area. The oral bioavailability of diflomotecan at the recommended dose was 67.1% which is much better than for other oral topoisomerase I inhibitors such as topotecan ( $F=30\text{--}44\%$ ), lurtotecan ( $F=12\text{--}21\%$ ), and 9-AC ( $F=48.6\%$ ) (166,252,265,323).

#### D. LURTOTECAN (GI147211 or GG211)

Like DX-8951f, lurtotecan (also known as GI147211 or GG211) is a hexacyclic CPT analog currently under clinical investigation as an anticancer drug. Lurtotecan is a water-soluble, totally synthetic derivative with a dioxalane moiety

between C-10 and C-11 (324). This agent has been evaluated clinically in various Phase I and II trials using a 30-min i.v. infusion given daily for 5 consecutive days (325,326), and as a 72-h (327) or 21-day continuous i.v. infusion (328). The DLT in all schedules was myelosuppression, including severe neutropenia and thrombocytopenia. Nonhematological toxicities were various and only mild to moderate. In Phase II trials, lurtotecan has shown modest activity in breast cancer, colorectal cancer, NSCLC (329), and SCLC (330). Overall, these data suggest that the hematological-toxicity profile and antitumor activity closely resemble that observed with topotecan, which remains the leading CPT analog for salvage treatment of lung cancer.

Because the oral bioavailability of lurtotecan was previously shown to be highly variable and as low as 10% (323), alternative ways of drug administration are currently being developed, including a new liposomal formulation (OSI-211; also known as NX 211). Preclinical data have been generated demonstrating that this unilamellar liposomal formulation of lurtotecan has significant therapeutic advantage over the free drug, showing increased antitumor activity in xenograft models, which is consistent with increased systemic exposure and enhanced tumor-specific delivery of the drug (331). Based on these exciting data, a Phase I clinical trial has been performed with OSI-211 given to cancer patients as a 30-min infusion in a once every 3-week regimen (332). As expected, the DLTs in this trial were neutropenia and thrombocytopenia, and pharmacological findings seem to corroborate the preclinical profile of this agent. Indeed, the clearance of total lurtotecan following administration of OSI-211 was approximately 25-fold slower than that of the free drug, which might prove to be beneficial for pharmacodynamic outcome of treatment.

### VIII. Conclusions

The CPTs are a class of effective anticancer drugs derived from plant alkaloids that exert their action against DNA topoisomerase I and have been developed in recent years. This specific mechanism of action and the activity against a broad spectrum of malignancies perpetuated a stimulus for research and clinical development of several CPT derivatives with improved physicochemical and pharmacological properties. At present, two analogs, viz. irinotecan and topotecan are registered for clinical use for the treatment of first- or second-line therapy in advanced colorectal cancer and second-line therapy in cisplatin-refractory ovarian cancer, respectively. Furthermore, in Japan irinotecan is also registered for the treatment of NSCLC. Other members of this promising class of cytotoxic agents, including 9-AC, 9-NC, exatecan, diflomotecan, and lurtotecan are in progress of clinical development to specify their definite place in the spectrum of anticancer treatment.

Several pharmacokinetic and pharmacodynamic factors, including poor aqueous solubility, a pH-dependent reversible interconversion between the active lactone and the inactive carboxylate form, increased lactone stability by

substitutions at specific sites on the molecule, cellular efflux, mechanism of resistance, and drug–drug interactions influence the antitumor efficacy and toxicity profile of these drugs.

The knowledge from preclinical studies that topoisomerase I inhibitors showed S-phase-specific cytotoxicity led to the development of protracted schedules of administration or prolonged exposure of the drug. Although this concept established greater tumor efficacy compared with bolus administration in experimental studies, the optimal treatment and dosing regimens such as chronic oral delivery, continuous i.v. infusion, liposomal encapsulation, or polymerized drug formulations have to be crystallized in further clinical investigations. So far, current insights derived from Phase II clinical trials suggested that prolonged drug exposure may be at least as effective and less toxic than more conventional schedules of intermittent administration of higher doses given as short bolus i.v. infusion. For a variety of reasons, oral regimens of anticancer drugs are more convenient for continuous drug administration, and, in general, more preferred by patients. But, the use of oral CPTs has to overcome some disadvantages. These include maintenance of stability of the drug in the low-pH environment of the stomach, absorption through the biochemical barrier of efflux pumps, i.e., drug transporters, and modulation by cytochrome P-450 isoenzymes in the epithelium of the intestine, the first-pass effect in the liver, and the excretion in the bile, all influence the relatively low, and highly variable, bioavailability of the CPTs. In addition, their narrow therapeutic index offers a potential risk of an accidental overdose and consequently unpredictable excessive toxicity, or suboptimal exposure and hence lower efficacy.

The biotransformation of the CPTs is a complex process, in which the hepatic metabolism significantly contributes to the elimination of the drug. Additionally, the pharmacokinetics of the CPTs can easily be altered by comedication that modulates the cytochrome P-450 isoenzymes. Furthermore, new insights of the genetic polymorphisms of the UGT1A1 enzyme, which detoxified SN-38 to SN-38 glucuronide (SN-38G), may lead to more individualized dosing of irinotecan guided by pharmacogenetics to overcome the variability in SN-38 glucuronidation, a major determinant of the severity of late diarrhea.

What will the future bring in the development of the CPTs? Efforts may focus on enhancement of the antitumor efficacy of the CPTs by combining these agents with other anticancer drugs, biological modifiers, or radiotherapy. Especially if these treatment modalities can modulate cell-cycle checkpoints which promote CPT activity. Furthermore, a new generation of CPTs with a broader spectrum of cytotoxicity or greater chemical stability of the lactone ring, e.g., exatecan and diflomotecan, respectively, and with more predictable side effects are now in clinical development. Also, protracted exposure to the drug can be achieved by using polymerized or macromolecular CPTs with prolonged half-lives. In addition, these macromolecular drugs penetrate in tumor tissue better due to their enhanced permeability and retention characteristics, and have lower systemic

toxicity associated with the free drug. Further investigations are required to demonstrate if these drugs show better antitumor activity.

### References

1. M. E. Wall, M. C. Wani, C. E. Cook, K. H. Palmer, A. T. McPhail, and A. T. Sim, *J. Am. Chem. Soc.* **88**, 3888 (1966).
2. M. E. Wall and M. C. Wani, in "Annals of the New York Academy of Sciences" (P. Pantazis, B. C. Giovanella and M. L. Rothenberg, eds.), vol. 803, pp. 1–12. The New York Academy of Sciences, New York, 1996.
3. M. E. Wall and M. C. Wani, *Cancer Res.* **55**, 753 (1995).
4. D. Costin and M. Potmesil, *Adv. Pharmacol.* **29B**, 51 (1994).
5. A. M. Abang, *Semin. Hematol.* **35**, 13 (1998).
6. S. G. Arbuck and C. H. Takimoto, *Semin. Hematol.* **35**, 3 (1998).
7. F. M. Muggia, P. J. Creaven, H. H. Hansen, M. H. Cohen, and O. S. Selawry, *Cancer Chemother. Rep.* **56**, 515 (1972).
8. C. G. Moertel, A. J. Schutt, R. J. Reitemeier, and R. G. Hahn, *Cancer Chemother. Rep.* **56**, 649 (1972).
9. J. A. Gottlieb and J. K. Luce, *Cancer Chemother. Rep.* **56**, 103 (1972).
10. R. H. Mathijssen, R. J. van Alphen, J. Verweij, W. J. Loos, K. Nooter, G. Stoter, and A. Sparreboom, *Clin. Cancer Res.* **7**, 2182 (2001).
11. J. C. Wang, *Annu. Rev. Biochem.* **54**, 665 (1985).
12. H. P. Vosberg, *Curr. Top. Microbiol. Immunol.* **114**, 19 (1985).
13. C. C. Juan, J. L. Hwang, A. A. Liu, J. Whang-Peng, T. Knutsen, K. Huebner, C. M. Croce, H. Zhang, J. C. Wang, and L. F. Liu, *Proc. Natl. Acad. Sci. USA* **85**, 8910 (1988).
14. N. Kunze, G. C. Yang, Z. Y. Jiang, H. Hameister, S. Adolph, K. H. Wiedorn, A. Richter, and R. Knippers, *Hum. Genet.* **84**, 6 (1989).
15. M. R. Redinbo, L. Stewart, J. J. Champoux, and W. G. Hol, *J. Mol. Biol.* **292**, 685 (1999).
16. N. Kunze, G. C. Yang, M. Dölberg, R. Sundarp, R. Knippers, and A. Richter, *J. Biol. Chem.* **266**, 9610 (1991).
17. S. Heiland, R. Knippers, and N. Kunze, *Eur. J. Biochem.* **217**, 813 (1993).
18. L. Stewart, G. C. Ireton, and J. J. Champoux, *J. Biol. Chem.* **274**, 32950 (1999).
19. J. L. Keck and J. M. Berger, *Nat. Struct. Biol.* **6**, 900 (1999).
20. L. Stewart, G. C. Ireton, and J. J. Champoux, *J. Biol. Chem.* **271**, 7602 (1996).
21. L. Stewart, M. R. Redinbo, X. Qiu, W. G. Hol, and J. J. Champoux, *Science* **279**, 1534 (1998).
22. M. R. Redinbo, L. Stewart, P. Kuhn, J. J. Champoux, and W. G. Hol, *Science* **279**, 1504 (1998).
23. Y. H. Hsiang, M. G. Lihou, and L. F. Liu, *Cancer Res.* **49**, 5077 (1989).
24. L. F. Liu and P. D'Arpa, *Important Adv. Oncol.* **442**, 79 (1992).
25. B. Drewinko, E. J. Freireich, and J. A. Gottlieb, *Cancer Res.* **34**, 747 (1974).
26. P. D'Arpa, C. Beardmore, and L. F. Liu, *Cancer Res.* **50**, 6919 (1990).
27. C. J. Gerrits, M. J. de Jonge, J. H. Schellens, G. Stoter, and J. Verweij, *Br. J. Cancer* **76**, 952 (1997).
28. K. W. Kohn and Y. Pommier, in "Annals of the New York Academy of Sciences" (J. G. Liehr, B. C. Giovanella and C. F. Verschraegen, eds.), vol. 922, pp. 11–26. The New York Academy of Sciences, New York, 2000.



29. H. A. Burris, 3rd, A. R. Hanauske, R. K. Johnson, M. H. Marshall, J. G. Kuhn, S. G. Hilsenbeck, and D. D. von Hoff, *J. Natl. Cancer Inst.* **84**, 1816 (1992).
30. J. Verweij and J. H. Schellens, *Ann. Oncol.* **6**, 102 (1995).
31. H. Hashimoto, S. Chatterjee, and N. A. Berger, *Clin. Cancer Res.* **1**, 369 (1995).
32. R. D. Anderson and N. A. Berger, *Mutat. Res.* **309**, 109 (1994).
33. B. C. Baguley and L. R. Ferguson, *Biochim. Biophys. Acta* **1400**, 213 (1998).
34. L. Cosentino and J. A. Heddle, *Environ. Mol. Mutagen.* **34**, 208 (1999).
35. P. M. Shaver-Walker, C. Urlando, K. S. Tao, X. B. Zhang, and J. A. Heddle, *Proc. Natl. Acad. Sci. USA* **92**, 11470 (1995).
36. S. Chatterjee, D. Trivedi, S. J. Petzold, and N. A. Berger, *Cancer Res.* **50**, 2713 (1990).
37. C. Holm, J. M. Covey, D. Kerrigan, and Y. Pommier, *Cancer Res.* **49**, 6365 (1989).
38. K. C. Chow and W. E. Ross, *Mol. Cell. Biol.* **7**, 3119 (1987).
39. N. A. Berger, S. Chatterjee, J. A. Schmotzer, and S. R. Helms, *Proc. Natl. Acad. Sci. USA* **88**, 8740 (1991).
40. M. K. Andersen, B. Johansson, S. O. Larsen, and J. Pedersen-Bjergaard, *Haematologica* **83**, 483 (1998).
41. M. J. Ratain and J. D. Rowley, *Ann. Oncol.* **3**, 107 (1992).
42. M. K. Andersen, D. H. Christiansen, B. A. Jensen, P. Ernst, G. Hauge, and J. Pedersen-Bjergaard, *Br. J. Haematol.* **114**, 539 (2001).
43. K. Seiter, E. J. Feldman, C. Sreekantiah, M. Pozzuoli, J. Weisberger, D. Liu, C. Papageorgio, M. Weiss, R. Kancherla, and T. Ahmed, *Leukemia* **15**, 963 (2001).
44. C. H. Pui, R. C. Ribeiro, M. L. Hancock, G. K. Rivera, W. E. Evans, S. C. Raimondi, D. R. Head, F. G. Behm, M. H. Mahmoud, J. T. Sandlund, and W. M. Christ, *N. Engl. J. Med.* **325**, 1682 (1991).
45. C. H. Pui, M. V. Relling, G. K. Rivera, M. L. Hancock, S. C. Raimondi, H. E. Heslop, V. M. Santana, R. C. Ribeiro, J. T. Sandlund, H. H. Mahmoud, W. E. Evans, and R. A. Krance, *Leukemia* **9**, 1990 (1995).
46. M. Yagita, Y. Ieki, R. Onishi, C. L. Huang, M. Adachi, S. Horiike, Y. Konaka, T. Taki, and M. Miyake, *Int. J. Oncol.* **13**, 91 (1998).
47. M. A. Smith, L. Rubinstein, L. Cazenave, R. S. Ungerleider, H. M. Maurer, R. Heyn, F. M. Khan, and E. Gehan, *J. Natl. Cancer Inst.* **85**, 554 (1993).
48. J. Pedersen-Bjergaard, P. Philip, S. O. Larsen, M. Andersson, G. Daugaard, J. Ersboll, S. W. Hansen, K. Hou-Jensen, D. Nielsen, T. C. Sigsgaard, L. Specht, and K. Osterlind, *Leukemia* **7**, 1975 (1993).
49. C. A. Felix, *Biochim. Biophys. Acta* **1400**, 233 (1998).
50. C. Kollmannsberger, J. Beyer, J. P. Droz, A. Harstrick, J. T. Hartmann, P. Biron, A. Flechon, P. Schoffski, M. Kuczyk, H. J. Schmoll, L. Kanz, and C. Bokemeyer, *J. Clin. Oncol.* **16**, 3386 (1998).
51. G. Leone, L. Mele, A. Pulsoni, F. Equitani, and L. Pagano, *Haematologica* **84**, 937 (1999).
52. F. E. van Leeuwen, in "Bailliere's Clinical Haematology" (B. Löwenberg, ed.), vol. 9, pp. 57-85. Bailliere Tindall, London, 1996.
53. M. Stanulla, J. Wang, D. S. Chervinsky, and P. D. Aplan, *Leukemia* **11**, 490 (1997).
54. P. L. Broeker, H. G. Super, M. J. Thirman, H. Pomykala, Y. Yonebayashi, S. Tanabe, N. Zeleznik-Le, and J. D. Rowley, *Blood* **87**, 1912 (1996).
55. L. F. Wang, C. Y. Ting, C. K. Lo, J. S. Su, L. A. Mickley, A. T. Fojo, J. Whang-Peng, and J. Hwang, *Cancer Res.* **57**, 1516 (1997).
56. T. Andoh, K. Ishii, Y. Suzuki, Y. Ikegami, Y. Kusunoki, Y. Takemoto, and K. Okada, *Proc. Natl. Acad. Sci. USA* **84**, 5565 (1987).

57. Y. Sugimoto, S. Tsukahara, T. Oh-hara, T. Isoe, and T. Tsuruo, *Cancer Res.* **50**, 6925 (1990).
58. H. Tamura, C. Kohchi, R. Yamada, T. Ikeda, O. Koiwai, E. Patterson, J. D. Keene, K. Okada, E. Kjeldsen, K. Nishikawa, and T. Andoh, *Nucleic Acids Res.* **19**, 69 (1991).
59. N. Kubota, F. Kanzawa, K. Nishio, Y. Takeda, T. Ohmori, Y. Fujiwara, Y. Terashima, and N. Saijo, *Biochem. Biophys. Res. Commun.* **188**, 571 (1992).
60. P. Benedetti, P. Fiorani, L. Capuani, and J. C. Wang, *Cancer Res.* **53**, 4343 (1993).
61. A. M. Knab, J. Fertala, and M. A. Bjornsti, *J. Biol. Chem.* **268**, 22322 (1993).
62. A. Tanizawa, R. Beirand, G. Kohlhagen, A. Tabuchi, J. Jenkins, and Y. Pommier, *J. Biol. Chem.* **268**, 25463 (1993).
63. E. Rubin, P. Pantazis, A. Bharti, D. Toppmeyer, B. Giovannella, and D. Kufe, *J. Biol. Chem.* **269**, 2433 (1994).
64. J. Tsurutani, T. Nitta, T. Hirashima, T. Komiya, H. Uejima, H. Tada, N. Syunichi, A. Tohda, M. Fukuoka, and K. Nakagawa, *Lung Cancer* **35**, 299 (2002).
65. R. H. Mathijssen, W. J. Loos, J. Verweij, and A. Sparreboom, *Curr. Cancer Drug Targets* **2**, 103 (2002).
66. L. Iyer, C. D. King, P. F. Whittington, M. D. Green, S. K. Roy, T. R. Tephly, B. L. Coffman, and M. J. Ratain, *J. Clin. Invest.* **101**, 847 (1998).
67. P. J. Bosma, J. R. Chowdhury, C. Bakker, S. Gantla, A. de Boer, B. A. Oostra, D. Lindhout, G. N. Tytgat, P. L. Jansen, and R. P. Oude Elferink, *N. Engl. J. Med.* **333**, 1171 (1995).
68. E. Wasserman, A. Myara, F. Lokiec, F. Goldwasser, F. Trivin, M. Mahjoubi, J. L. Misset, and E. Cvitkovic, *Ann. Oncol.* **8**, 1049 (1997).
69. E. K. Rowinsky, L. B. Grochow, D. S. Ettinger, S. E. Sartorius, B. G. Lubejko, T. L. Chen, M. K. Rock, and R. C. Donehower, *Cancer Res.* **54**, 427 (1994).
70. M. L. Rothenberg, J. G. Kuhn, H. A. Burris, 3rd, J. Nelson, J. R. Eckardt, M. Tristan-Morales, S. G. Hilsenbeck, G. R. Weiss, L. S. Smith, and G. I. Rodriguez, *J. Clin. Oncol.* **11**, 2194 (1993).
71. R. L. Drengler, J. G. Kuhn, L. J. Schaaf, G. I. Rodriguez, M. A. Villalona-Calero, L. A. Hammond, J. A., Jr., Hodges, S. Stephenson, M. A. Kraynak, B. A. Staton, G. L. Elfring, P. K. Locker, L. L. Miller, D. D. von Hoff, and M. L. Rothenberg, *J. Clin. Oncol.* **17**, 685 (1999).
72. E. Gupta, R. Mick, J. Ramirez, X. Wang, T. M. Lestingi, E. E. Vokes, and M. J. Ratain, *J. Clin. Oncol.* **15**, 1502 (1997).
73. C. H. Takimoto, G. Morrison, N. Harold, M. Quinn, B. P. Monahan, R. A. Band, J. Cottrell, A. Guemei, V. Llorens, H. Hehman, A. S. Ismail, D. Flemming, D. M. Gosky, H. Hirota, S. J. Berger, N. A. Berger, A. P. Chen, J. D. Shapiro, S. G. Arbuck, J. Wright, J. M. Hamilton, C. J. Allegra, and J. L. Grem, *J. Clin. Oncol.* **18**, 659 (2000).
74. R. Garcia-Carbonero and J. G. Supko, *Clin. Cancer Res.* **8**, 641 (2002).
75. D. F. Kehler, W. Yamamoto, J. Verweij, M. J. de Jonge, P. de Bruijn, and A. Sparreboom, *Clin. Cancer Res.* **6**, 3451 (2000).
76. V. M. Herben, J. H. Schellens, M. Swart, G. Gruia, L. Vernillet, J. H. Beijnen, and W. W. ten Bokkel Huinink, *J. Clin. Oncol.* **17**, 1897 (1999).
77. R. Xie, R. H. Mathijssen, A. Sparreboom, J. Verweij, and M. O. Karlsson, *J. Clin. Oncol.* **20**, 3293 (2002).
78. D. F. Kehler, A. Sparreboom, J. Verweij, P. de Bruijn, C. A. Nierop, J. van de Schraaf, E. J. Ruijgrok, and M. J. de Jonge, *Clin. Cancer Res.* **7**, 1136 (2001).
79. E. Gupta, A. R. Safa, X. Wang, and M. J. Ratain, *Cancer Res.* **56**, 1309 (1996).

80. L. P. Rivory, M. C. Haaz, P. Canal, F. Lokiec, J. P. Armand, and J. Robert, *Clin. Cancer Res.* **3**, 1261 (1997).
81. A. Sparreboom, M. J. de Jonge, P. de Bruijn, E. Brouwer, K. Nooter, W. J. Loos, R. J. van Alphen, R. H. Mathijssen, G. Stoter, and J. Verweij, *Clin. Cancer Res.* **4**, 2747 (1998).
82. P. Canal, C. Gay, A. Dezeuze, J. Y. Douillard, R. Bugat, R. Brunet, A. Adenis, P. Herait, F. Lokiec, and A. Mathieu-Boue, *J. Clin. Oncol.* **14**, 2688 (1996).
83. H. M. Dodds, M. C. Haaz, J. F. Riou, J. Robert, and L. P. Rivory, *J. Pharmacol. Exp. Ther.* **286**, 578 (1998).
84. L. P. Rivory, J. F. Riou, M. C. Haaz, S. Sable, M. Vuilhorgne, A. Commercon, S. M. Pond, and J. Robert, *Cancer Res.* **56**, 3689 (1996).
85. H. S. Friedman, W. P. Petros, A. H. Friedman, L. J. Schaaf, T. Kerby, J. Lawyer, M. Parry, P. J. Houghton, S. Lovell, K. Rasheed, T. Cloughsey, E. S. Stewart, O. M. Colvin, J. M. Provenzale, R. E. McLendon, D. D. Bigner, I. Cokgor, M. Haglund, J. Rich, D. Ashley, J. Malczyn, G. L. Elfring, and L. L. Miller, *J. Clin. Oncol.* **17**, 1516 (1999).
86. R. H. Mathijssen, J. Verweij, P. de Bruijn, W. J. Loos, and A. Sparreboom, *J. Natl. Cancer Inst.* **94**, 1247 (2002).
87. D. F. Kehler, R. H. Mathijssen, J. Verweij, P. de Bruijn, and A. Sparreboom, *J. Clin. Oncol.* **20**, 3122 (2002).
88. A. Falcone, A. Di Paolo, G. Masi, G. Allegrini, R. Danesi, M. Lencioni, E. Pfanner, S. Comis, M. Del Tacca, and P. Conte, *J. Clin. Oncol.* **19**, 3456 (2001).
89. M. L. Rothenberg, *Ann. Oncol.* **8**, 837 (1997).
90. U. Vanhoefer, A. Harstrick, W. Achterrath, S. Cao, S. Seeber, and Y. M. Rustum, *J. Clin. Oncol.* **19**, 1501 (2001).
91. B. C. Giovanella, J. S. Stehlin, M. E. Wall, M. C. Wani, A. W. Nicholas, L. F. Liu, R. Silber, and M. Potmesil, *Science* **246**, 1046 (1989).
92. I. Husain, J. L. Mohler, H. F. Seigler, and J. M. Besterman, *Cancer Res.* **54**, 539 (1994).
93. B. E. Staley, W. S. Samowitz, I. B. Bronstein, and J. A. Holden, *Mod. Pathol.* **12**, 356 (1999).
94. L. P. Rivory and J. Robert, *Cancer Chemother. Pharmacol.* **36**, 176 (1995).
95. H. C. Pitot, R. M. Goldberg, J. M. Reid, J. A. Sloan, P. A. Skaff, C. Erlichman, J. Rubin, P. A. Burch, A. A. Adjei, S. A. Alberts, L. J. Schaaf, G. Elfring, and L. L. Miller, *Clin. Cancer Res.* **6**, 2236 (2000).
96. S. Negoro, M. Fukuoka, N. Masuda, M. Takada, Y. Kusunoki, K. Matsui, N. Takifuji, S. Kudoh, H. Niitani, and T. Taguchi, *J. Natl. Cancer Inst.* **83**, 1164 (1991).
97. C. H. Takimoto and S. G. Arbuck, in "Cancer Chemotherapy and Biotherapy: Principles and Practice", 3rd ed. (B. A. Chabner and D. L. Longo, eds.), pp. 579–646. Lippincott Williams & Wilkins, Philadelphia, 2001.
98. D. D. von Hoff, M. L. Rothenberg, H. C. Pitot, G. L. Elfring, J. S. Mohrland, and L. J. Schaff, *Proc. Am. Soc. Clin. Oncol.* **16**, 228a (1997).
99. D. Cunningham, S. Pyrhonen, R. D. James, C. J. Punt, T. F. Hickish, R. Heikkila, T. B. Johannesen, H. Starkhammar, C. A. Topham, L. Awad, C. Jacques, and P. Herait, *Lancet* **352**, 1413 (1998).
100. P. Rougier, E. van Cutsem, E. Bajetta, N. Niederle, K. Possinger, R. Labianca, M. Navarro, R. Morant, H. Bleiberg, J. Wils, L. Awad, P. Herait, and C. Jacques, *Lancet* **352**, 1407 (1998).

101. P. Rougier, R. Bugat, J. Y. Douillard, S. Culine, E. Suc, P. Brunet, Y. Becouarn, M. Ychou, M. Marty, J. M. Extra, J. Bonneterre, A. Adenis, J. F. Seitz, G. Ganem, M. Namer, T. Conroy, S. Negrier, Y. Merrouche, F. Burki, M. Mousseau, P. Herait, and M. Mahjoubi, *J. Clin. Oncol.* **15**, 251 (1997).
102. M. L. Rothenberg, J. V. Cox, R. F. DeVore, J. D. Hainsworth, R. Pazdur, S. E. Rivkin, J. S. J. Macdonald, C. E., Jr., Sandbach, J. Geyer, D. L. Wolf, J. S. Mohrland, G. L. Elfring, L. L. Miller, and D. D. von Hoff, *Cancer* **85**, 786 (1999).
103. C. H. Takimoto, G. Morrison, N. Harold, M. Quinn, B. P. Monahan, R. A. Band, J. Cottrell, A. Guemei, V. Llorens, H. Hehman, A. S. Ismail, D. Flemming, D. M. Gosky, H. Hirota, S. J. Berger, N. A. Berger, A. P. Chen, J. D. Shapiro, S. G. Arbuck, J. Wright, J. M. Hamilton, C. J. Allegra, and J. L. Grem, *J. Clin. Oncol.* **18**, 659 (2000).
104. S. O'Reilly and E. K. Rowinsky, *Crit. Rev. Oncol. Hematol.* **24**, 47 (1996).
105. L. R. Wiseman and A. Markham, *Drugs* **52**, 606 (1996).
106. G. G. Chabot, *Clin. Pharmacokinet.* **33**, 245 (1997).
107. L. L. Siu and E. K. Rowinsky, *Drugs Safety* **18**, 395 (1998).
108. L. B. Saltz, J. V. Cox, C. Blanke, L. S. Rosen, L. Fehrenbacher, M. J. Moore, J. A. Maroun, S. P. Ackland, P. K. Locker, N. Pirota, G. L. Elfring, and L. L. Miller, *N. Engl. J. Med.* **343**, 905 (2000).
109. J. Y. Douillard, D. Cunningham, A. D. Roth, M. Navarro, R. D. James, P. Karasek, P. Jandik, T. Iveson, J. Carmichael, M. Alakl, G. Gruia, L. Awad, and P. Rougier, *Lancet* **355**, 1041 (2000).
110. J. P. Stevenson, M. Redlinger, L. A. Kluijtmans, W. Sun, K. Algazy, B. Giantonio, D. G. Haller, C. Hardy, A. S. Whitehead, and P. J. O'Dwyer, *J. Clin. Oncol.* **19**, 4081 (2001).
111. H. E. Ford, D. Cunningham, P. J. Ross, S. Rao, G. W. Aherne, T. S. Benepal, T. Price, A. Massey, L. Vernillet, and G. Gruia, *Br. J. Cancer* **83**, 146 (2000).
112. M. Fukuda, K. Nishio, F. Kanzawa, H. Ogasawara, T. Ishida, H. Arioka, K. Bojanowski, M. Oka, and N. Saijo, *Cancer Res.* **56**, 789 (1996).
113. M. Fukuoka and N. Masuda, *Cancer Chemother. Pharmacol.* **34**, S105 (1994).
114. K. Ikeda, M. Terashima, H. Kawamura, I. Takiyama, K. Koeda, A. Takagane, N. Sato, K. Ishida, T. Iwaya, C. Maesawa, H. Yoshinari, and K. Saito, *Jpn. J. Clin. Oncol.* **28**, 168 (1998).
115. J. Ma, M. Maliepaard, K. Nooter, A. W. Boersma, J. Verweij, G. Stoter, and J. H. Schellens, *Cancer Chemother. Pharmacol.* **41**, 307 (1998).
116. Y. Kano, K. Suzuki, M. Akutsu, K. Suda, Y. Inoue, M. Yoshida, S. Sakamoto, and Y. Miura, *Int. J. Cancer* **50**, 604 (1992).
117. S. Kudoh, M. Takada, N. Masuda, K. Nakagawa, K. Itoh, Y. Kusunoki, S. Negoro, K. Matsui, N. Takifuji, H. Morino, M. Fukuoka, *Jpn. J. Cancer Res.* **84**, 203 (1993).
118. E. J. Katz, J. S. Vick, K. M. Kling, P. A. Andrews, and S. B. Howell, *Eur. J. Cancer* **26**, 724 (1990).
119. R. Kim, N. Hirabayashi, M. Nishiyama, K. Jinushi, T. Toge, and K. Okada, *Int. J. Cancer* **50**, 760 (1992).
120. M. J. A. de Jonge, A. Sparreboom, and J. Verweij, *Cancer Treat. Rev.* **24**, 206 (1998).
121. F. Goldwasser, M. Valenti, R. Torres, K. W. Kohn, and Y. Pommier, *Clin. Cancer Res.* **2**, 687 (1996).

122. N. Masuda, M. Fukuoka, S. Kudoh, Y. Kusunoki, K. Matsui, N. Takifuji, K. Nakagawa, M. Tamanoi, T. Nitta, T. Hirashima, S. Negoro, and M. Takada, *Br. J. Cancer* **68**, 777 (1993).
123. N. Masuda, M. Fukuoka, M. Takada, Y. Kusunoki, S. Negoro, K. Matsui, S. Kudoh, N. Takifuji, K. Nakagawa, and S. Kishimoto, *J. Clin. Oncol.* **10**, 1775 (1992).
124. K. Shirao, Y. Shimada, H. Kondo, D. Saito, T. Yamao, H. Ono, T. Yokoyama, H. Fukuda, M. Oka, Y. Watanabe, A. Ohtsu, N. Boku, T. Fujii, Y. Oda, K. Muro, and S. Yoshida, *J. Clin. Oncol.* **15**, 921 (1997).
125. K. Mori, T. Ohnishi, K. Yokoyama, and K. Tominaga, *Cancer Chemother. Pharmacol.* **39**, 327 (1997).
126. N. Masuda, M. Fukuoka, S. Kudoh, Y. Kusunoki, K. Matsui, K. Nakagawa, T. Hirashima, M. Tamanoi, T. Nitta, T. Yana, S. Negoro, N. Takifuji, and M. Takada, *J. Clin. Oncol.* **12**, 90 (1994).
127. K. Mori, T. Hirose, S. Machida, K. Yokoyama, and K. Tominaga, *Eur. J. Cancer* **33**, 503 (1997).
128. M. J. A. de Jonge, J. Verweij, A.S.Th. Planting, M. E. L. van der Burg, G. Stoter, M. M. de Boer-Dennert, P. de Bruijn, E. Brouwer, L. Vernillet, and A. Sparreboom, *Clin. Cancer Res.* **5**, 2012 (1999).
129. K. Noda, Y. Nishiwaki, M. Kawahara, S. Negoro, T. Sugiura, A. Yokoyama, M. Fukuoka, K. Mori, K. Watanabe, T. Tamura, S. Yamamoto, and N. Saijo, *N. Engl. J. Med.* **346**, 85 (2002).
130. F. Goldwasser, M. Gross-Goupil, J. M. Tigaud, M. di Palma, J. Marceau-Suissa, E. Wasserman, A. Yovine, J. L. Misset, and E. Cvitkovic, *Ann. Oncol.* **11**, 1463 (2000).
131. E. Wasserman, C. Cuvier, F. Lokiec, F. Goldwasser, S. Kalla, D. Mery-Mignard, M. Ouldkaci, A. Besmaine, G. Dupont-Andre, M. Mahjoubi, M. Marty, J. L. Misset, and E. Cvitkovic, *J. Clin. Oncol.* **17**, 1751 (1999).
132. W. Scheithauer, G. V. Kornek, M. Raderer, J. Valencak, G. Weinlander, M. Hejna, K. Haider, W. Kwasny, and D. Depisch, *J. Clin. Oncol.* **17**, 902 (1999).
133. J. Valencak, M. Raderer, G. V. Kornek, M. H. Henja, and W. Scheithauer, *J. Natl. Cancer Inst.* **90**, 160 (1998).
134. E. Cvitkovic, M. Marty, E. Wasserman, C. Cuvier, F. Goldwasser, and J. L. Misset, *J. Natl. Cancer Inst.* **90**, 1016 (1998).
135. H. M. Dodds, J. F. Bishop, and L. P. Rivory, *J. Natl. Cancer Inst.* **91**, 91 (1999).
136. W. Scheithauer, G. V. Kornek, M. Raderer, H. Ulrich-Pur, W. Fiebigler, C. Gedlicka, B. Schull, S. Brugger, B. Schneeweiss, F. Lang, A. Lenauer, and D. Depisch, *J. Clin. Oncol.* **20**, 165 (2002).
137. A. Karato, Y. Sasaki, T. Shinkai, K. Eguchi, T. Tamura, Y. Ohe, F. Oshita, M. Nishio, H. Kunikane, H. Arioka, H. Ohmatsu, H. Nakashima, J. Shiraiishi, and N. Saijo, *J. Clin. Oncol.* **11**, 2030 (1993).
138. N. Masuda, M. Fukuoka, S. Kudoh, K. Matsui, Y. Kusunoki, M. Takada, K. Nakagawa, T. Hirashima, H. Tsukada, T. Yana, A. Yoshikawa, A. Kubo, E. Matsuura, T. Nitta, N. Takifuji, K. Terakawa, and S. Negoro, *J. Clin. Oncol.* **12**, 1833 (1994).
139. M. Ando, K. Eguchi, T. Shinkai, T. Tamura, Y. Ohe, N. Yamamoto, T. Kurata, T. Kasai, H. Ohmatsu, K. Kubota, I. Sekine, N. Hojo, T. Matsumoto, T. Kodama, R. Kakinuma, Y. Nishiwaki, and N. Saijo, *Br. J. Cancer* **76**, 1494 (1997).

140. F. Oshita, K. Noda, Y. Nishiwaki, A. Fujita, Y. Kurita, T. Nakabayashi, K. Tobise, S. Abe, S. Suzuki, I. Hayashi, Y. Kawakami, T. Matsuda, S. Tsuchiya, S. Takahashi, T. Tamura, and N. Saijo, *J. Clin. Oncol.* **15**, 304 (1997).
141. N. Masuda, K. Matsui, S. Negoro, N. Takifuji, K. Takeda, T. Yana, M. Kobayashi, T. Hirashima, Y. Kusunoki, S. Ushijima, I. Kawase, T. Tada, H. Sawaguchi, and M. Fukuoka, *J. Clin. Oncol.* **16**, 3329 (1998).
142. M. Fujishiro, T. Shinkai, M. Fukuda, T. Tamura, Y. Ohe, H. Kunitoh, Y. Nishiwaki, I. Sekine, H. Fukuda, and N. Saijo, *Jpn. J. Clin. Oncol.* **30**, 487 (2000).
143. M. Fukuda, M. Oka, H. Soda, K. Terashi, S. Kawabata, K. Nakatomi, H. Takatani, J. Tsurutani, K. Tsukamoto, Y. Noguchi, M. Fukuda, A. Kinoshita, and S. Kohno, *Clin. Cancer Res.* **5**, 3963 (1999).
144. N. Naka, M. Kawahara, K. Okishio, S. Hosoe, M. Ogawara, S. Atagi, Y. Takemoto, K. Ueno, T. Kawaguchi, T. Tsuchiyama, and K. Furuse, *Lung Cancer* **37**, 319 (2002).
145. M. Yamada, S. Kudoh, H. Fukuda, K. Nakagawa, N. Yamamoto, Y. Nishimura, S. Negoro, K. Takeda, M. Tanaka, and M. Fukuoka, *Br. J. Cancer* **87**, 258 (2002).
146. A. A. Adjei, A. Argiris, and J. R. Murren, *Semin. Oncol.* **26**, 32 (1999).
147. A. Font, J. M. Sanchez, R. Rosell, M. Taron, E. Martinez, M. Guillot, J. L. Manzano, M. Margeli, A. Barnadas, and A. Abad, *Lung Cancer* **37**, 213 (2002).
148. T. Kasai, M. Oka, H. Soda, J. Tsurutani, M. Fukuda, Y. Nakamura, S. Kawabata, K. Nakatomi, S. Nagashima, H. Takatani, M. Fukuda, A. Kinoshita, and S. Kohno, *Eur. J. Cancer* **38**, 1871 (2002).
149. D. A. Rushing, *Oncology (Huntingt.)* **14**, 63 (2000).
150. T. Yamao, K. Shirao, Y. Matsumura, K. Muro, Y. Yamada, M. Goto, K. Chin, and Y. Shimada, *Ann. Oncol.* **12**, 1729 (2001).
151. W. Scheithauer, G. V. Kornek, S. Brugger, H. Ullrich-Pur, J. Valencak, M. Raderer, W. Fiebigger, E. Kovats, F. Lang, and D. Depisch, *Cancer Invest.* **20**, 60 (2002).
152. D. Pectasides, A. Visvikis, A. Kouloubinis, J. Glotsos, N. Bountouroglou, N. Karvounis, N. Ziras, and A. Athanassiou, *Eur. J. Cancer* **38**, 1194 (2002).
153. A. Fujita, T. Ohkubo, H. Hoshino, H. Takabatake, S. Tagaki, and K. Sekine, *Anticancer Drugs* **13**, 505 (2002).
154. T. Ohtsu, Y. Sasaki, T. Igarashi, T. Murayama, Y. Kobayashi, and K. Tobinai, *Jpn. J. Clin. Oncol.* **28**, 502 (1998).
155. W. D. Kingsbury, J. C. Boehm, D. R. Jakas, K. G. Holden, S. M. Hecht, G. Gallagher, M. J. Caranfa, F. L. McCabe, L. F. Faucette, and R. K. Johnson, *J. Med. Chem.* **34**, 98 (1991).
156. H. Rosing, V. M. Herben, D. M. van Gortel-van Zomeren, E. Hop, J. J. Kettenes-van den Bosch, W. W. ten Bokkel Huinink, and J. H. Beijnen, *Cancer Chemother. Pharmacol.* **39**, 498 (1997).
157. H. A. Gelderblom, M. J. de Jonge, A. Sparreboom, and J. Verweij, *Invest. New Drugs* **17**, 401 (1999).
158. L. B. Grochow, E. K. Rowinsky, R. Johnson, S. Ludeman, S. H. Kaufmann, F. L. McCabe, B. R. Smith, L. Hurowitz, A. DeLisa, and R. C. Donehower, *Drug Metab. Dispos.* **20**, 706 (1992).
159. L. J. van Warmerdam, G. J. Creemers, S. Rodenhuis, H. Rosing, M. de Boer-Dennert, J. H. Schellens, W. W. ten Bokkel Huinink, B. E. Davies, R. A. Maes, J. Verweij, and J. H. Beijnen, *Cancer Chemother. Pharmacol.* **38**, 254 (1996).
160. H. Rosing, D. M. van Zomeren, E. Doyle, A. Bult, and J. H. Beijnen, *Anticancer Drugs* **9**, 587 (1998).

161. S. O'Reilly, E. Rowinsky, W. Slichenmyer, R. C. Donehower, A. Forastiere, D. Ettinger, T. L. Chen, S. Sartorius, K. Bowling, J. Smith, A. Brubaker, B. Lubejko, V. Ignacio, and L. B. Grochow, *J. Natl. Cancer Inst.* **88**, 817 (1996).
162. S. O'Reilly, E. K. Rowinsky, W. Slichenmyer, R. C. Donehower, A. A. Forastiere, D. S. Ettinger, T. L. Chen, S. Sartorius, and L. B. Grochow, *J. Clin. Oncol.* **14**, 3062 (1996).
163. P. J. O'Dwyer, F. P. LaCreta, N. B. Haas, T. Halbherr, H. Frucht, E. Goosenberg, and K. S. Yao, *Cancer Chemother. Pharmacol.* **34**, S46 (1994).
164. J. G. Wall, H. A. Burris, 3rd, D. D. von Hoff, G. Rodriguez, R. Kneuper-Hall, D. Shaffer, T. O'Rourke, T. Brown, G. Weiss, G. Clark, S. McVea, J. Brown, R. Johnson, C. Friedman, B. Smith, W. S. Mann, and J. Kuhn, *Anticancer Drugs* **3**, 337 (1992).
165. L. J. van Warmerdam, J. Verweij, J. H. Schellens, H. Rosing, B. E. Davies, M. de Boer-Dennert, R. A. Maes, and J. H. Beijnen, *Cancer Chemother. Pharmacol.* **35**, 237 (1995).
166. J. H. Schellens, G. J. Creemers, J. H. Beijnen, H. Rosing, M. de Boer-Dennert, M. McDonald, B. Davies, and J. Verweij, *Br. J. Cancer* **73**, 1268 (1996).
167. N. B. Haas, F. P. LaCreta, J. Walczak, G. R. Hudes, J. M. Brennan, R. F. Ozols, and P. J. O'Dwyer, *Cancer Res.* **54**, 1220 (1994).
168. L. J. van Warmerdam, W. W. ten Bokkel Huinink, S. Rodenhuis, I. Koier, B. E. Davies, H. Rosing, R. A. Maes, and J. H. Beijnen, *J. Clin. Oncol.* **13**, 1768 (1995).
169. J. L. Abbruzzese, T. Madden, S. M. Sugarman, A. L. Ellis, S. Loughlin, K. R. Hess, R. A. Newman, L. A. Zwelling, and M. N. Raber, *Clin. Cancer Res.* **2**, 1489 (1996).
170. G. J. Creemers, C. J. Gerrits, J. H. Schellens, A. S. Planting, M. E. van der Burg, V. M. van Beurden, M. de Boer-Dennert, M. Harteveld, W. Loos, I. Hudson, G. Stoter, and J. Verweij, *J. Clin. Oncol.* **14**, 2540 (1996).
171. V. M. Herben, W. W. ten Bokkel Huinink, M. E. Schot, I. Hudson, and J. H. Beijnen, *Anticancer Drugs* **9**, 411 (1998).
172. L. Saltz, M. Sirott, C. Young, W. Tong, D. Niedzwiecki, Y. Tzy-Jyun, Y. Tao, B. Trochanowski, P. Wright, and K. Barbosa, *J. Natl. Cancer Inst.* **85**, 1499 (1993).
173. C. F. Stewart, A. J. Gajjar, R. L. Heideman, and P. J. Houghton, *Onkologie* **21**, 22 (1998).
174. W. C. Zamboni, D. I. Lüftner, M. J. Egorgin, M. Schweigert, O. Sezer, T. Richter, J. J. Natale, and K. Possinger, *Ann. Oncol.* **12**, 119 (2001).
175. S. M. Blaney, C. Takimoto, D. J. Murry, N. Kuttesch, C. McCully, D. E. Cole, K. Godwin, and F. M. Balis, *Cancer Chemother. Pharmacol.* **41**, 464 (1998).
176. H. Gelderblom, W. J. Loos, J. Verweij, M. J. de Jonge, and A. Sparreboom, *Clin. Cancer Res.* **6**, 1288 (2000).
177. L. S. Hofstra, A. M. Bos, E. G. de Vries, A. G. van der Zee, J. H. Beijnen, H. Rosing, N. H. Mulder, J. G. Aalders, and P. H. Willemse, *Br. J. Cancer* **85**, 1627 (2001).
178. S. C. Plaxe, R. D. Christen, J. O'Quigley, P. S. Braly, J. L. Freddo, E. McClay, D. Heath, and S. B. Howell, *Invest. New Drugs* **16**, 147 (1998).
179. V. M. Herben, E. Schoemaker, H. Rosing, D. M. van Zomeren, W. W. ten Bokkel Huinink, R. Dubbelman, S. Hearn, J. H. Schellens, and J. H. Beijnen, *Cancer Chemother. Pharmacol.* **50**, 59 (2002).
180. B. E. Davies, E. A. Minthorn, M. J. Dennis, H. Rosing, and J. H. Beijnen, *Pharm. Res.* **14**, 1461 (1997).
181. J. W. Jonker, J. W. Smit, R. F. Brinkhuis, M. Maliepaard, J. H. Beijnen, J. H. Schellens, and A. H. Schinkel, *J. Natl. Cancer Inst.* **92**, 1651 (2000).

182. J. M. Gallo, P. B. Laub, E. K. Rowinsky, L. B. Grochow, and S. D. Baker, *J. Clin. Oncol.* **18**, 2459 (2000).
183. G. J. Creemers, B. Lund, and J. Verweij, *Cancer Treat. Rev.* **20**, 73 (1994).
184. E. K. Rowinsky, L. B. Grochow, C. B. Hendricks, D. S. Ettinger, A. A. Forastiere, L. A. Hurowitz, W. P. McGuire, S. E. Sartorius, B. G. Lubejko, S. H. Kaufmann, and R. C. Donehower, *J. Clin. Oncol.* **10**, 647 (1992).
185. J. Verweij, B. Lund, J. Beijnen, A. Planting, M. de Boer-Dennert, I. Koier, H. Rosing, and H. Hansen, *Ann. Oncol.* **4**, 673 (1993).
186. L. Saltz, M. Sirott, C. Young, W. Tong, D. Niedzwiecki, Y. Tzy-Jyun, Y. Tao, B. Trochanowski, P. Wright, K. Barbosa, F. Toomasi, and D. Kelsen, *J. Natl. Cancer Inst.* **85**, 1499 (1993).
187. J. H. Schiller, K. Kim, P. Hutson, R. DeVore, J. Glick, J. Stewart, and D. Johnson, *J. Clin. Oncol.* **14**, 2345 (1996).
188. V. M. Herben, W. W. ten Bokkel Huinink, M. E. Schot, I. Hudson, and J. H. Beijnen, *Anticancer Drugs* **9**, 411 (1998).
189. G. Frasci, G. Nicoletta, P. Comella, I. Carreca, G. DeCataldis, D. Muci, C. Brunetti, M. Natale, F. Piantedosi, A. Russo, S. Palmeri, G. Comella, and N. Panza, *Br. J. Cancer* **84**, 1166 (2001).
190. A. Ardizzoni, H. Hansen, P. Dombernowsky, T. Gamucci, S. Kaplan, P. Postmus, G. Giaccone, B. Schaefer, J. Wanders, and J. Verweij, *J. Clin. Oncol.* **15**, 2090 (1997).
191. W. ten Bokkel Huinink, M. Gore, J. Carmichael, A. Gordon, J. Malfetano, I. Hudson, C. Broom, C. Scarabelli, N. Davidson, M. Spanczynski, G. Bolis, H. Malmstrom, R. Coleman, S. C. Fields, and J. F. Heron, *J. Clin. Oncol.* **15**, 2183 (1997).
192. W. ten Bokkel Huinink, J. Carmichael, D. Armstrong, A. Gordon, and J. Malfetano, *Semin. Oncol.* **24**, S5-S19 (1997).
193. G. J. Creemers, G. Bolis, M. Gore, G. Scarfone, A. J. Lacave, J. P. Guastalla, R. Despax, G. Favalli, R. Kreinberg, S. van Belle, I. Hudson, J. Verweij, and W. W. ten Bokkel Huinink, *J. Clin. Oncol.* **14**, 3056 (1996).
194. A. P. Kudelka, D. Tresukosol, C. L. Edwards, R. S. Freedman, C. Levenback, P. Chantarakwiroj, C. Gonzalez de Leon, E. E. Kim, T. Madden, B. Wallin, M. Hord, C. Verschraegen, M. Raber, and J. J. Kavanagh, *J. Clin. Oncol.* **14**, 1552 (1996).
195. P. G. Rose, N. H. Gordon, N. Fusco, L. Fluellen, M. Rodriguez, S. T. Ingalls, and C. L. Hoppel, *Gynecol. Oncol.* **78**, 228 (2000).
196. M. Markman, J. A. Blessing, K. DeGeest, M. Morgan, K. Y. Look, T. J. Herzog, and P. G. Rose, *Gynecol. Oncol.* **75**, 444 (1999).
197. M. Markman, J. A. Blessing, R. D. Alvarez, P. Hanjani, S. Waggoner, and K. Hall, *Gynecol. Oncol.* **77**, 112 (2000).
198. T. J. Lynch, Jr., L. Kalish, G. Strauss, A. Elias, A. Skarin, L. N. Shulman, M. Posner, and E. Frei 3rd, *J. Clin. Oncol.* **12**, 347 (1994).
199. R. Perez-Soler, F. V. Fossella, B. S. Glisson, J. S. Lee, W. K. Murphy, D. M. Shin, B. L. Kemp, J. J. Lee, J. Kane, R. A. Robinson, S. M. Lippman, J. M. Kurie, M. H. Huber, M. N. Raber, and W. K. Hong, *J. Clin. Oncol.* **14**, 503 (1996).
200. G. J. Creemers, J. Wanders, T. Gamucci, S. Vallentin, L. Y. Dirix, P. Schoffski, I. Hudson, and J. Verweij, *Ann. Oncol.* **6**, 844 (1995).
201. J. S. Macdonald, J. K. Benedetti, M. Modiano, and D. S. Alberts, *Invest. New Drugs* **15**, 357 (1997).



202. B. A. Murphy, T. Leong, B. Burkey, C. Langer, and A. Forastiere, *Am. J. Clin. Oncol.* **24**, 64 (2001).
203. D. S. Miller, J. A. Blessing, L. C. Kilgore, R. Mannel, and L. van Le, *Am. J. Clin. Oncol.* **23**, 355 (2000).
204. J. S. Macdonald, J. L. Jacobson, S. J. Ketchel, G. Weiss, S. Taylor, G. Mills, J. P. Kuebler, S. Rivkin, and M. Conrad, *Invest. New Drugs* **18**, 199 (2000).
205. J. J. Weitz, R. F. Marschke, Jr., J. A. Sloan, J. P. Grill, J. R. Jett, J. A. Knost, A. K. Hatfield, D. W. Zenk, W. W. Bate, and P. L. Schaefer, *Lung Cancer* **28**, 157 (2000).
206. E. G. Levine, C. T. Cirrincione, T. P. Szatrowski, G. Canellos, L. Norton, and I. C. Henderson, *Am. J. Clin. Oncol.* **22**, 218 (1999).
207. A. W. Maksymiuk, R. F., Jr., Tazelaar, H. D. Marschke, J. Grill, S. Nair, R. S. Marks, B. J. Brooks, J. A. Mailliard, G. M. Burton, and J. R. Jett, *Am. J. Clin. Oncol.* **21**, 610 (1998).
208. R. S. Witte, J. Manola, P. A. Burch, T. Kuzel, E. L. Weinshel, and P. J. Loehrer, Sr., *Invest. New Drugs* **16**, 191 (1998).
209. H. L. Kindler, M. G. Kris, I. E. Smith, V. A. Miller, S. C. Grant, J. B. Krebs, G. A. Ross, and M. L. Slevin, *Am. J. Clin. Oncol.* **21**, 438 (1998).
210. J. P. Stevenson, R. M. Scher, R. Kosierowski, S. C. Fox, M. Simmonds, K. S. Yao, F. Green, C. Broom, S. Z. Fields, J. B. Krebs, and P. J. O'Dwyer, *Eur. J. Cancer* **34**, 1358 (1998).
211. L. B. Saltz, G. K. Schwartz, D. H. Ilson, V. Quan, and D. P. Kelsen, *Am. J. Clin. Oncol.* **20**, 621 (1997).
212. J. K. Benedetti, H. A. Burris, 3rd, S. P. Balcerzak, and J. S. Macdonald, *Invest. New Drugs* **15**, 261 (1997).
213. J. G. Wall, J. K. Benedetti, M. A. O'Rourke, R. B. Natale, and J. S. Macdonald, *Invest. New Drugs* **15**, 257 (1997).
214. E. H. Kraut, M. J. Walker, A. Staubus, D. Gochmour, and S. P. Balcerzak, *Cancer Invest.* **15**, 318 (1997).
215. S. O'Reilly, R. C. Donehower, E. K. Rowinsky, S. Ord, and L. B. Grochow, *Anticancer Drugs* **7**, 410 (1996).
216. D. Macdonald, G. Cairncross, D. Stewart, P. Forsyth, C. Sawka, N. Wainman, and E. Eisenhauer, *Ann. Oncol.* **7**, 205 (1996).
217. R. M. Scher, R. Kosierowski, C. Lusch, R. Alexander, S. Fox, I. Redei, F. Green, B. Raskay, K. Amfoh, P. F. Engstrom, and P. J. O'Dwyer, *Invest. New Drugs* **13**, 347 (1996).
218. D. Armstrong and S. O'Reilly, *Oncologist* **3**, 4 (1998).
219. J. F. Heron, *Oncologist* **3**, 390 (1998).
220. H. Hochster, L. Liebes, J. Speyer, J. Sorich, B. Taubes, R. Oratz, J. Wernz, A. Chachoua, B. Raphael, R. Z. Vinci, and R. H. Blum, *J. Clin. Oncol.* **12**, 553 (1994).
221. H. Hochster, S. Wadler, C. Runowicz, L. Liebes, H. Cohen, R. Wallach, J. Sorich, B. Taubes, and J. Speyer, *J. Clin. Oncol.* **17**, 2553 (1999).
222. G. J. Creemers, C. J. Gerrits, J. R. Eckardt, J. H. Schellens, H. A. Burris, A. S. Planting, G. I. Rodriguez, W. J. Loos, I. Hudson, C. Broom, J. Verweij, and D. D. von Hoff, *J. Clin. Oncol.* **15**, 1087 (1997).
223. J. Kuhn, J. Dizzo, J. Eckhardt, S. Fields, P. Cobb, R. Rodriguez, D. Rinaldi, R. Drendgler, L. Smith, N. Peacock, A. Thurman, P. Delacruz, S. Hodges, D. von Hoff, and H. Burris, *Proc. Am. Soc. Clin. Oncol.* **14**, 474 (1995) (abstr. 1538).

224. C. J. Gerrits, H. Burris, J. H. Schellens, J. R. Eckardt, A. S. Planting, M. E. van der Burg, G. I. Rodriguez, W. J. Loos, V. van Beurden, I. Hudson, S. Fields, D. D. von Hoff, and J. Verweij, *Clin. Cancer Res.* **4**, 1153 (1998).
225. H. Hochster, L. Liebes, J. Speyer, J. Soric, B. Taubes, R. Oratz, J. Wernz, A. Chachoua, R. H. Blum, and A. Zeleniuch-Jacquotte, *Clin. Cancer Res.* **3**, 1245 (1997).
226. C. J. Gerrits, H. Burris, J. H. Schellens, A. S. Planting, M. E. van den Burg, G. I. Rodriguez, V. van Beurden, W. J. Loos, I. Hudson, S. Fields, J. Verweij, and D. D. von Hoff, *Eur. J. Cancer* **34**, 1030 (1998).
227. C. J. Gerrits, J. H. Schellens, H. Burris, J. R. Eckardt, A. S. Planting, M. E. van der Burg, G. I. Rodriguez, W. J. Loos, V. van Beurden, I. Hudson, D. D. von Hoff, and J. Verweij, *Clin. Cancer Res.* **5**, 69 (1999).
228. E. K. Rowinsky, S. H. Kaufmann, S. D. Baker, C. B. Miller, S. E. Sartorius, M. K. Bowling, T. L. Chen, R. C. Donehower, and S. D. Gore, *Clin. Cancer Res.* **2**, 1921 (1996).
229. R. N. Brogden and L. R. Wiseman, *Drugs* **56**, 709 (1998).
230. F. Robert, S. Soong, and R. H. Wheeler, *Am. J. Clin. Oncol.* **20**, 298 (1997).
231. G. R. Hudes, R. Kosierowski, R. Greenberg, H. E. Ramsey, S. C. Fox, R. F. Ozols, C. A. McAleer, and B. J. Giantonio, *Invest. New Drugs* **13**, 235 (1995).
232. M. Gore, W. ten Bokkel Huinink, J. Carmichael, A. Gordon, N. Davidson, R. Coleman, M. Spaczynski, J. F. Heron, G. Bolis, H. Malmstrom, J. Malfetano, C. Scarabelli, P. Vennin, G. Ross, and S. Z. Fields, *J. Clin. Oncol.* **19**, 1893 (2001).
233. M. Gore, A. Oza, G. Rustin, J. Malfetano, H. Calvert, D. Clarke-Pearson, J. Carmichael, G. Ross, R. A. Beckman, and S. Z. Fields, *Eur. J. Cancer* **38**, 57 (2002).
234. J. von Pawel, J. H. Schiller, F. A. Shepherd, S. Z. Fields, J. P. Kleisbauer, N. G. Chrysson, D. J. Stewart, P. I. Clark, M. C. Palmer, A. Depierre, J. Carmichael, J. B. Krebs, G. Ross, S. R. Lane, and R. Gralla, *J. Clin. Oncol.* **17**, 658 (1999).
235. J. H. Schiller, K. Kim, P. Hutson, R. DeVore, J. Glick, J. Stewart, and D. Johnson, *J. Clin. Oncol.* **14**, 2345 (1996).
236. J. von Pawel, U. Gatzemeier, J. L. Pujol, L. Moreau, S. Bildat, M. Ranson, G. Richardson, C. Steppert, A. Riviere, I. Camlett, S. Lane, and G. Ross, *J. Clin. Oncol.* **19**, 1743 (2001).
237. H. Kantarjian, *Semin. Hematol.* **35**, 1 (1998).
238. M. Beran, H. Kantarjian, S. O'Brien, C. Koller, M. al-Bitar, S. Arbuck, S. Pierce, M. Moore, J. L. Abbruzzese, M. Andreeff, M. Keating, and E. Estey, *Blood* **88**, 2473 (1996).
239. M. Beran and H. Kantarjian, *Semin. Hematol.* **35**, 26 (1998).
240. E. H. Kraut, J. J. Crowley, J. L. Wade, L. R. Laufman, M. Alsina, S. A. Taylor, and S. E. Salmon, *J. Clin. Oncol.* **16**, 589 (1998).
241. E. H. Kraut, R. Ju, and M. Muller, *Semin. Hematol.* **35**, 32 (1998).
242. D. F. Kehler, O. Soepenber, W. J. Loos, J. Verweij, and A. Sparreboom, *Anticancer Drugs* **12**, 89 (2001).
243. P. J. Houghton, P. J. Cheshire, J. D. Hallman, 2nd, L. Lutz, H. S. Friedman, M. K. Danks, and J. A. Houghton, *Cancer Chemother. Pharmacol.* **36**, 393 (1995).
244. S. S. Daoud, M. I. Fetouh, and B. C. Giovanella, *Anticancer Drugs* **6**, 83 (1995).
245. B. C. Giovanella, H. R. Hinz, A. J. Kozielski, J. S. Stehlin, Jr., R. Silber, and M. Potmesil, *Cancer Res.* **51**, 3052 (1991).

246. P. Pantazis, H. R. Hinz, J. T. Mendoza, A. J. Kozielski, L. J. Williams, Jr., J. S. Stehlin, Jr., and B. C. Giovanella, *Cancer Res.* **52**, 3980 (1992).
247. H. Hochster, L. Liebes, J. Speyer, J. Sorich, B. Taubes, R. Oratz, J. Wernz, A. Chachoua, R. H. Blum, and A. Zeleniuch-Jacquotte, *Clin. Cancer Res.* **3**, 1245 (1997).
248. H. Hochster, S. Wadler, C. Runowicz, L. Liebes, H. Cohen, R. Wallach, J. Sorich, B. Taubes, and J. Speyer, *J. Clin. Oncol.* **17**, 2553 (1999).
249. G. Liu, E. Franssen, M. I. Fitch, and E. Warner, *J. Clin. Oncol.* **15**, 110 (1997).
250. A. Sparreboom, M. J. de Jonge, and J. Verweij, *Eur. J. Cancer* **38**, 18 (2002).
251. M. D. DeMario and M. J. Ratain, *J. Clin. Oncol.* **16**, 2557 (1998).
252. V. M. Herben, H. Rosing, W. W. ten Bokkel Huinink, D. Van Zomeren, D. Batchelor, E. Doyle, F. D. Beusenberg, J. H. Beijnen, and J. H. Schellens, *Br. J. Cancer* **80**, 1380 (1999).
253. C. M. Kruijtzter, J. H. Beijnen, H. Rosing, W. W. ten Bokkel Huinink, M. Schot, R. C. Jewell, E. M. Paul, and J. H. Schellens, *J. Clin. Oncol.* **20**, 2943 (2002).
254. G. Hudes, *J. Clin. Oncol.* **20**, 2918 (2002).
255. B. K. Sinha, *Drugs* **49**, 11 (1995).
256. V. M. Herben, R. van Gijn, J. H. Schellens, M. Schot, J. Lieverst, M. J. Hillebrand, N. E. Schoemaker, M. G. Porro, J. H. Beijnen, and W. W. ten Bokkel Huinink, *J. Clin. Oncol.* **17**, 1906 (1999).
257. L. L. Siu, A. M. Oza, E. A. Eisenhauer, P. S. Firby, J. J. Thiessen, M. Michael, N. Wainman, J. Manzo, R. Feld, R. A. Goldberg, and M. J. Moore, *J. Clin. Oncol.* **16**, 1122 (1998).
258. E. Rubin, V. Wood, A. Bharti, D. Trites, C. Lynch, S. Hurwitz, S. Bartel, S. Levy, A. Rosowsky, D. Toppmeyer, and D. Kufe, *Clin. Cancer Res.* **1**, 269 (1995).
259. W. Dahut, N. Harold, C. Takimoto, C. Allegra, A. Chen, J. M. Hamilton, S. Arbuck, M. Sorensen, F. Grollman, H. Nakashima, R. Lieberman, M. Liang, W. Corse, and J. Grem, *J. Clin. Oncol.* **14**, 1236 (1996).
260. J. P. Eder, Jr., J. G. Supko, T. Lynch, M. Bryant, E. Vosburgh, L. N. Shulman, G. Xu, and D. W. Kufe, *Clin. Cancer Res.* **4**, 317 (1998).
261. A. M. Langevin, D. T. Casto, P. J. Thomas, S. D. Weitman, C. Kretschmar, H. Grier, C. Pratt, R. Dubowy, M. Bernstein, S. Blaney, and T. Vietti, *J. Clin. Oncol.* **16**, 2494 (1998).
262. R. R. Thomas, W. Dahut, N. Harold, J. L. Grem, B. P. Monahan, M. Liang, R. A. Band, J. Cottrell, V. Llorens, J. A. Smith, W. Corse, S. G. Arbuck, J. Wright, A. P. Chen, J. D. Shapiro, J. M. Hamilton, C. J. Allegra, and C. H. Takimoto, *Cancer Chemother. Pharmacol.* **48**, 215 (2001).
263. N. Vey, H. Kantarjian, H. Tran, M. Beran, S. O'Brien, C. Bivins, F. Giles, J. Cortes, B. Cheson, S. Arbuck, and E. Estey, *Ann. Oncol.* **10**, 577 (1999).
264. F. Muggia, L. Liebes, M. Potmesil, A. Hamilton, H. Hochster, G. Hornreich, J. Sorich, A. Downey, and H. Wasserstrom, in "Annals of the New York Academy of Sciences" (J. G. Liehr, B. C. Giovanella and C. F. Verschraegen, eds.), vol. 922, pp. 178-187. The New York Academy of Sciences, New York, 2000.
265. A. Sparreboom, M. J. de Jonge, C. J. Punt, K. Nooter, W. J. Loos, M. G. Porro, and J. Verweij, *Clin. Cancer Res.* **4**, 1915 (1998).
266. S. Mani, L. Iyer, L. Janisch, X. Wang, G. F. Fleming, R. L. Schilsky, and M. J. Ratain, *Cancer Chemother. Pharmacol.* **42**, 84 (1998).
267. M. J. de Jonge, C. J. Punt, A. H. Gelderblom, W. J. Loos, V. van Beurden, A. S. Planting, M. E. van der Burg, L. W. van Maanen, B. K. Dallaire, J. Verweij, D. J. Wagener, and A. Sparreboom, *J. Clin. Oncol.* **17**, 2219 (1999).

268. E. H. Kraut, S. P. Balcerzak, D. Young, M. A. O'Rourke, J. J. Petrus, J. P. Kuebler, and D. G. Mayernik, *Cancer Invest.* **18**, 28 (2000).
269. R. Pazdur, E. Diaz-Canton, W. P. Ballard, J. E. Bradof, S. Graham, S. G. Arbuck, J. L. Abbruzzese, and R. Winn, *J. Clin. Oncol.* **15**, 2905 (1997).
270. L. B. Saltz, N. E. Kemeny, W. Tong, J. Harrison, R. Berkery, and D. P. Kelsen, *Cancer* **80**, 1727 (1997).
271. R. Pazdur, D. C. Medgyesy, R. J. Winn, S. R. Dakhil, D. F., Jr., Scalzo, A. Moore, P. M. Hoff, S. G. Arbuck, and J. L. Abbruzzese, *Invest. New Drugs* **16**, 341 (1998).
272. H. C. Pitot, J. A. Knost, M. R. Mahoney, J. Kugler, J. E. Krook, A. K. Hatfield, D. J. Sargent, and R. M. Goldberg, *Cancer* **89**, 1699 (2000).
273. F. Hochberg, S. A. Grossman, T. Mikkelsen, M. Glantz, J. D. Fisher, and S. Piantadosi, *Neuro-oncol.* **2**, 29 (2000).
274. T. Lad, F. Rosen, D. Sciortino, B. Brockstein, J. P. Keubler, R. Arietta, and E. Vokes, *Invest. New Drugs* **18**, 261 (2000).
275. W. H. Wilson, R. Little, D. Pearson, E. S. Jaffe, S. M. Steinberg, B. D. Cheson, R. Humphrey, D. R. Kohler, and P. Elwood, *J. Clin. Oncol.* **16**, 2345 (1998).
276. A. Argiris, P. Heald, T. Kuzel, F. M. Foss, S. DiStasio, D. L. Cooper, S. Arbuck, and J. R. Murren, *Invest. New Drugs* **19**, 321 (2001).
277. E. E. Vokes, R. H. Ansari, G. A. Masters, P. C. Hoffman, A. Klepsch, M. J. Ratain, D. F. Sciortino, T. E. Lad, S. Krauss, P. A. Fishkin, and H. M. Golomb, *Ann. Oncol.* **9**, 1085 (1998).
278. E. E. Vokes, G. S. Gordon, C. M. Rudin, A. M. Mauer, S. Watson, S. Krauss, R. Arrieta, H. M. Golomb, and P. C. Hoffman, *Invest. New Drugs* **19**, 329 (2001).
279. W. J. Loos, J. Verweij, H. J. Gelderblom, M. J. de Jonge, E. Brouwer, B. K. Dallaire, and A. Sparreboom, *Anticancer Drugs* **10**, 705 (1999).
280. M. L. Li, L. Horn, P. S. Firby, and M. J. Moore, *Clin. Cancer Res.* **7**, 168 (2001).
281. M. H. Kirstein, P. J. Houghton, P. J. Cheshire, L. B. Richmond, A. K. Smith, S. K. Hanna, and C. F. Stewart, *Clin. Cancer Res.* **7**, 358 (2001).
282. S. Sakuma, Z. R. Lu, P. Kopeckova, and J. Kopecek, *J. Controlled Release* **75**, 365 (2001).
283. Z. M. Prijovich, B. M. Chen, Y. L. Leu, J. W. Chern, and S. R. Roffler, *Br. J. Cancer* **86**, 1634 (2002).
284. F. de Groot, G. Busscher, R. Aben, and H. Scheeren, *Bioorg. Med. Chem. Lett.* **12**, 2371 (2002).
285. P. Pantazis, J. A. Early, J. T. Mendoza, A. R. DeJesus, and B. C. Giovanella, *Cancer Res.* **54**, 771 (1994).
286. E. Karaberis and D. Mourelatos, *Teratog. Carcinog. Mutagen.* **20**, 141 (2000).
287. H. R. Hinz, N. J. Harris, E. A. Natelson, and B. C. Giovanella, *Cancer Res.* **54**, 3096 (1994).
288. E. A. Natelson, B. C. Giovanella, C. F. Verschraegen, K. M. Fehir, P. D. de Ipolyi, N. Harris, and J. S. Stehlin, in "Annals of the New York Academy of Sciences" (P. Pantazis, B. C. Giovanella and M. L. Rothenberg, eds.), vol. 803, pp. 224–230. The New York Academy of Sciences, New York, 1996.
289. C. F. Verschraegen, E. A. Natelson, B. C. Giovanella, J. J. Kavanagh, A. P. Kudelka, R. S. Freedman, C. L. Edwards, K. Ende, and J. S. Stehlin, *Anticancer Drugs* **9**, 36 (1998).
290. C. F. Verschraegen, K. Jaeckle, B. Giovanella, V. Knight, and B. E. Gilbert, in "Annals of the New York Academy of Sciences" (J. G. Liehr, B. C. Giovanella and C. F. Verschraegen, eds.), vol. 922, pp. 237–246. The New York Academy of Sciences, New York, 2000.

291. N. V. Koshkina, E. S. Kleinerman, C. Waidrep, S. F. Jia, L. L. Worth, B. E. Gilbert, and V. Knight, *Clin. Cancer Res.* **6**, 2876 (2000).
292. J. S. Stehlin, B. C. Giovanella, E. A. Natelson, P. D. de Ipolyi, D. Coil, B. Davis, D. Wolk, P. Wallace, and A. Trojacek, *Int. J. Oncol.* **14**, 821 (1999).
293. M. M. Konstadoulakis, P. T. Antonakis, B. G. Tsibloulis, G. P. Stathopoulos, A. P. Manouras, D. B. Mylonaki, and B. X. Golematis, *Cancer Chemother. Pharmacol.* **48**, 417 (2001).
294. C. F. Verschraegen, E. Gupta, E. Loyer, J. J. Kavanagh, A. P. Kudelka, R. S. Freedman, C. L. Edwards, N. Harris, M. Steger, V. Steltz, B. C. Giovanella, and J. S. Stehlin, *Anticancer Drugs* **10**, 375 (1999).
295. P. Schoffski, A. Herr, J. B. Vermorken, J. van den Brande, J. H. Beijnen, H. Rosing, J. Volk, A. Ganser, S. Adank, H. J. Botma, and J. Wanders, *Eur. J. Cancer* **38**, 807 (2002).
296. E. Raymond, M. Campone, R. Stupp, J. Menten, P. Chollet, T. Lesimple, R. Fety-Deporte, D. Lacombe, X. Paoletti, and P. Fumoleau, *Eur. J. Cancer* **38**, 1348 (2002).
297. J. A. Ellerhorst, A. Y. Bedikian, T. M. Smith, N. E. Papadopoulos, C. Plager, and O. Eton, *Anticancer Drugs* **13**, 169 (2002).
298. I. Mitsui, E. Kumazawa, Y. Hirota, M. Aonuma, M. Sugimori, S. Ohsuki, K. Uoto, A. Ejima, H. Terasawa, and K. Sato, *Jpn. J. Cancer Res.* **86**, 776 (1995).
299. R. de Jager, P. Cheverton, K. Tamanoi, J. Coyle, M. Ducharme, N. Sakamoto, M. Satomi, and M. Suzuki, in "Annals of the New York Academy of Sciences" (J. G. Liehr, B. C. Giovanella and C. F. Verschraegen, eds.), vol. 922, pp. 260–273. The New York Academy of Sciences, New York, 2000.
300. T. Oguma, M. Yamada, T. Konno, K. Inukai, and M. Nakaoka, *Biol. Pharm. Bull.* **24**, 176 (2001).
301. R. A. Lawrence, E. Izbicka, R. L. de Jager, A. Tohgo, G. M. Clark, S. D. Weitman, E. K. Rowinsky, and D. D. von Hoff, *Anticancer Drugs* **10**, 655 (1999).
302. N. Vey, F. J. Giles, H. Kantarjian, T. L. Smith, M. Beran, and S. Jeha, *Clin. Cancer Res.* **6**, 731 (2000).
303. E. Kumazawa, T. Jimbo, Y. Ochi, and A. Tohgo, *Cancer Chemother. Pharmacol.* **42**, 210 (1998).
304. S. Takiguchi, E. Kumazawa, T. Shimazoe, A. Tohgo, and A. Kono, *Jpn. J. Cancer Res.* **88**, 760 (1997).
305. T. Nomoto, K. Nishio, T. Ishida, M. Mori, and N. Saijo, *Jpn. J. Cancer Res.* **89**, 1179 (1998).
306. M. Ishii, M. Iwahana, I. Mitsui, M. Minami, S. Imagawa, A. Tohgo, and A. Ejima, *Anticancer Drugs* **11**, 353 (2000).
307. T. Oguma, T. Konno, A. Inaba, and M. Nakaoka, *Biomed. Chromatogr.* **15**, 108 (2001).
308. T. Oguma, Y. Ohshima, and M. Nakaoka, *J. Chromatogr. B Biomed. Sci. Appl.* **740**, 237 (2000).
309. E. K. Rowinsky, T. R. Johnson, C. E. Geyer, Jr., L. A. Hammond, S. G. Eckhardt, R. Drengler, L. Smetzer, J. Coyle, J. Rizzo, G. Schwartz, A. Tolcher, D. D. von Hoff, and R. L. de Jager, *J. Clin. Oncol.* **18**, 3151 (2000).
310. M. E. Royce, P. M. Hoff, P. Dumas, Y. Lassere, J. J. Lee, J. Coyle, M. P. Ducharme, R. de Jager, and R. Pazdur, *J. Clin. Oncol.* **19**, 1493 (2001).
311. S. Sharma, N. Kemeny, G. K. Schwartz, D. Kelsen, E. O'Reilly, D. Ilson, J. Coyle, R. L. de Jager, M. P. Ducharme, S. Kleban, E. Hollywood, and L. B. Saltz, *Clin. Cancer Res.* **7**, 3963 (2001).

312. H. Minami, H. Fujii, T. Igarashi, K. Itoh, K. Tamanoi, T. Oguma, and Y. Sasaki, *Clin. Cancer Res.* **7**, 3056 (2001).
313. V. Boige, E. Raymond, S. Faivre, M. Gattineau, K. Meely, S. Mekhaldi, P. Pautier, M. Ducreux, O. Rixe, and J. P. Armand, *J. Clin. Oncol.* **18**, 3986 (2000).
314. F. J. Giles, J. E. Cortes, D. A. Thomas, G. Garcia-Manero, S. Faderl, S. Jeha, R. L. de Jager, and H. M. Kantarjian, *Clin. Cancer Res.* **8**, 2134 (2002).
315. C. F. Verschraegen, C. Levenback, M. Vincent, J. Wolf, M. Bevers, E. Loyer, A. P. Kudelka, and J. J. Kavanagh, in "Annals of the New York Academy of Sciences" (J. G. Liehr, B. C. Giovanella and C. F. Verschraegen, eds.), vol. 922, pp. 349–351. The New York Academy of Sciences, New York, 2000.
316. O. Lavergne, D. Demarquay, P. G. Kasprzyk, and D. C. Bigg, in "Annals of the New York Academy of Sciences" (J. G. Liehr, B. C. Giovanella and C. F. Verschraegen, eds.), vol. 922, pp. 100–111. The New York Academy of Sciences, New York, 2000.
317. H. Gelderblom, "Pharmacologic aspects of new classes of anti-cancer agents: inhibitors of topoisomerase I or tubulin." Ph.D. Thesis, Erasmus University at Rotterdam, The Netherlands, 2001.
318. L. Lesueur-Ginot, D. Demarquay, R. Kiss, P. G. Kasprzyk, L. Dassonneville, C. Bailly, J. Camara, O. Lavergne, and D. C. Bigg, *Cancer Res.* **59**, 2939 (1999).
319. O. Lavergne, D. Demarquay, C. Bailly, C. Lanco, A. Rolland, M. Huchet, H. Coulomb, N. Muller, N. Baroggi, J. Camara, C. Le Breton, E. Manginot, J. B. Cazaux, and D. C. Bigg, *J. Med. Chem.* **43**, 2285 (2000).
320. P. Philippart, L. Harper, C. Chaboteaux, C. Decaestecker, Y. Bronckart, L. Gordover, L. Lesueur-Ginot, H. Malonne, O. Lavergne, D. C. Bigg, P. M. da Costa, and R. Kiss, *Clin. Cancer Res.* **6**, 1557 (2000).
321. C. Bailly, A. Lansiaux, L. Dassonneville, D. Demarquay, H. Coulomb, M. Huchet, O. Lavergne, and D. C. Bigg, *Biochemistry* **38**, 15556 (1999).
322. R. H. Mathijssen, J. Verweij, M. J. de Jonge, K. Nooter, G. Stoter, and A. Sparreboom, *J. Clin. Oncol.* **20**, 81 (2002).
323. C. J. Gerrits, J. H. Schellens, G. J. Creemers, P. Wissel, A. S. Planting, J. F. Pritchard, S. DePee, M. de Boer-Dennert, M. Hartevelde, and J. Verweij, *Br. J. Cancer* **76**, 946 (1997).
324. D. L. Emerson, J. M. Besterman, H. R. Brown, M. G. Evans, P. P. Leitner, M. J. Luzzio, J. E. Shaffer, D. D. Sternbach, D. Uehling, and A. Vuong, *Cancer Res.* **55**, 603 (1995).
325. C. J. Gerrits, G. J. Creemers, J. H. Schellens, P. Wissel, A. S. Planting, R. Kunka, K. Selinger, M. de Boer-Dennert, Y. Marijnen, M. Hartevelde, and J. Verweij, *Br. J. Cancer* **73**, 744 (1996).
326. S. G. Eckhardt, S. D. Baker, J. R. Eckardt, T. G. Burke, D. L. Warner, J. G. Kuhn, G. Rodriguez, S. Fields, A. Thurman, L. Smith, M. L. Rothenberg, L. White, P. Wissel, R. Kunka, S. DePee, D. Littlefield, H. A. Burris, D. D. von Hoff, and E. K. Rowinsky, *Clin. Cancer Res.* **4**, 595 (1998).
327. L. Paz-Ares, R. Kunka, D. DeMaria, J. Cassidy, M. Alden, P. Beranek, S. Kaye, D. Littlefield, D. Reilly, S. Depee, P. Wissel, C. Twelves, and P. O'Dwyer, *Br. J. Cancer* **78**, 1329 (1998).
328. J. P. Stevenson, D. DeMaria, J. Sludden, S. B. Kaye, L. Paz-Ares, L. B. Grochow, A. McDonald, K. Selinger, P. Wissel, P. J. O'Dwyer, and C. Twelves, *Ann. Oncol.* **10**, 339 (1999).

329. T. Gamucci, R. Paridaens, B. Heinrich, J. H. Schellens, N. Pavlidis, J. Verweij, C. Sessa, S. Kaye, M. Roelvink, J. Wanders, and A. Hanauske, *Ann. Oncol.* **11**, 793 (2000).
330. C. Sessa, J. Wanders, M. Roelvink, P. Dombernowsky, D. Nielsen, R. Morant, P. Drings, P. Wissel, and A. R. Hanauske, *Ann. Oncol.* **11**, 207 (2000).
331. D. L. Emerson, R. Bendele, E. Brown, S. Chiang, J. P. Desjardins, L. C. Dihel, S. C. Gill, M. Hamilton, J. D. LeRay, L. Moon-McDermott, K. Moynihan, F. C. Richardson, B. Tomkinson, M. J. Luzzio, and D. Baccanari, *Clin. Cancer Res.* **6**, 2903 (2000).
332. D. F. Kehler, A. M. Bos, J. Verweij, H. J. Groen, W. J. Loos, A. Sparreboom, M. J. de Jonge, M. Hamilton, T. Cameron, and E. G. de Vries, *J. Clin. Oncol.* **20**, 1222 (2002).

## TREMORGENIC AND NONTREMORGENIC 2,3-FUSED INDOLE DITERPENOIDS

HEATHER SINGS AND SHEO SINGH

*Merck Research Laboratories, Rahway, NJ 07065, USA*

- I. Introduction
  - II. Isolation
  - III. Synthesis
  - IV. Biosynthesis
  - V. Structure and Tremorgenicity
- References

### I. Introduction

This chapter reviews the literature of indole diterpenoids consisting of a minimum of five fused rings that involve indole C-2 and C-3, as represented by structure **1**. Although these alkaloids have been reviewed in various forms (*1–3*), there is no published comprehensive review that covers this group of alkaloids. The reported biological activities of some of these alkaloids have included definitions of various tremors and staggers, which were reviewed in 1989, including a proposal for a pharmacophore model for  $\gamma$ -amino butyric acid (GABA) activity (*4*). This chapter includes details of the isolation and structure elucidation, chemical modifications, and biological activities of all alkaloids reported in the published literature until 2002 (*Table I*), synthetic studies toward total synthesis, and biosynthetic studies. We have divided these alkaloids into six groups based on the substitution around the phenyl ring of the indole moiety. These groups are the paspalanes (**2**), aflatremanes (**3**), penitremanes (**4**), janthitremanes (**5**), lolitremanes (**6**), and nodulisporanes (**7**).





*Penicillium janthinellum* growing on ryegrass produces all of the janthitrems. Lastly, the pharmacologically useful and biologically well-studied nodulisporanes, the only class of nontremorgenic indole diterpenoids, are produced by fermentable *Nodulisporium* species growing as an endophyte on twigs.

## II. Isolation

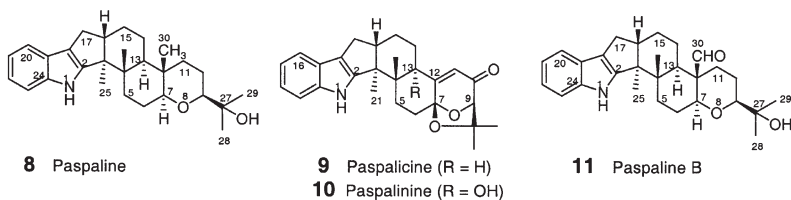
### A. PASPALANES

The paspalanes are structurally the simplest of the six groups because they lack substitution on the indole ring. This class constitutes the largest group of alkaloids, all characterized by the presence of four or five methyl groups, and two pairs each of aromatic doublets and triplets in the  $^1\text{H}$  NMR spectrum and the corresponding  $^{13}\text{C}$  NMR signals. For consistency, an atom numbering from Munday-Finch was adapted for this group in which the methyl group at C-12 is numbered as C-30, designating it as the last carbon atom. General HPLC conditions and the chemotaxonomic distribution of many indole diterpenoids were described by Frisvad in 1987 (5).

#### 1. Paspaline (8)

Paspaline was first isolated in 1966 from *C. paspali* Stevens et Hall by Fehr and Acklin (6) in Arigoni's lab. It displayed  $[\alpha]_{\text{D}} = -23^\circ$  and a molecular ion at  $m/z$  421. Elemental analysis led to a molecular formula of  $\text{C}_{28}\text{H}_{39}\text{NO}_2$ . It showed IR hydroxy group absorption ( $3500\text{ cm}^{-1}$ ) and a UV absorption band at  $\lambda_{\text{max}}$  282 nm, characteristic of an indole group. Fehr and Acklin elucidated the structure of this alkaloid by chemical methods as a hexacyclic indole diterpenoid possessing a 2,3-indole fused with a diterpenoid unit via a five-membered ring connection to a bis-cyclohexyl-pyran unit. They also deduced the stereochemistry of five of the seven asymmetric centers. The structure, including complete stereochemistry, was firmly established by Springer and Clardy in 1980 (7) by X-ray crystallographic analysis. The  $^{13}\text{C}$  NMR spectrum of paspaline (8) was first reported by Cole *et al.* (8) in 1977, followed by Nozawa *et al.* from a reisolation (9) from *Emericella striata*. However, many of the assignments were ambiguous. In 1996, Munday-Finch reported (10) the isolation of paspaline (8) from *P. paxilli* Bainier and established the  $^{13}\text{C}$  NMR assignments by 2D NMR (Table II), resulting in a reassignment of nine of the 28 carbon resonances.

Paspaline (8) was also isolated from *Albophoma yamanashiensis* (11) and *Lolium perenne* L. infected with *Neotyphodium lolii* (12), as well as from sclerotia of *Aspergillus alliaceus* (13), and *Aspergillus flavus* (14). A LC analysis method, including traces of UV and mass spectra, was reported for this and related alkaloids (15). Paspaline did not display tremorgenic activity in mice at 500 mg/kg (8).



### 2. Paspalicine (9)

In conjunction with paspaline (**8**), Fehr and Acklin reported the isolation of its congener paspalicine (**9**) from *C. paspali* Stevens et Hall (6). It showed an optical rotation of  $[\alpha]_D = +173^\circ$  which is opposite in sign to that of paspaline. Mass spectral and elemental analysis suggested a molecular weight of 417 and a molecular formula  $C_{27}H_{31}NO_3$ , which indicated paspalicine (**9**) contained one less carbon compared to paspaline. An absorption band corresponding to a conjugated ketone ( $1670$  and  $1620\text{ cm}^{-1}$ ) was observed in the IR spectrum, which was supported by an absorption band at  $\lambda_{\text{max}}$  244 nm in the UV spectrum. The latter spectrum exhibited the indole specific absorption band at  $\lambda_{\text{max}}$  275 nm. Like paspaline (**8**), the Zurich group elucidated the structure of this alkaloid by chemical degradation, and the stereostructure was firmly established by Springer and Clardy (7) by a single crystal X-ray analysis. A comparison of the structures of paspalicine (**9**) and congener paspaline (**8**) indicated that they differ in the sixth ring F. Demethylation of paspaline at C-12 followed by oxidation of C-10 and 11,12-dehydrogenation leads to the  $\Delta^{11,12}$ -enone of paspalicine. In addition, the C-27 hydroxy group of paspalicine forms a six-membered ring in the form of a spiro-hemiketal at C-7 ( $\delta_C$  104.4 versus  $\delta_C$  84.7) (8). It exhibited a positive Cotton effect in the CD spectrum at  $\lambda_{\text{max}}$  348 nm similar to paxilline (*vide infra*) indicating an identical absolute stereochemistry of the two alkaloids (7). A LC analysis method, including traces of UV and mass spectra, was reported for this and related alkaloids (15). Paspalicine did not induce tremors in mice at 250 mg/kg (8).

### 3. Paspalinine (10)

Paspalinine (**10**) was originally reported by Fehr and Acklin (6) in 1966 from the ergot fungus *C. paspali*, and was subsequently isolated by Cole *et al.* (8) in 1977 through a bioassay-guided isolation using Dekalb cockerels via oral administration. Paspalinine gave a molecular formula of  $C_{27}H_{31}NO_4$  (MW 433) indicating that it possessed an extra oxygen atom compared to paspalicine (**9**). Like paspalicine, it exhibited an UV spectrum with maxima at 232, 250, and 274 nm, and IR absorption bands corresponding to NH ( $3480\text{ cm}^{-1}$ ) and conjugated ketone groups ( $1669$  and  $1620\text{ cm}^{-1}$ ). In contrast to paspalicine (**9**), it displayed an absorption band for a hydroxy group ( $3590\text{ cm}^{-1}$ ) that could not be acetylated. The  $^{13}\text{C}$  NMR spectrum of paspalinine and paspalicine were essentially similar, except for the substitution of the C-13 methine ( $\delta_C$  39.2) with a quaternary oxygenated

TABLE I.  
Physicochemical Properties, Natural Occurrences, and Biological Activities of Indole Diterpenoids.

Alkaloid (#)	MW	MF	$[\alpha]_D$	Mp	Producing organism	Tremors in mice at (mg/kg) N,Y,NR <sup>a</sup>	Other activity	References
<i>Paspalanes</i>								
Paspaline (8)	421	C <sub>28</sub> H <sub>39</sub> NO <sub>2</sub>	-23°		<i>Claviceps paspali</i> <i>Emericella striata</i> <i>Penicillium paxilli</i> Bainier <i>Albophoma yamanashiensis</i> <i>Lolium perenne</i> L. ( <i>Neotyphodium lolii</i> ) <i>Aspergillus flavus</i> <i>Aspergillus alliaceus</i>	N (500)		(6-8,52) (9) (10) (11) (12) (14) (13)
Paspalicine (9)	417	C <sub>27</sub> H <sub>31</sub> NO <sub>3</sub>	+173°		<i>Claviceps paspali</i>	N (250)	Maxi-K	(6,7,52)
Paspalinine (10)	433	C <sub>27</sub> H <sub>31</sub> NO <sub>4</sub>			<i>Claviceps paspali</i> <i>Aspergillus flavus</i> <i>Eupenicillium shearii</i>	Y (80)	Maxi-K	(6,8,17,52) (18) (19)
Paspaline B (11)	435	C <sub>28</sub> H <sub>37</sub> NO <sub>3</sub>			<i>Penicillium paxilli</i>	NR	Anti-insectan	(10)
Emindole SB (12)	405	C <sub>28</sub> H <sub>39</sub> NO			<i>Emericella striata</i> <i>Albophoma yamanashiensis</i>	NR		(9,24) (11)
Paxilline (13)	435	C <sub>27</sub> H <sub>33</sub> NO <sub>4</sub>		253-255 °C	<i>Penicillium paxilli</i>  <i>Acantherum inebrians</i> <i>Eupenicillium shearii</i>	Y (4, 25)	Maxi-K, InsP <sub>3</sub>	(9,16,21, 22,37) (27) (19)

(continued)

TABLE I.  
Continued.

Alkaloid (#)	MW	MF	[ $\alpha$ ] <sub>D</sub>	Mp	Producing organism	Tremors in mice at (mg/kg) N, Y, NR <sup>a</sup>	Other activity	References
					<i>Acremonium lolii</i>			(23)
					<i>Emericella striata</i>			(24)
					<i>Emericella desertorum</i>			(25)
					<i>Emericella foveolata</i>			(24,26)
2,18-Dioxo-2,18-seco-paxilline (14)					<i>Eupenicillium shearii</i>	N (40)	Anti-insectan	(19)
13-Desoxypaxilline (20)	419	C <sub>27</sub> H <sub>33</sub> NO <sub>3</sub>			<i>Penicillium paxilli</i>	NR		(10)
					<i>Lolium perenne</i> ( <i>Neotyphodium lolii</i> )			(12)
					<i>Eupenicillium shearii</i>			(19)
					<i>Emericella striata</i>			(9)
27-O-Acetylpaxilline (21)	477	C <sub>29</sub> H <sub>35</sub> NO <sub>5</sub>			<i>Emericella striata</i>	Y (3.13)		(24)
7 $\alpha$ -Hydroxy-13-desoxypaxilline (22)	435	C <sub>27</sub> H <sub>33</sub> NO <sub>4</sub>	-20°		<i>Penicillium paxilli</i>	NR		(35)
					<i>Eupenicillium shearii</i>		Anti-insectan	(19)
7 $\alpha$ -Hydroxypaxilline (23)	451	C <sub>27</sub> H <sub>33</sub> NO <sub>5</sub>			<i>Penicillium paxilli</i>	N (4)		(35)
					<i>Acremonium lolii</i>			(35)
10 $\beta$ -Hydroxy-13-desoxypaxilline (24)	421	C <sub>27</sub> H <sub>35</sub> NO <sub>3</sub>			<i>Penicillium paxilli</i>	NR		(35)
					<i>Acremonium lolii</i>			(35)
PC-M5' (25)	479	C <sub>29</sub> H <sub>37</sub> NO <sub>5</sub>			<i>Penicillium crustosum</i>	NR		(36)
PC-M6 (26)	421	C <sub>27</sub> H <sub>35</sub> NO <sub>3</sub>			<i>Penicillium crustosum</i>	NR		(36)

Paxinorol (27)	377	C <sub>24</sub> H <sub>27</sub> NO <sub>3</sub>		<i>Penicillium paxilli</i>	NR		(37)
14-Hydroxypaspalinine (29)	449	C <sub>27</sub> H <sub>31</sub> NO <sub>5</sub>	+126°	<i>Aspergillus nomius</i>	NR	Anti-insectan	(38)
14-( <i>N,N</i> -dimethyl-L-valyloxy) Paspalinine (30)	577	C <sub>34</sub> H <sub>45</sub> N <sub>2</sub> O <sub>6</sub>	+102°	<i>Aspergillus nomius</i>	NR	Anti-insectan	(38)
Terpendole A (31)	536	C <sub>32</sub> H <sub>41</sub> NO <sub>6</sub>	+11.6°	<i>Albophoma yamanashiensis</i>	NR	ACAT inhibitor	(11,39)
Terpendole B (32)	421	C <sub>27</sub> H <sub>35</sub> NO <sub>3</sub>	-3.6°	<i>Albophoma yamanashiensis</i>	NR	ACAT inhibitor	(11,39)
Terpendole C (33)	519	C <sub>32</sub> H <sub>41</sub> NO <sub>5</sub>	-2.3°	<i>Albophoma yamanashiensis</i>		ACAT inhibitor	(11,39)
				<i>Lolium perenne</i> ( <i>Neotyphodium lolii</i> )	Y (8)		(41)
Terpendole D (34)	505	C <sub>32</sub> H <sub>43</sub> NO <sub>4</sub>	-31.2°	<i>Albophoma yamanashiensis</i>	NR	ACAT inhibitor	(11,39)
Terpendole E (35)	437	C <sub>28</sub> H <sub>39</sub> NO <sub>3</sub>	-36.4°	<i>Albophoma yamanashiensis</i>	NR	ACAT inhibitor	(40)
Terpendole F (36)	453	C <sub>28</sub> H <sub>39</sub> NO <sub>4</sub>	-35.8°	<i>Albophoma yamanashiensis</i>	NR	ACAT inhibitor	(40)
Terpendole G (37)	451	C <sub>28</sub> H <sub>37</sub> NO <sub>4</sub>	-28°	<i>Albophoma yamanashiensis</i>	NR	ACAT inhibitor	(40)
Terpendole H (38)	451	C <sub>27</sub> H <sub>33</sub> NO <sub>5</sub>	-47°	<i>Albophoma yamanashiensis</i>	NR	ACAT inhibitor	(40)
Terpendole I (39)	453	C <sub>27</sub> H <sub>35</sub> NO <sub>5</sub>	+7°	<i>Albophoma yamanashiensis</i>	NR	ACAT inhibitor	(40)
Terpendole J (40)	521	C <sub>32</sub> H <sub>43</sub> NO <sub>5</sub>	-30.3°	<i>Albophoma yamanashiensis</i>	NR	ACAT inhibitor	(40)
Terpendole K (41)	517	C <sub>32</sub> H <sub>39</sub> NO <sub>5</sub>	+21.8°	<i>Albophoma yamanashiensis</i>		ACAT inhibitor	(40)

(continued)

TABLE I.  
Continued.

Alkaloid (#)	MW	MF	$[\alpha]_D$	Mp	Producing organism	Tremors in mice at (mg/kg) N,Y,NR <sup>a</sup>	Other activity	References
Terpendole M (42)	535	C <sub>32</sub> H <sub>41</sub> NO <sub>6</sub>			<i>Lolium perenne</i> ( <i>Neotyphodium lolii</i> )	Y (8)		(12)
Thiersinines A (43)	523	C <sub>30</sub> H <sub>37</sub> NO <sub>7</sub>	-80°	255-258 °C	<i>Penicillium thiersii</i>	NR	Anti-insectan	(42)
Thiersinines B (44)	509	C <sub>29</sub> H <sub>35</sub> NO <sub>7</sub>	-93°		<i>Penicillium thiersii</i>	NR	Anti-insectan	(42)
<i>Aflatremanes</i> Aflatrem (45)	501	C <sub>32</sub> H <sub>39</sub> NO <sub>4</sub>			<i>Aspergillus flavus</i>	Y (4)	GABA <sub>A</sub> Cl Maxi-K	(14,30,43-50)
$\beta$ -Aflatrem (46)	501	C <sub>32</sub> H <sub>39</sub> NO <sub>4</sub>	+77.9°	188-190 °C	<i>Aspergillus flavus</i> <i>Aspergillus parasiticus</i> <i>Aspergillus oblivaceus</i>	NR	Anti-insectan	(14) (14) (14)
Paspalitrem A (47)	501	C <sub>32</sub> H <sub>39</sub> NO <sub>4</sub>			<i>Claviceps paspali</i> <i>Phomopsis sp.</i>	Y (< 14)	Maxi-K	(8,52) (30,51)
Paspalitrem B (48)	517	C <sub>32</sub> H <sub>39</sub> NO <sub>5</sub>			<i>Claviceps paspali</i>	Y (< 14)		(8)
Paspalitrem C (49)	501	C <sub>32</sub> H <sub>39</sub> NO <sub>4</sub>			<i>Claviceps paspali</i> <i>Phomopsis sp.</i>	NR	Maxi-K	(52) (30,51)
Sulpinine A (50)	503	C <sub>32</sub> H <sub>41</sub> NO <sub>4</sub>	-29.6°	149-152 °C	<i>Aspergillus sulphureus</i>	NR	Anti-insectan	(53)
Sulpinine B (51)	487	C <sub>32</sub> H <sub>41</sub> NO <sub>3</sub>	-43.2°	Oil	<i>Aspergillus sulphureus</i>	NR	Anti-insectan	(53)
Sulpinine C (52)	535	C <sub>32</sub> H <sub>41</sub> NO <sub>6</sub>	+17.1°	Oil	<i>Aspergillus sulphureus</i>	NR		(53)

Terpendole L (53)					<i>Albophoma yamanashiensis</i>	NR	ACAT inhibitor	(40)
21-Isopentenylpaxilline (54)	503	C <sub>32</sub> H <sub>41</sub> NO <sub>4</sub>	-12°	Oil	<i>Eupenicillium shearii</i>	NR	Anti-insectan	(19)
<i>Penitremanes</i>								
Penitrem A (55)	633	C <sub>37</sub> H <sub>44</sub> ClNO <sub>6</sub>		237–239 °C	<i>Penicillium cyclopium</i>	Y (0.25-0.6)	Maxi-K, GABA↑, Glu↑, Asp↑	(54,57–59, 65)
					<i>Penicillium crustosum</i>			(56)
					<i>Penicillium nigricans</i>			(68)
					<i>Penicillium sp.</i>		Anti-insectan	(64,70)
Penitrem B (58)	583	C <sub>37</sub> H <sub>45</sub> NO <sub>5</sub>	-4.9°	Solid	<i>Penicillium crustosum</i>	Y (5)		(57,58, 65)
					<i>Aspergillus sulphureus</i>		Anti-insectan	(53)
Penitrem C (59)	601	C <sub>37</sub> H <sub>44</sub> ClNO <sub>4</sub>		Solid	<i>Penicillium crustosum</i>	NR		(57,58,65)
Penitrem D (60)	567	C <sub>37</sub> H <sub>45</sub> NO <sub>4</sub>		> 300 °C	<i>Penicillium crustosum</i>	NR		(57,58,65)
Penitrem E (61)	599	C <sub>37</sub> H <sub>45</sub> NO <sub>6</sub>		Solid	<i>Penicillium crustosum</i>	Y (2)		(57,58,65)
					<i>Penicillium nigricans</i>			(68)
Penitrem F (62)	617	C <sub>37</sub> H <sub>44</sub> ClNO <sub>5</sub>		Solid	<i>Penicillium crustosum</i>	NR		(57,58,65)
Secopenitrem B (63)	585	C <sub>37</sub> H <sub>47</sub> NO <sub>5</sub>	-5.2°	185–189 °C	<i>Aspergillus sulphureus</i>	NR	Anti-insectan	(53)
Thomitrem A (64)	633	C <sub>37</sub> H <sub>44</sub> ClNO <sub>6</sub>			<i>Penicillium crustosum</i>	NR		(67)
Thomitrem E (65)	599	C <sub>37</sub> H <sub>45</sub> NO <sub>6</sub>			<i>Penicillium crustosum</i>	NR		(67)
Pennigritrem (66)	633	C <sub>37</sub> H <sub>44</sub> ClNO <sub>6</sub>			<i>Penicillium nigricans</i>	Y (80)		(68)
Penitremone A (67)	599	C <sub>37</sub> H <sub>45</sub> NO <sub>6</sub>			<i>Penicillium sp.</i>	Y (5.6)		(70,69)
					<i>Aspergillus sulphureus</i>			
Penitremone B (68)	633	C <sub>37</sub> H <sub>45</sub> NO <sub>7</sub>			<i>Penicillium sp.</i>	N (16.8)		(70)
Penitremone C (69)	583	C <sub>37</sub> H <sub>45</sub> NO <sub>5</sub>			<i>Penicillium sp.</i>	NR		(70)
<i>Janthitremans</i>								
Janthitrem A	601	C <sub>37</sub> H <sub>47</sub> NO <sub>6</sub>			<i>Penicillium janthinellum</i>	NR		(71,73)

(continued)



TABLE I.  
Continued.

Alkaloid (#)	MW	MF	$[\alpha]_D$	Mp	Producing organism	Tremors in mice at (mg/kg) N,Y,NR <sup>a</sup>	Other activity	References
Janthitrem B (72)	585	C <sub>37</sub> H <sub>47</sub> NO <sub>5</sub>			<i>Penicillium janthinellum</i>	Y (0.2)		(71, 73,165)
Janthitrem C (73)	569	C <sub>37</sub> H <sub>47</sub> NO <sub>4</sub>			<i>Penicillium janthinellum</i>	NR		(71,73)
Janthitrem D	NA	NA			<i>Penicillium janthinellum</i>	NR		(71,72)
Janthitrem E (74)	603	C <sub>37</sub> H <sub>49</sub> NO <sub>6</sub>			<i>Penicillium janthinellum</i>	NR		(74)
Janthitrem F (75)	645	C <sub>39</sub> H <sub>51</sub> NO <sub>7</sub>			<i>Penicillium janthinellum</i>	NR		(74)
Janthitrem G (76)	629	C <sub>39</sub> H <sub>51</sub> NO <sub>6</sub>			<i>Penicillium janthinellum</i>	NR		(74)
Shearinine A (77)	583	C <sub>37</sub> H <sub>45</sub> NO <sub>5</sub>	+16°	> 250 °C	<i>Eupenicillium shearii</i>	NR	Anti-insectan	(19)
Shearinine B (78)	585	C <sub>37</sub> H <sub>47</sub> NO <sub>5</sub>	-76°	165-170 °C	<i>Eupenicillium shearii</i>	NR	Anti-insectan	(19)
Shearinine C (79)	618	C <sub>37</sub> H <sub>47</sub> NO <sub>7</sub>	-146°	180-190 °C	<i>Eupenicillium shearii</i>	NR	Anti-insectan	(19)
<i>Lolitremanes</i>								
Lolitreman A (80)	701	C <sub>42</sub> H <sub>55</sub> NO <sub>8</sub>			<i>Lolium perenne</i> ( <i>Acremonium lolii</i> ) ( <i>Neotyphodium lolii</i> )	Y (2)		(78-80,82)
Lolitreman B (81)	685	C <sub>42</sub> H <sub>55</sub> NO <sub>7</sub>		303-304 °C	<i>Lolium perenne</i> ( <i>Acremonium lolii</i> ) <i>Acantherum inebrians</i> ( <i>Acremonium lolii</i> )	Y (0.5-1)		(27,79,85) (27,87)
Lolitreman C (83)	619	C <sub>37</sub> H <sub>49</sub> NO <sub>7</sub>			<i>Lolium perenne</i> ( <i>Neotyphodium lolii</i> )	N (20)		(16,80)

10- <i>O</i> -Acetylloliritriol ( <b>84</b> )	661	C <sub>39</sub> H <sub>51</sub> NO <sub>8</sub>	<i>Lolium perenne</i> ( <i>Neotyphodium lolii</i> )	NR	(16,80)
Lolitrems C ( <b>86</b> )	687	C <sub>42</sub> H <sub>57</sub> NO <sub>7</sub>	<i>Lolium perenne</i> ( <i>Acremonium lolii</i> )	NR	(79,85)
Lolitrems D			<i>Lolium perenne</i> ( <i>Acremonium lolii</i> )	NR	(84)
Lolitrems E ( <b>87</b> )	687	C <sub>42</sub> H <sub>57</sub> NO <sub>7</sub>	<i>Lolium perenne</i> ( <i>Acremonium lolii</i> )	N (2)	(85)
Lolitrems F ( <b>88</b> )	685	C <sub>42</sub> H <sub>55</sub> NO <sub>7</sub>	<i>Lolium perenne</i> ( <i>Acremonium lolii</i> )	Y (0.5-1)	(84)
Lolilline ( <b>90</b> )	601	C <sub>37</sub> H <sub>47</sub> NO <sub>6</sub>	<i>Lolium perenne</i> ( <i>Acremonium lolii</i> )	N (8)	(41)
Lolicine A ( <b>91</b> )	603	C <sub>38</sub> H <sub>53</sub> NO <sub>5</sub>	<i>Lolium perenne</i> ( <i>Neotyphodium lolii</i> )	NR	(80)
Lolicine B ( <b>92</b> )	617	C <sub>38</sub> H <sub>51</sub> NO <sub>6</sub>	<i>Lolium perenne</i> ( <i>Neotyphodium lolii</i> )	NR	(80)
Lolitrems N ( <b>93</b> )	619	C <sub>37</sub> H <sub>49</sub> NO <sub>7</sub>	<i>Lolium perenne</i> ( <i>Neotyphodium lolii</i> )	NR	(80)
11- <i>O</i> -Propionyllicine A ( <b>94</b> )	659	C <sub>41</sub> H <sub>57</sub> NO <sub>6</sub>	<i>Lolium perenne</i> ( <i>Neotyphodium lolii</i> )	NR	(80)
11- <i>O</i> -Propionyllicine B ( <b>95</b> )	673	C <sub>41</sub> H <sub>55</sub> NO <sub>8</sub>	<i>Lolium perenne</i> ( <i>Neotyphodium lolii</i> )	NR	(80)
10- <i>O</i> -Propionylolitrems N ( <b>96</b> )	675	C <sub>40</sub> H <sub>53</sub> NO <sub>8</sub>	<i>Lolium perenne</i> ( <i>Neotyphodium lolii</i> )	NR	(80)
26- <i>epi</i> -10- <i>O</i> -Acetyllolitrems N ( <b>97</b> )	661	C <sub>39</sub> H <sub>51</sub> NO <sub>8</sub>	<i>Lolium perenne</i> ( <i>Neotyphodium lolii</i> )	NR	(80)
26- <i>epi</i> -lolitrems N ( <b>98</b> )	619	C <sub>37</sub> H <sub>49</sub> NO <sub>7</sub>	<i>Lolium perenne</i> ( <i>Neotyphodium lolii</i> )	NR	(80)

(continued)

TABLE I.  
Continued.

Alkaloid (#)	MW	MF	$[\alpha]_D$	Mp	Producing organism	Tremors in mice at (mg/kg) N, Y, NR <sup>a</sup>	Other activity	References
<i>Nodulisporanes</i>								
Nodulisporic acid A ( <b>99</b> )	679	C <sub>43</sub> H <sub>53</sub> NO <sub>6</sub>	+13°	250–255 °C	<i>Nodulisporium sp.</i>	N	Insecticidal	(89)
Nodulisporic acid A <sub>1</sub> ( <b>101</b> )	695	C <sub>43</sub> H <sub>53</sub> NO <sub>7</sub>	–10.5°		<i>Nodulisporium sp.</i>	N	Insecticidal	(91)
Nodulisporic acid A <sub>2</sub> ( <b>102</b> )	713	C <sub>43</sub> H <sub>55</sub> NO <sub>8</sub>	–21°		<i>Nodulisporium sp.</i>	N	Insecticidal	(91)
Nodulisporic acid B ( <b>103</b> )	665	C <sub>43</sub> H <sub>55</sub> NO <sub>5</sub>	–40°		<i>Nodulisporium sp.</i>	N	Insecticidal	(92)
Nodulisporic acid B <sub>1</sub> ( <b>107</b> )	681	C <sub>43</sub> H <sub>55</sub> NO <sub>6</sub>	–36°		<i>Nodulisporium sp.</i>	N	Insecticidal	(92)
Nodulisporic acid B <sub>2</sub> ( <b>108</b> )	699	C <sub>43</sub> H <sub>57</sub> NO <sub>7</sub>	–30°		<i>Nodulisporium sp.</i>	N	Insecticidal	(92)
Nodulisporic acid C ( <b>109</b> )	667	C <sub>43</sub> H <sub>57</sub> NO <sub>5</sub>	–42.5°		<i>Nodulisporium sp.</i>	N	Insecticidal	(93)
Nodulisporic acid C <sub>1</sub> ( <b>111</b> )	683	C <sub>43</sub> H <sub>57</sub> NO <sub>6</sub>	–30°		<i>Nodulisporium sp.</i>	N	Insecticidal	(93)
Nodulisporic acid C <sub>2</sub> ( <b>112</b> )	701	C <sub>43</sub> H <sub>59</sub> NO <sub>7</sub>	–42.5°		<i>Nodulisporium sp.</i>	N	Insecticidal	(93)

<sup>a</sup>N = No; Y = Yes; NR = specific tremorgenic experimental data has not been reported.

TABLE II.

$^1\text{H}$  and  $^{13}\text{C}$  NMR Spectral Assignments of Paspaline (**8**) in  $\text{CDCl}_3$  and Paxilline (**13**) in  $\text{DMSO}-d_6+\text{CDCl}_3$  (1:2).

#	Paspaline <sup>a</sup>		Paxilline <sup>b</sup>	
	$\delta_{\text{C}}$	$\delta_{\text{H}}$ , m, $J$ (Hz)	$\delta_{\text{C}}$	$\delta_{\text{H}}$ , m, $J$ (Hz)
2	150.9		152.6	
3	53.0		50.4	
4	40.1		42.6	
5	34.0	1.96, 1.63	26.4	$\alpha$ : 2.55, $\beta$ : 1.81
6	24.7	1.72, 1.82	28.5	$\alpha$ : 2.26, $\beta$ : 1.80
7	85.8	3.04	71.7	4.87
9	84.8	3.23	83.0	3.69
10	22.0	1.45, 1.66	198.8	
11	37.7	1.14, 1.85	119.3	5.80
12	36.6	–	169.6	
13	46.5	1.50, m	75.9	
14	22.0	1.46, m 1.69, m	32.9 20.9	$\alpha$ : 1.72, $\beta$ : 1.87
15	25.3	1.61, m 1.79, m		$\alpha$ : 2.02, $\beta$ : 1.69
16	48.8	2.76, m	49.5	2.78
17	27.6	2.34, dd, $J=13.0$ , 10.4 2.68, dd, $J=13.0$ , 6.4	27.0	$\alpha$ : 2.37, $\beta$ : 2.64
18	118.3	–	115.3	
19	125.2	–	124.6	
20	118.4	7.43, m	117.7	7.29
21	119.6	7.08, m	118.5	6.93
22	120.5	7.08, m	118.8	6.91
23	111.5	7.30, m	111.8	7.28
24	140.0	–	139.9	
25	14.6	1.03, s	16.2	1.29, s
26	20.0	1.14, s	18.9	0.96, s
27	72.0	–	72.6	
28	23.8	1.19, s	24.7	1.22, s
29	26.1	1.21, s	26.3	1.24, s
30	12.7	0.88, s	–	

<sup>a</sup>Taken from Munday-Finch *et al.* (10)

<sup>b</sup>Taken from Miles *et al.* (16)

carbon ( $\delta_{\text{C}}$  76.0), thus the hydroxy group was placed at C-13 (17). The structure was confirmed by single crystal X-ray crystallographic analysis. The absolute stereochemistry of paspaline was determined by biosynthetic conversion of paspaline to paspalinine (17).

Cole *et al.* reported in 1977 that paspalinine (**10**) was one of three components responsible for the neurological disorder called Dalhsggrass poisoning or “paspalum staggers”, a syndrome found in animals, which graze on fungal-infected *Paspalum* sp. in Georgia and Louisiana. Paspalinine was also isolated from the aflatoxin-producing fungus, *A. flavus* Link Fr (18) and from *Eupenicillium shearii* (19). A LC analysis method, including traces of UV and mass spectra, was reported for this and related alkaloids (15).

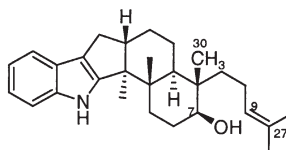
Paspalinine caused tremors in mice at 80 and 160 mg/kg when dosed IP and the clinical effect was indistinguishable from that of paxilline (**13**) (*vide infra*) (4,8). It was even more tremorgenic to sheep and caused tremors at 1 mg/kg iv (4). Paspalinine (**10**) was tremorgenic to one-day-old chickens at 25 mg/kg ( $ED_{50} < 25$  mg/kg) (18).

#### 4. Paspaline B (**11**)

Munday-Finch reported (10) the isolation of paspaline B (**11**) from *P. paxilli* in 1996 along with paspaline, and 13-desoxypaxilline (**20**) (*vide infra*) from the mother liquor of paxilline (*vide infra*) crystallization. It had a molecular weight of 435 and molecular formula  $C_{28}H_{37}NO_3$ . A comparison of the  $^1H$  NMR spectra of paspaline B (**11**) and paspaline (**8**), suggested that the C-30 methyl group ( $\delta_C$  12.7) of paspaline (**11**) was substituted with an aldehyde ( $\delta_C$  207.3) moiety. This substitution was supported by the reciprocal nOe between the aldehyde H-30 and H<sub>3</sub>-26 ( $\delta_H$  0.94) and an aldehyde substitution-induced downfield shift of C-12 ( $\delta_C$  50.7 versus  $\delta_C$  36.6 in paspaline) (10). The proposed structure of paspaline (**11**) was fully established as paspalin-30-al by 2D NMR. No specific biological activity has been reported for this alkaloid.

#### 5. Emindole SB (**12**)

Emindole SB (**12**) was isolated (9) from *E. striata* as a congener of paspaline (**8**), and 13-desoxopaxilline (**20**) (*vide infra*). A molecular weight of 405 and molecular formula of  $C_{28}H_{39}NO$  was determined by mass spectral analysis. The difference between the structures of emindole SB (**12**) and paspaline (**8**) lies in the right hand side of the molecule. The 8,9-ether bond of the tetrahydropyran ring of paspaline (**8**) is opened in emindole SB (**12**) and an olefin is present at  $\Delta^{9,27}$ . The structure was elucidated by the comparison of the NMR spectra of the respective alkaloids (9,20). The isolation of emindole SB was also reported (11) from *A. yamanashiensis* as a congener of terpendoles (*vide infra*). Emindole SB is the simplest member of the family and is a likely biosynthetic precursor of paspaline and other advanced alkaloids. No biological activity has been reported for this alkaloid.



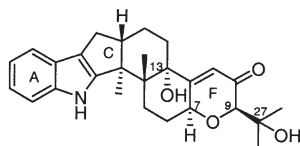
**12** Emindole SB

### 6. Paxilline (13)

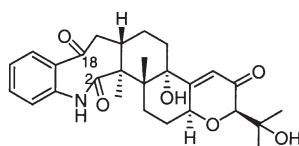
Paxilline (13) is a tremorogenic metabolite originally produced by a strain of *P. paxilli* isolated from insect-damaged pecans (21). Paxilline was isolated from the chloroform extract of the fungus by silica gel chromatography, and the purification was followed by measurement of tremorogenic activity by oral dosing of the fractions to one-day old Dekalb cockerels. It produced plates from acetone and showed a melting point of 252 °C. It showed a characteristic indole diterpene UV spectrum (230 and 281 nm), displayed a molecular ion at  $m/z$  435 and molecular formula of  $C_{27}H_{33}NO_4$ . The structure and relative stereochemistry of paxilline (13) were elucidated by single crystal X-ray analysis by Springer *et al.* (22). They reported the CD spectral data and showed that paxilline exhibited two positive ( $\lambda_{max}$  335 and 330 nm) and a third shorter band negative Cotton effects. The  $^1H$  and  $^{13}C$  NMR assignments (Table II) of this alkaloid were reported by Nozawa *et al.* (9,20). However, the complete 2D NMR based assignment was reported by Miles *et al.* (16). The major structural difference between paspalicine (9) and paxilline (13) is the presence of the hydroxy group at C-13 and absence of the dioxane ring.

Paxilline was subsequently isolated from many fungal sources, including *E. shearii* (19), and *Acremonium lolii* (23), Nozawa *et al.* (24) studied the distribution of paxilline in 19 species of *Emericella* and found that it was produced by three species, namely *Emericella desertorum* (25), *E. foveolata*, and *E. striata* (24,26). Paxilline was detected in the endophytic fungus *Acantherum inebrians* by ELISA and HPLC assays (27). Paxilline was also detected in the extracts of other indigenous Australian grazing grasses, such as *Echinopogon* sp. infected by *Neotyphodium* sp., by ELISA detection (28). Several HPLC procedures have been reported for the analysis and isolation of this class of indole diterpenoids, including paxilline, paspaline, paspalicine, and paspalinine (15).

Paxilline (13) has been reported to cause strong tremors in mice at 25 mg/kg, which are sustained for several hours. Unlike many nonindole diterpenoid tremorgens, paxilline is less toxic with a  $LD_{50}$  of 150 mg/kg (4,21).



13 Paxilline

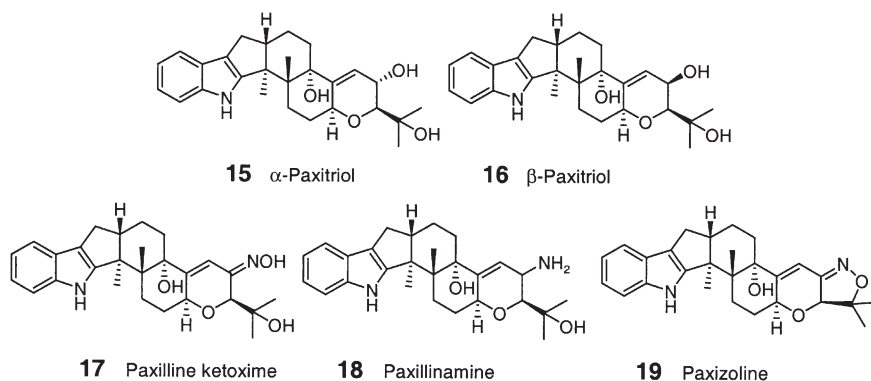


14 Dioxoindole-paxilline

Incubation of paxilline (13) in bile from pasture fed sheep efficiently produced the indole oxidation product 2,18-dioxo-2,18-seco-paxilline (14). Active enzyme is not required for this oxidation as there was no effect on the reaction using boiled bile. Ozonolysis of paxilline mimicked the biotransformation reaction and small amounts of dioxoindole paxilline were produced when a methanolic solution of paxilline was stirred in air (19). The oxidized product was nontremorogenic in mice at 40 mg/kg ip, thus this route may be used by animals

as a potential detoxification mechanism (29). It is proposed that the increased polarity of the oxidized product may increase its xenobiotic elimination.

Several semisynthetic paxilline derivatives have been made as follows. Reduction of paxilline (13) with  $\text{NaBH}_4$  produced two epimeric alcohols (15 and 16) in a ratio of 1:5.5 as a result of 1,2-reduction of the C-10 ketone. These alkaloids were named  $\alpha$ - and  $\beta$ -paxitriol. These alkaloids have not been reported as natural products and did not cause tremors (16). In addition, paxilline was reacted with hydroxylamine to give ketoxime (17, 60%), which, on reduction with  $\text{NaBH}_4$ , produced paxillinamine (18). Treatment of paxilline ketoxime (17) with diphenyl disulfide and tributyl phosphine afforded paxizoline (19) in 75% yield (30).



Paxilline binds with high affinity to maxi-K channels and enhances charybdotoxin binding to Maxi-K channels in vascular smooth muscle and blocks these channels in electrophysiological experiments (30). These data indicate that the paxilline binding site is distinct from the charybdotoxin binding site and is located at an external entrance of the pore of the channel, which is important for channel gating. This is distinct from the paxilline-binding site, which is blocked by elevated levels of calcium (31). Paxilline potently inhibited the large conductance, calcium-activated potassium outward currents sensitive to iberiotoxin by a single site interaction ( $K_i = 35.7$  nM) in rat mesenteric arterial cells (32). In another study, paxilline increased the spontaneous contractility of guinea pig and rat urinary bladders, as well as rat duodenum, and induced tension in guinea pig trachea as a result of blockade of large-conductance, calcium-activated potassium ( $\text{BK}_{\text{Ca}}$ ) channels (33). Paxilline is also a reversible antagonist of the cerebellar inositol 1,4,5-triphosphate ( $\text{InsP}_3$ ) receptor (34). See paspalitrem C in the aflatremes section for further discussion of the biological activity of paxilline and its derivatives.

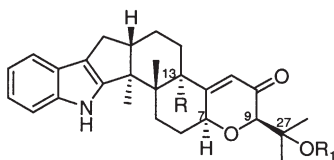
### 7. 13-Desoxypaxilline (20)

In a targeted search for indole diterpenoids Nozawa *et al.* (9,20) reported 13-desoxypaxilline 20 (a.k.a. dehydroxypaxilline) from extracts of *E. striata* as a

minor congener of paxilline in 1988. It lacked one oxygen atom compared to paxilline and showed a molecular formula of  $C_{27}H_{33}NO_3$  (MW 419). Comparison of the  $^{13}C$  NMR spectral data of this alkaloid with paxilline revealed the absence of the oxygenated quaternary carbon signal at  $\delta_C$  76.78 and the presence of a methine at  $\delta_C$  42.69 with appropriate changes in the chemical shifts of the surrounding carbons, thus confirming the absence of the C-13 hydroxy group. This alkaloid was reported from *E. shearii* (19), *P. paxilli* (10), and *N. lolii* (12). No biological activity was reported.

#### 8. 27-O-Acetylpaxilline (Original Name 1'-O-Acetylpaxilline, **21**)

This alkaloid was isolated from *E. striata* together with paxilline (**13**) (20,24). It showed a molecular formula of  $C_{29}H_{35}NO_5$  (MW 477), indicating that it was the acetylated version of paxilline. The acetyl group was placed on the paxilline C-27 hydroxy group on the basis of the downfield shift ( $\Delta\delta_H$  0.23) of the C-29 and C-30 methyl groups, as compared to paxilline. Acetylation of paxilline produced acetylpaxilline **21**, which was identical to the isolated material, thus confirming the structure and stereochemistry of natural 27-O-acetylpaxilline (**21**). The tremorogenic activity of acetylpaxilline was as strong as paxilline, showing sustained tremors in mice at 3.125 mg/kg (24).

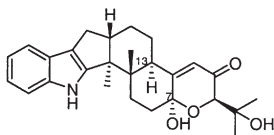


**20** 13-Desoxypaxilline (R = R<sub>1</sub> = H)

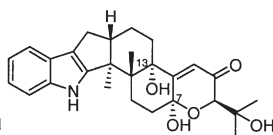
**21** 27-O-Acetylpaxilline (R = OH, R<sub>1</sub> = Ac)

#### 9. 7 $\alpha$ -Hydroxy-13-Desoxy-Paxilline (**22**)

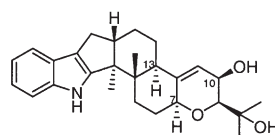
This alkaloid was originally isolated by Mantle *et al.* (35) from *P. paxilli*, and subsequently reported from ascostromata of *E. shearii* (19). It showed a molecular formula  $C_{27}H_{33}NO_4$  that is isomeric to paxilline (**13**). The NMR spectra of **22** easily distinguished it from paxilline by the absence of the C-7 oxymethine and the oxygenated quaternary carbon at C-13, and the presence of a bis-oxy quaternary carbon ( $\delta_C$  93.7), which was easily assigned to C-7, and a methine ( $\delta_C$  41.9) assigned to C-13. No biological data was reported for this alkaloid.



**22** 7 $\alpha$ -Hydroxy-13-desoxypaxilline



**23** 7 $\alpha$ -Hydroxypaxilline



**24** 10 $\beta$ -Hydroxy-13-desoxypaxilline



### 10. 7 $\alpha$ -Hydroxypaxilline (**23**)

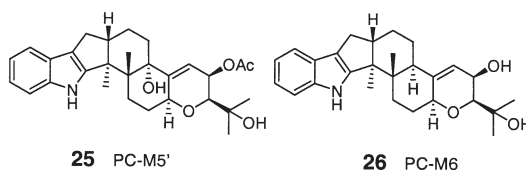
This alkaloid was isolated (35) from *P. paxilli* and was detected in *A. lolii*. It showed a molecular formula of C<sub>27</sub>H<sub>33</sub>NO<sub>5</sub> indicating the presence of an extra oxygen atom when compared to paxilline (**13**). The structure was assigned as 7 $\alpha$ -hydroxypaxilline based on the absence of the H-7 signal in the <sup>1</sup>H NMR spectrum (recorded in DMSO-*d*<sub>6</sub>); the observation of an additional OH singlet ( $\delta_{\text{H}}$  3.62); and the small chemical shift differences observed for some of the methyl groups, particularly H<sub>3</sub>-25 ( $\Delta\delta_{\text{H}}$  0.24). Unfortunately, no <sup>13</sup>C NMR data were reported which would have enabled the unambiguous assignment of the substitution pattern at C-7. The stereochemistry of the hydroxy group was assumed to be  $\alpha$ , based on the argument that enzymatic transformations of this type proceed with retention of configuration (35). Alkaloid **23** did not show any sign of tremor at 4 mg/kg in mice, while in a parallel experiment, paxilline produced significant tremors, indicating that oxidation at C-7 is detrimental for tremorgenic activity (35).

### 11. 10 $\beta$ -Hydroxy-13-Desoxypaxilline (**24**)

This metabolite was isolated from *P. paxilli* as a congener of 7 $\alpha$ -hydroxypaxilline (**23**) and 7 $\alpha$ -hydroxy-13-desoxypaxilline (**22**), and exhibited a molecular formula of C<sub>27</sub>H<sub>33</sub>NO<sub>3</sub> (35). The presence of **24** was also detected in extracts of *A. lolii*. The <sup>1</sup>H NMR spectrum of **24** in DMSO-*d*<sub>6</sub> lacked the C-13 hydroxyl singlet observed in paxilline and showed an additional downfield doublet at  $\delta_{\text{H}}$  4.80 ( $J=6.3$  Hz) and a doublet of triplets at  $\delta_{\text{H}}$  4.05 ( $J=2.5, 6.3$  Hz). These latter signals were assigned to the OH at C-10 and H-10 $\alpha$  by <sup>1</sup>H-<sup>1</sup>H COSY. Reduction of the C-10 ketone of **13** to a  $\beta$ -paxitriol (**16**) resulted in the loss of W-coupling between H-7 $\alpha$  and H-9 $\alpha$ , similar to what is observed in PC-M6 (**26**) (*vide infra*) (35). No tremorgenic activity data was reported for this alkaloid.

### 12. PC-M5' (**25**)

PC-M5' (**25**) was isolated from *Penicillium crustosum*, a fungus known to contaminate cream cheese, walnuts, and hamburger meat, and to cause tremorgenic intoxication in dogs and other animals in California and Australia (36). The tremor-causing metabolites have been identified as the penitrems (*vide infra*). During the course of mycotoxicological investigation of *P. crustosum* isolated from retail cocoa and bread at the Shinagawa Ward Institute of Public Health Research, Tokyo, the alkaloids PC-M5' (**25**) and PC-M6 (**26**) (*vide infra*) were isolated as congeners of the penitrems. PC-M5' produced a molecular formula of C<sub>29</sub>H<sub>37</sub>NO<sub>5</sub> (MW 479). It showed <sup>1</sup>H and <sup>13</sup>C NMR spectra characteristic for paxilline (**13**), except for the absence of the <sup>13</sup>C NMR signal for the C-10 keto group and the presence of an acetylated oxygen-bearing methine ( $\delta_{\text{C}}$  66.0) assigned to C-10 (36). The structure and stereochemistry of PC-M5' (**25**) was confirmed by comparison with the major NaBH<sub>4</sub> reduction product of paxilline, followed by acetylation. No biological activity was reported for this alkaloid.

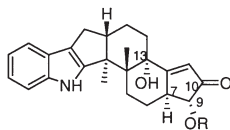


### 13. PC-M6 (**26**)

PC-M6 (**26**) was isolated (**36**) from *P. crustosum* as a congener of PC-M5' and the penitremes. It gave a molecular formula of  $C_{27}H_{35}NO_3$  (MW 421) which was 14 amu less than paxilline. Like PC-M5', the signal for the C-10 keto group was absent in the  $^{13}C$  NMR spectrum of PC-M6 (**26**) and was replaced by an oxymethine carbon. Unlike PC-M5', the  $^{13}C$  NMR spectrum of **26** lacked the signal corresponding to the oxygenated C-13 of paxilline ( $\delta_C$  77.5), displaying instead a methine ( $\delta_C$  40.5). The  $^1H$  NMR of **26** also showed small couplings ( $J=1.8$  Hz) between H-9 and H-10, as observed for PC-M5', thus confirming the  $\beta$ -configuration of the hydroxy group at C-10. Based on these data, PC-M6 was assigned as 10-dihydro-13-dehydroxy-paxilline (**26**) (**36**). No biological activity was reported for this alkaloid.

### 14. Paxinorol (**27**)

Miles *et al.* (**37**) reported the isolation of paxinorol (**27**) from the fermentation broth of *P. paxilli* Bainier as a trace component. They successfully employed TLC-based ELISAGram to aid in the isolation of this minor component. Paxinorol (**27**) showed a molecular formula of  $C_{24}H_{27}NO_3$  (MW 377). The mass spectrum produced a prominent ion at  $m/z$  182, characteristic of the unsubstituted, intact A-C ring of paxilline (**13**). The NMR spectrum of paxinorol lacked signals for the gem-dimethyl groups observed in paxilline (C-28 and C-29), and showed several differences for the signals corresponding to C-7 to C-13. In particular, the  $^{13}C$  NMR signals of the C-10 keto group and C-12 were significantly downfield shifted to  $\delta_C$  206.9 and  $\delta_C$  183.4, respectively. This indicated a substantial structural change in the F ring. In addition, the  $^{13}C$  NMR spectrum indicated that C-7 was no longer connected to an oxygen atom ( $\delta_H$  46.6,  $\delta_H$  3.73) and was coupled to an oxymethine ( $\delta_C$  80.9,  $\delta_H$  4.30). Therefore, based on these arguments, and by comparison of the  $^{13}C$  NMR shifts of model alkaloids, and measurements of  $^1J_{CH}$  coupling constants, structure **27** was assigned for paxinorol. The stereochemistry of paxinorol was firmly established by measurements of nOe's after irradiations of H-9, H-7, H-6 $\alpha$ , and H-6 $\beta$ . Standard acetylation of paxinorol yielded the C-9 monoacetate (**28**). Biological activity of paxinorol was not reported.



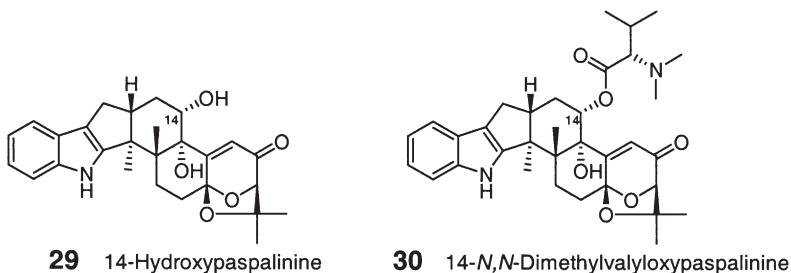
**27** Paxinorol (R = H)  
**28** Paxinorol-9-acetate (R = Ac)

15. 14-Hydroxypaspalinine (**29**)

14-Hydroxypaspalinine (**29**) is among the first reported alkaloids of the paspalane class to be oxygenated in the D-ring. It was isolated from the sclerotia of *Aspergillus nomius* by Gloer's group at the University of Iowa (**38**) by a bioassay-guided isolation using corn earworm, *Helicoverpa zea*. It possessed a molecular formula of  $C_{27}H_{31}NO_5$  (MW 449),  $[\alpha]_D = +126^\circ$ , indicating that it contained an extra oxygen atom compared to paspalinine. The extra oxygen was unambiguously placed at C-14 by HMBC correlation of the new methine proton ( $\delta_H$  4.25) to C-12, C-13, C-15, and C-16. Scalar couplings and NOESY correlations established the stereochemistry of the new chiral center. For example, the methine proton (H-14) showed NOESY cross peaks with H-16 and H<sub>3</sub>-26, thus establishing their 1,3,5-triaxial relation. No tremorgenic activity was reported for this alkaloid.

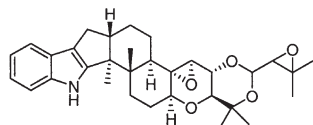
16. 14-(*N,N*-Dimethyl-L-Valyloxy)-Paspalinine (**30**)

Gloer's group isolated this C-14 ester as a congener of 14-hydroxypaspalinine (**38**). It showed a molecular formula of  $C_{34}H_{44}N_2O_6$  (MW 577) and  $[\alpha]_D = +102^\circ$ . The difference in molecular formulae of the two alkaloids suggested the presence of a dimethyl valine group, which was elucidated by NMR analysis and confirmed by hydrolysis that led to the isolation of *N,N*-dimethyl-L-valine. Esterification of the C-14 hydroxy group with dimethyl valine was unequivocally confirmed by the downfield shift of H-14 ( $\delta_H$  4.25–5.36), and requisite HMBC correlations of H-14, including correlation to the ester carbonyl (C-1') of valine. Both C-14 oxygenated alkaloids (**29** and **30**) gave virtually identical activity against larvae of *H. zea* and resulted in 91% and 88% weight gain reduction at 100 ppm when these alkaloids were fed to *H. zea* with a standard pinto bean diet. Paspalinine (**10**) showed no anti-insectan activity under the same assay conditions. No other biological activity was reported for this alkaloid.

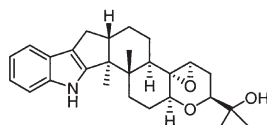
17. Terpendoles (**31–42**)

These alkaloids are a class of indole diterpenoids of the paspalane subfamily that contain either an 11,12-epoxide group or a C-11 hydroxy group. Twelve of the thirteen members (A–L) of the terpendoles were isolated from the soil fungus *A. yamanashiensis* by Omura's group (**11,39,40**). The last member, terpendole M

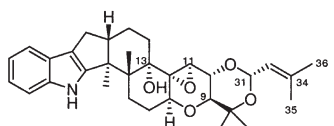
(42), was isolated by the Miles group (12) from *L.perenne* infected with *N. lolii*. Because of prenyl substitution in the aromatic ring, terpendole L has been grouped with the aflatremanes and is discussed later. These alkaloids were isolated by bioassay-guided fractionation using an acyl-CoA cholesteryl transferase (ACAT) inhibition assay. The ratio of these alkaloids in *A. yamanashiensis* was determined to be as follows: A (0.20), B (0.97), C (1.18), D (0.22), E (0.26), F (0.24), G (0.14), H (0.04), I (0.26), J (0.19), K (0.11), and L (0.14), respectively (40). Representative  $^1\text{H}$  and  $^{13}\text{C}$  NMR spectral data of terpendole C, E, and L are presented in Table III.



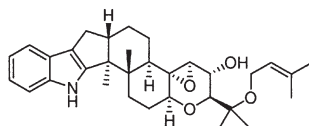
31 Terpendole A



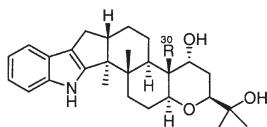
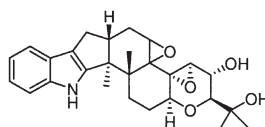
32 Terpendole B



33 Terpendole C



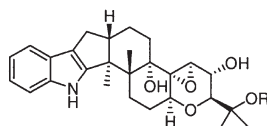
34 Terpendole D

35 R = CH<sub>3</sub> (Terpendole E)

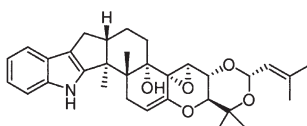
38 Terpendole H

36 R = CH<sub>2</sub>OH (Terpendole F)

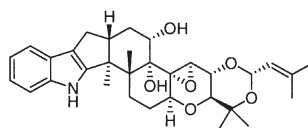
37 R = CHO (Terpendole G)



39 Terpendole I (R = H)



41 Terpendole K

40 Terpendole J (R = CH<sub>2</sub>CHC(CH<sub>3</sub>)<sub>2</sub>)

42 Terpendole M

TABLE III.  
<sup>1</sup>H and <sup>13</sup>C NMR spectral assignments of terpendoles C (33), E (35) and L (53) in  
DMSO-*d*<sub>6</sub>.

#	Terpendole C <sup>a</sup>		Terpendole E <sup>b</sup>		Terpendole L <sup>b</sup>	
	δ <sub>C</sub>	δ <sub>H</sub> , m, <i>J</i> (Hz)	δ <sub>C</sub>	δ <sub>H</sub> , m, <i>J</i> (Hz)	δ <sub>C</sub>	δ <sub>H</sub> , m, <i>J</i> (Hz)
1-NH		10.69, s		10.54, s		10.64, s
2	152.7		151.3		152.0	
3	50.2		52.7		49.9	
4	42.2		40.1		42.2	
5	25.6	2.41, m; 1.69, m	32.1	1.86, m; 1.69, m	25.5	2.42, m
6	28.5	2.14, m; 1.64, m	25.0	1.67, m	28.4	1.63, m; 2.14, m
7	70.7	4.26, brt, <i>J</i> =9.0	76.9	3.48, dd, <i>J</i> =11.0, 4.0	70.7	4.26, t, <i>J</i> =9.0
9	71.1	3.39, d, <i>J</i> =9.5	78.9	3.42, dd, <i>J</i> =12.0, 2.5	71.1	3.40, d, <i>J</i> =9.0
10	70.2	4.05, brd, <i>J</i> =9.5	29.3	1.45, dt, <i>J</i> =14.0, 2.5; 1.78, dd, <i>J</i> =14.0, 6.0	70.1	4.06, d, <i>J</i> =9.0
11	59.0	3.51, s	68.4	3.59, brd, <i>J</i> =3.0	58.9	3.51, s
12	67.1		39.2		67.0	
13	76.5		37.0	2.13, dd, <i>J</i> =12.5, 2.0	76.5	
14	28.4	1.53, m; 1.47, m	21.0	1.62, m; 1.23, m	28.6	1.46–1.50, m
15	20.5	1.79, m; 1.47, m	24.3	1.57, m	20.4	1.48, m; 1.78, m
16	49.6	2.68, m	48.6	2.63, m	49.7	2.69, brs
17	26.9	2.26, dd, <i>J</i> =13.0, 10.8; 2.56, dd, <i>J</i> =13.0, 6.2	27.1	2.22, dd, <i>J</i> =13.0, 2.0; 2.54, dd, <i>J</i> =13.0, 6.0	28.5	2.42, m; 2.70, m
18	114.9		115.7		114.4	
19	124.5		124.4		123.9	
20	117.6	7.24, m	117.5	7.24, m	131.4	
21	118.4	6.87, m	118.3	6.87, td, <i>J</i> =7.0, 1.5	117.6	6.64, d, <i>J</i> =7.0
22	119.2	6.91, m	119.2	6.91, td, <i>J</i> =7.0, 1.5	119.5	6.81, dd, <i>J</i> =8.0, 7.0
23	111.8	7.24, m	111.8	7.25, m	109.6	7.06, d, <i>J</i> =8.0
24	139.8		140.2		139.8	
25	16.1	1.17, s	14.5	0.95, s	16.0	1.16, s

(continued)

TABLE III.  
Continued.

#	Terpendole C <sup>a</sup>		Terpendole E <sup>b</sup>		Terpendole L <sup>b</sup>	
	$\delta_C$	$\delta_H$ , m, $J$ (Hz)	$\delta_C$	$\delta_H$ , m, $J$ (Hz)	$\delta_C$	$\delta_H$ , m, $J$ (Hz)
26	18.0	1.02, s	19.4	1.03, s	18.0	1.03, s
27	74.1		70.3		74.1	
28	16.7	1.22, s	24.8	1.02, s	16.7	1.22, s
29	28.3	1.12, s	26.7	1.06, s	28.3	1.13, s
30			13.1	0.77, s		
31	92.0	5.51, d, $J=6.5$			92.0	5.51, d, $J=6.5$
33	122.5	5.09, brd, $J=6.5$			122.5	5.10, dt, $J=6.5, 1.0$
34	137.5				137.4	
35	18.4	1.63, d, $J=1.2$			25.0	1.65, d, $J=1.0$
36	25.1	1.65, d, $J=1.2$			18.3	1.64, d, $J=1.0$
37					31.6	3.46, d, $J=7.0$
38					124.0	5.30, dt, $J=7.0, 1.5$
39					130.6	
40					17.7	1.69, d, $J=0.5$
41					25.5	1.66, d, $J=0.5$

<sup>a</sup>Taken from Huang *et al.* (39).<sup>b</sup>Taken from Tomoda *et al.* (40).

### 18. Terpendole A (31)

Terpendole A (**31**) exhibited a MF of C<sub>32</sub>H<sub>41</sub>NO<sub>6</sub> (MW 536) and  $[\alpha]_D = +11.6^\circ$ . The molecular formula indicated that it had the same hydrogen count as terpendole C (**33**), and possessed an extra oxygen atom. The <sup>1</sup>H NMR spectral comparison of terpendoles C and A indicated that terpendole A lacked the olefinic methyl groups H<sub>3</sub>-35 and H<sub>3</sub>-36 ( $\delta_H$  1.63 and 1.65) and the olefinic methine (H-33,  $\delta_H$  5.09) observed in terpendole C, and contained instead a shielded methyl pair ( $\delta_H$  1.22, 1.29) and an oxymethine ( $\delta_C$  64.7,  $\delta_H$  2.79). These signals were assigned to the C-35 and C-36 methyl groups and the oxymethine at C-33, respectively. This led to the placement of an epoxide group at C-33, C-34 that was confirmed by HMBC correlations (39). The stereochemistry of terpendole A (**31**) was reported later based on the analogy with other terpendoles (40).

### 19. Terpendole B (32)

Terpendole B possessed a molecular formula of C<sub>27</sub>H<sub>35</sub>NO<sub>3</sub>, a molecular weight of 421, and an optical rotation of  $[\alpha]_D = -3.6^\circ$ . The NMR spectra of terpendole B (in comparison with C) lacked the signals for the prenyl group (C-31–C-36) and the C-10 oxymethine was replaced with a methylene ( $\delta_C$  27.7,  $\delta_H$  1.76, 2.07). These assignments were corroborated by COSY correlations among

H-9 ( $\delta_{\text{H}}$  3.53), H<sub>2</sub>-10 ( $\delta_{\text{H}}$  1.96, 2.07), and H-11 ( $\delta_{\text{H}}$  3.46) and confirmed by requisite HMBC correlations (39). This is the simplest member of the terpendole family. Like terpendole A, the stereochemistry of this alkaloid was also reported based on the analogy with other terpendoles (40).

#### 20. Terpendole C (33)

Terpendole C had a molecular formula of C<sub>32</sub>H<sub>41</sub>NO<sub>5</sub>, (MW = 519),  $[\alpha]_{\text{D}} = -2.3^\circ$ , and showed a characteristic indole UV spectrum ( $\lambda_{\text{max}}$  225, 275 nm). The structure was thoroughly elucidated by extensive 2D NMR (COSY, HMQC, HMBC, and NOESY) experiments and complete NMR assignments (Table III) have been reported (39). Terpendole C (33) possessed an additional isoprene unit, the tail of which was part of a new 1,3-dioxane ring fused with tetrahydropyran ring F as deduced by HMBC correlations of H-31 to C-27 and C-10. The nOe's of H-31 with H-10; H<sub>3</sub>-29 with H-9; H-9 with H-7; and H-11 with H-14 $\alpha$ , established the stereochemistry of the new stereocenters of terpendole C. The nOe's of the remainder of the molecule verified the stereochemistry of the remaining stereocenters to be that found in all paspalanes. Terpendole C was subsequently reisolated from the ryegrass *L.perenne* infected with the endophytic fungus *N. lolii* (12). Terpendole C caused more intense tremors than paxilline in mice at 8 mg/kg when administered ip (41).

#### 21. Terpendole D (34)

Terpendole D (34) showed a molecular formula of C<sub>32</sub>H<sub>43</sub>NO<sub>4</sub> (MW 505) indicating that it was the dihydro derivative of terpendole C (33) and lacked one oxygen atom. Analysis of the NMR spectra indicated the absence of the hydroxy group at C-13, leading to a methine ( $\delta_{\text{C}}$  40.6,  $\delta_{\text{H}}$  2.13, coupled with H-14) and the appearance of an oxymethylene ( $\delta_{\text{C}}$  58.0,  $\delta_{\text{H}}$  3.96) at the expense of the C-31 hemiketal carbon, thus establishing the structure of terpendole D (34), which was confirmed by X-ray crystallographic analysis (39).

#### 22. Terpendole E (35)

Terpendole E (35) showed a molecular formula of C<sub>28</sub>H<sub>39</sub>NO<sub>3</sub> (MW 437) and  $[\alpha]_{\text{D}} = -36.4^\circ$ . The comparison of the spectral data (Table III) of 35 and other terpendoles, particularly of terpendole B (32) indicated that the 11,12-epoxide group of 35 was replaced with an angular methyl ( $\delta_{\text{C}}$  13.1) at C-12 ( $\delta_{\text{C}}$  39.2) and a hydroxy at C-11 ( $\delta_{\text{C}}$  68.4). This was verified by HMBC correlations. In addition, it lacked the hydroxy group at C-13 ( $\delta_{\text{C}}$  37.0,  $\delta_{\text{H}}$  21.3) as in terpendole D (34). The structure of 35 was also confirmed by X-ray crystallography (40).

#### 23. Terpendole F (36)

Terpendole F displayed a molecular formula of C<sub>28</sub>H<sub>39</sub>NO<sub>4</sub> (MW 453) and  $[\alpha]_{\text{D}} = -35.8^\circ$ . This alkaloid differs from terpendole E (35) by an additional oxygen atom, which was present as a hydroxymethyl ( $\delta_{\text{C}}$  59.8,  $\delta_{\text{H}}$  3.72, 3.90) group located

at C-12, and was confirmed by HMBC correlations of the hydroxymethyl protons to C-11, C-12, and C-13. The stereochemistry was similar to other terpendoles (40).

#### 24. Terpendole G (37)

A molecular formula  $C_{28}H_{37}NO_4$  (MW 451) and  $[\alpha]_D = -28.0^\circ$  was determined for terpendole G (37). The NMR spectrum showed the presence of an aldehyde group ( $\delta_C$  208.0,  $\delta_H$  10.1) and an absence of the hydroxymethyl group of terpendole F. The HMBC correlations of the aldehyde proton to C-12 and the correlation of H-7 ( $\delta_H$  3.64) to the aldehyde carbonyl confirmed the location of the aldehyde group at C-12 (40). The stereochemistry was found to be identical to terpendoles D and E.

#### 25. Terpendole H (38)

It produced a molecular formula of  $C_{27}H_{33}NO_5$  (MW 451) and  $[\alpha]_D = -47^\circ$ . The comparison of the NMR spectra of terpendoles H (38) with those of B (32) and C (33), indicated that it possessed the C-11, C-12 epoxide group like terpendole C (33) and lacked the prenyl group like terpendole B (32). In addition, it showed the presence of two shielded oxygenated carbons including a methine, which was assigned to a second epoxide group placed at C-13, C-14 and confirmed by HMBC correlations of H<sub>2</sub>-15 with C-13 ( $\delta_C$  67.1) and C-14 ( $\delta_C$  54.9,  $\delta_H$  3.22) (40). The stereochemistry was identical to terpendole C.

#### 26. Terpendole I (39)

Terpendole I (39) showed a molecular formula  $C_{27}H_{35}NO_5$  (MW 453) and  $[\alpha]_D = +7^\circ$ . The formula of this alkaloid differs from terpendole H (38) by two extra hydrogen atoms. The  $^{13}C$  NMR spectrum indicated the absence of the signals for the 13,14-epoxide carbons of terpendole H and showed the presence of a quaternary oxygenated carbon at  $\delta_C$  78.7 which was assigned to C-13, consistent with other C-13 hydroxylated terpendoles such as C (40). The stereochemistry of terpendole I was similar to terpendoles D and E.

#### 27. Terpendole J (40)

A molecular formula of  $C_{32}H_{43}NO_5$  (MW 421) and optical rotation of  $[\alpha]_D = -30.3^\circ$  was determined for terpendole J (40). The molecular formula of this alkaloid indicated that it contained an isopentenyl group, which was corroborated by the NMR spectra. The structures of terpendoles I (39) and J (40) differed by the presence and the absence of the isopentenyl group that was placed at the C-27 oxygen in the form of an ether bridge, as in terpendole D, and was confirmed by the HMBC correlations of H<sub>2</sub>-31 ( $\delta_H$  3.96) with C-27 ( $\delta_C$  79.1) (40).

#### 28. Terpendole K (41)

This isolate showed a molecular formula of  $C_{32}H_{39}NO_5$  (MW 419) and  $[\alpha]_D = +21.8^\circ$ . The formula of this alkaloid has two hydrogen atoms less than that



of terpendole C (**33**). The NMR spectral comparison of the two alkaloids indicated that the signals for the C-7 oxymethine and the C-6 methylene were replaced by a trisubstituted olefin ( $\delta_C$  145.0 and  $\delta_C$  105.4,  $\delta_H$  5.25). The assignment was confirmed by HMBC correlations of H<sub>2</sub>-5 to C-6 and C-7 (**40**). The stereochemistry was similar to terpendole C.

### 29. *Terpendole M* (**42**)

The discovery of this alkaloid was reported by the Miles group (**12**) as a very minor congener of lolitrem B, together with minor, but significantly higher amounts of paspaline (**8**) and 13-desoxypaxilline (**20**) from the ryegrass *L. perenne* infected with the endophytic fungus *N. lolii*. Terpendole M is produced presumably by the fungus. The molecular formula of C<sub>32</sub>H<sub>41</sub>NO<sub>6</sub> and molecular weight 535 as determined by mass spectrometry indicated that it had an extra oxygen atom compared to terpendole C (**33**), also isolated from this ryegrass. This oxygen was placed at C-14 by HMBC correlations of H-15 ( $\delta_H$  1.89) to two oxygenated carbons i.e., C-13 ( $\delta_C$  77.3), and C-14 ( $\delta_C$  70.5), and two nonoxygenated carbons i.e., C-3 ( $\delta_C$  50.7), and C-16 ( $\delta_C$  46.0). The stereochemistry at this new center was established by ROESY correlations of the H<sub>3</sub>-26 methyl group to H-14, thus proving the equatorial ( $\alpha$ ) orientation of the hydroxy group at C-14, as seen in 14-hydroxypaspalinine (**29**).

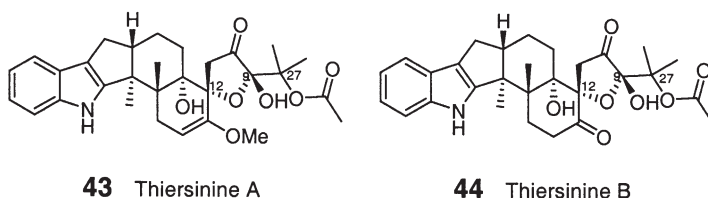
### 30. *Biological Activity of the Terpendoles*

Terpendoles inhibited ACAT activity in a dose dependent manner and showed the following IC<sub>50</sub> values: A (15.1  $\mu$ M), B (26.8  $\mu$ M), C (2.1  $\mu$ M), D (3.2  $\mu$ M), E (288  $\mu$ M), F (221  $\mu$ M), G (388  $\mu$ M), H (230  $\mu$ M), I (145  $\mu$ M), J (38.8  $\mu$ M), K (38  $\mu$ M), and L (32.4  $\mu$ M). The most potent of the terpendoles is C followed by D, A, and B. The activity of the other terpendoles are significantly weaker. The presence of an additional prenyl group at the C-27 oxygen appears to be important for the activity. Terpendole C (**33**) produced tremors at 8 mg/kg in mice and was faster acting, but of shorter duration, than paxilline (**41**). The tremorgenic activity of terpendole M (**42**) was significantly reduced compared to terpendole C (**33**), as measured in a standard mouse assay. This is a clear indication that in contrast to the C-13 hydroxy group that appears to be critical (e.g., paspaline (**10**) vs. paspalicine (**9**) for tremorgenic activity, a hydroxy group at C-14 causes diminution of such activity, even in the presence of C-13 hydroxy group. Molecular modeling indicates that a potential H-bond between the C-13 and C-14 hydroxy groups may occur, however whether or not that plays a role in the reduction of the tremorgenic activity is not clear (**12**). The tremorgenicity of other terpendoles is unknown.

### 31. *Thiersinines A* (**43**) and *B* (**44**)

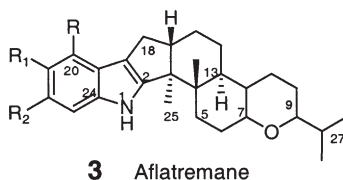
Thiersinines A (C<sub>30</sub>H<sub>37</sub>NO<sub>7</sub>, MW 523) and B (C<sub>29</sub>H<sub>35</sub>NO<sub>7</sub>, MW 509) were isolated from cultured *Penicillium thiersii* following anti-insectan bioassay by Gloer

and coworkers (42). The EI mass spectrum produced a characteristic paspalane fragment ion at  $m/z$  182 due to the cleavage of C3–C4 and C14–C15. They elucidated the structure of these alkaloids by extensive application of 2D NMR (600 MHz) techniques and showed that these alkaloids contain a novel (for this class) C-12 spiro tetrahydrofuran ring with an acetylated C-27 hydroxy group. Structurally, the two alkaloids differ by having either a C-7 ketone (thiersinine B) or enolic methyl ether at C-7 (thiersinine A). These alkaloids exhibited equal anti-insectan activity and displayed 83% and 84% reduction in growth rate of the agriculturally important armyworm *Spodoptera frugiperda* at 100 ppm (42). No tremorgenic activity was reported.



## B. AFLATREMANES

The aflatremanes are a group of indole diterpenoids that contain one or more acyclic isoprene substitutions on the indole ring and are represented by  $\alpha$ - (3a),  $\beta$ - (3b) and  $\gamma$ - (3c) aflatremanes due to substitution at C-20, C-21, and C-22, respectively.



- 3a**  $\alpha$  ( $R = C_5H_9$ ,  $R_1 = R_2 = H$ )  $\alpha$ -aflatremane  
**3b**  $\beta$  ( $R_1 = C_5H_9$ ,  $R = R_2 = H$ )  $\beta$ -aflatremane  
**3c**  $\gamma$  ( $R_2 = C_5H_9$ ,  $R = R_1 = H$ )  $\gamma$ -aflatremane

### 1. Aflatrem (45)

Aflatrem, a toxin that is produced by several sclerotia-forming strains of *A. flavus*, a common fungus that grows on various foodstuffs. It was originally discovered in 1964 by Wilson and Wilson, who recovered the organism from moistened cracked corn, which caused tremors and convulsions to animals feeding on infected corn (43). It produced tremors and convulsions to mice at 0.5–1.0 mg, resulting in death at higher doses. Mass spectral analysis revealed a molecular formula of  $C_{32}H_{39}NO_4$ , and, like most of the indole diterpenoids, it showed UV

absorption bands at 231, 282, and 292 nm. In addition, it also showed strong absorption at 250 nm, indicative of an  $\alpha,\beta$ -unsaturated ketone, as seen in paspalinine (**10**). Clardy and coworkers (44,45) elucidated the structure of this isolate in 1978–1980 by comparison of mass spectral and NMR data with paspalinine (**10**). The  $^{13}\text{C}$  NMR spectra of aflatrem (**45**) and paspalinine (**10**) were identical, except for the presence of five additional carbons and a  $\sim 20$  ppm downfield shift of one of the aromatic carbons. The  $^1\text{H}$  NMR spectrum indicated that one of the four available positions of the aromatic ring of the aflatrem indole was substituted, as only three aromatic protons, each with *ortho*-couplings, were observed. The five new carbons were assigned to an  $\alpha,\alpha$ -dimethylallyl group by  $^1\text{H}$  and  $^{13}\text{C}$  NMR spectral data and were attached to the downfield-shifted aromatic carbon (C-20) by reasoning of the shielding effects on the  $^1\text{H}$  and  $^{13}\text{C}$  NMR chemical shifts of the aromatic ring.

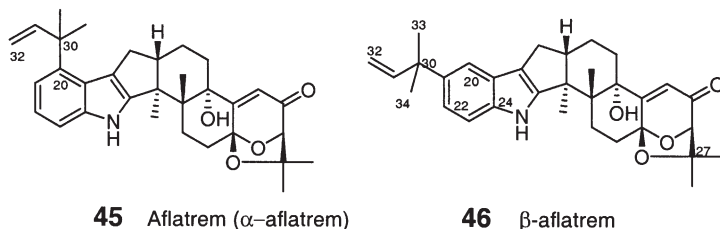
Aflatrem (**45**) appears to be the first reported example of the tremorgenic indole diterpenoids. However, its structure elucidation was hampered at the time due to a significantly major focus on the highly hepatotoxic and carcinogenic toxin, aflatoxin, which is also produced by *A. flavus* and *A. parasiticus*. Hence, although aflatrem was discovered in 1964, its structure was not reported until 1978, and only after the structures of the paspaline class were elucidated (45). This is first example of the  $\alpha$ -aflatremene class and should be renamed as  $\alpha$ -aflatrem.

Wicklow and Cole reported (46) that aflatrem was produced by sclerotia of *A. flavus* and not by mycelia. It was subsequently reported from other isolates of *A. flavus* (14,30).

Aflatrem exhibited tremors in mice in a dose-dependent manner when tested ip at 0.5, 1.0, 2.0, and 4.0 mg/kg. It gave a sharp tremor with maximal response at 30 min post injection, with subsequent sharp fall off with barely detectable effect after 24 h. After one week post injection, the behavior of all murine subjects were normal, including feeding behavior (4,47).

In a study with isolated hippocampal nerve terminals, Valdes *et al.* (48) reported that aflatrem caused a decrease in the capacity of the GABA and glutamate uptake systems, which were interpreted as a loss of nerve terminals. The study also showed that aflatrem caused a decrease in the release of these transmitters and induced degeneration of neuronal processes in hippocampal neurotransmitter systems. Therefore, it was suggested that aflatrem represented a long-term health hazard (48). Aflatrem allosterically potentiates the GABA<sub>A</sub> induced chloride channel expressed in *Xenopus oocytes* at  $< 5 \mu\text{M}$ , and the site of its action on this channel is different from that of the benzodiazepines, pentobarbital, and picrotoxin (49). At  $10 \mu\text{M}$ , it has no significant effect on the co-expressed voltage-dependent sodium, calcium, and kainate channels. The potentiating effect of aflatrem on the GABA<sub>A</sub> channel does not directly explain its tremorgenic effect on animals (49). However, in a separate report Gant *et al.* reported (50) that

aflatrem inhibited GABA-induced chloride influx in rat brain, thus putting these two findings at odds with each other. It is fair to mention that the concentrations used in both studies were different, and some of the experiments could not be repeated in the later (49) studies due to the poor solubility of aflatrem. Aflatrem and paspalinine (10) were tremorgenic to one-day old chickens at 25 mg/kg ( $ED_{50} < 25$  mg/kg) (18).



## 2. $\beta$ -Aflatrem (46)

An alkaloid isomeric ( $C_{32}H_{39}NO_4$ ) to aflatrem was isolated (14) as a major congener of aflatrem from the sclerotia of *A. flavus*. The structure of  $\beta$ -aflatrem differs from aflatrem in the location of the  $\alpha,\alpha$ -dimethylallyl chain, which was placed at C-21 by selective INEPT NMR experiments in which irradiation of the aromatic proton doublet ( $\delta_H$  7.43,  $J=1.5$  Hz) resulted in strong polarization transfer to C-18 and C-30. The full NMR assignments are listed in Table IV.  $\beta$ -Aflatrem (46) is the first member of the  $\beta$ -aflatremane family.

Minor amounts of  $\beta$ -aflatrem (46) were also detected in both aflatoxin containing and nonaflatoxin containing strains of *A. parasiticus* and a strain of *A. sublivaceus*.

$\beta$ -Aflatrem (46) exhibited significant activity against *H. zea* causing a 57% reduction in weight gain relative to controls when fed at 100 ppm mixed with a standard diet. No specific tremorgenic activity was reported.

## 3. Paspalitrem A (47)

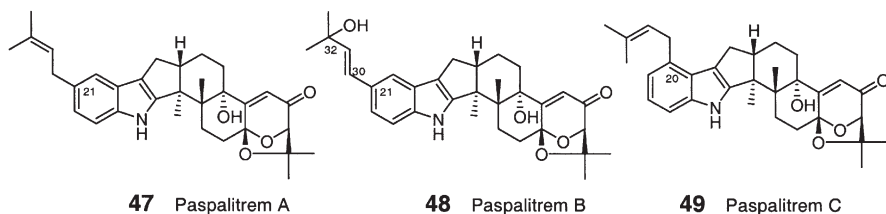
Paspalitrem A (47),  $C_{32}H_{39}NO_4$ , a member of a  $\beta$ -aflatremane group, was isolated from the sclerotia of *C. paspali* collected from the cattle grazing grass *Paspalum dilatatum*, along with paspalitrem B (*vide infra*) (8). It was reported that paspalitremes A and C (*vide infra*) could not be resolved by TLC, but were easily separated by reversed phase HPLC. The UV and most of the  $^1H$  and  $^{13}C$  NMR spectra of this alkaloid were similar to paspalinine. The structural difference of the two alkaloids was attributed to the presence of an additional isoprene (3-methyl-2-butenyl) unit which was attached to C-21 on the basis of comparison between the observed and calculated  $^{13}C$  NMR shifts of the aromatic carbons. It was

TABLE IV.  
 $^1\text{H}$  and  $^{13}\text{C}$  NMR Spectral Assignments of  $\beta$ -aflatrem (**46**)<sup>a</sup> in  $\text{CDCl}_3$ .

#	$\delta_{\text{C}}$	$\delta_{\text{H}}$ , m, $J$ (Hz)
1-NH		7.73, s
2	152.5	
3	51.5	
4	39.9	
5	26.9	2.26, m; 2.69, m
6	21.1	1.75, m; 1.82, m
7	104.4	
9	88.0	4.32, s
10	197.3	
11	117.6	5.86, s
12	169.8	
13	77.6	
14	28.3	2.73, m; 2.83, m
15	33.8	1.97, m; 1.92, m
16	48.6	2.83, m
17	27.6	2.45, dd, $J = 12.5, 10.3$ 2.73, m
18	117.2	
19	124.9	
20	115.3	7.43, d, $J = 1.5$
21	140.1	
22	119.5	7.13, dd, $J = 8.8, 1.5$
23	111.0	7.27, d, $J = 8.8$
24	138.1	
25	23.5	1.19, s
26	16.3	1.23, s
27	78.7	
28	23.1	1.14, s
29	28.8	1.42, s
30	41.1	
31	149.0	6.12, dd, $J = 17.3, 10.5$
32	109.9	5.05, brd, $J = 10.5$ 5.09, brd, $J = 17.3$
33	28.8	1.48, brs
34	28.8	1.48, brs

<sup>a</sup>Taken from TePaske *et al.* (14).

reisolated from *Phomopsis* sp. (30,51). Paspalitrem A caused tremors at < 14 mg/kg ip in mice (4)



#### 4. Paspalitrem B (48)

Paspalitrem B (48),  $C_{32}H_{39}NO_5$ , also a member of a  $\beta$ -aflatremene group, was isolated as a congener of paspalitrem A (8). The molecular formula of 48 indicated that it had an extra oxygen atom compared to paspalitrem A, the location of which was deduced to be at the terminal carbon of the isoprene unit by  $^{13}C$  NMR ( $\delta_{C32}$  71.2). The UV spectrum of paspalitrem B (48) showed a bathochromic shift of the indole absorption bands ( $\lambda_{max}$  305, 336 nm) indicating an extended conjugation of the indole ring with the side chain in the form of a *trans*-olefin. Both paspalitrem A (47) and B (48) were isolated along with paspalinine. Like paspalitrem A, it exhibited tremors at < 14 mg/kg ip in mice (4).

#### 5. Paspalitrem C (49)

Paspalitrem C (49),  $C_{32}H_{39}NO_4$ , a member of an  $\alpha$ -aflatremene group, was isolated from sclerotia of *P. paspali* by Dorner *et al.* in 1984 as a congener of paspaline, paspalinine, paspalicine, and paspalitrem A (52). The structure of paspalitrem C was elucidated by comparison of its  $^{13}C$  NMR spectrum with the corresponding spectrum of the isomeric alkaloids paspalitrem A and aflatrem. The  $^1H$  NMR spectrum of paspalitrem C (49) showed the presence of the 3-methyl-2-butenyl group like paspalitrem A (47). Unlike paspalitrem A, the  $^1H$  NMR spectrum of paspalitrem C showed the presence of three contiguous aromatic protons, each showing *ortho* couplings ( $J=7.3$  Hz) as seen in aflatrem. Therefore, the isoprene unit was connected to C-20 in paspalitrem C (52). It is noteworthy that the sclerotia of *P. paspali* perform normal isoprenylation of both the C-20 (e.g., paspalitrem C), and C-21 (e.g., paspalitrem A) positions of the indole ring, whereas the sclerotia of *A. flavus* perform the reversed isoprenylation of C-20 (e.g., aflatrem) and C-21 (e.g.,  $\beta$ -aflatrem). Paspalitrem C (49) was reisolated from *Phomopsis* sp. (30,51).

Aflatrem (45), paspalitrem A (47), paspalitrem C (49), and paspalinine (10) inhibited the binding of [ $I^{125}$ ] charybdotoxin (ChTX) to large-conductance,  $Ca^{2+}$ -activated  $K^+$  (maxi-K) channels in bovine aortic smooth muscle sarcolemmal membranes (30). In contrast, paxilline and paspalicine (9) enhanced toxin binding. The binding activity ( $K_{1/2}$ ) of these alkaloids was in the range of 100–1700 nM.

Despite these differences in binding, these alkaloids (both inhibitors and stimulators) potently inhibited the maxi-K channels in electrophysiological measurements, thus indicating allosteric effects on ChTX binding. Chemical modification of paxilline led to a defined SAR. Reduction of the C-10 keto group to the epimeric alcohols **15** and **16** rendered these alkaloids inactive at 100  $\mu\text{M}$ . Likewise, C-10 amino **18** and oxime **17** derivatives were also inactive. Paxizoline (**19**) exhibited biphasic activity, but demonstrated identical activity as paxilline (**13**) in the ChTX binding assay. These studies indicated a preference for the enone type of arrangement around C-10 for activity. These indole diterpenes are among the most potent nonpeptide inhibitors of maxi-K channels, and some of their physiological activities could be explained by the inhibition of maxi-K channels. However, since both tremorgenic (e.g., paspalinine, **10**) and nontremorgenic (e.g., paspalicine **9**) alkaloids exhibit no difference in their ability to block maxi-K channels, tremorgenicity is probably not related to the channel blocking activity (**30**). Paspalitre C was suggested to be tremorgenic based on its structural similarity with related alkaloids, but no experimental tremorgenic data has been reported (**52**).

#### 6. Sulpinine A (**50**)

Sulpinine A (**50**),  $\text{C}_{32}\text{H}_{41}\text{NO}_4$ , a member of the  $\gamma$ -aflatremene group, was isolated from *A. sulphureus* through bioassay-guided purification following anti-insectan activity against the agriculturally important lepidopteran *H. zea* (**53**). The structure was thoroughly elucidated by NMR spectral studies. Sulpinine A exhibited a slow decomposition in  $\text{CDCl}_3$ , which hampered initial structure elucidation. The diterpene portion of the molecule is similar to penitrem B (*vide infra*), a congener, as evidenced by the identical  $^1\text{H}$  and  $^{13}\text{C}$  NMR spectra of the two alkaloids. Like penitrem B, it showed the presence of long-range coupling between H-7 and H-11 and a lack of vicinal coupling between H-9 and H-10 (**53**). The  $^1\text{H}$  NMR spectrum of sulpinine A indicated the presence of an  $\alpha,\alpha$ -dimethylallyl group like aflatrem, and the aromatic portion of the spectrum showed the presence of three aromatic signals [ $(\delta_{\text{H}} 7.20, \text{d}, J = 8.3 \text{ Hz}, \text{H-20})$ ,  $(\delta_{\text{H}} 6.95, \text{dd}, J = 8.3, 1.7 \text{ Hz}, \text{H-21})$ , and  $(\delta_{\text{H}} 7.28, \text{d}, J = 1.3 \text{ Hz}, \text{H-23})$ ], two with *ortho* couplings ( $J = 8.3 \text{ Hz}$ ) and one with *meta* coupling ( $J = 1.3 \text{ Hz}$ ) indicating substitution at either C-21 or C-22. A selective INEPT experiment (H-20 to C-18, C-19, C-22 and C-24; H-23 to C-21, C-22, C-24, C-19, and C-30) confirmed the location of the reversed isoprene unit at C-22. The stereochemistry was deduced by comparison of the reported stereochemistry of penitrem B and was substantiated by NOESY data (**53**). The EIMS spectrum of sulpinine A exhibited a base peak at  $m/z$  250 due to simultaneous cleavage of the C3–C4 and C14–C15 bonds, a characteristic phenomenon observed in other aflatrems with similar substitutions.

Sulpinine A showed potent activity against *H. zea* showing a 96% reduction in weight gain at 100 ppm relative to control, with 10% mortality (**53**). It was not evaluated for its tremorgenic activity.

### 7. Sulpinine B (51)

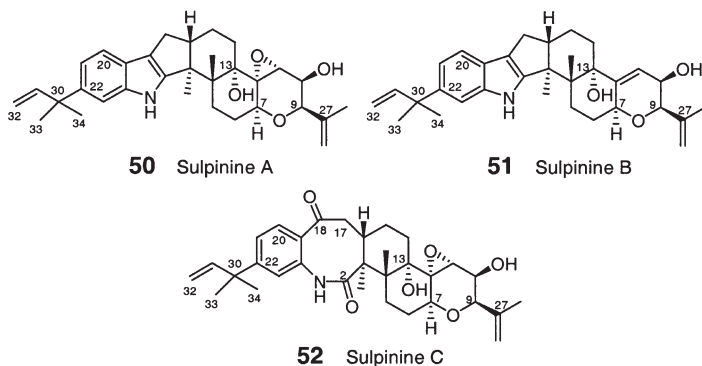
Sulpinine B (**51**), also a  $\gamma$ -aflatremene, was isolated from *A. sulphureus* as a congener of sulpinine A (**50**) by bioassay-guided purification following anti-insectan activity against the agriculturally important lepidopteran *H. zea* (**53**). A comparison of the molecular formulae of the two alkaloids (sulpinine B =  $C_{32}H_{41}NO_3$ ) indicated a difference of only an oxygen atom, which was attributed to the lack of an epoxide ring in sulpinine B, resulting in a  $\Delta^{10}$ -olefin. The EIMS spectrum of sulpinine B showed a base peak at  $m/z$  250 like sulpinine A (**50**), indicating that the difference between the two alkaloids resided in the right hand portion. The NMR spectra of sulpinines A (**50**) and B (**51**) were similar with the following exceptions: the signal for H-10 ( $\delta_H$  3.47,  $J = 2$  Hz) of sulpinine A was shifted downfield to  $\delta_H$  5.82 (brd,  $J = 4.7$  Hz), with a corresponding downfield shift observed in the  $^{13}C$  NMR spectrum of sulpinine B (**51**). Structurally, the sulpinines differ from afatrem and the paspalitrems in the position of the substitution of the prenyl group on the aromatic ring, and the lack of an oxygen atom at C-27.

Sulpinine B (**51**) displayed similar activity to sulpinine A (**50**), showing 87% reduction in weight gain at 100 ppm for *H. zea* (**53**). It was not evaluated for its tremorogenic activity.

### 8. Sulpinine C (52)

This biological oxidation product of sulpinine A (**50**) displayed a molecular formula of  $C_{32}H_{41}NO_6$  indicating a higher level of oxygenation (**53**). The EIMS spectrum of sulpinine C did not exhibit the ion at  $m/z$  250, indicating that the additional two oxygen atoms were present in the left side of the molecule. The  $^{13}C$  NMR spectrum of sulpinine C showed the presence of two carbonyl groups ( $\delta_C$  176.6 and 202.4) indicative of an oxidized indole ring like that in paxilline and other indole diterpenoids.

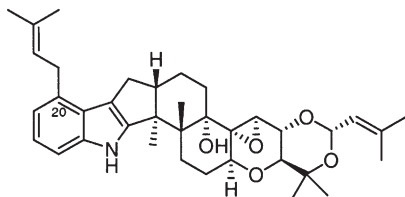
Sulpinine C (**52**) is significantly less active than the other two sulpinines in corresponding anti-insectan assays. It was not evaluated for its tremorogenic activity.





9. *Terpendole L (53)*

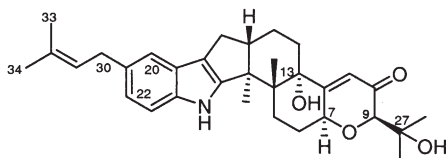
Terpendole L was isolated from *A. yamanashiensis* with the other terpendoles (*vide supra*) (40). Terpendole L (53) is an  $\alpha$ -aflatremene, displaying a molecular formula of  $C_{37}H_{49}NO_5$  (MW 587) and an optical rotation of  $[\alpha]_D = +16.5^\circ$ . The formula of terpendole L differs from that of terpendole C (33) by an extra isopentenyl group as confirmed by COSY, and was placed at the  $\alpha$ -position (C-20) by HMBC correlations of the methylene protons ( $\delta_H$  3.46) of the isopentenyl group to C-19, C-20, and C-21 (see Table III for NMR assignments). It was not evaluated for its tremorgenic activity.



**53** Terpendole L

10. *21-Isopentenylpaxilline (54)*

21-Isopentenylpaxilline (54) is a  $\beta$ -aflatremene and was isolated from ascostromata of *E. shearii* as a congener of the shearinines (*vide infra*) and paxilline (13) (19). The mass spectral data led to a molecular formula of  $C_{32}H_{41}NO_4$  for this alkaloid, indicating that it was related to paxilline (13), and contained an extra isoprene unit, which was placed at C-21 by expected HMBC correlations from H-20 to the isoprene carbons, and the isoprene  $CH_2$  to the aromatic carbons C-20, C-21, and C-22 (19). It was not evaluated for its tremorgenic activity.

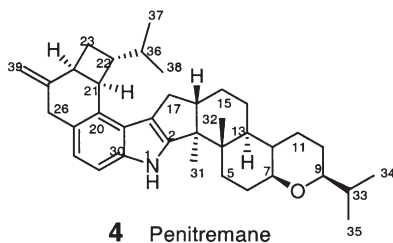


**54** 21-Isopentenylpaxilline

## C. PENITREMANES

The penitremenes are a group of indole diterpenoids that have two *ortho* positions of the phenyl ring substituted with two isoprenes that are cyclized in fused cyclohexyl-cyclobutyl rings and differ by chlorine, hydroxy, and epoxide substituents. The early work of penitremes A–F has been reviewed previously, and this review included details of the structure elucidation (2). The atom

numbering of the penitremes has been modified for this review to make it consistent with the other indole diterpenoids, which are discussed here.



### 1. Penitrem A (55)

The first member of decacyclic indole diterpenoids, penitrem A (MF  $C_{37}H_{44}NO_6Cl$ ) was initially isolated in 1968 by Wilson *et al.* (54) from *Penicillium cyclopium* growing on feedstuff, which subsequently caused outbreaks of disease among farm animals. This class of alkaloids was originally called “tremortins”, but was later renamed to penitremes. Penitrem A was subsequently isolated in 1971 by Hou *et al.* (55) from *Penicillium palitans*, together with two new alkaloids, penitrem B ( $C_{37}H_{45}NO_5$ ), and penitrem C (no formula given). In a study of the production of penitremes, Pitt (56) concluded that all of the fungal isolates which produced penitremes belong to the soil borne fungus *P. crustosum*. The structural studies of these alkaloids were hampered due to extreme acid sensitivities, compound availability and molecular complexity, and were not resolved until 1981 when Steyn and his group (57) reisolated penitremes A–F and the first structural information was reported.

Penitrem A (55), the major metabolite, was isolated by prep TLC along with other penitremes (57,58). It displayed an UV spectrum ( $\lambda_{max}$  233 and 295 nm) that is characteristic of the indole diterpenoids. It differs from other indole diterpenoids such as paspaline (8) by virtue of possessing two extra isoprenes, which are cyclized to form a cyclohexyl–cyclobutyl bicycle, and are fused at C-20 and C-21 (C-27 in penitrem numbering) of the indole phenyl ring. In addition, C-17 and C-36 are connected via an oxygen atom to form an eight-membered ring. Like sulpinine A, the hydroxy group classically present in most of these alkaloids at C-33 is dehydrated to form a  $\Delta^{33,35}$ -olefin and the classically present  $\Delta^{11,12}$ -olefin is oxidized to form an epoxide. The  $^1H$  NMR analysis indicated the presence of only one of the aromatic protons, suggesting that three positions of the indole ring were substituted. The  $^1H$  and  $^{13}C$  NMR spectrum of penitrem A indicated the presence of two vinyl groups, one olefinic methyl, and two extra angular methyls when compared with paspaline (8), with additional signals accounting for the presence of two isoprene residues attached to the indole aromatic ring. The final structure was elucidated by extensive application of

the NMR techniques available at the time including  $^1\text{H}$ - $^1\text{H}$  decoupling, nuclear Overhauser enhancements, deuterium-induced shift measurements, proton-noise-decoupled, single frequency off-resonance proton-decoupled, selective proton-decoupled  $^{13}\text{C}$  NMR spectra, and selective population inversion (SPI) experiments (58). The structural assignments were supported through biosynthetic studies by feeding  $^{13}\text{C}$ -labeled acetate and mevalonate, with subsequent analysis of the resulting  $^{13}\text{C}$  NMR spectra (57-59). The NMR assignment and thorough discussion of structure elucidation has been detailed. The NMR assignments have been excerpted and are presented in Table V. The relative stereochemistry of penitrem A (55), including eastern and western hemispheres, was elucidated by application of scalar couplings and nOe measurements. De Jesus and coworkers used Horeau's esterification method (60) by applying 'partial resolution' to deduce the absolute stereochemistry. In this method, penitrem A (55) was reacted with racemic  $\alpha$ -phenylbutyric acid to yield 10-*O*- $\alpha$ -phenylbutyrate penitrem A and recovered  $\alpha$ -phenylbutyric acid that had  $[\alpha]_{\text{D}} = -7.5^\circ$ , indicating an *S*-configuration at C-10 of penitrem A (58). Acetylation of penitrem A produced 25-*O*-acetylpenitrem A (56) and hydrogenation over  $\text{PtO}_2$  gave tetrahydropenitrem A (57) (58).

Penitrem A (55) elicited sustained tremors, discoordination, and convulsions in laboratory and farm animals. In 1980, Norris *et al.* (61) directly measured the release of the amino acid neurotransmitter from rat synaptosomes and reported that penitrem A (55) affected the presynaptic transmission in central synapses by excessive release of transmitter amino acids e.g., glutamic, aspartic, and  $\gamma$ -aminobutyric acids, but without impairing neurotransmitter synthesis (61). Penitrem A inhibited binding of charybdotoxin to maxi-K channels in bovine aortic smooth muscle sarcolemmal membrane (30). In order to clarify the neurotoxic effect of penitrem A, in 1998, Cavanagh *et al.* studied the pathological effect of penitrem A on the rat brain and reported that it caused a three- to four-fold increase in cerebellar cortical blood flow. It caused mitochondrial swelling in cerebellar stellate and basket cells within 30 min of administration, which persisted for more than 12 h without causing cell death. It also caused a massive degeneration of Purkinje cells, which was both time and dose dependent. Despite the morphological changes and degeneration of these cells, the effect of the drug disappeared over time and the animal behavior became almost normal within a week. Penitrem A did not show any observable morphological changes to other parts of the brain (62). A similar result of dose-dependent injuries in the cerebellum with massive degeneration of Purkinje cells was simultaneously reported by Breton *et al.* (63) though the precise mechanism of these effects is not clear.

Penitrem A caused significant tremors (250-600  $\mu\text{g}/\text{kg}$ , ip in mice, 20  $\mu\text{g}/\text{kg}$ , iv in sheep, 2 mg/kg, po. in sheep) in vertebrates and was highly toxic to mice ( $\text{LD}_{50} = 1.05$  mg/kg ip). Details of the various activities of penitrem A have been reviewed (4). Penitrem A caused significant mortality to *Heliothis zea* (corn

TABLE V.  
 $^1\text{H}$  and  $^{13}\text{C}$  NMR Spectral Assignment of Penitrem A (**55**)<sup>a</sup> in  $\text{CD}_3\text{OD}$ .

#	$\delta_{\text{C}}$	$\delta_{\text{H}}$ , m, $J$ (Hz)
2	154.4	
3	50.1	
4	43.6	
5	26.9	2.61, ddd, $J = 13.4, 13.4, 5.2$ 1.58, ddd, $J = 13.4, 6.0, 2.0$
6	28.9	2.22, dddd, $J = 13.5, 8.0, 5.2, 2.0$ 2.04, dddd, $J = 13.5, 13.4, 10.0, 6.0$
7	72.0	4.29, ddd, $J = 10.0, 8.0, 1.4$
9	74.7	4.04, ddd, $J = 1.5, 1.4, < 1$
10	66.3	4.04, dd, $J = 7.5, 2.6$
11	61.9	3.57, dd, $J = 2.6, 1.4$
12	66.1	
13	78.2	
14	30.6	1.68, ddd, $J = 13.5, 3.3, 2.6$ 1.48, dddd, $J = 13.5, 12.5, 4.3, 2.6$
15	18.6	1.92, dddd, $J = 12.5, 12.5, 13.1, 3.3$ 1.78, dddd, $J = 12.5, 4.3, 2.6, 2.6$
16	58.8	2.63, ddd, $J = 13.1, 8.2, 2.6$
17	72.4	4.93, d, $J = 8.2$
18	120.6	
19	122.0	
20	133.3	
21	81.0	
22	52.7	2.49, ddd, $J = 11.1, 9.3, 1.0$
23	24.7	2.41, dd, $J = 11.1, 9.2$ 2.26, ddd, $J = 11.1, 9.3, 2.6$
24	47.0	2.98, m
25	149.5	
26	35.1	3.63, d, $J = 15.6$ 3.26, dddd, $J = 15.6, 1.6, 1.6, 1.6$
27	125.8	
28	124.6	
29	111.9	7.24, s
30	139.7	
31	21.4	1.40, s
32	19.0	1.22, s
33	143.3	
34	19.7	1.71, ddd, $J = 1.5, < 1, 0.9$
35	111.6	5.07, ddd, $J = 2.6, 1.5, 0.9$ 4.87, ddd, $J = 2.6, 1.5, 1.4$

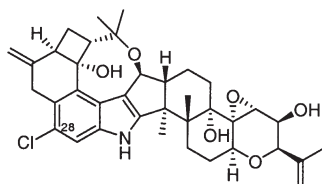
(continued)

TABLE V.  
Continued.

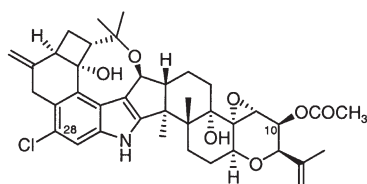
#	$\delta_C$	$\delta_H$ , m, $J$ (Hz)
36	76.1	
37	20.3	1.07, s
38	31.1	1.75, s
39	107.1	5.01, ddd, $J=2.9, 1.6, 1.6$ 4.86, ddd, $J=3.0, 1.6, 1.6$

<sup>a</sup>Taken from DeJesus *et al.* (58).

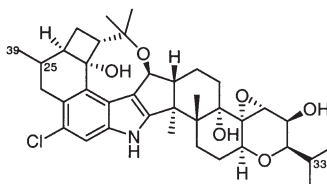
earworm) at 25 ppm. In contrast, while it is toxic to insects such as *H. zea*, it did not show any tremorgenic effect in insects (64).



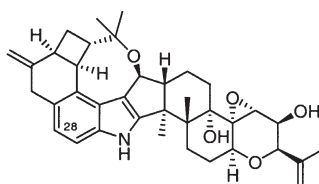
**55** Penitrem A



**56** 10-O-Acetylpenitrem A



**57** 33,35,25,39-Tetrahydropenitrem A



**58** Penitrem B

## 2. Penitrem B (58)

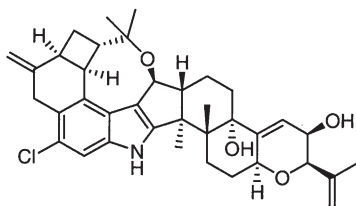
Penitrem B was one of the penitrems isolated in the early 1970s and was reisolated as a congener of other penitrems in 1981 (57,65). It displayed a molecular formula of  $C_{37}H_{45}NO_5$  suggesting that it was a deoxy-deschloro analog of penitrem A (55), which was supported by the presence of a methine ( $\delta$  39.4 vs.  $\delta$  81.0) at C-21 like penitrem F, and two *ortho*-coupled aromatic protons like penitrem E (*vide infra*) (65). A *cis* stereochemistry at C-21 was assigned based on  $^1H$ - $^1H$  coupling constants and the *cis*-stereochemical requirements for a six- and four-membered ring fusion (65).

Penitrem B (58) was reisolated (53) from *Aspergillus sulphureus* as a congener of the sulpinines and exhibited similar anti-insectan activity as was

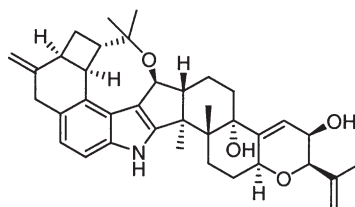
observed for sulpinine B (**51**) and secopenitrem B (*vide infra*) and showed weight reduction of 87.4% of *H. zea* at 100 ppm without any apparent larval mortality (**53**). Penitrem B was less tremorgenic than penitrem A and caused tremors at 5 mg/kg, ip in mice (**4**).

### 3. Penitrem C (**59**)

Penitrem C showed a molecular formula of  $C_{37}H_{44}NO_4Cl$  indicating that it was a dideoxy analog of penitrem A (**55**) or a chloro derivative of penitrem D (*vide infra*) (**60**). The  $^{13}C$  NMR spectrum of penitrem C was identical to the corresponding spectrum of penitrem D (**60**) except for the 5 ppm downfield shift of C-28 ( $\delta_C$  125.3) and other chlorine-induced shifts of the corresponding signals in the vicinity of C-28. The  $^1H$  NMR spectrum of penitrem C (**59**) was similar to penitrem F (*vide infra*) except for the differences caused by substitution of the C9–C10 epoxide with an olefin.



**59** Penitrem C



**60** Penitrem D

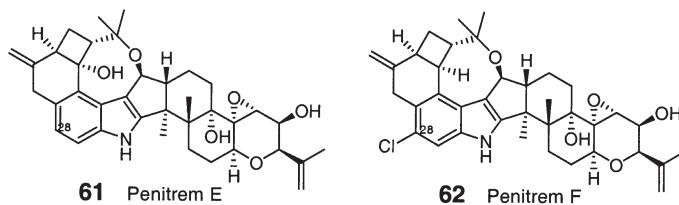
### 4. Penitrem D (**60**)

Penitrem D was also isolated from *P. crustosum* together with other penitrems (**65**), and showed a molecular formula of  $C_{37}H_{45}NO_4$  which suggested that it was a dideoxy-deschloro analog of penitrem A (**55**). Like penitrems B (**58**) and F (**62**), the  $^1H$  NMR spectrum of penitrem D showed an *ortho*-coupled pair of aromatic protons ( $\delta_H$  6.70 and 7.02) and a resonance corresponding to the C-21 methine ( $\delta_H$  3.86). In addition, an olefinic proton doublet of doublets at  $\delta_H$  5.75 ( $J = 5.75, 1.8$  Hz) was present at the expense of the oxymethine proton at C-10 and was supported by the presence of olefinic carbons at  $\delta_C$  119.6 (C-11) and  $\delta_C$  148.4 (C-12) confirming the replacement of epoxide with an olefin. Later, Wilkins *et al.* (**66**) reported the reversal of the  $^{13}C$  NMR signal assignment of C-7 and C-9 of penitrems C (**59**) and D (**60**) based on the 2D NMR of janthitrem B (**72**).

### 5. Penitrem E (**61**)

Penitrem E (**61**) was isolated (**65**) as a congener of penitrem A (**55**), and showed a molecular formula of  $C_{37}H_{44}NO_6$  indicating that it was a C-28 deschloro analog of penitrem A (**55**). This was supported by the presence of two *ortho*-coupled ( $J = 8.3$  Hz) aromatic ( $\delta_H$  6.70 and 7.09) protons in the  $^1H$  NMR spectrum of penitrem E. The remainder of the  $^1H$  NMR spectrum of penitrem E was identical

to penitrem A except for the observation of chlorine-induced shifts. A separation of  $\Delta[\delta_{\text{Ha}}-\delta_{\text{Hb}}]=0.57$  ppm was observed between the two C-26 geminal methylene protons in penitrem A (**55**) while the corresponding separation was  $\Delta=-0.26$  ppm in penitrem E (**61**), indicating strong steric influence exerted by the bulky chlorine atom. The H-9 and H-10 protons of penitrem E (two magnetically equivalent protons in penitrem A) were somewhat resolved and displayed a separation of  $\Delta=0.1$  ppm in the  $^1\text{H}$  NMR spectrum of penitrem E allowing for the measurement of the scalar coupling ( $J=1.5$  Hz) between these two protons (65). Penitrem E caused tremors at 2 mg/kg ip in mice and was more tremorgenic than penitrem B (4)



#### 6. Penitrem F (**62**)

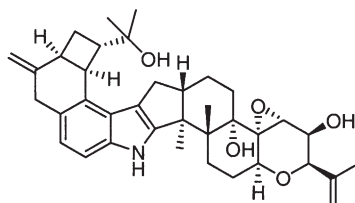
Penitrem F (**62**) was isolated (65) in conjunction with penitrems A–E and exhibited a molecular formula of  $\text{C}_{37}\text{H}_{44}\text{ClNO}_5$ , indicating that it was a deoxy analog of penitrem A. The absence of the oxygenated carbon signal at  $\delta_{\text{C}}$  81.0 and the presence of a methine carbon at  $\delta_{\text{C}}$  39.5 and the corresponding proton at  $\delta_{\text{H}}$  3.87 (a multiplet with couplings to all protons of the cyclobutyl ring) in the  $^{13}\text{C}$  and  $^1\text{H}$  NMR spectra of penitrem F corroborated the replacement of the hydroxy group with a proton at C-21 (65).

Like penitrem B, a *cis* stereochemistry was assigned to C-21. Like penitrem A, the absolute stereochemistry of penitrem D (**60**) was deduced by the partial resolution method developed by Horeau in 1961 (60). Since penitrems A–F all produced similar CD spectra it was concluded that they must have the identical absolute stereochemistry (58).

#### 7. Secopenitrem B (**63**)

Secopenitrem B,  $\text{C}_{37}\text{H}_{47}\text{NO}_5$ , was isolated from *A. sulphureus* as a congener of the sulpinines (**50–52**) and penitrem B (**58**) (53). The formula indicated that it had one degree of unsaturation less than penitrem B. A comparison of the  $^1\text{H}$  and  $^{13}\text{C}$  NMR spectra of secopenitrem B with those of penitrem B and the sulpinines indicated the absence of the C-17 oxygen atom present in penitrem B ( $\delta_{\text{C}}$  72.1), and the presence of a methylene group ( $\delta_{\text{C}}$  29.4,  $\delta_{\text{H}}$  2.99, dd,  $J=13.0, 6.1$ ;  $\delta_{\text{H}}$  2.47, m) as observed in the sulpinines, suggesting a severed ether linkage between C-17 and C-36. The HMBC correlations of H-16 to three methylenes C-17, C-15 and C-14, and one of the methylene protons  $\text{H}_{2-17}$  to C-2 and C-18, confirmed this assignment.

Secopenitrem B (**63**) exhibited similar anti-insectan activity as was observed for sulphinine B and penitrem B and showed weight reduction of 87% of *H. zea* at 100 ppm with 32% larval mortality (53). The tremorgenic activity was not determined.



**63** Secopenitrem B

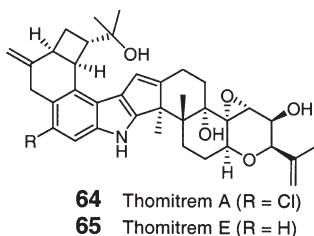
#### 8. Thomitrem A (**64**)

Thomitrem A (**64**),  $C_{37}H_{44}ClNO_6$ , was isolated as a minor component from *P. crustosum* recovered from Norwegian foodstuff and grown on rice (67). It was isolated by reverse phase HPLC from this strain along with the major component, penitrem A (**55**). Thomitrem A was isomeric to penitrem A, however, the mass spectrum of **64** showed fragment ions for a loss of  $[M-18-68]^+$ , as was seen in secopenitrem B (**63**), and was different from penitrem A, which showed fragment ions for  $[M-18-58]^+$ . Comparison of the  $^1H$  NMR spectra of thomitrem A with secopenitrem B and penitrem A indicated a severed ether bond between C-17 and C-36, a lack of the C-17 oxygen atom, and the presence of an olefinic doublet ( $\delta_H$  6.82,  $J=1.8$  Hz) in **64**. The COSY, HSQC, and 1D-SELTCOSY experiments helped to assign the 16,17-olefin, which was confirmed by HMBC correlations of the  $H_{3-31}$  methyl protons to two olefinic (C-2 and C-16) and two aliphatic (C-3 and C-4) carbons. The severed ether linkage caused a significant upfield shift of  $H_{3-38}$  ( $\delta_H$  1.01 or 1.17 vs  $\delta_H$  1.73 of penitrem A). In addition, the presence of the  $\Delta^{16}$ -olefin in **64** caused significant shielding of the C-32 methyl group ( $\delta_H$  0.51 vs  $\delta_H$  1.22 in **55**). These authors performed a detailed conformational analysis of **55** and **64** by NOESY and ChemDraw 3D modeling, and found that despite having identical stereochemistries of the A and B rings, not surprisingly, their conformations were different. The B-ring adopted  $\alpha$ -, and  $\beta$ -half-chair conformations in **64** and **55**, respectively with the C-39 methylene oriented toward the  $\beta$ -face in each case (67). Thus, structure **64** was assigned to thomitrem A, which can be named as 16,17-dehydrosecopenitrem A. No biological activity was reported.

#### 9. Thomitrem E (**65**)

Thomitrem E was isolated as a significantly minor congener of thomitrem A, and showed a molecular formula of  $C_{37}H_{45}NO_6$ . A C-28 deschloro thomitrem A (16,17-dehydrosecopenitrem E) structure was assigned to **65** by NMR spectral comparisons, and named as thomitrem E due to the structural similarity with penitrem E (**61**). No biological activity was reported (67).

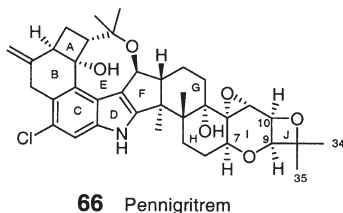




### 10. Pennigritrem (**66**)

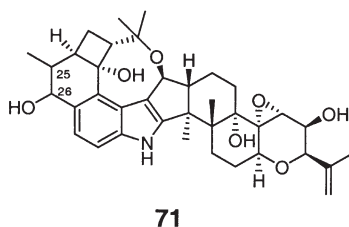
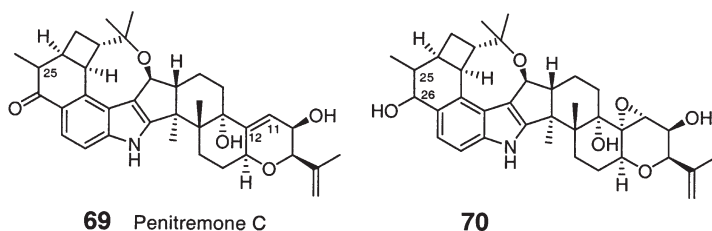
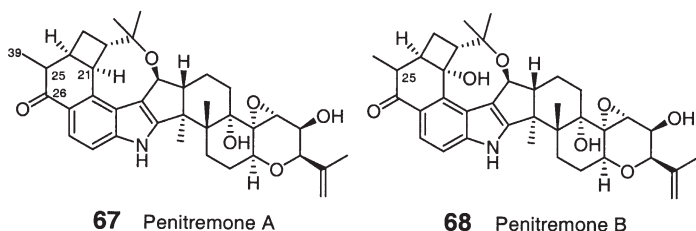
Pennigritrem was isolated (*68*), along with penitrem A, from *Penicillium nigricans* by silica gel chromatography followed by reversed phase HPLC, as a minor component, which eluted between penitrem E (**61**) and A (**55**). It had a molecular formula of  $C_{37}H_{44}NO_6Cl$  indicating that it was isomeric with penitrem A. The  $^1H$  NMR spectra of the two alkaloids were mostly identical, except for the protons in ring I of **66**, where H-9 ( $\delta_H$  3.87, d,  $J = 4.17$  Hz) and H-10 ( $\delta_H$  4.60, dd,  $J = 4.17, 0.75$  Hz) were well resolved from each other with associated  $J$  values of 4.17 Hz. The spectrum of pennigritrem lacked the signals for an isopropenyl group (vinyl and olefinic methyl), and showed the presence of two methyl singlets at  $\delta_H$  1.40 and  $\delta_H$  1.20. In addition, signal splitting of H-7 ( $\delta_H$  3.51) was simplified to a doublet of doublets with  $J$  values of 7.2 and 4.2 Hz compared to a multiplet observed in the  $^1H$  NMR spectrum of most of penitremes. These observations indicated the formation of oxetane ring J, which was corroborated by measurement of various  $J_{CH}$  values and comparison of these values with known rings. It was confirmed by the observation of several nOe effects of H-9 to H-10, and H-10 to H-34 (*68*). These nOe's also established the *cis*-fusion of rings I and J. The oxetane ring J exhibits a new cyclization motif in this series of alkaloids and contrasts with other cyclizations involving C-33 such as paxilline (**13**), paspalinine (C-27 in paspaline numbering), and the lolitrems (*vide infra*). While penitrem A and pennigritrem were produced equally in submerged culture of *P. nigricans*, the latter alkaloid was the principal product of mycelia when grown in stationary conditions using the same media. The isolation of pennigritrem has not been reported from *P. crustosum*, but it is not clear whether the culture was specifically examined for the production of pennigritrem.

Pennigritrem (**66**) was reported to be considerably less active as an acute tremorgen than penitrem A (**55**), and its activity was of the same order as paspalinine. The presence of the oxetane ring J clearly would impair the binding of this alkaloid to its neurological receptors, leading to diminished tremorgenic activity (*68*).



## 11. Penitremones A (67)

Penitremones (67) were first isolated from the sclerotia of *A. sulphureus* (69). Penitremones A (67), B (68), and C (69) were subsequently isolated by Naik *et al.* (70) from the culture of a *Penicillium* sp. along with penitrem A (55). The later isolation of the penitremones was prompted by an earlier report by Frisvad (5) that this *Penicillium* sp. was different from the species that produced the penitremes. Penitremones A (67) produced a molecular formula of  $C_{37}H_{45}NO_6$  and was isomeric with penitrem E (61). However, the UV spectrum ( $\lambda_{max}$  260, 286 nm) of penitremones A–C showed a bathochromic shift of one of the absorption bands. The NMR spectrum of penitremones A showed the absence of the vinyl protons at C-39. These protons were replaced by a secondary methyl group ( $\delta_H$  1.11, d,  $J = 5.5$  Hz;  $\delta_C$  12.7), which was coupled to a methine multiplet at  $\delta_H$  2.77 ( $\delta_C$  45.9) positioned next to a ketone group at C-26 ( $\delta_C$  200.2). Like penitrem F (62), the quaternary carbon bearing the hydroxy group at C-21 is replaced by a methine ( $\delta_C$  35.2,  $\delta_H$  3.82) in penitremones A (67). The stereochemistry at C-25 has not been determined. Reduction of penitremones A with  $NaBH_4$  produced the dihydro derivative 70 (70).



### 12. Penitremone B (68)

Penitremone B (68) had the same UV spectrum as penitremone A (67) and showed a molecular formula of  $C_{37}H_{45}NO_7$  indicating that it had an additional oxygen atom compared with penitremone A (70). The  $^1H$  and  $^{13}C$  NMR spectrum of penitremone B (68) was similar to penitremone A (67) except for the exchange of a hydrogen for a hydroxy group at C-21 ( $\delta_C$  76.5). Like penitremone A, reduction of this alkaloid gave the dihydro derivative 71.

### 13. Penitremone C (69)

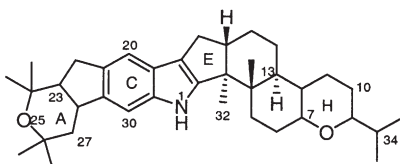
Penitremone C (69) produced a molecular formula of  $C_{37}H_{45}NO_5$  indicating that it had one less oxygen atom than penitremone A (67). This was attributed to replacement of the 11,12-epoxide with an olefin, as in penitremes C (59) and D (60) and was supported by the NMR and mass spectral data (70).

### 14. Biological Activity of Penitremones

Penitremone A (67) exhibited three-fold less tremorgenic activity than the potent penitrem A, and the activity was similar to penitrem E at a dose of 0.14 mg/25 g (per mouse) tested with albino mice (70). The reduced product 70 was inactive at the same dose. In contrast, penitremone B was not tremorgenic at doses up to three-fold higher than penitremone A. The hydroxy derivative B 71 was inactive at the same dose, but at a ten-fold higher dose evidence of marked tremor was observed (70). These observations point out the significance of the molecular architecture of the eastern side of the molecule present in penitrem A. Any modification, either the substitution of the chlorine atom or changes in the level of oxidation in the B ring, caused significant loss of tremorgenic activity.

## D. JANTHITREMANES

The janthitremes are a group of indole diterpenoids that have two *ortho* positions on the phenyl ring of the indole unit substituted with two isoprenes that are cyclized in fused cyclohexyl-pyranyl rings.



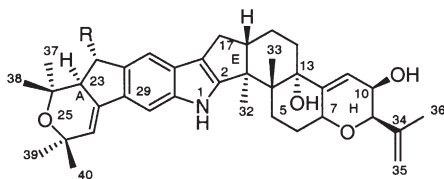
5 Janthitremone

### 1. Janthitremes A–D

Janthitremes A–D were isolated (71) from the fermentation of *P. janthinellum* (a fungus which is associated with ryegrass staggers), using TLC chromatographic separations, by monitoring their purple-blue fluorescence properties under

longwave UV light. The crude extract and TLC bands were tested for tremorgenic properties in a mouse bioassay. These alkaloids produced grey-green colored spots on TLC plates when sprayed with Ehrlich reagent (1% *p*-dimethylamino benzaldehyde in 95% ethanol, followed by 5–10 min exposure to HCl vapor). These alkaloids showed  $\lambda_{\max}$  228, 258, 265, and 329 nm, indicating a 2,3-substituted indole with an extended conjugation to the aromatic ring, as evidenced by the bathochromic shift of the indolic absorption ( $\lambda_{\max}$  290–300 to  $\lambda_{\max}$  329 nm). High-resolution MS measurements provided a molecular formula of  $C_{37}H_{47}NO_6$  (MW 601),  $C_{37}H_{47}NO_5$  (MW 585), and  $C_{37}H_{47}NO_4$  (MW 569) for janthitrems A–C, respectively. The different oxidation states differentiate these three alkaloids, however no full structures have been reported. Janthitrem D was reported as a component of the same extract by HPLC analysis without any structural information (72). Janthitrems A–C were reisolated (73) from the same New Zealand strain of *P. janthinellum* as was used for the first isolation of these tremorgens, resulting in the structure elucidation of janthitrems B (72) and C (73). The structure of A was not reported due to paucity of material.

The structures of janthitrems B and C were elucidated (73) by comparison of their  $^1H$  and  $^{13}C$  NMR spectra with the corresponding spectra of janthitrems E (74) and G (76) (*vide infra*), respectively. The spectral data of these alkaloids were similar, except for the absence of the resonances for the acetate group and the signals for the 2-hydroxypropyl (C34–C36) group, which were replaced with propenyl group signals in both alkaloids. Like janthitrem E (74), janthitrem B (72) has a C-22 hydroxy group, while janthitrem C lacks this hydroxy group, as does janthitrem G (76) (73). These assignments were fully corroborated by a full complement of NMR spectral data including nOe measurements. The eastern part of the structures of janthitrem B (72) and C (73) is identical to penitrem D (60), and the spectral data of that part were identical. The relative stereochemistry of C-22 and C-23 in rings A and B of janthitrem B (as well as E and F, *vide infra*) was reported for the first time by Wilkins *et al.* (66) in 1992 by the application of nOe difference experiments. They reversed the methyl assignments of H<sub>3</sub>-32/H<sub>3</sub>-37 and H<sub>3</sub>-39/H<sub>3</sub>-40 of janthitrem E (74) and B (72) reported by De Jesus *et al.* (74) on the basis of 2D NMR, which was critical for the nOe experiments (66). Irradiation of H-37 of janthitrem B produced strong enhancement to the *gem*-methyl H<sub>3</sub>-38 and the methine H-23, and a weak enhancement to H-22. Similar irradiation of H-22 afforded strong enhancements of H-20, 22-OH, and H<sub>3</sub>-38, and a weak enhancement of H-23. There was a nOe enhancement observed between H-27 and H-30. H-22 and H-23 exhibited a *J* value of 6 Hz, consistent with a pseudo-*trans* relationship between H-22 and H-23 in a half-chair ring system. Based on these and molecular mechanics calculations, the relative stereochemistry was assigned as shown, but unfortunately, the relative stereochemistry of the rings A and B was not unambiguously related to the relative stereochemistry of the rings F–H, which is identical in all indole diterpenoids. Janthitrem B exhibited characteristic tremors at 200  $\mu g/kg$  ip in mice, which was accompanied by incoordination and hypersensitivity to sound and touch (71).

**72** Janthitrem B (R = OH)**73** Janthitrem C (R = H)

### 2. Janthitrem E (74)

Janthitrem E (**74**) was isolated (**74**) by De Jesus *et al.* in 1984, by silica gel chromatography, from the fungus *P. janthinellum* collected in New Zealand. It showed an UV spectrum similar to other janthitrems, including the absorption maxima at  $\lambda_{\max}$  330 nm. It produced a molecular formula of  $C_{37}H_{49}NO_6$  (MW 603), which has an additional mole of hydrogen compared to janthitrem A. De Jesus *et al.* (**74**) elucidated the eight-ringed structure of janthitrem E (**74**) by high resolution NMR analysis using  $^1H$ - $^1H$  decoupling, SPI deuterium isotope shift, and nOe experiments. The right hand part of the structure containing rings C-H was identical to  $\beta$ -paxitriol. The allylic and homoallylic coupling of H-22 to H-20 and H-27, and the subsequent *para*-coupling of H-20 to H-30, along with enhancements of C-23, C-24, and C-38 by irradiation of H<sub>3</sub>-37; C-26, C-27, and C-40 by irradiation of H<sub>3</sub>-39; and C-26 and C-29 by irradiation of H-27 established the connectivity of rings A and B with aromatic ring C, and establishing the structure of janthitrem E (**74**). The full  $^1H$  and  $^{13}C$  NMR assignments of janthitrem E (**74**) are listed in Table VI. The relative stereochemistry of rings E-H of janthitrem E (**74**) was deduced by  $^1H$ - $^1H$  coupling constants and comparison with known alkaloids and was found to be identical to other indole diterpenoids, such as paxilline (**13**) and  $\beta$ -paxitriol (**15**). The stereochemistry at C-22 and C-23 was not determined at the time, but these centers were later determined through nOe measurements by Wilkins *et al.* (**66**).

### 3. Janthitrem F (75)

Janthitrem F (**75**) was isolated as a congener of janthitrem E (**74**) from *P. janthinellum* by De Jesus *et al.* (**74**). The molecular formula ( $C_{39}H_{51}NO_7$ ) of janthitrem F indicated that it was an acetylated derivative of janthitrem E (**74**), which was unequivocally elucidated to be 10-*O*-acetyljanthitrem E (**75**) based on the downfield shift of H-10 ( $\delta_H$  5.21) by  $\Delta\delta$  1.07 ppm with concomitant effects on H-7 and H-9.

### 4. Janthitrem G (76)

Janthitrem G (**76**),  $C_{39}H_{51}NO_6$ , another congener of janthitrem E and F, contained one oxygen less than janthitrem F (**74**). The C-22 oxymethine ( $\delta_H$  4.90,  $\delta_C$  76.5) group of janthitrem E and F was replaced by a methylene group ( $\delta_H$  3.07, 2.65,  $\delta_C$  33.5) in the respective NMR spectra. The new methylene protons showed

TABLE VI.  
 $^1\text{H}$  and  $^{13}\text{C}$  NMR Spectral Assignments of Janthitrem E (**74**) in Acetone- $d_6$  and Shearinine A (**77**) in  $\text{CDCl}_3$ .

#	Janthitrem E <sup>a</sup>		Shearinine A <sup>b</sup>	
	$\delta_{\text{C}}$	$\delta_{\text{H}}$ , m, $J$ (Hz)	$\delta_{\text{C}}$	$\delta_{\text{H}}$ , m, $J$ (Hz)
1-NH				7.62, s
2	155.9		153.2	
3	51.8		51.6	
4	43.4		39.9	
5	27.9	2.61, m; 1.58, m	27.0	2.67, m; 1.80, m
6	29.2	2.05, m; 1.78, m	28.2	2.78, m; 2.03, m
7	75.0	4.56, m	104.4	
9	81.8	3.04, d, $J=2.0$	88.0	4.30, d, $J=1.0$
10	64.5	4.15, m	197.0	
11	119.2	5.63, dd, $J=5.8, 1.7$	117.7	5.82, d, $J=1.0$
12	148.6		169.9	
13	77.5		77.7	
14	34.5	1.56, m; 1.65, m	33.9	1.97, m; 1.87, brd, $J=13.6$
15	22.0	2.01, m; 1.56, m	21.1	2.04, m; 1.76, m
16	50.3	2.66, m	48.5	2.77, m
17	28.0	2.35, d, $J=14.7$ 2.66, dd, $J=14.7, 2.8$	27.5	2.39, dd, $J=13.0, 10.7$ 2.68, m
18	116.9		117.0	
19	127.8		126.7	
20	114.0	7.38, m	114.0	7.24, s
21	139.9		137.0	
22	76.5	4.90, ddd, $J=7.8, 6.0, 1.0$	33.0	3.10, dd, $J=15.7, 9.3$ 2.66, m
23	60.3	2.66, dd, $J=6.0, 2.9$	48.8	2.91, m
24	74.3		74.5	
26	72.8		72.6	
27	120.1	5.99, d, $J=2.99$	119.9	5.91, d, $J=3.0$
28	137.1		139.5	
29	131.5		133.5	
30	103.7	7.37, d, $J=0.8$	102.9	7.32, s
31	142.1		139.9	
32	16.6	1.32 <sup>c</sup> , s	16.2	1.36, s
33	20.2	0.87, s	23.6	1.21, s
34	72.7		78.8	
35	27.3	1.25, s	23.1	1.17, s

(continued)

TABLE VI.  
Continued.

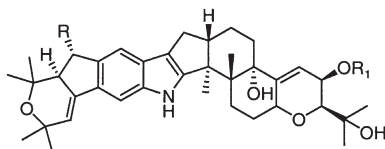
#	Janthitrem E <sup>a</sup>		Shearinine A <sup>b</sup>	
	$\delta_C$	$\delta_H$ , m, <i>J</i> (Hz)	$\delta_C$	$\delta_H$ , m, <i>J</i> (Hz)
36	27.2	1.28, s	28.9	1.43, s
37	30.4	1.41 <sup>c</sup> , s	30.0	1.32, s
38	23.8	1.09, s	22.0	1.07, s
39	30.6	1.25 <sup>d</sup> , s	31.9	1.32, s
40	32.5	1.29 <sup>d</sup> , s	30.1	1.35, s

<sup>a</sup>Taken from DeJesus *et al.* (74).

<sup>b</sup>Taken from Belofsky *et al.* (19) in CDCl<sub>3</sub>.

<sup>c,d</sup>Assignment reversal, see Ref. (66).

<sup>1</sup>H–<sup>1</sup>H couplings with H-23 and H-27, thus unequivocally establishing the structure of janthitrem G as 22-deoxyjanthitrem F (76).



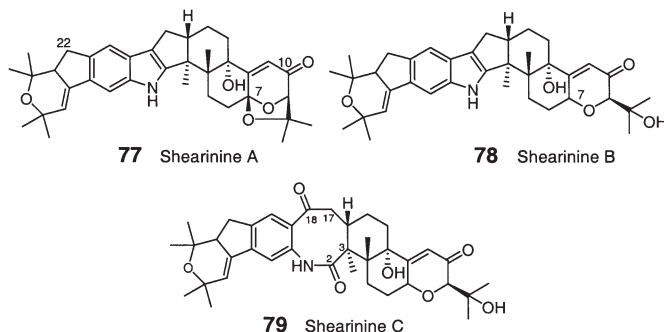
- 74** Janthitrem E (R = OH, R<sub>1</sub> = H)  
**75** Janthitrem F (R = OH, R<sub>1</sub> = Ac)  
**76** Janthitrem G (R = H, R<sub>1</sub> = Ac)

It has been reported that the janthitrem-producing organisms either produce janthitrem A–D or E–G, and are found both in Australia and New Zealand (73). Although it is assumed that these alkaloids are tremorgenic, no specific data has been provided, except for janthitrem B.

### 5. Shearinine A (77)

Shearinine A (77), C<sub>37</sub>H<sub>45</sub>NO<sub>5</sub>, was isolated from the organic extract of ascostromata, produced by solid-substrate fermentation of *E. shearii*, through bioassay guided separation using a feeding assay against the larvae of *H. zea* (corn earworm) (19). The UV spectrum indicated that it was an indole diterpenoid of the janthitrem class, which was confirmed by comparison of the <sup>1</sup>H and <sup>13</sup>C NMR spectra of shearinine A (77) with janthitrem E (74). The NMR spectra of shearinine A indicated the replacement of the oxymethines assigned for C-7, C-10 and C-22 in janthitrem E, with a bis-oxy quaternary carbon ( $\delta_C$  104.4), a ketone ( $\delta_C$  197.0), and a methylene ( $\delta_C$  33.0), respectively, by COSY, NOESY and HMBC experiments, thus establishing the structure and relative stereochemistry of shearinine A (77).

The full NMR assignments of shearinine A are listed in Table VI.



#### 6. Shearinine B (78)

Shearinine B (**78**), a congener of shearinine A, was isolated from ascostromata of *E. shearii* (19). It gave a molecular formula  $C_{37}H_{47}NO_5$  that contains two extra hydrogen atoms compared to shearinine A (**77**). This was attributed to the opening of the dioxane ring (I) as evidenced by the presence of the C-7 methine group ( $\delta_H$  4.83,  $\delta_C$  72.6) and the absence of the bis-oxy quaternary carbon ( $\delta_C$  104.4). These data established the structure of shearinine B and were corroborated by extensive 2D NMR experiments.

#### 7. Shearinine C (79)

Shearinine C (**79**),  $C_{37}H_{47}NO_7$ , is an artifact of isolation, presumably due to the auto-oxidation of shearinine B (19). In fact, it was produced in reasonable amounts when a methanolic solution of shearinine B was stirred in air. The structure was elucidated by standard NMR techniques. It showed two additional carbonyl groups at  $\delta_C$  203.0 and  $\delta_C$  176.2 assigned to C-18 and C-2. Paxilline (**13**) converts to a dioxoindole **14** when treated with thermally inactivated sheep bile via a nonenzymatic oxidation process (*vide supra*). Many members of this class of alkaloids, including shearinine A (**77**) and paspalinine (**10**), undergo these transformations. However, the rate of the oxidation of paxilline under similar conditions appears to be much slower. There has been an increased preponderance of reports of dioxoindole type structures, suggesting that this oxidation process may be a key pathway for the degradation of the paspalane class of alkaloids and plausibly common among the members of this class as well (19). Monosubstituted indoles do not appear to undergo similar oxidation reactions. Therefore, it has been suggested that the 2,3-bis-substitution of the indole, particularly in the form of strained 5,5-fused rings, contributes to the susceptibility of this class of alkaloids towards auto-oxidation to the dioxoindole (19).

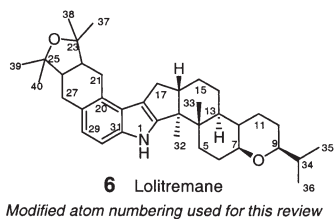
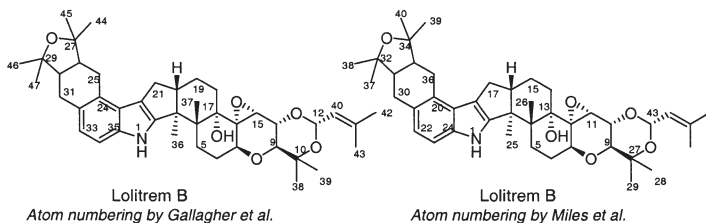
Shearinines A and B exhibited significant anti-insectan activity and showed 89 and 94% reduction in growth rate of *H. zea* relative to control. The oxidized product, shearinine C, was substantially less active. Paxilline was only slightly less



active than shearinine A in the *H. zea* assay. Shearinine B and paxilline also showed similar activities against *S. frugiperda* (fall armyworm) (19). No tremorgenic activity data were reported for any of these three alkaloids.

### E. LOLITREMANES

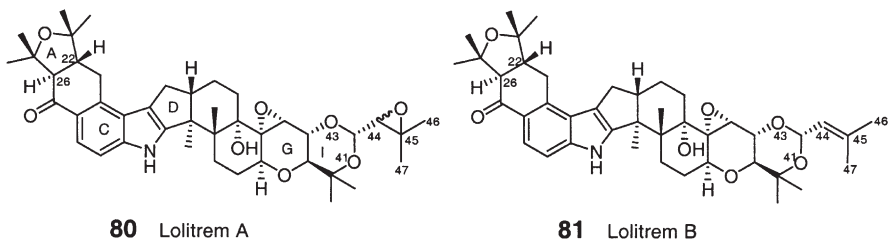
The lolitremanes are a group of indole diterpenoids that have two *ortho* positions of the phenyl ring substituted with two isoprene units. These isoprene moieties are then cyclized to form fused cyclohexyl-tetrahydrofuran rings. These alkaloids also contain an isoprene unit in the extreme right hand portion of the diterpenoid, connected either in the form of 1,3-dioxane, forming ring I, or as an ether. Cattle that graze perennial ryegrass (*L. perenne* L.) infected with endophytic fungi such as *N. lolii*, *A. lolii* and others experienced severe tremor, as well as discoordination and hypersensitivity to external stimuli as a result of nervous disorders. Although this was predominantly observed in New Zealand, and Australia, *Neotyphodium* infected grass is indigenous to every continent except Antarctica, and has now been implicated in the poisoning of grazing animals (28), including a ryegrass staggers outbreak reported in Cumbria, UK in 1997 (75). Although this phenomenon and evidence of the fungal infection of the ryegrass was reported as early as 1902 (28,76), the role of endophytic fungi in the toxicity of *L. perenne* was not firmly demonstrated until 1980 (28,77). Subsequently, Gallagher *et al.* isolated lolitrem A (80) and B (81) from ryegrass pastures (78) infected with the endophyte and established that these alkaloids were responsible for ryegrass stagger syndrome and reported the structure of the major alkaloid lolitrem B (81) in 1984 (79). Since then, numerous lolitremes and related alkaloids have been isolated from ryegrass (*L. perenne*) pastures (41,80) and ryegrass seed (81). No lesions were observed and animals return to normalcy after they ceased grazing on such infected grasses.



### 1. Lolitrem A (80)

Lolitrem A was isolated as the second most abundant albeit minor (8% of total lolitremes), congener of the ryegrass pastures and seed extract (78,82). It exhibited a molecular formula of  $C_{42}H_{55}NO_8$  indicating that it had an extra oxygen atom and the same degree of unsaturation as seen in lolitrem B (81, *vide infra*). The mass spectrum produced the characteristic fragment at  $m/z$  348, suggesting the oxygen was present in the diterpenoid part. It was assigned a structure of 44,45-epoxylolitrem B (80), which exists as a 7:3 mixture of  $\alpha$  and  $\beta$  diastereomers at C-44, as indicated by the  $^1H$  and  $^{13}C$  NMR spectra ( $\delta_{H44} = 2.88$ , d,  $J = 6.3$  Hz;  $2.86$ , d,  $J = 6$  Hz;  $\delta_{C44} = 62.8, 63.0$ ;  $\delta_{C45} = 57.88, 57.9$ ). The NMR spectra were assigned by 2D NMR, including HMBC experiments, and the stereochemistry was confirmed by nOe measurements and molecular modeling.

The tremorgenic activity exhibited by lolitrem A (80) in the mouse was equal to that of lolitrem B (81), both in potency (2 mg/kg) and duration of action (82).



### 2. Lolitrem B (81)

Lolitrem B ( $C_{42}H_{55}NO_7$ ) was isolated (78,79) from ryegrass *L. perenne* pastures and seeds infected with the endophyte *A. lolii*. It displayed a UV spectrum ( $\lambda_{max}$  267 and 290 nm) similar to the penitremes, indicating the presence of a ketone conjugated with the aromatic ring of the indole. It produced a major, characteristic, indole-containing fragment ion at  $m/z$  348, due to concomitant cleavage of C3-C4 and C14-C15 (79). The  $^1H$  and  $^{13}C$  NMR spectra of lolitrem B (Table VII) were related to other indole diterpenoids and were assigned (79) by decoupling, nOe, and SPI experiments, and were later verified by 2D NMR experiments, which led to the revision the assignments of C-20, C-28, and C-29 (80). The location of the ketone group at C-27 was established by a SPI experiment by irradiation of H-29, which gave population inversion of the ketone carbonyl at  $\delta_C$  196.5. The location of the 2-methylprop-1-enyl moiety at C-42 was evident from its proton ( $\delta_H$  5.52, d,  $J = 6.6$  Hz) and carbon ( $\delta_C$  92.7) chemical shift values (80) which were confirmed by HMBC (80). The *trans*-fusion of rings H and I, and the relative stereochemistry at C-10 and C-42, were confirmed by the nOe effects of the axial methyl group at C-34 to H-10 and H-42 (16). A *trans* A/B ring fusion was proposed by Gallagher *et al.* based on the vicinal  $J$  value of 14.3 Hz between H-22

TABLE VII.

<sup>1</sup>H and <sup>13</sup>C NMR Spectral Assignments of Lolitrem B (**81**)<sup>a</sup> in CDCl<sub>3</sub>.

#	$\delta_C$	$\delta_H$ , m, $J$ (Hz)
1-NH		
2	152.8	
3	50.7	
4	42.4	
5	27.4	2.70, m 1.36, m
6	28.0	2.27, m 1.76, m
7	71.5	4.33, brt, $J=9.0$
9	71.2	3.57, d, $J=9.4$
10	71.1	3.92, d, $J=9.4$
11	61.3	3.63
12	67.7	
13	78.1	
14	30.3	1.56, m; 1.42, m
15	20.5	1.95, m; 1.64, m
16	50.1	2.86, m
17	29.2	2.63, m; 2.94, m
18	118.6	
19	123.9	
20	137.0	
21	28.3	2.98, dd, $J=15.9, 12.3$ 3.44, dd, $J=15.9, 3.9$ 2.68, m
22	49.9	
23	79.3	
25	79.9	
26	59.9	2.78, d, $J=14.3$
27	196.5	
28	125.4	
29	120.2	7.87, d, $J=8.7$
30	110.4	7.22, d, $J=8.7$
31	142.0	
32	15.9	1.28, s
33	18.9	1.15, s
34	74.7	
35	28.3	1.30, s
36	16.6	1.30, s
37	30.6	1.54, s
38	25.1	1.32, s
39	25.0	1.26, s

(continued)

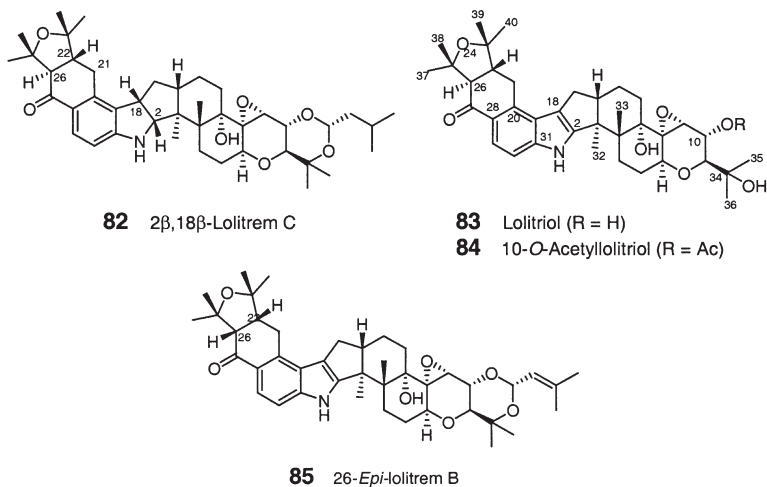
TABLE VII.  
Continued.

#	$\delta_C$	$\delta_H$ , m, $J$ (Hz)
40	29.3	1.39, s
42	92.7	5.54, d, $J = 6.7$
44	122.0	5.30, m
45	139.5	
46	18.6	1.73, brs
47	25.6	1.75, brs

<sup>a</sup>Taken from Munday-Finch *et al.* (80,84).

and H-26 (79). Finally, the H-22 $\beta$  and H-26 $\alpha$  stereochemistry was unambiguously elucidated by Ede *et al.* (80,83) by hydrogenation of lolitrem B to 2 $\beta$ , 18 $\beta$ , 44, 45-tetrahydrololitrem B (2 $\beta$ , 18 $\beta$ -lolitrem C, **82**) followed by the observation of molecular modeling-supported nOe effects of H-18 to H-17 $\beta$  and H-21 $\beta$  (83).

Acid hydrolysis of lolitrem B (**81**) produced exclusively lolitriol (**83**) (16), which was also detected (16) in the extracts of *L. perenne*. Acetylation of lolitriol with acetic anhydride in pyridine produced 10-*O*-acetyllolitriol (**84**) (80). It was reported that lolitrem B (**81**) was unstable in moist CDCl<sub>3</sub>-DMSO (16). Lolitrem B was easily prepared by PTSA-catalyzed reaction of lolitriol with 3-methyl-2-butenal dimethyl acetal (16). Base (NaOH) catalyzed epimerization of lolitrem B gave 26-*epi*-lolitrem B (**85**) (84).



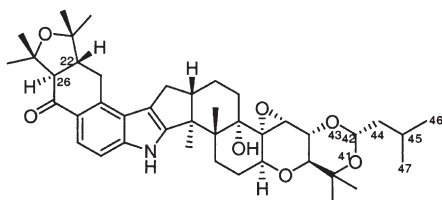
Miles *et al.* reported a modified method for the isolation of lolitrem B by Soxhlet extraction with petroleum followed by solvent partitioning, flash chromatography, and crystallization, leading to a much better recovery (85).

The low-level production of lolitrem B (**81**) and lolitriol (**83**) was recently demonstrated (16) in the axenic cultures of *A. lolii* which are also capable of producing large amounts of paxilline (**13**), indicating a biosynthetic association between the lolitremes and paxilline (16,23). A HPLC method for the analysis of lolitrem B was reported (86). Lolitrem B was detected in perennial drunken horse grass *A. inebrians* infected with the endophytic fungus *Acremonium* sp. by ELISA and HPLC assays (27). *Acremonium* sp. was reported to have caused intoxicating effect to horses grazing this grass in northwestern China and Mongolia (87).

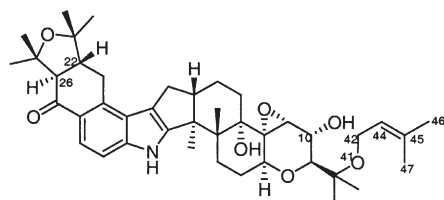
Lolitrem B (**81**) exhibited dose-dependent tremors in mice when tested ip at 0.5, 1.0, 2.0, 4.0, and 8.0 mg/kg. All doses gave a sustained and detectable tremor at 30-min post injection with a maximal response after 2–3 h. The maximal tremor responses plateau between 2.5–5 h with a slow decline in intensity. The response was still observed 24 h-post injection, but was essentially gone after 48 h. Mice became normal after one week (47). In a parallel experiment, Miles *et al.* reported that the tremorigenic activity of lolitrem B (**81**) was five-fold higher than paxilline (**13**). In this experiment they reported (16) that paxilline is much more tremorigenic than reported earlier and this was attributed to a variance in the test vehicle [DMSO-water (16) vs. corn oil (21)]. Lolitriol was nontremorigenic to mice at 20 mg/kg, indicating that lolitriol (**83**) is at least 20 times less tremorigenic than lolitrem B (**81**), but appears to be lethal at 16 mg/kg, depending on the type of administration (16). 26-*Epi*-lolitrem B (**85**) was at least three times less tremorigenic than lolitrem B. It was postulated by Munday-Finch *et al.* (84) that the *cis*-ring fusion in the 26-*epi*-lolitrem B (**85**) results in an  $\alpha$ -bend of the A ring, placing the methyl groups at the  $\alpha$ -face. This may result in steric hindrance which prevents its binding to the receptor.  $\beta$ -Face bend (c.f., lolitrem F) has no effect on the activity (*vide infra*) (84).

### 3. Lolitrem C (**86**)

Lolitrem C (C<sub>42</sub>H<sub>57</sub>NO<sub>7</sub>) was isolated as a minor congener of lolitrem B (**81**) and was reported as the 44,45-dihydro derivative of lolitrem B without spectral or physical data (79). The existence of this structure was since disputed based on its lack of solubility in CDCl<sub>3</sub> and HPLC analysis of a sample labeled lolitrem C found in Gallagher's collection, which showed that it coeluted with lolitrem E (**87**). Thus it has been postulated that lolitrem C has the same structure as lolitrem E (*vide infra*) (85).



**86** Lolitrem C



**87** Lolitrem E

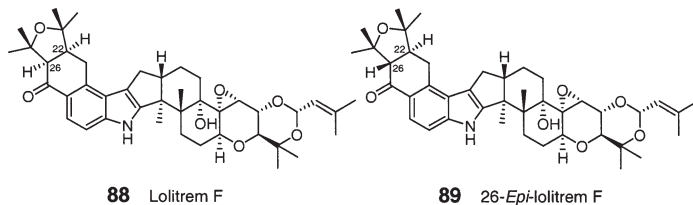
4. *Lolitrem D*

It was reported as one of the four alkaloids obtained during original isolation, but no further data and structural information have been reported (84).

5. *Lolitrem E (87)*

Lolitrem E (87) was isolated as the second most abundant (15% of total lolitrem) of the lolitremes and was isolated during a large-scale isolation of lolitrem B from ryegrass seeds and gave a molecular formula of  $C_{42}H_{57}NO_7$ , the same formula assigned to lolitrem C (85). The NMR spectra of this alkaloid were similar to those of lolitrem B (81), differing only in the ring H, and showed the absence of the signals for the acetal (C-42) carbon and proton, indicating opening of the 1,3-dioxane ring I. The presence of an oxymethylene, two-proton doublet ( $\delta_H$  4.06,  $J=7.2$  Hz), which was coupled to the C-43 olefin ( $\delta_H$  5.36, t), which in turn was coupled to two methyl groups, indicated the presence of an intact isoprene unit. This was located at the C-34 oxygen versus the C-10 oxygen based on the observed couplings between H-10 and the attached OH group and the observation of the acetylation induced shift of H-10 (85).

Lolitrem E (87) is not tremorgenic at 2 mg/kg in mice, while, in comparison, lolitrem B (81) exhibited significant tremor at 1 mg/kg (85).

6. *Lolitrem F (88)*

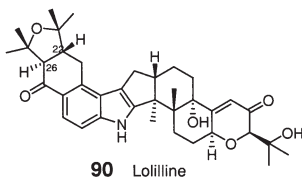
Lolitrem F was isolated as an extremely minor congener of lolitrem B (81) that eluted as a small polar shoulder by HPLC. It was isolated by silica gel chromatography of the mother liquor from lolitrem B crystallization, followed by acetylation and HPLC purification (84). It showed a molecular formula of  $C_{42}H_{55}NO_7$  suggesting an isomeric relationship with lolitrem B. A 22-epimeric lolitrem B (88) structure was assigned to lolitrem F based on the  $^1H$  and  $^{13}C$  NMR spectral analysis. The  $^1H$  NMR spectrum of lolitrem F showed downfield shifts of  $\Delta\delta=0.57$  and 0.34 ppm of H-26 ( $\delta_H$  3.35, d,  $J=6.5$  Hz) and H-36 $\alpha$  ( $\delta_H$  3.30, dd,  $J=6.9, 16.6$  Hz), respectively (84). The lower  $J$  value of H-26 was indicative of a *cis*-fusion of the A/B rings, which was confirmed by the observation of a nOe between H-26 and H-22. This was further verified by base (NaOH) catalyzed epimerization of lolitrem F which yielded 26-*epi*-lolitrem F (89), an alkaloid that displayed an upfield shifted H-26 ( $\delta_H$  2.78) with a larger  $J$  value of 14.1 Hz, as seen in lolitrem B (81). The  $^1H$  NMR spectral pattern of 26-*epi*-lolitrem B (85) was essentially identical to the spectrum of lolitrem F (88), and *vice versa* was the case for 26-*epi*-lolitrem F (89) and lolitrem B (81) (84).

Lolitrems F (**88**) and 26-*epi*-lolitrems F (**89**) were as tremorgenic as lolitrem B (**81**) in mice, both in terms of their potency and their duration of action (**84**).

### 7. Lolilline (**90**)

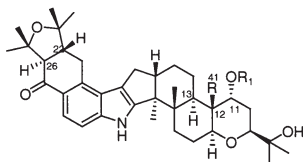
Lolilline (**90**) was also isolated as a minor component from perennial ryegrass *L. perenne* infected by the endophytic fungus *A. lolii* during the large-scale isolation of lolitrem B (**81**). It had a molecular weight of  $C_{37}H_{47}NO_6$  indicating that it differed from lolitriol (**83**) by a mole of water (**41**). The mass spectral data showed a prominent ion at  $m/z$  348 characteristic of the indole part of the molecule of lolitrem B (**81**). The comparison of the NMR spectral data of lolilline (**90**) with lolitrem B (**81**) and paxilline (**13**), followed by complete NMR assignment by 2D NMR, allowed Munday-Finch *et al.* (**41**) to assign a lolitrem B-paxilline hybrid structure for lolilline (**90**), whereby the diterpenoid structure was identical to paxilline (**13**); hence the name lolilline.

Lolilline (**90**) did not exhibit any tremorgenic activity at 8 mg/kg in mice, and is much less active than paxilline (**13**) and lolitrem B (**81**) (**41**).



### 8. Lolicine A (**91**), lolicine B (**92**), and lolitrem N (**93**)

Lolicines A and B, and lolitrem N were purified (**80**) after separation of the propionate ester derivatives of the extract of the perennial ryegrass *L. perenne* infected with the endophytic fungus *N. lolii*. These three alkaloids could not be isolated in their natural state due to their poor chromatographic resolution. Therefore, all of the data reported for these alkaloids are of their respective propionate esters (**80**). No biological activity was reported.



- 91** Lolicine A (R = CH<sub>3</sub>, R<sub>1</sub> = H)  
**92** Lolicine B (R = CHO, R<sub>1</sub> = H)  
**94** 11-*O*-Propionyllolicine A (R = CH<sub>3</sub>, R<sub>1</sub> = COCH<sub>2</sub>CH<sub>3</sub>)  
**95** 11-*O*-Propionyllolicine B (R = CHO, R<sub>1</sub> = COCH<sub>2</sub>CH<sub>3</sub>)

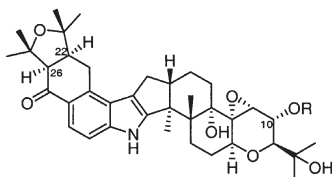
### 9. 11-*O*-Propionyllolicine A (**94**)

A molecular formula of  $C_{41}H_{57}NO_6$  was determined for the propionate ester of lolicine A (**94**) by mass spectral analysis, suggesting a molecular formula of

$C_{38}H_{53}NO_5$  for lolicine A, indicating that it contained an extra  $CH_4$  and had lost two oxygen atoms when compared with lolitriol (**83**) (80). The presence of the characteristic fragment ion at  $m/z$  348 and the absorption bands in the UV spectrum indicated the presence of the intact A–E rings of lolitrem B (**81**), including the ketone at C-27. The  $^1H$  and  $^{13}C$  NMR spectra indicated the presence of an extra angular methyl group ( $\delta_{H41}$  0.96, s;  $\delta_{C41}$  12.8), and a methine ( $\delta_{H13}$  1.95,  $\delta_{C13}$  39.0). Based on 2D NMR experiments (including HMBC) Munday-Finch *et al.* (80) elucidated the structure of lolicine A-11-*O*-propionate ester, which like paspaline (**8**), contains a methyl group at C-12, lacks the C-13 hydroxy group, and possesses an  $\alpha$ -hydroxy group ( $\delta_{H11}$  4.96, s;  $\delta_{C11}$  72.3) at C-11, as determined by the ROESY correlation of H-11 with  $H_3$ -41 (80). No biological activity was reported.

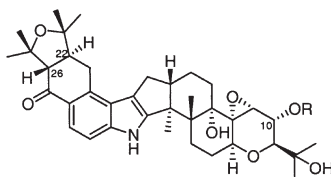
#### 10. 11-*O*-Propionyllolicine B (**95**)

It showed a molecular formula of  $C_{41}H_{55}NO_7$  ( $C_{38}H_{51}NO_6$  for lolicine B) and indicated the presence of an additional oxygen atom and two hydrogen atoms less than lolicine A-11-*O*-propionate ester (**94**). This was attributed to the substitution of the C-12 methyl group with an aldehyde ( $\delta_{H41}$  10.15,  $\delta_{C41}$  204.6), and the structure was thoroughly established by 2D NMR (80). No biological activity was reported.



**93** Lolitrem N (R = H)

**96** 10-*O*-Propionyllolitrem N (R =  $COCH_2CH_3$ )



**97** 26-*Epi*-10-*O*-acetyllolitrem N (R =  $COCH_3$ )

**98** 26-*Epi*-lolitrem N (R = H)

#### 11. 10-*O*-Propionyllolitrem N (**96**)

The mass spectrum of lolitrem N-10-*O*-propionate (**96**) produced a molecular formula of  $C_{40}H_{53}NO_8$  ( $C_{37}H_{49}NO_7$  for lolitrem N) and suggested that it was isomeric to lolitriol (**83**) (80). A comparison of the NMR spectrum of lolitrem N-propionate (**96**) and lolitriol acetate (**84**) suggested that the difference between the two alkaloids resided in the stereochemistry at C-22, aside from the acetate and propionate. Like lolitrem F (**88**), a *cis*-ring fusion of the A/B rings was established based on 2D-NMR experiments and a  $J$  value of 7.3 Hz between H-22 ( $\delta_H$  2.68, ddd) and H-26 ( $\delta_H$  3.35, d) (80). No biological activity was reported.

#### 12. 26-*Epi*-10-*O*-acetyllolitrem N (a.k.a., 31-*Epi*-10-*O*-acetyllolitrem N) (**97**)

This alkaloid was not purified, but it was detected by  $^1H$  and COSY NMR as a 15% contaminant of lolitriol-10-*O*-acetate (**84**), which was prepared by the acetylation of natural lolitriol isolated from ryegrass *L. perenne* infected with *N. lolii* (80). The NMR spectrum of the mixture of the two acetates (**84** and **97**)

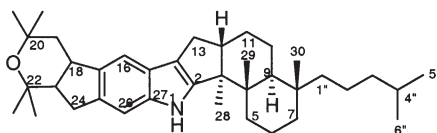


indicated that the minor component was the 22 $\alpha$ , 26 $\beta$ -epimer of lolitriol acetate, which is same as the 26 $\beta$ -epimer of lolitrem N-acetate (**97**). The  $^1\text{H}$  NMR spectrum of the mixture displayed the chemical shifts and coupling constants of H-21 $\alpha$  ( $\delta_{\text{H}}$  3.34, dd,  $J=15.9, 3.9$  Hz), H-21 $\beta$  ( $\delta_{\text{H}}$  3.01), and H-22 $\alpha$  ( $\delta_{\text{H}}$  2.70) identical to those observed for 26-*epi*-lolitrem F. Therefore, Munday-Finch *et al.* (80) assigned 26-*epi*-lolitrem N-10-*O*-acetate to the acetylated product and 26-*epi*-lolitrem N (**98**) as the natural product, present with natural lolitriol (**83**), which apparently was not observed in the synthetic lolitriol from lolitrem B (*vide supra*). No biological activity was reported.

## F. NODULISPORANES

Nodulisporanes are a group of indole diterpenoids, represented by the nodulisporic acids, whereby two *ortho* positions of the phenyl ring of the indole are substituted with two isoprene units, which are cyclized to produce fused cyclohexyl-pyranyl rings, but with a different spacial arrangement than the janthitremanes. These alkaloids are grouped here with the other indole diterpenoids, however, they are characteristically different from the classical indole diterpenoids for the following reasons. While most of the indole diterpenoids form a fused pyran ring at C-7 and C-9, all of the nodulisporanes are devoid of that ring. In addition, these alkaloids have not shown toxicity to any animals tested to date, and are a potent and important class of insecticide, particularly for the treatment of flea and tick infestation of dogs and cats.

Nodulisporic acid A (**99**), the first member of the nodulisporane family, was originally isolated in low yield ( $\sim 2$  mg/L) from an extract of laboratory cultured endophytic fungus *Nodulisporium* sp. (ATCC 74245), which was recovered from a woody plant (*Bontia daphnoides*) collected in Hawaii. These alkaloids were isolated as a part of an insecticidal screening program using *in vitro* blowfly larvae (*Lucilia sericata*) followed by an *in vivo* evaluation using compound medicated diets fed to mice, which were infested with bed bug (*Cimex lectularius*). It is noteworthy that like many other indole diterpenoids, the fungus that produces nodulisporic acids is also an endophyte, but unlike the lolitrem producers, *Nodulisporium* sp. could be cultured in the laboratory. A review describing many of these alkaloids, including the chronology of their discovery and biological activities, was published recently by Meinke *et al.* (88). The original atom-numbering scheme has been adapted for the discussion of these alkaloids.



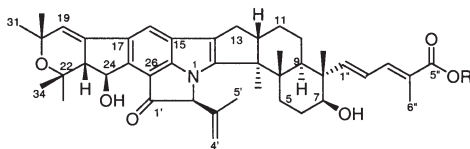
**7** Nodulisporane

1. *Nodulisporic Acid A* (**99**)

*Nodulisporic acid A* (**99**) was the first alkaloid isolated (*89*) at a level of  $\sim 2$  mg/L from *Nodulisporium* sp. as a yellow solid. It produced a molecular formula of  $C_{43}H_{53}NO_6$  and gave an UV spectrum similar to other indole diterpenoids. Its structure was originally elucidated by NMR spectroscopic studies (Table VIII) supported by extensive 2D NMR techniques, including HMBC and computerized INADEQUATE analysis of Dunkel. Some of the critical features of the structure of this alkaloid were the presence of a dienoic acid chain, a highly strained  $\beta$ -ketodihydropyrrole, and a fused cyclopentyl-dihydropyranyl ring. The latter two fused rings are present in the janthitrems, but the fusion of these two rings is reversed in *nodulisporic acids*.

The relative stereochemistries of the eastern and western hemispheres of *nodulisporic acid A* were independently deduced by scalar couplings,  $nOe$  difference, and NOESY experiments. The Merck group established the stereochemical relationship of the two remote hemispheres by a novel method in which they prepared the C-24 *O*-MOM ether of methyl ester **100**, and reduced the keto group of the  $\beta$ -ketodihydropyrrole ring by  $NaBH_4$ , thus creating a stereochemical bridge between the two hemispheres. The link was established by  $nOe$  measurements between the H-2', H-1', H-24, MOM-CH<sub>2</sub>, and C-1' OH groups (*89*). The structure and relative stereochemistry was finally confirmed by X-ray crystallographic studies of a 7-*O*-*p*-bromobenzoate methyl ester. Finally, the absolute stereochemistry was deduced by application of advanced the Mosher method to the methyl ester **100**. *Nodulisporic acids* and the *penitrems* are the only examples in which the stereochemistries of the eastern and western hemispheres have been correlated (*89*). Ether protection of the C-24 alcohol caused the alkaloids to be more labile, resulting in a loss of the C-24 oxygen and the formation of  $\Delta^{23,24}$ . This observation lead to the hypothesis that the natural product was stabilized by a 6-center hydrogen bond involving the C-24 hydroxy group and the C-1' ketone (*89*).

Of the 448 *Nodulisporium* sp. isolates (370 from tropical sources and 78 from temperate sources) that were identified during screening efforts, only 13 species produced *nodulisporic acid A* (**90**). All of the *nodulisporic acid* producers were endophytes and were isolated from plant leaf litters, twigs, stems, herbivore dung, and fruticose lichen, and were collected from such diverse places as Hawaii, Colombia, Mauritius, French Polynesia, Equatorial Guinea, Puerto Rico, and Peru (*90*).



**99** *Nodulisporic acid A* (R = H)

**100** *Nodulisporic acid A methyl ester* (R = CH<sub>3</sub>)

TABLE VIII.

$^1\text{H}$  and  $^{13}\text{C}$  NMR Assignments of Nodulisporic Acids A (**99**)<sup>a</sup> A<sub>1</sub> (**101**)<sup>b</sup> and A<sub>2</sub> (**102**)<sup>b</sup> in CD<sub>2</sub>Cl<sub>2</sub>.

#	Nodulisporic acid A		Nodulisporic acid A <sub>1</sub>		Nodulisporic acid A <sub>2</sub>	
	$\delta_{\text{C}}$	$\delta_{\text{H}}$ , m, <i>J</i> (Hz)	$\delta_{\text{C}}$	$\delta_{\text{H}}$ , m, <i>J</i> (Hz)	$\delta_{\text{C}}$	$\delta_{\text{H}}$ , m, <i>J</i> (Hz)
2	154.7	—	154.8		154.7	
3	56.1	—	55.5		55.4	
4	39.1	—	39.5		39.6	
5	32.3	1.93 m, 1.76 m	30.0	~ 1.90 m	30.7	~ 1.83 m ~ 2.00 m
6	25.95	1.78 m, 1.81 m	30.4	~ 1.70 m ~ 1.91 m	30.1	
7	76.8	3.45 m	106.9		105.5	
8	47.8	—	49.6		49.2	
9	45.2	1.65 m	41.3	1.68 m	47.4	~ 1.70 m
10	24.7	1.47 m, 1.47 m	24.8	~ 1.56 m	23.2	~ 1.48 m ~ 1.92 m
11	25.7	1.55 m, 1.49 m	26.0	~ 1.9	25.8	~ 1.78 m ~ 1.83 m
12	48.0	2.85 m	48.1	2.93 m	48.2	2.87 m
13	27.75	$\alpha$ : 2.33 dd, <i>J</i> =10.8, 13.9 $\beta$ : 2.76 dd, <i>J</i> =6.5, 13.9	27.8	2.35 dd, 2.75 dd, <i>J</i> =6.5, 14.0	27.8	2.33 dd, 2.77 dd, <i>J</i> =6.6, 13.9
14	122.7	—	122.6		122.5	
15	121.8	—	121.8		121.8	
16	116.7	7.73 s	116.7	7.72 s	116.7	7.70 s
17	134.0	—	135.9		135.9	
18	135.9	—	134.0		134.0	
19	122.0	6.07 d, <i>J</i> =3.2	122.0	6.06 d, <i>J</i> =2.9	122.0	6.06 d, <i>J</i> =2.9
20	72.6	—	72.6		72.6	
22	73.9	—	73.9		73.9	
23	58.2	2.82 dd, <i>J</i> =3.0, 6.2	58.2	2.81 dd, <i>J</i> =2.9, 6.3	58.2	2.81 dd, <i>J</i> =2.9, 6.3
24	75.3	5.24 d, <i>J</i> =6.2	75.3	5.21 d, <i>J</i> =6.3	75.3	5.21 d, <i>J</i> =6.3
25	138.4	—	138.3		138.4	
26	113.1	—	113.2		113.2	
27	162.0	—	162.0		162.0	
28	15.1	0.97 s	29.9	1.34 s	29.9	1.33 s
29	19.6	1.15 s	32.0	1.31 s	32.0	1.31 s
30	11.24	1.07 s	23.4	1.122 s	23.4	1.118 s
31	29.9	1.34 s	30.1	1.42 s	30.0	1.42 s

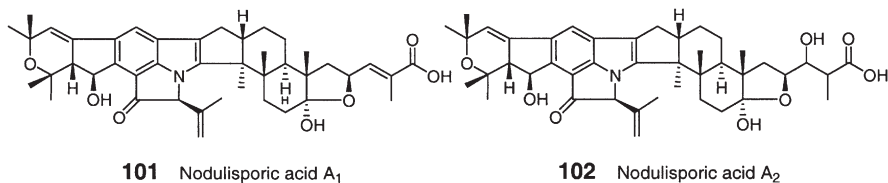
(continued)

TABLE VIII.  
Continued.

#	Nodulisporic acid A		Nodulisporic acid A <sub>1</sub>		Nodulisporic acid A <sub>2</sub>	
	$\delta_C$	$\delta_H$ , m, $J$ (Hz)	$\delta_C$	$\delta_H$ , m, $J$ (Hz)	$\delta_C$	$\delta_H$ , m, $J$ (Hz)
32	31.95	1.31 s	15.3	0.95 s	15.1	0.92 s
33	23.45	1.13 s	16.7	1.06 s	16.7	1.05 s
34	30.1	1.43 s	17.7	1.126 s	17.6	1.112 s
1'	198.0	–	198.1		198.1	
2'	76.4	5.11 s	76.6	5.10 s	76.6	5.10 s
3'	140.0	–	140.1		140.1	
4'	117.5	5.23 br.s, 4.99 brs	117.8	5.0 br s 5.20 dq, $J = \sim 1.2$	117.9	5.00 br s 5.20 br s
5'	18.1	1.48 brs	18.0	1.42 s	17.8	1.42 s
1''	154.6	5.96 d, $J = 15.2$	44.5	1.73 dd, $J = 9.3, 12.6$ ; 2.34 dd, $J = 7.3, 12.6$	40.3	1.48 dd, $J = \sim 9, \sim 13$ ; 1.72 dd, $J = 7.5, 12.7$
2''	125.9	6.42 dd, $J = 11.2, 15.2$	73.3	4.88 br dt, $J = \sim 8$	78.9	4.3 m
3''	140.8	7.34 brd, $J = 11.2$	147.1	6.93 dq, $J = 8.0, 1.3$	81.1	3.96 m
4''	125.1	–	126.8		40.4	2.70 m
5''	172.6	–	172.0		176.3	
6''	12.65	1.96 d, $J = 1.2$	12.5	1.86 d, $J = 1.3$	13.2	1.09 d, $J = 7.0$

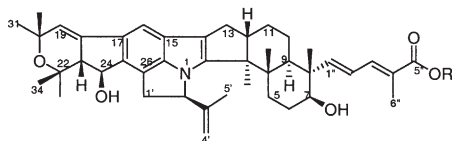
<sup>a</sup>Taken from Ondeyka *et al.* (89).<sup>b</sup>Taken from Hensens *et al.* (91).2. Nodulisporic Acid A<sub>1</sub> (101)

Nodulisporic acid A<sub>1</sub>, C<sub>43</sub>H<sub>53</sub>NO<sub>7</sub> (MW 695), was isolated (91) as the second most abundant congener, and its structure was elucidated by 2D NMR and mass spectrometry. It differed from nodulisporic acid A by an extra oxygen atom, which was placed in the form of tetrahydrofuran ring I formed as a result of the formal addition of water across C1''-C2'' followed by cyclization at C-7 ( $\delta_C$  106.9) presumably via a putative C-7 keto group. The structure was fully corroborated by <sup>1</sup>H and <sup>13</sup>C NMR spectral assignments (Table VIII) which revealed an ABMX spin system (–CH<sub>A</sub>H<sub>B</sub>–CH<sub>M</sub>(O)–CH<sub>X</sub>=) assigned to C1''-C3'' (91).



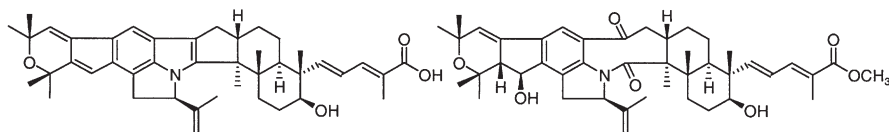
### 3. *Nodulisporic Acid A<sub>2</sub>* (**102**)

Nodulisporic acid A<sub>2</sub>, C<sub>43</sub>H<sub>55</sub>NO<sub>8</sub> (MW 713), was isolated (91) as a third most abundant congener from the cultured extract of *Nodulisporium* sp. along with nodulisporic acids A (99) and A<sub>1</sub> (102) and the structure was elucidated by 2D NMR and the mass spectrometry. It differed from nodulisporic acid A<sub>1</sub> by an extra mole of water, which was added across the C3''-C4'' olefin. The hydroxy group was placed at C-3'' with the assistance of the <sup>1</sup>H and <sup>13</sup>C NMR spectra (Table VIII) (91).



**103** Nodulisporic acid B (R = H)

**104** Nodulisporic acid B methyl ester (R = CH<sub>3</sub>)



**105** Δ<sup>23</sup>-Dehydronodulisporic acid B

**106**

### 4. *Nodulisporic Acid B* (**103**)

Nodulisporic acid B, C<sub>43</sub>H<sub>55</sub>NO<sub>5</sub> (MW 665), was initially detected in the original natural isolate of *Nodulisporium* sp., but was eventually isolated from a mutant culture ATCC74382 as a result of a targeted screening for nodulisporic acid analogs (92). The structure of this alkaloid differed from nodulisporic acid A (99) by the absence of an oxygen atom and the presence of two additional hydrogens. This was attributed to the substitution of the C-1' ketone ( $\delta_C$  198.0) with a CH<sub>2</sub> ( $\delta_C$  41.1) group in nodulisporic acid B (Table IX). The structure was supported by the 2D NMR analysis. Nodulisporic acid B formed a chemically stable methyl ester **104** on reaction with diazomethane. The C-24 hydroxy group of nodulisporic acid B readily dehydrated to produce Δ<sup>23</sup>-dehydronodulisporic acid B (**105**), particularly when it is present in the free acid form, and therefore it was isolated as a sodium salt. The higher propensity of intra-molecular acid-catalyzed dehydration of nodulisporic acid B was attributed to the lack of the six-center hydrogen bond between the C-24 hydroxy group and the C-1' keto group of nodulisporic acid A (99) (92). The dehydration reaction was observed in all nodulisporic acids lacking the C-1' keto group, including all B- and C-series of nodulisporic acids, but the rate of dehydration was much more pronounced in the B-series. The indole oxidation product **106** of the methyl ester **104** was also reported (92).

TABLE IX.  
<sup>1</sup>H and <sup>13</sup>C NMR Assignments<sup>a</sup> of Nodulisporic Acids B (103), B<sub>1</sub> (107), and B<sub>2</sub> (108)  
 in Acetone-*d*<sub>6</sub>.

#	Nodulisporic acid B		Nodulisporic acid B <sub>1</sub>		Nodulisporic acid B <sub>2</sub>	
	$\delta_C$	$\delta_H$ , m, <i>J</i> (Hz)	$\delta_C$	$\delta_H$ , m, <i>J</i> (Hz)	$\delta_C$	$\delta_H$ , m, <i>J</i> (Hz)
2	151.9		152.0		152.1	
3	56.1		55.6		55.7	
4	39.6		41.4		41.1	
5	32.8	1.8, m; 2.0, m	30.0	2.0, m, 2H	33.1	1.8, m; 1.95, m
6	27.3	1.78, m	30.7	1.7, m; 1.85, m	30.5	1.75, m; 1.9, m
7	76.9	3.48, m	106.4		105.9	
8	47.9		48.0		49.6	
9	45.4	1.75, m	41.1	1.8, m	42.0	1.7, m
10	25.0	1.62, m, 2H	25.3	1.74, m, 2H	25.4	1.55, m; 1.7, m
11	26.2	1.45, m, 2H	26.6	1.45, m, 1.65, m	26.6	1.4, m; 1.65, m
12	47.9	2.70, m	49.9	2.75, m	50.3	2.75, m
13	28.5	2.25, m; 2.60, m	28.5	2.20, m; 2.60, m	28.5	2.2, m; 2.6, m
14	120.9		120.3		120.8	
15	124.1		124.0		124.1	
16	107.9	7.25, s	107.8	7.20, s	107.9	7.20, s
17	133.9		133.9		133.9	
18	135.6		135.3		135.3	
19	119.6	5.93, d, <i>J</i> = 3.0	119.4	5.95, d, <i>J</i> = 3.0	119.6	5.95, d, <i>J</i> = 3.0
20	72.6		72.9		72.9	
22	74.1		74.0		74.4	
23	60.5	2.67, dd, <i>J</i> = 3.0, 6.0	60.2	2.64, dd, <i>J</i> = 3.0, 6.0	60.3	2.64, dd, <i>J</i> = 3.0, 6.0
24	75.6	4.92, d, <i>J</i> = 6.0	75.5	4.92, d, <i>J</i> = 6.0	75.5	4.90, d, <i>J</i> = 6.0
25	137.4		137.3		137.4	
26	118.5		118.8		118.6	
27	155.7		155.6		155.7	
28	15.3	0.96, s	15.3	0.90, s	16.8	0.85, s
29	19.5	1.13, s	17.6	1.07, s	17.7	1.04, s
30	11.7	1.07, s	17.1	1.00, s	16.3	0.95, s
31	30.3	1.29, s	30.3	1.27, s	30.5	1.27, s
32	32.4	1.25, s	32.3	1.23, s	32.3	1.23, s
33	23.6	1.10, s	23.5	1.07, s	23.5	1.07, s
34	30.5	1.40, s	30.2	1.40, s	30.5	1.38, s
1'	41.1	3.5, d, <i>J</i> = 16.0; 4.0, dd, <i>J</i> = 8.0, 16.0	41.0	3.5, d, <i>J</i> = 16.0; 4.0, dd, <i>J</i> = 8.0, 16.0	41.1	3.5, d, <i>J</i> = 16.5; 4.0, dd, <i>J</i> = 8.0, 16.5

(continued)

TABLE IX.  
Continued.

#	Nodulisporic acid B		Nodulisporic acid B <sub>1</sub>		Nodulisporic acid B <sub>2</sub>	
	$\delta_C$	$\delta_H$ , m, <i>J</i> (Hz)	$\delta_C$	$\delta_H$ , m, <i>J</i> (Hz)	$\delta_C$	$\delta_H$ , m, <i>J</i> (Hz)
2'	69.8	5.35, d, <i>J</i> = 8.0	69.9	5.35, d, <i>J</i> = 8.0	69.7	5.35, d, <i>J</i> = 8.0
3'	147.5		147.4		147.6	
4'	112.7	4.79, s, 4.82, s	112.9	4.78, s, 2H	112.9	4.78, s, 2H
5'	17.0	1.24, s	16.7	1.17, s	17.4	1.15, s
1''	154.8	5.96, d, <i>J</i> = 15.0	45.3	1.7, m, 2.3, m	37.9	1.8, 2.0, m
2''	125.7	6.38, dd, <i>J</i> = 15.0, 13.5	74.3	4.3, t, <i>J</i> = 6.0	79.3	4.20, m
3''	139.6	7.22, d, <i>J</i> = 13.5	140	6.56, d, <i>J</i> = 6.0	74.7	3.90, m
4''	125.7		120.3		42.9	2.3, m
5''	170.4		171.5		175.6	
6''	12.9	1.9, brs	13.9	1.78, brs	16.2	1.16, brs

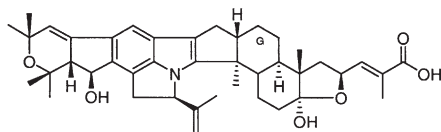
<sup>a</sup>Taken from Ondeyka *et al.* (92).

### 5. Nodulisporic Acid B<sub>1</sub> (107)

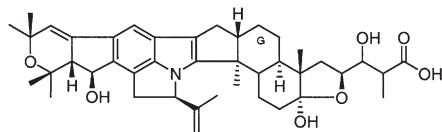
Nodulisporic acid B<sub>1</sub>, C<sub>43</sub>H<sub>55</sub>NO<sub>6</sub> (MW 681), was also isolated as a sodium salt from a mutant culture of *Nodulisporium* sp. (ATCC74382) as a result of a targeted screening for nodulisporic acid analogs (92). The molecular formula of this alkaloid differed from nodulisporic acid B (103) by one oxygen atom, which was attributed to oxidation of the side chain, followed by cyclization to produce tetrahydrofuran ring I, as seen in nodulisporic acid A<sub>1</sub> (101). This structure was fully supported by the NMR spectral data (Table IX) (92).

### 6. Nodulisporic Acid B<sub>2</sub> (108)

Nodulisporic acid B<sub>2</sub>, C<sub>43</sub>H<sub>57</sub>NO<sub>7</sub> (MW 699), is a minor component that was also isolated as a sodium salt from the same mutant culture of *Nodulisporium* sp. (ATCC 74382) as a result of similar targeted screening designed for the isolation of nodulisporic acid analogs, like nodulisporic acids B (103) and B<sub>1</sub> (107) (92). The molecular formula of this alkaloid differed from nodulisporic acid B<sub>1</sub> (103) by a mole of water, which was added across the C3''-C4'' olefin, similar to nodulisporic acid A<sub>2</sub> (102). The structure was thoroughly assigned by 2D NMR and the assignments are presented in Table IX (92).



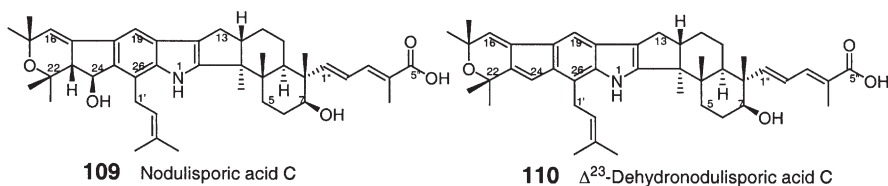
**107** Nodulisporic acid B<sub>1</sub>



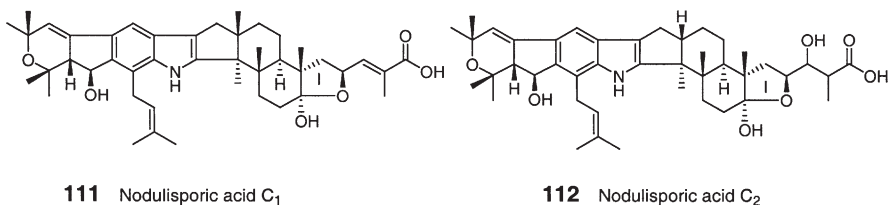
**108** Nodulisporic acid B<sub>2</sub>

7. *Nodulisporic Acid C* (**109**)

Nodulisporic acid C,  $C_{43}H_{57}NO_5$  (MW 667), like nodulisporic acid B, was initially detected in extracts of the original, naturally isolated culture, but was eventually isolated as a sodium salt from a mutant culture of *Nodulisporium* sp. (ATCC 74383) as a result of a targeted screening for nodulisporic acid analogs, similar to the nodulisporic acids B series (93). The molecular formula of this alkaloid differed from nodulisporic acid B by a mole of hydrogen. A structure possessing an opened D-ring was assigned to nodulisporic acid C by the  $^1H$  and  $^{13}C$  NMR spectral comparisons with nodulisporic acids A (**99**) and B (**103**), which showed the absence of the isopropylidene methyl and the presence of a dimethylallyl group (Table X) (93). Dehydration of the C-24 hydroxy group of nodulisporic acid C was also observed when it was concentrated, particularly in its free acid form, leading to the formation of  $\Delta^{23}$ -dehydro-nodulisporic acid C (**110**). The dehydration propensity was lower for this class of alkaloids compared to the more strained nodulisporic acid B (**103**).

8. *Nodulisporic Acid C<sub>1</sub>* (**111**)

Nodulisporic acid  $C_1$ ,  $C_{43}H_{57}NO_6$  (MW 683), a minor component, was also isolated as a sodium salt from the same mutant culture of *Nodulisporium* sp. that produced nodulisporic acid C (**109**) (93). Structurally, it differed from nodulisporic acid C by an extra oxygen atom, which was found to be present in the form of tetrahydrofuran ring I, similar to nodulisporic acids  $A_1$  (**101**) and  $B_1$  (**103**), and was fully assigned by 2D NMR spectral analysis (Table X) (93).

9. *Nodulisporic Acid C<sub>2</sub>* (**112**)

Nodulisporic acid  $C_2$ ,  $C_{43}H_{59}NO_7$  (MW 701), another minor component, was also isolated as a sodium salt from the same mutant culture of *Nodulisporium* sp. (ATCC 74383) in a similar targeted screening used for other C-series of nodulisporic acids (93). Like nodulisporic acids  $A_2$  and  $B_2$ , it contained a



TABLE X.

$^1\text{H}$  and  $^{13}\text{C}$  NMR Assignments<sup>a</sup> of Nodulisporic Acids C (**109**), C<sub>1</sub> (**111**), and C<sub>2</sub> (**112**) in Acetone-*d*<sub>6</sub>.

#	Nodulisporic acid C		Nodulisporic acid C <sub>1</sub>		Nodulisporic acid C <sub>2</sub>	
	$\delta_{\text{C}}$	$\delta_{\text{H}}$ , m, <i>J</i> (Hz)	$\delta_{\text{C}}$	$\delta_{\text{H}}$ , m, <i>J</i> (Hz)	$\delta_{\text{C}}$	$\delta_{\text{H}}$ , m, <i>J</i> (Hz)
2	153.0		153.0		153.1	
3	54.3		53.7		53.7	
4	39.7		40.1		40.0	
5	33.4	1.85, m	30.5	1.90, m, 2H	30.5	1.90, m, 2H
6	27.6	1.78, m; 1.81, m	27.9	1.75, m, 2H	27.9	1.75, m, 2H
7	76.9	3.45, dd, <i>J</i> = 4.5, 10.5	106.6		105.7	
8	47.9		49.7		49.6	
9	45.0	1.75, m	41.1	1.90, m	41.5	1.80, m
10	25.4	1.46, m, 2H	25.6	1.58, m, 2H	25.5	1.75, m; 1.9, m
11	26.0	1.60, m, 2H	26.4	1.65, m, 2H	26.4	1.50, m; 1.75, m
12	49.7	2.75, m	50.0	2.80, m	50.0	2.80, m
13	27.9	2.25, dd, <i>J</i> = 10.5, 13.0 2.60, dd, <i>J</i> = 6.5, 13.0	28.0	2.28, brt, <i>J</i> = 13.0 2.62, dd, <i>J</i> = 6.4, 13.0	28.0	2.30, m  2.60, m
14	118.8		118.8		118.7	
15	127.4		127.4		127.3	
16	107.6	7.31, s	107.5	7.31, s	107.5	7.30, s
17	132.2		132.2		132.2	
18	137.2		137.2		137.2	
19	119.8	5.96, d, <i>J</i> = 3.0	119.7	5.95, d, <i>J</i> = 6.0	119.7	5.94, brs
20	72.7		72.7		72.7	
22	74.2		74.2		74.2	
23	60.7	2.70, dd, <i>J</i> = 3.0, 6.0	60.7	2.68, dd, <i>J</i> = 3.0, 6.0	60.6	2.68, brs
24	76.5	5.00, d, <i>J</i> = 6.0	76.5	5.02, d, <i>J</i> = 6.0	76.3	5.05, brs
25	137.1		137.2		137.5	
26	123.3		123.2		123.2	
27	142.1		142.1		142.0	
28	14.7	1.05, s	14.9	1.02, s	14.9	1.00, s
29	19.4	1.13, s	17.7	1.15, s	17.7	1.12, s
30	11.7	1.07, s	17.0	1.06, s	17.4	1.05, s
31	30.3	1.26, s	30.4	1.27, s	30.4	1.26, s
32	32.3	1.27, s	32.4	1.25, s	32.4	1.25, s
33	23.1	1.00, s	23.1	1.00, s	23.1	1.00, s
34	30.3	1.40, s	30.4	1.40, s	30.4	1.40, s

(continued)

TABLE X.  
Continued.

#	Nodulisporic acid C		Nodulisporic acid C <sub>1</sub>		Nodulisporic acid C <sub>2</sub>	
	$\delta_C$	$\delta_H$ , m, $J$ (Hz)	$\delta_C$	$\delta_H$ , m, $J$ (Hz)	$\delta_C$	$\delta_H$ , m, $J$ (Hz)
1'	26.6	3.70, dd, $J=6.0, 15.0$ ; 4.00, dd, $J=8.0, 15.0$	26.4	3.70, dd, $J=6.0, 15.0$ ; 4.00, dd, $J=8.0, 15.0$	26.4	3.70, brm  4.00, brm
2'	124.4	5.30, t, $J=6.0, 8.0$	124.4	5.30, m	124.4	5.29, m
3'	131.7		132.2		131.1	
4'	25.4	1.80, s	26.4	1.82, s	25.8	1.82, s
5'	18.1	1.67, s	18.1	1.67, s	18.1	1.66, s
1''	155.2	5.96, d, $J=15.0$	45.0	1.73, m; 2.34, m	31.3	1.60, m; 2.0, m
2''	125.6	6.38, dd, $J=11.5, 15.0$	74.2	4.94, m	78.4	4.32, m
3''	140.1	7.22, d, $J=11.5$	146.0	6.90, brd	74.6	3.85, m
4''	125.4		123.2		44.5	2.35, m
5''	170.0		170.5		174.8	
6''	12.7	1.90, d, $J=1.2$	12.7	1.82, d, $J=1.3$	12.5	1.16, brs
NH		9.00, brs		9.00, brs		9.00, brs

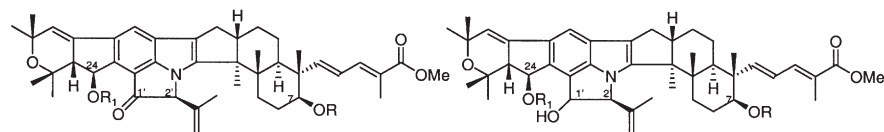
<sup>a</sup>Taken from Ondeyka *et al.* (93).

tetrahydrofuran ring I and a C-4'' hydroxy group, which was assigned by the comparison of the NMR spectra (Table X) (93).

#### 10. Chemistry of Nodulisporic Acid A (99)

Nodulisporic acid A (99) was methylated with diazomethane at  $-78^\circ\text{C}$  to produce methyl ester 100, which was selectively acylated with *p*-bromobenzoyl chloride to afford crystalline 7-*O*-*p*-bromobenzoate 113 that was reacted with MOMCl to yield 24-*O*-MOM ether 114. The MOM ether appeared to be unstable in chlorinated NMR solvents such as  $\text{CDCl}_3$  and  $\text{CD}_2\text{Cl}_2$ , exclusively yielding the  $\Delta^{23}$ -dehydronodulisporic acid A 115, but was stable in nonchlorinated solvents such as  $\text{CD}_3\text{CN}$ . The formation of dehydro alkaloid 115 also predominated during various attempts to methylate the C-24 hydroxy group (89). While sodium borohydride reduction of the 24-*O*-MOM ether 114 exclusively furnished the 1'- $\beta$ -hydroxy derivative 116, similar reduction of the unprotected derivative 113 provided a mixture of the  $\alpha$ - and  $\beta$ -epimeric 1'-hydroxy derivatives 117 and 118 in a 1:9 ratio, indicating the steric crowding on the  $\beta$ -face, which was enhanced by the MOM group in 114 (89). The C-2' center  $\alpha$  to the ketone group of the  $\beta$ -ketodihydropyrrole ring was prone to epimerization under basic conditions. For example, 4-(dimethylamino) pyridine (in a mixture of  $\text{CH}_3\text{CN}-\text{CH}_2\text{Cl}_2$ )

readily epimerized the methyl ester **100**, affording the 2'-*R*-nodulisporic acid A methyl ester derivative **119**.



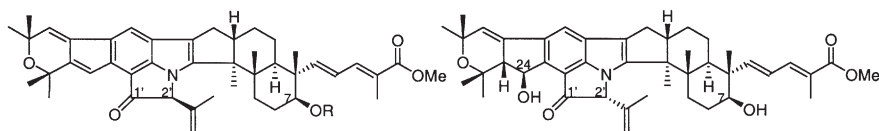
**113** (R = *p*-Br-C<sub>6</sub>H<sub>4</sub>CO, R<sub>1</sub> = H)

**114** (R = *p*-Br-C<sub>6</sub>H<sub>4</sub>CO, R<sub>1</sub> = MOM)

**116** (R = *p*-Br-C<sub>6</sub>H<sub>4</sub>CO, R<sub>1</sub> = MOM, 1'-β-OH)

**117** (R = *p*-Br-C<sub>6</sub>H<sub>4</sub>CO, R<sub>1</sub> = H, 1'-β-OH)

**118** (R = *p*-Br-C<sub>6</sub>H<sub>4</sub>CO, R<sub>1</sub> = H, 1'-α-OH)



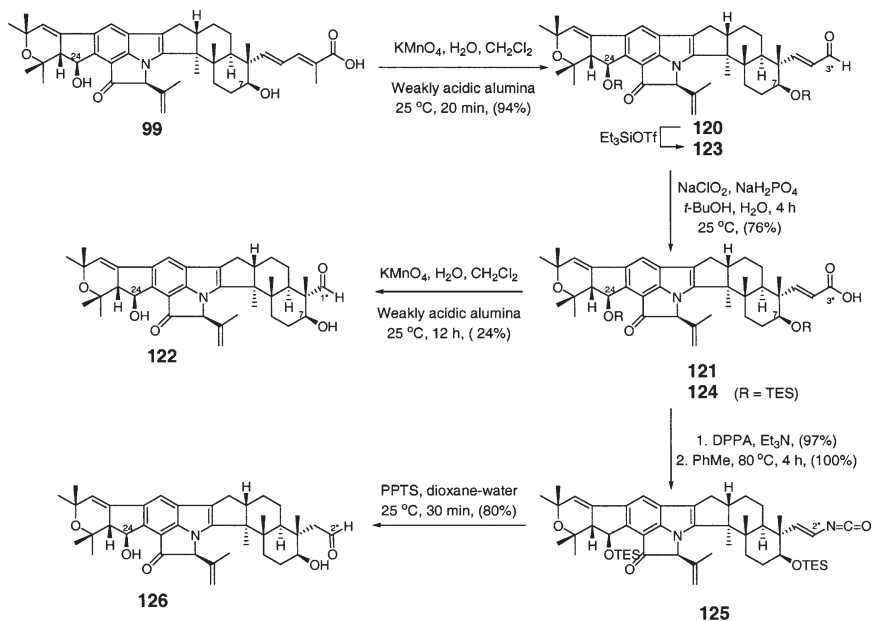
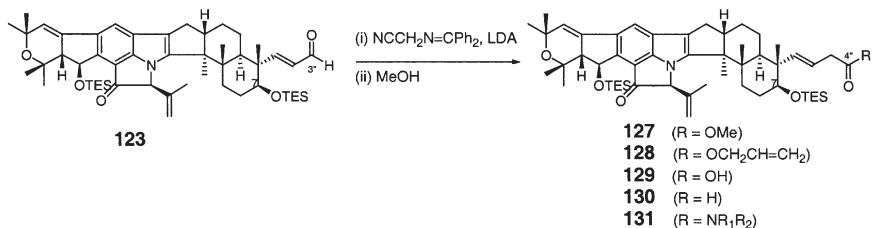
**115** (R = *p*-Br-C<sub>6</sub>H<sub>4</sub>CO)

**119**

### 11. Oxidative Cleavage of the Side Chain of Nodulisporic Acid A (**99**)

After extensive studies, Chakravarty *et al.* (*94*) developed a specific method for the oxidation of the side chain of nodulisporic acid A (**99**). In this method, reaction of nodulisporic acid A with KMnO<sub>4</sub> preadsorbed on weakly acidic alumina produced a 94% yield of 3''-aldehyde **120** on a gram scale, requiring no chromatography. The subsequent oxidation of this aldehyde with sodium chlorite gave the 3''-acid **121** in 76% yield, which, on repeat oxidation with KMnO<sub>4</sub>, gave the 1''-aldehyde **122** in 24% yield (*Scheme 1*). The steric factors around C-1'' caused longer reaction times, which led to poor yields of the 1''-aldehyde (*88,94*). Protection of the hydroxy groups of **120** as the triethylsilyl (TES) ethers led to the formation of the bis-TES ether **123**, which, on sodium chlorite oxidation of the aldehyde group, gave the protected acid **124**. Subsequent reaction of **124** with diphenylphosphoryl azide (DPPA), followed by thermolysis-induced Curtius rearrangement, produced vinyl isocyanate intermediate **125**. Hydrolysis of the isocyanate intermediate with pyridinium *p*-toluenesulfonate (PPTS) afforded the deprotected 2''-acid **126** in a very good yield (*88,95*).

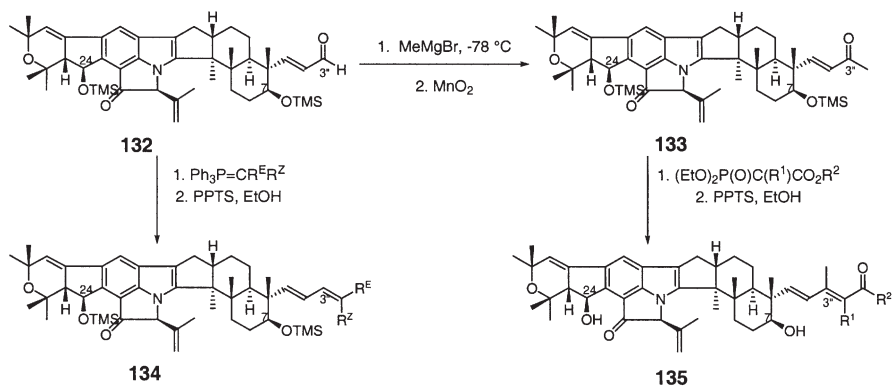
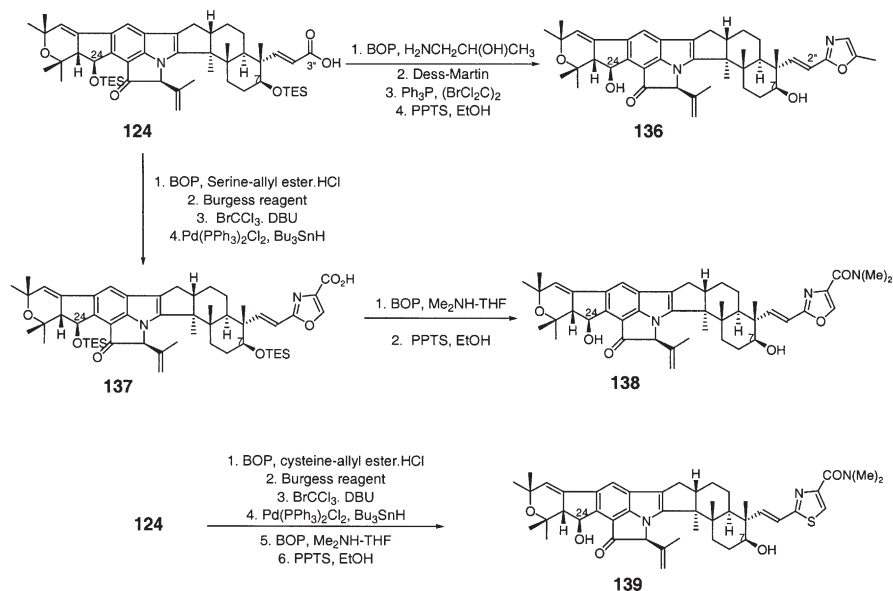
The synthesis of the 4''-carboxylic acid required a different strategy and is illustrated in *Scheme 2*. The bis-TES ether **123** was treated with the lithium enolate of NCCH<sub>2</sub>N=CPh<sub>2</sub> to produce an unstable dienyl intermediate, which on methanolic hydrolysis, gave the methyl ester **127** (*95*). Direct saponification of the methyl ester to the corresponding carboxylic acid was not successful. However, titanium isopropoxide-mediated transesterification led to the formation of the 4''-allyl ester **128**, which was converted to the 4''-acid **129**, the 4''-aldehyde **130**, and a series of simple and substituted amides **131** (*88,95*).

Scheme 1. Oxidative cleavages of the side chain of nodulisporic acid A (**99**).Scheme 2. Side-chain modifications of nodulisporic acid A (**99**).

Methyl Grignard reaction of the bis-TMS-protected 3''-aldehyde **132**, followed by allylic oxidation produced the 3''-methyl ketone **133**. Subsequent olefination of either aldehyde **132** or methyl ketone **133** produced homologs of nodulisporic acids of the types **134** and **135** (Scheme 3) (**96**). However, these reactions were mostly unsuccessful for the formation of the 3''- and 4''-dimethyl homologated derivatives (**88**).

## 12. 2''-Oxazole and 2''-Thiazole Derivatives

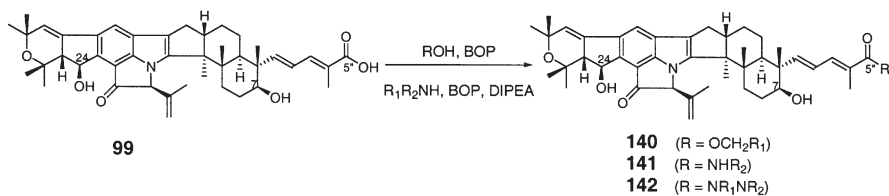
Berger *et al.* (**97**) reported the synthesis of the oxazoles **136**–**138** and the thiazole **139** derivatives from the 3''-carboxy acid **124** following a procedure developed by Wipf and coworkers (Scheme 4) (**98,99**).

Scheme 3. Homologation and other side-chain reactions of nodulisporic acid A (**99**).

Scheme 4. Synthesis of 2''-oxazole and 2''-thiazole derivatives.

### 13. Nodulisporamides

The esters **140** or thioesters of nodulisporic acid A (**99**) were synthesized using Coste's conditions ( $\text{ROH}$ ,  $\text{CH}_2\text{Cl}_2$ , BOP,  $-20^\circ\text{C}$  to rt), whereas BOP-mediated coupling with primary and secondary amines in Castro's conditions efficiently produced the respective amides **141** and **142** (Scheme 5). Meinke and coworkers synthesized a series of esters and amides using these methods and reported the structure activity relationships (100).



Scheme 5. Esterification and amidation of nodulisporic acid A (**99**).

#### 14. Biological Activities of Nodulisporic Acids and Derivatives

The nodulisporic acids were originally discovered by screening natural product extracts against *L. sericata* in an *in vitro* assay, followed by *in vivo* evaluation of the crude extract, fractions, and purified alkaloids against the bedbug *Cimex lectularius*. The details have been recently reviewed by Meinke *et al.* (88). Nodulisporic acid A (**99**), the most potent of the series showed LC<sub>50</sub> (lethal concentration to kill 50% of *L. sericata* larvae) of 300–1000 parts-per-billion (ppb) and was much more potent than known insecticides, except ivermectin, which exhibited an LC<sub>50</sub> of 40 ppb. Among the remaining eight natural nodulisporic acids, only nodulisporic acid A<sub>1</sub> (**101**) was as active as **99**, and exhibited an LC<sub>50</sub> of 300 ppb. The remaining seven were less active (88,92,93). A similar activity profile was also observed when they were evaluated against *Aedes aegypti* mosquito larvae (88,89). Nodulisporic acid A (**99**) was about 10-fold (LD<sub>90</sub> = 0.4 mg/kg) more active than ivermectin (LD<sub>90</sub> = 5 mg/kg) when dosed orally against bedbug infected mice. It exhibited complete paralysis of the parasite (88).

After confirmation of the activity of nodulisporic acid A (**99**) against the aforementioned, commercially nonrelevant targets, *L. sericata* and *A. aegypti*, it was evaluated for its effect against a commercially relevant flea target (*Ctenocephalides felis*) using an artificial membrane flea feeding method (88,101). Nodulisporic acid A (**99**) exhibited 10-fold better activity than ivermectin and displayed an LD<sub>90</sub> of 1 parts-per-million (ppm) compared to an LD<sub>90</sub> of 10 ppm for ivermectin. The remaining natural nodulisporic acids were 5–> 100-fold less active (92,93). This assay provided a method to measure systemic flea efficacy and was a key bioassay used for the evaluation of derivatives from the medicinal chemistry efforts, which provided predictive SAR data.

The systemic evaluation of nodulisporic acid A (**99**) against hard tick (*Dermacentor variabilis*) in a mouse assay did not show any efficacy at 2.5 mg/kg (97). Similarly, nodulisporic acid A (**99**) did not have any effect against either *in vitro* nematocidal assays or an *in vivo* nematode-infected rodent assay (88).

Mechanistically, like ivermectin, nodulisporic acid A (**99**) activates the glutamate-gated chloride ion channel in invertebrates, and, unlike ivermectin, it has no effect against glycine- and GABA-gated chlorine ion channels, which are found in mammals (102,103). The exquisite specificity of nodulisporic acids for

insect-specific neuronal chloride channels leads this alkaloid to selectively paralyze the insects, while having no effect on mammals which naturally lack these channels, thus providing a superior safety profile. The details of the mechanistic studies have been reviewed (88). These studies were made possible by performing binding studies using radiolabeled nodulisporamides and [<sup>3</sup>H]-ivermectin. From these studies, it was observed that there were high affinity binding sites for the radiolabeled nodulisporamides in fly head membranes, but essentially none in the fly body membrane (104). However, there was ample binding observed for [<sup>3</sup>H]-ivermectin in both types of membranes, again indicating the exquisite specificity of nodulisporic acids for those channels present only in fly heads (88,102).

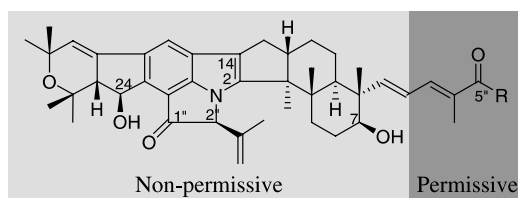
Most importantly, nodulisporic acid A (99) exhibited systemic efficacy against flea infested dogs. In a trial using eight dogs in the treatment group and four dogs in the control group, dogs were challenged with an equal number of fleas, and the treatment group was dosed once orally with 15 mg/kg of nodulisporic acid A (99). Fleas were counted after 48 h post-dosing. Fleas were completely eliminated from the nodulisporic acid A treated animals showing 99.7% efficacy. Repeated flea challenge of dogs with new fleas after every 48 h and examination of dogs after 48 h post-dosing revealed 96.6% and 50.5% efficacy after 4 and 6 days, respectively. No efficacy was observed after 6 days. A large number of dead fleas were recovered from the treatment group and none from the control group of dogs. Furthermore, the dogs did not exhibit any adverse effects (88).

Nodulisporic acid A (99) showed a maximum blood plasma concentration ( $C_{max}$ ) of 2  $\mu$ g/mL 8 h post oral dosing at 15 mg/kg and a plasma half life of 19.3 h. It exhibited first-order kinetics of drug elimination from blood. A similar pharmacokinetic profile was exhibited by nodulisporic acid A (99) when dosed at 1.5 mg/kg iv, except for the expected observation of the  $C_{max}$  at one hour earlier, and a half life of 23 h (88). A 20% bioavailability was observed for nodulisporic acid A. Nodulisporic acid A did not show any toxicity to mice at 100 ppm (of feed) and dogs at 15 mg/kg orally, the highest dose tested.

### 15. Medicinal Chemistry and SAR of Nodulisporic Acid A

It was very clear from the *in vivo* activity of nodulisporic acid A (99) that it had great potential as a significant chemical lead for further development as a flea control drug. Therefore, a significant medicinal-chemistry effort was launched at Merck Research Laboratories. Chemical modification of the various accessible sites of nodulisporic acid A, including preparation of a variety of esters and amides of the 5''-carboxylic acid, derivatization of the C-7 and C-24 alcohols, including ethers, acylation, and oxidation, 1''-carbonyl reductions with either hydride or Grignard reagents, 2'-epimerizations, 23,24-dehydrations, indole-2,14-oxidative cleavage, and oxidative cleavages (94) of the two olefins followed by subsequent modifications (95–97) of resulting alkaloids (as described earlier) led to the identification of a number of more potent and pharmacologically more desirable anti-flea alkaloids. This allowed for the definition of the “permissive” and

TABLE XI.

Amide Derivatives of Nodulisporic Acid A (**99**) and Anti-Flea Activity.

Compound	R	Flea (ppm)
<b>99</b>	OH	1
<b>143</b>	NHCH <sub>2</sub> CH <sub>2</sub> OH	0.5
<b>144</b>	N(Me)Et	0.1
<b>145</b>	NHCH <sub>2</sub> (2-tetrahydrofurfuryl)	0.1
<b>146</b>	NHCH <sub>2</sub> OPh(4-OMe)	0.1
<b>147</b>	NMe <sub>2</sub>	~0.1
<b>148</b>	NHC(Me <sub>2</sub> )C(O)NMe <sub>2</sub>	0.01
<b>149</b>	N-1-[4-SO <sub>2</sub> Me]piperaziny]	0.01

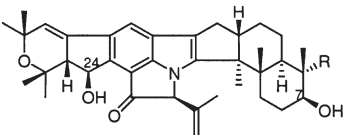
“non-permissive” structural regions of nodulisporic acid A as illustrated in Table XI (88). The most pharmacologically important series were the C-5' amides. Selected amides are listed in Table XI. In general, nodulisporic acid A esters, aliphatic amides with polar groups other than hydroxyls (e.g., **143**) were biologically not interesting. However, a variety of other intermediate-sized structurally diverse amides, exemplified by **143–149**, were some of the better compounds that showed enhanced systemic flea efficacy (Table XI) (88,100). Nodulisporamides **148** and **149** were at least 100-fold better than nodulisporic acid A (**99**) in the artificial membrane feeding assay. Recently, a comparison of flea and *L. sericata* activity of nodulisporamides was reported. In general, the derivatives that were more active against flea were also more active against *L. sericata* (105).

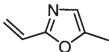
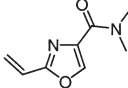
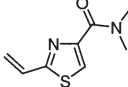
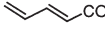
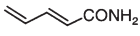
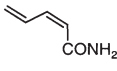
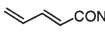
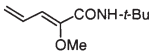
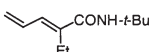
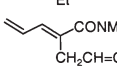
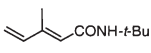
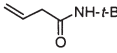
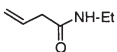
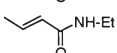
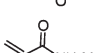
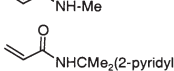
Nodulisporamides **144**, **145**, and **146** were further evaluated *in vivo* as a flea control agent in a dog model. Like nodulisporic acid A (**99**), 15 mg/kg of each alkaloid was administered once orally to two dogs each. It was found that these alkaloids were more efficacious than nodulisporic acid A. They were 100% effective against fleas for 8 days. Nodulisporamides **144** and **145** were >90% efficacious for 2 weeks postdosing. The amide **146** was slightly less efficacious. The efficacy of these alkaloids was consistent with their improved pharmacokinetic profiles (88,106).

Selected analogs were derived from other modifications of C-2' to C-4' and their activity is presented in Table XII. While some of the alkaloids showed



TABLE XII.  
Selected Nodulisporic Acid A Derivatives and Their Anti-Flea Activity.



Compound	R	Flea (ppm)	Flea/dog (mg/kg/days)	Ref.
150		10	10/< 14	(97)
151		1	10/~ 14	(97)
152		1	NR	(97)
153		1	NR	(96)
154		~ 1	NR	(96)
155		10	NR	(96)
156		~ 0.1	NR	(96)
157		~ 1	NR	(96)
158		1	NR	(96)
159		~ 1	NR	(96)
160		1	NR	(96)
161		1	NR	(95)
162		~ 10	NR	(95)
163		~ 10	NR	(95)
164		~ 10	NR	(95)
165		1	NR	(95)

NR, not reported.

enhanced activity over nodulisporic acid A (**99**), none were profoundly better than the simple amides presented in the Table XI.

Nodulisporic acids are a novel class of nontremorgenic indole diterpenoids with insecticidal properties and a mechanism of action similar to the avermectins, but with an improved therapeutic index and an unparalleled safety profile. This class of alkaloids represents an unprecedented structural type for the control of fleas on dogs and cats.

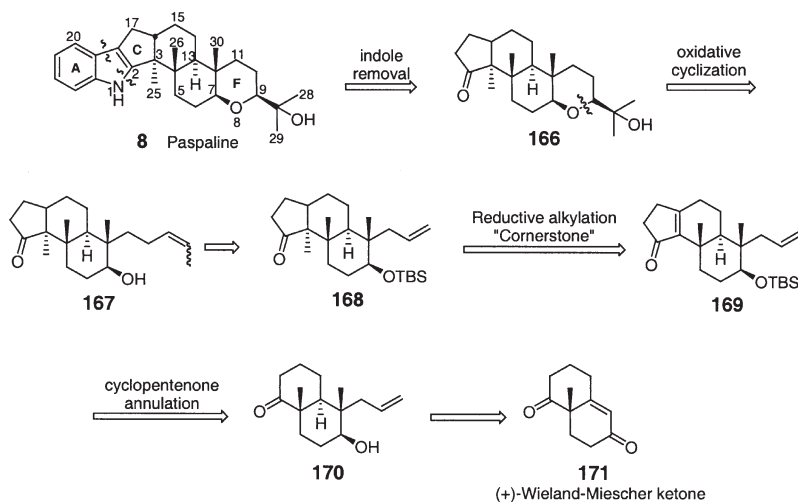
### III. Synthesis

The total synthesis of paspaline by Smith and coworkers (107–109) represents the first effort toward the synthesis of the tremorgenic indole alkaloids. To date, the total syntheses of four tremorgenic indoles have been achieved: paspaline, paspalicine, paspalinine, and penitrem D. In addition, the total synthesis of nodulisporic acid A is close to fruition. This section will outline the published total syntheses and the efforts toward total syntheses.

#### A. THE PASPALANES

##### 1. The Total Synthesis of Paspaline

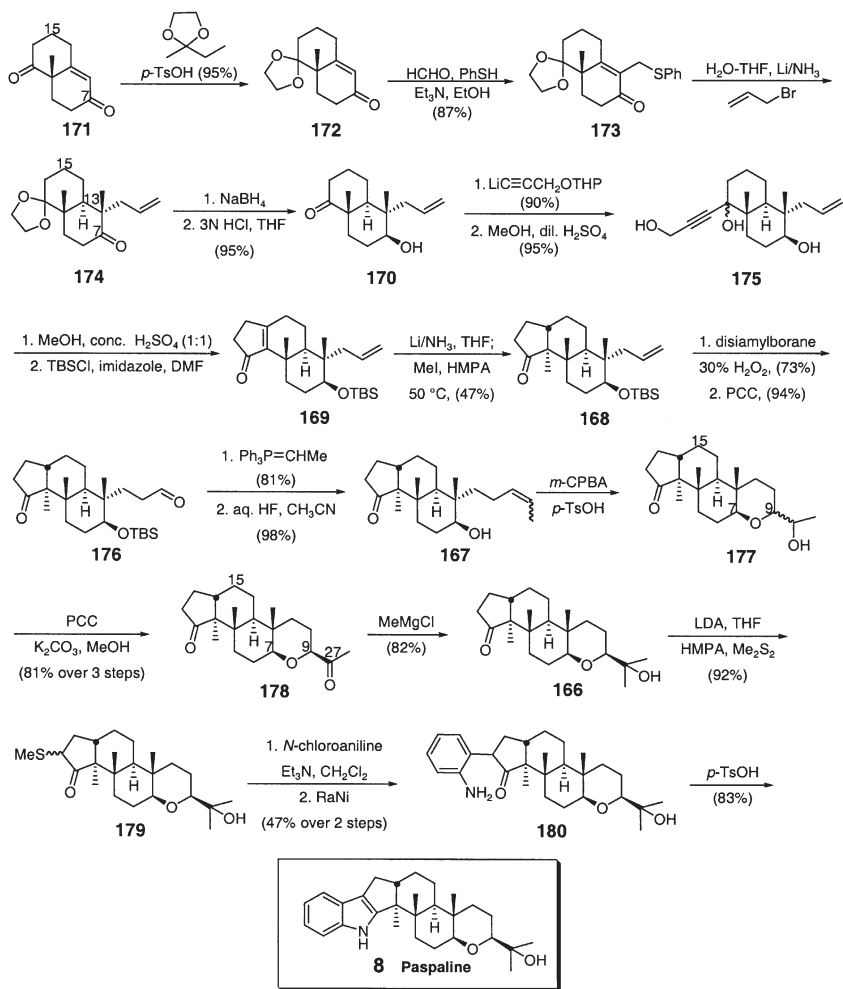
*a. First Generation Synthesis of Paspaline.* The retrosynthetic analysis of paspaline, as outlined in Scheme 6, begins with removal of the indole ring, to be introduced ultimately via a Fisher (110) or Gassman (111) indole synthesis.



Scheme 6. Retrosynthetic analysis of paspaline (**8**).

Intermediate **166** would then arise from the acid-promoted cyclization of tricyclic ketone **167**. Ketone **167** would evolve from a two-carbon extension of the allyl side chain of **168**, thus leading to what the authors describe as the “Cornerstone” of their synthetic strategy: reductive alkylation of enone **169** to afford the *trans*-cyclopentenone **168**. Enone **169** would be derived from the Wieland–Miescher ketone **171** (*112*).

As outlined in [Scheme 7](#), the synthesis commences with the (+)-Wieland–Miescher ketone **171** (*112*). A three-step sequence, involving the chemoselective



Scheme 7. First generation total synthesis of paspaline (**8**) (*107–109*).

transketalization protocol of Kirk and Petrow, afforded enone **173** in 87% overall yield (113). Reductive alkylation of **173** with allyl bromide gave ketone **174**, which was stereoselectively reduced with sodium borohydride (114). Subsequent deketalization afforded a 4:1 mixture of the desired alcohol **170** and its C-7 epimer. Alcohol **170** was then treated with the lithium anion derived from the THP ether of propargyl alcohol to generate, after acid catalyzed removal of the THP protecting group, triol **175**. Triol **175** was briefly exposed to a mixture of concentrated H<sub>2</sub>SO<sub>4</sub> and MeOH, followed by reaction of the product mixture with *tert*-butyldimethylsilyl chloride and imidazole to afford enone **169**. It should be noted that in addition to the desired product **169**, formed in 25% yield, the authors also report three minor side products whose structures are not listed here. The key synthetic step in this sequence was the stereoselective reductive alkylation of cyclopentenone **169** to generate the core structure **168**. Here the authors describe in excellent detail their failed attempts to generate the desired *trans* alkylation product **168**. Eventually however, the authors were able to generate **168** in synthetically useful yields by reduction of **169** with lithium in liquid ammonia followed by inverse addition of the derived enolate to a warm solution of MeI–HMPA. Completion of the diterpene unit of paspaline was subsequently achieved via a two-carbon extension of the allyl group of **168** over four steps to give the homologated keto olefin **167** as an 85:15 *E–Z* mixture. Treatment of alcohol **167** with *m*-CPBA followed by a catalytic amount of *p*-TsOH afforded a mixture of C-9 epimeric alcohols **177**. The mixture was subsequently treated with PCC to generate the corresponding diketones, which, after equilibration with K<sub>2</sub>CO<sub>3</sub> in MeOH, followed by recrystallization from hexane–ether, gave a 95:5 mixture of **178** (major isomer shown) in 81% yield (initial ratio before equilibration and recrystallization was 2.2:1). Methylation of the C-27 ketone proceeded with high chemoselectivity, completing the diterpene portion of paspaline, namely **166**.

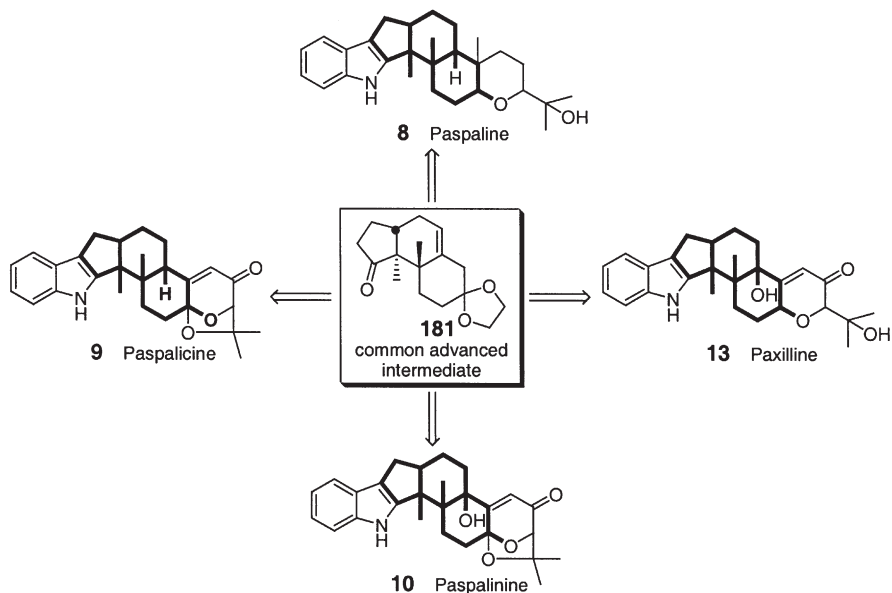
The final stage in the synthesis of paspaline was the nontrivial introduction of the indole ring. After successful construction of indoles using model ketones, the authors proceeded to incorporate the indole following the Gassman protocol (111). Thus advanced intermediate **166** was converted to the epimeric methylthio keto anilines which were reduced with Raney nickel to furnish aminophenyl ketone **180** in 47% yield from **179**. Acid-catalyzed cyclization to the indole completed the synthesis of paspaline (**8**), which was spectroscopically identical to an authentic sample.

In summary, the first total synthesis of (–)-paspaline was achieved in 23 steps from the Wieland–Miescher ketone, affording the target alkaloid in high enantiomeric purity. The authors also describe an analogous synthesis of C-3-epi-paspaline, the details of which can be found in Ref. (106).

*b. Second Generation Synthesis of Paspaline: Development of a Unified Synthetic Strategy.* With the first account in 1985 of the total synthesis of (–)-paspaline, Smith and coworkers reported extreme difficulty with the stereoselective introduction of the quaternary vicinal centers at C-3 and C-4, and acknowledge

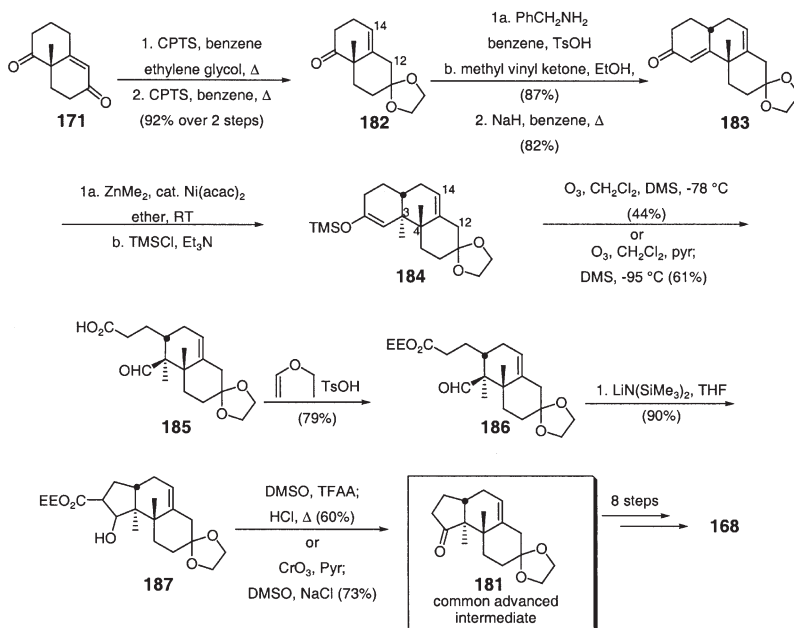
that the route was not readily amenable to other members of this class. Thus they embarked on the development of a stereocontrolled synthesis of a common intermediate, which would lead to a more efficient, second-generation synthesis of (–)-paspaline, and provide what they describe as a “unified strategy . . . applicable to the entire class of simple indole diterpenes” (115). This effort led to the synthesis of the advanced intermediate **181** (Scheme 8), which was used in the second-generation syntheses of paspaline (**8**), as well as paspalicine (**9**) and paspalinine (**10**).

In 1988, Smith and coworkers reported an efficient synthesis of intermediate **181** in 9 steps (9.4% overall yield) from (+)-Wieland–Miescher ketone (**171**) (108,115,116). A full account of this synthesis, including an alternate 14-step route is described (115). Later, when Smith and coworkers reported the synthesis of paspalinine and paspalicine, they described an improved synthesis of intermediate **181**, whereby the yield was increased from 9.4% to 21%, and it is this improved synthesis, which will be described here (Scheme 9) (117). In summary, ketone **171** was converted into ketal **182** using a modified Paquette ketalization protocol (118) to afford a (1:1) mixture of  $\Delta^{13,14}$ - and  $\Delta^{12,13}$ -ketals (67%). Subsequent equilibration of the products by exposing the mixture to the same acidic conditions in the absence of ethylene glycol, increased the amount of the more thermodynamically stable  $\Delta^{13,14}$ -ketal **182** to 9:1, in 85% overall yield. A two-step Robinson annulation (119) then afforded tricyclic enone **183**. With **183** in hand, the most efficient approach to the introduction of the C-3 quaternary methyl



Scheme 8. Common advanced intermediate for the synthesis of the paspalane family of indole diterpenes (115).

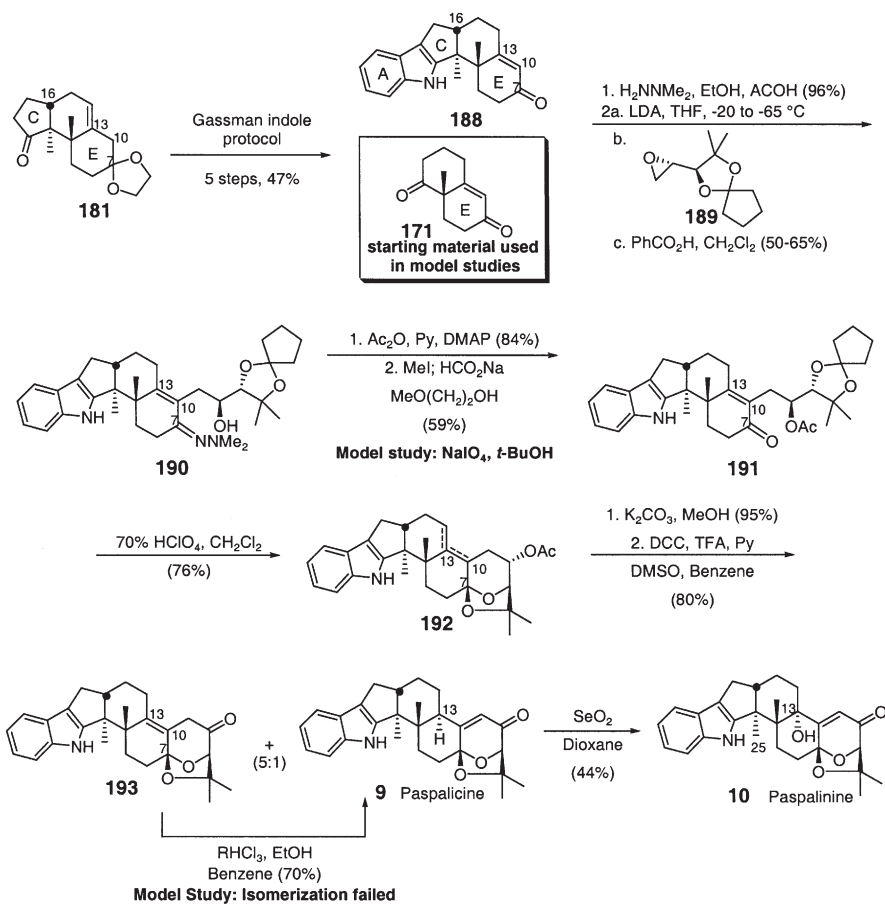
group would be through direct 1,4-conjugate addition. Here, the authors examined several routes to effect this transformation without success, given the steric hindrance at the  $\beta$ -carbon. In spite of the difficulty, the authors were able to generate the desired 1,4-adduct **184** using conditions described by Luche (*120*). Thus, treatment of **183** with dimethylzinc and a catalytic amount of nickel acetylacetonate, followed by quenching with trimethylsilyl chloride gave the elusive 1,4-adduct in 90–95% yield! This highly effective 1,4-addition procedure is presumed to be a direct result of the thermal stability of the organozinc reagent, which allows for the addition to take place at room temperature. Silyl enol ether **184** was then ozonized to the corresponding carboxy aldehyde **185**, which was subsequently esterified to afford **186**. Closure of the five-membered ring using lithium hexamethyldisilazide generated a mixture of  $\beta$ -hydroxy esters **187**. Oxidation following the Swern trifluoroacetic anhydride-DMSO protocol (*121*) gave the corresponding  $\beta$ -keto esters that were hydrolyzed with concomitant decarboxylation to afford target compound **181**. The yield for this final transformation was later improved (*117*) by replacing the Swern conditions with the Collins oxidation protocol (chromium trioxide, pyridine)(*122*) which, after decarboxylation following the Krapcho procedure (sodium chloride in hot DMSO)(*123*) afforded **181** in 73% versus 60% yield. Completion of the second-generation synthesis of paspaline (**8**) involved an eight-step transformation of **181** to **168**, an advanced intermediate in the first total synthesis of paspaline (**8**) (Scheme 9).



Scheme 9. Second generation synthesis of paspaline (**8**) (*117*).

## 2. The Total Syntheses of Paspalicine (9) and Paspalinine (10)

*a. First Generation Synthesis.* The total syntheses of paspalicine (9) and paspalicine (10) (Scheme 10) were initially reported by Smith and coworkers as a communication in 1990 (124), with the full paper appearing in 1992 (117). Unlike the paspaline synthesis, whereby the indole ring was incorporated late in the synthesis, here the authors chose to convert advanced intermediate **181** into the indole derivative **188**, thus first constructing the ABCDE-ring system (following Gassman protocol, see Scheme 7, 166–180). Before embarking on the next key step involving the coupling of enone **188** with epoxide **189** (generated in six steps starting from 3-methyl-2-buten-1-ol) the authors investigated these final reactions on model systems, resulting in the independent synthesis of the D–G rings of



Scheme 10. First generation syntheses of paspalicine (9) and paspalinine (10) (117,124).

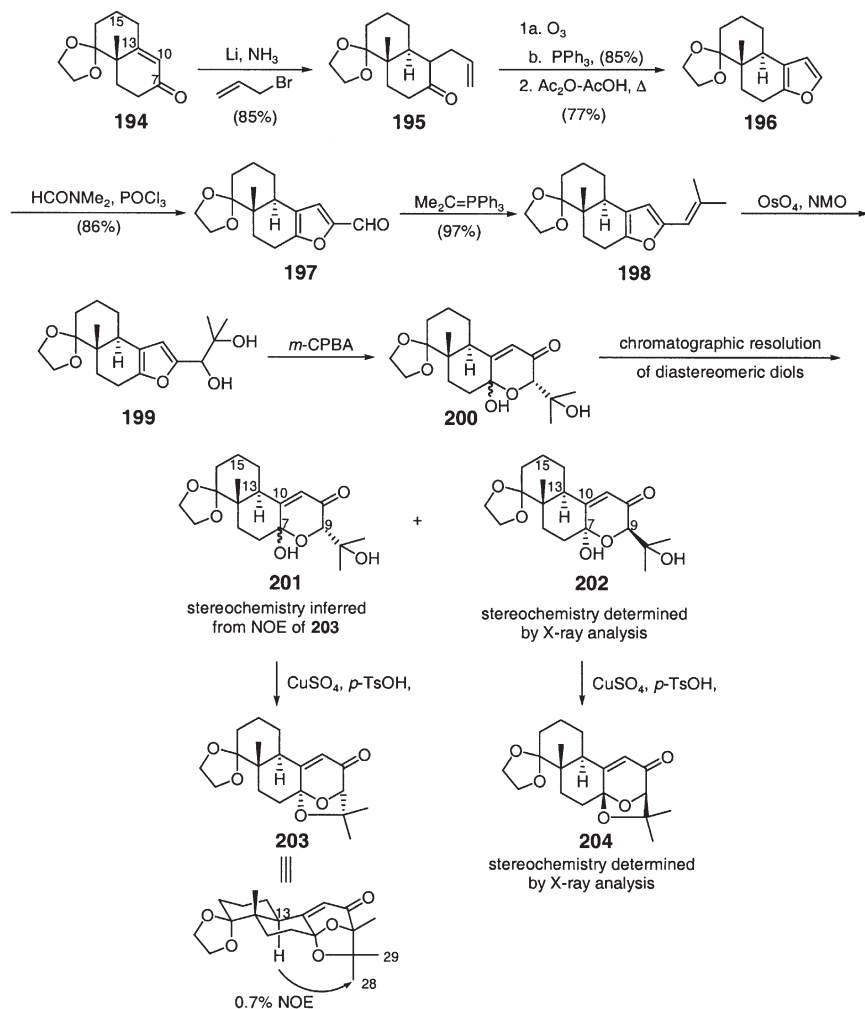
paspalicine. The authors were also able to construct the equivalent D–G rings of paspalinine, but only as the C-13 epimer. The steps whereby the chemistry developed in the model system differed from the real system are noted in [Scheme 10](#).

Following the Stork metalloenamine protocol, enone **188** was successfully coupled to epoxide **189** to generate a mixture of  $\Delta^{10,13}/\Delta^{13,14}$  double-bond isomers. However, brief exposure to benzoic acid gave exclusively the desired  $\alpha,\beta$ -hydrazone **190**. Acetylation of **190** was followed by removal of the hydrazine moiety via quaternization with MeI and hydrolysis of the derived sodium salt with sodium formate to afford **191** as the major product in 59% yield. Acid-catalyzed deketalization with concomitant cyclization afforded **192** as a 2:1 mixture of  $\Delta^{10,13}$ - and  $\Delta^{13,14}$ -bicyclic ketals. Deacetylation of the mixture **192** furnished, after chromatographic separation, the corresponding  $\Delta^{10,13}$ -alcohol (67%) and the  $\Delta^{13,14}$ -alcohol (28%). Moffatt oxidation of the desired  $\Delta^{10,13}$  alcohol gave a 5:1 mixture of  $\beta,\gamma$ -enone **193**, and paspalicine (**9**). In contrast to their findings with their model systems, the authors could successfully isomerize the olefin of **193** using the Clive modification of Grieco's rhodium chloride protocol ([125](#)), thus affording paspalicine (**9**) as the only product in 70% yield. The structure of synthetic paspalicine was confirmed via single-crystal X-ray analysis and by comparison with an authentic sample. Allylic oxidation of paspalicine (**9**) to generate paspalinine (**10**) was achieved with selenium dioxide in 44% yield. The synthetic material **10** was found to be spectroscopically identical to a sample of authentic alkaloid.

*b. Toward Paspalicine: Synthesis of Rings D–G.* In 1991 a group at the University of Leeds reported an independent approach to the D–G rings of paspalicine (**9**), which they believed offered an efficient alternative to the route developed by Smith and coworkers (preliminary communication 1989, full paper 1991) ([126,127](#)). In this approach, synthesis of the D–G rings revolved around the synthesis of the crucial intermediate aldehyde **197**, which could be generated from the monoketal of the (+)-Wieland–Miescher ketone, namely **194** ([Scheme 11](#)). Thus, reductive alkylation of **194** with lithium–liquid ammonia, followed by allyl bromide addition generated the  $\alpha$ -substituted ketone **195**. The product **195** was subsequently ozonized and the resulting keto-aldehyde cyclized to the furanodecalin derivative **196**. Formylation of **196** by the Vilsmeier–Haack procedure afforded intermediate aldehyde **197**. Wittig condensation of aldehyde **197** with the appropriate triphenylphosphorane gave alkene **198**, which, upon treatment with OsO<sub>4</sub>, followed by oxidative ring expansion with *m*-chloroperbenzoic acid, gave a mixture of diols, **201** and **202**, which were readily separated. X-ray crystallography showed one of these diols to have structure **202**, as shown in [Scheme 11](#), possessing the desired C-9 paspalinine/paspalicine stereochemistry alpha to the carbonyl group. Cyclization with copper sulfate via the oxonium ion generated the desired  $\beta$ -pyrone ketal **204**, having the paspalinine/paspalicine stereochemistry, as determined by single crystal X-ray analysis.

The second diol generated from the oxidative ring expansion of **199** was deduced to have the structure **201** shown in [Scheme 11](#). Cyclization of **201** with





Scheme 11. The synthesis of the D-G rings of paspalicine (126,127).

copper sulfate generated  $\beta$ -pyrone ketal **203**, possessing the undesired stereochemistry at C-9 as determined by the observation of the small NOE between H-13 and Me-28/29. It should be noted that in the preliminary 1989 communication, the authors reported that *both* of the individual diols **201** and **202** cyclized in the presence of copper (II) sulfate to give the *same* undesired  $\beta$ -pyrone ketal **203**. This was based on comparison of the  $^1\text{H}$  NMR spectra of the semi-purified products of very small-scale cyclizations. Unfortunately, the authors reported that the original samples and NMR data were misplaced, so it was not possible to re-examine the data (128).

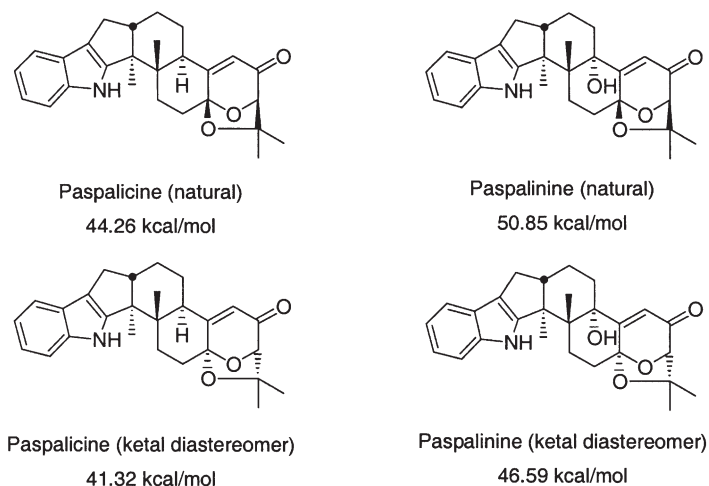
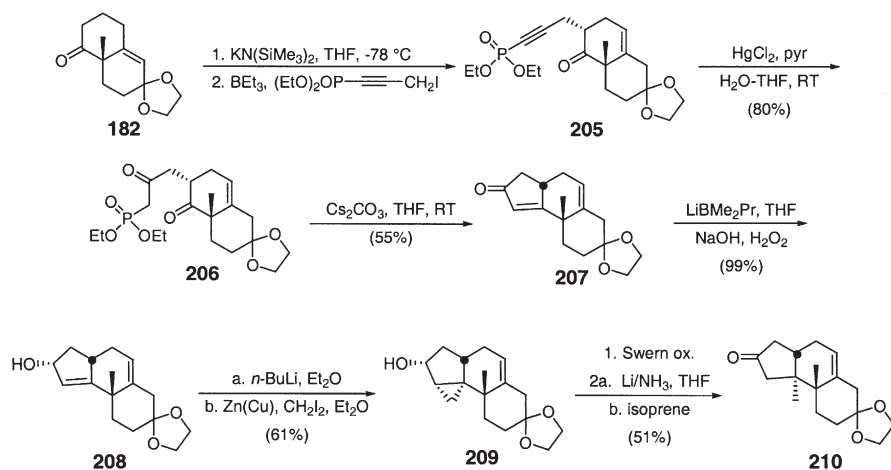


Figure 1. MM2 energy minima for paspalcine, paspalinine, and ketal diastereomers (117).

The 1989 communication by the Saxton group, which reported that both diols **201** and **202** furnished the undesired ketal **203**, prompted the Smith group to examine whether or not the unnatural ketal **203** was in fact thermodynamically preferred. Thus they calculated the enthalpy differences for a model pair of diastereomeric ketals (data not shown here), as well as for paspalcine and paspalinine (Fig. 1) (117). The computations were done with the MM2 forcefield (MACROMODEL v 2.5) (129). For each structure listed in Fig. 1, two geometries were used: a chair conformation for ring D and both chair and boat conformations for ring E. Each system was allowed to minimize until the gradient RMS was  $< 0.01$  and these results are summarized in Fig. 1. The calculations revealed that in the model and paspalinine/paspalcine systems, the unnatural bicyclic ketal moiety was the thermodynamically preferred, with energy differences of 4.26 (paspalinine diastereomeric pairs) and 2.94 (paspalcine diastereomer pairs) kcal/mol.

*c. Toward Paspalinine (10): Synthesis of the C/D Rings.* After the successful construction of the D–G ring system of paspalinine (Scheme 11), the Saxton group focused their effort of the preparation of the C/D ring system (130). The difficulties encountered by Smith and coworkers in the synthesis of the *trans* C/D ring system prompted the authors to investigate a different approach, whereby an isomer of the Smith ketone **181** was envisioned to serve as the key synthetic intermediate, namely **207**. Ketone **207** was readily accessible from monoketal **182** of the (+)-Wieland–Miescher ketone. Alkylation of **182** gave the ketophosphonate **205**, whereby the introduced alkyl group is equatorial. Hydration of **205**, following Corey's method (131), gave the diketo phosphonate **206**, which was subsequently cyclized via an intramolecular Wadsworth–Emmons reaction to afford the desired



Scheme 12. Synthesis of the C/D rings of paspalinine (**130**).

cyclopentenone **207**. Intermediate **207** was then stereoselectively reduced to the  $\alpha$ -allylic alcohol **208** in excellent yield. Cyclopropanation of **208** with butyl-lithium and the Simmons–Smith reagent gave the hydroxycyclopropane **209**. Oxidation and cleavage of the cyclopropane ring then gave the target ketone **210**, comprising the C/D rings of paspalinine, the structure and stereochemistry of which was confirmed by X-ray analysis. Though the synthesis of **210** appeared in 1992, further elaboration of **210** to generate paspalinine has not yet been reported (Scheme 12).

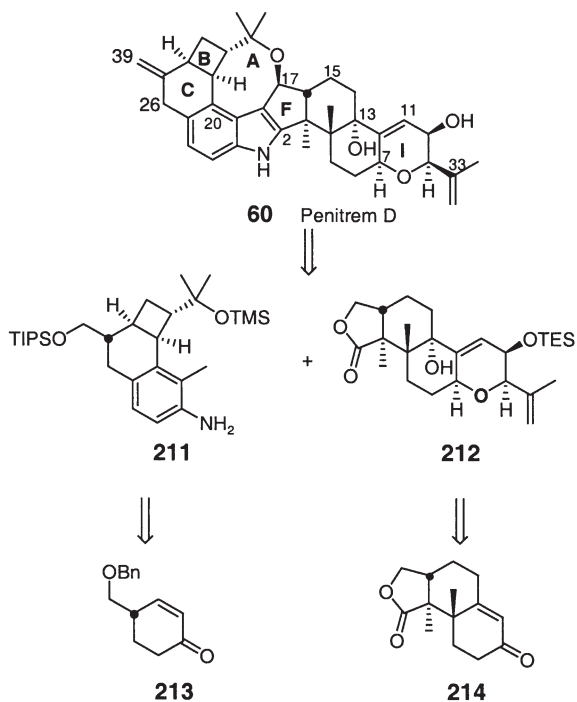
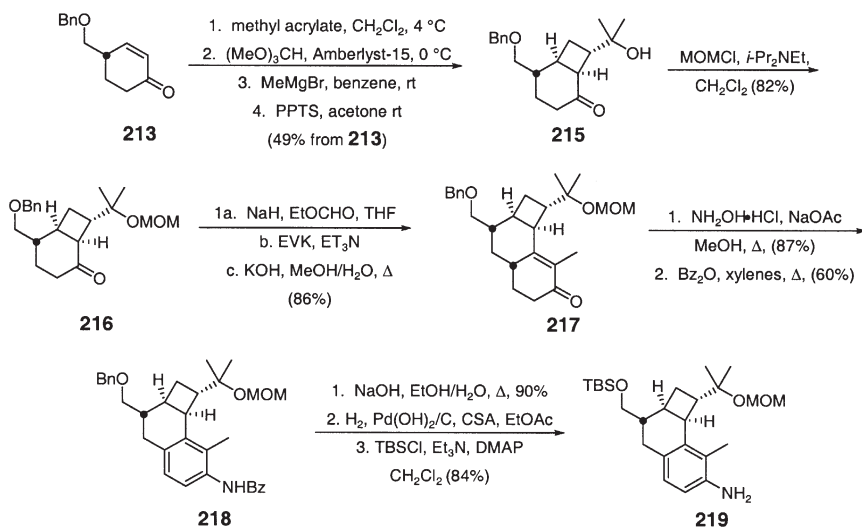
## B. PENITREM D

### 1. Retrosynthetic Analysis

With the syntheses of paspaline, paspalicine, and paspalinine completed, Smith and coworkers embarked on the next target, the more complex penitrem D, with penitrem D (**60**) as the initial synthetic goal (**132**). Penitrem D possesses several synthetically challenging structural elements, namely, a highly substituted indole core, an eight-membered oxocane, nine fused rings, eleven stereogenic centers, and two allylic hydroxyl groups. The molecule was thus divided into western and eastern hemispheres, **211** and **212**, with the eastern hemisphere being derived from lactone **214**, and the western hemisphere ultimately arising from enone **213** (Scheme 13). A summary of the key transformations involved in the synthesis of penitrem D will be presented.

### 2. Synthesis of the Western Hemisphere

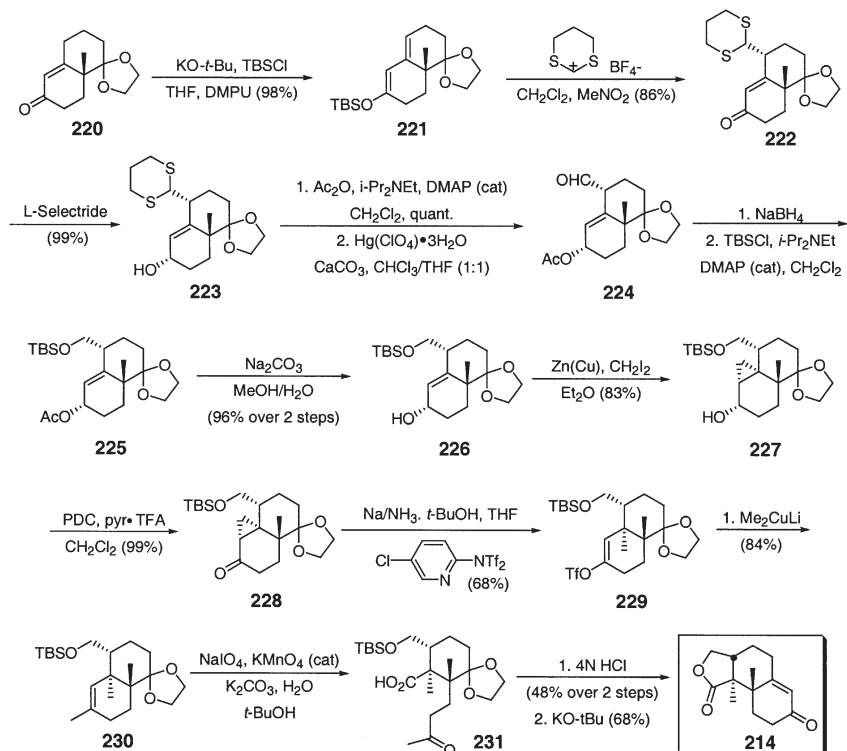
The synthesis of the western hemisphere **211** of penitrem D (Scheme 14) was reported as a communication in 1988 (**132**). The synthesis of **211** began with enone **213**, which was obtained in 77% yield from 3-ethoxy-2-cyclohexenone by the

Scheme 13. Retrosynthetic analysis of penitrem D (**60**) (*132*).Scheme 14. Synthesis of the western hemisphere of penitrem D (**60**) (*132*).

method of Stork and Danheiser (133). Enone **213** was irradiated in the presence of methyl acrylate to furnish a complex mixture of photoproducts, which were carried through the next synthetic sequence without purification (Scheme 14). Thus, the mixture was subjected to ketalization, followed by Grignard addition, and deketalization to afford, after purification, the keto alcohol **215** in 49% yield from **213**. Protection of **215** as the MOM ether, followed by Robinson annulation of **216** introduced the D ring of penitrem D, in the form of enone **217**. Enone **217** was then converted into the corresponding oxime, which was subjected to a Semmler–Wolff reaction to aromatize ring D (134,135). Hydrolysis of the benzamide, followed by a benzyl ether to TBS protecting group switch, completed the construction of the western subunit **219**. The overall yield for this 15-step sequence was 10.5% (132).

### 3. Synthesis of Eastern Hemisphere

The eastern portion of penitrem D is derived from tricyclic lactone **214** (Scheme 15). For the more complex penitrem class of indole diterpenes, lactone **214** serves as a common advanced intermediate, as **181** did in the syntheses of the

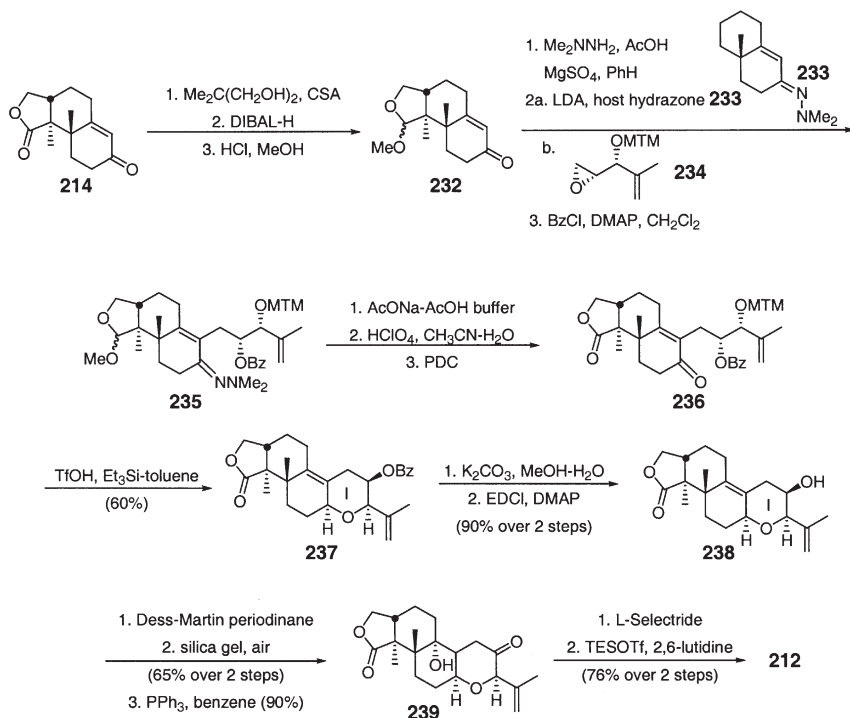


Scheme 15. Construction of the advanced F–H ring precursor for the synthesis of penitrem D (137).

paspalanes. Here, the lactone **214** is required for the successful construction of the indole nucleus, as the structural complexity of the penitremes prevents use of the Gassman protocol for the incorporation of the indole moiety. To this end, Smith and coworkers reported three asymmetric syntheses of **214** (*136,137*). The most improved, third-generation synthesis will be summarized here (*137*).

Lactone **214** is ultimately derived from the monoketal of the (–)-Wieland–Miescher ketone, **220** (the enantiomer of **170**). The monoketal **220** was exposed to potassium *tert*-butoxide and the derived thermodynamic enolate trapped with TBSCl to afford the silyl dienol ether **221**. Alkylation of **221** with 1,3-dithienium tetrafluoroborate generated the desired  $\gamma$ -alkylation product **222** ( $\alpha:\beta=3.5:1$ , major product shown) in 86% yield. Crystallization of the epimeric mixture afforded pure **222**, whose structure was confirmed via X-ray analysis. Ketone **222** was then stereoselectively reduced with L-selectride to afford the desired  $\alpha$ -alcohol **223**. Acylation, followed by dithiane removal, generated aldehyde **224**, which was reduced, and the resulting alcohol protected as the TBS ether. Removal of the acetate protection group of **225** afforded cyclopropanation substrate **226**. This five-step sequence to transform **223** to **226** proceeded with an overall yield of 84%. The authors report an alternative three-step sequence to generate **226** from **223**, however, diminished yields (42%) for the shorter sequence were observed. The hydroxyl-directed cyclopropanation/reductive ring opening, which transformed **226** into the *trans* ring fused product **229**, was the key step for the successful generation of lactone **214**. In summary, Simmons–Smith (*138,139*) cyclopropanation of allylic alcohol **226** generated cyclopropane **227**, whose relative stereochemistry was deduced by NOE. Oxidation of **227** was followed by dissolving metal reduction to generate the *trans* ring fusion product **229**.  $\sigma$ -Bond olefination of **229** with lithium dimethylcuprate then provided **230** in 84% yield. After several attempts to effect oxidative cleavage of the trisubstituted olefin **230**, the authors found success using a modification of the Lemieux–von Rudloff protocol (*140*) to generate the keto acid **231**. Without purification, **231** was exposed to 4N HCl, which removed the TBS and ketal protecting groups and promoted lactonization. Ring closure of the corresponding diketone then furnished the tricyclic lactone **214**. Thus, lactone **214** was synthesized in 15 steps from the (–)-Wieland–Miescher ketone in 8.3% overall yield.

With lactone **214** in hand, completion (Scheme 16) of the eastern hemisphere commenced with a three-step sequence to furnish a mixture of  $\alpha$ - and  $\beta$ -acetals **232** (*141*). The mixture of isomers **232** was separated (on a preparative scale, the  $\alpha$ - and  $\beta$ -acetals **232** were carried forward without separation) and individually converted into the corresponding dimethyl hydrazones. Metalloenamine coupling with epoxide **234** (*142*) in the presence of host dimethyl hydrazone **233**, followed by benzoate protection of the hydroxyl groups, afforded the individual  $\alpha$ - and  $\beta$ -isomers **235**. Concomitant hydrolysis of the hydrazone and acetal groups was followed by PDC oxidation to generate lactone **236**. Treatment of **236** with TfOH removed the MTM moiety, which induced cyclization to generate ring I and silane reduction of the resulting hemiacetal furnished exclusively the *cis* pyran **237**. Removal of the benzoyl group caused partial hydrolysis of the

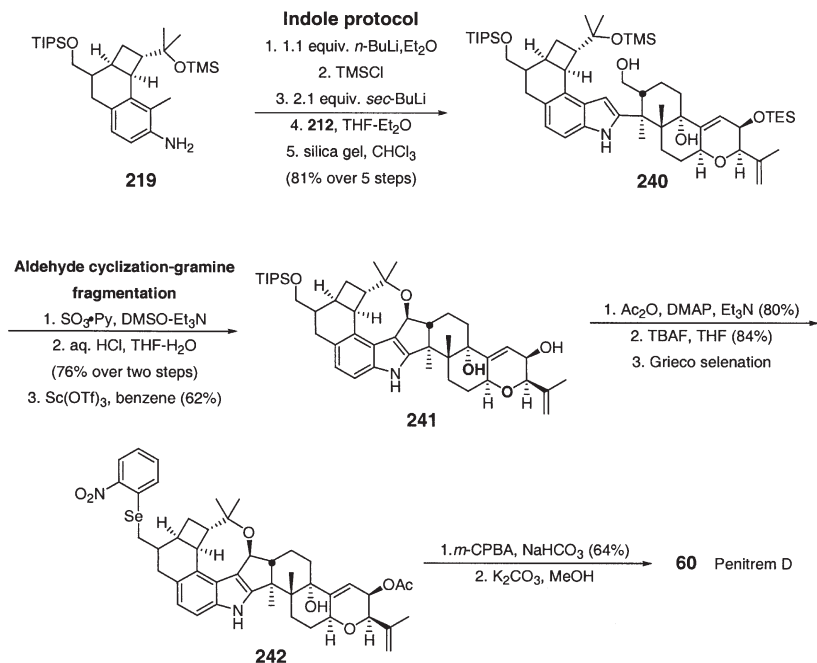


Scheme 16. Completion of the eastern hemisphere of penitrem D (**60**) (141).

lactone, which was restored with EDCI. Dess–Martin oxidation of **238** gave the  $\beta,\gamma$ -unsaturated ketone, which was auto-oxidized to the corresponding tertiary hydroperoxide, reduction of which with  $\text{PPh}_3$  gave alcohol **239**. Stereoselective reduction of the ketone followed by protection as the TES ether completed the synthesis of the eastern hemisphere **212** (Scheme 16), the structure of which was confirmed by X-ray analysis.

#### 4. Completion of Penitrem D (**60**)

To complete the synthesis of penitrem D (**60**), the authors first explored routes for the synthesis of 2-substituted indoles. This led to the report of an efficient synthesis of such indoles whereby *o*-toluidine derivatives were condensed with esters and lactones (143,144) and this synthetic protocol was then applied to the synthesis of penitrem D (141). Here, treatment of the western hemisphere **219** with *n*-BuLi, followed the by addition of **212** resulted in acylation of the lactone carbonyl. *In situ* Peterson olefination generated intermediate **240** in 81% overall yield (Scheme 17). Parikh–Doering (145) oxidation followed by TMS and TES removal afforded an equilibrium mixture of alkaloids (intermediates not shown here) which were treated with  $\text{Sc}(\text{OTf})_3$ . The  $\text{Sc}(\text{OTf})_3$  promoted an aldehyde

Scheme 17. Completion of penitrem D (**60**) (141).

cyclization-gramine fragmentation which was followed by capture of the intermediate carbocation by the tertiary C-17 hydroxyl group to construct rings A and F in a highly stereoselective manner (>95:5). Acylation of the C-10 hydroxyl and removal of the TIPS group was followed by selenation, following Grieco's (146) protocol, to generate **242**. Subsequent oxidative-elimination of the selenide generated the C-39 *exo* olefin, and hydrolytic removal of the acetate completed the synthesis of penitrem D (**60**). The authors confirmed the identity of synthetic penitrem D with that of natural material by direct comparisons.

## C. NODULISPORIC ACID A

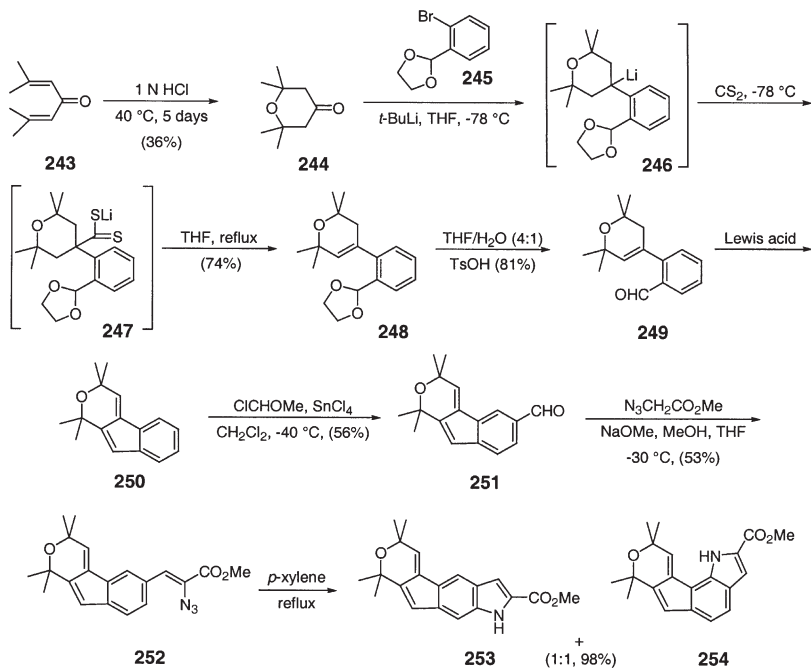
### 1. Introduction

In 1997, Merck reported a new member of the indole diterpenoid natural product family with potent insecticidal and antiparasitic activity, which is not tremorgenic, namely nodulisporic acid A (NodA, **99**) (89). Subsequently, several papers have been published describing medicinal chemistry efforts initiated to identify the nodulisporic acid A pharmacophore, and to improve the ectoparasiticidal activity and pharmacokinetic profiles. For a summary of the SAR for the nodulisporic acids, see Section II.F (94,96,97,100). This section will focus only on efforts toward the total synthesis of the natural product.



## 2. Synthesis of the A–D Rings

As pointed out by Smith and coworkers, NodA is a most formidable synthetic target. To summarize, the molecule contains an N1-C26 bridge with an epimerizable isoprenyl side chain, a dihydropyran, and a cyclopentyl ring possessing a labile secondary benzylic hydroxyl group. The first report on efforts toward the synthesis of NodA appeared in 1999 (147), two years after the Merck group reported its isolation (89). Magnus and Mansley successfully synthesized the ABCD-rings of nod A starting from phorone (243) as outlined in Scheme 18. Addition of the corresponding aryl lithium product of 245 to ketone 244 generated alkoxide 246. The authors found that the product obtained on workup was rather acid sensitive, thus 246 was treated *in situ* with carbon disulfide and heated at reflux to give 248 (presumably through intermediate 247). Acid catalyzed hydrolysis of ketal 248 afforded aldehyde 249 in 81% yield. Aldehyde 249 was exposed to several reaction conditions to generate 250, the details of which can be found in Ref (147). Installation of the indole ring required regioselective formylation of 250, which was accomplished with dichloromethyl methyl ether and tin(IV) chloride. Exposure of 251 to  $\alpha$ -azido methyl acetate gave the vinyl azide 252 in 53% yield. The isomeric indoles 253 and 254 were then formed by heating 252 in xylene. Indoles 253 and 254 were readily separated, with 253 representing the ABCD-rings of nod A. Further elaboration of 253 to generate NodA has not been reported.



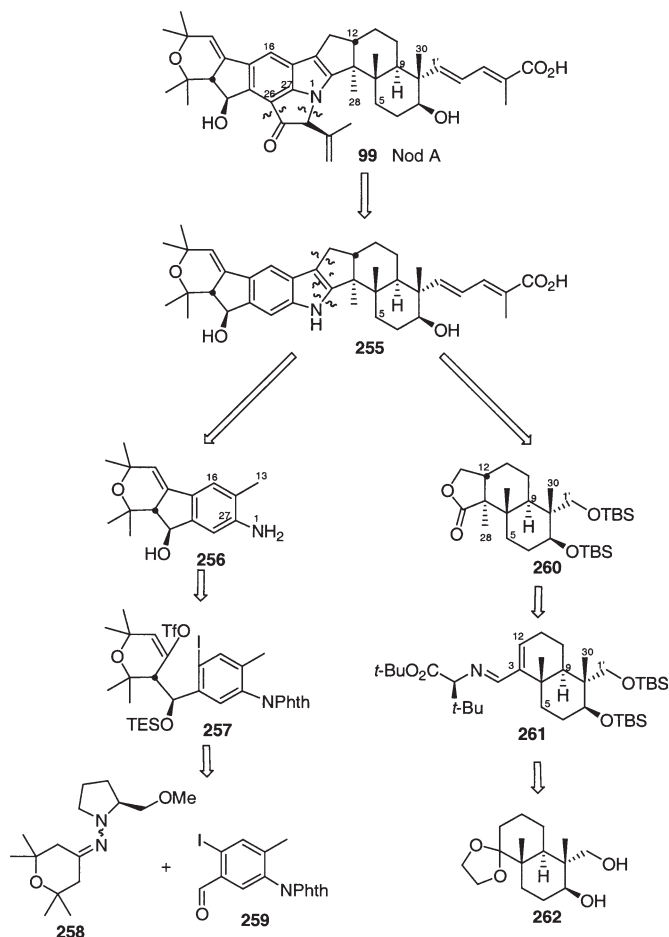
Scheme 18. Synthesis of the A–D rings of nodulisporic acid A (99) (147).

### 3. Alternative Synthetic Approach by Smith and Coworkers

*a. Retrosynthetic Analysis.* In 2001, Smith and coworkers reported sequential papers their overall strategy for the synthesis of nod A and the synthesis of the ABC- and FGH-rings (149,150). In their retrosynthetic analysis (Scheme 19), removal of the five-membered-ring isoprenyl unit reveals indole **255**. Indole **255** is predicted to arise from the union of the corresponding western and eastern halves of the molecule, via the indole ring synthetic protocol utilized in the synthesis of penitrem D (*vide supra*). The western hemisphere **256** would arise from a palladium-catalyzed tandem transmetalation-cyclization of **257**. Triflate **257** would come about from the asymmetric addition of SAMP hydrazone **258** to aldehyde **259**, which, after removal of the chiral auxiliary and hydroxyl protection would provide the appropriate precursor to enol triflate **257**. Eastern hemisphere **260** was envisioned to arise from tandem installation of a vinyl moiety and the C-8 quaternary methyl group via a Koga three-component conjugate addition-alkylation protocol via intermediate **261**. Further disconnection of **261** leads to the known diol **262** (148) (Scheme 19).

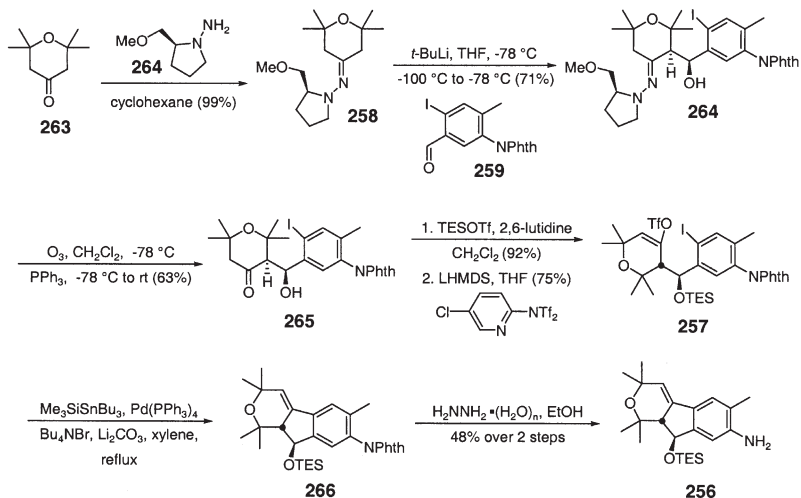
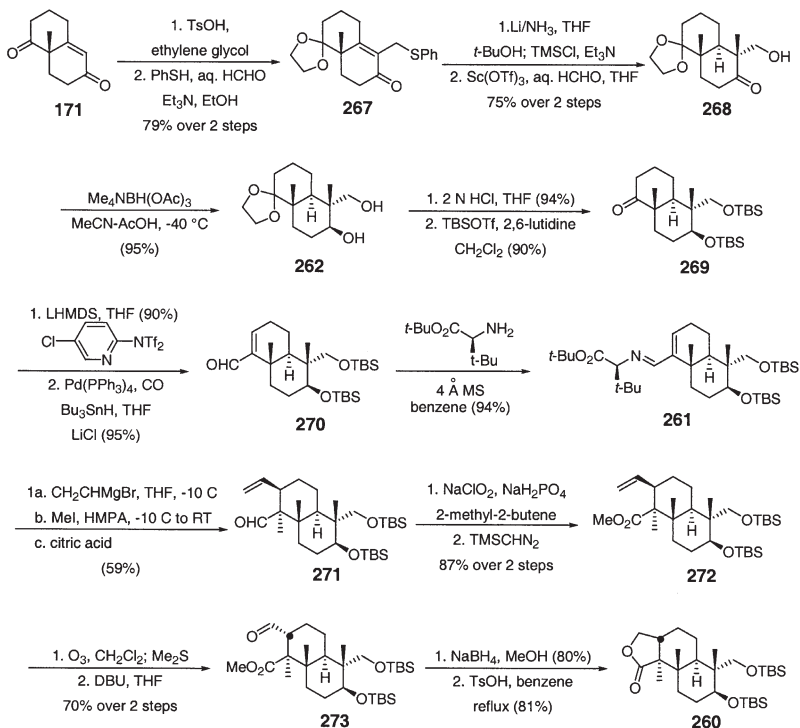
*b. Synthesis of the western hemisphere.* The synthesis of western hemisphere **256** proceeded (149) as outlined in Scheme 20. Ketone **263** was converted into the Enders hydrazone **258** by refluxing **263** with hydrazone **264** in cyclohexane. Subsequent treatment of **258** with *t*-BuLi at  $-78\text{ }^{\circ}\text{C}$ , followed by addition of aldehyde **259** (synthesized in five steps from commercially available 3-amino-4-methylbenzyl alcohol) (149) at  $-100\text{ }^{\circ}\text{C}$ , generated an 11:2 mixture of  $\beta$ -hydroxyhydrazones, which after separation by flash chromatography afforded **264** in 71% yield. Ozonolysis provided the  $\beta$ -hydroxyketone **265** whose absolute configuration was assigned by advanced Mosher ester analysis. (151) Vinyl triflate **257** was prepared from **265** via protection of the secondary hydroxyl group, followed by formation of the enol triflate with Comins (152) reagent. Conversion of **257** to the vinylstannane and subsequent cyclization with aryl iodide (Shibasaki-Mori protocol) (153) afforded **266**. Completion of the western hemisphere **256** was realized by deprotection of the aniline moiety.

*c. Synthesis of the Eastern Hemisphere.* The synthesis of the eastern hemisphere began with the familiar (+)-Wieland-Miescher ketone (**171**) (150). Chemoselective transketalization followed by (phenylthio)-methylation (Kirk-Petrow protocol) (113) gave enone **267** (Scheme 21).  $\beta$ -Hydroxyketone **268** arose from reductive alkylation of **267** using aqueous formaldehyde and Sc(OTf)<sub>3</sub> (154) catalyst. Stereoselective reduction of **268** afforded the previously reported *trans* diol **262** (148). Ketal hydrolysis and disilylation, followed by sulfonation with the Comins reagent, gave the corresponding enol triflate, which underwent palladium-catalyzed carbonylation to give aldehyde **270**. The relative stereochemistry at C-7 and C-8 of aldehyde **270** was determined by single-crystal X-ray analysis. Condensation of aldehyde **270** with a leucine derivative gave imine **261**, the substrate for the Koga three-component conjugate addition-alkylation (155). Addition of vinylmagnesium bromide to imine **261**, followed by quenching of the resulting anion with iodomethane afforded, after hydrolysis, aldehyde **271**. Methyl ester **272** was prepared by



Scheme 19. Retrosynthetic analysis of nodulisporic acid A (**99**) (149,150).

oxidation of aldehyde **271** to the carboxylic acid and esterification with TMS-diazomethane. As shown in structure **272**, the undesired stereochemistry at C-12 was obtained, contrary to the expectation based on the Koga precedent. However, the C-3 quaternary center did possess the requisite stereochemistry for nodulisporic acid A. The stereochemistry at C-12 could be easily corrected by ozonolysis, followed by epimerization to give the desired stereochemical precursor **273**, the structure of which was assigned by 2D NOESY. Reduction of aldehyde **273** and treatment of the resulting alcohol with TsOH was the final step in the construction of the eastern hemisphere  $\gamma$ -lactone **260**. The synthesis of **260** was achieved in 17 steps and 9% overall yield (Scheme 21). The union of the eastern and western hemispheres, resulting in the total synthesis of nodulisporic acid A, has yet to be reported.

Scheme 20. Synthesis of the western hemisphere of nodulisporic acid A (**99**) (149).Scheme 21. Synthesis of the eastern hemisphere of nodulisporic acid A (**99**) (150).

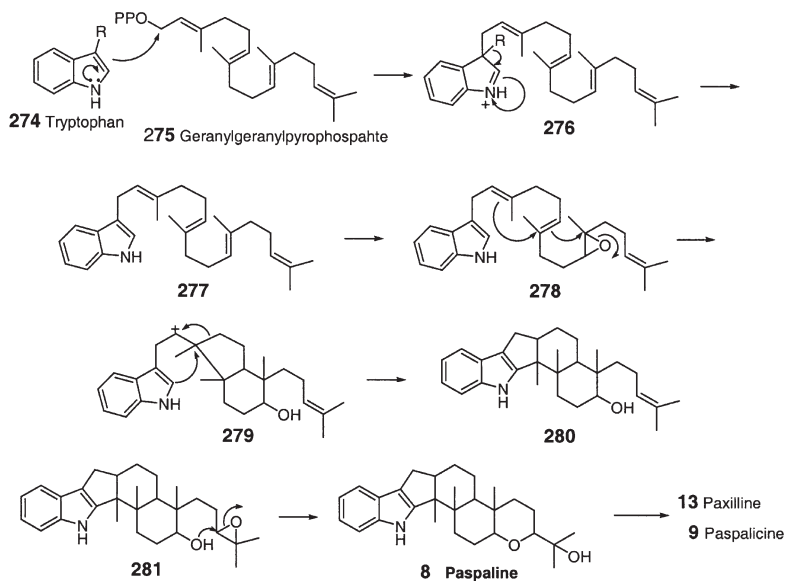
## IV. Biosynthesis

## A. INTRODUCTION

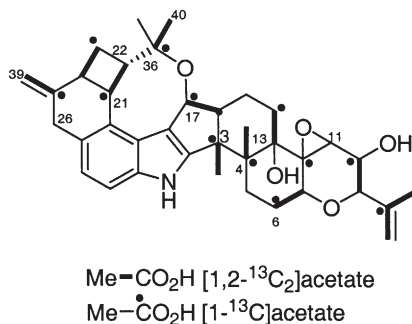
The study of the biosynthesis of the tremorgenic indole alkaloids is a formidable task, and though much groundwork has been covered, very little is known about the nature of the biochemical intermediates, or the enzymology of their biosynthesis. Most biogenetic schemes that have been published are based on radiolabeling studies and the isolation of proposed intermediates. The following section will chronologically trace the progress that has been made in the biosynthesis of the tremorgenic indole alkaloids.

### B. GERANYL-GERANYL-PYROPHOSPHATE (GGPP) AND TRYPTOPHAN AS THE PRIMARY METABOLIC PRECURSORS FOR THE PASPALANES AND PENITREMANES

As early as 1977, Arigoni and coworkers (156) reported that paspaline is formed via condensation of tryptophan (274) and GGPP (275), and proposed that a migration of the carbon skeleton occurs during the course of the biosynthesis (157). The studies were presumably done in submerged fermentation as no fermentation conditions were published. As shown in Scheme 22, the authors proposed that condensation of tryptophan with GGPP followed by dealkylation to produce intermediate 277. Epoxidation of the penultimate olefin results in ring closure to the



Scheme 22. Proposed biogenesis of paspaline (8) (156,157).



Scheme 23. Labeling pattern for Penitrem A (**55**) (59).

carbocation intermediate **279**. A 1,2-migration of the carbon skeleton then occurs to afford **280** and the A–E pascalane rings. A second epoxidation-ring closure affords paspaline, the proposed precursor to paxilline and paspalicine.

In 1983, de Jesus reported that penitrem A (**55**) is also derived from tryptophan and GGPP, along with two isopentenyl-pyrophosphate units (59). The incorporation of the indole portion into penitrem A (Scheme 23) was established by feeding, in separate experiments, either side-chain labeled, or benzene-ring labeled, <sup>14</sup>C tryptophan to cultures of *P. crustosum*. The benzene-ring labeled <sup>14</sup>C tryptophan gave an eight-fold higher incorporation of radioactivity into penitrem A than did side-chain labeled tryptophan. However, the overall incorporation was still quite low (0.16%). In a separate set of experiments, cultures which were fed [1-<sup>13</sup>C]-acetate showed enhancement of 12 carbon signals in the NMR spectrum, pointing to the involvement of six mevalonate units in the formation of the terpene unit of penitrem A. The authors also reported several one-bond couplings between C-3/C-4, C-36/C-37, and C-16/C-17. The observed one-bond coupling between C-3 and C-4 suggests that a rearrangement in the form of a 1,2-shift occurs during the biosynthesis of penitrem A, as proposed for the biosynthesis of paspaline (*vide supra*, **279** to **280**). The two other, low intensity, one-bond couplings between C-36/C-37 and C-16/C-17 were presumed to be due to coupling between a <sup>13</sup>C-enriched carbon and the adjacent carbon atom present at the natural abundance level (1.11%).

In response to the eight-fold higher incorporation of benzene-ring labeled <sup>14</sup>C tryptophan and the lower level of incorporation of side-chain labeled tryptophan reported by de Jesus, Mantle and Laws sought to find more definitive evidence that indeed the indole moiety of penitrem A is derived from tryptophan. To Laws and Mantle, the question remained: “is eight times a spurious value, due only to metabolic scrambling of the radiolabel in the putative precursor, compelling evidence?” (158). The study Laws and Mantle thus involved a side by side comparison of the amount of radioactivity incorporated into penitrem A (**55**) and E (**61**), with that incorporated into roquefortine, a substituted tryptophan-histidine diketopiperazine in which the whole carbon skeleton of tryptophan is retained.

Thus roquefortine was viewed as an internal standard against which incorporation into the penitremes of tryptophan radiolabeled in the indole moiety could be measured. A comparative biosynthetic incorporation of radiolabeled putative precursors into **55** and **61** and roquefortine is shown in Table XIII. Entries 1–5 list the % incorporation of precursors when administered to *P. crustosum* in stationary liquid culture. As shown in Table XIII,  $^{14}\text{C}$  labeled tryptophan was incorporated into roquefortine with >20% efficiency, regardless of the position of the radiolabel (entries 2–3). In contrast, very little labeled tryptophan was incorporated into the penitremes, and only three times more radioactivity was observed from benzene-ring labeled tryptophan as compared to side-chain labeled tryptophan (entries 2–3). In addition,  $^{14}\text{C}$  phenylalanine and  $^{14}\text{C}$  tyrosine (entries 4–5) gave similar values for the extent of incorporation when compared to side-chain labeled tryptophan, presumably through metabolic recycling through pathways leading to acetate, phosphoenolpyruvate, or erythrose-4-phosphate (158). Therefore, the experiment failed to provide compelling evidence that the indole moiety of the penitremes is derived from tryptophan.

TABLE XIII.  
Comparative Biosynthetic Incorporation of Radiolabeled Precursors in Alkaloid  
Metabolites of *P. crustosum* (158).

Entry	Precursor	Stage of fermentation	Amount ( $\mu\text{Ci}$ )	Metabolite yield (mg/100 ml medium)	% incorporation
1 <sup>a</sup>	DL-[benzene ring $^{14}\text{C}$ ] Tryptophan	Day 2	5	Penitremes (4.9) Roquefortine (5.0)	1.0 10.5
2 <sup>a</sup>	DL-[benzene ring $^{14}\text{C}$ ] Tryptophan	Day 5	5	Penitremes (7.2) Roquefortine (10.3)	1.4 23.4
3 <sup>a</sup>	DL-[methylene $^{14}\text{C}$ ] Tryptophan	Day 5	5	Penitremes (6.4) Roquefortine (10.1)	0.5 21.5
4 <sup>a</sup>	L-[U- $^{14}\text{C}$ ] Phenylalanine	Day 5	5	Penitremes (6.3) Roquefortine (10.6)	0.2 0.1
5 <sup>a</sup>	L-[U- $^{14}\text{C}$ ]Tyrosine	Day 5	5	Penitremes Roquefortine	0.4 0.2
6 <sup>b</sup>	DL-[benzene ring $^{14}\text{C}$ ] Tryptophan	Day 5	5	Penitremes (7.2) Roquefortine (10.3)	3.6 10

<sup>a</sup>Radioactive precursors administered to stationary liquid culture.

<sup>b</sup>Radioactive precursors applied to fungal mat.

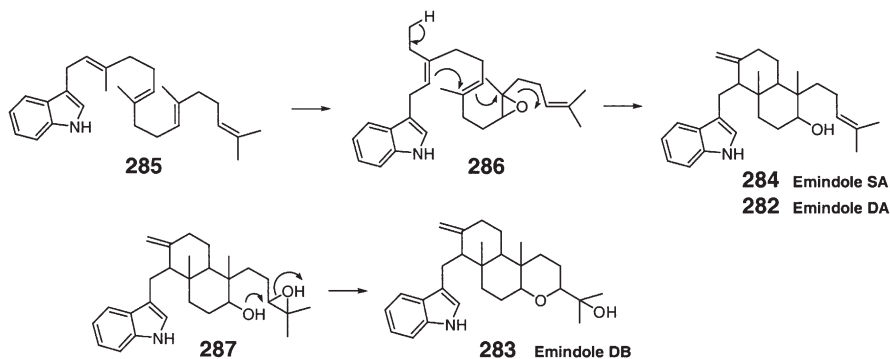
In a separate set of experiments, the authors administered the radiolabeled precursors via the hydrophobic spores that form the upper surface of *P. crustosum* mycelia. Here they obtained a greater incorporation of aromatic ring labeled tryptophan (3.6%, entry 6, Table XIII), providing what the authors believe to be definitive evidence that tryptophan is indeed the precursor of the penitrem indole.

### C. ALTERNATIVE CYCLIZATION PATHWAY: ROUTE TO EMINDOLES

In 1988, Nozawa and coworkers isolated Emindoles DA (**282**) and DB (**283**), followed by emindole SA (**284**), and paxilline from *Emericella* (157,159). The isolation of emindole SA, along with paxilline suggested that there is a second possible cyclization pathway for the diterpene moiety at an early stage of the biosynthesis (157). The first pathway, leading to paspaline, involves migration of the carbon skeleton as described in Scheme 22. The alternative pathway outlined in Scheme 24 gives emindole SA by direct cyclization/epoxide opening without migration of the carbon skeleton.

### D. PAXILLINE: A PUTATIVE PRECURSOR TO OTHER INDOLE DITERPENES

The core structure of the tremorgenic indole diterpenes is well exemplified by paxilline (**13**), and it can be postulated that paxilline may serve as a biosynthetic intermediate for other tremorgens. In 1989, Mantle and Penn administered radiolabeled paxilline (obtained biosynthetically using [2-<sup>14</sup>C]-mevalonate) to *P. janczewskii* fermentations (160). After four days, the major penitremes were extracted and isolated by preparative TLC. The most abundant metabolite, penitrem A, was further purified by reversed-phase HPLC to ensure removal of residual <sup>14</sup>C-labeled paxilline. The authors found that between 3.1 and 8.7% of the <sup>14</sup>C-paxilline administered was incorporated into penitrem A (**55**). Other, less abundant penitremes were also radiolabeled. In particular, radiolabeled penitrem E



Scheme 24. Alternative cyclization pathway: route to emindoles (157).



(61) was isolated, and when combined with penitrem A biosynthesis, the percent incorporation ranged from 3.3 to 17%. It would appear therefore that paxilline (13) may serve as a biosynthetic intermediate for the penitrem.

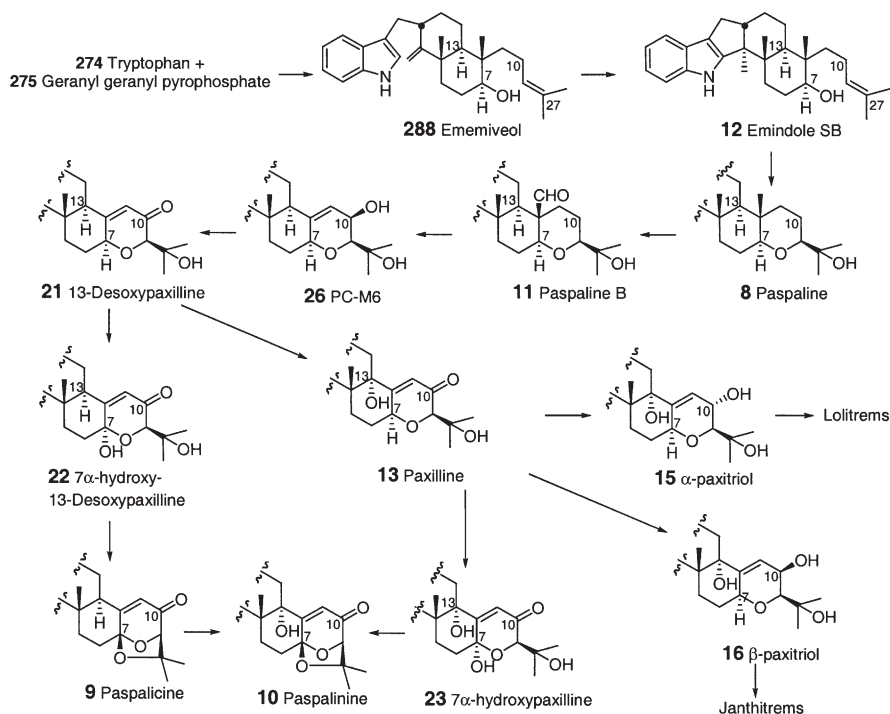
Further evidence that paxilline (13) is the precursor to other indole diterpenoids was obtained in 1994, when Penn and Mantle fed paxilline derivatives, biosynthetically radiolabeled with  $^{14}\text{C}$  in the diterpene, to submerged fermentation of *P. janczewskii* and *P. janthinellum*, organisms which produce both the penitrem and janthitrem alkaloids (161). In addition, the authors examined the potential biosynthetic role of  $\alpha$ - and  $\beta$ -paxitriol (15 and 16) obtained by sodium borohydride reduction of the C-10 carbonyl of radiolabeled paxilline. It was found that addition of [ $^{14}\text{C}$ ]-paxilline and  $\beta$ -[ $^{14}\text{C}$ ]-paxitriol to *P. janczewskii* and *P. janthinellum* fermentations resulted in incorporation of both precursors into penitrem A and E, pennigritrem (66), and janthitrem B (72) and C (73) (Table XIV). On the other hand,  $\alpha$ -[ $^{14}\text{C}$ ]-paxitriol was not significantly incorporated into these metabolites. This result is not surprising, as the stereochemistry at the C-10 positions of these metabolites is  $\beta$ . The authors also reported that  $\beta$ -[ $^{14}\text{C}$ ]-paxitriol was transformed into some unidentified metabolites, which were chromatographically identical to those observed in fermentations receiving [ $^{14}\text{C}$ ]-paxilline. Thus, the authors speculated that these unidentified metabolites could be intermediates or by-products leading to other indole diterpene alkaloids (161).

In 1994, Mantle and Weedon fed [ $^{14}\text{C}$ ]-tryptophan or [ $^{14}\text{C}$ ]-mevalonate to *P. paxilli* and isolated, in addition to paxilline, three minor alkaloids that were radiolabeled from either or both precursors (35). The new metabolites were elucidated to be  $7\alpha$ -hydroxypaxilline (23),  $7\alpha$ -hydroxy-13-desoxy paxilline (22),

TABLE XIV.

Incorporation of [ $^{14}\text{C}$ ]-Paxilline and [ $^{14}\text{C}$ ]  $\alpha$ - and  $\beta$ -Paxitriols into the Principal Indole-Diterpenoid Metabolites of *P. janczewskii* and *P. janthinellum* Biomass in Submerged Fermentations (161).

Entry	Radiolabeled precursor	Incorporation of $^{14}\text{C}$ (% of the $^{14}\text{C}$ -labeled precursor that became cell associated)			
1	<i>P. janczewskii</i>	Penitrem A (55)	Penitrem E (61)	Pennigritrem (66)	Total
2	Paxilline (13)	8.13	1.87	3.73	13.7
3	$\beta$ -Paxitriol (16)	6.05	2.47	2.16	10.7
4	$\alpha$ -Paxitriol (15)	0.11	0.33	0.28	0.72
	<i>P. janthinellum</i>	Janthitrem B (72)	Janthitrem C (73)		Total
5	Paxilline (13)	11.1	12.1		23.2
6	$\beta$ -Paxitriol (16)	15.0	19.5		34.5
7	$\alpha$ -Paxitriol (15)	6.05	1.1	0.00	1.1



Scheme 25. Proposed biogenetic pathway for the indole diterpenoids (10,35).

and 10 $\beta$ -hydroxy-13-desoxypaxilline (24) (Scheme 25). In consideration of the structural range of indole-diterpenoid alkaloids thus far described from *Acremonium*, *Aspergillus*, *Claviceps*, and *Penicillium*, the authors generated a scheme describing the putative biosynthetic relationships of some of these alkaloids. This scheme was later modified by Munday-Finch to include emeniveol (286) and paspaline B (11), and a combination of these proposed grids is summarized in Scheme 25 [adapted from Munday-Finch *et al.* (10) and Mantle *et al.* (35)]. As shown in Scheme 25, GGPP and tryptophan serve as the primary metabolic precursors. Paspaline (8) is placed early in the scheme as it contains all the requisite carbons present in the diterpene unit. Oxidation of C-30 to the aldehyde would convert paspaline (8) to paspaline B (11), the first oxidized analogue of paspaline to have been isolated (10). Paspaline B (11) may thus represent one of the early stages in the transformation of paspaline to form the diterpene unit on which most of the other tremorgens are based (10). This could occur via elimination of the C-30 aldehyde to generate the corresponding 11,12-alkene (this proposed intermediate has not yet been isolated) followed by oxidation of C-10 to generate the known alkaloid PC-M6 (26). Further oxidation of the C-10 hydroxyl to the  $\alpha,\beta$ -unsaturated ketone would afford 13-desoxypaxilline (21) and could then be converted to paxilline (8) through allylic oxidation of C-13.

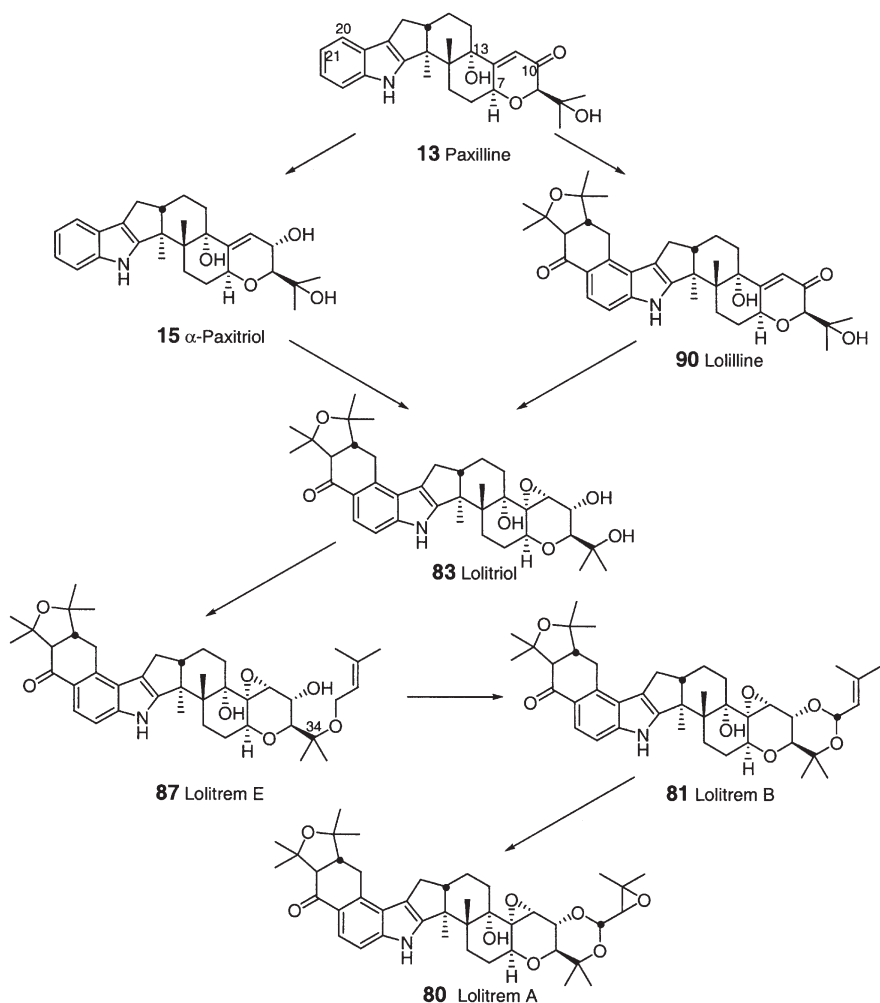
A separate fate of 13-desoxypaxilline would involve oxidation at C-7 to afford 7 $\alpha$ -hydroxy-13-desoxypaxilline, an alkaloid isolated by Mantle and coworkers following [ $^{14}$ C]-tryptophan or [ $^{14}$ C]-mevalonate administration to *P. paxilli* (*vide supra*). This alkaloid could serve as direct precursor to paspalicine (**9**) and paspalinine (**10**). Reduction of the C-10 ketone in paxilline would lead to the  $\alpha$  and  $\beta$ -paxitriols, the putative precursors of the lolitrems and janthitrems. Alternatively, the C-10 hydroxy group of the latter alkaloids may be derived from the reduction of putative enone derivatives of the fully assembled skeletons of the lolitrems and janthitrems.

In 1997 Munday-Finch and coworkers isolated lolilline (**90**), an alkaloid containing structural features present in both paxilline and the lolitrems (**41**). The isolation of lolilline and the putative metabolic grid, which traces paxilline (**13**) to the lolitrems, is consistent with previously published biogenetic schemes. An extension of the metabolic grid illustrated in [Scheme 25](#) is shown in [Scheme 26](#), and sketches a possible biogenesis of the lolitrem family of indole-diterpenoids (**41**). The incorporation of two isoprene units into the paxilline skeleton at C-20 and C-21 would form the *trans*-fused A/B ring system of lolilline (**90**). Reduction of the C-10 keto group and epoxidation of the C-11 alkene would generate lolitriol (**83**) (alternatively,  $\alpha$ -paxitriol could serve as the precursor to lolitriol). Subsequent isoprene addition to the C-27 hydroxyl of lolitriol would lead to lolitrem E (**87**). Ring closure to afford lolitrem B (**81**) could then be followed by epoxidation to generate lolitrem A (**80**).

In 1998 Munday-Finch and coworkers reported the isolation of lolicine A (**91**), lolicine B (**92**), lolitriol (**83**), lolitrem N (**93**), 26-*epi*-lolitrem N (**98**), and 26-*epi*-lolitrem F (**89**) from *L. perenne* infected with *N. lolii* (**80**). These findings suggest that assembly of the A/B ring system of the lolitrems lacks stereospecificity, resulting in a series of lolitrem B analogs, which differ only in the stereochemistry at C-22 and C-26 (**80**). The fact that lolicines A and B contain either a methyl or formyl group at C-41 suggests they are not biosynthesized directly from paxilline or  $\alpha$ -paxitriol. Rather, they might be produced from paspaline (**8**) and paspaline B (**11**) via terpendoles E (**35**) and G (**37**). This is supported by the identification of terpendoles in endophyte-infected *L. perenne* (**11,39,40**). Thus, the authors proposed the metabolic grid shown in [Scheme 27](#) for the biosynthesis of the lolicines (**80**). The authors also point out the possibility that the lolicines could be metabolized to the lolitrems via the intermediacy of lolitriol. Therefore, it can be postulated that biosynthesis of the lolitrems may not involve paxilline (**13**) or  $\alpha$ -paxitriol (**15**).

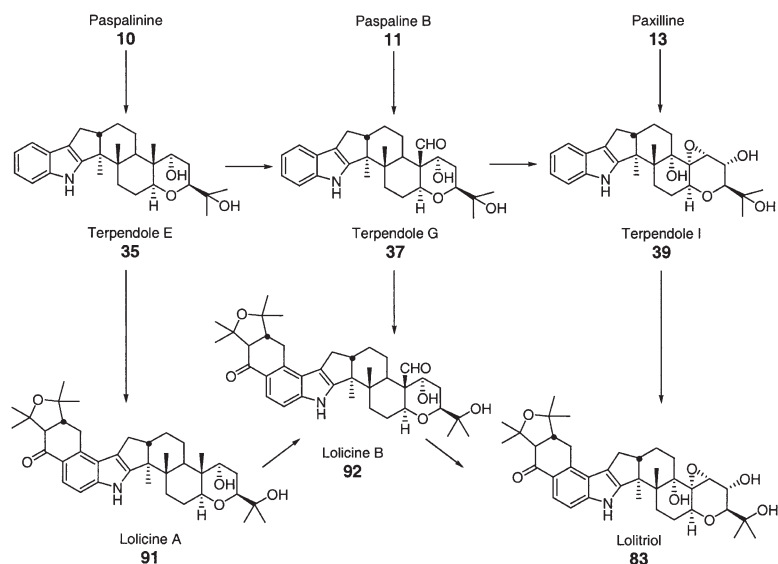
#### E. GENETIC ANALYSIS OF *PENICILLIUM PAXILLI*

In 1998, Scott and coworkers identified a locus on chromosome Va of *P. paxilli* that was involved in paxilline biosynthesis (**162**). Three paxilline-negative (Pax $^-$ ) mutants were isolated and all were shown to have deletions of 100–200 kb at a single locus. In 2001, this group then demonstrated that the Pax $^-$  phenotype



Scheme 26. Proposed biogenetic pathway for the lolitremes (41).

resulted from deletion of the gene cluster responsible for paxilline biosynthesis, resulting in the first report of the molecular cloning and genetic analysis of an indole-diterpene gene cluster (163). The cluster was predicted to lie within a 50-kb region of chromosome Va and is believed to contain 17 genes. As shown in Table XV, 12 genes have significant similarity to genes of known function, 4 have a function yet to be identified, and 1 has no significant similarity to genes within the searched database. The identified functions include a GGPP, two FAD-dependent mono-oxygenases, a dimethylallyl-tryptophan synthase, and two transcription factors. The identification of a GGPP (*paxG*) in the paxilline biosynthesis gene



Scheme 27. Proposed biogenic grid for the lolicines (80).

TABLE XV.  
The Paxilline Gene Cluster of *P. paxilli*<sup>a</sup>.

Gene	Proposed function	Homolog	Size <sup>b</sup>
PaxO	Oxidoreductase	PirlG7510	423
PaxD	DMAT synthase	EmblCAB39314.1	438
PaxQ	P450 monooxygenase	EmblCAA76703	512
PaxP	P450 monooxygenase	EmblCAA76703	515
PaxC	Prenyltransferase	RefNP_004827.1	317
PaxM	Monooxygenase	gil2290996	477
PaxG	GGPP synthase	sp.lP24322	371
PaxU	Unknown	PirlT33520	291
PaxT	Transporter	RefNP_01022.1	478
PaxV	Unknown	No similarity	877
PaxW	Unknown	GblAAD44757.1	518
PaxH	Dehydrogenase	EmblCAB88427.1	385
PaxX	Unknown	DbjlBAA84094.1	435
PaxR	Transcription factor	sp.IP52958	684
PaxS	Transcription factor	GblAAB05250.1	495
PaxY	Glucanosyltransferase	GlbAAF40140	489
PaxM	Monooxygenase	EmblCAB94646.1	402

<sup>a</sup>Adapted from Ref. (163).<sup>b</sup>Predicted sizes of the pax polypeptide given in amino acids.

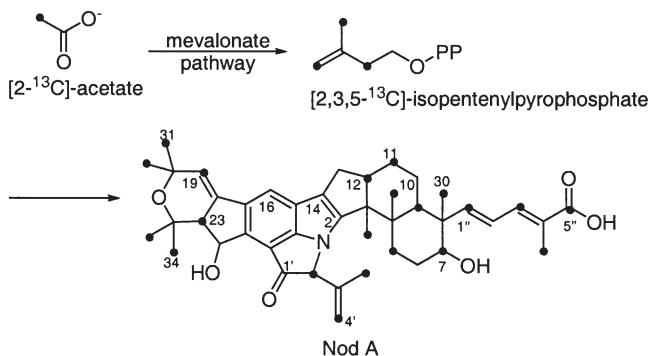
cluster was unexpected, as this gene is typically essential for growth. Targeted replacement of *paxG* confirmed that it was essential for paxilline biosynthesis, but not necessary for primary metabolism. The GGPP for primary metabolism was identified (*ggs1*) and was mapped to chromosome IV. It was also found that the mRNA levels for *paxG*, *paxM*, and *paxP* were upregulated just before the onset of paxilline biosynthesis, which occurs at about 60 h. These results suggest that within the *pax* gene cluster there is a coregulation of expression corresponding to the onset of paxilline biosynthesis.

## F. NODULISPORIC ACID A

In 2002, Merck Research Laboratories published the biosynthesis of nodulisporic acid A (nod A, **99**) (166). The study was undertaken to investigate whether the biosynthesis of nod A by *Nodulisporium* sp. used the mevalonate-tryptophan biosynthetic pathway as proposed for paspaline and penitrem A (*C. paspali* and *P. crustosum*) (59,156,158). The authors reported that incorporation of [2-<sup>13</sup>C]-acetate and [2-<sup>13</sup>C]-mevalonolactone in nod A occurred in the classical mevalonic acid pattern. However, contrary to what has been found with other alkaloids, the authors found that tryptophan was not the precursor for the indole nucleus, rather the indole moiety was derived from anthranilic acid and ribose. A novel pathway for the biosynthesis of nod A was thus proposed, the details of which are presented here.

Radiolabeled precursors were applied to washed cells of *Nodulisporium* sp. (MF6244 and MF6299). Addition of [2-<sup>13</sup>C]-acetate resulted in enrichment at carbons 5, 7, 9, 11, 19, 23, 28, 29, 30, 31, 32, 33, 34, 2', 5', 1'', 3'', 5'', and 6'' as determined by the <sup>13</sup>C NMR. This enrichment pattern was consistent with the model that [2-<sup>13</sup>C]-acetate is incorporated into four units of [2,4,5-<sup>13</sup>C<sub>3</sub>]-IPP, which then condenses to form GGPP. The <sup>13</sup>C NMR spectrum also revealed a strong coupling between C-11 and C-12 ( $J=34.0$  Hz), suggesting that a rearrangement had occurred during the condensation and cyclization of GGPP with the indole precursor. This 1,2-bond shift is consistent with the rearrangement proposed for the cyclization of paspaline (**8**) and penitrem A (**55**) (*vide supra*) (59,156). The addition of [2-<sup>13</sup>C]-mevalonolactone to washed cells confirmed the acetate-labeling pattern shown in Scheme 28 and the involvement of the mevalonic acid pathway.

In contrast to previously reported biosynthetic studies for penitrem A and paxilline (35,59,158), all attempts to label nod A with radiolabeled tryptophan or radiolabeled indole were unsuccessful. However, anthranilic acid incorporation into nod A was 1.6%, and greater than 6% of the added [ring-<sup>14</sup>C<sub>6</sub>]-anthranilic acid was incorporated into the entire family of nod A alkaloids. To substantiate this observation, the Merck group conducted several control experiments. For example, unlabeled tryptophan was added to washed cells in conjunction with [ring-<sup>14</sup>C<sub>6</sub>]-anthranilic acid, which led to a 2.5-fold increase in anthranilic acid incorporation into nod A. This result is significant, for if tryptophan was indeed a precursor, the addition of excess tryptophan should have led to a dilution of the label. The

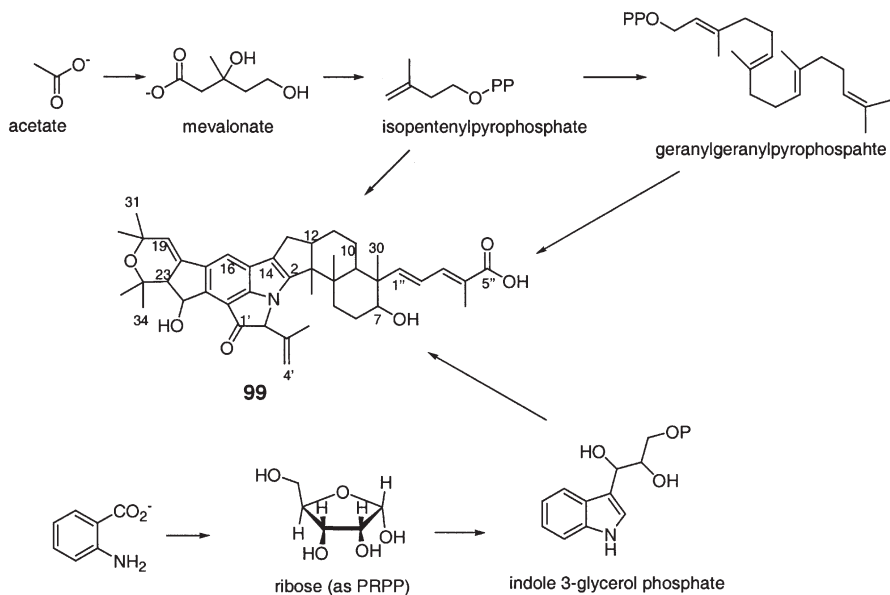


Scheme 28. Incorporation of [2- $^{13}\text{C}$ ]-acetate into nodulisporic acid A (**99**) (166).

apparent increase in incorporation of anthranilic acid in the presence of excess tryptophan would be expected if tryptophan was in fact not a precursor, as down-regulation of tryptophan synthesis could occur, allowing for increased shunting of anthranilic acid in nod A (**99**).

The authors proposed that if anthranilic acid were being incorporated in nod A (**99**) using a pathway analogous to tryptophan biosynthesis, the carboxyl group of anthranilic acid would be lost as  $\text{CO}_2$ , and thus not be incorporated into nod A. Therefore, in a separate set of experiments, a comparison of [ring- $^{14}\text{C}_6$ ]-anthranilic acid and [carboxyl- $^{14}\text{C}$ ]-anthranilic acid incorporation was investigated. A 48 h incubation resulted in 2.0% incorporation of ring-labeled anthranilic acid into nod A (**99**), while no incorporation was obtained from carboxyl-labeled anthranilic acid. This result was in agreement with that observed by Laws, whereby [carboxyl- $^{14}\text{C}$ ]-anthranilic acid resulted in only 0.016% incorporation into the penitremes (158). However, the counter experiment with [ring- $^{14}\text{C}_6$ ]-anthranilic acid was not performed. Finally, incubation of both ring-labeled anthranilic acid and  $^{15}\text{N}$ -anthranilic acid confirmed the origin of the six benzene indole carbon atoms, as well as the single nitrogen atom. The six benzene carbons of nod A (**99**) were labeled at an enrichment level of two- to three-fold, and two signals with distinct satellites resulting from  $^{13}\text{C}$ - $^{15}\text{N}$  coupling at C-2 and C-27 were observed.

To elucidate the origin of the remaining two carbons of the indole nucleus of nod A (**99**), MF6299 cells were supplemented with either [1- $^{13}\text{C}$ ]-D-ribose or [UL- $^{13}\text{C}_5$ ]-D-ribose. The  $^{13}\text{C}$  NMR spectrum of the isolated nod A produced in the presence of [1- $^{13}\text{C}$ ]-D-ribose showed a two-fold enrichment of carbon 2 of nod A, the expected site of enrichment if the indole is formed by condensation of anthranilic acid and phosphoribosyl-pyrophosphate (PRPP). The  $^{13}\text{C}$  NMR spectrum of nod A (**99**) isolated from incubation of the resting cells with [UL- $^{13}\text{C}_5$ ]-D-ribose revealed a two-fold enrichment of C-2 and C-14, demonstrating that these carbon atoms arise intact from two adjacent carbons of ribose. Comparison with



Scheme 29. Proposed biogenetic scheme for nodulisporic acid A (**99**) (166).

known aromatic amino acid biosynthesis would suggest that phosphoribosyl-anthranilate (PRPP) would proceed to form indole-3-glycerol phosphate, which is then proposed to serve as the activated indole intermediate which condenses with GGPP to form the indole-diterpenoid core of **99**. Thus, the novel pathway described in Scheme 29 was proposed for nodulisporic acid A (**99**) biosynthesis.

## V. Structure and Tremorgenicity

Paspalinine (**10**) exhibited tremorgenic activity at 80 mg/kg ip in mice, while its congeners paspaline (**8**) and paspalinine (**9**) did not cause any tremors. The only structural difference between **9** and **10** is the presence of the tertiary hydroxy group at C-13. This led to a hypothesis by Cole in 1981 (164) that the hydroxy group at C-13 modulates tremorgenicity (52). This basic hypothesis remains valid 20 years later whereby all reported indole diterpenoids that have been reported to be tremorgens possess a C-13 hydroxy group. However, there is a significant hole in the published data for many alkaloids either with or without a C-13 hydroxy group, and there are several C-13 hydroxy-containing alkaloids that are not tremorgenic. For example, paxitriol, lolitriol, and lolitrem E possess a C-13 hydroxy group, but lack tremorgenic activity at the highest dose tested. In addition, lolilline (**90**), which has the identical diterpenoid unit as paxilline, was not tremorgenic at 8 mg/kg, indicating that the presence of the furanyl-cyclohexenone unit of **90** contributes to diminished tremorgenicity in the presence of a paxilline type  $\Delta^{11,12}$ -en-10-one



substructure. From these data it is clear that in order to explain the tremorgenic SAR of the indole diterpenoids, a new model is needed. In the absence of data generated in tightly controlled parallel experiments, it is rather difficult to compare and understand the SAR based on the available data. However, an attempt is made here to compare these data, as well as to define the basic pharmacophore for tremorgenic activity, and to discuss the structural requirements for tremorgenic potency.

There is a 20-fold difference in the reported tremorgenic activities of paspalinine (**10**) and paxilline (**13**), the latter being more active. A comparison of the two structures reveals that paxilline lacks the dioxane-ring and has a lower level of oxidation at C-7 than paspalinine. The higher level of oxidation at C-7 does cause diminution of the tremorgenic activity. For example, 7 $\alpha$ -hydroxypaxilline (**23**) is not tremorgenic at 4 mg/kg ip in mice, while paxilline caused significant tremors at the same dose. Unfortunately, no titration data was provided. The presence of an  $\alpha$ -hydroxy group at C-14 also appears to cause a reduction of tremorgenic activity [e.g., terpendole C (**33**) is more tremorgenic than terpendole M (**38**) at 8 mg/kg ip in mice]. Whether or not the presence of the additional hydroxy group at C-14 will have a similar effect in lowering the tremorgenic activity of 14-hydroxypaspalinine (**29**) and 14-(*N,N*-dimethyl-L-valyloxy)-paspalinine (**30**), in comparison with paspalinine, remains to be verified.

Aflatrem (**45**), structurally identical to paspalinine (**10**) except for the presence of an isoprenyl chain at C-20, exhibited tremorgenic activity at 4 mg/kg, which was similar to the activity of paxilline (**13**). Paspalitrem A (**47**) and B (**48**) exhibited similar tremorgenic activity at < 14 mg/kg, indicating that a lipophilic chain at C-20 or C-21 compensated for the loss of activity due to the C-7 oxygen and dioxane ring. If this were true then isopentenylpaxilline (**54**) would be predicted to be more tremorgenic than paxilline (**13**). However, this could not be verified due to lack of the data for **54**. Tremors caused by paspalanes and the aflatremes were fast acting, but were of shorter duration.

Penitrem A (**55**) caused significant tremors at 250  $\mu$ g/kg ip in mice, and is one of the most potent tremorgens of the indole diterpenoid class. However, unlike the paspalanes and aflatremes, it was lethal (LD<sub>50</sub>) at 1.05 mg/kg. In addition to being the most potent, tremors caused by penitrem A were slow acting, but longer lasting. There were 8–20-fold differences in the tremorgenic activity of penitrems A (**55**), B (**58**), and E (**61**). Structurally, the three alkaloids are similar and possess a common 11,12- $\alpha$ -epoxy-10- $\beta$ -ol, and differ only in the presence or absence of a chorine and/or a hydroxy group at C-21 and C-28. In the case of paxilline (**13**), reduction of the C-10 keto group to generate  $\beta$ -paxitriol led to loss of the tremorgenic activity. Penitrem A however, has a  $\beta$ -hydroxy group at the equivalent position on the terpene skeleton, therefore it appears that the substitution of a  $\Delta^{11,12}$ -en-10-one with an 11,12- $\alpha$ -epoxy-10- $\beta$ -ol, together with the presence of a cyclohexyl-cyclobutyl ring, more than compensates for the tremorgenic activity. The presence of both the hydroxy and the chloride groups at C-21 and C-28,

respectively in penitrem A (**55**) rendered it a 20-fold more potent tremorgen compared to penitrem B (deschloro, desoxy) and eight-fold more potent compared to penitrem E (deschloro).

Janthitrem B (**72**) was also tremorgenic at 200  $\mu\text{g}/\text{kg}$  while possessing a C-10- $\beta$ -hydroxy group like the penitrems. It also contains an additional bicyclic lipophilic substitution on the indole ring. Based on the SAR known for paxilline derivatives, one could predict stronger tremorgenic activity for shearinine B (**78**) due to the presence of  $\Delta^{11,12}$ -en-10-one as in paxilline (i.e., an analogous comparison to paxilline and  $\beta$ -paxitriol) if it behaves like the paxilline class. The activity would be diminished if it behaved like lolilline and lolitrems.

Lolitrems A (**80**) and lolitrem B (**81**) showed strong tremors at 0.5 to 2 mg/kg ip in mice, peaking at 2.5 to 5 h, and was detectable until 48 h. Lolitrem B was five-times more tremorgenic than paxilline (**13**) as measured in a parallel experiment. Lolitriol (**83**), which lacks one of the isoprene ethers present in **80** and **81**, was not tremorgenic at 20 mg/kg, indicating at least a 20-fold lower activity caused by the loss of one of the isoprene groups, probably due to increased polarity. Lolitriol turned out to be lethal at 16 mg/kg, however, no comparative data was available for lolitrem B. The stereochemistry of the A/B ring has a significant effect on the tremorgenic activity of the lolitrems. For example, 26-*epi*-lolitrem B (**85**), with the  $\alpha$ -*cis*-fused A/B rings, is three-times less tremorgenic than lolitrem B (**81**) with the *trans*-fused A/B rings. However, lolitrem F (**88**), with the  $\beta$ -*cis*-fused A/B rings, and 26-*epi*-lolitrem F (**89**), with the alternative *trans*-fused A/B rings, exhibited tremorgenic activity that was identical to lolitrem B. This observation led to a proposal that the  $\alpha$ -bend caused by the  $\alpha$ -*cis* fusion in **85** may orient the molecule away from the receptor binding site, and thus indicated that this part of the molecule is probably important for putative receptor binding for this group of tremorgens. This may be responsible, at least in part, for the slow acting, long duration of action or both behaviors of these alkaloids.

The tremorgenic activity of these alkaloids can be classified into two groups: (a) alkaloids that are fast acting (peaking at 15–20 min), but with short duration of action (<20 h) following a normal decay slope exemplified by paspalanes and aflatremanes; and (b) alkaloids that are slow acting (peaking at 2–5 h) with long duration of action (> 48 h) exemplified by the lolitrems, penitrems, and possibly the janthitrems (no details of tremor behavior have been reported for janthitrem B). This would suggest that these two groups of alkaloids exert their tremorgenic effect by different mechanisms of action, with possible binding to different neuronal receptors. This may explain the difference in the SAR exhibited by the two classes of tremorgens. In one case the C-10 keto group is essential (paspalanes, aflatremanes), in the other case it appears not to be essential (penitremanes, janthitremanes, lolitremanes).

Finally, it is clear that there are two-tremorgenic pharmacophores operating within the indole diterpenoids. One pharmacophore exerts fast-acting

and short-duration tremorgenic activity (e.g., paspalanes and aflatremanes) in which additional oxidations at C-7 or C-14 render the alkaloids to be less tremorgenic. A second pharmacophore causes slow-acting and long-lasting activity, represented by the more complex indole diterpenoids (e.g., penitremanes, janthitremanes, and lolitremanes). However, in order to propose any definitive model that could explain these alkaloids, careful systematic and parallel studies of many of these, both active and inactive, alkaloids are needed. Until then, a definitive structure–function relationship of the tremorgenicity of these indole diterpenoids cannot be elucidated. In addition, the molecular mechanism of the tremorgenicity of the indole diterpenoids requires elucidation.

### References

1. V. Betina, in “Mycotoxins-Production, Isolation, Separation and Purification” (V. Betina, ed.), pp. 415. Elsevier Science Publishers BV, Amsterdam, 1984.
2. P. S. Steyn and R. Vleggaar, *Prog. Chem. Org. Nat. Prod.* **48**, 1 (1985).
3. R. X. Tan and W. X. Zou, *Nat. Prod. Rep.* **18**, 448 (2001).
4. M. I. Selala, F. Daelemans, and P. J. C. Schepens, *Drug Chem. Toxicol.* **12**, 237 (1989).
5. J. Frisvad, *J. Chromatogr.* **392**, 333 (1987).
6. T. Fehr and W. Ackin, *Helv. Chem. Acta* **49**, 1907 (1966).
7. J. P. Springer and J. Clardy, *Tetrahedron Lett.* **21**, 231 (1980).
8. R. J. Cole, J. W. Dorner, J. A. Lansden, R. H. Cox, C. Pape, B. M. Cunfer, S. S. Nicholson, and D. M. Bedell, *J. Agric. Food Chem.* **25**, 1197 (1977).
9. K. Nozawa, S. Nakajima, K. Kawai, and S. Udagawa, *J. Chem. Soc., Perkin Trans. 1* **9**, 2607 (1988).
10. S. C. Munday-Finch, A. L. Wilkins, and C. O. Miles, *Phytochemistry* **41**, 327 (1996).
11. X. H. Huang, H. Tomoda, H. Nishida, R. Masuma, and S. Omura, *J. Antibiot.* **48**, 1 (1995).
12. W. A. Gatenby, S. C. Munday-Finch, A. L. Wilkins, and C. O. Miles, *J. Agric. Food Chem.* **47**, 1092 (1999).
13. J. A. Laakso, E. D. Narske, and J. B. Gloer, *J. Nat. Prod.* **57**, 128 (1994).
14. M. R. TePaske, J. B. Gloer, D. T. Wicklow, and P. F. Dowd, *J. Nat. Prod.* **55**, 1080 (1992).
15. M. I. Selala, A. Musuku, and P. J. C. Schepens, *Anal. Chim. Acta* **244**, 1 (1991).
16. C. O. Miles, A. L. Wilkins, R. T. Gallagher, A. D. Hawkes, S. C. Munday, and N. R. Towers, *J. Agric. Food Chem.* **40**, 234 (1992).
17. R. T. Gallagher, J. Finer, J. Clardy, A. Leutwiler, F. Weibel, W. Ackin, and D. Arigoni, *Tetrahedron Lett.* **21**, 235 (1980).
18. R. J. Cole, J. W. Dorner, J. P. Springer, and R. H. Cox, *J. Agric. Food Chem.* **29**, 293 (1981).
19. G. N. Belofsky, J. B. Gloer, D. T. Wicklow, and P. F. Dowd, *Tetrahedron* **51**, 3959 (1995).
20. K. Kawai and K. Nozawa, in “Mycotoxins and Phycotoxins '88” (S. Natori, S. Hashimoto and Y. Ueno, eds.), pp. 205. Elsevier Science Publishers BV, Amsterdam, 1989.
21. R. J. Cole and J. W. Kirksey, *Can. J. Microbiol.* **20**, 1159 (1974).
22. J. P. Springer, J. Clardy, J. M. Wells, R. J. Cole, and J. W. Kirksey, *Tetrahedron Lett.* **30**, 2531 (1975).

23. C. M. Weedon and P. G. Mantle, *Phytochemistry* **26**, 969 (1987).
24. K. Nozawa, Y. Horie, S. Udagawa, K. Kawai, and M. Yamazaki, *Chem. Pharm. Bull.* **37**, 1387 (1989).
25. K. Nozawa, H. Seyea, S. Nakajima, S. Udagawa, and K. Kawai, *J. Chem. Soc., Perkin Trans. 1*, 1735 (1987).
26. H. Seya, K. Nozawa, S. Udagawa, S. Nakajima, and K. Kawai, *Chem. Pharm. Bull.* **34**, 2411 (1986).
27. C. O. Miles, G. A. Lane, M. E. diMenna, I. Garthwaite, E. L. Piper, O. J.-P. Ball, G. C. M. Latch, J. M. Allen, M. B. Hunt, L. P. Bush, F. K. Min, I. Fletcher, P. S. Harris, *J. Agric. Food Chem.* **44**, 1285 (1996).
28. C. O. Miles, M. E. Di Menna, S. W. L. Jacobs, I. Garthwaite, G. A. Lane, R. A. Prestidge, S. L. Marshall, H. H. Wilkinson, C. L. Schardl, O. J.-P. Ball, G. C. M. Latch, *Appl. Environ. Microbiol.* **64**, 601 (1998).
29. P. G. Mantle, S. J. Burt, K. M. MacGeorge, J. N. Bilton, and R. N. Sheppard, *Xenobiotica* **20**, 809 (1990).
30. H. G. Knaus, O. B. McManus, S. H. Lee, W. A. Schmalhofer, M. Garcia-Calvo, L. M. H. Helms, M. Sanchez, K. Giangiacomo, J. P. Reuben, A. B., III, Kaczorowski, G. J. Smith, M. L. Garcia, *Biochemistry* **33**, 5819 (1994).
31. M. Sanchez and O. B. McManus, *Neuropharmacology* **35**, 963 (1996).
32. G. D. Li and D. W. Cheung, *Eur. J. Pharmacol.* **372**, 103 (1999).
33. F. P. DeFarias, M. F. Carvalho, S. H. Lee, G. J. Kaczorowski, and G. Suarez-Kurtz, *Eur. J. Pharmacol.* **314**, 123 (1996).
34. C. L. Longland, J. L. Dyer, and F. Michelangeli, *Eur. J. Pharmacol.* **408**, 219 (2000).
35. P. G. Mantle and C. M. Weedon, *Phytochemistry* **36**, 1209 (1994).
36. T. Hosoe, K. Nozawa, S. Udagawa, S. Nakajima, and K. Kawai, *Chem. Pharm. Bull.* **38**, 3473 (1990).
37. C. O. Miles, A. L. Wilkins, I. Garthwaite, R. M. Ede, and S. C. Munday-Finch, *J. Org. Chem.* **60**, 6067 (1995).
38. G. M. Staub, K. B. Gloer, and J. B. Gloer, *Tetrahedron Lett.* **34**, 2569 (1993).
39. X. H. Huang, H. Nishida, H. Tomoda, N. Tabata, K. Shiomi, D. J. Yang, H. Takayanagi, and S. Omura, *J. Antibiot.* **48**, 5 (1995).
40. H. Tomoda, N. Tabata, D. J. Yang, H. Takayanagi, and S. Omura, *J. Antibiot.* **48**, 793 (1995).
41. S. C. Munday-Finch, A. L. Wilkins, C. O. Miles, H. Tomoda, and S. Omura, *J. Agric. Food Chem.* **45**, 199 (1997).
42. C. Li, J. B. Gloer, D. T. Wicklow, and P. F. Dowd, *Org. Lett.* **4**, 3095 (2002).
43. B. J. Wilson and C. H. Wilson, *Science* **144**, 177 (1964).
44. R. T. Gallagher, J. Clardy, and B. J. Wilson, *Tetrahedron Lett.* **21**, 239 (1980).
45. R. T. Gallagher and B. J. Wilson, *Mycopathologia* **66**, 183 (1978).
46. D. T. Wicklow and R. J. Cole, *Can. J. Bot.* **60**, 525 (1982).
47. R. T. Gallagher and A. D. Hawkes, *Experientia*, 823 (1986).
48. J. J. Valdes, J. E. Cameron, and R. J. Cole, *Environ. Health Perspect.* **62**, 459 (1985).
49. Y. Yao, A. B. Peter, R. Baur, and E. Sigel, *Mol. Pharmacol.* **35**, 319 (1989).
50. D. B. Gant, R. J. Cole, J. J. Valdes, M. E. Eldefrawi, and A. T. Eldefrawi, *Life Sci.* **41**, 2207 (1987).
51. G. F. Bills, R. A. Giacobbe, S. H. Lee, F. Pelaez, and J. S. Tkacz, *Mycol. Res.* **96**, 977 (1992).
52. J. W. Dorner, R. J. Cole, R. H. Cox, and B. M. Cunfer, *J. Agric. Food Chem.* **32**, 1069 (1984).

53. J. A. Laakso, J. B. Gloer, D. T. Wicklow, and P. F. Dowd, *J. Org. Chem.* **57**, 2066 (1992).
54. B. J. Wilson, C. H. Wilson, and A. W. Hayes, *Nature* **220**, 77 (1968).
55. C. T. Hou, A. Ciegler, and C. W. Hesseltine, *Can. J. Microbiol.* **17**, 599 (1971).
56. J. I. Pitt, *Mycologia* **71**, 1166 (1979).
57. A. E. DeJesus, P. S. Steyn, F. R. van Heerden, R. Vleggaar, and P. L. Wessels, *J. Chem. Soc., Chem. Commun.*, 289 (1981).
58. A. E. DeJesus, P. S. Steyn, F. R. van Heerden, R. Vleggaar, and P. L. Wessels, *J. Chem. Soc., Perkin Trans. 1*, 1847 (1983).
59. A. E. DeJesus, C. P. Gorst-Allman, P. S. Steyn, F. R. van Heerden, R. Vleggaar, and P. L. Wessels, *J. Chem. Soc., Perkin Trans. 1*, 1863 (1983).
60. A. Horeau, *Tetrahedron Lett.*, 506 (1961).
61. P. J. Norris, C. C. T. Smith, J. de Belle Roche, H. F. Bradford, P. G. Mantle, A. J. Thomas, and R. H. C. Penny, *J. Neurochem.* **34**, 33 (1980).
62. J. B. Cavanagh, J. L. Holton, C. C. Nolan, D. E. Ray, J. T. Naik, and P. G. Mantle, *Vet. Pathol.* **35**, 53 (1998).
63. P. Breton, J. C. Bizot, J. Buee, and I. De la Manche, *Toxicon* **36**, 645 (1998).
64. P. F. Dowd, R. J. Cole, and R. F. Vesonder, *J. Antibiot.* **41**, 1868 (1988).
65. A. E. DeJesus, P. S. Steyn, F. R. van Heerden, R. Vleggaar, and P. L. Wessels, *J. Chem. Soc., Perkin Trans. 1*, 1857 (1983).
66. A. L. Wilkins, C. O. Miles, R. M. Ede, R. T. Gallagher, and S. C. Munday, *J. Agric. Food Chem.* **40**, 1307 (1992).
67. T. Rundberget and A. L. Wilkins, *Phytochemistry* **61**, 979 (2002).
68. J. Penn, J. R. Biddle, P. G. Mantle, J. N. Bilton, and R. N. Sheppard, *J. Chem. Soc., Perkin Trans. 1* **1**, 23 (1992).
69. J. A. Laakso, J. B. Gloer, D. T. Wicklow, and P. F. Dowd, *J. Agric. Food Chem.* **41**, 973 (1993).
70. J. T. Naik, P. G. Mantle, R. N. Sheppard, and E. S. Waight, *J. Chem. Soc., Perkin Trans. 1*, 1121 (1995).
71. R. T. Gallagher, G. C. M. Latch, and R. G. Keogh, *Appl. Environ. Microbiol.* **39**, 272 (1980).
72. D. R. Lauren and R. T. Gallagher, *J. Chromatogr.* **248**, 150 (1982).
73. J. Penn, R. Swift, L. J. Wigley, P. G. Mantle, J. N. Bilton, and R. N. Sheppard, *Phytochemistry* **32**, 1431 (1993).
74. A. E. DeJesus, P. S. Steyn, F. R. van Heerden, and R. Vleggaar, *J. Chem. Soc., Perkin Trans. 1*, 697 (1984).
75. L. A. Holmes, N. W. Frame, R. K. Frame, J. P. Duff, and G. C. Lewis, *Vet. Rec.* **145**, 462 (1999).
76. E. M. Freeman, *Proc. R. Soc. Lond.* **71**, 27 (1902).
77. L. R. Fletcher and I. C. Harvey, *N. Z. Vet. J.* **29**, 185 (1981).
78. R. T. Gallagher, E. P. White, and P. H. Mortimer, *N. Z. Vet. J.* **29**, 189 (1981).
79. R. T. Gallagher, A. D. Hawkes, P. S. Steyn, and R. Vleggaar, *J. Chem. Soc., Chem. Commun.*, 614 (1984).
80. S. C. Munday-Finch, A. L. Wilkins, and C. O. Miles, *J. Agric. Food Chem.* **46**, 590 (1998).
81. R. T. Gallagher, A. G. Campbell, A. D. Hawkes, P. T. Holland, D. A. McGaveston, E. A. Pansier, and I. C. Harvey, *N. Z. Vet. J.* **30**, 183 (1982).
82. S. C. Munday-Finch, C. O. Miles, A. L. Wilkins, and A. D. Hawkes, *J. Agric. Food Chem.* **43**, 1283 (1995).

83. R. M. Ede, C. O. Miles, L. P. Meagher, S. C. Munday, and A. L. Wilkins, *J. Agric. Food Chem.* **42**, 231 (1994).
84. S. C. Munday-Finch, A. L. Wilkins, C. O. Miles, R. M. Ede, and R. A. Thomson, *J. Agric. Food Chem.* **44**, 2782 (1996).
85. C. O. Miles, S. C. Munday, A. L. Wilkins, R. M. Ede, and N. R. Towers, *J. Agric. Food Chem.* **42**, 1488 (1994).
86. R. T. Gallagher, A. D. Hawkes, and J. M. Stewart, *J. Chromatogr.* **321**, 217 (1985).
87. G. W. Bruehl and R. E. Klein, *Mycologia* **86**, 773 (1994).
88. P. T. Meinke, M. M. Smith, and W. L. Shoop, *Curr. Top. Med. Chem.* **2**, 655 (2002).
89. J. G. Ondeyka, G. L. Helms, O. D. Hensens, M. A. Goetz, D. L. Zink, A. Tspirouras, W. L. Shoop, L. Slayton, A. W. Dombrowski, J. D. Polishook, D. A. Ostlind, N. N. Tsou, R. G. Ball, S. B. Singh, *J. Am. Chem. Soc.* **119**, 8809 (1997).
90. J. D. Polishook, J. G. Ondeyka, A. W. Dombrowski, F. Pelaez, G. Platas, and A. M. Teran, *Mycologia* **93**, 1125 (2001).
91. O. D. Hensens, J. G. Ondeyka, A. W. Dombrowski, D. A. Ostlind, and D. L. Zink, *Tetrahedron Lett.* **40**, 5455 (1999).
92. J. G. Ondeyka, A. M. Dahl-Roshak, J. S. Tkacz, D. L. Zink, M. Zakson-Aiken, W. L. Shoop, M. A. Goetz, and S. B. Singh, *Bioorg. Med. Chem. Lett.* **12**, 2941 (2002).
93. J. G. Ondeyka, K. Byrne, D. Vesey, D. L. Zink, W. L. Shoop, M. A. Goetz, and S. B. Singh, *J. Nat. Prod.* **66**, 121 (2003).
94. P. K. Chakravarty, S. Tyagarajan, T. L. Shih, S. Salva, C. Snedden, M. J. Wyvratt, M. H. Fisher, and P. T. Meinke, *Org. Lett.* **4**, 1291 (2002).
95. P. K. Chakravarty, T. L. Shih, S. L. Colletti, M. B. Ayer, C. Snedden, H. Kuo, S. Tyagarajan, L. M. Gregory, M. Zakson-Aiken, W. L. Shoop, D. M. Schmatz, M. J. Wyvratt, M. H. Fisher, P. T. Meinke, *Bioorg. Med. Chem. Lett.* **12**, 147 (2003).
96. D. Ok, C. Li, T. L. Shih, S. Salva, M. B. Ayer, S. L. Colletti, P. K. Chakravarty, M. J. Wyvratt, M. H. Fisher, L. Gregory, M. Zakson-Aiken, W. L. Shoop, D. M. Schmatz, P. T. Meinke, *Bioorg. Med. Chem. Lett.* **12**, 1751 (2002).
97. R. Berger, W. L. Shoop, J. V. Pivnichny, L. M. Warmke, M. Zakson-Aiken, K. A. Owens, P. deMontigny, D. M. Schmatz, M. J. Wyvratt, M. H. Fisher, P. T. Meinke, S. L. Colletti, *Org. Lett.* **3**, 3715 (2001).
98. P. Wipf and S. Lim, *J. Am. Chem. Soc.* **117**, 558 (1995).
99. P. Wipf and C. P. Miller, *Tetrahedron Lett.* **33**, 907 (1992).
100. P. T. Meinke, M. B. Ayer, S. L. Colletti, C. S. Li, J. Lim, D. Ok, S. Salva, D. M. Schmatz, T. L. Shih, W. L. Shoop, L. M. Warmke, M. J. Wyvratt, M. Zakson-Aiken, M. H. Fisher, *Bioorg. Med. Chem. Lett.* **10**, 2371 (2000).
101. W. L. Shoop, L. M. Gregory, M. Zakson-Aiken, B. F. Michael, H. W. Haines, J. G. Ondeyka, P. T. Meinke, and D. M. Schmatz, *J. Parasitol.* **87**, 419 (2001).
102. M. M. Smith, V. A. Warren, B. S. Thomas, R. M. Brochu, E. A. Ertel, S. Rohrer, J. Schaeffer, D. Schmatz, B. R. Petuch, Y. S. Tang, P. T. Meinke, G. J. Kaczorowski, C. J. Cohen, *Biochemistry* **39**, 5543 (2000).
103. N. S. Kane, B. Hirschberg, S. Qian, D. Hunt, B. Thomas, R. Brochu, S. W. Ludmerer, Y. C. Zheng, M. Smith, J. P. Arena, C. J. Cohen, D. Schmatz, J. Warmke, D. F. Cully, *Proc. Natl. Acad. Sci. USA* **97**, 13949 (2000).
104. S. W. Ludmerer, V. A. Warren, B. S. Williams, Y. C. Zheng, D. C. Hunt, M. B. Ayer, M. A. Wallace, A. G. Chaudhary, M. A. Egan, P. T. Meinke, D. C. Dean, M. L. Garcia, D. F. Cully, M. M. Smith, *Biochemistry* **41**, 6548 (2002).

105. T. Felcetto, J. Ondeyka, S. L. Colletti, P. T. Meinke, and W. L. Shoop, *J. Parasitol.* **88**, 223 (2002).
106. W. L. Shoop, M. Zakson-Aiken, L. M. Gregory, B. F. Michael, J. Pivnichny, P. T. Meinke, M. H. Fisher, M. J. Wyrvatt, B. Pikounis, D. M. Schmatz, *J. Parasitol.* **87**, 1150 (2001).
107. A. B., III and Mewshaw, R. Smith, *J. Am. Chem. Soc.* **107**, 1769 (1985).
108. A. B., III and Leenay, T. L. Smith, *Tetrahedron Lett.* **29**, 2791 (1988).
109. R. E. Mewshaw, M. D. Taylor, and Smith, A. B., III, *J. Org. Chem.* **54**, 3449 (1989).
110. B. Robinson, *Chem. Rev.* **62**, 373 (1962).
111. P. G. Gassman, T. J. van Bergen, D. P. Gilbert, and Cue, B. W., Jr., *J. Am. Chem. Soc.* **96**, 5495 (1974).
112. Z. G. Hajos and D. R. Parrish, *J. Org. Chem.* **39**, 1615 (1974).
113. D. N. Kirk and V. J. Petrow, *J. Chem. Soc.*, 1091 (1962).
114. A. B., III and Mewshaw, R. E. Smith, *J. Org. Chem.* **49**, 3685 (1984).
115. A. B., III and Leenay, T. L. Smith, *J. Am. Chem. Soc.* **111**, 5761 (1989).
116. A. B., III and Leenay, T. L. Smith, *Tetrahedron Lett.* **29**, 2787 (1988).
117. A. B., III, Kingery-Wood, J. Smith, T. L. Leenay, E. G. Nolen, and T. Sunazuka, *J. Am. Chem. Soc.* **114**, 1438 (1992).
118. T. Nitz and L. A. Paquette, *Tetrahedron Lett.*, 3047 (1984).
119. M. Jung, *Tetrahedron* **32**, 3 (1976).
120. A. E. Greene, J. P. Lansard, J. L. Luche, and C. Petrier, *J. Org. Chem.* **49**, 931 (1984).
121. S. L. Huang, K. Omura, and D. Swern, *J. Org. Chem.* **41**, 3329 (1976).
122. J. C. Collins, W. W. Hess, and F. J. Frank, *Tetrahedron Lett.*, 3363 (1968).
123. A. P. Krapcho and A. J. Lovey, *Tetrahedron Lett.*, 957 (1973).
124. A. B., III, Sunazuka, T. Smith, T. L. Leenay, and J. Kingery-Wood, *J. Am. Chem. Soc.* **112**, 8197 (1990).
125. D. L. J. Clive and A. C. Joussef, *J. Org. Chem.* **55**, 1096 (1990).
126. A. Ali and J. E. Saxton, *Tetrahedron Lett.* **30**, 3197 (1989).
127. A. Ali, S. Guile, J. E. Saxton, and M. Thornton-Pett, *Tetrahedron Lett.* **47**, 6407 (1991).
128. S. Guile, J. E. Saxton, and M. Thornton-Pett, *Tetrahedron Lett.* **32**, 1381 (1991).
129. W. C. Still, F. Mohamadi, N. G. J. Richards, W. C. Guida, M. Lipton, R. Liskamp, G. Chang, T. Hendrickson, F. DeGunst, and W. Hasel, Department of Chemistry, Columbia University, New York, NY 10027.
130. S. Guile, J. E. Saxton, and M. Thornton-Pett, *J. Chem. Soc., Perkin Trans. 1*, 1763 (1992).
131. E. J. Corey and S. C. Virgil, *J. Am. Chem. Soc.* **112**, 6429 (1990).
132. J. Haseltine, M. Visnick, and Smith, A. B., III, *J. Org. Chem.* **53**, 6160 (1988).
133. G. Stork and R. L. Danheiser, *J. Org. Chem.* **38**, 1775 (1973).
134. W. Semmler, *Chem. Ber.* **25**, 3352 (1892).
135. L. Wolff, *Annalen* **322**, 351 (1902).
136. A. B., III, Nolen, E. G., Jr., Shirai, R. Smith, F. R. Blase, M. Ohta, N. Chida, R. A. Hartz, D. M. Fitch, W. M. Clark, P. A. Sprengeler, *J. Org. Chem.* **60**, 7837 (1995).
137. A. B., III, Hartz, R. A. Smith, P. G. Spoor, and J. D. Rainier, *Isr. J. Chem.* **37**, 69 (1997).
138. A. B. Charette and J.-F. Marcous, *Synlett*, 1197 (1995).
139. A. H. Hoveyda, D. A. Evans, and G. C. Fu, *Chem. Rev.* **93**, 1307 (1993).
140. R. U. Lemieux and E. von Rudloff, *Can. J. Chem.* **33**, 1701 (1955).

141. A. B., III, Kanoh, N. Smith, H. Ishiyama, and R. A. Hartz, *J. Am. Chem. Soc.* **122**, 11254 (2000).
142. A. B., III, Ohta, M. Smith, W. M. Clark, and J. W. Leahy, *Tetrahedron Lett.* **34**, 3033 (1993).
143. A. B., III, Visnick, M. Smith, J. N. Haseltine, and P. A. Sprengeler, *Tetrahedron* **42**, 2957 (1986).
144. A. B., III and Visnick, M. Smith, *Tetrahedron Lett.* **26**, 3757 (1985).
145. J. R. Parikh and W. E. Doering, *J. Am. Chem. Soc.* **89**, 5505 (1967).
146. P. A. Grieco, S. Gilman, and M. Nishizawa, *J. Org. Chem.* **41**, 1485 (1976).
147. P. Magnus and T. E. Mansley, *Tetrahedron Lett.* **40**, 6909 (1999).
148. T. Nagamitsu, T. Sunazuka, R. Obata, H. Tomoda, H. Tanaka, Y. Harigaya, K. Omura, and Smith, A. B., III, *J. Org. Chem.* **60**, 8126 (1995).
149. A. B., III, Ishiyama, H. Smith, Y. S. Cho, and K. Ohmoto, *Org. Lett.* **3**, 3967 (2001).
150. A. B., III, Cho, Y. S. Smith, and H. Ishiyama, *Org. Lett.* **3**, 3971 (2001).
151. I. Ohtani, T. Kusumi, Y. Kashman, and H. Kakisawa, *J. Am. Chem. Soc.* **113**, 4092 (1991).
152. D. L. Comins and A. Dehghani, *Tetrahedron Lett.* **33**, 6299 (1992).
153. M. Mori, N. Kaneta, and M. Shibasaki, *J. Org. Chem.* **56**, 3486 (1991).
154. S. Kobayashi, *Chem. Lett.*, 2187 (1991).
155. H. Kogen, K. Tomioka, S. Hashimoto, and K. Koga, *Tetrahedron* **37**, 3951 (1981).
156. W. Ackin, F. Weibel, and D. Arigoni, *Chimia* **31**, 63 (1977).
157. K. Nozawa, M. Yuyama, S. Nakajima, and K. Kawai, *J. Chem. Soc., Perkin Trans. I*, 2155 (1988).
158. I. Laws and P. G. Mantle, *J. Gen. Microbiol.* **135**, 2679 (1989).
159. K. Nozawa, H. Nakajima, and S. Udagawa, *J. Chem. Soc., Perkin. Trans. I*, 1689 (1988).
160. P. G. Mantle and J. Penn, *J. Chem. Soc., Perkin Trans. I*, 1539 (1989).
161. J. Penn and P. G. Mantle, *Phytochemistry* **35**, 921 (1994).
162. C. Young, Y. Itoh, R. Johnson, I. Garthwaite, C. O. Miles, S. C. Munday-Finch, and B. Scott, *Curr. Genet.* **33**, 368 (1998).
163. C. Young, L. McMillan, E. Telfer, and B. Scott, *Mol. Microbiol.* **39**, 754 (2001).
164. R. J. Cole, *J. Food Prot.* **44**, 715 (1981).
165. A. L. Wilkins, C. O. Miles, R. M. Ede, R. T. Gallagher, and S. C. Munday, *J. Agric. Food Chem.* **40**, 1307 (1992).
166. K. M. Byrne, S. K. Smith, and J. G. Ondeyka, *J. Am. Chem. Soc.* **124**, 7055 (2002).



## THE *DAPHNIPHYLLUM* ALKALOIDS

JUN'ICHI KOBAYASHI AND HIROSHI MORITA

*Graduate School of Pharmaceutical Sciences, Hokkaido University,  
Sapporo 060, Japan*

- I. Introduction
  - II. Structures of Representative Alkaloids
  - III. Biosynthesis and Biogenesis
  - IV. Synthesis
  - V. Conclusions
- References

### I. Introduction

*Daphniphyllum* alkaloids are a structurally diverse group of natural products, which are elaborated by the oriental tree “Yuzuriha” (*Daphniphyllum macropodum*; Daphniphyllaceae) which are dioecious evergreen trees and shrubs native to central and southern Japan. *Daphniphyllum* comes from the Greek and refers to “Daphne” and “leaf.” “Yuzuri-ha” means that the old leaf is replaced by a new leaf in the succeeding season. That is, to take over or take turns, with the old leaf dropping after the new leaf emerges, thus there is no interruption of the foliage. “Yuzuri-ha” in Japan is used as an ornamental plant for the New Year to celebrate the good relationships of the old and new generations. There are three *Daphniphyllum* species in Japan, *D. macropodum*, *D. teijsmanni*, and *D. humile*. The other several species, such as *D. calycinum*, *D. gracile*, and *D. glaucescens* are closely distributed in New Guinea, China, and Taiwan, respectively.

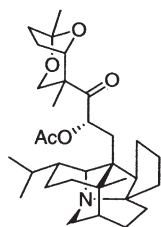
Since the previous review by Yamamura and Hirata in Volume 15 (1) and by Yamamura in Volume 29 (2) of this treatise, a number of new *Daphniphyllum* alkaloids have been discovered. As a result, the number of known *Daphniphyllum* alkaloids has grown markedly in recent years to a present count of 63 (compounds 1–63). These alkaloids, isolated chiefly by Yamamura and Hirata *et al.* are classified into six different types of backbone skeletons (1–3). These unusual ring systems

have attracted great interest as challenging targets for total synthesis or biosynthetic studies. This chapter covers the reports on *Daphniphyllum* alkaloids that have been published between 1987 and 2002, and provides an update of the previous review by Yamamura in 1984 (2). Since the structures and stereochemistry of these alkaloids are quite complex and the representation of the structure formula has not been unified, all of the natural *Daphniphyllum* alkaloids (compounds 1–63) are listed in Table I. Classification of the alkaloids basically follows that of the previous reviews (1,2), but sections on the newly found skeletons have been added.

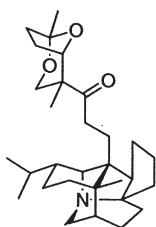
It was of substantial interest when Heathcock and coworkers proposed a biogenetic pathway for *Daphniphyllum* alkaloids (4,5) and demonstrated a biomimetic total synthesis of several *Daphniphyllum* alkaloids.

TABLE I.  
Skeletal Types of *Daphniphyllum* Alkaloids.

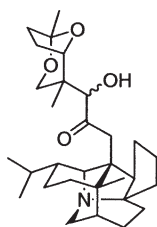
A. Daphnane-Type Alkaloids



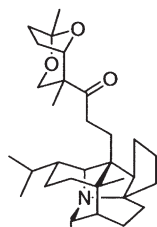
Daphniphylline (1)<sup>7-10</sup>  
(Daphniphyllamine)  
(C<sub>32</sub>H<sub>49</sub>NO<sub>5</sub>)



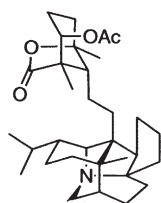
Codaphniphylline (2)<sup>10-12</sup>  
(C<sub>30</sub>H<sub>47</sub>NO<sub>3</sub>)



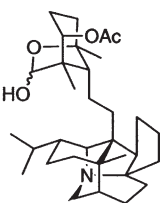
Daphniphyllidine (3)<sup>13</sup>  
(C<sub>30</sub>H<sub>47</sub>NO<sub>4</sub>)



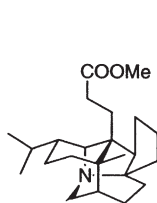
Daphnimacropine (4)<sup>14</sup>  
(C<sub>30</sub>H<sub>47</sub>NO<sub>4</sub>)



Daphmacrine (5)<sup>15-17</sup>  
(C<sub>32</sub>H<sub>49</sub>NO<sub>4</sub>)



Daphmacropodine (6)<sup>15,18</sup>  
(C<sub>32</sub>H<sub>51</sub>NO<sub>4</sub>)

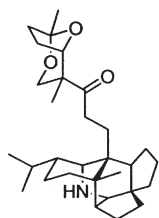
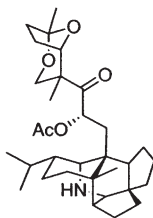
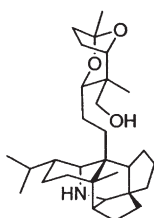
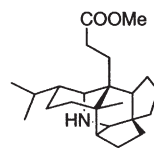


Methyl Homodaphniphyllate (7)<sup>19,20,37</sup>  
(C<sub>23</sub>H<sub>37</sub>NO<sub>2</sub>)

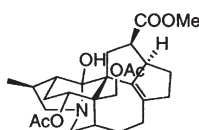
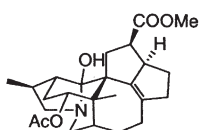
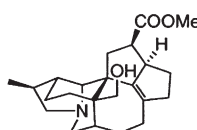
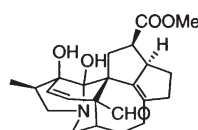
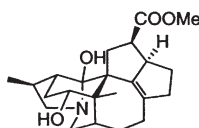
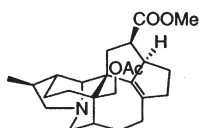
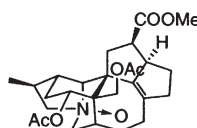
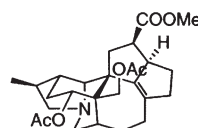
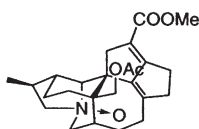
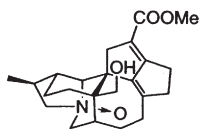
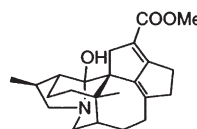
(continued)

TABLE I.  
Continued.

## B. Secodaphnane-Type Alkaloids

Secodaphniphylline (**8**)<sup>19,21,22</sup>  
(C<sub>30</sub>H<sub>47</sub>NO<sub>3</sub>)Daphniteijsmine (**9**)<sup>23</sup>  
(C<sub>33</sub>H<sub>49</sub>NO<sub>5</sub>)Daphniteijsmanine (**10**)<sup>24</sup>  
(C<sub>30</sub>H<sub>49</sub>NO<sub>3</sub>)Methyl Homoseco-  
daphniphyllate (**11**)<sup>19,21,22</sup>  
(C<sub>23</sub>H<sub>37</sub>NO<sub>2</sub>)

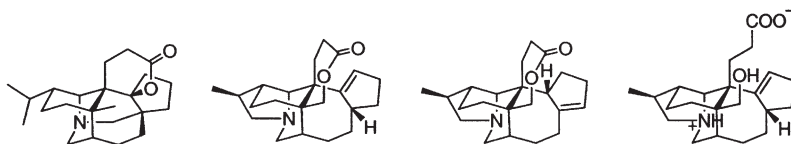
## C. Yuzurimine Skeletal Types

Yuzurimine (**12**)<sup>7, 15,25,26</sup>  
(Macrodaphnidine)  
(C<sub>27</sub>H<sub>37</sub>NO<sub>7</sub>)Yuzurimine-A (**13**)<sup>26,27</sup>  
(C<sub>25</sub>H<sub>35</sub>NO<sub>5</sub>)Yuzurimine-B (**14**)<sup>26,27</sup>  
(C<sub>23</sub>H<sub>33</sub>NO<sub>3</sub>)Yuzurimine-C (**15**)<sup>28</sup>  
(C<sub>23</sub>H<sub>29</sub>NO<sub>5</sub>)Macrodaphniphyllamine (**16**)<sup>15</sup>  
(Deacetyl yuzurimine-A)  
(C<sub>23</sub>H<sub>33</sub>NO<sub>4</sub>)Macrodaphniphyllidine (**17**)<sup>15</sup>  
(Acetyl yuzurimine B)  
(C<sub>25</sub>H<sub>35</sub>NO<sub>4</sub>)Macrodaphnine (**18**)<sup>15,29</sup>  
(C<sub>27</sub>H<sub>37</sub>NO<sub>7</sub>)Deoxyyuzurimine (**19**)<sup>30</sup>  
(C<sub>27</sub>H<sub>37</sub>NO<sub>6</sub>)Daphnijsmine (**20**)<sup>23</sup>  
(C<sub>25</sub>H<sub>33</sub>NO<sub>5</sub>)Deacetyl daphnijsmine (**21**)<sup>23</sup>  
(C<sub>23</sub>H<sub>31</sub>NO<sub>4</sub>)Calycine A (**22**)<sup>31</sup>  
(C<sub>23</sub>H<sub>31</sub>NO<sub>3</sub>)

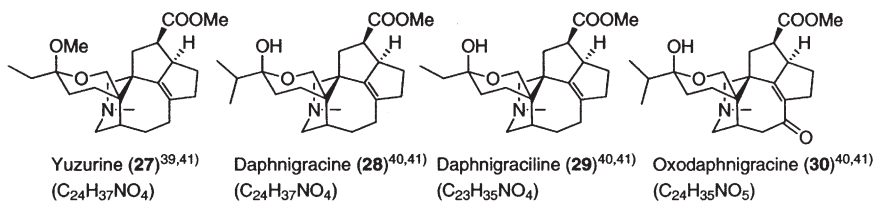
(continued)

TABLE I.  
 Continued.

## D and E. Daphnilactones A and B type Alkaloids

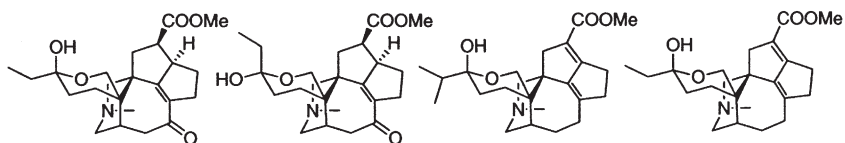

 Daphnilactone A (**23**)<sup>32,33</sup> Daphnilactone B (**24**)<sup>34-37</sup> Isodaphnilactone B (**25**)<sup>30</sup> Zwitterionic alkaloid (**26**)<sup>38</sup>  
 (C<sub>23</sub>H<sub>35</sub>NO<sub>2</sub>) (C<sub>22</sub>H<sub>31</sub>NO<sub>2</sub>) (C<sub>22</sub>H<sub>31</sub>NO<sub>2</sub>) (C<sub>22</sub>H<sub>33</sub>NO<sub>3</sub>)

## F. Yuzurine-Type and Other Alkaloids


 Yuzurine (**27**)<sup>39,41</sup>  
 (C<sub>24</sub>H<sub>37</sub>NO<sub>4</sub>)

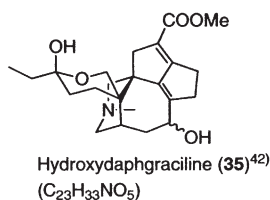
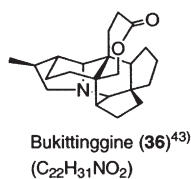
 Daphnigracine (**28**)<sup>40,41</sup>  
 (C<sub>24</sub>H<sub>37</sub>NO<sub>4</sub>)

 Daphnigraciline (**29**)<sup>40,41</sup>  
 (C<sub>23</sub>H<sub>35</sub>NO<sub>4</sub>)

 Oxodaphnigracine (**30**)<sup>40,41</sup>  
 (C<sub>24</sub>H<sub>35</sub>NO<sub>5</sub>)

 Oxodaphnigraciline (**31**)<sup>40,41</sup>  
 (C<sub>23</sub>H<sub>33</sub>NO<sub>5</sub>)

 Epioxodaphnigraciline (**32**)<sup>40,41</sup>  
 (C<sub>23</sub>H<sub>33</sub>NO<sub>5</sub>)

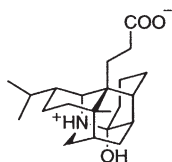
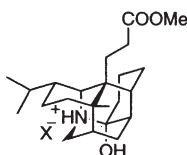
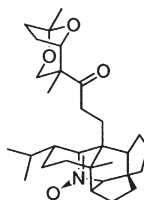
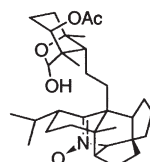
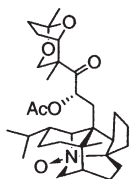
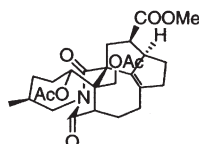
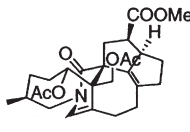
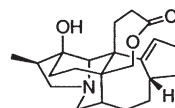
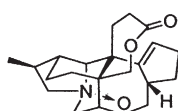
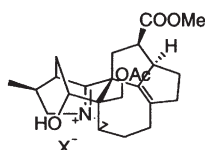
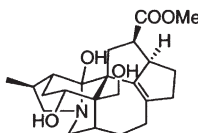
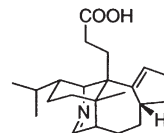
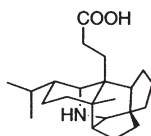
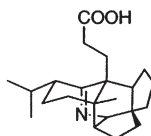
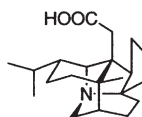
 Daphgracine (**33**)<sup>42</sup>  
 (C<sub>24</sub>H<sub>35</sub>NO<sub>4</sub>)

 Daphgraciline (**34**)<sup>42</sup>  
 (C<sub>23</sub>H<sub>33</sub>NO<sub>4</sub>)

 Hydroxydaphgraciline (**35**)<sup>42</sup>  
 (C<sub>23</sub>H<sub>33</sub>NO<sub>5</sub>)

 Bukittinggine (**36**)<sup>43</sup>  
 (C<sub>22</sub>H<sub>31</sub>NO<sub>2</sub>)

(continued)

TABLE I.  
Continued.

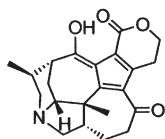
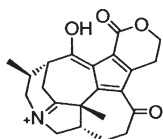
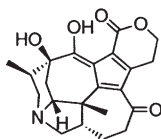
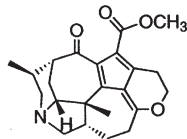
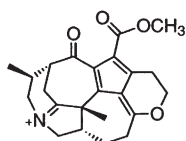
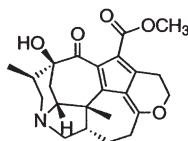
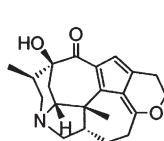
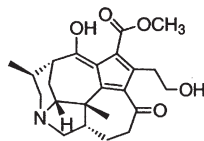
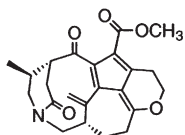
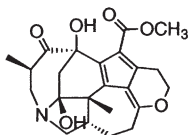
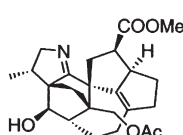
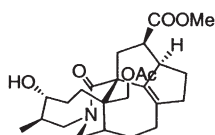
## G. Daphnezomines

Daphnezimine A (37)<sup>44</sup>  
(C<sub>22</sub>H<sub>35</sub>NO<sub>3</sub>)Daphnezimine B (38)<sup>44</sup>  
(C<sub>23</sub>H<sub>39</sub>NO<sub>3</sub>)Daphnezimine C (39)<sup>45</sup>  
(C<sub>30</sub>H<sub>45</sub>NO<sub>4</sub>)Daphnezimine D (40)<sup>45</sup>  
(C<sub>32</sub>H<sub>49</sub>NO<sub>5</sub>)Daphnezimine E (41)<sup>45</sup>  
(C<sub>22</sub>H<sub>49</sub>NO<sub>6</sub>)Daphnezimine F (42)<sup>46</sup>  
(C<sub>27</sub>H<sub>35</sub>NO<sub>8</sub>)Daphnezimine G (43)<sup>46</sup>  
(C<sub>27</sub>H<sub>35</sub>NO<sub>7</sub>)Daphnezimine H (44)<sup>47</sup>  
(C<sub>22</sub>H<sub>31</sub>NO<sub>3</sub>)Daphnezimine I (45)<sup>47</sup>  
(C<sub>22</sub>H<sub>31</sub>NO<sub>3</sub>)Daphnezimine J (46)<sup>47</sup>  
(C<sub>25</sub>H<sub>34</sub>NO<sub>5</sub>)Daphnezimine K (47)<sup>47</sup>  
(C<sub>23</sub>H<sub>33</sub>NO<sub>5</sub>)Daphnezimine L (48)<sup>48</sup>  
(C<sub>22</sub>H<sub>33</sub>NO<sub>2</sub>)Daphnezimine M (49)<sup>48</sup>  
(C<sub>22</sub>H<sub>35</sub>NO<sub>2</sub>)Daphnezimine N (50)<sup>48</sup>  
(C<sub>22</sub>H<sub>33</sub>NO<sub>2</sub>)Daphnezimine O (51)<sup>48</sup>  
(C<sub>21</sub>H<sub>33</sub>NO<sub>2</sub>)

(continued)

TABLE I.  
 Continued.

H and I. Daphnicyclidins and Daphmanidins


 Daphnicyclidin A (**52**)<sup>49</sup>  
 (C<sub>22</sub>H<sub>25</sub>NO<sub>4</sub>)

 Daphnicyclidin B (**53**)<sup>49</sup>  
 (C<sub>22</sub>H<sub>24</sub>NO<sub>4</sub>)

 Daphnicyclidin C (**54**)<sup>49</sup>  
 (C<sub>22</sub>H<sub>25</sub>NO<sub>5</sub>)

 Daphnicyclidin D (**55**)<sup>49</sup>  
 (C<sub>23</sub>H<sub>27</sub>NO<sub>4</sub>)

 Daphnicyclidin E (**56**)<sup>49</sup>  
 (C<sub>23</sub>H<sub>26</sub>NO<sub>4</sub>)

 Daphnicyclidin F (**57**)<sup>49</sup>  
 (C<sub>23</sub>H<sub>27</sub>NO<sub>5</sub>)

 Daphnicyclidin G (**58**)<sup>49</sup>  
 (C<sub>21</sub>H<sub>25</sub>NO<sub>3</sub>)

 Daphnicyclidin H (**59**)<sup>49</sup>  
 (C<sub>23</sub>H<sub>29</sub>NO<sub>5</sub>)

 Daphnicyclidin J (**60**)<sup>50</sup>  
 (C<sub>23</sub>H<sub>25</sub>NO<sub>5</sub>)

 Daphnicyclidin K (**61**)<sup>50</sup>  
 (C<sub>23</sub>H<sub>27</sub>NO<sub>6</sub>)

 Daphmanidin A (**62**)<sup>51</sup>  
 (C<sub>25</sub>H<sub>33</sub>NO<sub>5</sub>)

 Daphmanidin B (**63**)<sup>51</sup>  
 (C<sub>25</sub>H<sub>35</sub>NO<sub>6</sub>)

This chapter describes the recent studies on *Daphniphyllum* alkaloids isolated from the genus *Daphniphyllum*, the proposed biogenetic pathway, and the syntheses of *Daphniphyllum* alkaloids based on these biogenetic proposals. In Section II, all of the *Daphniphyllum* alkaloids isolated so far and including our recent work are surveyed, while Sections III and IV mainly deal with the biogenetic pathways, the total syntheses, and the biomimetic synthesis of the *Daphniphyllum* alkaloids.

## II. Structures of Representative Alkaloids

### A. DAPHNANE-TYPE ALKALOIDS

In 1909, Yagi isolated daphnimacrine, one of the C<sub>30</sub>-type *Daphniphyllum* alkaloids (6). The structure elucidation of daphniphylline (1), one of the major

C<sub>30</sub>-type *Daphniphyllum* alkaloids, was carried out by X-ray crystallographic analysis of the hydrobromide (7–10). Yamamura and Hirata also reported the structures of codaphniphylline (2) (10–12) and daphniphyllidine (3) (13), both of which are closely related to daphniphylline (1). Furthermore, they isolated methyl homodaphniphyllate (7), and the structure lacking the C8 unit of daphniphylline (3) was elucidated by chemical correlations from daphniphylline (1) (19,20,37). On the other hand, Nakano isolated daphnimacropine (4) (14), daphmacrine (5) (15–17), and daphmacropodine (6) (15,18), the structures of which were elucidated by X-ray crystallographic analysis of their methiodides. The structures and molecular formulae of these alkaloids are listed in Table I.

#### B. SECODAPHNANE-TYPE ALKALOIDS

Two secodaphnane-type alkaloids (Table I), secodaphniphylline (8) (19,21,22) and methyl homosecodaphniphyllate (11) (19,21,22), were isolated by Yamamura and Hirata and their structures were elucidated by X-ray analysis of methyl *N*-bromoacetyl homosecodaphniphyllate and chemical correlations between 8 and 11. The structures of the two related alkaloids, daphnitejsmine (9) (23) and daphnitejsmanine (10) (24), were elucidated by spectroscopic analysis coupled with an exhaustive comparison of the NMR data of secodaphniphylline (8) and methyl homosecodaphniphyllate (11).

#### C. YUZURIMINE-TYPE ALKALOIDS

In 1966, Hirata *et al.* isolated yuzurimine (12) as one of the major alkaloids from *D. macropodum* and reported the crystal structure of yuzurimine hydrobromide (25). They also isolated the two related alkaloids, yuzurimines A (13) and B (14), whose structures were elucidated through spectroscopic data and chemical evidence in 1972. At almost the same time, Nakano *et al.* isolated macrodaphniphyllamine (16), macrodaphniphyllidine (17), and macrodaphnine (18) (15,29), whose structures were identical with deacetyl yuzurimine A, acetyl yuzurimine B, and dihydroyuzurimine, respectively. Yamamura *et al.* isolated deoxyyuzurimine (19) from *D. humile* (30), and daphnijsmine (20) and deacetyl daphnijsmine (21) from the seeds of *D. teijsmanni* (23). From *D. calycinum* distributed in China, calycinine A (22) was isolated, together with deacetyl daphnijsmine (21), deacetyl yuzurimine, and the zwitterionic alkaloid 26 (31).

#### D. DAPHNILACTONE A-TYPE ALKALOIDS

Hirata and Sasaki isolated daphnilactone A (23) as one of the minor alkaloids from *D. macropodum*, and the structure was determined by X-ray analysis (32,33). The skeleton of daphnilactone A (23) is considered to be constructed by the insertion of a Cl unit into a nitrogen–carbon bond in the daphnane type skeleton, such as methyl homodaphniphyllate (7), followed by lactonization.

## E. DAPHNILACTONE B-TYPE ALKALOIDS

Daphnilactone B (**24**) was isolated as one of the major alkaloids from the fruits of three *Daphniphyllum* species in Japan, *D. macropodum*, *D. teijsmanni*, and *D. humile*, and the structure was estimated by extensive spectral analysis, as well as by chemical evidence, and finally assigned by X-ray crystallographic analysis (34,35,37). Isodaphnilactone B (**25**) was isolated from the leaves of *D. humile* and the structure was analyzed by spectroscopic methods (30). A zwitterionic alkaloid **26**, the hydration product of daphnilactone B (**24**), was isolated from the fruits of *D. teijsmanni*, and the structure determined on the basis of its spectral and chemical properties (38).

## F. YUZURINE-TYPE AND OTHER ALKALOIDS

Nine alkaloids belonging to the yuzurine group were isolated from *D. macropodum* and *D. gracile* distributed in New Guinea. The structure of yuzurine (**27**) was established by X-ray crystallographic analysis of yuzurine methiodide (39). The other alkaloids belonging to this group, daphnigracine (**28**), daphnigraciline (**29**), oxodaphnigracine (**30**), oxodaphnigraciline (**31**), epioxodaphnigraciline (**32**), daphgracine (**33**), daphgraciline (**34**), and hydroxydaphgraciline (**35**), were isolated from *D. gracile* and their structures were assigned by spectroscopic methods.

A new skeletal alkaloid, bukittingine (**36**), was isolated from *Sapium baccatum* (Euphorbiaceae). The structure, which is closely related to both methyl homosecodaphniphyllate (**11**) and daphnilactone B (**24**), was determined by X-ray analysis of its hydrobromide (43). The presence of bukittingine (**36**) indicates that this species may be closely related to the genus *Daphniphyllum*.

## G. DAPHNEZOMINES

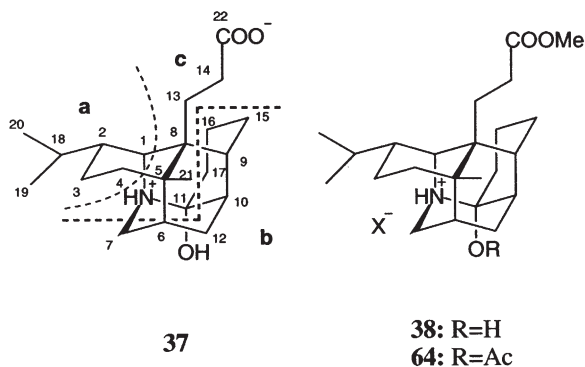
During the course of our studies for biogenetic intermediates of the *Daphniphyllum* alkaloids, a project was initiated on the alkaloids of *D. humile*. A series of new *Daphniphyllum* alkaloids, daphnezomines A–O (**37–51**), which were isolated from the leaves, stems, and fruits of *D. humile*, are of considerable interest from a biogenetic point of view. All of the structures are listed in Table I.

The leaves, stems, and fruits of *D. humile* collected in Sapporo were extracted with MeOH, and the MeOH extract was partitioned between EtOAc and 3% tartaric acid. Water-soluble materials, which were adjusted to pH 9 with sat. Na<sub>2</sub>CO<sub>3</sub>, were partitioned with CHCl<sub>3</sub>, and the CHCl<sub>3</sub>-soluble materials were subjected to a C<sub>18</sub> column (CH<sub>3</sub>CN/0.1% TFA), silica gel column (CHCl<sub>3</sub>/MeOH), and gel filtration on Sephadex LH-20 (MeOH) to afford daphnezomines A (**37**, 0.01% yield), B (**38**, 0.008%), C (**39**, 0.0001%), D (**40**, 0.00007%), E (**41**, 0.001%), F (**42**, 0.0002%), G (**43**, 0.0001%), H (**44**, 0.0002%), I (**45**, 0.005%), J (**46**, 0.002%), and K (**47**, 0.002%), as unspecified salts (44–47). The structures of these daphnezomines A–G (**37–43**) were elucidated mainly on the basis of

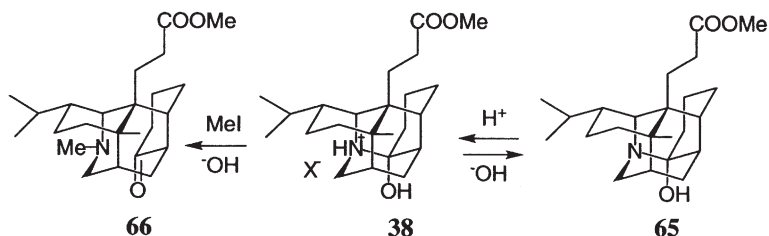


extensive spectroscopic studies, including several types of two-dimensional NMR experiments (e.g.,  $^1\text{H}$ - $^1\text{H}$  COSY,  $^1\text{H}$ - $^{13}\text{C}$  COSY, HMBC, HMQC, and NOESY spectra).

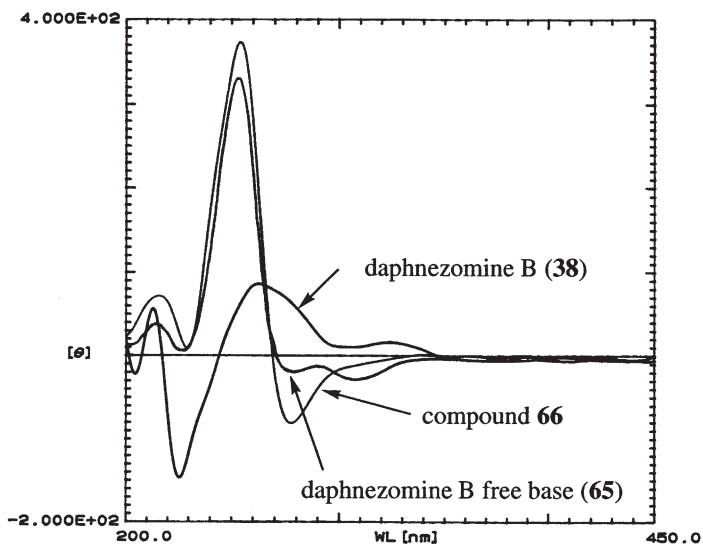
Daphnezomine A (**37**),  $\text{C}_{22}\text{H}_{35}\text{NO}_3$ , was suggested to possess OH ( $3600\text{ cm}^{-1}$ ), NH ( $3430\text{ cm}^{-1}$ ), and carboxylate ( $1570$  and  $1390\text{ cm}^{-1}$ ) functionalities from the IR absorptions.  $^1\text{H}$  and  $^{13}\text{C}$  NMR data revealed signals due to a methine ( $\delta_{\text{C}} 59.82$ ;  $\delta_{\text{H}} 3.79$ ) and a methylene ( $\delta_{\text{C}} 45.99$ ;  $\delta_{\text{H}} 3.44$  and  $3.97$ ), which were ascribed to those bearing a nitrogen, while a quaternary carbon ( $\delta_{\text{C}} 89.64$ ) was assigned as an amino ketal carbon. Detailed analysis of the  $^1\text{H}$ - $^1\text{H}$  COSY, HOHAHA, and HMQC-HOHAHA spectra allowed the assignment of all of the proton signals and clearly established the proton-connectivities. HMBC correlations to connect the above several partial units completed the gross structure of **37**, consisting of an azaadamantane core (N-1, C-1, and C-5-C-12) fused to a cyclohexane ring (C-1-C-5 and C-8) and another cyclohexane ring (C-9-C-11 and C-15-C-17), and three substituents at C-2, C-5, and C-8 (**44**).



Daphnezomine B (**38**),  $\text{C}_{23}\text{H}_{37}\text{NO}_3$ , which was larger than **37** by a  $\text{CH}_2$  unit, possessed a methoxy signal ( $\delta_{\text{H}} 3.67$ ) absent in **37**. Acetylation of **38** afforded the monoacetate **64**, in which the axially oriented tertiary hydroxyl group was acetylated. When daphnezomine B (**38**) was treated with aqueous  $\text{Na}_2\text{CO}_3$ , it was converted into its free base **65**, showing spectroscopic anomalies as follows (Scheme 1). The  $^{13}\text{C}$  signals (C-9, C-12, C-16, C-17, and C-18) of the free base showed extreme broadening, while the quaternary carbon (C-11) was not observed. NMR evidence indicating a differently directed nitrogen lone pair was obtained by the  $^{15}\text{N}$  NMR spectra (**38**:  $\delta_{\text{N}} 93.7$ ; free base of **38**:  $\delta_{\text{N}} 63.0$ ). On the other hand, in the IR spectrum, the close proximity of the carbonyl and the nitrogen permits pronounced interaction of these two functions to result in a lower shift of the carbonyl peak ( $\nu_{\text{max}} 1680\text{ cm}^{-1}$ ) for **66**, whereas it was not observed for the free base of **38**. In order to examine these spectroscopic anomalies, yuzurimine (**12**) free base with the similar amino ketal functionality was prepared under the same conditions, but the spectroscopic anomalies were not observed. When the free base



Scheme 1.

Figure 1. CD spectra of daphnezomine B (**38**), daphnezomine B free base (**65**), and compound **66** (**44**).

was treated with acetic acid, it was easily converted into **38** again. Compound **66** was obtained by treatment of **38** with  $\text{CH}_3\text{I}/\text{K}_2\text{CO}_3$  (Scheme 1) (**40**). Production of **66** could have resulted from *N*-methylation of the free base followed by the alkaline-induced N–C-11 bond cleavage to generate a ketone at C-11. In the CD spectra (Fig. 1), the structural similarity between the free bases of **38** showing spectroscopic anomalies and **66** were obtained by the CD spectra (MeOH) [free base of **38**:  $\lambda_{\text{max}}$ , 255 ( $\theta$  +400) and 280 ( $-80$ ) nm; **66**:  $\lambda_{\text{max}}$  260 ( $\theta$  +350), 280 ( $-20$ ), and 305 ( $-30$ ) nm], showing a different CD curve from that of **38** [ $\lambda_{\text{max}}$  225 ( $\theta$   $-150$ ) and 265 ( $+100$ ) nm]. These data indicated that the balance of the amino ketal in the free base of **38** declined in the keto form in solution. Thus the structure of daphnezomine B was elucidated to be **38**. The spectral data and the  $[\alpha]_{\text{D}}$  value of the methyl ester of **37**, which was obtained by treatment of **37** with

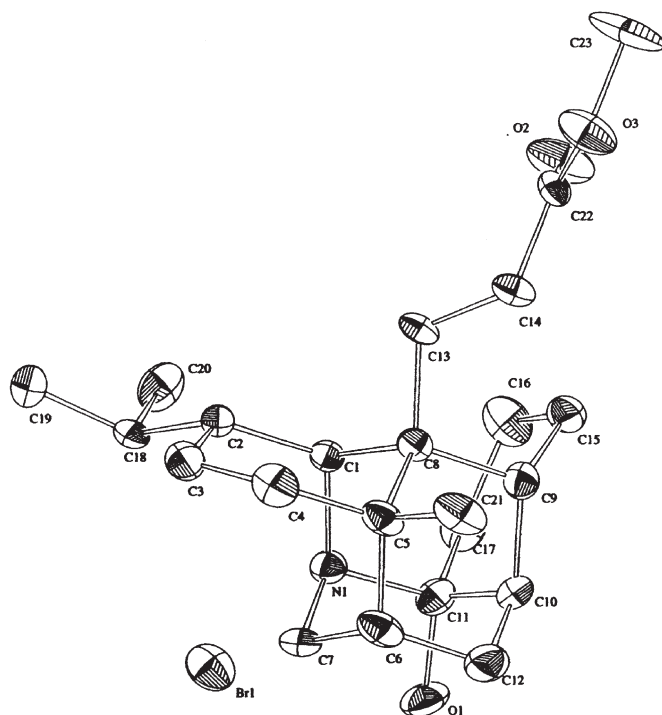


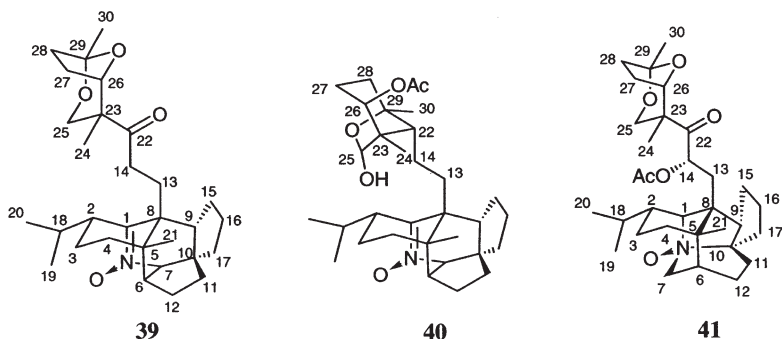
Figure 2. Molecular structure of daphnezomine B (**38**) hydrobromide obtained by X-ray analysis (ORTEP drawing; ellipsoids are drawn at the 30% probability level). Hydrogen atoms are omitted for clarity (44).

trimethylsilyldiazomethane, were in complete agreement with those of natural daphnezomine B (**38**) (44).

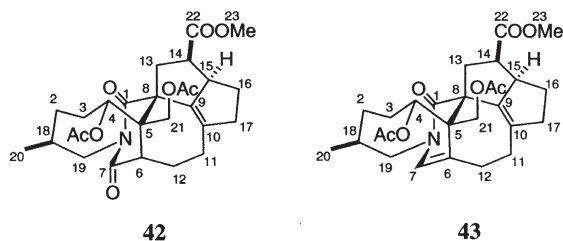
In order to determine the absolute stereochemistry of **37** and **38**, a crystal of the hydrobromide of **38** generated from MeOH–acetone (1:9) was submitted to X-ray crystallographic analysis (44). The crystal structure containing the absolute configuration, which was determined through the Flack parameter (52),  $\chi = -0.02(2)$ , is shown in Fig. 2. Daphnezomines A (**37**) and B (**38**) consisting of all six-membered rings are the first natural products containing an aza-adamantane core (53–56) with an amino ketal bridge, although there are reports on a number of *Daphniphyllum* alkaloids containing five-membered rings, which may be generated from a nitrogen-involved squalene intermediate via the secodaphnane skeleton (1,2).

Daphnezomines C (**39**) and D (**40**), possess the secodaphniphylline-type skeleton with a nitrone functionality, while daphnezomine E (**41**) is the first *N*-oxide

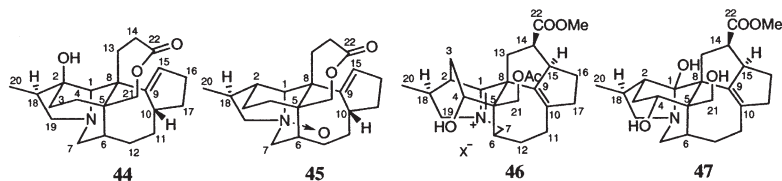
of a daphniphylline-type alkaloid, though the *N*-oxides of several yuzurimine-type alkaloids have been reported (45).



Spectral investigations of daphnezomines F (42) and G (43), whose molecular formulae are  $C_{27}H_{35}NO_8$  and  $C_{27}H_{35}NO_7$ , respectively, revealed that they are structurally related and possess an 1-azabicyclo[5.2.2]undecane moiety. The conformation of the 1-azabicyclo[5.2.2]undecane ring in 43 was elucidated by a low temperature NMR study and computational analysis (46).

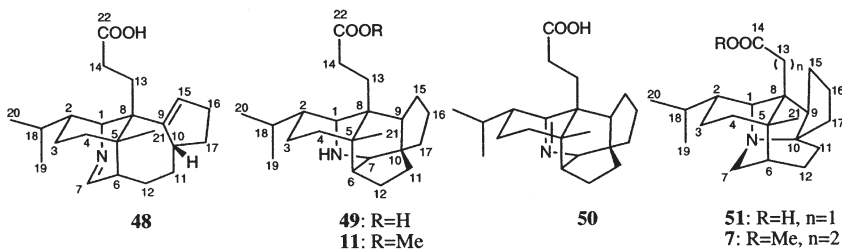


The structures, including relative stereochemistry, of daphnezomines H (44), I (45), J (46), and K (47), four new alkaloids possessing a daphnilactone-type (44 and 45) or a yuzurimine-type skeleton (46 and 47) were elucidated on the basis of spectroscopic data (47). Daphnezimine I (45) is the first *N*-oxide alkaloid having a daphnilactone-type skeleton, while daphnezimine J (46) is the first alkaloid possessing a yuzurimine-type skeleton with an anti-Bredt-rule imine (57,58).



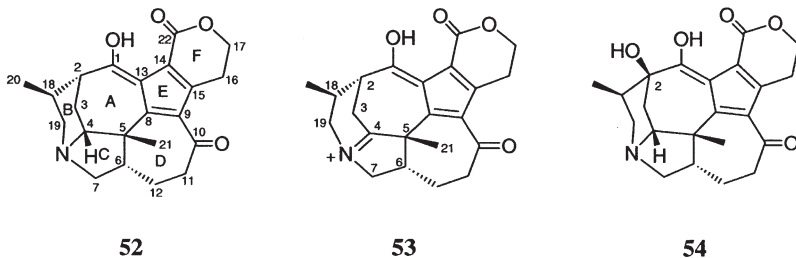
Relatively polar fractions prepared from the stems of *D. humile* were subjected to an amino silica gel column followed by  $C_{18}$  HPLC ( $CH_3CN/0.1\%$  TFA)

to afford daphnezomines L (**48**, 0.0001%), M (**49**, 0.00007%), N (**50**, 0.00007%), and O (**51**, 0.001%) as colorless solids, together with the known zwitterionic alkaloid **26** (0.0005%) (**48**). Daphnezomine L (**48**) was close structurally to a biogenetic intermediate between the secodaphnane and daphnane skeletons.



### H. DAPHNICYCLIDINS

Eight highly modified *Daphniphyllum* alkaloids with unprecedented fused hexa- or pentacyclic skeletons, daphnicyclidins A (**52**, 0.003% yield), B (**53**, 0.0003%), C (**54**, 0.001%), D (**55**, 0.002%), E (**56**, 0.001%), F (**57**, 0.001%), G (**58**, 0.001%), and H (**59**, 0.004%) were isolated as colorless solids from alkaloidal fractions prepared from the stems of *D. teijsmanni* and *D. humile* (**49**).



Daphnicyclidin A (**52**),  $C_{22}H_{25}NO_4$ , showed IR absorptions which implied the presence of OH and/or NH ( $3440\text{ cm}^{-1}$ ) and conjugated carbonyl ( $1680\text{ cm}^{-1}$ ) functionalities. Three partial structures, **a** (from C-2 to C-4 and from C-18 to C-19 and C-20), **b** (from C-6 to C-7 and C-12 and from C-11 to C-12), and **c** (from C-16 to C-17) were deduced from extensive analyzes of 2D NMR data, including the  $^1\text{H}$ - $^1\text{H}$  COSY, HOHAHA, HMQC, and HMBC spectra in  $\text{CDCl}_3$ - $\text{CD}_3\text{OD}$  (9:1). The connections of the three partial structures through a nitrogen atom (N-1) and also through a quaternary carbon (C-5) were established by the  $^1\text{H}$ - $^{13}\text{C}$  long-range (two- and three-bond) couplings detected in the HMBC spectrum to afford a proposed structure. The X-ray crystal structure (**Fig. 3**) of daphnicyclidin A TFA salt revealed a unique fused-hexacyclic ring system consisting of two each of five, six, and seven-membered rings containing a nitrogen atom and two methyls at C-5 and C-18, in which an intramolecular hydrogen bond was observed between the

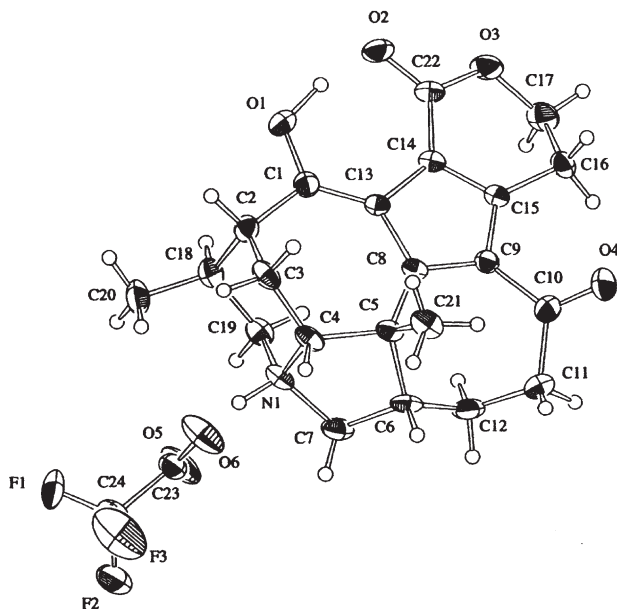
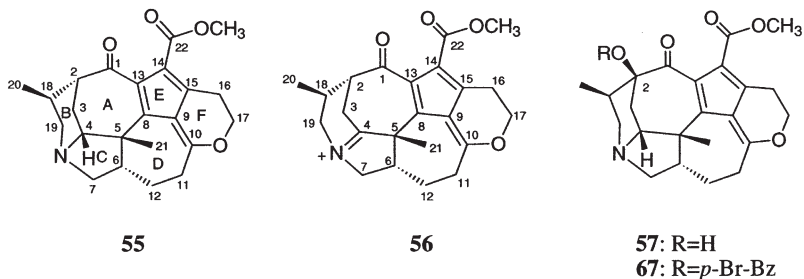


Figure 3. Molecular structure of daphnicyclidin A (**52**) TFA salt obtained by X-ray analysis (ORTEP drawing; ellipsoids are drawn at the 30% probability level) (49).

C-1 hydroxyl proton and the C-22 carbonyl oxygen. The relative configurations at C-4, C-5, C-6, and C-18 were deduced from NOESY correlations, together with a stable chair conformation of ring B as depicted in the computer-generated 3D drawing (Fig. 4).

The FABMS spectrum of daphnicyclidin B (**53**) showed the molecular formula,  $C_{22}H_{24}NO_4$ . The 2D NMR data of **53**, including the  $^1H$ - $^1H$  COSY, HOHAHA, HMQC, and HMBC spectra, corroborated well with those of the imine (C-4 and N-1) from of daphnicyclidin A (**52**). Spectral investigation of daphnicyclidin C (**54**), whose molecular formula is  $C_{22}H_{25}NO_5$ , revealed that it was the 2-hydroxy form of daphnicyclidin A (**52**) (49).



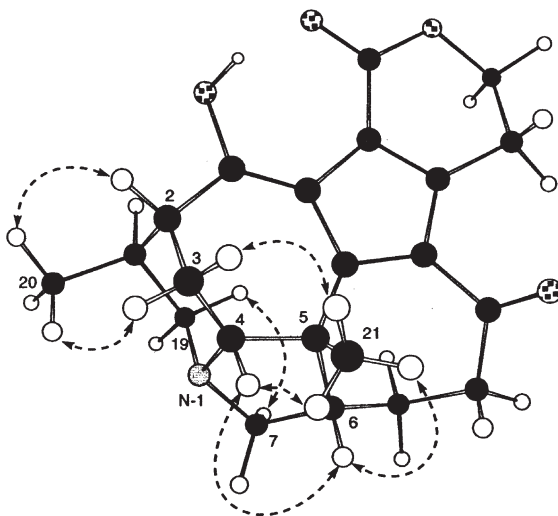
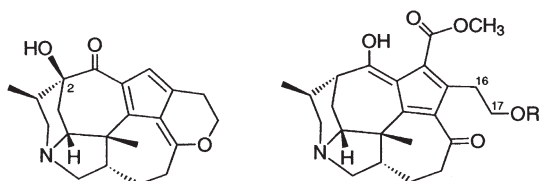


Figure 4. Selected NOESY correlations (dotted arrows) and relative configurations for daphnicyclidin A (**52**) (49).

The molecular formula,  $C_{23}H_{27}NO_4$  of daphnicyclidin D (**55**), was larger than that of daphnicyclidin A (**52**) by a  $CH_2$  unit.  $^1H$  and  $^{13}C$  NMR data of **55** were analogous to those of **52** in the left hand part consisting of rings A to C with a nitrogen atom, except that a methoxy signal ( $\delta_H$  3.76) absent for **52** was observed for **55**. The structure of **55** was elucidated by 2D NMR ( $^1H$ - $^1H$  COSY, HOHAHA, HMQC, and HMBC) data. HMBC cross-peaks indicated that C-10 and C-17 ( $\delta_C$  69.1) were connected to each other through an oxygen atom to form a dihydropyran ring. In addition, the presence of a conjugated cyclopentadiene moiety (C-8-C-9 and C-13-C-15) as in **52** was suggested by HMBC correlations. Treatment of **52** with methanolic *p*-TsOH gave daphnicyclidin D (**55**) (Scheme 2). Thus, the structure of daphnicyclidin D was assigned as **55** (49).

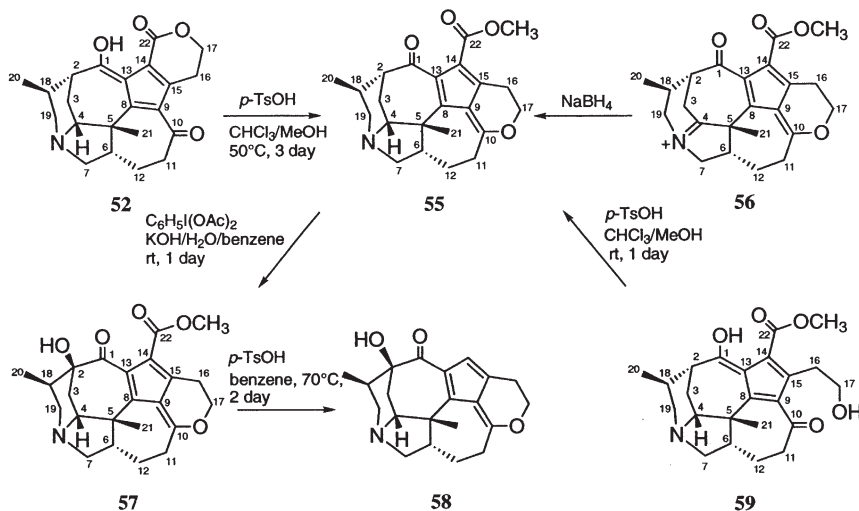
The IR spectrum of daphnicyclidin E (**56**),  $C_{23}H_{25}NO_4$  was indicative of the presence of conjugated carbonyl and/or imine ( $1680\text{ cm}^{-1}$ ) functionalities.  $^1H$  and  $^{13}C$  NMR data of **56** were analogous to those of daphnicyclidin D (**55**). The presence of an iminium carbon [C-4,  $\delta_C$  197.5 (s)] was elucidated by HMBC correlations for  $H_3$ -21 and  $H_B$ -3 to C-4, and  $H_2$ -7 and  $H_a$ -19 to C-4 through a nitrogen atom. Treatment of **56** with  $NaBH_4$  afforded daphnicyclidin D (**55**) (Scheme 2). Thus, daphnicyclidin E (**56**) was concluded to be the imine form at C-4 of daphnicyclidin D (**55**) (49).

2D NMR analysis of daphnicyclidin F (**57**),  $C_{23}H_{27}NO_5$ , and chemical correlation of daphnicyclidin D (**55**) with **57**, indicated that daphnicyclidin F (**57**) was the 2-hydroxy form of daphnicyclidin D (**55**) (49).

**58****59:** R=H**68:** R=Ac

The molecular formula,  $C_{21}H_{25}NO_3$ , of daphnicyclidin G (**58**), was less than that of daphnicyclidin F (**57**) by a  $C_2H_2O_2$  unit. Though the  $^1H$  and  $^{13}C$  NMR data were close to those of daphnicyclidin F (**57**), differences were observed for the methoxy carbonyl moiety. Daphnicyclidin F (**57**) possessed a methoxy carbonyl moiety at C-14, while the  $^1H$  and  $^{13}C$  NMR data of **58** showed signals due to an  $sp^2$  methine [ $\delta_H$  6.51 (1H, s),  $\delta_C$  118.4 (d)]. Treatment of **57** with *p*-TsOH at  $70^\circ C$  for 2 days gave daphnicyclidin G (**58**) (Scheme 2). Therefore, daphnicyclidin G (**58**) was elucidated to be the 14-demethoxycarbonyl form of daphnicyclidin F (**57**) (**49**).

Daphnicyclidin H (**59**),  $C_{23}H_{29}NO_5$  showed IR absorptions at  $3435$  and  $1680\text{ cm}^{-1}$  indicating the presence of hydroxyl and conjugated carbonyl groups, respectively.  $^1H$  NMR signals assignable to H-17 ( $\delta_H$  3.70) were observed to be equivalent. Treatment of **59** with acetic anhydride afforded the monoacetate



Scheme 2. Chemical correlations for daphnicyclidins A (**52**) and D–H (**55**–**59**) (**49**).



**68**, in which the hydroxyl group at C-17 was acetylated. On the other hand, the presence of a methoxy carbonyl group at C-14 and rings A–E with a ketone at C-10 ( $\delta_{\text{C}}$  204.5) was deduced from the 2D NMR analysis. The 2D NMR data indicated that the conjugated keto-enol moiety of **59** was the same as that of daphnicyclidin A (**52**). Treatment of daphnicyclidin H (**59**) with *p*-TsOH gave daphnicyclidin D (**55**) (Scheme 2) (49).

The absolute stereochemistry of daphnicyclidin F (**57**) was analyzed by applying the exciton chirality method (61) after introduction of a *p*-bromobenzoyl chromophore into the hydroxyl group at C-2. As the sign of the first Cotton effect [ $\lambda_{\text{max}}$  280 ( $\theta$ +20,000) and 225 ( $-16,000$ ) nm] was positive, the chirality between the cyclopentene moiety and the benzoate group of the *p*-bromobenzoyl derivative **67** of **57** was assigned as shown in Fig. 5 (right-handed screw), indicating that the absolute stereochemistry at C-2 was *S* (49).

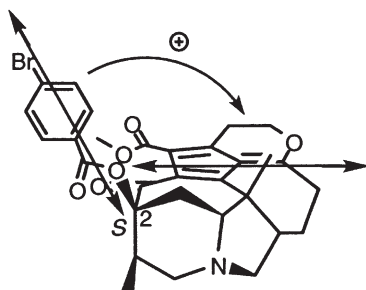
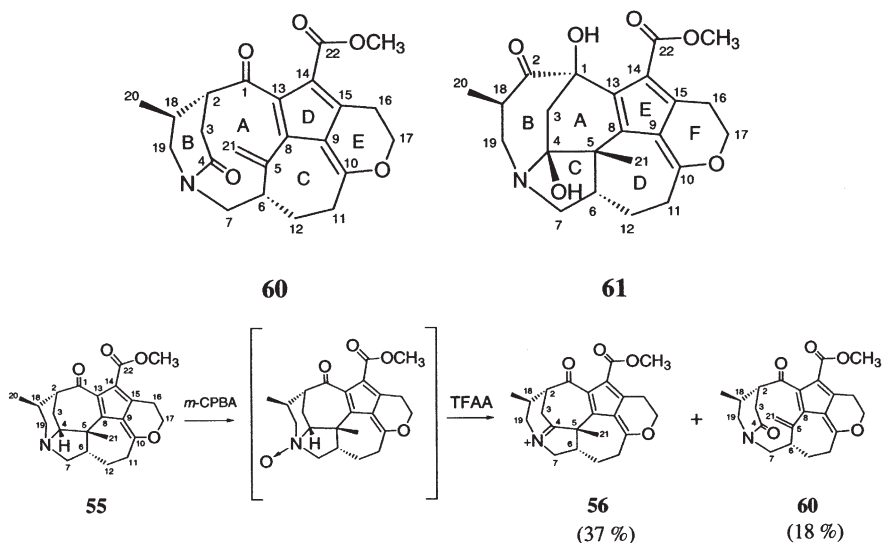


Figure 5. Stereostructure of *p*-bromo benzoate (**67**) of daphnicyclidin F (**57**). Arrows denote the electric transition dipole of the chromophore (49).

Daphnicyclidins J (**60**) and K (**61**), two alkaloids with unprecedented fused penta- or hexacyclic skeletons, respectively, were isolated from the stems of *D. humile* (50).

Daphnicyclidin J (**60**),  $\text{C}_{23}\text{H}_{25}\text{NO}_5$ , showed IR absorptions at 1690 and  $1660\text{ cm}^{-1}$ , corresponding to ketone and amide carbonyl functionalities, respectively. The  $^1\text{H}$ - $^1\text{H}$  COSY and HOHAHA spectra provided information on the proton-connectivities for three partial structures **a** (C-2 to C-3 and C-18 and C-18 to C-19 and C-20), **b** (C-6 to C-7 and C-12, and C-11 to C-12), and **c** (C-16 to C-17). The partial structures were revealed to be linked to each other by long range  $^1\text{H}$ - $^{13}\text{C}$  correlations. The presence of a fulvene functionality (C-8–C-10 and C-13–C-15), which was conjugated with two carbonyl groups (C-1 and C-22) and an exo-methylene group (C-5 and C-21), was elucidated by comparison of the carbon chemical shifts with those of daphnicyclidin D (**55**). UV absorptions

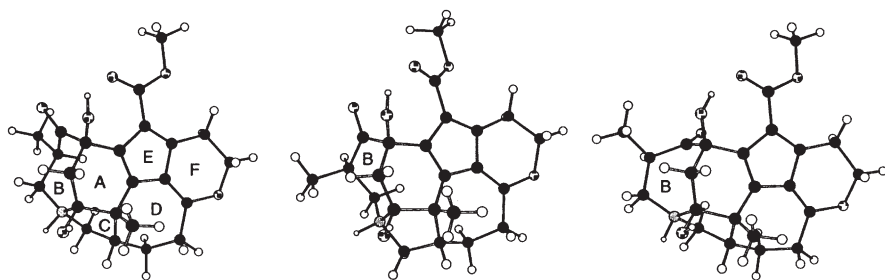


Scheme 3. Chemical transformation of daphnicyclidin D to daphnicyclidins E and J by a modified Polonovski reaction.

(245, 320, and 330 nm) also supported the existence of the conjugated fulvene functionality. Thus, the structure of daphnicyclidin J was assigned as **60** having a uniquely fused-pentacyclic ring system (one five-, two six-, one seven-, and one ten-membered rings) containing a  $\delta$ -lactam and a pyran ring. The absolute stereochemistry was established by chemical correlation with a known-related alkaloid, daphnicyclidin D (**55**), through a modified Polonovski reaction (Scheme 3) (50).

Daphnicyclidin K (**61**) was shown to have the molecular formula  $C_{23}H_{27}NO_6$ . IR absorptions implied the presence of hydroxyl ( $3600\text{ cm}^{-1}$ ), ester carbonyl ( $1700\text{ cm}^{-1}$ ), and conjugated carbonyl ( $1650\text{ cm}^{-1}$ ) functionalities. The structure of **61** was elucidated by analyzes of 2D NMR data including  $^1\text{H}$ - $^1\text{H}$  COSY, HOHAHA, HMBC spectra to have an unusual skeleton consisting of a 6/7/5/7/5/6 hexacyclic ring system (50).

The relative stereochemistry was assigned from NOESY correlations and conformational calculations by Monte Carlo simulation (59), which suggested that the seven-membered ring (ring B) with a chair conformation (**61a**) was the most stable, whereas those with a twist chair (**61b**) and a boat (**61c**) conformations had considerably higher energy (Fig. 6). In addition, the NOESY correlations indicated that another seven-membered ring (ring D) assumed a twist-boat conformation similar to the crystal structure of daphnicyclidin A (**52**).

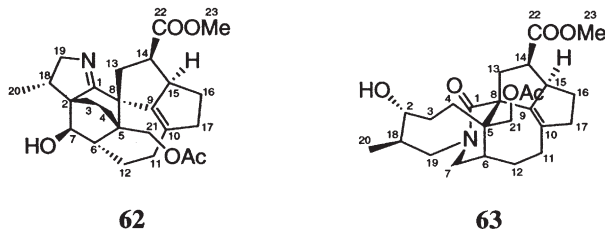


**61a** (chair, 252.3 kJ/mol)    **61b** (twist chair, 282.6 kJ/mol)    **61c** (boat, 290.9 kJ/mol)

Figure 6. Three representative stable conformers (**61a–61c**) for daphnicyclidin K (**61**) analyzed by Monte Carlo simulation followed by minimization and clustering analysis (50).

### I. DAPHMANIDINS

Further investigation on extracts of the leaves of *D. teijsmanii* resulted in the isolation of daphmanidin A (**62**, 0.0001% yield), an alkaloid with an unprecedented fused-hexacyclic ring system, and daphmanidin B (**63**, 0.00003%) with a pentacyclic ring system (51).



The IR absorptions of daphmanidin A (**62**),  $C_{25}H_{33}NO_5$ , implied the presence of hydroxyl ( $3616\text{ cm}^{-1}$ ), ester carbonyl ( $1730\text{ cm}^{-1}$ ), and imine ( $1675\text{ cm}^{-1}$ ) functionalities. Detailed spectroscopic analysis revealed that the gross structure of daphmanidin A possesses a fused-hexacyclic ring system consisting of a dihydropyrrole ring (N-1, C-1, C-2, C-18, and C-19) with a methyl group at C-18, a bicyclo[2.2.2]octane ring (C-1–C-8) with a hydroxyl at C-7, and a decahydrocyclopenta[*cd*]azulene ring (C-5, C-6, C-8–C-17) with a methoxy carbonyl group at C-14 and an acetoxy methyl group at C-5. The relative and absolute stereochemistry of **62** was determined by a combination of NOESY correlations (Fig. 7) and the modified Mosher method.

The structure of daphmanidin B (**63**),  $C_{25}H_{36}NO_6$ , was elucidated by 2D NMR ( $^1\text{H}$ – $^1\text{H}$  COSY, HOHAHA, HMQC, and HMBC) data to possess a 1-azabicyclo[5.2.2]undecane moiety, like daphnezomines F (**42**) and G (**43**) (46).

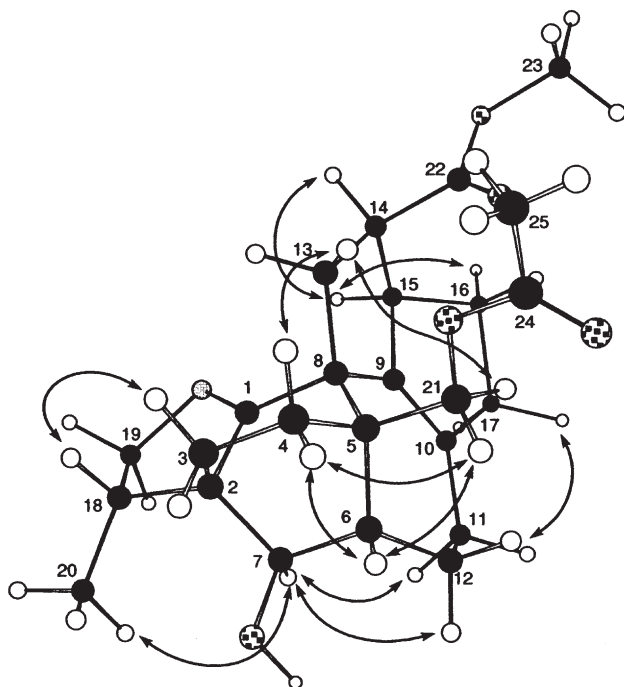


Figure 7. Key NOESY correlations (arrows) and relative stereochemistry for daphmanidin A (**62**) (51).

The relative stereochemistry was deduced from NOESY correlations. The conformation of the unit (C-2-C-5, C-18 to C-2, C-19, and N) in the 1-azabicyclo[5.2.2]undecane moiety taking a twist-chair form, as shown in Fig. 8, was consistent with the results of a conformational search using MMFF force field (60) implemented in the Macromodel program (59).

### III. Biosynthesis and Biogenesis

#### A. BIOSYNTHESIS OF *DAPHNIPHYLLUM* ALKALOIDS

Suzuki and Yamamura conducted feeding experiments on the *Daphniphyllum* alkaloids using the leaves of *D. macropodum* (62). Alkaloids, as well as their amounts, varied with season, and the highest incorporation of DL-mevalonic acid (69, MVA) and squalene (70) into daphniphylline (1) was recorded in June and July. From the feeding experiments, followed by degradation studies, daphniphylline (1) and codaphniphylline (2) were biosynthesized from six moles of MVA (69) through a squalene-like intermediate (Fig. 9). In addition, the feeding experiments using the fruits of *D. teijsmannii* resulted in the incorporation of four

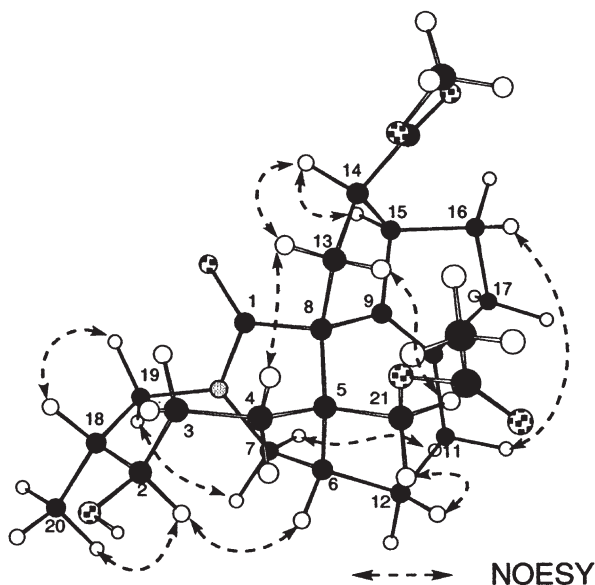


Figure 8. Selected 2D NMR correlations and relative stereochemistry for daphmanidin B (**63**) (51).

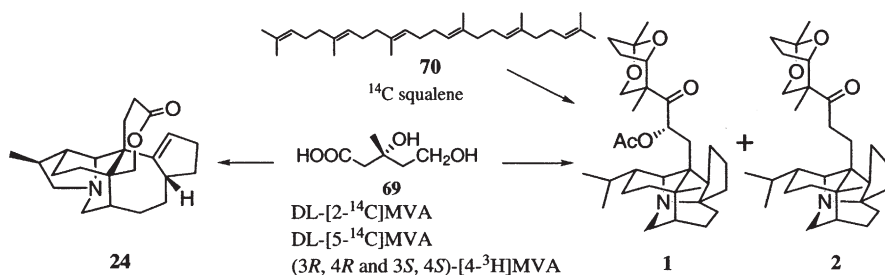


Figure 9. Feeding experiments with labeled mevalonic acid (**69**) and squalene (**70**) into daphniphylline (**1**), codaphniphylline (**2**), and daphnilactone B (**24**) (62).

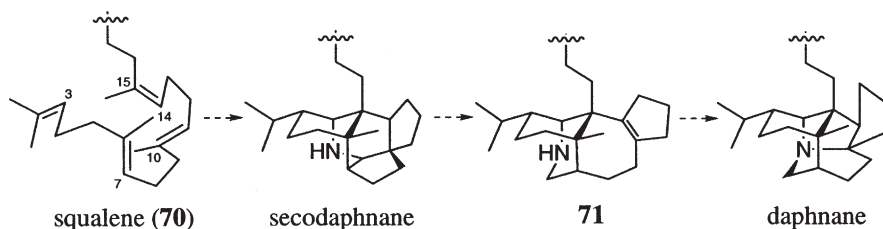
moles of MVA (**69**) into one of the major C22 type *Daphniphyllum* alkaloids, daphnilactone B (**24**) (36).

## B. BIOGENESIS OF THE DAPHNANE AND SECODAPHNANE SKELETONS

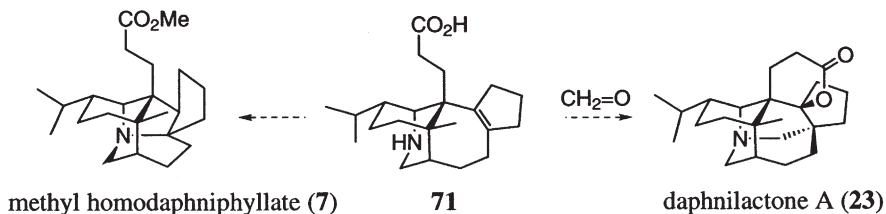
Heathcock proposed the biosynthetic pathway of the *Daphniphyllum* alkaloids (4,5). In the skeleton of secodaphniphylline (**8**), the linear squalene (**70**)

molecule may be traced in the pentacyclic domain of **8**. To convert squalene into secodaphniphylline (**8**), four C–C bonds must be formed: C-10 to C-14; C-6 to C-15; C-3 to the C-15 methyl group; and C-7 to the C-10 methyl group. In addition, the nitrogen atom is inserted between C-7 and the C-15 methyl group. For daphniphylline (**1**), however, the nitrogen seems to have been inserted between C-10 and its methyl group, which is also connected to C-7. Thus, it is likely that secodaphniphylline (**8**) precedes daphniphylline (**1**) in the biosynthetic pathway, and that an unsaturated amine such as compound **71** provides a biogenetic link between the two skeletons (**5**) (Scheme 4). The hypothetical unsaturated amine **71** also contains the bicyclo[4.4.1]undecane feature that is seen in yuzurimine (**12**), and could account for the extra carbon that is found in daphnilactone A (**23**) (Scheme 5).

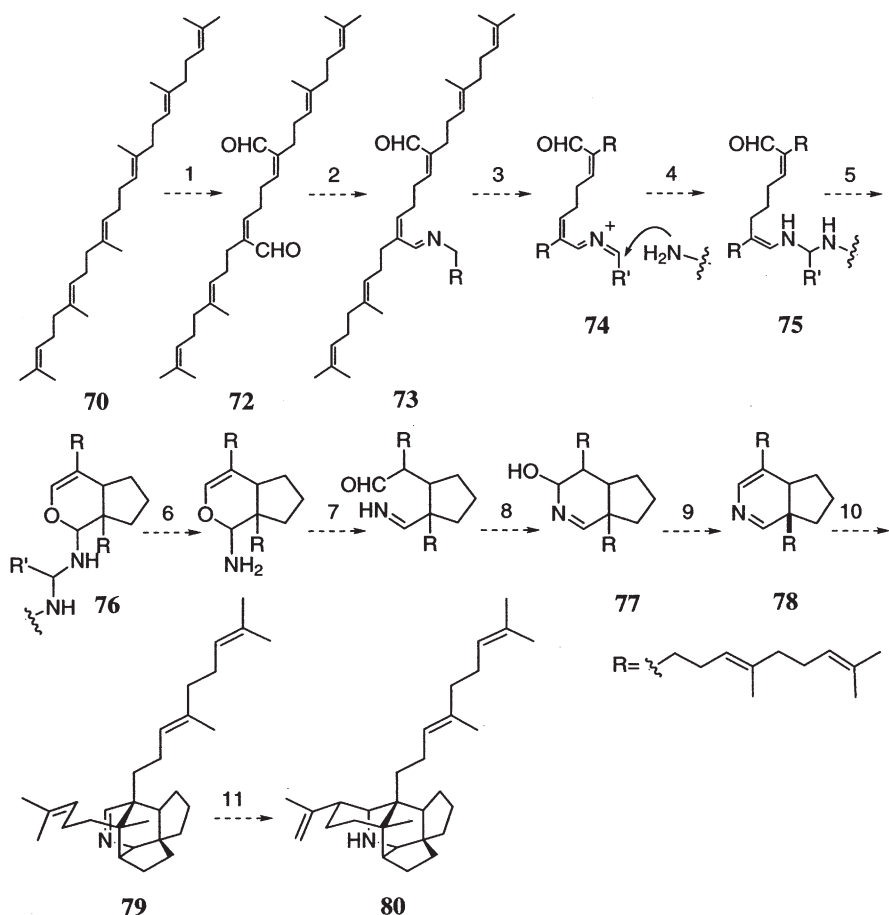
This hypothesis led to the postulation of various scenarios whereby squalene (**70**) might acquire a nitrogen atom and be transformed into the pentacyclic secodaphniphylline skeleton. The outline of this proposal is shown in Scheme 6. Step 1 is an oxidative transformation of squalene **70** into a dialdehyde, **72**. In step 2, it is proposed that some primary amine, perhaps pyridoxamine or an amino acid, condenses with one of the carbonyl groups of compound **72**, affording the imine **73**. Step 3 is the prototypic rearrangement of an 1-azadiene **73** to a 2-azadiene **74**. A nucleophilic species adds to the imine bond of **74** in step 4 to give the product **75**, followed by subsequent cyclization to give compound **76**. In steps 6–9, the resulting bicyclic dihydropyran derivative **76** is transformed into a dihydropyridine derivative **78** by a sequence of proton-mediated addition and elimination processes. Alkaloid **78** would then be converted into **79** by a catalyzed



Scheme 4.



Scheme 5.

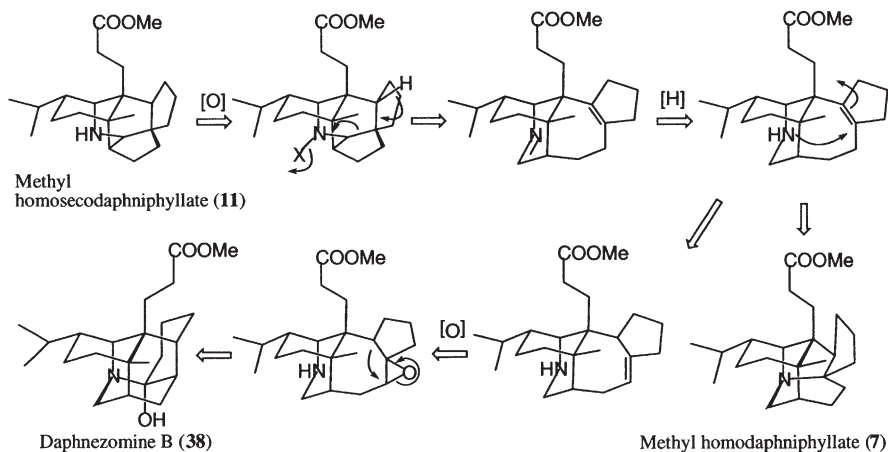


Scheme 6. Biogenesis of proto-daphniphylline (**80**).

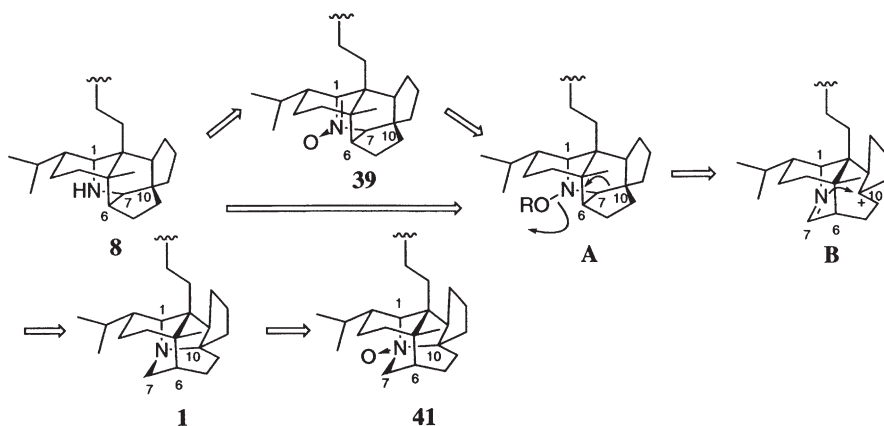
Diels-Alder reaction, and the final ring would result from an ene-like cyclization, giving alkaloid **80**. Because **80** is the first pentacyclic alkaloid to occur in the biogenesis of the *Daphniphyllum* alkaloids, it was named proto-daphniphylline (**80**).

### C. BIOGENESIS OF THE DAPHNEZOMINES

Daphnezomines A (**37**) and B (**38**) consisting of all six-membered rings are the first natural products containing an aza-adamantane core with an amino ketal bridge. A biogenetic pathway for daphnezomine B (**38**) is proposed in Scheme 7. Daphnezomines A (**37**) and B (**38**) might be generated through ring expansion accompanying backbone rearrangement of a common fragmentation intermediate.



Scheme 7. Biogenesis of daphnezomine B (38).



Scheme 8. Biogenesis of the daphniphylline skeleton of 1.

Daphnezomines C (39) and D (40) are the first alkaloids possessing the secodaphniphylline-type skeleton with a nitron functionality, while daphnezomine E (3) is the first *N*-oxide of a daphniphylline-type alkaloid, although the *N*-oxides of yuzurimine-type alkaloids have been reported (23,29). Heathcock and Pietre offered a biogenetic conversion of the secodaphniphylline-type skeleton to the daphniphylline-type skeleton, in which an initial oxidation of the secodaphniphylline-type skeleton occurs on the nitrogen atom, followed by transformation into the daphniphylline-type skeleton through a ring-opened intermediate such as **B** (Schemes 4 and 8) (4,5). The structures of daphnezomines C (39) and D (40) are very similar to that of a nitron intermediate synthesized by Heathcock *et al.* (73).

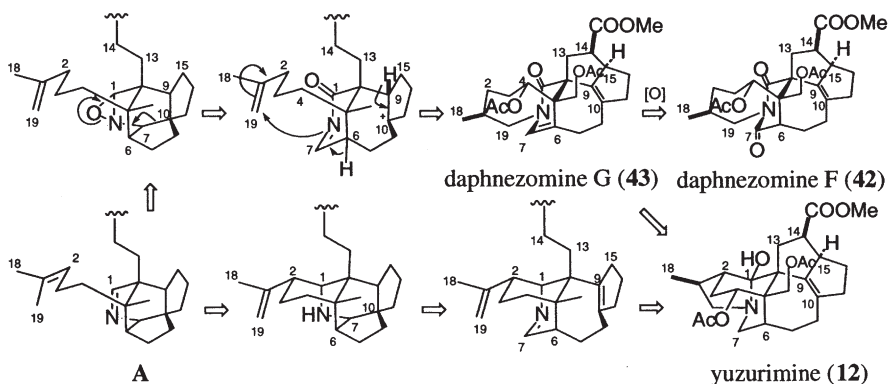


Biogenetically, the daphniphylline-type skeleton (e.g., **1**) may be generated from the secodaphniphylline-type skeleton (e.g., **8**) through *N*-oxidation to generate an intermediate (**A**) or a nitron such as **39**. Cleavage of the C-7–C-10 bond, generation of a ring-opened imine intermediate (**B**), and formation of another C–N bond between N-1 and C-10, follows Heathcocks' proposal (Schemes 4 and 8).

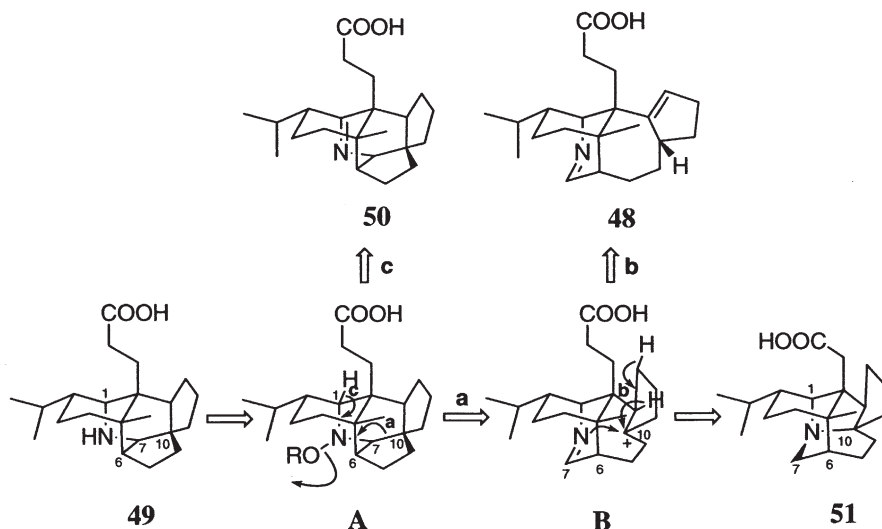
The structures of daphnezomines F (**42**) and G (**43**) are similar to that of yuzurimine (**12**), but they lack the C-1–C-2 bond. A biogenetic pathway for daphnezomines F (**42**) and G (**43**) is proposed in Scheme 9. Daphnezomine G (**43**) might be generated through oxidation of a common imine intermediate **A** (proposed as a precursor of the secodaphniphylline-type skeleton by Heathcock *et al.*), and subsequent cleavage of the C-7–C-10 bond, followed by formation of the C-19–N-1 and C-14–C-15 bonds to give daphnezomine G (**43**). Daphnezomine F (**42**) may be derived from daphnezomine G (**43**) through oxidation of the C-7–C-6 bond. On the other hand, yuzurimine (**12**) might be generated from the intermediate **A** through the secodaphniphylline-type skeleton, although an alternative pathway through **43** is also possible.

Biogenetically, daphnezomine I (**45**) may be derived from daphnilactone B (**24**) through oxidation at N-1, while daphnezomine J (**46**) may be generated from yuzurimine (**12**) through dehydroxylation at C-1.

Daphnezomine L (**48**) is structurally close to a biogenetic intermediate on the pathway from the secodaphnane to the daphnane skeleton (**48**). Yamamura *et al.* suggested that a pentacyclic skeleton such as **48** is a biogenetic intermediate to the daphnane skeleton **51** (**77**), while Heathcock *et al.* proposed a biogenetic route from the secodaphnane (**49**) to the daphnane (**51**) skeletons through intermediates **A** and **B** (Scheme 10) (**73**). Daphnezomines L (**48**) and O (**51**) might be biosynthesized through intermediates **A** and **B**, while daphnezomine N (**50**) might be generated through intermediate **A** (**48**).



Scheme 9. Biogenesis of daphnezomines F (**42**) and G (**43**).

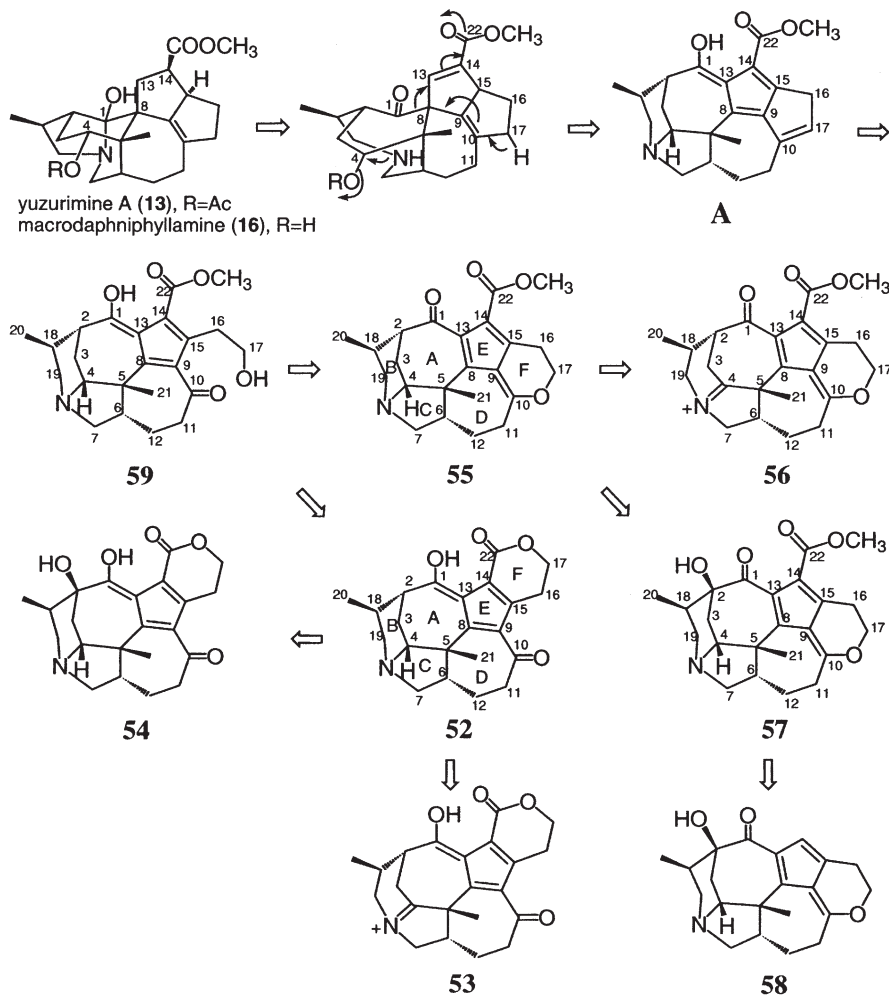


Scheme 10.

#### D. BIOGENESIS OF THE DAPHNICYCLIDINS

Daphnicyclidins A–G (**52–58**) and H (**59**) are novel alkaloids consisting of fused hexa or penta-cyclic ring systems, respectively. A biogenetic pathway for daphnicyclidins A–H (**52–59**) is proposed in [Scheme 11](#). The biogenetic origin of these alkaloids seems to be yuzurimine-type alkaloids, such as yuzurimine A (**13**) and macrodaphniphyllamine (**16**), with an appropriate leaving group at C-4 and a methyl group at C-21. Rings B and C might be constructed by loss of the leaving group at C-4 followed by N-1–C-4 bond formation. Subsequently, cleavage of the C-1–C-8 bond followed by formation of the C-1–C-13 bond would result in enlargement of ring A, and aromatization of ring E to generate an intermediate A. Furthermore, oxidative cleavage of the C-10–C-17 bond could lead to daphnicyclidin H (**59**), followed by cyclization and dehydration to produce daphnicyclidin D (**55**), which may be oxidized to give daphnicyclidins E (**56**) and F (**57**). On the other hand, cyclization of the 17-OH to C-22 in **59** to form ring F would generate daphnicyclidins A (**52**), B (**53**), and C (**54**).

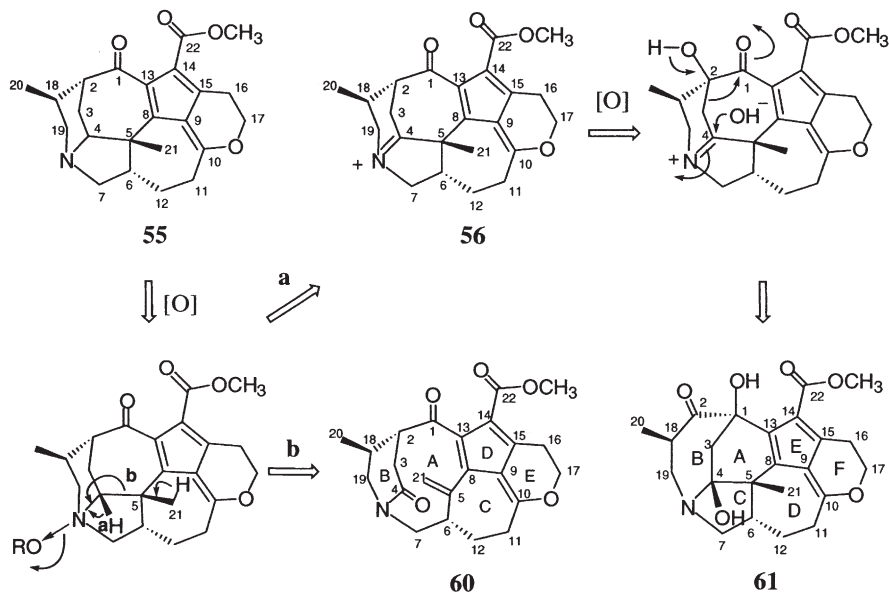
A biogenetic pathway for daphnicyclidins J (**60**) and K (**61**) is proposed in [Scheme 12](#). Daphnicyclidins J (**60**) and K (**61**), as well as daphnicyclidins A–H reported more recently, might be derived from the yuzurimine-type alkaloids such as yuzurimine A (**13**) and macrodaphniphyllamine (**16**). Daphnicyclidin J (**60**) might be generated through *N*-oxidation of daphnicyclidin D (**55**), while daphnicyclidin K (**61**) might be derived from an imine form (**56**) of daphnicyclidin D (**55**) through introduction of hydroxy groups at C-2 and C-4, followed by acyloin rearrangement ([Scheme 12](#)).



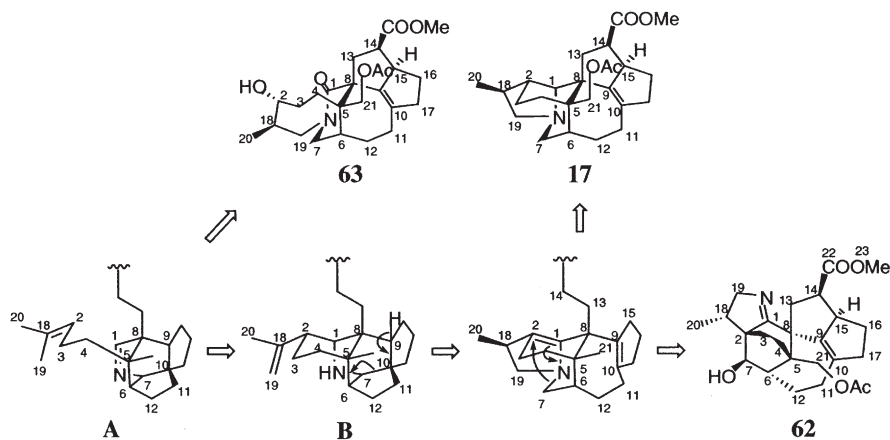
Scheme 11. Biogenetic pathway of daphnicyclidins A-H (52-59).

## E. BIOGENESIS OF THE DAPHMANIDINS

A biogenetic pathway for daphmanidins A (62) and B (63) is proposed in [Scheme 13](#). Daphmanidin A (62) might be generated from a common imine intermediate **A**, which has been proposed as a precursor of the secodaphniphylline-type skeleton (**B**) by Heathcock *et al.* (4,5). Cleavage of the C-7-C-10 bond in **B** will afford an intermediate with the yuzurimine-type skeleton, such as



Scheme 12. Biogenetic pathway of daphnicyclidins J (60) and K (61).



Scheme 13. Biogenesis of daphmanidins A (62) and B (63).

macrodaphniphyllidine (17), while subsequent cleavage of the N-1-C-7 bond, followed by formation of the C-7-C-2 bond will afford daphmanidin A (62). On the other hand, daphmanidin B (63) might be derived from the imine intermediate A through formation of the N-1-C-19 bond.

## IV. Synthesis

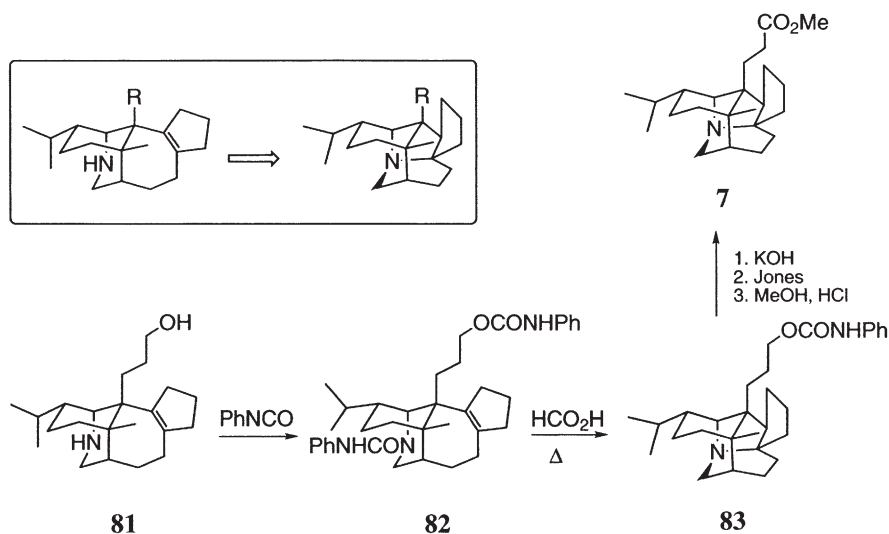
## A. BIOMIMETIC CHEMICAL TRANSFORMATIONS

## 1. Transformation of an Unsaturated Amine to the Daphnane Skeleton

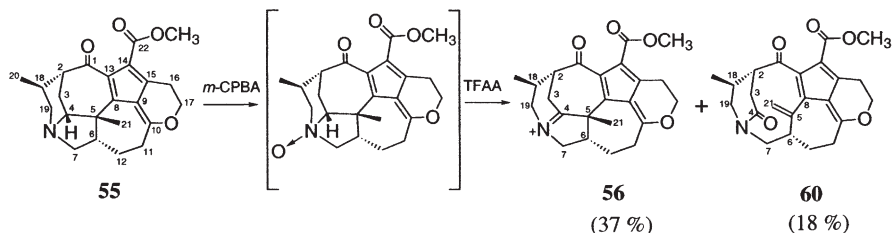
Heathcock *et al.* suggested that the daphnane skeleton, such as methyl homodaphniphyllate (**7**), might arise by the cyclization of an unsaturated amine **81** (**63**). Failure of this transformation under various acidic conditions presumably results from the preferential protonation of the amine. In contrast, the bis-carbamoyl derivative **82**, obtained by treatment of the amino alcohol **81** with phenyl isocyanate, cyclizes smoothly in refluxing formic acid to provide the carbamate **83** (Scheme 14) (**63**). The ease of cyclization of **82** raises an interesting question of whether a similar process might also be involved in the biosynthetic formation of the daphnane skeleton. The biogenetic carbamoylating agent could be carbamoyl phosphate.

2. Transformation of Daphnicyclidin D (**55**) to Daphnicyclidins E (**56**) and J (**60**)

Daphnicyclidin J (**60**) was obtained together with daphnicyclidin E (**56**) from daphnicyclidin D (**55**) through a modified Polonovski reaction (**64**) as shown in Scheme 15. Treatment of **55** with *m*-chloroperbenzoic acid (*m*-CPBA) followed by reaction with trifluoroacetic anhydride (TFAA) gave two compounds in 37 and 18% yields, whose spectral data were identical with those of natural daphnicyclidins E (**56**) and J (**60**), respectively (**50**). This result indicated



Scheme 14. Chemical transformation of **81** to methyl homodaphniphyllate (**7**) (**63**).



Scheme 15. Chemical transformation of daphnicyclidin D (**55**) to daphnicyclidins E (**56**) and J (**60**) (50).

that daphnicyclidin J (**60**) might be generated through *N*-oxidation of daphnicyclidin D (**55**).

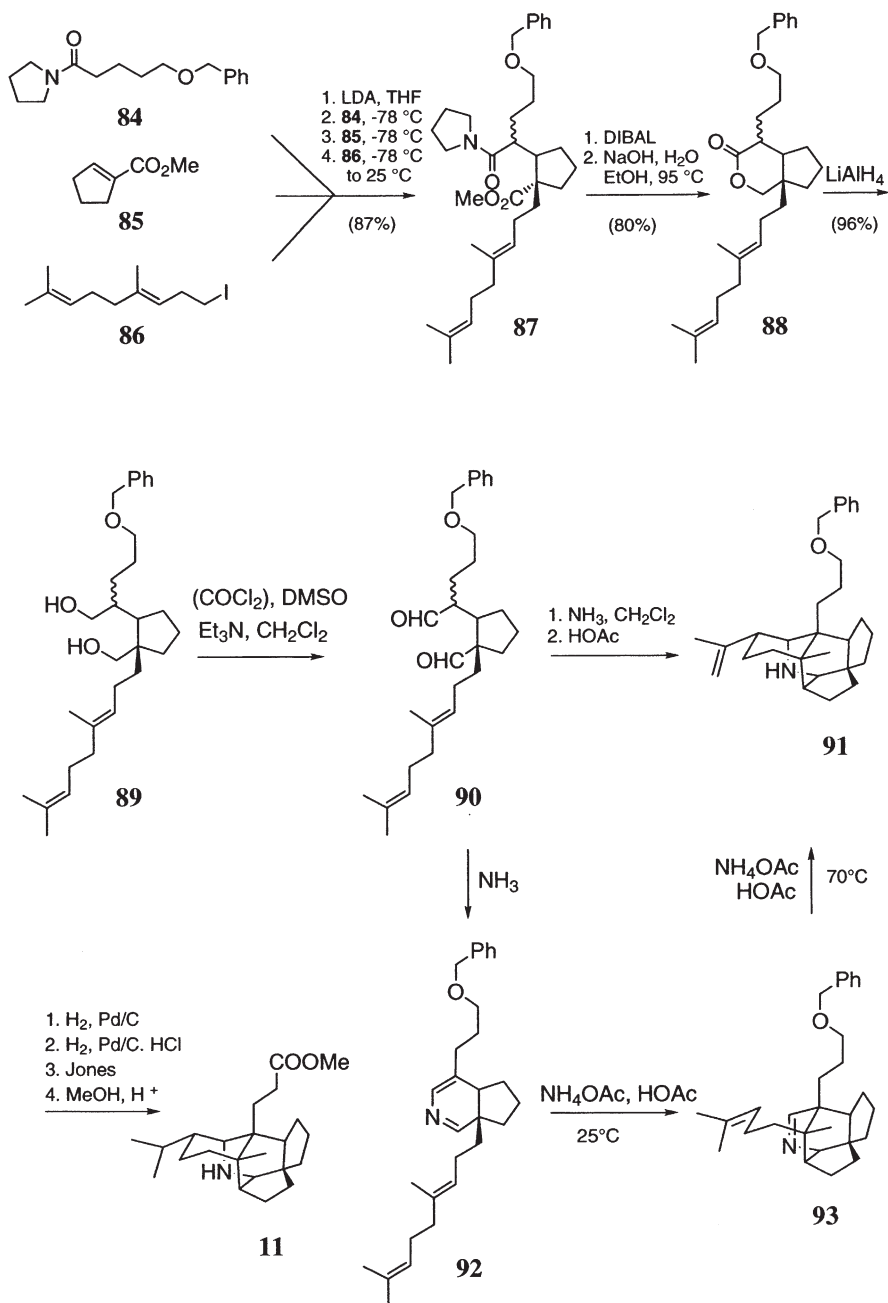
## B. BIOMIMETIC TOTAL SYNTHESIS

### 1. Methyl Homosecodaphniphyllate and Protodaphniphylline

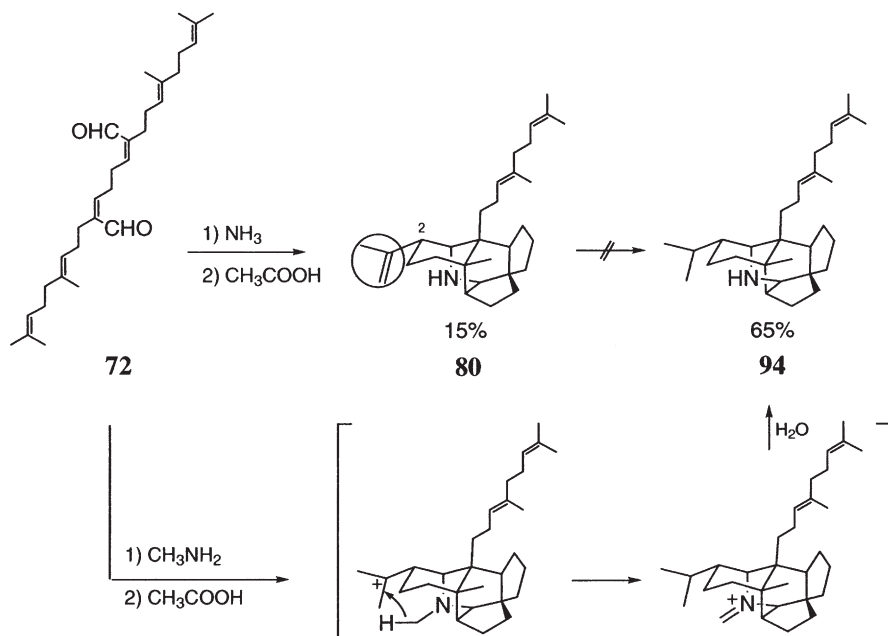
Heathcock *et al.* have embarked on a program to establish experimental methods to accomplish their proposals for the transformations of these alkaloids (4,5). They initially focused their attention on the final stages of the polycyclization reaction leading to the secodaphniphylline skeleton (65,66). Three simple building blocks, amide **84**, unsaturated ester **85**, and unsaturated iodide **86**, were combined in a highly convergent conjugate addition/enolate alkylation process to obtain the ester amide **87** in high yield. Straightforward methods were then employed to convert this substance into the dialdehyde **90**. Compound **90** was treated with ammonia, and then buffered acetic acid, to obtain the unsaturated amine **91** in excellent yield (64% overall from **87** to **91**). The additional functional groups are used to convert **91** into racemic methyl homosecodaphniphyllate (**11**) (65,66).

The transformation of compound **90** to **91** involves a cascade of reactions and the two intermediates can be isolated. Thus, treatment of compound **90** with ammonia causes almost instantaneous transformation of the nonpolar dialdehyde to a complex mixture of polar materials, from which the dihydropyridine **92** can be isolated in about 45% yield. This compound reacts rapidly on being treated with ammonium acetate in acetic acid at room temperature to give compound **93**, as the result of a formal intramolecular Diels-Alder reaction. Continued treatment with warm acetic acid converts compound **93** into compound **91** (65,66) (Scheme 16).

In addition, Heathcock and coworkers have intervened at an earlier stage in the biogenetic pathway depicted in Scheme 6. They prepared the dihydrosqualene dialdehyde **72** and treated it sequentially with ammonia and warm acetic acid. It was gratifying to find proto-daphniphylline **80** in the product of this reaction (67). Although the isolation yield of **80** was only modest (15%), a great deal has been accomplished, theoretically and practically, by the use of the simple reaction



Scheme 16.



Scheme 17. Synthesis of dihydroprotodaphniphylline (**94**) (67).

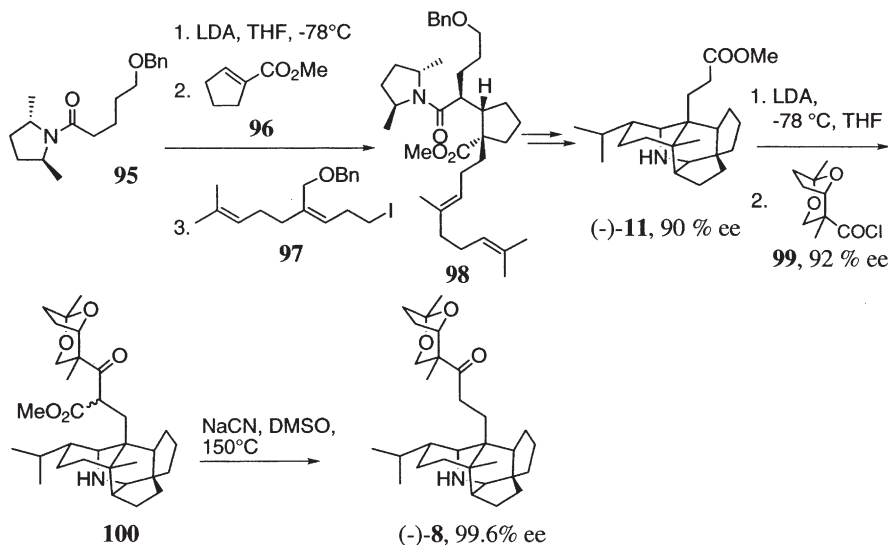
conditions. The fortuitous discovery of using methylamine in place of ammonia suggested a possible solution to the problem of low yield in the pentacyclization process with dihydrosqualene dialdehyde **72**. When compound **72** was treated successively with methylamine and warm acetic acid dihydroprotodaphniphylline (**94**) was formed in 65% yield (Scheme 17) (67).

This marvelous transformation results in the simultaneous formation of seven new sigma bonds and five rings. It is fully diastereoselective, and a necessary consequence of the reaction mechanism is that one of three similar carbon-carbon double bonds is regioselectively saturated.

## 2. Secodaphniphylline

An asymmetric total synthesis of (–)-secodaphniphylline (**8**) was carried out using a mixed Claisen condensation between (–)-methyl homosecodaphniphyllate (**11**) and a carboxylic acid derivative **99** with the characteristic 2,8-dioxabicyclo[3.2.1]octane structure commonly found in the *Daphniphyllum* alkaloids (Scheme 18) (68,69). The necessary chirality was secured by an asymmetric Michael addition reaction of the lithium enolate of the C<sub>2</sub>-symmetric amide **95** to the  $\alpha,\beta$ -unsaturated ester **96** to give ester amide **98**. The conversion of **98** to (–)-**11** was performed by the same route as in the racemic series. Ester (–)-**11** and acid





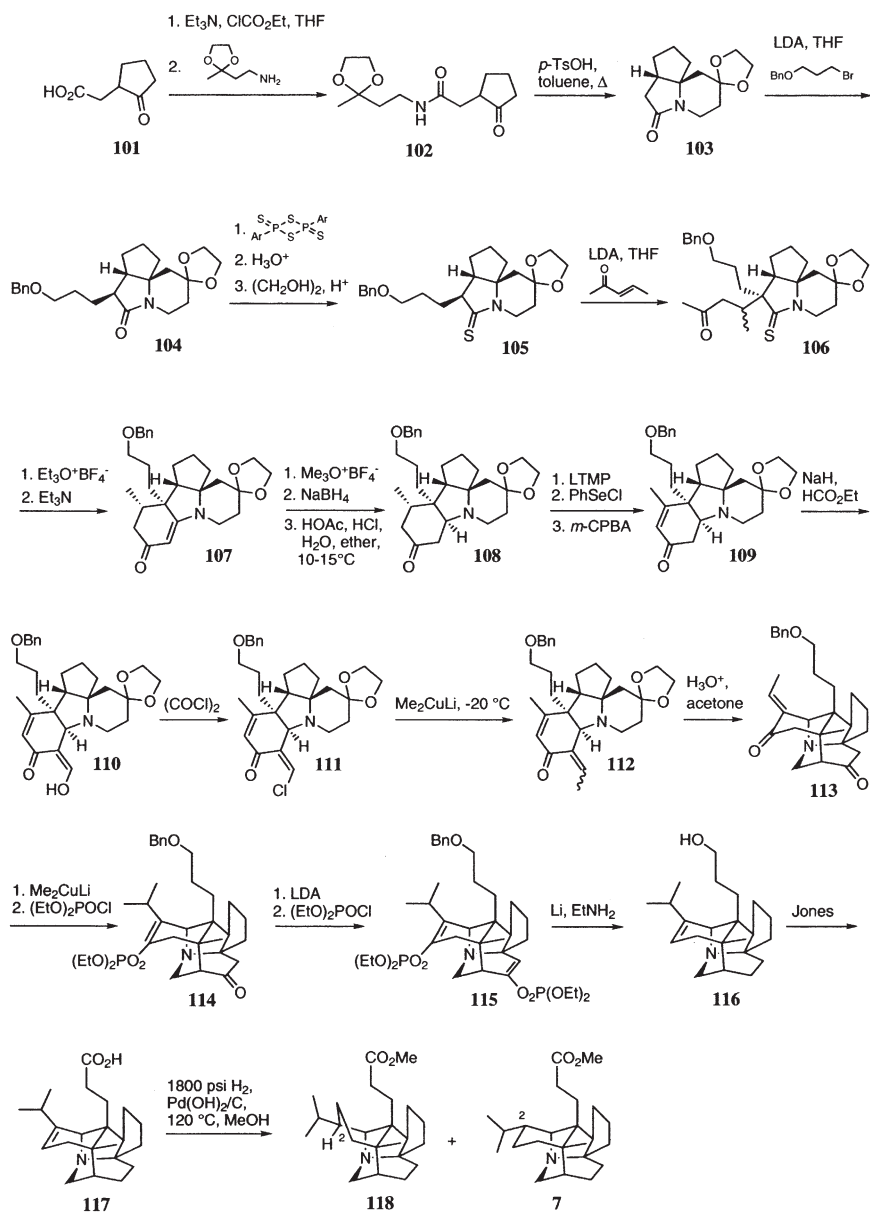
Scheme 18. Synthesis of (–)-secodaphniphylline (**8**) (68,69).

chloride **99** were joined by a mixed Claisen condensation and the resulting diastereomeric  $\beta$ -keto ester was demethylated and decarboxylated by treatment with NaCN in hot DMSO to obtain (–)-secodaphniphylline (**8**).

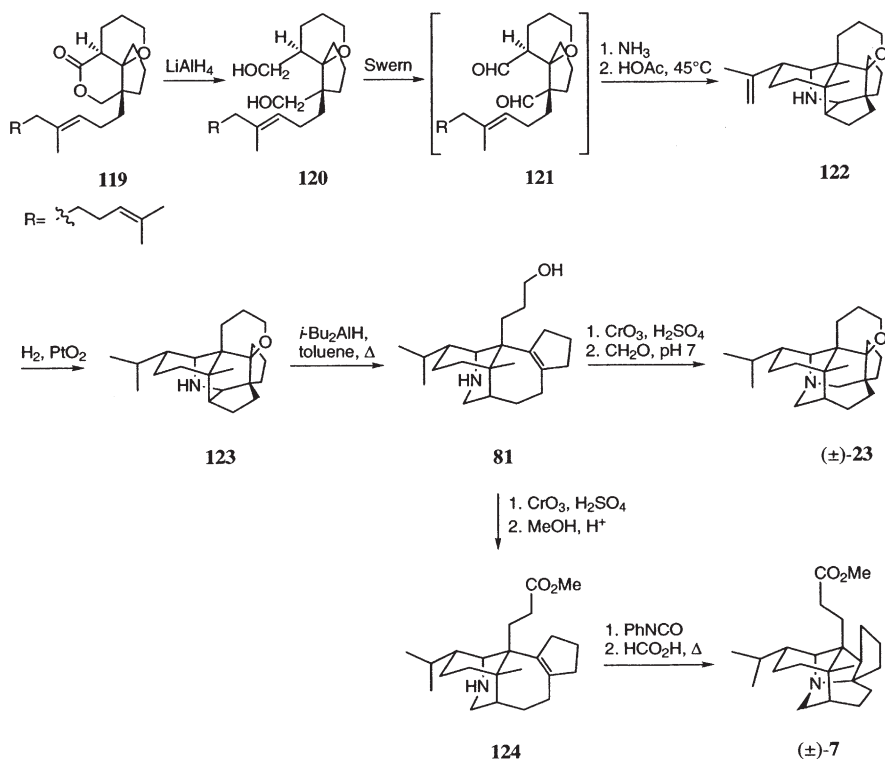
### 3. Methyl Homodaphniphyllate and Daphnilactone A

Synthetic work on the *Daphniphyllum* alkaloids has been dominated by the versatile biomimetic synthesis developed by Heathcock and his collaborators. The first total synthesis of *Daphniphyllum* alkaloids was achieved for methyl homodaphniphyllate (**7**) (Scheme 19) (70,71). The overall yield was about 1.1%. They employed network analysis outlined by Corey and chose an intramolecular Michael reaction for the strategic bond formation, since examination of molecular models of the hypothetical intermediate showed that there are conformations in which the indicated carbon in the tetrahydropyridone ring is within easy bonding distance of the  $\beta$  carbon of the cyclohexenone ring. The pentacyclic intermediate **112**, synthesized from the known keto acid **101**, was treated with a mixture of HCl and  $\text{H}_2\text{SO}_4$  in aqueous acetone for 2 days to give two isomers in a ratio of 3 : 1. The major isomer was in full agreement with the expected Michael cyclization product **113**. Finally, racemic methyl homodaphniphyllate (**7**) was obtained by reduction of **117** with hydrogen in the presence of Pearlman's catalyst,  $\text{Pd}(\text{OH})_2$  in ethanol at  $120^{\circ}\text{C}$  and 1800 psi hydrogen pressure for 20 h, together with its isomer **118** at C-2 in the ratio of 1 : 1 (Scheme 19).

In addition, biomimetic total synthesis of ( $\pm$ )-methyl homodaphniphyllate (**7**) has been carried out (63,72). The synthesis began with the preparation of the



Scheme 19. Synthesis of methyl homodaphniphyllate (7) (70,71).



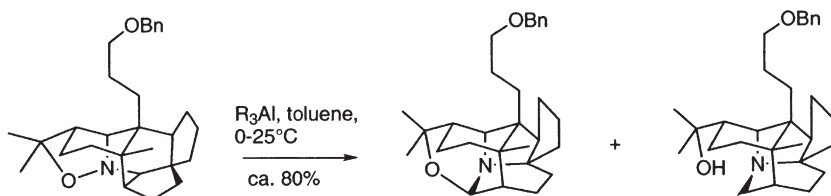
Scheme 20. Synthesis of (±) methyl homodaphniphyllate (**7**) (63,72).

tricyclic lactone ether **119**, which was reduced to the diol **120** with  $\text{LiAlH}_4$ . Oxidation of **120** gave a sensitive dialdehyde **121**, which was treated sequentially with ammonia and warm acetic acid to obtain the hexacyclic amino ether **122**. The tetracyclization process leading from **120** to **122** proceeded in 47% yield and resulted in the formation of five new  $\sigma$ -bonds and four new rings. Unsaturated amino alcohol **81** derived from **122** was converted into (±)-methyl homodaphniphyllate (**7**) by a biomimetic process utilizing a urea derivative as described previously. Furthermore, (±)-daphnilactone **A** (**23**) was synthesized from the unsaturated amino alcohol **81** by oxidation to the unsaturated amino acid, which was cyclized by treatment with aqueous formaldehyde at pH 7 (Scheme 20) (72).

A possibly biomimetic transformation of the secodaphnane to the daphnane skeleton with various Lewis acids has been investigated (Scheme 21) (73).

#### 4. Codaphniphylline

(+)-Codaphniphylline (**2**), one of the  $\text{C}_{30}$  *Daphniphyllum* alkaloids, was synthesized by a modification of Heathcock's biomimetic approach (74)



Scheme 21.

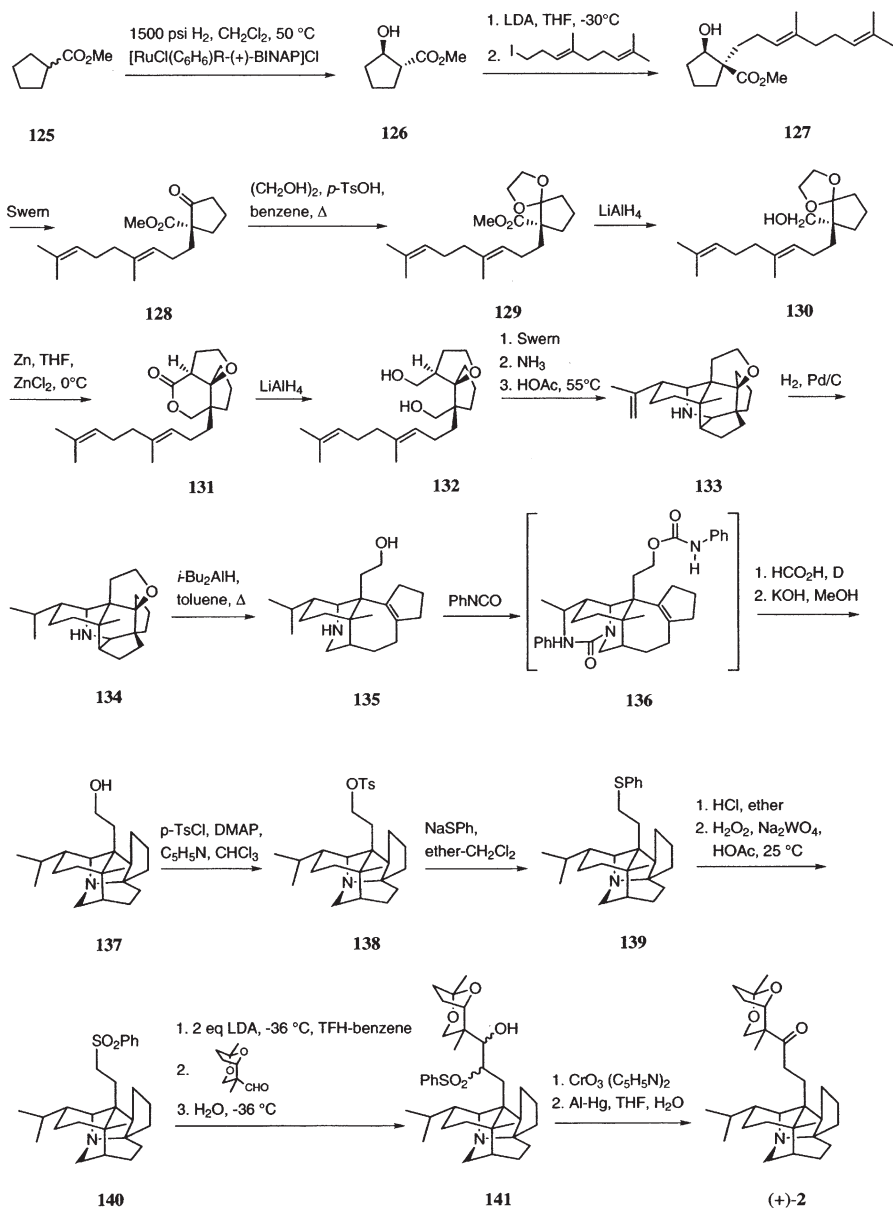
(Scheme 22). Modification was carried out by changing the tetrahydropyran to a tetrahydrofuran as in **131** (Scheme 22). This modification resulted in a yield improvement for the pentacyclization process from 47 to 66%. Treatment of the amino ether **134** with diisobutylaluminum hydride in refluxing toluene accomplished Eschenmoser-Grob fragmentation, and reduction of the initially formed immonium ion to give the unsaturated amino alcohol **135** in 86% yield. It was gratifying to find that **135** was the only product formed in this reaction. In the tetrahydropyran derivative, reduction of **134** to **135** is accompanied by about 15% simple elimination. Displacement of the tosyl group in **138** gives sulfide **139**, which is oxidized to sulfone **140**. This material is metalated and coupled with enantiomerically pure aldehyde to secure the codaphniphylline skeleton (**74**).

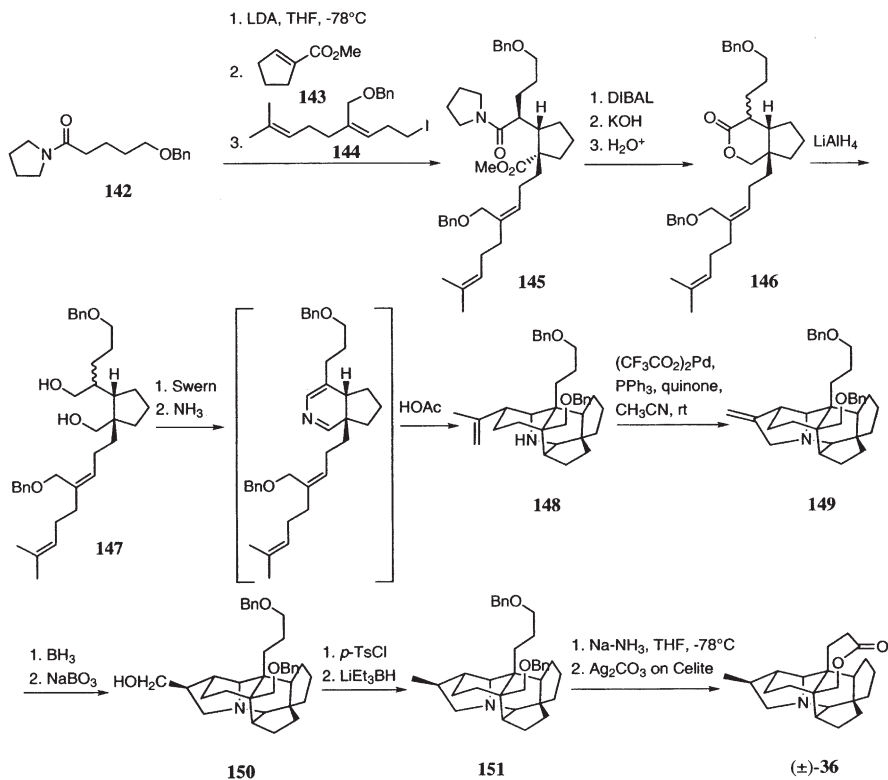
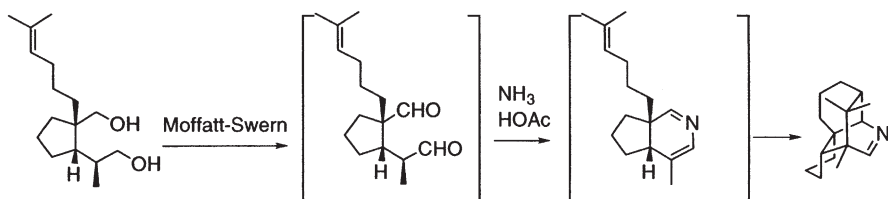
### 5. Bukittinggine

Bukittinggine (**36**) possesses key structural elements of both secodaphniphylline (**8**) and yuzurimine (**12**). Consequently, the biogenesis of the heptacyclic alkaloid, bukittinggine (**36**) isolated from *Sapium baccatum*, may be similar to that of the *Daphniphyllum* alkaloids. The basic secodaphnane nucleus was synthesized in one step by application of the tetracyclization process to produce dihydroxy diether **147**. The pyrrolidine ring was formed by a Pd(II)-catalyzed oxidative cyclization of **148** to give the hexacyclic amine **149**. Hydrogenation of **149** proceeded with little diastereoselectivity in establishing the final stereocenter. However, the sequence of hydroboration/oxidation, tosylation, and reduction of **149** gave **151** under excellent stereocontrol. Debenzylation of **151**, followed by regiospecific oxidative lactonization of the diol, afforded ( $\pm$ )-bukittinggine (**36**) (Scheme 23) (**75**).

### 6. Polycyclization Cascade

Recently, the scope of the 2-azadiene intramolecular Diels-Alder cyclization, employed for the synthesis of the *Daphniphyllum* alkaloids, has been further investigated by Heathcock *et al.* (**76**). The protocol involves Moffatt-Swern oxidation of the 1,5-diol to the dialdehyde, and treatment of the crude methylene chloride solution with ammonia followed by solvent exchange from methylene chloride to a buffered acetic acid solution. The cyclopentyl ring, quaternary carbon and tertiary carbon centers in the diol starting material all play a role in providing a selective and high-yielding cyclization (Scheme 24) (**76**).

Scheme 22. Synthesis of (+)-codaphniphylline (**2**) (74).

Scheme 23. Synthesis of (±)-bukittingine (**36**) (75).

Scheme 24.

## V. Conclusions

Studies on the *Daphniphyllum* alkaloids from 1966 to 2002 have been reviewed, particularly focusing on recent developments in the biomimetic synthesis of these alkaloids, and the structures of the new alkaloid types, such as the daphnezomines, the daphnicyclidins, and the daphmanidins. There are currently

more than 60 *Daphniphyllum* alkaloids of known structure. Further phytochemical investigations will bring increasing structural variation to this alkaloid group. Although the total syntheses of some of the daphnane and seco-daphnane skeletons have been accomplished, the other skeletal variants remain an attractive subject. Since the pharmacological activity of the *Daphniphyllum* alkaloids is poorly studied, this area should also be developed. Similarly, the biosynthesis of *Daphniphyllum* alkaloids has been only preliminarily studied, and the pathways have not been characterized with respect to the intermediates and the relevant enzymes. Widespread efforts for understanding the properties of these complex and fascinating alkaloids will result in further developments in this field.

### References

1. S. Yamamura and Y. Hirata, "The Alkaloids" (R. H. F. Manske, ed.), vol. 15, pp. 41. Academic Press, New York, 1975.
2. S. Yamamura, "The Alkaloids" (A. Bossi, ed.), vol. 29, pp. 265. Academic Press, New York, 1986.
3. M. Toda, H. Irikawa, S. Yamamura, and Y. Hirata, *Nippon Kagaku Zasshi* **91**, 103 (1970). [*C.A.* 73, 22137j (1970)].
4. S. Piettre and C. H. Heathcock, *Science* **248**, 1532 (1990).
5. C. H. Heathcock, *Proc. Natl. Acad. Sci. USA* **93**, 14323 (1996).
6. S. Yagi, *Kyoto Igaku Zasshi* **6**, 208 (1991).
7. N. Sakabe, H. Irikawa, H. Sakurai, and Y. Hirata, *Tetrahedron Lett.*, 963 (1966).
8. N. Sakabe and Y. Hirata, *Tetrahedron Lett.*, 965 (1966).
9. S. Yamamura, H. Irikawa, and Y. Hirata, *Tetrahedron Lett.*, 3361 (1967).
10. H. Irikawa, N. Sakabe, S. Yamamura, and Y. Hirata, *Tetrahedron* **24**, 5691 (1968).
11. H. Irikawa, H. Sakurai, N. Sakabe, and Y. Hirata, *Tetrahedron Lett.*, 5363 (1966).
12. H. Irikawa, S. Yamamura, N. Sakabe, and Y. Hirata, *Tetrahedron Lett.*, 553 (1967).
13. M. Toda, H. Niwa, Y. Hirata, and S. Yamamura, *Tetrahedron Lett.*, 797 (1973).
14. N. Kamijo, T. Nakano, S. Terao, and K. Osaki, *Tetrahedron Lett.*, 2889 (1966).
15. T. Nakano and Y. Saeki, *Tetrahedron Lett.*, 4791 (1967).
16. T. Nakano, Y. Saeki, C. S. Gibbons, and J. Trotter, *Chem. Commun.*, 600 (1968).
17. C. S. Gibbons and J. Trotter, *J. Chem. Soc., B*, 840 (1969).
18. T. Nakano, M. Hasegawa, and Y. Saeki, *J. Org. Chem.* **38**, 2404 (1973).
19. H. Irikawa, M. Toda, S. Yamamura, and Y. Hirata, *Tetrahedron Lett.*, 1969 (1821).
20. M. Toda, S. Yamamura, and Y. Hirata, *Tetrahedron Lett.*, 2585 (1969).
21. K. Sasaki and Y. Hirata, *J. Chem. Soc., B*, 1565 (1971).
22. M. Toda, Y. Hirata, and S. Yamamura, *Tetrahedron* **28**, 1477 (1972).
23. S. Yamamura and Y. Hirata, *Tetrahedron Lett.*, 2849 (1974).
24. S. Yamamura and Y. Hirata, *Tetrahedron Lett.*, 3673 (1974).
25. H. Sakurai, N. Sakabe, and Y. Hirata, *Tetrahedron Lett.*, 6309 (1966).
26. H. Irikawa, S. Yamamura, and Y. Hirata, *Tetrahedron* **28**, 3727 (1972).
27. H. Sakurai, H. Irikawa, S. Yamamura, and Y. Hirata, *Tetrahedron Lett.*, 2883 (1967).
28. S. Yamamura, H. Irikawa, Y. Okumura, and Y. Hirata, *Bull. Chem. Soc. Jpn.* **48**, 2120 (1975).
29. T. Nakano and B. Nilsson, *Tetrahedron Lett.*, 2883 (1969).
30. S. Yamamura and Y. Terao, *Chem. Lett.*, 1381 (1976).

31. X.-J. Hao, J. Zhou, M. Node, and K. Fuji, *Acta Botanica Yunnanica* **15**, 205 (1993).
32. K. Sasaki and Y. Hirata, *J. Chem. Soc., Perkin Trans. 2*, 1411 (1972).
33. K. Sasaki and Y. Hirata, *Tetrahedron Lett.*, 1275 (1972).
34. K. Sasaki and Y. Hirata, *Tetrahedron Lett.*, 1891 (1972).
35. H. Niwa, M. Toda, Y. Hirata, and S. Yamamura, *Tetrahedron Lett.*, 2697 (1972).
36. H. Niwa, Y. Hirata, K. T. Suzuki, and S. Yamamura, *Tetrahedron Lett.*, 2129 (1973).
37. M. Toda, H. Niwa, H. Irikawa, Y. Hirata, and S. Yamamura, *Tetrahedron* **30**, 2683 (1974).
38. S. Yamamura, M. Toda, and Y. Hirata, *Bull. Chem. Soc. Jpn.* **49**, 839 (1976).
39. S. Yamamura, K. Sasaki, M. Toda, and Y. Hirata, *Tetrahedron Lett.*, 2023 (1974).
40. S. Yamamura, J. A. Lambertson, H. Irikawa, Y. Okumura, and Y. Hirata, *Chem. Lett.*, 923 (1975).
41. S. Yamamura, J. A. Lambertson, H. Irikawa, Y. Okumura, M. Toda, and Y. Hirata, *Bull. Chem. Soc. Jpn.* **50**, 1836 (1977).
42. S. Yamamura, J. A. Lambertson, M. Niwa, K. Endo, and Y. Hirata, *Chem. Lett.*, 393 (1980).
43. D. Arbain, L. T. Byrne, J. R. Cannon, V. A. Patrick, and A. H. White, *Aust. J. Chem.* **43**, 185 (1990).
44. H. Morita, N. Yoshida, and J. Kobayashi, *J. Org. Chem.* **64**, 7208 (1999).
45. H. Morita, N. Yoshida, and J. Kobayashi, *Tetrahedron* **55**, 12549 (1999).
46. H. Morita, N. Yoshida, and J. Kobayashi, *J. Org. Chem.* **65**, 3558 (2000).
47. H. Morita, N. Yoshida, and J. Kobayashi, *Tetrahedron* **56**, 2641 (2000).
48. H. Morita and J. Kobayashi, *Tetrahedron* **58**, 6637 (2002).
49. J. Kobayashi, Y. Inaba, M. Shiro, N. Yoshida, and H. Morita, *J. Am. Chem. Soc.* **123**, 11402 (2001).
50. H. Morita, N. Yoshida, and J. Kobayashi, *J. Org. Chem.* **67**, 2278 (2002).
51. J. Kobayashi, S. Ueno, and H. Morita, *J. Org. Chem.* **67**, 6546 (2002).
52. H. D. Flack, *Acta Cryst.* **A39**, 876 (1983).
53. T. Goto, Y. Kishi, S. Takahashi, and Y. Hirata, *Tetrahedron Lett.* 779 (1964); *idem*, *Tetrahedron* **21**, 2059 (1965); R. B. Woodward, *Pure Appl. Chem.* **9**, 49 (1964).
54. D. M. Roll, J. E. Biskupiak, C. L. Mayne, and C. M. Ireland, *J. Am. Chem. Soc.* **108**, 6680 (1986).
55. Y. Morita, M. Hesse, H. Schmid, A. Banerji, J. Banerji, A. Chatterjee, and W. E. Oberhansli, *Helv. Chim. Acta* **60**, 1419 (1977).
56. H.-J. Borschberg, *Helv. Chim. Acta* **67**, 1878 (1984).
57. G. Kobrich, *Angew. Chem. Int. Ed. Engl.* **12**, 464 (1973).
58. M. Toda, Y. Hirata, and S. Yamamura, *J. Chem. Soc. Chem. Commun.* 1597 (1970).
59. F. Mohamadi, N. G. J. Richards, W. C. Guida, R. Liskamp, M. Lipton, C. Caufield, G. Chang, T. Hendrickson, and W. C. Still, *J. Comput. Chem.* **11**, 440 (1990).
60. T. Halgren, *J. Am. Chem. Soc.* **112**, 4710 (1990).
61. N. Harada, K. Nakanishi, and S. Tatsuoka, *J. Am. Chem. Soc.* **91**, 5896 (1969).
62. K. T. Suzuki, S. Okuda, H. Niwa, M. Toda, Y. Hirata, and S. Yamamura, *Tetrahedron Lett.*, 799 (1973).
63. R. B. Ruggeri and C. H. Heathcock, *J. Org. Chem.* **55**, 3714 (1990).
64. D. Grierson, *Organic Reactions* **39**, 85 (1990).
65. R. B. Ruggeri, M. M. Hansen, and C. H. Heathcock, *J. Am. Chem. Soc.* **110**, 8734 (1988).
66. C. H. Heathcock, M. M. Hansen, R. B. Ruggeri, and J. C. Kath, *J. Org. Chem.* **57**, 2544 (1992).



67. C. H. Heathcock, S. Piettre, R. B. Ruggeri, J. A. Ragan, and J. C. Kath, *J. Org. Chem.* **57**, 2554 (1992).
68. J. A. Stafford and C. H. Heathcock, *J. Org. Chem.* **55**, 5433 (1990).
69. C. H. Heathcock and J. A. Stafford, *J. Org. Chem.* **57**, 2566 (1992).
70. C. H. Heathcock, S. K. Davidsen, S. Mills, and M. A. Sanner, *J. Am. Chem. Soc.* **108**, 5650 (1986).
71. C. H. Heathcock, S. K. Davidsen, S. Mills, and M. A. Sanner, *J. Org. Chem.* **57**, 2531 (1992).
72. C. H. Heathcock, R. B. Ruggeri, and K. F. McClure, *J. Org. Chem.* **57**, 2585 (1992).
73. C. H. Heathcock and D. Joe, *J. Org. Chem.* **60**, 1131 (1995).
74. C. H. Heathcock, J. C. Kath, and R. B. Ruggeri, *J. Org. Chem.* **60**, 1120 (1995).
75. C. H. Heathcock, J. A. Stafford, and D. L. Clark, *J. Org. Chem.* **57**, 2575 (1992).
76. G. A. Wallace and C. H. Heathcock, *J. Org. Chem.* **66**, 450 (2001).
77. H. Niwa, M. Toda, S. Ishimaru, Y. Hirata, and S. Yamamura, *Tetrahedron* **30**, 3031 (1974).

## THE MANZAMINE ALKALOIDS

JIN-FENG HU<sup>1</sup>, MARK T. HAMANN<sup>1</sup>, RUSSELL HILL<sup>2</sup>, AND  
MICHELLE KELLY<sup>3</sup>

<sup>1</sup>*Department of Pharmacognosy and National Center for the Development of Natural Products (NCNPR), School of Pharmacy, The University of Mississippi, University, Mississippi, USA;* <sup>2</sup>*The Center of Marine Biotechnology (COMB), University of Maryland Biotechnology Institute, Columbus Center, Baltimore, Maryland, USA;* <sup>3</sup>*National Center for Aquatic Biodiversity & Biosecurity, National Institute of Water & Atmospheric Research (NIWA) Ltd., Newmarket, Auckland, New Zealand*

- I. Introduction
  - II. Isolation and Structure Elucidation from Marine Sponges
  - III. Biogenesis and Biosynthesis
  - IV. Synthesis
  - V. Pharmacology
  - VI. Conclusions
- References

### I. Introduction

The number of alkaloids identified from marine organisms continues to grow at an increasing rate, but few, if any, provide comparable sophistication in molecular architecture or as promising a biological significance as the manzamine class. The manzamines are a unique class of  $\beta$ -carboline-containing alkaloids with an unusual polycyclic system identified from marine sponges beginning in the late 1980s. The first representative of this class of alkaloids isolated by Higa's group was identified as manzamine A (**1**) (Fig. 1) (*1*), and the relative, as well as absolute, configuration was considered unprecedented at the time. X-ray diffraction crystallographic analysis of manzamine A hydrochloride (**1a**), showed that apart from the  $\beta$ -carboline substituent, the molecule comprises a complicated array of 5-, 6-, 8-, and 13-membered rings. The piperidine and cyclohexene ring systems

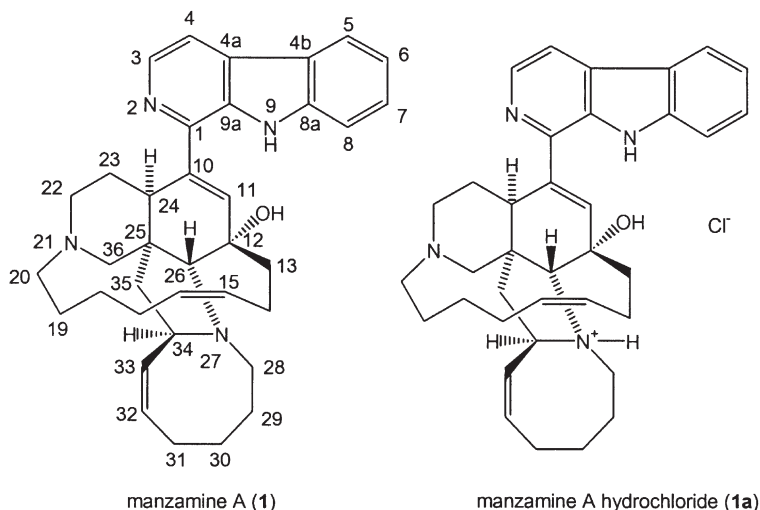
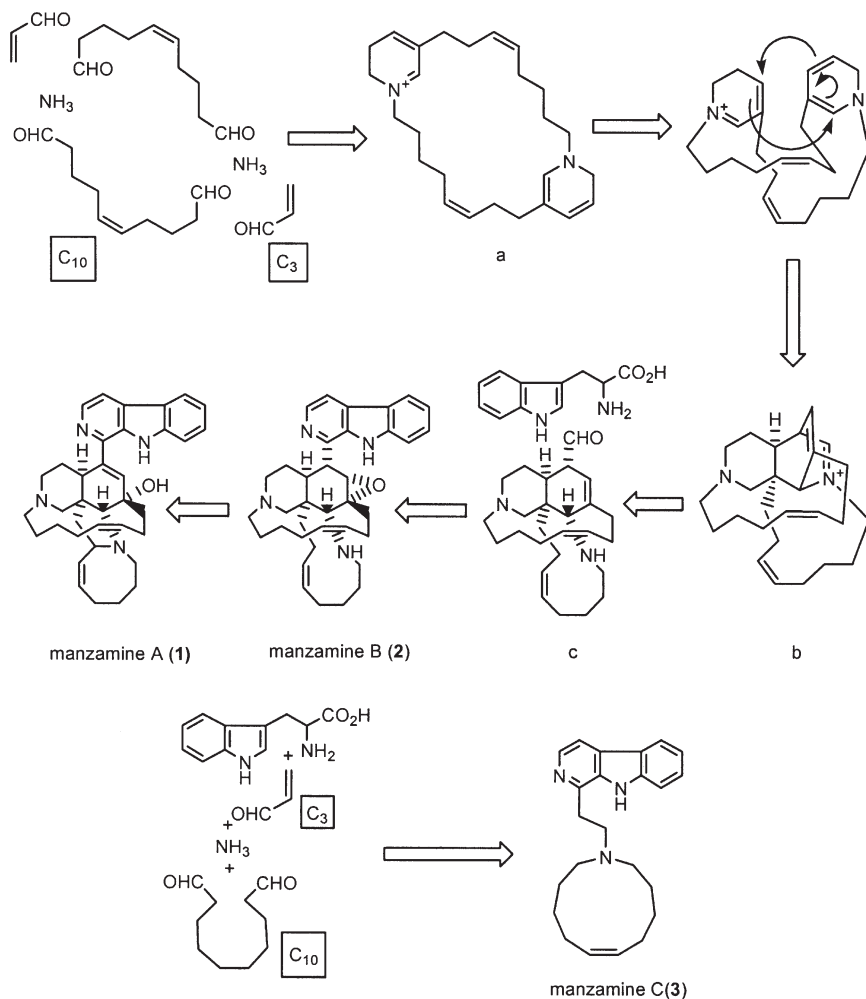


Figure 1. The structures of manzamine A (**1**) and its hydrochloride (**1a**).

adopt chair and boat conformations, respectively, while the pyrrolidinium ring forms an envelope. The conformation of the 8-membered *Z*-olefinic ring is in an envelope-boat, with a mirror plane passing through C-32 and C-28. The two, six-membered rings of manzamine A are bridged by a chain of eight carbon atoms constituting a 13-membered macrocycle with a quadrangular conformation. The six bonds joining C-12 to C-19 of manzamine A form a “convex side” and a pseudo mirror plane transfixing the double bond and the C-36 atom (*1*).

In recent years, the manzamines have been regarded as an intriguing group of marine alkaloids with extraordinary biological activity, and as a result these compounds have been the subject of several reviews regarding their chemistry and pharmacology (*2–4*). In addition, the manzamines have also provoked a great deal of interest in their unprecedented biosynthetic pathway. In 1992 Baldwin *et al.* (*5*) first proposed a plausible biogenetic pathway involving an intramolecular Diels-Alder reaction for manzamines A (**1**) and B (**2**). This biogenetic scheme suggested that a macrocyclic bisdihydropyridine maybe derived from ammonia, a C3 unit, and a C10 unit. The bisdihydropyridine could then be converted through a Diels-Alder-type [4+2] intramolecular cycloaddition into a pentacyclic intermediate, which, in turn, would provide manzamines A and B via a tetracyclic intermediate. Manzamine C (**3**) could then easily be formed as a related product through a straightforward process involving four units including: tryptophan, ammonia, a C3 acrolein, and a C10 symmetrical dialdehyde (*Scheme 1*) (*5*).

Following manzamine A (**1**) (*1*), a series of  $\beta$ -carboline-containing manzamine alkaloids (**2–29**) (*Fig. 2*) (*2,6–21*) have been isolated from marine sponges over the past two decades, including the fascinating unsymmetrical



Scheme 1. Biogenetic path of manzamines A (1), B (2), and C (3) proposed by Baldwin *et al.* (5).

manzamine dimer from the Scheuer group called kauluamine (**25**) (15) and a nearly symmetrical dimer called *neo*-kauluamine (**26**) (18). Based on Scheme 1, keramaphidin C (**30**) (22) may be regarded as the precursor of manzamine C (3). Keramaphidin C (**30**) and the closely related marine alkaloids **31** (23), **32–34** (24) (Fig. 3) are regarded as manzamine-related alkaloids due to their relationship to manzamine C presented in Scheme 1, despite the fact that they lack both the  $\beta$ -carboline and isoquinoline ring systems. From this same scheme it is also clear that ircinal A (**35**) (10) may be a key precursor to manzamine A (1). Therefore,

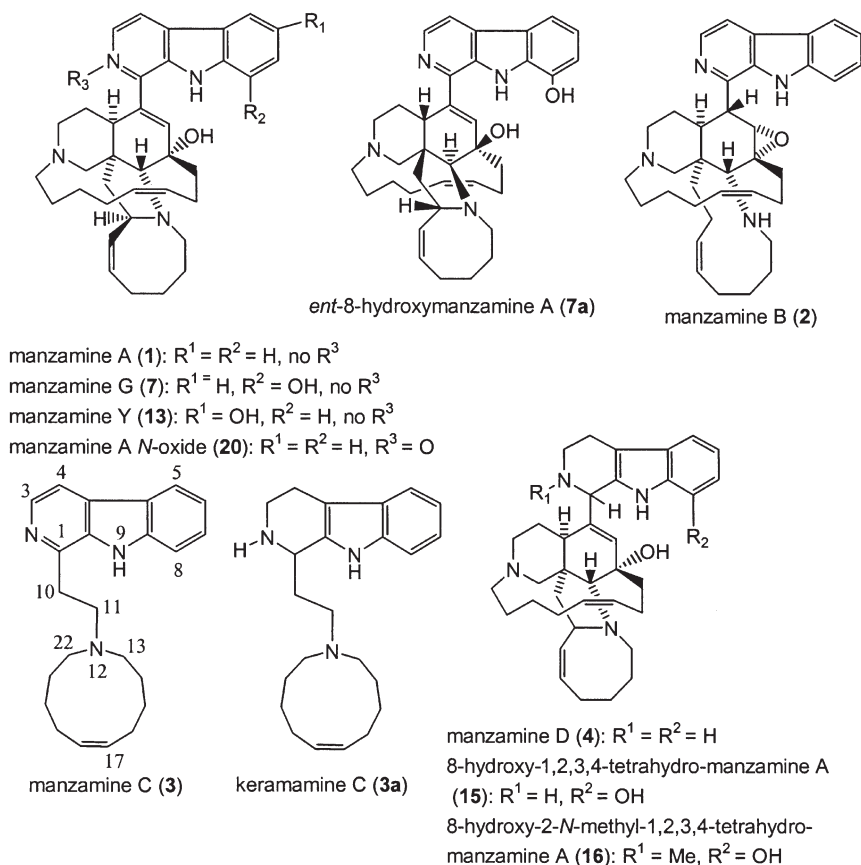


Figure 2.  $\beta$ -Carboline-containing manzamines.

ircinal A, as well as the related marine alkaloids **36** (10), **37** (25), and **38** (25), are also regarded as part of the manzamine class of alkaloids (Fig. 3). Keramaphidin B (39) (26) is considered a key precursor to ircinal A (35) and B (36) (27), and, as a result, 39 and its related marine alkaloids **40** (28,29), **41** (28), **42** (30), **43** (30), **44** (31), **45–49** (32), **50** (33,34), **51–54** (35), and **55** (36) (Fig. 3) are also included in this review of manzamine-related alkaloids. In addition, there is a series of macrocyclic alkaloids isolated from marine sponges (37–52), which are similar in structure to compounds 39–55. However, these structures are not detailed in this review due to a diminished relationship to the manzamine alkaloids. Nakadomarin A (56) (53) is an example of a manzamine-related alkaloid that could be biogenetically derived from ircinal A (35) (3).

The manzamine alkaloids have shown a diverse range of bioactivities including: antitumor and cytotoxicity (1,7,9,10,12,15,16,54), anti-inflammatory

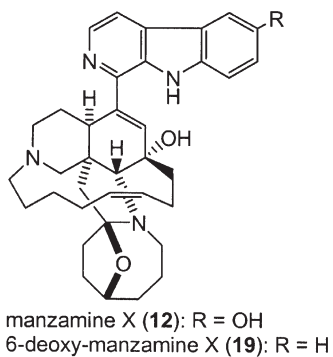
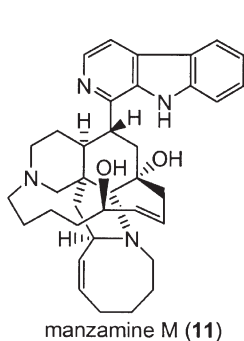
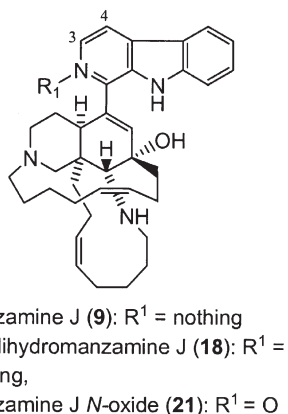
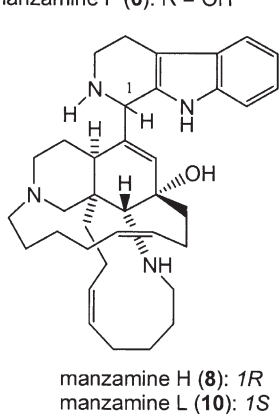
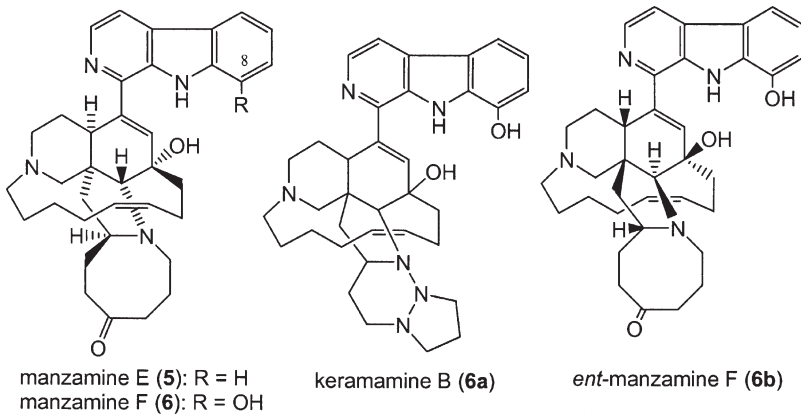


Figure 2. (continued)

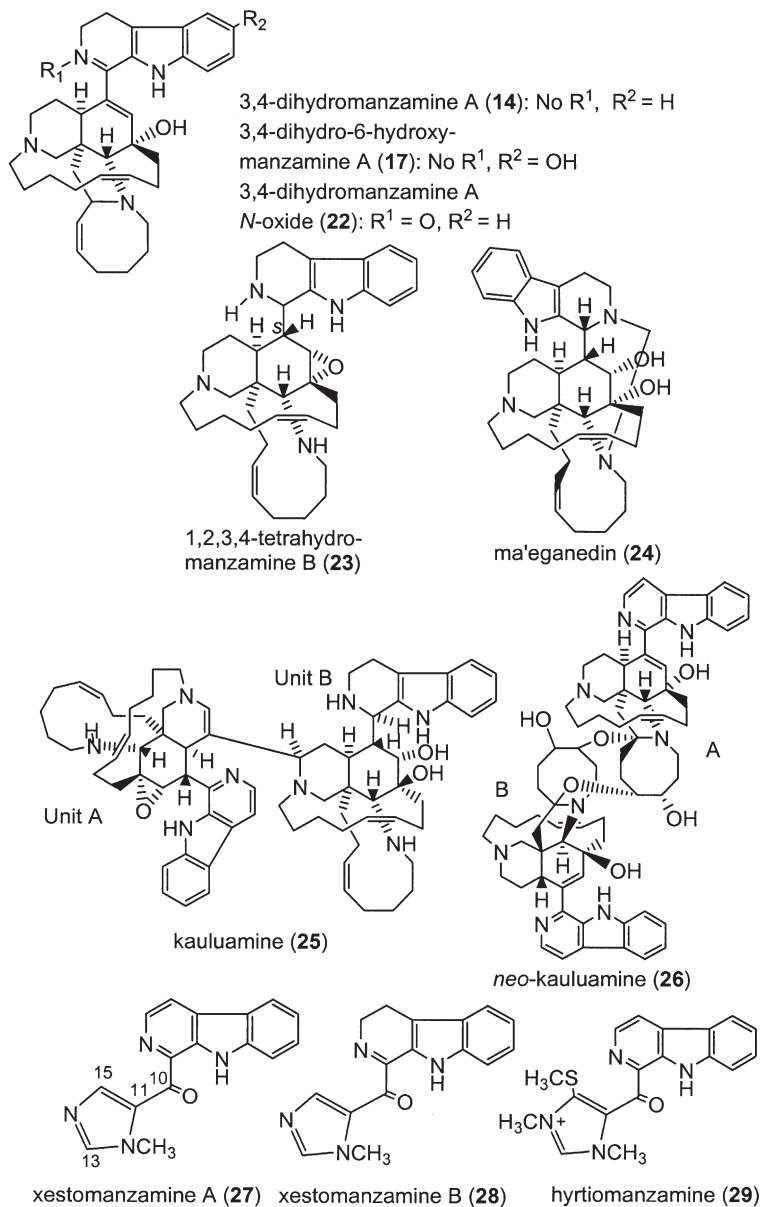


Figure 2. (continued)

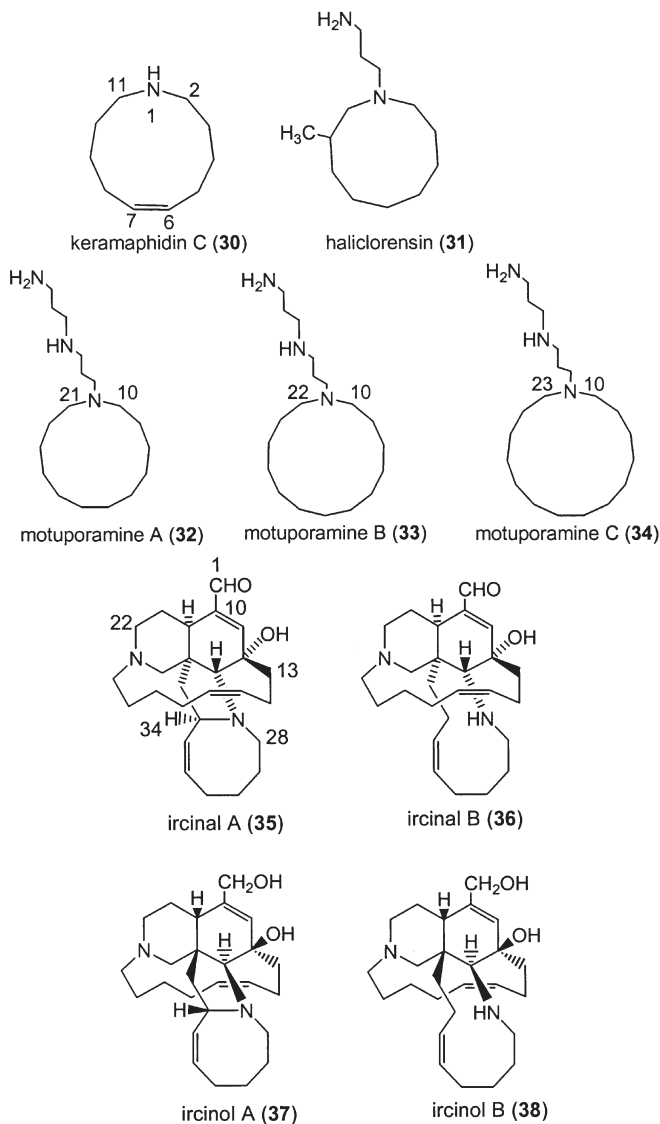


Figure 3. Manzamine-related marine alkaloids.

(55), insecticidal (16,56), anti-infective and antiparasitic (17,27), with the greatest anti-infective activity against malaria and Mtb (18). The diversity of biological activity for this class of compounds provides additional evidence that they may be of microbial origin and ultimately a novel class of lead, broad-spectrum, antiparasitic-antibiotics. To date, the greatest potential for the manzamine



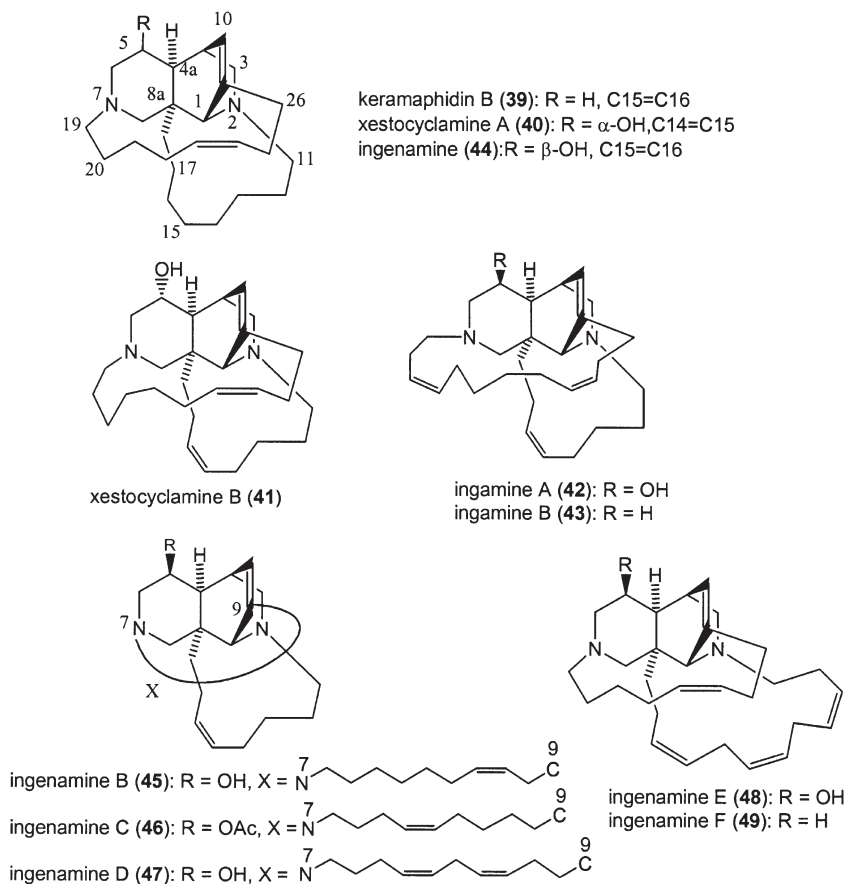


Figure 3. (continued)

alkaloids appears to be against malaria with manzamine A (**1**), ent-8 hydroxymanzamine A (**7a**), as well as *neo*-kauluamine (**26**) showing improved activity over the clinically used drugs chloroquine and artemisinin in animal models (**18**). The isolation of the manzamine alkaloids from a growing number of sponge genera further implies the existence of a sponge-associated microorganism as the actual biosynthetic source for the manzamine alkaloids. A key tool for the study of the biosynthesis of these intriguing structures will clearly be the identification of such a microorganism.

## II. Isolation and Structure Elucidation from Marine Sponges

To date, there are 17 or more species belonging to 5 families of marine sponges that have been reported to yield the  $\beta$ -carboline-containing manzamine

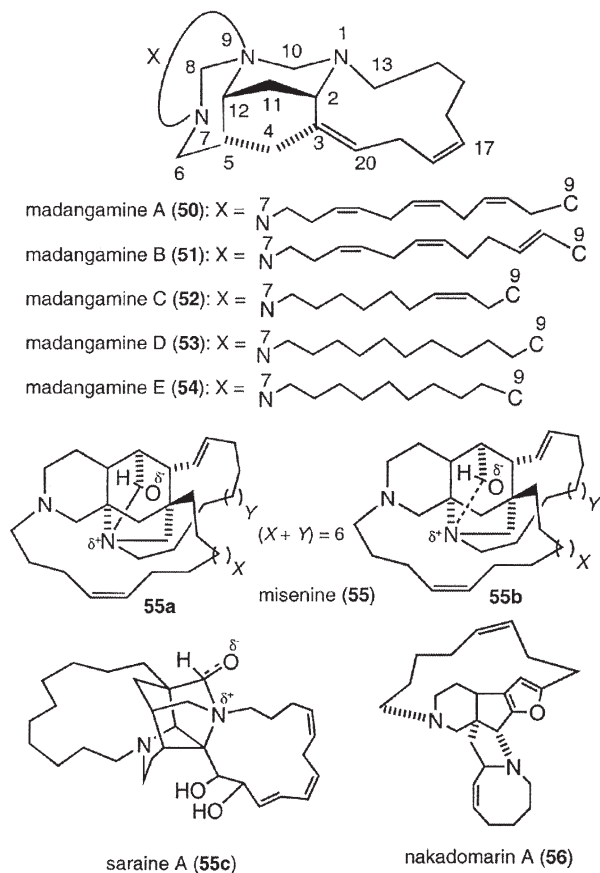


Figure 3. (continued)

and manzamine-related alkaloids (Table I). These sponges have been collected from Okinawa, Philippines, Indonesia, Red Sea, Italy, South Africa, and Papua New Guinea. Most species yielded a number of  $\beta$ -carboline-containing manzamine and manzamine-related alkaloids. The most productive species are those in the genera *Amphimedon* sp. (2,27), and *Acanthostrongylophora* ((58,59)); see Table I), which to date has yielded the greatest number of  $\beta$ -carboline-containing manzamine and manzamine-related alkaloids. Some species are particularly unusual due to their generation of enantiomers, such as **6** and **6b**, as well as **7** and **7a** (18).

#### A. $\beta$ -CARBOLINE-CONTAINING MANZAMINE ALKALOIDS

The  $\beta$ -carboline moiety is a distinct feature, which has been utilized in the classification of these alkaloids since the first report of manzamine A (1).

TABLE I.  
Marine Sponges Yielding Manzamines and Related Alkaloids.

Taxonomy	Collection localities	Alkaloids	References
Order HAPLOSCLERIDA Topsent			
Family CHALINIDAE Gray			
Genus <i>Haliclona</i> Grant			
<i>Haliclona</i> spp.	Manzamo and Amitori Bay (Iriomote Island), Okinawa	<b>1, 2, 3, 4, 13</b>	<i>1,7,8,14</i>
<i>Haliclona tulearensis</i> VV&L <sup>a</sup>	Sodwana Bay, South Africa	<b>31</b>	<i>23</i>
Genus <i>Reniera</i> Nardo			
<i>Reniera</i> sp.	Capo Miseno, Naples, Italy	<b>55</b>	<i>36</i>
<i>Reniera sarai</i> Pulitzeri-Finali	Bay of Naples	<b>55c</b>	<i>53</i>
Family NIPHATIDAE van Soest			
Genus <i>Amphimedon</i> D&M <sup>a</sup>			
<i>Amphimedon</i> spp.	Kerama Islands, Okinawa	<b>1, 2, 3, 3a, 4, 7, 8, 10, 11, 13, 14, 17, 18, 23, 24, 30, 35, 36, 37, 38, 39, 56</b>	<i>2,12,17,19,20, 22,25–27,57</i>
Genus <i>Cribochalina</i> Schmidt			
<i>Cribochalina</i> sp.	Madang, Papua New Guinea	<b>16</b>	<i>13</i>
Family PETROSIIDAE van Soest			
Genus <i>Acanthostrongylophora</i> Hooper <sup>b</sup>			
<i>Xestospongia</i> spp.*	Miyako Island and Amitori Bay (Iriomote Island), Okinawa	<b>1, 2, 3, 4, 5, 6, 12, 27, 28, 40, 41</b>	<i>9,14,28,29</i>
[ <i>Prianos</i> sp.]	Manado Bay, Sulawesi, Indonesia	<b>25</b>	<i>15</i>
[ <i>Xestospongia ashmorica</i> Hooper]	Mindoro Island, Philippines	<b>1, 5, 6, 9, 19, 20, 21, 22</b>	<i>16</i>
[ <i>Xestospongia ingens</i> Thiele]	Papua New Guinea	<b>42, 43, 44, 45, 46, 47, 48, 49, 50, 51, 52, 53, 54</b>	<i>30–33,35</i>

[Petrosiidae n.g.] n. sp.	Manado Bay, Sulawesi, Indonesia	<b>6b, 7a, 26, 57, 58, 59, 62, 63, 64, 65, 66</b>	<i>18,58–60</i>
[ <i>Pachypellina</i> sp.]	Manado Bay, Sulawesi, Indonesia	<b>1, 7</b>	<i>11</i>
<i>Pellina</i> sp.*	Kerama islands, Okinawa	<b>1, 6</b>	<i>6</i>
Genus <i>Xestospongia</i> de Laubenfels			
<i>Xestospongia exigua</i> Kirkpatrick	Papua New Guinea	<b>32, 33, 34</b>	<i>24</i>
Genus <i>Petrosia</i> Vosmaer			
<i>Petrosia contignata</i> Thiele	Milne Bay, Papua New Guinea	<b>15, 16</b>	<i>13</i>
Order DICTYOCERATIDA Minchin			
Family THORECTIDAE Bergquist			
Genus <i>Hyrtios</i> D&M <sup>a</sup>			
<i>Hyrtios erecta</i> Keller	Red Sea	<b>29</b>	<i>21</i>
Family IRCINIIDAE Gray			
Genus <i>Ircinia</i> Nardo			
<i>Ircinia</i> sp.	Kise, Okinawa	<b>1, 2, 4, 5, 8, 9, 35, 36</b>	<i>2,10</i>
Undetermined	Palau	<b>60, 61</b>	<i>61</i>

<sup>a</sup>Taxonomic authorities: VV&L = Vacelet, Vasseur & Lévi; D&M = Duchassaing & Michelotti.

<sup>b</sup>The genus *Acanthostrongylophora* Hooper has been recently confirmed as the appropriate genus name for the group of sponges listed in square brackets above (63).

\*Those taxa followed by an asterisk have not been examined by MK but their descriptions conform to our understanding of the genus *Acanthostrongylophora*.

In addition to manzamine A (**1**) (*1*), the following  $\beta$ -carboline-containing manzamines have since been reported and include: B (**2**) (*7,8*), C (**3**) (*7,8*), D (**4**) (*7,8*), E (**5**) (*9*), F (**6**) (*9*), G (**7**) (*11,27*), H (**8**) (*10*), J (**9**) (*10*), L (**10**) (*27*), M (**11**) (*17*), X (**12**) (*14*), Y (**13**) (*12,27*), 3,4-dihydropanzamine A (**14**) (*12*), 8-hydroxy-1,2,3,4-tetrahydropanzamine A (**15**) (*13*), 8-hydroxy-2-*N*-methyl-1,2,3,4-tetrahydropanzamine A (**16**) (*13*), 3,4-dihydro-6-hydroxypanzamine A (**17**) (*17*), 3,4-dihydropanzamine J (**18**) (*17*), and 6-deoxy-manzamine X (**19**) (*19*). Panzamines A (**1**) and F (**6**) were independently isolated almost at the same time and named as kerampamine-A and B (**6**), respectively. The incorrect structural assignment of kerampamine-B (**6a**) was revised quickly to be manzamine F (**6**) (*9*).

Panzamine G (**7**) (*27*) was first described using the name 8-hydroxypanzamine A (*11*), and it was also called manzamine K at a national meeting (34th Annual Meeting of The American Society of Pharmacognosy, July 18–22, 1993, San Diego, CA, Abstract No. P. 46) (*11*). 6-Hydroxypanzamine A (*12*) was named later as manzamine Y (**13**) (*14,27*). The Philippine sponge *Xestospongia* (= *Acanthostrongylophora*) *ashmorica* Hooper is an unusual species, which yielded the following manzamine *N*-oxides (*16*): manzamine A *N*-oxide (**20**), manzamine J *N*-oxide (**21**), and 3,4-dihydropanzamine A *N*-oxide (**22**) (*Fig. 2*).

Panzamine B (**2**) was the first epoxy alkaloid isolated in 1986 (*7,8*), and more than 10 years later the second epoxy 1,2,3,4-tetrahydropanzamine B (**23**) was isolated from a sponge identified as *Amphimedon* sp. (*19*). Ma'eganedin (**24**) is a tetrahydro- $\beta$ -carboline alkaloid with a similar core structure to panzamine B (**2**), but possessing the unusual structural features of a methylene bridge between *N*-2 and *N*-27 and a C-11, C-12 vicinal *cis*-diol (*20*). The unsymmetrical panzamine dimer kauluamine (**25**) (*15*) and the nearly symmetrical panzamine *neo*-kauluamine (**26**) (*18*) were isolated from two species of Indonesian sponges independently. Panzamines H (**8**) and L (**10**) are C-1 isomers, (*10,27*) which were isolated from a single Okinawan species. Moreover, a striking feature of the panzamine series is that the two enantiomers of the  $\beta$ -carboline-containing panzamines, *ent*-8-hydroxypanzamine A (**7a**) (*18*) and *ent*-panzamine F (**6b**) (*18*) were obtained from the same sample collected in Manado, Indonesia. Compounds **7a** and **6b** possess opposite absolute configurations to those of 8-hydroxy panzamine A (panzamine G) and F. The  $\beta$ -carboline alkaloid kerampamine C (**3a**) (*22,27*), regarded as the precursor of panzamine C (**3**), was isolated from the Okinawan sponge *Amphimedon* sp. Two  $\beta$ -carboline alkaloids xestopanamines A (**27**) and B (**28**) (*14*) were identified from another Okinawan panzamine sponge *Xestospongia* sp. Hyrtiopanzamine (**29**) is structurally very similar to xestopanamine A (**27**), and was isolated from the phylogenetically distant Red Sea sponge *Hyrtios erecta* (*21*).

Panzamine A (**1**) was first isolated as the major constituent from a sponge identified as belonging to the genus *Haliclona* (*1*). Subsequent studies with this same species have led to the isolation of the minor constituents panzamine B (**2**), C (**3**), and D (**4**) (*7,8*). The cytotoxic extract was purified over Si gel by successive elution with chloroform and acetone. The acetone eluate gave panzamine A hydrochloride

(**1a**, 100 mg) as colorless crystals after recrystallization from methanol: mp > 240°C dec,  $[\alpha]_D^{20} +50^\circ$  (*c* 0.28, CHCl<sub>3</sub>) (*1*). Almost at the same time, the brownish Okinawan marine sponge *Pellina* sp. was collected at the Kerama Islands. The chloroform soluble part of the 80% ethanol portion was chromatographed twice on Sephadex LH-20 columns (chloroform–methanol 1 : 1 and ethanol), followed by Si gel column chromatography (chloroform–methanol 98 : 2) to give pure manzamine A (called keramamine-A in the publication) hydrochloride (**1a**) (0.026% from wet sponge) (*6*).

Manzamine E (**5**) and F (**6**) were isolated from an Okinawan *Xestospongia* sp. (*9*). Both **5** and **6** possess a ketonic carbonyl group in the eight-membered ring portion of the molecule. Manzamine F was found earlier from a sponge, *Pellina* sp., and named as keramamine B with an incorrectly assigned 1,2,3-triazacyclohexane moiety (*6*). Later, the unusual structure of keramamine B (**6a**) was revised as **6** (*9*). A sample (6 kg) of *Xestospongia* sp. was extracted by steeping in methanol. Purification of the fractions containing alkaloids by HPLC (LiChrosorb–NH<sub>2</sub>, CHCl<sub>3</sub>–MeOH 30 : 1) gave the free bases of manzamine E (**5**, 31 mg) and F (**6**, 111 mg) (*9*).

8-Hydroxymanzamine A (**7**, also called manzamine G or K) was isolated from an Indonesian sponge thought to be an undescribed species of *Pachypellina* by Ichiba *et al.* (*11*). The CH<sub>2</sub>Cl<sub>2</sub>-soluble fraction (320 mg) was separated by high-speed countercurrent chromatography with a solvent system of hexane–MeCN–CH<sub>2</sub>Cl<sub>2</sub> (10 : 7 : 3, lower mobile phase) providing semi-pure 8-hydroxymanzamine A, which could be further purified by recrystallization from CH<sub>2</sub>Cl<sub>2</sub>/MeOH to furnish pure 8-hydroxymanzamine A (0.3%, based on dry weight) (*11*). This sponge was recently confirmed by MK to be in the genus *Acanthostrongylophora* Hooper.

Manzamines H (**8**) and J (**9**) were isolated from the Okinawan sponge *Ircinia* sp. (*10*). From this sponge, ircinals A (**35**) and B (**36**), two plausible biogenetic precursors of the manzamine alkaloids were also isolated. The sponge *Ircinia* sp. was collected off Kise Island, Okinawa, and kept frozen until processing. The methanol extract of the sponge was partitioned between ethyl acetate and water. The ethyl acetate soluble material was subjected to silica gel chromatography (hexane/acetone 4 : 1, CHCl<sub>3</sub>/MeOH 95 : 5, and hexane/acetone 9 : 1) to afford manzamines H (**8**, 0.0007% wet weight of the sponge) and J (**9**, 0.0022%) and ircinals A (**35**, 0.0057%) and B (**36**, 0.0020%) (*10*).

Manzamine M (**11**, 0.0015% wet weight), 3,4-dihydro-6-hydroxymanzamine A (**17**, 0.0015%), and 3,4-dihydromanzamine J (**18**, 0.0004%) were isolated from the sponge *Amphimedon* sp. collected off the Kerama Islands (*17*). Manzamine M (**11**) is the first manzamine congener with a hydroxyl group on the C-13–C-20 chain. 6-Hydroxymanzamine A (**13**) and 3,4-dihydromanzamine A (**14**) were obtained from another Okinawan sponge *Amphimedon* sp. (*12*). The sponge (1.5 kg) *Amphimedon* sp. was collected from Okinawa and kept frozen until extracted with MeOH and then evaporated under reduced pressure to give 68.4 g of extract.

A fraction eluting from Si gel with  $\text{CHCl}_3/\text{MeOH}$  (95 : 5) was further purified with a Si gel column (cyclohexane– $\text{Me}_2\text{CO}$ – $\text{Et}_2\text{NH}$ , 70 : 30 : 2) to give manzamine Y, also called 6-hydroxymanzamine A (**13**, 0.005%, wet weight). The fraction eluting with  $\text{CHCl}_3/\text{MeOH}$  (98 : 2) was separated over a Si gel column ( $\text{C}_6\text{H}_6$ – $\text{Me}_2\text{CO}$ – $\text{Et}_2\text{NH}$ , 95 : 5 : 2) to afford 3,4-dihydromanzamine A (**14**, 0.002%) (**12**).

8-Hydroxy-1,2,3,4-tetrahydromanzamine A (**15**) and its *N*-methylated derivatives 8-hydroxy-2-*N*-methyl-1,2,3,4-tetrahydromanzamine A (**16**) were isolated from sponges of the genus *Petrosia* (**13**). The sponge *P. contignata* was preserved immediately after collection by immersion in an alcohol:H<sub>2</sub>O (1 : 1) solution. After approximately 24 h this solution was decanted and discarded. The damp organisms were placed in Nalgene™ bottles and shipped at ambient temperature. Final purification by HPLC (normal phase, hexane:EtOAc 1 : 1) provided 40 mg of 8-hydroxy-1,2,3,4-tetrahydromanzamine A (**15**) and 35 mg of 8-hydroxy-2-*N*-methyl-1,2,3,4-tetrahydromanzamine A (**16**). At the same time, compound **16** was also isolated from a *Cribrochalina* sp. (**13**). The manzamine-containing fractions were combined and further resolved with HPLC using a Si gel column and acetone:hexane (1 : 4). A less polar fraction was rechromatographed on Si gel HPLC (acetone:hexane 1 : 5) to give 50 mg of 8-hydroxy-2-*N*-methyl-1,2,3,4-tetrahydromanzamine A (**16**) (**13**).

Manzamine X (**12**) and the  $\beta$ -carboline alkaloids xestomanzamine A (**27**) and B (**28**) were isolated from an Okinawan marine sponge *Xestospongia* sp. (**14**). This sponge was collected in the shallow water (–2 m) off Amitori Bay, Okinawa. 6-Deoxymanzamine X (**19**) and the *N*-oxides of manzamine J (**20–22**) have been isolated from the Philippine sponge *Xestospongia* (= *Acanthostrongylophora ashmorica*) (Hooper), which was collected off the shores of Mindoro Island (**16**). The samples were freeze-dried prior to transport and extraction. The *n*-BuOH-soluble material was subjected to Si gel column chromatography, and seven major fractions were obtained. The first fraction yielded 6-deoxymanzamine X (**19**) together with manzamine J (**9**), and 6-deoxy-manzamine X (**19**) was obtained from the methanolic supernatant upon precipitation of manzamine J (**9**) at 5 °C for 24 h. The final three polar fractions yielded the manzamine *N*-oxides (**20–22**). The presence of manzamine *N*-oxides was evident in an HPLC chromatogram of the crude extract, indicating that these alkaloids are present as natural products and not as oxidation artifacts formed during isolation. The three *N*-oxides (**20–22**) were more polar and lack the characteristic fluorescence on Si 60 TLC plates when compared with their parent alkaloids (365 nm). In all cases, the mass spectral data of the *N*-oxides indicate that the molecular weight is 16 mass units higher than that expected after analysis of the NMR spectra. For each of the *N*-oxides, the 1D and 2D NMR spectra allowed signal assignments that readily confirm the chemical shift changes found in the aromatic system. These differences between the shifts of the *N*-oxides compared with those of their parent compounds appear to be characteristic, with large upfield shifts for aromatic carbons in the *ortho* and *para* positions to the substituent, caused by mesomeric redistribution of electron density and downfield shifts for directly bound  $\text{sp}^3$  carbon atoms. The decisive experiment for ascertaining

the *N*-oxide character of the  $\beta$ -carboline moiety was its reduction with zinc dust and 1 N HCl, which is a specific reducing agent for the conversion of an *N*-oxide to its corresponding tertiary base (16).

Manzamine L (10, 0.0056% wet weight,  $[\alpha]_D^{24} - 15^\circ$ ) together with the known manzamines A (1), B (2), C (3), D (4), G (7), H (8), Y (13), and 3,4-dihydromanzamine A (14) were isolated from *Amphimedon* sp. collected off Kerama Islands, Okinawa (27). From this sponge, keramamine C (3a), ircinals A (35) and B (36), ircinols A (37) and B (38), keramaphidins B (40) and C (30) were also isolated.

Both enantiomers of keramaphidin B were separated by using chiral HPLC (27), of which one may be a plausible biogenetic precursor for both ircinals as well as manzamines A and B, while the other may be associated with the antipodes of the manzamine alkaloids, such as ircinols A and B. Ircinols A (37) and B (38), are the first reported antipodes of manzamine-related alkaloids and were isolated from an Okinawan sponge *Amphimedon* sp. collected off the Kerama Islands, Okinawa (25). The structures were determined to be enantiomers of the alcoholic forms at C-1 of ircinals A (35) and B (36) (10), respectively. Treatment of ircinal A (35), which was isolated from this sponge, with DIBALH afforded a reduced product, the spectral data of which were identical with those of ircinol A except for the optical rotation [reduction product of ircinal A,  $[\alpha]_D^{18} + 20^\circ$  (*c* 0.2, MeOH); ircinol A,  $[\alpha]_D^{18} - 19^\circ$  (*c* 0.5, MeOH)]. This result revealed that ircinol A was an enantiomer of the alcoholic derivative of ircinal A which has been shown to have the same absolute configuration as that of manzamine A. Manzamines A ( $[\alpha]_D^{20} + 46^\circ$ ) and B ( $[\alpha]_D^{20} + 93^\circ$ ) and ircinals A ( $[\alpha]_D^{15} + 42^\circ$ ) and B ( $[\alpha]_D^{15} + 15^\circ$ ) isolated from this sponge had the same absolute configurations as those reported previously (25,27).

Manzamines H (8) and L (10) were isolated from the same sponge, and both were shown to have the same 2D structure with a significant difference in the  $^{13}\text{C}$  NMR chemical shift of C-1 (8: 59.9 ppm, 10: 56.1 ppm,  $\text{CDCl}_3$ ). The absolute configuration of C-1 of manzamine L (10) was deduced to be *1S* from a negative Cotton effect, while 8 showed the opposite sign implying the *1R*-configuration. At the same time, manzamine D (4) was also isolated from this sponge, and showed a *1R*-configuration as per a positive Cotton effect (27).

Dimeric manzamines: kauluamine (25) is the first report of a manzamine dimer, adding yet another level of complexity to the manzamine-type of alkaloids. Kauluamine was isolated by Scheuer's group from an Indonesian sponge originally identified as *Prianos* sp. collected in Manado Bay, Indonesia (15). The fact that just a single bond holds two of these complex polycyclic systems together gives the molecule kauluamine the unusual appearance of being fragile. This sponge was also recently identified as a species of *Acanthostrongylophora* Hooper. The second unprecedented manzamine dimer isolated by Hamann's group was named *neo*-kauluamine (26) and was isolated from what was originally identified as an undescribed petrosid genus, together with the new enantiomers



of 8-hydroxymanzamine A (*ent*-8-hydroxymanzamine A, **7a**) and manzamine F (*ent*-manzamine F, **6b**) (18). *neo*-Kauluamine was also isolated from a sponge collected in Manado Bay, Indonesia as kauluamine. The relative stereochemistry of the nearly symmetric manzamine dimer *neo*-kauluamine (**26**) was established through a detailed analysis of the NOE-correlations combined with molecular modeling, while the enantiomers were elucidated through NOE measurements combined with optical rotation values (18). The undescribed petrosid genus is now known to conform to our understanding of the genus *Acanthostrongylophora* (63).

## B. MANZAMINE-RELATED MARINE ALKALOIDS

Keramaphidin C (**30**) was isolated from *Amphimedon* sp. (22). Haliclorensins (**31**) was isolated from *Haliclona* sp. collected off Sodwana Bay, South Africa (23). Motuporamines A (**32**), B (**33**) and C (**34**) were isolated as an inseparable mixture from *Xestospongia exigua* collected in Papua New Guinea (24). Ircinals A (**35**) and B (**36**), two plausible biogenetic precursors of the manzamine alkaloids, were isolated from the Okinawan sponge *Ircinia* sp. (10). The antipodes of the manzamine-related alkaloids ircinols A (**37**) and B (**38**) were obtained from another Okinawan sponge *Amphimedon* sp., together with keramaphidins B (**39**) and C (**30**) (22,25–27). Ircinols A and B were determined to be enantiomers of the C-1 alcoholic forms of ircinals A and B, respectively. Xestocyclamine A (**40**) was first isolated from the Papua New Guinea marine sponge *Xestospongia* (= *Acanthostrongylophora*) *ingens*, and its structure was revised in the following year with the isolation of xestocyclamine B (**41**) (28,29). Ingamines A (**42**) and B (**43**) (30), ingenamine (**44**) (31), ingenamines B (**45**), C (**46**), D (**47**), E (**48**) and F (**49**) (32) were also isolated from the Papua New Guinea marine sponge *Xestospongia* (= *A.*) *ingens* (Fig. 3).

Madangamine A (**50**) was isolated from *Xestospongia* sp. collected off Madang, Papua New Guinea (33,34), and later madangamines B (**51**), C (**52**), D (**53**), and E (**54**) were also obtained from this same sponge (35). Misenine (**55**), a polycyclic ‘cage-like’ alkaloid, was isolated from an unidentified Mediterranean species *Reniera* sp. (36). The <sup>1</sup>H-NMR spectrum of this unusual alkaloid showed significant variations with pH and it was concluded that the dominant species in neutral and basic solutions was **55a** whereas under acidic conditions the structure **55b** was preferred. A similar transannular N/C=O “proximity effect” had previously been observed in saraine A (**55c**) although, in this case, a lowering of pH enhanced the C–N linkage (53). Nakadomarin A (**56**) was isolated from *Amphimedon* sp., and its structure was reported to contain an unprecedented 8/5/5/5/15/6 ring system (57).

## C. RECENTLY ISOLATED $\beta$ -CARBOLINE-CONTAINING MANZAMINE ALKALOIDS

Recently, a number of Indo-Pacific sponges have yielded a novel class of manzamines, named 12,34-oxamanzamines (58). These alkaloids possess a novel

ring system generated through a new ether bridge formed between carbons 12 and 34 of the typical manzamine structure. *ent*-12,34-Oxamanzamines E (**57**) and F (**58**), as well as 12,34-oxamanzamine A (**59**), were obtained from three Indo-Pacific sponges. The biocatalytic transformation of *ent*-8-hydroxymanzamine A (**7a**) to **58**, using *Nocardia* sp. ATCC 21145 and *Fusarium oxysporium* ATCC 7601, has also been achieved, suggesting that these alkaloids maybe formed through biocatalysis by a sponge-associated microbe. In fact, the *epi*-isomers such as manzamines H (**8**, *1R* configuration) and L (**10**, *1S* configuration) were isolated from different sponges, but at the same time the sponge samples also yielded a series of manzamine-related compounds with *1R* and/or *1S* configuration. In 2000, Kingston's group reported two new *epi*-manzamines (**60**, **61**) (*61*). These two new  $\beta$ -carboline containing manzamines were isolated from a Palauan sponge, and both *epi*-manzamine D (**60**) and 2-*N*-methyl-*epi*-manzamine D (**61**) possess negative optical rotation values. Most recently, two unprecedented manzamine-related alkaloids called manadomanzamines A (**62**) and B (**63**) have been reported from an unidentified Indonesian sponge (*59*). Manadomanzamines A and B represent an unprecedented rearrangement of the manzamine skeleton. In addition three new  $\beta$ -carboline containing manzamines: 32,33-dihydro-31-hydroxymanzamine A (**64**), 32,33-dihydro-6,31-dihydroxymanzamine A (**65**), and 32,33-dihydro-6-hydroxymanzamine A-35-one (**66**) have recently been reported (*60*). Based on biogenetic considerations, compounds **64** and **65** are likely the reduced derivatives of manzamine E. Alkaloid **66** is unique in that it possesses a ketone moiety at C-35, instead of a typical C-31 ketone as seen in manzamine E and F (Fig. 4).

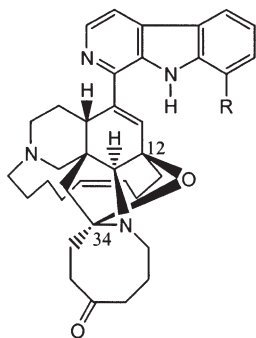
#### D. PHYSICAL AND SPECTRAL PROPERTIES

The physico-chemical properties of the manzamines are shown in Table II. Manzamines are solid powders or crystals, and most show strong UV absorption due to the  $\beta$ -carboline moiety. The majority of the manzamine alkaloids possess a positive optical rotation, except for *ent*-manzamine F (**6b**), *ent*-8-hydroxymanzamine A (**7a**), manzamine L (**10**), ircinols A (**37**) and B (**38**), *epi*-manzamine D (**60**), and 2-*N*-methyl-*epi*-manzamine D (**61**). The structures were completed by spectroscopic methods such as HR-MS, high-field 2D NMR, and X-ray diffraction analysis. The  $^{13}\text{C}$ - and  $^1\text{H}$ -NMR spectral data were recorded primarily in  $\text{CDCl}_3$ , and their data are shown in Tables III and IV, respectively.

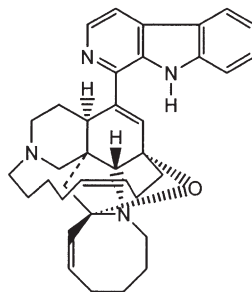
### III. Biogenesis and Biosynthesis

#### A. BIOGENETIC PATHWAYS

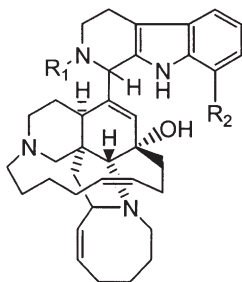
Since the first representative, manzamine A (**1**) with a fused and bridged pentacyclic ring system joined to a  $\beta$ -carboline moiety, was isolated in 1986, the manzamines have been regarded as an intriguing group of marine alkaloids (*2-4*), which have provoked a great interest in their unprecedented biosynthetic pathway. In 1992 Baldwin *et al.* (*5*) proposed a biogenetic pathway with an intramolecular Diels-Alder reaction for manzamines A (**1**) and B (**2**).



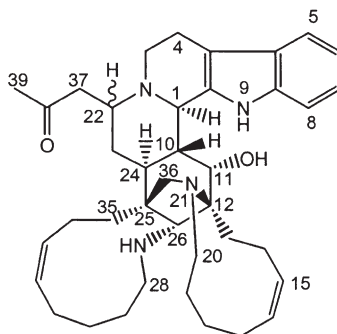
*ent*-12,34-oxamanzamine E (**57**): R = H  
*ent*-12,34-oxamanzamine F (**58**): R = OH



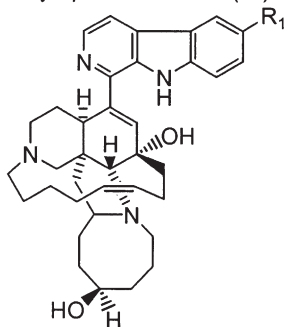
12,34-oxamanzamine A (**59**)



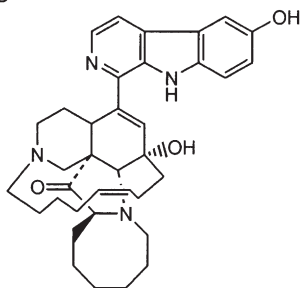
manzamine D (**4**): R<sup>1</sup> = R<sup>2</sup> = H, 1*R*  
*epi*-manzamine D (**60**): R<sup>1</sup> = R<sup>2</sup> = H, 1*S*  
*N*-methyl-*epi*-manzamine D (**61**): R<sup>1</sup> = Me, R<sup>2</sup> = H, 1*S*



manadomanzamine A (**62**): 22β-H  
 manadomanzamine B (**63**): 22α-H



32,33-dihydro-31-hydroxymanzamine A (**64**): R<sup>1</sup> = H  
 32,33-dihydro-6,31-dihydroxymanzamine A (**65**): R<sup>1</sup> = OH



32,33-dihydro-6-hydroxymanzamine A (**66**)

Figure 4. Recently isolated β-carboline manzamine alkaloids.

TABLE II.  
Physico-chemical Properties of Manzamine Alkaloids.

Alkaloids <b>1</b> , <b>2</b> , <b>3</b> , <b>3a</b> and <b>4</b>	<b>1</b> ( <i>1,9</i> ) <sup>a</sup>	<b>2</b> ( <b>8</b> )	<b>3</b> ( <b>8</b> )	<b>3a</b> ( <b>22</b> )	<b>4</b> ( <b>7</b> )
Appearance	Colorless powder	Colorless crystals (EtOAc)	Colorless plates (CHCl <sub>3</sub> -CH <sub>3</sub> CN)	Colorless oil	Colorless powder
Molecular formula	C <sub>36</sub> H <sub>44</sub> N <sub>4</sub> O	C <sub>36</sub> H <sub>46</sub> N <sub>4</sub> O	C <sub>23</sub> H <sub>29</sub> N <sub>3</sub>	C <sub>23</sub> H <sub>33</sub> N <sub>3</sub>	C <sub>36</sub> H <sub>48</sub> N <sub>4</sub> O
HR-MS <i>m/z</i>	548.3510 <sup>a</sup> (Δ 0.5 mmu) (HREIMS)			351.2687 (Δ 1.3 mmu) (HREIMS)	552.3837 (Δ 0.9 mmu) (HREIMS)
MP (°C)	> 200 (dec.)	198–203	77–82		165–168
[α] <sub>D</sub>	+ 44.3° ( <i>c</i> 1.09, CHCl <sub>3</sub> )	+ 89° ( <i>c</i> 1.8, CHCl <sub>3</sub> )		+ 20° ( <i>c</i> 0.92, MeOH)	+ 60.6° ( <i>c</i> 0.66, CHCl <sub>3</sub> )
UV λ <sub>max</sub> (MeOH) nm (ε)	219 (22900), 236 (18600), 280 (10800), 290 (sh, 9800), 346 (5300), 357 (5600)	212 (18000), 235 (22000), 240 (sh, 20000), 250 (sh, 15000), 282 (sh, 6900), 288 (11000), 338 (3500), 351 (3500)	212 (13500), 234 (22000), 239 (sh, 21000), 248 (sh, 14000), 282 (sh, 6100), 287 (9500), 335 (3000), 349 (3000)	225 (sh), 271 (5600) 285 (sh), 290 (sh)	223 (28800), 275 (sh, 6300), 281 (6700), 288 (5400)
IR ν <sub>max</sub> (KBr) cm <sup>-1</sup>	3280, 3150, 3050, 3000, 2920, 2800, 2760, 2630, 2560, 1617, 1555, 1488, 1448, 1418, 1385, 1370, 1315, 1270, 1230, 1180, 1142, 1110, 1095, 1065, 1025, 820, 740, 725, 700	3340, 3200, 3140, 3060, 3000, 2920, 2845, 1620, 1510, 1495, 1470, 1445, 1420, 1400, 1320, 1275, 1255, 1235, 1210, 1120, 870, 745, 710, 660, 620	3000, 2910, 2840, 2810, 1640, 1495, 1465, 1440, 1425, 1350, 1335, 1320, 1290, 1230, 1215, 1200, 1120, 740, 715, 660	3400, 2940	3460, 3000, 2920, 1450, 1440, 1365, 1340, 1290, 1240, 1210, 1145, 1105, 1070, 995, 970

(continued)

TABLE II.  
Continued.

Alkaloids <b>5</b> , <b>6</b> , <b>6b</b> , <b>7</b> and <b>7a</b>	<b>5</b> ( <i>9</i> )	<b>6</b> ( <i>9</i> )	<b>6b</b> ( <i>18</i> )	<b>7</b> ( <i>11</i> )	<b>7a</b> ( <i>18</i> )
Appearance	Colorless crystals (CH <sub>3</sub> CN)	Colorless crystals (CH <sub>3</sub> CN)	Yellowish powder	Pale yellow crystals, (CH <sub>2</sub> Cl <sub>2</sub> /MeOH)	Yellowish powder
Molecular formula	C <sub>36</sub> H <sub>44</sub> N <sub>4</sub> O <sub>2</sub>	C <sub>36</sub> H <sub>44</sub> N <sub>4</sub> O <sub>3</sub>	C <sub>36</sub> H <sub>44</sub> N <sub>4</sub> O <sub>3</sub>	C <sub>36</sub> H <sub>44</sub> N <sub>4</sub> O <sub>2</sub>	C <sub>36</sub> H <sub>44</sub> N <sub>4</sub> O <sub>2</sub>
HR-MS <i>m/z</i>	565.3555 (M <sup>+</sup> +H, Δ 1.2 mmu) (HRFABMS)	581.3496 (M <sup>+</sup> + H, Δ 0.4 mmu) (HRFABMS)	581.3434 (Δ -5.8 mmu) [M+H] <sup>+</sup> (HRESIMS)	565.3507 (M <sup>+</sup> +H, Δ 1.8 mmu) (HRFABMS)	565.3433 (Δ -11.0 mmu) [M+H] <sup>+</sup> (HRESIMS)
MP (°C)	174–176	> 200 (dec.)	194 (dec)	> 230 (dec)	196–198 (dec)
[α] <sub>D</sub>	+ 63.7° ( <i>c</i> 2.51, CHCl <sub>3</sub> )	+ 59.9° ( <i>c</i> 0.67, CHCl <sub>3</sub> )	- 44.6° ( <i>c</i> 0.11, CHCl <sub>3</sub> )	+ 118.5° ( <i>c</i> 1.94, CHCl <sub>3</sub> )	- 112.0° ( <i>c</i> 0.12, CHCl <sub>3</sub> )
UV λ <sub>max</sub> (MeOH) nm ( <i>ε</i> )	220 (35800), 237 (28100), 279 (18000), 290 (sh, 15300), 346 (8700), 359 (9300)	220 (36000), 244 (31000), 265 (13900), 3559 (8100)	266 (3.04), 300 (3.02), 380 (2.92)	206 (sh, 22700), 222 (32300), 245 (30600), 268 (14000), 360 (8100)	266 (2.95), 282 (2.94), 390 (2.85)
IR ν <sub>max</sub> (KBr) cm <sup>-1</sup>	3400 (br), 3050, 3010, 2940, 2850, 2800, 1700, 1625, 1560, 1495, 1465, 1455, 1420, 1370, 1350, 1320, 1270, 1230, 1150, 1110, 1065, 1020, 820, 785, 740	3400, 3060, 3020, 2950, 2860, 2810, 1695, 1595, 1570, 1465, 1445, 1420, 1375, 1350, 1335, 1275, 1245, 1230, 1115, 1075, 790, 780, 740	3498–3260, 3026–2802, 1699, 1670, 1564, 1446, 1221	3280, 2900, 1570, 1540, 1420, 1410, 1330, 1260, 1230, 1220, 1200, 1055, 1035, 1010, 970, 940, 745, 720	3499–3267, 3017–2807, 1680, 1563, 1446, 1220

Compounds 8–12	8 (10,27)	9 (10)	10 (27)	11 (17)	12 (14)
Appearance	Colorless solid	Colorless amorphous solid		Colorless amorphous solid	Yellow prisms ( <i>n</i> -hexane–acetone)
Molecular formula	C <sub>36</sub> H <sub>50</sub> N <sub>4</sub> O	C <sub>36</sub> H <sub>46</sub> N <sub>4</sub> O	C <sub>36</sub> H <sub>50</sub> N <sub>4</sub> O	C <sub>36</sub> H <sub>44</sub> N <sub>4</sub> O <sub>2</sub>	C <sub>36</sub> H <sub>44</sub> N <sub>4</sub> O <sub>3</sub>
HR-MS <i>m/z</i>	554.3980 (Δ −0.5 mmu) (HREIMS)	550.3660 (Δ −1.2 mmu) (HREIMS)	554.3975 (M <sup>+</sup> , Δ −0.9 mmu) (HREIMS)	564.3459 (Δ −0.5 mmu) (HREIMS)	581.3470 [M+H] <sup>+</sup> (Δ −2.0 mmu) (HRFABMS)
MP (°C)	145	140	143		> 250
[α] <sub>D</sub>	+17° ( <i>c</i> 1.1, CHCl <sub>3</sub> )	+47° ( <i>c</i> 2.0, CHCl <sub>3</sub> )	−15° ( <i>c</i> 0.42, CHCl <sub>3</sub> )	+16° ( <i>c</i> 0.48, MeOH)	+ 66.1° ( <i>c</i> 1.93, CHCl <sub>3</sub> )
UV λ <sub>max</sub> (MeOH) nm (ε)	225 (29000), 277 (6600), 282 (6800), 290 (5500)	218 (26000), 236 (21000), 280 (11000), 290 (11000), 348 (5500), 356 (5600)	223 (34000), 283 (6400)	205 (14000), 233 (3000), 276 (1500), 359 (1000)	215 (29500), 300 (17000), 378 (4800)
IR ν <sub>max</sub> (KBr) cm <sup>−1</sup>	3400, 3300, 2990, 2910, 2850, 2780, 1650, 1450, 1360, 1340, 1290, 1260, 1210, 1110, 1070, 1035, 1000, 910	3400, 3220, 2990, 2920, 2850, 2790, 1620, 1560, 1490, 1450, 1420, 1320, 1280, 1230, 1110, 1070, 1040	3400, 2900	3410 (br), 2925, 1630, 1405, 1070	3290, 2930, 1640, 1562, 1462
CD (MeOH) λ <sub>ext</sub> (Δε) nm			202 (+13.6), 222 (−10.8), 270 (+4.2)		

(continued)

TABLE II.  
Continued.

Compounds <b>13–16</b>	<b>13</b> ( <i>12</i> ) <sup>b</sup>	<b>13'</b> ( <i>14</i> ) <sup>b</sup>	<b>14</b> ( <i>12</i> )	<b>15</b> ( <i>13</i> )	<b>16</b> ( <i>13</i> )
Appearance	Yellowish amorphous solids	Yellow solid ( <i>n</i> -hexane–acetone)	Colorless amorphous solids		White powder
Molecular formula	C <sub>36</sub> H <sub>44</sub> N <sub>4</sub> O <sub>2</sub>	C <sub>36</sub> H <sub>44</sub> N <sub>4</sub> O <sub>2</sub>	C <sub>36</sub> H <sub>46</sub> N <sub>4</sub> O	C <sub>36</sub> H <sub>48</sub> N <sub>4</sub> O <sub>2</sub>	C <sub>37</sub> H <sub>50</sub> N <sub>4</sub> O <sub>2</sub>
HR-MS <i>m/z</i>	564.3465 (M <sup>+</sup> , Δ –1.8 mmu) (HREIMS)	565.3530 [M+H] <sup>+</sup> (Δ –1.0 mmu) (HRFABMS)	550.3653 (Δ –1.9 mmu)	569.3832 [M+H] <sup>+</sup> (Δ 2.3 mmu) (HRFABMS)	583.4025 [M+H] <sup>+</sup> (Δ –1.3 mmu) (HREIMS)
MP (°C)	253	> 250	237–241		
[α] <sub>D</sub>	+139° ( <i>c</i> 1.10, MeOH)	+33° ( <i>c</i> 2.50, CHCl <sub>3</sub> )	+86° ( <i>c</i> 0.25, CHCl <sub>3</sub> )		+5° ( <i>c</i> 0.03, CH <sub>2</sub> Cl <sub>2</sub> )
UV λ <sub>max</sub> (MeOH) nm (ε)	210 (32000), 293 (sh, 15000), 300 (16000), 370 (5100)	215 (29500), 300 (11000), 378 (3000)	230 (sh, 25000), 244 (21000), 323 (10000)		240, 270, 326, 370
IR ν <sub>max</sub> (KBr) cm <sup>-1</sup>	3300, 2920, 1450	3228, 2930, 1670, 1562, 1462, 1200	3280, 2940, 1470, 1450		3005, 2935, 2847, 1648, 1627, 1578

Compounds 17–22	17 (17)	18 (17)	19 (16)	20 (16)	21 (16)	22 (16)
Appearance	Colorless amorphous solid	Colorless amorphous solid	Pale yellow amorphous powder	Yellow crystalline powder	Yellow crystalline powder	Yellow crystalline powder
Molecular formula	C <sub>36</sub> H <sub>46</sub> N <sub>4</sub> O <sub>2</sub>	C <sub>36</sub> H <sub>48</sub> N <sub>4</sub> O	C <sub>36</sub> H <sub>44</sub> N <sub>4</sub> O <sub>2</sub>	C <sub>36</sub> H <sub>44</sub> N <sub>4</sub> O <sub>2</sub>	C <sub>36</sub> H <sub>46</sub> N <sub>4</sub> O <sub>2</sub>	C <sub>36</sub> H <sub>46</sub> N <sub>4</sub> O <sub>2</sub>
HR-MS <i>m/z</i>	566.3604 ( $\Delta$ -1.7 mmu) (HREIMS)	552.3815 ( $\Delta$ -1.4 mmu) (HREIMS)	565 [M+H] <sup>+</sup> (FABMS)	565 [M+H] <sup>+</sup> (FABMS)	567 [M+H] <sup>+</sup> (FABMS)	567 [M+H] <sup>+</sup> (FABMS)
MP (°C)	140					
[ $\alpha$ ] <sub>D</sub>	+ 28.0° ( <i>c</i> 1.2, MeOH)	+ 50.0° ( <i>c</i> 0.10, MeOH)	+ 30.1° ( <i>c</i> 0.35, CHCl <sub>3</sub> )	+ 18.6° ( <i>c</i> 0.35, CHCl <sub>3</sub> )	+ 15.0° ( <i>c</i> 0.40, CHCl <sub>3</sub> )	+ 34.1° ( <i>c</i> 0.59, CHCl <sub>3</sub> )
UV $\lambda_{\max}$ (MeOH)	207 (9000), 225 (6500),	209 (13000), 242 (9000),	210 (26000), 260 (11800),	201 (26000), 241 (23000),	261 (25000), 325 (19000)	201 (25000), 355 (11000)
nm ( $\epsilon$ )	250 (3500), 337 (2500)	322 (4500)	312 (sh, 10000), 378 (3000)	261 (23000), 310 (21000)		
IR $\nu_{\max}$ (KBr) cm <sup>-1</sup>	3420 (br), 2920, 1630, 1400, 1070	3420 (br), 2920, 1630, 1090				

(continued)



TABLE II.  
 Continued.

Compounds <b>25–28, 35</b>	<b>25 (15)</b>	<b>26 (18)</b>	<b>27 (14)</b>	<b>28 (14)</b>	<b>35 (10)</b>
Appearance	Unstable pale yellow solid	Colorless needles	Yellow needles (CHCl <sub>3</sub> –MeOH)	Yellow oil	Colorless solid
Molecular formula	C <sub>72</sub> H <sub>94</sub> N <sub>8</sub> O <sub>3</sub>	C <sub>72</sub> H <sub>88</sub> N <sub>8</sub> O <sub>6</sub>	C <sub>16</sub> H <sub>12</sub> N <sub>4</sub> O	C <sub>16</sub> H <sub>14</sub> N <sub>4</sub> O	C <sub>26</sub> H <sub>38</sub> N <sub>2</sub> O <sub>2</sub>
HR–MS <i>m/z</i>	1101.7426 (Δ –0.4 mmu) for C <sub>72</sub> H <sub>93</sub> N <sub>8</sub> O <sub>2</sub> [MH–H <sub>2</sub> O] <sup>+</sup> (HRFABMS)	1161.6905 (Δ –5.1 mmu) for C <sub>72</sub> H <sub>89</sub> N <sub>8</sub> O <sub>6</sub> [M+H] <sup>+</sup> (HRFABMS)	277.1100 [M+H] <sup>+</sup> (Δ –4.0 mmu) (HRFABMS)	279.1250 [M+H] <sup>+</sup> (Δ 0 mmu) (HRFABMS)	410.2924 [M] <sup>+</sup> (Δ –0.9 mmu) (HREIMS)
MP (°C)		184	185–186		70
[α] <sub>D</sub>	+ 0.7° ( <i>c</i> 0.18, CHCl <sub>3</sub> )	+ 94.6° ( <i>c</i> 0.1, CHCl <sub>3</sub> )			+ 48.0° ( <i>c</i> 2.9, CHCl <sub>3</sub> )
UV λ <sub>max</sub> (MeOH) nm (ε)		252 (4.20), 357 (3.85)	221 (7400), 257 (1700), 300 (3900), 395 (1600)	222 (27200), 270 (10300), 298 (16500), 388 (4500)	231 (8500)
IR ν <sub>max</sub> (KBr) cm <sup>–1</sup>	3380, 3150, 2990, 2900, 2840, 1645, 1620, 1450, 1440, 1320, 1235, 1150	3592, 3475–3250 (br), 3007–2802, 1626, 1560, 1454, 1215	3427, 3075, 1612, 1211, 1128	3451, 3110, 2926, 1641, 1190, 1130	3420, 2950, 2920, 2850, 2790, 1680, 1670, 1560, 1450, 1400, 1200, 1150, 1100, 1070, 730

Compounds <b>30</b> , <b>36–39</b>					
	<b>30 (22)</b>	<b>36 (10)</b>	<b>37 (25)</b>	<b>38 (25)</b>	<b>39 (26,27)</b>
Appearance	colorless amorphous solid	colorless solid	colorless amorphous solid	colorless amorphous solid	colorless needle
Molecular formula	C <sub>10</sub> H <sub>19</sub> N	C <sub>26</sub> H <sub>40</sub> N <sub>2</sub> O <sub>2</sub>	C <sub>26</sub> H <sub>40</sub> N <sub>2</sub> O <sub>2</sub>	C <sub>26</sub> H <sub>42</sub> N <sub>2</sub> O <sub>2</sub>	C <sub>26</sub> H <sub>40</sub> N <sub>2</sub>
HR–MS m/z	153.1493 [M] <sup>+</sup> (Δ –2.4 mmu) (HRFABMS)	412.3118 [M] <sup>+</sup> (Δ +2.9 mmu) (HREIMS)	412.3107 [M] <sup>+</sup> (Δ +1.7 mmu) (HREIMS)	414.3248 [M] <sup>+</sup> (Δ +0.2 mmu) (HREIMS)	380.3199 [M] <sup>+</sup> (Δ +0.8 mmu) (HREIMS)
MP (°C)	106–109	95	83–85	78–79	131–132
[α] <sub>D</sub>	0	+18.0° (c 1.1, CHCl <sub>3</sub> )	–19.0° (c 0.54, MeOH)	–2.8° (c 0.12, MeOH)	+22.2° <sup>c</sup>
UV λ <sub>max</sub> (MeOH) nm (ε)		224 (12000)			
IR ν <sub>max</sub> (KBr) cm <sup>–1</sup>	3400, 2940	3400, 2920, 2850, 2800, 1680, 1450, 1190, 1170, 1120, 1040, 700	3400, 2940	3400, 2940	2940

(continued)

TABLE II.  
Continued.

Compounds <b>57–61</b>	<b>57 (58)</b>	<b>58 (58)</b>	<b>59 (58)</b>	<b>60 (61)</b>	<b>61(61)</b>
Appearance	Brown amorphous solid	Yellowish powder	White powder	Amorphous powder	Orthorhombic crystals
Molecular formula	C <sub>36</sub> H <sub>42</sub> N <sub>4</sub> O <sub>2</sub>	C <sub>36</sub> H <sub>42</sub> N <sub>4</sub> O <sub>3</sub>	C <sub>36</sub> H <sub>42</sub> N <sub>4</sub> O	C <sub>36</sub> H <sub>48</sub> N <sub>4</sub> O	C <sub>37</sub> H <sub>50</sub> N <sub>4</sub> O
HR–MS m/z	563.3386 [M+H] <sup>+</sup> (Δ –3.0 mmu) (HRFABMS)	579.3335 [M+H] <sup>+</sup> (Δ +0.4 mmu) (HRFABMS)	347.3408 [M+H] <sup>+</sup> (Δ –5.0 mmu) (HRFABMS)	552.3830 [M] <sup>+</sup> (Δ +0.2 mmu) (HREIMS)	566.3974 [M] <sup>+</sup> (Δ –1.0 mmu) (HREIMS)
MP (°C)	152	158	164		185–188
[α] <sub>D</sub>	–54.6° (c 0.3, CHCl <sub>3</sub> )	–49.2° (c 0.10, CHCl <sub>3</sub> )	+40.0° (c 0.6, CHCl <sub>3</sub> )	+77.3° (c 0.165, CHCl <sub>3</sub> )	+91.4° (c 0.27, CHCl <sub>3</sub> )
UV λ <sub>max</sub> (MeOH) nm (ε)	252 (3.82) 275 (3.65) 354 (3.41)	251 (3.83) 273 (3.69) 356 (3.42)	252 (3.823) 271 (3.71) 358 (3.41)	225 (4.23) 281 (3.79)	223 (4.24) 281 (3.74)
IR ν <sub>max</sub> (KBr) cm <sup>–1</sup>	3650, 3001–2818, 1714, 1620, 1592, 1533, 1452, 1267, 1144, 1052.	3658, 3377, 3002–2822, 1714, 1620, 1592, 1533, 1452, 1267, 1144, 1052	3635, 3368, 3001–2815, 1715, 1625, 1590, 1535, 1451, 1265, 1145, 1050	3600–3200, 3004, 2931, 1650, 1620, 1454, 1071.	3500–3200, 3004, 2937, 1651, 1616, 1454, 1070, 1060.
CD (MeOH) λ <sub>ext</sub> (Δε) nm				204 (+22.1), 221.5 (–14.3), 226 (sh, –13.7), 269.5 (+11.7), 291.5 (+6.8).	205 (+26.8), 223.5 (–13.7), 229 (sh, –12.2), 271 (+6.3), 295 (+3.4).

Compounds <b>62–66</b>	<b>62 (59)</b>	<b>63 (59)</b>	<b>64 (60)</b>	<b>65 (60)</b>	<b>66 (60)</b>
Appearance	White powder	White powder	Colorless crystals	Pale yellow powder	Pale yellow powder
Molecular formula	C <sub>39</sub> H <sub>54</sub> N <sub>4</sub> O <sub>2</sub>	C <sub>39</sub> H <sub>54</sub> N <sub>4</sub> O <sub>2</sub>	C <sub>36</sub> H <sub>46</sub> N <sub>4</sub> O <sub>2</sub>	C <sub>36</sub> H <sub>46</sub> N <sub>4</sub> O <sub>3</sub>	C <sub>36</sub> H <sub>44</sub> N <sub>4</sub> O <sub>3</sub>
HR–MS <i>m/z</i>	611.4348 [M+H] <sup>+</sup> (Δ +2.9 mmu) (HRESIMS)	611.4310 [M+H] <sup>+</sup> (Δ –0.9 mmu) (HRESIMS)	567.4052 [M+H] <sup>+</sup> (Δ –3.5 mmu) (HRESIMS)	583.3477 [M+H] <sup>+</sup> (Δ –16.6 mmu) (HRESIMS)	581.3467 [M+H] <sup>+</sup> (Δ –2.5 mmu) (HRESIMS) > 200 (dec.)
MP (°C)	–19°	–18°	+ 34.44°	+ 25.9°	+ 10.0°
[α] <sub>D</sub>	( <i>c</i> 0.11, MeOH)	( <i>c</i> 0.11, MeOH)	( <i>c</i> 0.9, CHCl <sub>3</sub> )	( <i>c</i> 0.5, MeOH)	( <i>c</i> 1.0, MeOH)
UV λ <sub>max</sub> (MeOH) nm (ε)	282 (7700)	282 (7200)	215, 248, 281, 291, 352, 359	218, 240, 280, 291, 356, 359	219, 248, 268, 356, 395
IR ν <sub>max</sub> (KBr) cm <sup>–1</sup>	3372, 3002, 2919, 1707, 1468, 1354, 1164, 736	3387, 3001, 2917, 1711, 1460, 1355, 1162, 736	3280, 2954, 2927, 1560, 1493, 1453, 1370, 1276, 1150, 748, 665	3324, 2928, 1649, 1559, 1461, 1194, 675	3324, 2935, 1661, 1559, 1461, 1197, 664
CD (MeOH) λ <sub>ext</sub> (Δε) nm	226 (+ 13.4) 271 (–3.62)	224 (+ 15.9) 269 (–3.68)			

<sup>a</sup>Manzamine A hydrochloride (**1a**): Colorless crystals (MeOH); MP (°C) > 240 °C (dec.); [α]<sub>D</sub><sup>20</sup> + 50° (*c* 0.28, CHCl<sub>3</sub>).

<sup>b</sup>Compound **13** and compound **13'** should have the same structure as manzamine Y (6-hydroxymanzamine A), but the spectral data especially their optical rotations showed great difference between two different reports (*12,14*).

<sup>c</sup>A small amount of crystals of keramaphidin B (**39**) obtained from CH<sub>3</sub>CN or CHCl<sub>3</sub> was racemic (*26*).

TABLE III.  
<sup>13</sup>C-NMR Data of Manzamine-type Alkaloids in CDCl<sub>3</sub>.

Alkaloids 1–8 Atom	1 (9)	2 (8)	3 (8)	3a (22) <sup>a</sup>	4 (7) <sup>b</sup>	5 (9)	6 (9)	7 (11)	8 (10,27)
1	143.6s	146.2s	145.8s	53.9d	60.0d	142.8s	142.5s	143.3s	59.9d
3	137.5d	137.0d	137.4d	42.1t	66.9t	138.4d	137.8d	137.9d	43.2t
4	113.8d	113.7d	113.0d	21.7t	43.6t	113.4d	113.7d	114.7d	22.4t
4a	129.3s	129.2s	128.1s	109.5s	127.7s	129.4s	130.2s	129.8s	109.0s
4b	121.1s	121.1s	121.9s	128.0s	109.4s	121.6s	122.8s	123.2s	127.8s
5	120.9d	121.3d	121.6d	119.0d	119.2d	121.3d	112.0d	112.6d	118.0d
6	119.2d	118.8d	119.0d	120.3d	118.0d	119.9d	120.9d	120.7d	119.3d
7	127.9d	128.8d	127.6d	123.1d	129.8d	128.3d	113.0d	114.3d	121.4d
8	112.8d	111.3d	111.8d	112.2d	111.0d	111.9d	143.4s	143.8s	111.0d
8a	141.4s	140.5s	140.6s	138.1s	141.0s	140.6s	129.9s	130.6s	135.5s
9a	133.3s	134.9s	135.5s	115.9s	133.8s	133.3s	133.2s	132.9s	134.2s
10	141.2s	44.5d	34.7t	27.7t	135.4s	140.3s	140.9s	141.9s	143.9s
11	135.1d	60.2d	52.8t	52.9t	134.5d	138.0d	137.3d	134.6d	130.1d
12	71.3s	60.4s			69.8s	68.4s	69.0s	71.2s	70.1s
13	39.1t	18.6t	48.9t	48.9t	40.9t	40.5t	39.9t	39.2t	40.6t
14	20.6t	22.7t	26.0t	23.0t	21.9t	21.2t	21.4t	20.7t	21.9t
15	126.8d	127.7d	23.3t	25.0	128.7d	127.9d	127.9d	126.7d	129.4d
16	132.8d	131.8d	24.9t	26.8t	132.2d	132.0d	130.1d	133.0d	129.1d
17	24.9t	23.5t	130.9d	132.1d	33.3t	25.2t	25.5t	24.7t	29.1t
18	26.4t	26.7t	130.9d	132.1d	27.1t	26.3t	26.6t	26.5t	28.6t
19	24.5t	24.3t	24.9t	26.8t	22.7t	24.8t	25.0t	24.5t	29.2t
20	53.3t	50.8t	23.3t	25.0t	53.6t	52.5t	52.8t	53.4t	53.4t
21			26.0t	23.0t	23.0t				
22	49.1t	47.5t	48.9t	48.9t	49.8t	49.3t	49.6t	49.1t	49.6t

23	33.5t	32.3t			32.0t	33.2t	34.0t	33.4t	32.3t
24	41.0d	32.5d			37.9d	41.7d	42.3d	41.3d	44.6d
25	46.9s	44.0s			47.6s	46.5s	47.3s	47.1s	43.5s
26	78.0d	59.7d			75.5d	80.8d	81.7d	78.3d	59.2d
28	53.3t	39.4t			55.1t	52.6t	53.0t	53.7t	59.2t
29	26.2t	23.4t			26.2t	32.4t	32.7t	26.4t	29.2t
30	24.2t	18.1t			25.9t	44.3t	45.1t	24.2t	29.2t
31	28.3t	27.9t			28.4t	214.8s	216.2s	28.4t	25.0t
32	142.3d	132.3d			136.4d	38.7t	38.8t	142.8d	131.6d
33	123.5d	131.3d			121.4d	24.4t	24.4t	123.3d	131.1d
34	57.0d	27.3t			51.0t	63.2d	63.6d	57.4d	26.2t
35	44.7t	44.7t			44.8t	46.5t	46.6t	44.8t	37.3t
36	70.3t	56.6t			68.8t	68.4t	69.0t	70.2t	65.7t

Alkaloids 9–17

Atom	9 (10)	10 (27)	11 (17)	12 (14)	13 (14)	14 (12)	15 (13)	16 (13)	17 (17)
1	144.1s	56.1d	145.6s	142.9s	143.3s	158.9s	60.8d	69.5d	158.8s
3	138.6d	41.3t	139.6d	137.9d	137.0d	48.8t	43.9t	53.0t	48.8t
4	113.4d	21.7t	115.3d	113.4d	113.9d	19.1t	22.3t	21.9t	19.2t
4a	129.4s	109.7s	123.5s	129.0s	129.1s	117.1s	110.3s	110.3s	116.2s
4b	121.9s	126.6s	132.1s	122.3s	121.7s	125.5s	129.5s	129.0s	126.0s
5	121.6d	117.1d	123.1d	106.7d	106.0d	119.7d	109.5d	109.3d	103.4d
6	120.0d	118.6d	121.7d	150.3s	149.8s	120.2d	119.9d	119.9d	149.8s
7	129.4d	120.6d	130.3d	118.5d	118.4d	124.3d	106.8d	106.9d	114.5d
8	111.7d	110.0d	114.1d	112.3d	113.3d	121.1d	143.0s	143.1s	112.9d
8a	140.2s	134.8s	135.7s	134.7s	136.2s	136.1s	125.1s	125.3s	135.2s
9a	133.8s	132.6s	141.3s	134.3s	134.0s	127.6s	144.8s	144.9s	128.3s
10	142.5s	143.3s	143.5s	139.8s	141.3s	139.0s	132.8s	131.6s	138.9s
11	131.7d	128.6d	138.4d	136.6d	134.9d	140.8d	132.7d	132.1d	140.2d
12	70.4s	68.9s	70.7s	69.4s	71.2s	69.9s	70.6s	71.1s	69.9s

(continued)

TABLE III.  
Continued.

13	40.9t	39.6t	50.5t	41.7t	39.2t	40.5t	39.6t	39.8t	40.3t
14	22.2t	21.0t	128.3d	21.8t	20.8t	21.6t	20.6t	20.6t	21.4t
15	128.2d	128.4d	140.6d	128.5d	126.9d	128.4d	127.6d	126.8d	128.9d
16	131.2d	127.9d	74.4d	132.3d	132.8d	132.3d	131.7d	132.9d	132.4d
17	32.5t	28.1t	37.2t	26.1t	25.0t	25.9t	24.9t	24.8t	25.5t
18	28.7t	27.5t	27.4t	26.3t	26.4t	25.8t	26.4t	26.3t	26.2t
19	29.2t	28.2t	22.5t	22.9t	24.6t	25.6t	24.4t	24.4t	25.1t
20	53.5t	52.8t	55.9t	53.2t	53.4t	53.4t	53.3t	53.2t	53.4t
22	49.7t	48.6t	45.3t	49.8t	49.2t	49.5t	49.1t	49.1t	49.4t
23	29.2t	31.7t	33.3t	32.5t	33.4t	32.5t	33.7t	33.4t	32.6t
24	46.7d	46.2d	42.2d	39.3d	40.8d	40.8d	37.5d	37.4d	38.2d
25	43.5s	42.9s	49.1s	45.4s	47.0s	46.9s	46.7s	44.6s	46.8s
26	59.2d	58.1d	74.7d	75.2d	78.0d	75.1d	78.9d	78.9d	75.2d
28	37.5t	58.1t	53.1t	55.3t	53.4t	50.9t	53.5t	53.3t	51.2t
29	26.2t	28.2t	34.5t	28.0t	26.4t	31.3t	26.3t	26.3t	29.6t
30	25.1t	28.2t	27.2t	26.8t	24.3t	25.6t	24.0t	24.0t	28.2t
31	29.2t	24.1t	30.1t	79.6d	28.3t	28.1t	28.6t	28.7t	25.8t
32	131.0d	130.6d	136.9d	40.7t	142.4d	134.9d	142.5d	142.1d	135.2d
33	129.4d	130.0d	131.4d	36.9t	123.6d	129.6d	123.6d	123.6d	128.2d
34	59.2t	25.1t	57.3d	103.9s	57.1d	55.0t	57.5d	57.5d	55.2d
35	29.2t	37.0t	45.3t	51.4t	44.7t	44.5t	43.2t	42.5t	44.6t
36	65.6t	64.9t	65.6t	66.5t	70.3t	68.6t	70.9t	70.9t	68.9t
N-Me								44.4q	

Alkaloids **18–22**, and **25**

Atom	<b>18 (17)</b>	<b>19 (16)<sup>c</sup></b>	<b>20 (16)<sup>c</sup></b>	<b>21 (16)<sup>c</sup></b>	<b>22 (16)<sup>c</sup></b>	<b>25 (15)</b> Unit A	<b>25 (15)</b> Unit B
1	159.8s	143.8s	135.0s	135.0s	136.6s	147.6s	57.5d
3	48.8t	137.8d	132.9d	133.1d	61.9t	136.6d	38.4t

4	19.1t	113.5d	115.2d	115.3d	20.3t	113.6d	23.3t
4a	117.1s	129.4s	120.5s	120.3s	108.3s	129.3s	107.7s
4b	125.5s	122.1s	122.5s	122.5s	126.5s	120.9s	127.2s
5	119.7d	121.8d	121.2d	121.2d	119.1d	121.0d	117.9d
6	120.1d	120.3d	121.3d	121.4d	121.0d	118.5d	118.2d
7	124.2d	129.0d	127.8d	127.8d	123.5d	127.4d	120.2d
8	112.0d	112.0d	112.0d	111.9d	112.0d	110.6d	110.5d
8a	136.1s	140.5s	141.3s	141.1s	137.8s	140.7s	135.9s
9a	127.7s	133.9s	136.8s	136.9s	129.9s	135.8s	135.3s
10	140.1s	140.0s	141.3s	137.8s	134.5s	53.0d	38.8d
11	133.5d	138.8d	140.8d	134.6d	141.1d	58.8d	74.7d
12	70.2s	69.7s	70.0s	70.5s	69.9s	60.3s	64.2s
13	40.7t	41.9t	41.3t	41.0t	41.2t	40.1t	31.1t
14	21.9t	22.2t	22.0t	26.5t	21.9t	24.0t	18.7t
15	129.3d	128.6d	128.8d	131.1d	128.8d	130.8d	130.2d
16	129.2d	132.6d	132.9d	132.4d	132.9d	132.2d	130.8d
17	29.1t	NR	NR	NR	NR	24.9t	24.9t
18	28.6t	NR	NR	NR	NR	28.2t	27.6t
19	29.1t	NR	NR	NR	NR	26.1t	26.9t
20	53.4t	NR	NR	NR	NR	52.8t	46.8t
22	49.5t	NR	NR	NR	NR	127.3d	62.0d
23	32.3t	NR	NR	NR	NR	116.3s	23.0t
24	45.0d	NR	NR	NR	NR	34.6d	40.3d
25	43.2s	NR	NR	NR	NR	35.6s	45.2s
26	59.2d	78.8d	75.3d	59.4d	75.1d	60.6d	66.8d
28	59.2t	55.8t	51.4t	54.8t	51.3t	47.7t	48.3t
29	29.1t	23.2t	33.7t	29.8t	33.9t	26.9t	27.6t
30	29.1t	37.4t	26.0t	29.0t	26.0t	28.1t	26.6t
31	25.0t	79.8d	28.4t	32.9t	28.4t	23.4t	24.2t



TABLE III.  
Continued.

Atom	<b>18</b> (17)	<b>19</b> (16) <sup>c</sup>	<b>20</b> (16) <sup>c</sup>	<b>21</b> (16) <sup>c</sup>	<b>22</b> (16) <sup>c</sup>	<b>25</b> (15) Unit A	<b>25</b> (15) Unit B
32	131.0d	28.4t	134.7d	130.0d	134.8d	129.5d	130.6d
33	131.4d	41.0t	130.4d	129.5d	130.3d	132.5d	131.2d
34	26.2t	104.2s	55.7d	25.4t	55.0d	18.4t	20.9t
35	37.4t	51.9t	43.9t	22.8t	44.1t	32.9t	32.7t
36	65.6t	67.1t	69.3t	65.8t	63.9t	49.9t	56.3t

<sup>13</sup> C-, <sup>15</sup> N-NMR Data of Manzamine-type Alkaloids <b>26</b> , <b>57-59</b> in CDCl <sub>3</sub> <sup>d</sup>							
Atom	<b>26</b> (18) Unit A	<b>26</b> (18) Unit B	<b>57</b> (58)	<b>58</b> (58)	<b>59</b> (58)		
1	142.8s	143.0s	143.9s	142.6s	143.8s		
N2	273.7s	273.7s	298.0s	299.0s	ND		
3	138.7d	138.8d	138.8d	138.3d	138.2d		
4	113.4d	113.5d	114.2d	114.3d	113.9d		
4a	129.3s	129.4s	129.9s	130.1s	130.1s		
4b	121.8s	121.8s	122.0s	123.4s	112.0s		
5	121.6d	121.6d	121.8d	111.9d	122.1d		
6	120.1d	120.1d	120.4d	120.9d	120.6d		
7	128.4d	128.4d	128.8d	113.6d	128.4d		
8	111.5d	111.5d	112.3d	143.6s	111.9d		
8a	139.8s	139.9s	140.8s	130.6s	140.3s		
N9	83.6p	83.6p	109.0p	105.4p	ND		
9a	133.5s	133.6s	133.8s	133.2s	133.2s		

10	139.8s	140.8s	142.8s	140.1s	142.9s
11	137.2d	137.2d	132.7d	132.2d	135.5d
12	70.8s	69.3s	80.5s	80.3s	80.4s
13	40.4t	41.6t	40.3t	39.8t	41.4t
14	21.7t	21.8t	23.1t	22.5t	23.6t
15	128.0d	128.3d	129.9d	129.3d	127.8d
16	132.5d	132.8d	129.8d	129.4d	133.2d
17	25.9t	25.8t	25.4t	25.0t	24.6t
18	26.7t	26.7t	30.0t	29.7t	29.7t
19	25.6t	26.1t	30.1t	29.6t	30.1t
20	44.6t	53.1t	59.3t	58.9t	58.8t
N21	13.5s	13.0s	36.1s	NO	ND
22	49.6t	49.7t	50.1t	49.7t	49.3t
23	32.4t	32.2t	32.1t	32.8t	33.8t
24	39.8d	39.2d	46.3d	45.9d	43.2d
25	45.3s	45.3s	38.6s	38.0s	39.9s
26	75.5d	75.9d	67.2d	66.8d	68.8d
N27	57.4s	37.4s	73.5s	73.2s	ND
28	47.2t	44.6t	54.1t	53.7t	54.1t
29	29.7t	30.0t	23.3t	22.7t	22.4t
30	72.2d	72.7d	33.1t	31.7t	33.9t
31	84.4d	67.2d	206.2s	205.1s	29.6t
32	39.5t	22.8t	30.9t	30.5t	133.4d
33	26.5t	26.6t	30.5t	30.0t	124.1d
34	89.7s	104.5s	101.8s	101.6s	94.9s
35	53.1t	51.2t	47.4t	47.2t	49.1t
36	68.7t	67.0t	66.3t	66.0t	69.9t

(continued)

TABLE III.  
Continued.

<sup>13</sup> C-NMR Data of Manzamine-related Natural Alkaloids <b>27</b> , <b>28</b> , <b>30</b> , <b>35-39</b> in CDCl <sub>3</sub> .								
Atom	<b>27</b> (14)	<b>28</b> (14)	<b>30</b> (22) <sup>a</sup>	<b>35</b> (10)	<b>36</b> (10)	<b>37</b> (25)	<b>38</b> (25)	<b>39</b> (26)
1	136.4s	155.8s		193.3d	194.3d	66.0t	65.2t	64.3d
2			42.8t					
3	137.9d	49.1t	23.8t					53.6t
4	118.4d	18.8t	25.1t					38.0d
4a	131.5s	118.0s						43.3d
4b	120.6s	124.7s						
5	121.7d	120.3d	26.5t					27.6t
6	120.5d	119.9d	132.2d					47.4t
7	129.6d	125.1d	132.2d					
8	111.8d	112.2d	26.5t					50.8t
8a	140.8s	136.9s						45.1s
9			25.1t					141.8s
9a	136.5s	125.1s						
10	184.2s	182.9s	23.8t	142.6s	144.7s	144.3s	143.8s	122.6d
11	129.7s	126.3s	42.8t	157.6d	151.7d	130.4d	126.8d	54.1t
12				70.2s	69.9s	71.6s	70.6s	26.1t
13	143.6d	144.2d		38.9t	40.4t	42.1t	41.2t	25.6t
14				21.0t	21.4t	23.0t	22.6t	22.9t
15	143.3d	144.2d		127.9d	129.3d	129.1d	130.5d	131.2d
16				132.5d	131.4d	134.6d	128.9d	130.9d
17				25.6t	29.2t	27.1t	30.0t	21.0t
18				26.7t	29.2t	28.6t	29.6t	41.6t
19				25.3t	26.2t	26.9t	25.5t	56.2t
20				53.5t	37.1t	55.0t	59.4t	21.1t

21							27.2t
22			49.4t	49.5t	51.2t	49.9t	25.0t
23			31.6t	31.4t	33.6t	30.2t	131.5d
24			34.0d	40.2d	39.9d	44.1d	132.0d
25			46.4s	42.6s	48.7s	43.9s	25.6t
26			76.3d	59.8d	78.8d	60.3d	37.0t
28			51.4t	53.5t	54.5t	52.4t	
29			29.8t	29.2t	30.1t	29.4t	
30			25.3t	25.0t	26.5t	29.7t	
31			28.2t	28.6t	29.7t	23.0t	
32			137.1d	131.2d	141.5d	130.9d	
33			127.7d	129.2d	127.6d	132.0d	
34			55.4d	59.3d	55.8d	29.7d	
35			44.6t	29.2t	46.3t	37.5t	
36			69.2t	65.6t	71.3t	65.3t	
<i>N</i> -Me	35.2q	35.2q					

<sup>13</sup>C-, <sup>15</sup>N-NMR Data of Manzamine-type Alkaloids **60–66** in CDCl<sub>3</sub><sup>d</sup>

Atom	<b>60</b> ( <i>6I</i> )	<b>61</b> ( <i>6I</i> )	<b>62</b> ( <i>59</i> )	<b>63</b> ( <i>59</i> )	<b>64</b> ( <i>60</i> )	<b>65</b> ( <i>60</i> )	<b>66</b> ( <i>60</i> )
1	61.3	69.2	53.5	60.1	143.1s	143.5,s	139.4,s
N2	ND	ND	46.3	40.4	ND	ND	ND
3	43.7	53.0	49.3	23.0	137.7d	136.7d	116.2d
4	22.2	22.0	23.0	108.3	113.7d	113.6d	129.5d
4a	109.4	109.4	108.7	127.4	130.3s	129.9s	134.8s
4b	136.2	136.5	127.4	118.2	121.6s	122.2s	123.5s
5	117.4	117.4	118.2	111.9	121.3d	105.3d	105.6d
6	120.8	120.8	119.0	118.9	119.9d	151.4s	153.2s
7	118.5	118.6	121.3	121.3	128.5d	118.5d	123.1d
8	112.0	111.9	111.3	111.3	112.3d	113.0d	114.1d

(continued)

TABLE III.  
Continued.

Atom	60 (61)	61 (61)	62 (59)	63 (59)	64 (60)	65 (60)	66 (60)
8a	127.0	126.7	136.1	136.1	141.1s	134.7s	139.4s
N9	ND	ND	123.8	ND	ND	ND	ND
9a	132.5	143.3	134.7	134.9	133.8s	136.1s	136.9s
10	144.1	143.3	43.0	40.4	141.7s	139.5s	143.7s
11	132.5	133.4	74.5	74.7	137.2d	136.9d	143.7d
12	70.7	71.0	64.7	64.6	68.6s	69.9s	72.5s
13	39.5	39.6	31.0	31.4	40.5t	41.0t	41.2t
14	20.6	20.6	18.6	18.7	21.7t	21.9t	21.6t
15	127.2	127.0	130.0	130.1	127.8d	128.7d	134.8d
16	132.8	132.9	131.1	131.0	132.7d	132.0d	127.5d
17	24.9	24.9	25.0	25.0	25.7t	26.3t	23.6t
18	26.4	26.4	27.6	27.6	26.9t	27.1t	26.1t
19	24.5	24.5	27.0	27.0	25.0t	22.8t	22.8t
20	53.3	53.2	46.6	46.7	52.8t	53.5t	53.2t
N21	ND	ND	36.9	ND	ND	ND	ND
22	49.1	49.3	57.9	58.6	49.8t	50.2t	49.7t
23	33.9	33.6	26.8	27.9	33.4t	32.5t	31.5t
24	37.1	37.5	33.6	39.4	42.4d	40.1d	39.5d
25	46.8	46.9	45.2	45.3	45.9s	45.5s	42.7s
26	78.8	78.8	66.9	66.7	81.9d	75.6d	79.7d
N27	ND	ND	32.6	ND	ND	ND	ND
28	53.3	53.3	48.0	48.1	53.5t	53.5t	53.2t
29	26.2	26.2	27.3	27.4	31.7t	32.4t	38.1t
30	24.4	24.4	26.2	26.2	48.2t	48.2t	41.2t

31	28.3	28.3	24.3	24.3	70.6d	79.9d	25.8t
32	141.9	141.8	131.1	130.8	36.8t	37.2t	23.6t
33	124.1	124.1	130.8	130.6	25.0t	26.3t	31.5t
34	57.1	57.2	21.4	21.2	63.8d	65.4d	66.9d
35	43.1	42.6	33.3	33.1	46.2t	47.3t	197.2s
36	70.8	71.1	57.5	57.2	68.9t	66.9t	63.5t
37		44.2	45.2	49.6			
38			208.6	207.4			
39			30.9	30.6			

<sup>a</sup>Recorded in CD<sub>3</sub>OD.

<sup>b</sup>Recorded in C<sub>6</sub>D<sub>6</sub>+CD<sub>3</sub>OD

<sup>c</sup>**19–22** were recorded in CD<sub>2</sub>Cl<sub>2</sub>. NR = not reported in the original literature.

<sup>d</sup>Nitromethane was used as external standard for <sup>15</sup>N-NMR, s = quaternary, p = protonated nitrogens. NO = not observed. ND = not determined.

TABLE IV.  
<sup>1</sup>H-NMR Data of Manzamine-type Alkaloids in CDCl<sub>3</sub>.

Alkaloids 1-4 Atom	1 (9)	2 (8)	3 (8)	3a (22) <sup>a</sup>	4 (7) <sup>b</sup>
1					4.51, s
3	8.34, d, 5.1-5.3	8.26, d, 5	8.26, d, 5	3.36, m 3.13, m	2.35, 2H, m
4	7.85, d, 5.1-5.3	7.84, d, 5	7.81, d, 5	2.83, m 2.88, m	2.98, 2H, m
5	8.08, d, 7.9	8.07, d, 7.8	8.11, d, 7.8	7.43, d, 7.8	7.49, d, 7.6
6	7.23, t, 7.9	7.46, dd, 7.8, 7.8	7.51, m	7.02, t, 7.8	7.08, t, 7.3
7	7.52, t, 7.9	7.18, dd, 7.8, 7.8	7.34 m	7.11, t, 7.8	7.14, t, 7.5
8	7.83, d, 7.9	7.40, d, 7.8	7.51, m	7.32, d, 7.8	7.42, d, 7.9
10		3.80, dd, 9.5, 4.5	2.90, dd, 2H, 5.1, 5.1	2.22, m 2.31, m	
11	6.52, s	3.52, d, 4.4	3.31, dd, 2H, 5.1, 5.1	3.04, m 2.92, m	5.71, s
13	2.15, m	1.75, m 2.6-1.4, overlapped	2.82, dd, 2H, 7.5, 7.5	2.99, m 2.95, m	2.2-1.2, overlapped
14	2.1-2.2, m	2.6-1.4, overlapped	2.32, 2H, m	1.68, 2H, m	2.2-1.2, overlapped
15	5.57, m	5.62, ddd, 10.8, 10.8, 5.4	1.75, 2H, m	1.52, 2H, m	5.85, m
16	5.57, m	5.47, ddd, 10.8, 10.8, 4.3	1.52, 2H, m	2.27, 2H, m	5.52, m
17	2.50, m	1.60, m 2.6-1.4, overlapped	5.47, m	5.43, m	2.2-1.2, overlapped
18	1.45, m	1.20, m 2.6-1.4, overlapped	5.47, m	5.43, m	2.2-1.2, overlapped
19	1.81, m	1.45, m 2.6-1.4, overlapped	1.52, 2H, m	2.27, 2H, m	2.2-1.2, overlapped
20	2.58, m	2.38, m 2.6-1.4, overlapped	1.75, 2H, m	1.52, 2H, m	2.62, 2H, m
21			2.32, 2H, m	1.68, 2H, m	2.2-1.2, overlapped
22	2.93, m; 1.88, m	2.80, 2H, m	2.82, dd, 2H, 7.5, 7.5	2.99, m; 2.95, m	2.81, 2H, m
23	2.95, m	1.78, m 2.6-1.4, over- lapped 1.30, dd, 13.2, 13.2			2.2-1.2, overlapped
24	2.55, m	2.6-1.4, overlapped			2.2-1.2, overlapped
26	3.72, s	2.95, s			3.40, s
28	4.03, m	3.27, m 3.09, br			3.16, m 2.51, m

(continued)

TABLE IV.  
Continued.

Atom	1 (9)	2 (8)	3 (8)	3a (22) <sup>a</sup>	4 (7) <sup>b</sup>	
29	2.60, m	2.00, m	2.6-1.4, overlapped		2.2-1.2, overlapped	
30	1.95, m	1.45, m	2.6-1.4, overlapped		2.2-1.2, overlapped	
31	2.30, m		2.6-1.4, overlapped		2.2-1.2, overlapped	
32	6.29, m		5.30, brs		5.64, m	
33	5.39, t, 7		5.30, brs		5.20, dd, 9.3, 9.8	
34	4.94, m		2.6-1.4, overlapped		4.18, t, 7.8	
35	2.40, m	1.85, m	1.14, d, 13.9 0.92, dd, 13.9, 7.9		2.2-1.2, overlapped	
36	2.88, m	2.32, m	2.6-1.4, overlapped		2.2-1.2, overlapped	
<b>Alkaloids 5-10</b>						
Atom	5 (7,9)	6 (7,9)	7 (11)	8 (10)	9 (10)	10 (27)
1				4.64,s		4.65, m
3	8.42, d, 5.1	8.38, d, 5.3	8.33, d, 5.1	3.40-3.10 overlapped	8.44, d5.4	3.6-1.0, m
4	7.83, d, 5.1	7.80, d, 5.3	7.83, d, 5.1	3.40-3.10 overlapped	7.83, d, 5.1	3.6-1.0, m
5	8.10, d, 7.9	7.62, d, 7.7	7.62, brd, 7.2	7.48, d, 7.6	8.11, d, 7.8	7.48, d, 7.7
6	7.26, dt, 7.9, 1.1	7.14, m	7.15, t, 7.2	7.14, m	7.27, m	7.14, t, 8.0
7	7.53, dt, 7.9, 1.1	7.14, m	7.09, dd, 7.5, 0.9	7.09, m	7.53, m	7.09, t, 8.0
8	7.59, d, 7.9			7.33, d, 7.8	7.53, m	7.31, d, 8.1
11	6.50, s	6.65,s	6.46,s	5.61,s	6.24,s	5.64,s
13	1.88, m	2.05, m	2.06, m	3.40-3.10 overlapped		3.6-1.0, m
14	1.73, m	1.87, m	1.80, m	3.40-3.10 overlapped		3.6-1.0, m
15	2.2-2.1, m	2.3-2.1, m	2.23, m	5.62, m	5.64, brt, 11.1	5.58, m
16	5.54, dt, 10.6, 7.8	5.63, dt, 10.3, 7.9	5.59, m	5.45, m	5.46, brtd, 11.1, 3.8	5.43, m
17	5.45, td, 10.8, 4.6	5.52, ddd, 10.8, 10.8, 4.4	5.55, m			
	2.50, m	2.50, m	2.47, m	3.40-3.10		3.6-1.0,m
	1.64, m	2.50, m	2.47, m	3.40-3.10		3.6-1.0, m
		1.64, m	1.64,m	overlapped		

(continued)



TABLE IV.  
Continued.

Atom	5 (7,9)	6 (7,9)	7 (11)	8 (10)	9 (10)	10 (27)
18	1.42, m 1.30, m	1.42, m 1.30, m	1.54, m 1.23, m	3.40–3.10 overlapped		3.6–1.0, m
19	1.70, m 1.35, m	1.75, m 1.40, m	1.85, m 1.50, m	3.40–3.10 overlapped		3.6–1.0, m
20	2.60, m 2.38, m	2.60, m m	2.38, 2.62, m 2.43, m	3.40–3.10 overlapped		3.6–1.0, m
22	2.80, m 1.90, m	2.80, m 1.90, m	2.97, m 1.88, m	3.40–3.10 overlapped		3.6–1.0, m
23	2.03, m 1.45, m	2.25, m 1.56, m	2.97, m 1.86, m	3.40–3.10 overlapped		3.6–1.0, m
24	3.20, m	3.20, m	2.53, m	3.40–3.10 overlapped	3.33, brd, 11.0	3.6–1.0, m
26	3.53, s	3.70, s	3.77, d, 6.9	3.71, brs	3.85, brs	3.74, brs
28	3.23, m 2.65, m	3.32, m 2.75, m	4.03, dd, 12.06.9 3.32, q, 10.1	3.40–3.10 overlapped		3.6–1.0, m
29	1.90, m 1.80, m	2.05, m 1.95, m	2.50, m 2.30, m	3.40–3.10 overlapped		3.6–1.0, m
30	2.48, m 2.23, m	2.49, m 2.22, m	2.03, m 1.54, m	3.40–3.10 overlapped		3.6–1.0, m
31			2.35, m	3.40–3.10 overlapped		3.6–1.0, m
32	2.35, m 2.15, m	2.63, m 2.33, m	6.34, dt, 10.8, 6.8	5.31, m	5.36, brt, 9.9	5.32, m
33	1.95, m 1.60, m	2.10, m 1.70, m	5.42, t, 9.8	5.20, m	5.25, brt, 10.7	5.19, m
34	2.85, m	2.98, m	4.98, brq, 6.9	3.40–3.10 overlapped		3.6–1.0, m
35	1.60, m 1.49, m	1.65, m 1.57, m	2.39, m 1.92, m	3.40–3.10 overlapped		3.6–1.0, m
36	2.50, m 2.35, m	2.49, m 2.30, m	2.92, m 2.40, m	3.40–3.10 overlapped		3.6–1.0, m
<b>Alkaloids 11–15</b>						
Atom	11 (17) <sup>a</sup>	12 (14)	13 (14)	14 (12)		15 (13)
1						4.80, brs
3	8.35, d, 5.2	8.31, d, 5.1	8.13, d, 4.8	3.96, m 3.84, m		3.27, brd, 11.0 2.94, dt, 11.0
4	8.00, d, 5.2	7.59, d, 5.1	7.48, d, 4.8	2.82, 2H, m		2.81, m 2.62, brd, 13.8
5	8.19, d, 7.7	7.49, d, 2.5	7.39, d, 2.4	7.60, d, 7.9		6.96, d, 8.0
6	7.30, dd, 7.7, 7.1			7.13, t, 7.9		6.91, dt, 8.1, 4.0

(continued)

TABLE IV.  
Continued.

Atom	11 (17) <sup>a</sup>	12 (14)	13 (14)	14 (12)	15 (13)
7	7.59, dd, 7.1, 8.2	7.13, dd, 2.5, 8.6	7.08, dd, 2.4, 7.5	7.28, t, 7.9	6.63, d, 8.1
8	7.72, d, 8.2	7.26, d, 8.6	7.54, d, 7.5	7.41, d, 7.9	
11	6.54, s	6.45, s	6.51, s	6.32, s	5.84, s
13	2.95, m	2.13, m	2.02, 2H, m	1.93, m	2.00, m
	2.73, dd, 10.0, 14.4	1.68, m		1.67, m	1.52, m
14	5.73, ddd, 14.8, 10.0, 4.3	2.36, m 2.13, m	2.26, 2H, m	2.35, m 2.13, m	2.13, 2H, m
15	5.65, dd 14.8, 8.3	5.64, m	5.51, m	5.63, m	5.55, m
16	4.06, brt, 7.5	5.53, m	5.51, m	5.53, dt, 10.6, 4.7	5.53, m
17	1.72, m 1.52, m	2.58, m 1.70, m	2.47, m 1.57, m	2.53, m 1.70, m	2.38, m 1.42, m
18	1.68, m 1.45, m	1.44, 2H, m	1.42, m 1.24–1.17, m	1.70, m 1.33, m	1.38, m 1.13, m
19	1.66, m 1.45, m	1.69, m 1.43, m	1.83, m 1.42, m	1.73, m 1.42, m	1.85, m 1.42, m
20	2.60, tt, 4.4, 8.6 2.30, m	2.67, m 2.45, m	2.55, m 2.42, m	2.60, dt, 13.2, 5.2 2.44, m	2.27, m 2.45, dd, 12.0, 5.1
22	2.81, m 2.18, m	2.71, m 1.95, m	2.86, m 1.86, m	2.76, brd, 10.8 1.95, m	2.77, m 1.67, m
23	1.98, m 1.72, m	1.93, m 1.51, m	2.86, m 1.74, m	1.97, m 1.45, m	2.16, m 1.33, m
24	2.93, m	3.00, dd, 12.0, 6.0	2.55, m	2.00, m	1.97, m
26	4.20, s	3.62, s	3.67, s	3.44, s	3.55, s
28	2.95, 2H, m	3.34, m 2.88, dd, 11.1, 10.3	3.98, m 3.21, m	3.17, 2H, m	3.82, m 3.16, t, 11.4
29	1.99, m 1.67, m	1.70, m 1.58, m	2.60, m 1.24–1.17, m	1.96, m 1.62, m	2.45, m 1.84, m
30	1.95, m 1.45, m	1.93, m 1.44, m	1.95, m 1.42, m	1.87, m 1.34, m	1.90, m 1.42, m
31	2.34, m 2.22, m	4.55, m	2.26, m	2.35, m 2.13, m	2.32, m (2H)
32	5.98, dt, 10.9, 7.1	2.40, m 2.13, m	6.20, m	5.95, m	6.14, m
33	5.36, brt, 8.8	1.44, m	5.30, m	5.26, brd, 10.6	5.18, t, 9.9
34	4.32, brt, 8.3		4.89, m	4.19, m	4.70, t, 8.7
35	2.41, dd, 8.6, 13.2 1.68, m	2.40, d-like, 12.7 2.34, d-like, 12.7	2.45, m 1.83, m	2.14, m 1.69, m	1.71, m 1.42, m

(continued)

TABLE IV.  
Continued.

Atom	11 (7) <sup>a</sup>	12 (14)	13 (14)	14 (12)	15 (13)
36	2.95, d, 11.6 1.95, d, 11.6	3.14, d, 12 2.27, d, 12	2.86, m 2.40, m	2.78, d, 11.6 2.27, d, 11.6	2.78, m 2.10, m
<b>Alkaloids 16–20</b>					
Atom	16 (13)	17 (17)	18 (17)	19 (16) <sup>c</sup>	20 (16) <sup>c</sup>
1	3.92, s				
3	3.00, dd, 11.0, 4.0 2.44, dd, 12.0, 3.0	3.93, m 3.89, m	3.45, m 3.35, m	8.42, d, 5.1	8.06, d, 6.7
4	2.85, t, 12.0 2.65, brd, 15.0	2.81, m 2.79, m	2.88, m 2.86, m	7.87, d, 5.2	7.77, d, 6.7
5	6.96, d, 8.0	6.97, brs	7.59, d, 7.7	8.16, d, 7.8	8.04, d, 8.0
6	6.91, dt, 8.0, 4.0		7.14, dd, 7.7, 7.1	7.33, m	7.32, t, 8.0
7	6.64, d, 8.0	6.86, brd, 8.2	7.26, dd, 7.1, 8.2	7.57, m	7.51, m
8		7.29, d, 8.2	7.40, d, 8.2	7.57, m	7.54, m
11	5.91, s	6.36, s	6.15, s	6.41, s	6.07, s
13	1.92, m 1.75, m	1.92, m 1.72, m	2.05, m 1.48, m	2.10, m 1.69, m	2.15, m 1.85, m
14	2.17, 2H, m	1.73, m 1.43, m	2.27, m 1.98, m	2.40, m 2.14, m	2.40, m 2.10, m
15	5.56, dt, 8.0, 3.0	5.63, ddd, 7.3, 8.3, 10.8	5.32, ddd, 7.0, 8.3, 10.6	5.68, q, 10.0	5.72, m
16	5.54, dt, 11.0, 4.0	5.54, dt, 10.8, 7.3	5.28, dt, 10.6, 7.6	5.58, dt, 10.8, 5.0	5.60, dt, 7.9, 4.7
17	2.36, m 1.55, m	1.77, m 1.43, m	2.93, m 2.90, m	2.64, m 1.86–1.76, m	2.55, m 1.75, m
18	1.45, m 1.14, m	1.91, m 1.43, m	1.90, m 1.55, m	1.51, 2H, m	1.41, m 1.30, m
19	1.72, m 1.40, m	1.73, m 1.43, m	1.70, m 1.20, m	1.47, 2H, m	1.81, m 1.41, m
20	2.48, dd, 13.0, 5.0 2.26, m	2.61, m 2.43, m	2.91, m 2.82, m	2.78, m 2.54, m	2.80, m 2.38, m
22	2.75, m 1.61, brd, 11.0	2.78, m 1.95, m	2.95, m 1.94, m	2.80, m 2.01, m	2.98, m 2.50, m
23	2.16, m 1.43, m	2.01, m 1.48, m	2.17, m 1.72, m	1.58, 2H, m	3.15, m 1.75, m
24	1.86, m	2.78, m	2.45, m	3.01, dt, 9.3, 6.4	3.00, dd, 11.5, 7.3
26	3.56, d, 7.5	3.47, s	3.78, s	3.62, s	3.72, s
28	3.88, m 3.16, q, 10.0	3.19, m 3.08, s	2.62, m 2.35, m	3.36, m 2.89, m	3.96, m 3.20, m

(continued)

TABLE IV.  
Continued.

Atom	16 (13)	17 (17)	18 (17)	19 (16) <sup>c</sup>	20 (16) <sup>c</sup>	
29	2.44, m 1.91, m	1.93, m 1.27, m	1.78, m 1.70, m	1.86–1.76, 2H, m	2.84, m 1.98, m	
30	1.97, m 1.42, m	2.29, m 2.16, m	1.78, m 1.28, m	1.86–1.76, m 1.66, m	1.91, m 1.38, m	
31	2.34, m 2.20, m	1.74, m 1.48, m	1.74, m 1.48, m	4.54, brd, 7.9	2.30, 2H, m	
32	6.17, dt, 12.0, 6.0	5.97, t, 10.4, 7.6	5.61, dt, 10.9, 7.1	3.20, d, 11.9 2.05, m	5.95, m	
33	5.18, t, 10.0	5.25, brt, 9.5	5.36, brt, 8.8	2.25–2.16, m 1.63, m	5.35, m	
34	4.73, q, 8.1	4.30, m	2.72, m 2.19, m		4.29, m	
35	1.69, dd, 14.0, 8.0 1.30, brd, 14.0	2.78, m 1.72, m	2.18, m 1.45, m	2.33, d, 1 3.9 1.94, d, 13.9	2.43, m 1.68, m	
36	2.74, brd, 12.1 2.09, brd, 12.0	2.80, m 2.37, m	3.30, d, 12.1 2.08, d, 12.1	2.27, d, 11.9	2.80, d, 11.6 2.33, d, 11.3	
<i>N</i> -Me	2.26, s					
Alkaloids <b>21</b> , <b>22</b> , <b>25</b> and <b>26</b>						
Atom	21 (16) <sup>c</sup>	22 (16) <sup>c</sup>	25 (15) unit A	25 (15) unit B	26 (18) unit A	26 (18) unit B
1				2.43, m		
3	8.08, d, 6.6	4.36, m 4.21, m	8.17, d, 5.0	2.57, m 2.34, m	8.45, d, 5.1	8.46, d, 5.1
4	7.79, d, 6.2	3.22, 2H, m	7.62, d, 5.0	2.13, m 1.89, m	7.83, d, 5.3	7.83, d, 5.3
5	8.04, d, 7.5	7.51, d, 7.8	7.27, m	6.84, brd, 8.0	8.10, d, 7.9	8.10, d, 7.9
6	7.32, m	7.15, d, 8.0	6.51, brt, 8.0	6.78, brt, 8.0	7.29, dd, 8.0, 7.9	7.29, dd, 8.0, 7.9
7	7.51, m	7.21, dt, 7.6, 1.1	7.11, m	6.97, t, 8.0	7.55, dd, 8.3, 8.0	7.55, dd, 8.3, 8.0
8	7.51, m	7.41, d, 8.0	7.17, brd, 8.0	7.14, d, 8.0	7.51, d, 8.4	7.51, d, 8.4
10			3.50, m	1.22, m		
11	6.06, s	5.97, s	3.44, d, 4.2	3.07, brs	6.37, s	6.41, s
13	2.08, m	2.02, m	2.48, m	2.33, m 1.11, dt, 14.5, 5.0	2.11, 2H, m	2.13, m 1.70, m
14	1.59, br 2.18, 2H, br	1.75, m 2.41, m 2.14, m	1.30, m 2.49, m 2.16, m	2.51, m 1.68, m	2.37, m 2.09, m	2.37, m 2.11, m
15	5.66, dt, 10.8, 4.4	5.69, m	5.24, m	5.44, dt, 11.0, 6.5	5.64, m	5.64, m
16	5.47, d, 10.9	5.59, dt, 10.8, 4.7	5.34, brt, 11.0	5.25, m	5.58, m	5.58, m
17		2.52, m 1.85, m	2.49, m 1.91, m	2.64, m 1.78, m	1.78, m 1.59, m	1.77, m 1.55, m

(continued)

TABLE IV.  
Continued.

Atom	21 (16) <sup>c</sup>	22 (16) <sup>c</sup>	25 (15) unit A	25 (15) unit B	26 (18) unit A	26 (18) unit B
18		1.70, m 1.34, m	1.57, m 1.51, m	1.67, m 1.08, m	1.44, 2H, m	1.44, 2H, m
19	1.20, brd, 10.1	1.70, m 1.34, m	1.73, m 1.53, m	1.24, m 1.24, m	1.76, m 1.39, m	1.77, m 1.41, m
20	2.59, brd, 11.6 2.38, br	2.63, dt, 11.7, 4.8 2.42, m	2.75, dt, 14.0, 4.5 3.47, m	2.33, m 1.85, m	2.64, m 2.49, m	2.46, m 1.96, m
22	2.88, br 1.81, br	2.79, m 1.95, m	5.47, brs	2.88, m	2.75, m 1.98, m	2.76, m 1.99, m
23		1.97, m 1.60, m		1.29, m 0.96, m	1.88, mm 1.54, m	1.89, m 1.53, m
24	2.90, brs	2.98, m	2.81, d, 8.5	1.36, m	3.06, m	3.05, m
26	3.77, brs	3.45, s	3.13, s	2.91, brs	3.85, s	3.66, s
28	2.98, m 2.88, m	3.19, 2H, m	3.41, m 2.47, m	3.15, m 2.62, m	3.15, 2H, m	3.57, m 3.18, m
29		1.70, m 1.55, m	1.95, m 1.62, m	1.82, m 1.57, m	2.05, m 1.56, m	2.27, m 2.12, m
30	1.50, m	1.85, m 1.34, m	1.82, m 1.67, m	1.63, m 1.54, m	3.76, brd, 6.1	4.14, d, 7.5
31	1.75, m 1.59, br	2.35, m 2.15, m	2.50, m 2.07, m	2.26, m 1.95, m	4.41, d, 8.7	3.69, brd, 6.1
32	5.35, m	5.94, m	5.53, td, 11.0, 3.5	5.63, m	2.07, m 1.55, m	2.12, m 1.52, m
33	5.50, m	5.30, t, 9.5	5.69, td, 11.0, 4.0	5.65, m	1.75, m 1.45, m	1.78, m 1.40, m
34	1.48, m	4.21, m	2.40, m 1.94, m	2.24, m 1.92, m		
35	2.47, br 2.19, br	2.95, m 1.65, m	2.34, m 0.91, m	1.74, m 1.26, m	2.65, m 2.45, m	2.36, d, 13.1 2.05, d, 12.9
36		2.80, d, 11.6 2.30, d, 11.6	2.98, d, 10.5 2.69, d, 10.5	2.86, d, 9.5 2.07, d, 9.5	3.42, dd, 11.3, 2.0 2.30, m	3.10, dd, 11.8, 2.1 2.28, d, 11.9
Alkaloids 27, 28, 30 and 39						
Atom	27 (14)	28 (14)	30 (22) <sup>d</sup>		39 (26)	
1				3.01, s		
2			3.08, 2H, t, 7.6			
3	8.55, d, 5.0	4.16, dd, 9.0, 9.0	1.76, 2H, m	2.86, dd, 8.5, 1.5	2.91, dd, 20.7, 9.7	1.64, dd, 9.0, 2.3
4	8.09, d, 5.0	2.97, dd, 9.0, 9.0	1.58, 2H, m	2.22, m		
4a				0.93, ddd, 11.6, 5.6, 1.9		
5	8.12, d, 8.2	7.60, d, 7.9	2.30, 2H, m	1.36, m	1.17, ddd, 13.0, 8.7, 4.4	

(continued)

TABLE IV.  
Continued.

Atom	27 (14)	28 (14)	30 (22) <sup>d</sup>	39 (26)
6	7.30, dd, 8.2, 6.2	7.13, dd, 7.9, 7.0	5.46, m	2.75, m 2.63, dt, 12.3, 3.6
7	7.55, dd, 7.3, 6.2	7.29, dd, 7.3, 7.0	5.46, m	
8	7.57, d, 7.3	7.40, d, 7.3	2.30, 2H, m	2.23, d, 12.3 2.08, d, 10.7
9			1.58, 2H, m	
10			1.76, 2H, m	5.81, brd, 6.3
11			3.08, 2H, t, 7.6	2.23, m
12				1.45, m 1.24, m
13	8.93, s	8.37, s		1.58, m 1.46, m
14				2.35, m 1.57, m
15	7.66, s	7.63, s		5.64, ddd, 13.6, 10.1, 5.2
16				5.69, ddd, 13.6, 10.1, 6.3
17				2.27, m 1.78, m
18				1.88, dt, 12.3, 7.6 1.61, m
19				3.07, m 2.24, m
20				1.55, m 1.34, m
21				1.48, m 1.32, m
22				2.14, m 1.96, brd, 15.2
23				5.24, brd, 10.8
24				5.36, brd, 10.8
25				2.29, m 2.12, m
26				2.33, m 2.25, m
<b>Alkaloids 35-38</b>				
Atom	35 (10)	36 (10)	37 (25) <sup>a</sup>	38 (25)
1	9.45, s	9.50, s	4.00, s (2H)	3.88, s (2H)
11	6.75, s	6.53, s	5.68, s	5.70, s
13	1.77, m 1.61, m	3.10-1.0 (overlapped)	1.80, m 1.61, m	2.18, brd, 10.8 1.64, m
14	2.24, m 2.11, m	3.10-1.0 (overlapped)	2.26, m 1.96, m	2.15, m 1.91, m
15	5.56, m	5.58, m	5.49, m	5.42, m
16	5.50, dddd 10.7, 10.7, 10.7, 4.6	5.44, m	5.52, m	5.29, m
17	2.43, m 1.63, m	3.10-1.0 (overlapped)	2.52, m 1.63, m	2.98, brt, 12.7 1.74, m
18	1.41, m 1.25, m	3.10-1.0 (overlapped)	1.42, m 1.22, dt, 9.2, 4.3	1.65, m 1.19, m
19	1.71, m 1.38, m	3.10-1.0 (overlapped)	1.77, m 1.46, m	1.36, m 1.34, m
20	2.57, m 2.39, m	3.10-1.0 (overlapped)	2.67, dt, 12.0, 5.2 2.34, m	2.49, dt, 12.1, 1.3 2.25, ddd, 16.9, 11.6, 4.6
22	2.77, m 1.86, m	3.10-1.0 (overlapped)	2.87, dd, 11.3, 5.5 1.83, m	2.77, dd, 9.4, 4.7 1.74, m

(continued)

TABLE IV.  
Continued.

Atom	35 (10)	36 (10)	37 (25) <sup>a</sup>	38 (25)
23	1.78, m 1.22, m	3.10–1.0 (overlapped)	1.90, m 1.41, m	1.68, m 1.59, m
24	2.58, dd, 12.2, 6.8	3.10–1.0 (overlapped)	2.05, dd, 12.0, 6.8	1.71, m
26	3.44, s	3.71, s	3.59, s	3.66, s
28	3.38, m 3.04, m	3.25, m 3.10–1.0 (overlapped)	3.56, dt, 12.7, 7.0 3.32, m	3.00, m 2.90, m
29	1.93, m 1.73, m	3.10–1.0 (overlapped)	1.98, m 1.58, m	1.61, m 1.47, m
30	1.89, m 1.35, m	3.10–1.0 (overlapped)	1.77, m 1.45, m	1.65, m 1.34, m
31	2.29, m 2.14, m	3.10–1.0 (overlapped)	2.36, m 2.24, m	2.55, m 1.94, m
32	6.03, dddd 11.0, 7.1, 7.1, 1.5	5.27, m	6.18, dt, 10.7, 7.1	5.32, brt, 10.1
33	5.26, ddd 10.5, 10.3, 1.2	5.19, m	5.40, dd, 10.7, 9.4	5.54, brt, 10.8
34	4.36, brt, 8.1	3.10–1.0 (overlapped)	4.52, brt, 7.9	1.99, m 1.96, m
35	1.86, m 1.67, m	3.10–1.0 (overlapped)	2.11, dd, 13.6, 8.0 1.71, m	2.23, m 1.08, brt, 12.7
36	2.81, d, 11.2 2.29, d, 11.2	3.10–1.0 (overlapped)	2.94, brd, 1 1.5 2.29, d, 11.5	3.30, brd, 11.9 1.84, d, 11.9
<b>Alkaloids 57–59 and 61</b>				
Atom	57 (58)	58 (58)	59 (58)	61 (61)
1				3.97, s
3	8.41, d, 5.2	8.39, d, 5.6	8.46, d, 5.0	2.49, m 3.03, ddd, 12.9, 4.7, 1.4
4	7.84, d, 5.2	7.82, d, 5.6	7.84, d, 5.0	2.73, ddd, 14.9, 12.9, 1.5 2.89, m
5	8.08, d, 7.8	7.63, d, 7.7	8.12, d, 7.7	7.43, d, 7.6
6	7.26, t, 8.0	7.13, dd, 7.8, 7.7	7.29, t, 7.5	7.09, d, 7.6
7	7.51, t, 7.4	7.02, d, 7.8	7.53, t, 7.6	7.02, dt, 7.6, 1.1
8	7.55, d, 8.0	—	7.49, d, 7.6	7.59, d, 7.6
N9	8.85, s	9.12, s		
11	6.24, s	6.33, s	6.58, s	5.94, s
13	2.35, m 1.66, m	2.27, m 2.09, m	2.25, m 2.12, m	1.75, m, 1.92, m
14	2.85, m, 2.45, m	2.24, m, 1.83, m	2.31, m, 2.01, m	2.17, m
15	5.34, brs	5.33, brs	5.65, m	5.59, dt, 3.1, 7.4
16	5.29, brs	5.30, brs	5.57, m	5.54, dt, 10.6, 4.0
17	1.86, m, 1.73, m	1.61, m, 1.49, m	1.65, m, 1.53, m	1.59, m, 2.41, m
18	1.52, m, 1.24, m	1.81, m, 1.63, m	1.64, m, 1.73, m	1.15, m, 1.45, m

(continued)

TABLE IV.  
Continued.

Atom	57 (58)	58 (58)	59 (58)	61 (61)	
19	1.46, m 1.38, m	1.79, m 1.60, m	1.81, m 1.67, m	1.40, m, 1.72, m	
20	2.71, m 2.28, m	2.67, m 2.36, m	2.65, m 2.34, m	2.26, m 2.53, dd, 12.2, 5.7	
22	3.02, m 2.04, m	3.03, brd, 9.3 2.07, m	3.05, m 2.15, m	2.76, m	
23	2.59, m 2.67, m	2.59, m 2.20, m	2.46, m 2.31, m	1.43, m, 2.16, m	
24	2.52, dd, 11.8, 5.5	2.57, dd, 12.0, 5.6	2.47, dd, 12.0, 5.4	1.84, dd, 7.0, 11.9	
26	4.36, s	4.39, s	4.38, s	3.53, brs	
28	3.38, dd, 12.5, 11.3 2.84, dd, 12.5, 4.4	3.37, dd, 12.8, 11.9 2.84, dd, 12.8, 4.7	3.35, dd, 1 2.7, 11.6, 2.83, dd, 12.8, 4.6	3.12, dd, 9.6, 11.4 3.94, m	
29	1.72, m 1.76, m	1.57, m 1.48, m	1.63, m 1.46, m	1.91, m, 2.48, m	
30	1.64, m 1.78, m	1.83, 2H, m	1.58, m 1.82, m	1.42, m, 1.97, m	
31	—	—	2.32, m 1.86, m	2.34, m	
32	3.20, m 2.75, m	1.79, m 1.51, m	5.37, brs	6.18, dt, 9.9, 7.1	
33	2.25, m, 2.15, m	2.53, m, 1.57, m	5.38, brs	5.21, dd, 9.9, 9.7 4.68, m	
34					
35	2.27, d, 12.5 2.34, d, 12.5	2.34, d, 12.4 2.24, d, 12.4	2.35, d, 12.5 2.21, d, 12.3	1.26, dd, 12.5, 1.3 1.69, m	
36	3.15, d, 11.0 2.24, d, 11.0	3.16, d, 11.1 2.30, d, 11.1	3.14, d, 11.2 2.26, d, 11.1	2.09, d, 11.3 2.76, d, 12.3 2.30, s	
37					
Alkaloids 62-66					
Atom	62 (59)	63 (59)	64 (60)	65 (60)	66 (60)
1	4.16, d, 9.6	4.13, d, 9.3			
3	3.25, m, 2.84, m	2.96, m 2.90, m	8.30, d, 5.2	8.22, d, 5.3	8.44, d, 5.3
4	2.80, 2H, m	2.77, 2h, m	7.93, d, 5.2	7.84, d, 5.3	8.35, d, 5.3
5	7.46, d, 7.6	7.45, d, 7.6	8.14, d, 8.14	7.49, d, 2.3	7.63, d, 2.3
6	7.04, t, 7.6	7.03, t, 7.6	7.24, t, 8.0		
7	7.11, t, 7.6	7.10, t, 7.6	7.53, t, 8.0	7.09, dd, 2.3, 8.8	7.33, dd, 2.3, 8.8
8	7.31, d, 8.0	7.30, d, 7.6	7.66, d, 8.5	7.52, d, 8.8	7.68, d, 8.8
N9	9.17, s	9.04, s			
10	1.58, m	1.63, m			
11	3.52, m	3.39, m	6.44, s	6.29, s	6.65, s
13	2.48, m, 1.37, m	2.45, m 1.20, m	1.83, m, 1.88, m	1.81, m, 1.89, m	1.85, m, 1.99, m
14	2.63, m, 1.80, m	2.54, m 1.73, m	2.15, m, 2.18, m	2.11, m, 2.20, m	2.11-2.20, m
15	5.48, m	5.46, m	5.63, q, 12.08	5.65, dt, 4.7, 11.38	5.62, q, 9.8

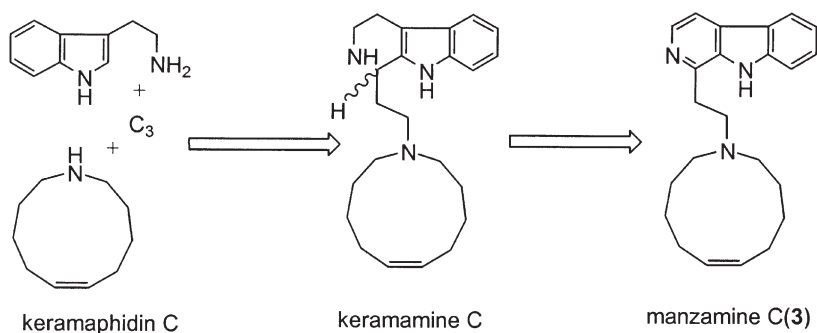
(continued)



TABLE IV.  
Continued.

Atom	62 (59)	63 (59)	64 (60)	65 (60)	66 (60)
16	5.29, m	5.30, m	5.52, dt, 4.4, 10.8	5.52, q, 9.09	5.66, q, 10.1
17	2.70, m, 1.81, m	2.68, m, 1.82, m	1.64, m, 2.49, m	1.66, m, 2.48 m	1.65, m, 2.51, m
18	1.15, m, 1.77, m	1.16, m, 1.76, m	1.35, m, 1.42, m	1.35, m, 1.41, m	1.32, m, 1.40, m
19	1.73, m, 1.41, m	1.37, m, 1.74, m	1.36, m, 1.69, m	1.34, m, 1.71, m	1.42, m, 1.73, m
20	2.54, m, 2.12, m	2.52, m, 2.08, m	2.39, m, 2.60, m	2.37, m, 2.62, m	2.36, m, 2.59, m
22	3.75, m	3.54, m	1.82, m, 2.70, m	1.83, m, 2.71, m	1.93, m, 2.81, m
23	1.43, m, 1.78, m	1.49, m, 1.74, m	1.48, m, 1.95, m	1.46, m, 1.85, m	1.55, m, 2.75, m
24	2.11, m	1.98, m	3.15, dt, 6.4, 9.3	3.15, dd, 7.3, 11.2	3.05, dd, 7.1, 10.8
26	2.93, s	2.95, s	3.79, s	3.64, s	5.01, s
28	3.07, m, 2.70, m	3.10, m, 2.69, m	2.66, m, 3.56, m	2.66, m, 3.56, m	
29	1.74, 2H, m	1.65, 2H, m	1.83, m, 1.90, m	1.83, m, 1.90, m	1.83, m, 2.10, m
30	1.47, m, 1.86, m	1.46, m, 1.72, m	2.65, m, 2.98, m	2.65, m, 2.98, m	2.45, m, 2.87, m
31	2.22, m, 2.03, m	2.25, m, 1.98, m	4.05, m	4.05, m	2.05, m
32	5.53, m	5.55, m	1.80, m, 2.21, m	1.80, m, 2.21, m	1.98, m, 2.31, m
33	5.53, m	5.55, m	1.60, m, 1.79, m	1.60, m, 1.79, m	1.70, m, 2.10, m
34	2.05, m, 2.24, m	2.26, m, 2.00, m	3.05, m	3.2, m	4.13, m
35	1.50, m, 1.60, m	1.63, m, 1.44, m	1.35, m, 1.42, m	1.34, m, 1.42, m	
36	2.89, d, 10.0 2.39, d, 10.0	2.93, d, 9.6 2.28, d, 9.6	2.30, m, 2.65, m	2.31, m, 2.65, m	2.33, m, 2.55, m
37	3.06, m, 2.63, m	2.54, dd, 15.8, 7.6 2.89, m			
39	2.17, 3H, s	2.27, s			

<sup>a</sup>Recorded in CD<sub>3</sub>OD<sup>b</sup>Recorded in C<sub>6</sub>D<sub>6</sub>+CD<sub>3</sub>OD<sup>c</sup>Recorded in CD<sub>2</sub>Cl<sub>2</sub><sup>d</sup>Recorded in CD<sub>3</sub>OH



Scheme 2. Biogenetic Pathway for Manzamine C (3) Proposed by Tsuda *et al.* (2).

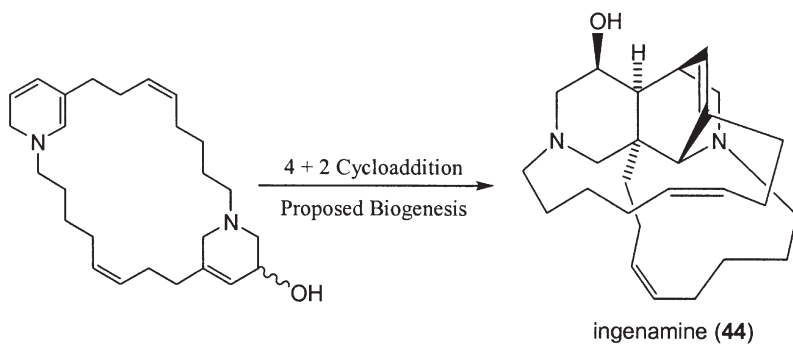
The proposal by Tsuda *et al.* suggested that the macrocyclic bisdihydropyridine maybe derived from ammonia, a C<sub>3</sub> unit, and a C<sub>10</sub> unit. The bisdihydropyridine could then be converted through a Diels-Alder-type [4+2] intramolecular cycloaddition into a pentacyclic intermediate, which in turn could provide manzamines A and B via a tetracyclic intermediate (Scheme 1) (5). 8-hydroxy-1,2,3,4-tetrahydromanzamine A (15) and its *N*-methylated derivative 8-hydroxy-2-*N*-methyl-1,2,3,4-tetrahydromanzamine A (16) are of further interest as it provides yet another intermediate in the biosynthetic path from acyclic precursors to the fully aromatized manzamines (13).

The isolation of keramaphidin C and keramamine C, together with manzamine C (3) and tryptamine, appears to substantiate, in part, the biogenetic path of manzamine C (3), which may be derived from the coupling of keramaphidin C with tryptamine and a C<sub>3</sub> unit via keramamine C. On the other hand, keramaphidin C is probably generated from a C<sub>10</sub> unit and ammonia (Scheme 2) (2). The biogenesis has not yet been investigated experimentally.

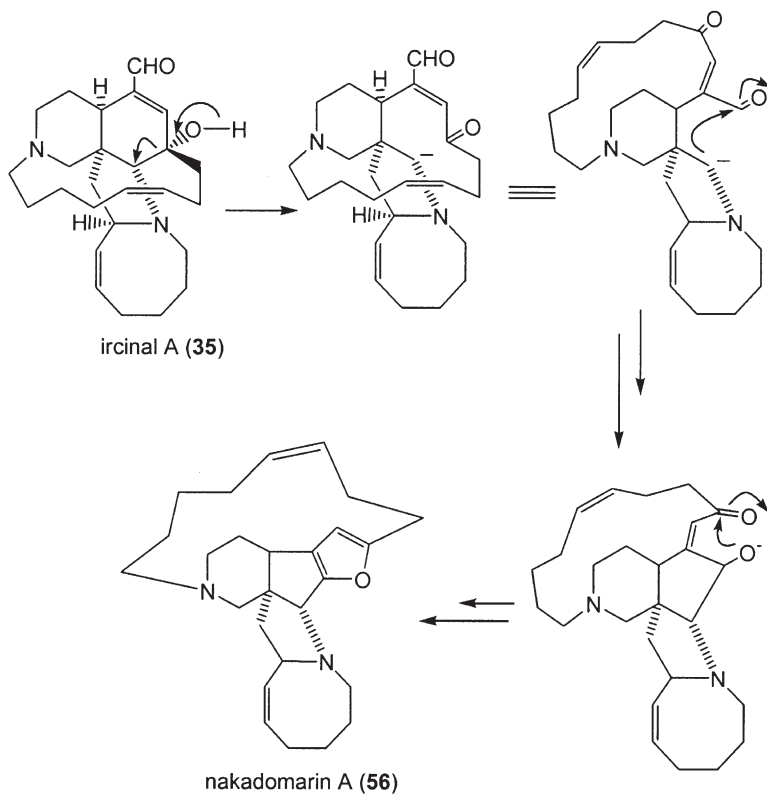
The following proposed schemes have been published for the rational biogenesis of a number of the manzamine and manzamine-related alkaloids and are shown in Schemes 3–6.

## B. INTERMEDIATES

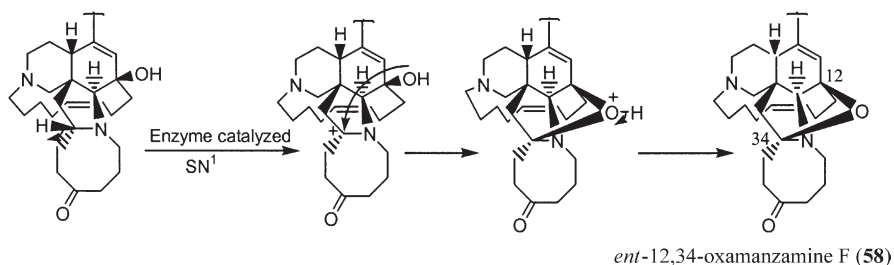
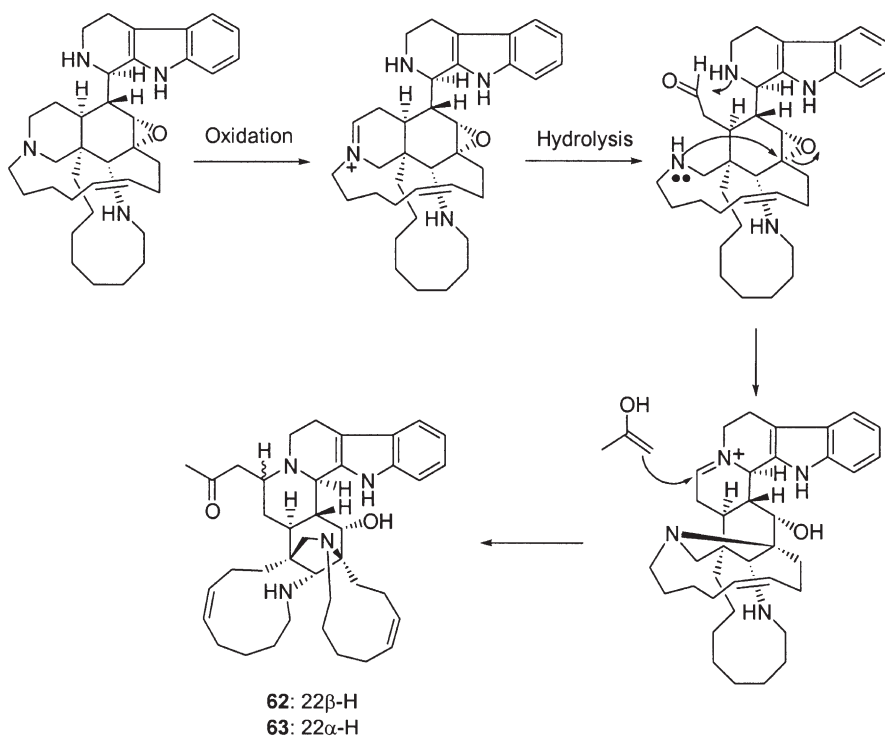
As shown in the Scheme 1, Baldwin *et al.* proposed a biogenetic pathway for manzamines A–C, where the manzamines were presumed to be biosynthesized from an intermediate composed of two dihydropyridine rings with an alkyl residue and a tryptophan unit (5). The proposal was based on the isolation of several reasonable intermediates in the biosynthetic pathway, which include structures similar to the *bis*-3-alkyldihydropyridine macrocyclic intermediate (a) and the pentacyclic intermediate (b). While the isolation of the plausible biosynthetic intermediates ircinals A (35) and B (36) (10), ircinol A (37) (25), ingenamine (31), keramaphidin B



Scheme 3. Biogenesis of ingenamine (**44**), proposed by Kong *et al.* (31).



Scheme 4. Biogenesis of nakadomarin A (**56**) from ircinal A (**35**) (3,57).

Scheme 5. Biogenesis of the 12,34-oxaether bridge in alkaloid **58** (58).Scheme 6. Biogenetic pathway of manadomanzamine A (**62**) and B (**63**) (59).

(2,26), and xestocyclamine B (**28**) have facilitated piecing together a reasonable biogenesis, it is noteworthy to mention that these alkaloids have been isolated from sponges belonging to a number of different genera. As a result, the manzamines are certain to be the key to a better understanding of the bioorganic evolution of the sponges that produce these alkaloids, as well as the evolutionary pressures that

have allowed for the accumulation of metabolites that fit so neatly as intermediates into a sophisticated biosynthetic scheme. In addition, it would seem clear that the microbial associations with the manzamine-producing sponges will play a critical role in understanding the biosynthesis of many of these manzamine or manzamine-related alkaloids.

### C. A TAXONOMIC SURVEY OF SPONGES THAT PRODUCE MANZAMINES AND RELATED ALKALOIDS

A large variety of manzamines and related alkaloids thought to be their biogenetic precursors have been reported primarily from the Order Haplosclerida (Porifera: Demospongiae); 15 or more species in 7 genera and 3 families have been listed as producers (Table I). Two species in 2 genera and 2 families within the phylogenetically distant Order Dictyoceratida have also been found to produce manzamines and related alkaloids.

#### *Haliclona*, *Reniera*, and *Prianos* (Order Haplosclerida: Family Chalinidae)-

The first manzamine identified (A (1)) was extracted from a sponge identified as a *Haliclona* sp. collected off Manzamo Island, Okinawa, in April 1985 by Higa's group (1). Manzamines B, C, and D (2,3,4) were subsequently extracted from possibly the same species after further collections (8). In 1992, Kobayashi *et al.* (14) collected another unidentified *Haliclona* sp. from Iriomote Island, Okinawa, reporting the new alkaloid manzamine Y (13) (12,27). No taxonomic description of the sponge was given in these early papers, other than the sponge was "brownish", and no taxonomic authority was acknowledged for identification.

A further species of *Haliclona* collected from Sodwana Bay, Durban in September 1992 (23), containing haliclorensins (31), was identified as *Haliclona tulearensis* Vacelet, Vasseur & Lévi (62) by an unknown taxonomic authority. The sponge was described as a "fine muddy orange laminate sponge with large oscules on ridges on the surface", but no details of the skeleton were given. Although this sponge appears to be somewhat similar to the description of this type of species (62), spiculation and arrangement of the skeleton will need to be checked to confirm the generic identification. A species of the manzamine-containing genus *Acanthostrongylophora* (Table I) is known from Pemba Island, off Zanzibar. The sponge is a bright orange hemisphere with flush oscules, and has a *Haliclona*-like skeleton of small strongyles. To the inexperienced eye, this sponge could easily be mis-identified as an "unusual species of *Haliclona*" or a thick species of *Prianos*.

Misenine (55) and saraine A (55c), the only two manzamines reported from Mediterranean waters, were isolated from an unidentified species of *Reniera* (36) and *Reniera sarai* Pulitzer-Finali (37), both sponges were collected from the vicinity of Naples, Italy. Neither report contains descriptive details of morphology, skeletal architecture, or spiculation, nor is there a taxonomic authority named.

Confirmation of these identifications can only come from examination of the vouchers that are available (36,37).

The genus *Haliclona* contains species that are characterized by a very simple spiculation of small oxea spicules joined together at their ends to form a regular network. In some species, the spicules form tracts, but the sponges are always soft, compressible and often feel soggy and slightly velvety to the touch. *Reniera* is considered by some taxonomists to be a subgenus of *Haliclona*. These sponges are typically brightly colored and quite small; it is doubtful whether the identifications for the material are correct, as “brownish” is not a common chalinid color, and rather a large amount of material was harvested (8 kg) (8) suggesting a more dense sponge of a different, perhaps petrosid genus. However, without recourse to examination of the specimens that the compounds were isolated from (no sample numbers were given or retained for reference), it is impossible to confirm the taxonomic identity of these sponges.

It is now known that the sponge described as *Prianos* sp., from Manado, Indonesia (15) is closely related to the sponges identified as *Pachypellina* (11), *Xestospongia* (16,28–33,35), and to those reported as an undescribed new genus and species from the Family Petrosiidae (18,58,59) (Table I). These taxa have all been confirmed as species of *Acanthostrongylophora* Hooper, which was previously unrecognizable (63).

***Amphimedon*, *Cribrochalina* (Order Haplosclerida: Family Niphatidae):**

Some 22 alkaloids have been isolated from at least 8 specimens of a sponge identified as an undescribed species of *Amphimedon* (see Table I). Examination of the specimen SS-264 (17,20,57) from Kerama Island, Okinawa, kindly supplied by the original taxonomic authority, Dr J. Fromont, Museum of Western Australia, confirms that the generic identification is correct. Several specimens, SS-326 (12), and SS-932 (19) from Okinawa Island, Okinawa, also appear to be correctly identified by the descriptions given of spicule complement and skeletal arrangements in the literature. However, the remaining reports contain no taxonomic or morphological information, other than that the specimens were collected from Kerama Island, Okinawa. Although we cannot assume that these latter specimens are the same undescribed species of *Amphimedon*, the likelihood that they are is quite high since the material had been collected many times by the same groups. Although no description of the sponge material, spiculation or skeletal arrangements is reported for *Cribrochalina* sp. (13), the taxonomic authority was reputable and thus the identification is most probably correct.

*Amphimedon* and *Cribrochalina* are sister taxa within the Family Niphatidae and are characterized by the possession of small oxeas usually embedded in well-developed spongin. Differences in fiber size and architecture, especially at the sponge surface, and spicule dimensions, differentiate the genera.

***Acanthostrongylophora*, *Xestospongia*, *Petrosia* (Order Haplosclerida: Family Petrosiidae):** All of the species listed in brackets under *Acanthostrongylophora* in Table I are now considered to be species of that genus (MK, R. van Soest, University of Amsterdam, unpublished data), recently re-described by Desqueyroux-Faundez (2002) in (63). Along with the specimens in publications (18,58,59) (Table I), these specimens clearly comprise several species, possibly up to five (58), and are the subject of ongoing taxonomic evaluation. The genus is characterized by the possession of small curved to slightly sinuous strongyles arranged in loose ladder-like tracts to large loose irregular rounded meshes. The sponges are usually quite crumbly, soft and compressible, and have a rough surface due to projecting tracts of spicules. They form irregular thick encrustations to massive lumps with raised oscular chimneys, or can form columns with apical oscular vents. The color is usually brown externally with a deep yellow interior, and the surface is frequently tinged with the maroon of a symbiotic cyanobacteria.

One of the authors (11) considered the blackish-brown sponge that they collected in Sulawesi, Indonesia, to be reminiscent of *Xestospongia* collected off the Coast of Miyako Island, Okinawa in June, 1986 (9). The former sponge was identified as *Pachypellina* (11), but has since been confirmed as a species of *Acanthostrongylophora* (58). Thus, it is highly likely that the material extracted in publication (9) is also a species of *Acanthostrongylophora*. However, confirmation can only be given by examination of voucher material. It seems quite possible that the “brownish” sponge from Kerama Island, Okinawa, identified as *Pellina* sp. (6) by Hoshino, may also be a species of *Acanthostrongylophora*, as this genus typically possesses oxeas or strongyles in tracts.

In contrast to the above specimens, it is likely that the identification of *Xestospongia exigua* (Kirkpatrick), given to the material extracted by Williams *et al.* (24) is correct, as the taxonomic authority is reputable and *Acanthostrongylophora* is exceedingly rare in southern Papua New Guinea, having been found in only two locations: Eastern Fields and the Louisiade Archipelago (MK, unpublished data). The great majority of species are found in Indonesia, with some species known from the Philippines, the northern coast of Papua New Guinea, Micronesia, Fiji, and Tanzania (MK, unpublished data). The geographic distribution is very similar to that of the genus *Diacarnus* (Poecilosclerida: Podospongiidae) (64), but, unlike *Diacarnus*, *Acanthostrongylophora* is less common in the southern Indo-Pacific locations such as the Great Barrier Reef and southern Papua New Guinea, and absent, as far as is known, from New Caledonia.

The identification of *Petrosia contignata* Thiele (13) is probably correct, as the sponge was described as being gray to tan, barely compressible, with oxeas in two size categories, arranged in a dense isotropic multispicular reticulate skeleton.

***Hyrtios* (Order Dictyoceratida: Family Thorectidae) and *Ircinia* (Order Dictyoceratida: Family Irciniidae):** A manzamine alkaloid has been obtained from Red Sea specimens of *Hyrtios erecta* (Keller) (21) and Okinawan specimens of *Ircinia*

sp. (10), both of which would be very difficult to mistake taxonomically, as dictyoceratid sponges do not contain spicules as haplosclerid sponges do. These sponges are fleshy and rubbery and contain only sand-grains embedded in large spongin (collagen) fibres. These sponges are very distantly related to the haplosclerid sponges considered above, and are in completely different taxonomic orders. It is interesting to note that a similar situation exists with the distribution of cytotoxic latrunculins found typically in the Red Sea sponge genus *Negombata* (65a), latrunculins are also found in the dictyoceratid sponge *Petrosaspongia mycofijiensis* (Bakus).

Following this survey (Table I), it now appears that manzamines and related alkaloids are restricted to eight genera (*Haliclona*, *Reniera*, *Amphimedon*, *Cribrochalina*, *Acanthostrongylophora*, *Petrosia*, *Hyrtios*, *Ircinia*) within five families (Chalinidae, Niphatidae, Petrosiidae, Thorectidae, Irciniidae) in two orders (Haplosclerida, Dictyoceratida). The isolation of these alkaloids from such a range of genera has led to the speculation that production of these alkaloids may be due to the biosynthetic participation of microorganisms (6,9,14). While there is an increasing level of data to support a microbial origin, the vast majority of alkaloids are produced by petrosid species, particularly those in *Acanthostrongylophora* (Table I). It may thus be interesting to investigate the potential congruence between the producer microorganisms and sponge phylogenies once the sponge species are confirmed and the microorganism populations are fully characterized. Future taxonomic studies based on morphological examination and comparison of all relevant voucher specimens should reveal the taxonomic and chemotaxonomic relationships within *Acanthostrongylophora* in particular, and shed further light on the distribution of the manzamines and related alkaloids across the Orders Haplosclerida and Dictyoceratida.

#### D. MANZAMINE SPONGE-ASSOCIATED MICROBES

Sixteen different species of sponges from five families have been shown to produce manzamine-related alkaloids to date and the discovery of additional manzamine producing sponges seems highly likely (Table I). One interpretation for the fact that these compounds can be isolated from a diverse array of sponges is that the manzamines are produced by common or closely related microorganism(s) present as symbionts in all of these sponges. This possibility was proposed by Kobayashi *et al.* in 1995 (14) after six species of sponges were known to contain manzamines and appears even more likely now that an even greater diversity of sponges are known to yield manzamines. This possibility warrants careful investigation as the pharmaceutical potential of manzamine alkaloids continues to grow. If these compounds are actually produced by symbiotic bacteria within the sponge, isolation and culture of the producing bacteria may provide an efficient method for production of the compound in fermentation systems. This could ensure a ready supply of a particular manzamine in the high likelihood that one of these drug-leads will advance into clinical trials and applications. Certainly, if it could be shown that manzamines are microbial products, the pharmaceutical and biotechnology community would express a greater interest in this group of



compounds and sponge metabolites in general. The marine natural products community in particular is highly sensitive to the difficulty associated with the supply of sufficient quantities of invertebrate metabolites to allow the preclinical and clinical development. Sustainable sourcing for development has been a strong justification for thorough microbiological evaluation of manzamine-producing sponges. In addition, evidence that sponge-associated microbes may play a significant role in the bioconversion of manzamines to the growing number of alkaloids found in manzamine producing sponges is provided by the biotransformation of 8-hydroxymanzamine A (**7**) and the enantiomer **7a** to manzamine A (**1**) and *ent*-12,34-oxamazamine F (**58**), respectively (**58**).

The culturable microbial communities associated with two undescribed *Acanthostrongylophra* species also known as 01IND35 (**58**) and 01IND52 (**59**), were investigated to obtain isolates that could be examined for manzamine production.

A full molecular community analysis of the entire bacterial community (both culturable and unculturable) was completed for sponge 01IND35 (**Fig. 5**). This molecular approach is essential to explore the full diversity of microbes associated with sponges since typically less than 1% of the bacteria present are culturable by conventional approaches.

Culturable isolates of heterotrophic bacteria were obtained from sponges 01IND 35 and 01IND52 and unequivocally identified by 16S ribosomal RNA gene sequence analysis. Ten isolates were obtained and the nearest relative of each isolate was found by BLAST analysis (**Table V**). Phylogenetic trees can then be inferred for selected isolates, exemplified in **Fig. 5**. Homologous nucleotides were compared using the neighbor-joining, Fitch–Margoliash and maximum parsimony algorithms in the PHYLIP package. Tree topologies were evaluated after 1000 bootstrap re-samplings of the neighbor-joining data. Isolates of this undescribed Petrosiidae genus included several closely-related strains of  $\alpha$ -proteobacteria (**Fig. 5** and **Table V**), a group previously found to be important in culturable sponge-associated bacteria (**65b**). Interestingly, two actinomycetes (designated M41 and M42) were also present in the culturable assemblage (**Table V**). Actinomycetes are recognized as a significant component of sponge-associated microbiota (**65c**) and are of particular interest considering the excellent track-record of these microbes in production of bioactive compounds. The great diversity of bacteria present in the total bacterial community associated with sponge 01IND35 (**Fig. 5**) is striking. Clearly, sponges can be a valuable source of novel microbial isolates for biological screening if methods can be developed to culture a greater proportion of these microbes. Microbiological analysis of manzamine-containing sponges provides valuable insights into the potential of the bacterial communities to produce bioactive metabolites, including manzamines, considering the diversity of these communities and the presence of bacteria known to be producers of important compounds. The role that these microbes play in the biosynthesis or metabolism of the manzamine alkaloids remains to be determined.

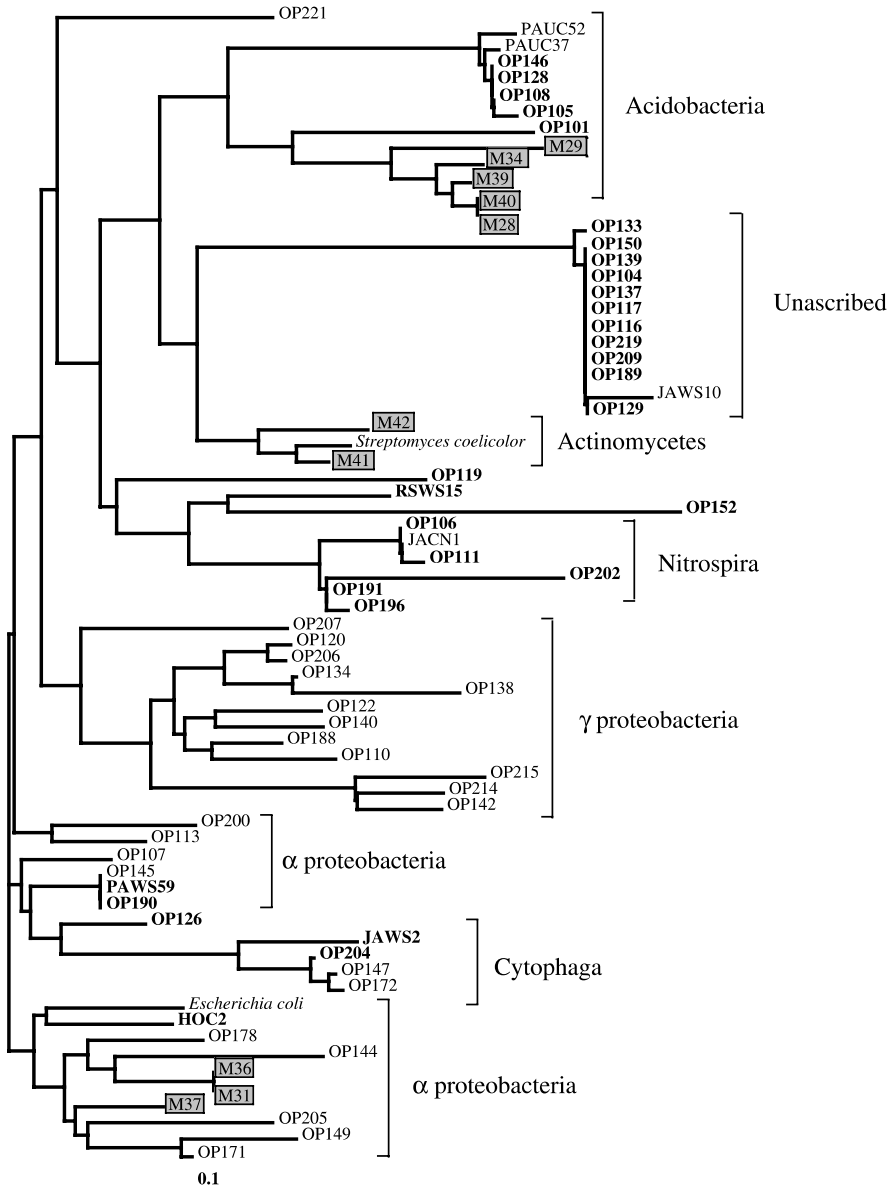


Fig. 5. Neighbor-joining phylogenetic tree from analysis of ca. 500 bp of 16S rRNA gene sequence from clones obtained from *Acanthostrongylophora* sp. (01IND035) (58). The scale bar represents 0.1 substitutions per nucleotide position. Culturable isolates from the sponge are boxed. Sequences shown in **bold** are those whose nearest relatives, based on BLAST searches, are also from sponges.

TABLE V.

Nearest Relatives of Isolates from Two Undescribed Sponges from *Acanthostrongylophora* sp. (01IND035) (58) and (01IND052) (59) Based on BLAST.

Strain designation	Source sponge	Closest relative from BLAST analysis	Accession no. of closest relative
M28	01IND35	<i>Bacillus</i> sp. strain VAN35	AF286486
M29	01IND35	<i>Staphylococcus arlettae</i>	AB009933
M30	01IND35	<i>Brevibacillus borstelensis</i>	AF378230
M31	01IND35	Alpha proteobacterium MBIC3368	AB012864
M34	01IND35	Unidentified firmicute strain HTE831	AB010863
M36	01IND35	Alpha proteobacterium strain NW001	AF295099
M37	01IND35	<i>Pseudomonas</i> sp. strain PB1	AF482708
M39	01IND35	Unidentified eubacterium clone BSV04	AJ229178
M40	01IND35	<i>Bacillus</i> sp. strain VAN35	AF286486
M41	01IND35	<i>Microbacterium barkeri</i>	X77446
M42	01IND35	<i>Micromonospora</i> sp. strain IM-7416	AF131427
M44	01IND52	Shewanella alga	U91547
M45	01IND52	Alpha proteobacterium strain NW001	AF295099
M46	01IND52	Alpha proteobacterium strain NW001	AF295099
M47	01IND52	Alpha proteobacterium MBIC3368	AB012864
M52	01IND52	<i>Shewanella woodyi</i>	AF003549
M53	01IND52	Alpha proteobacterium NW001	AF295099
M56	01IND52	<i>Pseudomonas</i> sp. strain PB1	AF482708

#### IV. Synthesis

The unusual ring system of the manzamines has attracted great interest as one of the most challenging natural product targets for total synthesis. Synthetic studies of the manzamines have been reported by a number of groups and this part of the review is limited to the most recently completed total syntheses, as well as semisynthetic studies that have been the key for the structural and stereochemical determination of these alkaloids.

## A. TOTAL SYNTHESIS

Among the more reasonable manzamine targets is manzamine C (**3**), which has been synthesized by Torisawa *et al.* (Scheme 7) (66,67). A number of research groups have contributed syntheses of manzamine C or its precursors (68–73).

A total synthesis of the sophisticated manzamine A (**1**) skeleton was not achieved until Pandit's group published their work in 1996 (Scheme 8) (74). They first reported a total synthesis of the pentacyclic nuclei of manzamine A (**1**) (74). Before Pandit's report, Nakagawa *et al.* reported the synthesis of a tetracyclic core of manzamine A (**1**) (Scheme 9) (75).

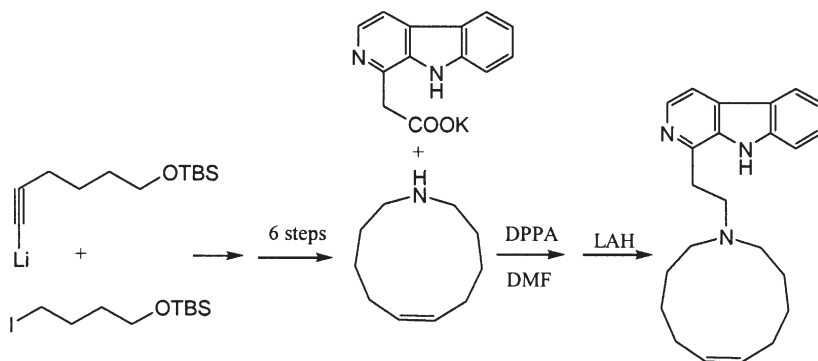
In 1998, Winkler's group reported the first total syntheses of ircinol A, ircinal A, and manzamines A & D (Scheme 10) (76). There are over 77 publications reporting the total synthesis of manzamine A, related alkaloids, potential key intermediates and substructures, attesting to the level of interest and challenge involved in the synthesis of the manzamine alkaloids (77–153).

## B. SEMISYNTHESIS

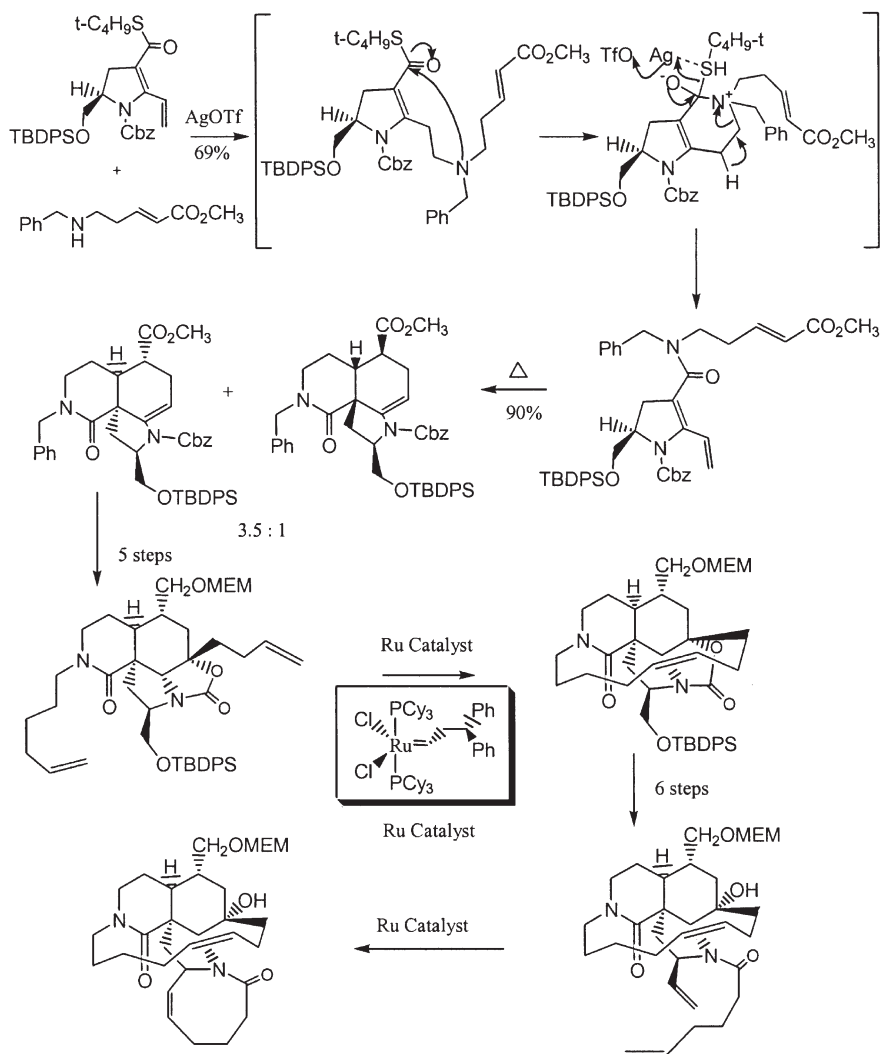
Ircinals A (**35**) and B (**36**), the biogenetic precursors of the manzamine alkaloids, were isolated from an Okinawan sponge *Ircinia* sp. (10). Aldehydes **35** and **36** were successfully converted into manzamines A (**1**) and J (**9**), respectively, through a Pictet-Spengler cyclization (154) with tryptamine (step I, yield: 37%) followed by 2,3-dichloro-5,6-dicyano-*p*-benzoquinone (DDQ) oxidation (step II, yield: 54%) (Scheme 11) (10).

## C. BIOMIMETIC METHODS

8-Methoxymanzamine A was generated from 8-hydroxymanzamine A (manzamine G, **7**) by using TMSCHN<sub>2</sub> (11). Treatment of manzamine L (**10**)

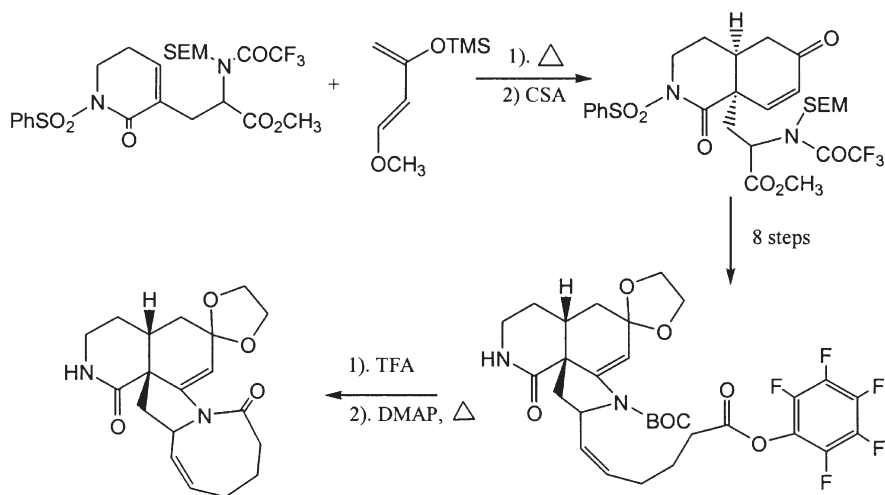


Scheme 7. Synthesis of Manzamine C (**3**) by Torisawa *et al.* (66,67).



Scheme 8. Synthesis of the pentacyclic core of manzamine A (**1**) by Pandit *et al.* (74).

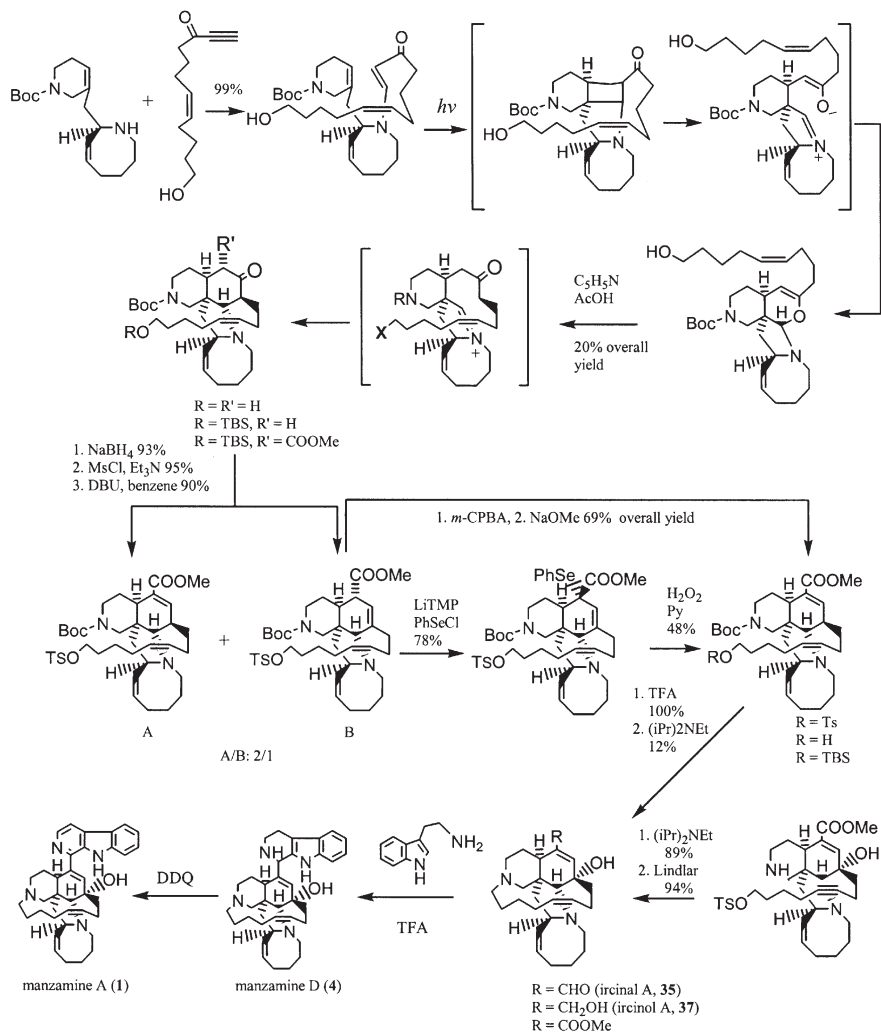
with DDQ yielded the corresponding manzamine J (**9**) (27). DDQ oxidation of 3,4-dihydro-6-hydroxymanzamine A (**17**) and 3,4-dihyromanzamine J (**18**) yielded 6-hydroxymanzamine A (manzamine Y, **13**) and manzamine J (**9**), respectively (17). Manzamine A (**1**) was shown to be generated from 8-hydroxy manzamine A (**7**) in good yields using *Fusarium solani* and *Streptomyces seokies* providing further evidence for the biogenesis of some of these alkaloids from a sponge-associated



Scheme 9. Synthesis of the tetracyclic core of manzamine A (**1**) by Nakagawa *et al.* (75).

microbe and the potential biocatalysis and biotransformations have for the production of analogs of these complex alkaloids (58*b*). The 3,4-dihydro analogs of the manzamine alkaloids, e.g., 3,4-dihydromanzamine A (**14**), are likely the direct precursors which generate manzamine A through dehydrogenation (12). In fact, **14** can be easily converted into **1** by daylight (2). Manzamines X (**12**) and Y (**13**) are examples of 6-hydroxymanzamine-type alkaloids (12,14), and **13** is presumed to follow manzamine A (**1**) via oxidation at the C-6 position. The tetrahydrofuran ring moiety in **12** is then presumed to be biosynthesized from **13** via initial allylic oxidation at C-31 in **13**, subsequent migration of the double bond ( $\Delta^{32} \rightarrow \Delta^{33}$ ), and cyclization between the hydroxyl at C-31 and C-34 as depicted in Scheme 12 (14). On the other hand, a biogenetic pathway of the xestomanzamines A (**27**) and B (**28**) is presumed to occur as depicted in Scheme 13 (14). That is, these alkaloids could potentially be biosynthesized from an *N*-methyl histidine and a tryptamine unit.

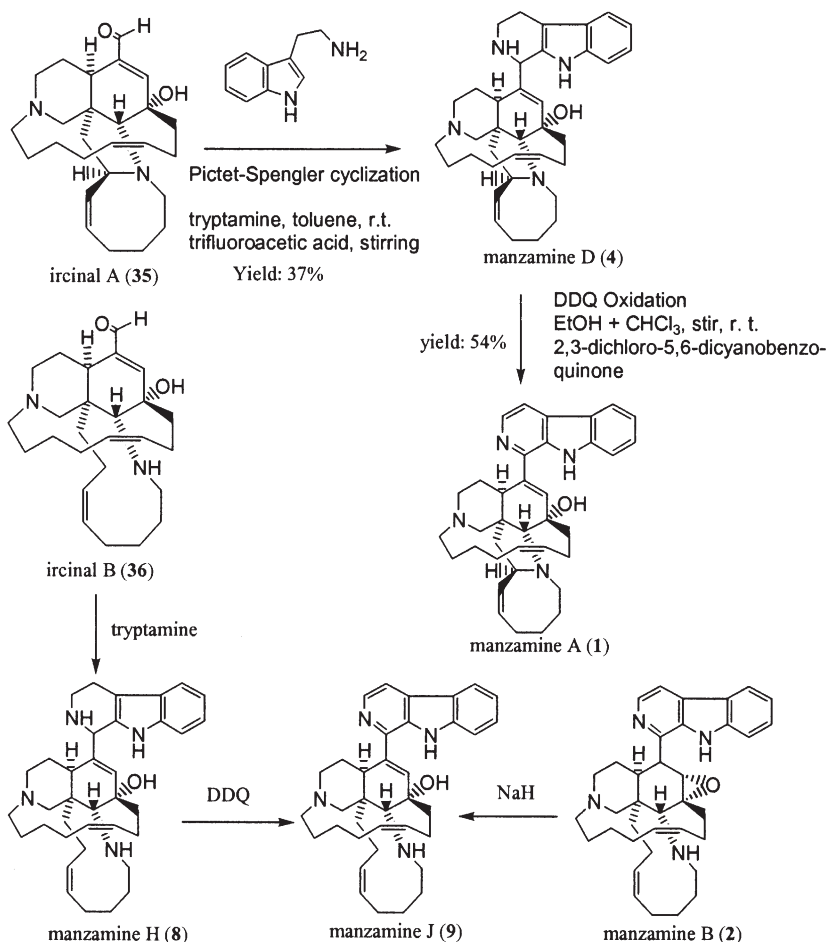
As discussed earlier, a species of *Amphimedon* sp. yielded ircinal A (**35**) and B (**36**), as well as ircinol A (**37**) and B (**38**) (27). Ircinal A (**35**) and B (**36**) were then converted into manzamines A (**1**) and J (**9**), respectively, through a Pictet-Spengler cyclization with tryptamine, followed by DDQ oxidation. Treatment of ircinal A (**35**) with DIBALH afforded a reductive product (**35a**), whose spectral data were identical with those of ircinol A (**37**). However, the sign of the optical rotation was opposite {**35a**,  $[\alpha]_D^{18} +20^\circ$  (*c* 0.2, MeOH); **37**,  $[\alpha]_D^{18} -19^\circ$  (*c* 0.5, MeOH)} (Scheme 14) (2,25). This result revealed that compound **37** is clearly an enantiomer of the alcoholic form at C-1 of ircinal A (**35**) (2,25). In the same way, **38** was shown to be an enantiomer of the alcoholic form at C-1 of **36** (2,25). Alkaloids **37** and **38** were the first examples possessing the opposite absolute configurations to those of the



Scheme 10. The Total Synthesis of Ircinal A (**35**), Ircinol A (**37**), Manzamines A (**1**) and D (**4**) by Winkler *et al.* (**76**).

previously reported manzamine alkaloids, followed by the recently reported new enantiomers (**6b** and **7a**) of manzamine F (**6**) and 8-hydroxymanzamine A (manzamine G, **7**).

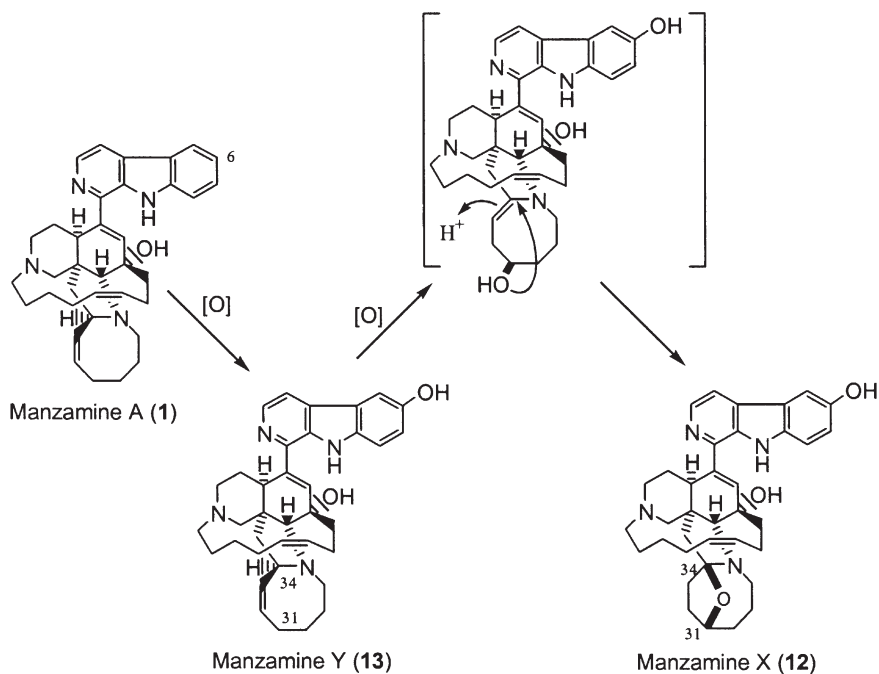
Keramaphidin B (**39**) is a unique pentacyclic alkaloid with an unprecedented skeleton isolated from *Amphimedon* sp., and in addition, several alkaloids with similar skeletons to that of **39** such as ingenamine, ingenamines B–F,



Scheme 11. Semisynthesis of Manzamines A (1), D (4), H (8) and J (9) via Pictet-Spengler Cyclization (2,10).

ingamines A and B, and xestocyclamines A and B from *Xestospongia* have also been reported. These structures are very close to those of the corresponding biogenetic intermediate of manzamines A (1) and B (2) proposed by Baldwin *et al.*, in which a *bis*-3-alkyldihydropyridine macrocycle may be converted through a Diels-Alder-type [4+2] intramolecular cycloaddition into a pentacyclic intermediate like 39, which in turn provides manzamines A (1) and B (2) via a tetracyclic intermediate such as ircinals A (35) and B (36). This may explain the fact that manzamines A (1) and B (2) and keramaphidin B (39) possess the same absolute configurations, and indeed, ircinals A (35) and B (36) were found to have the same absolute configurations as those of manzamines A (1) and B (2). Keramaphidin B



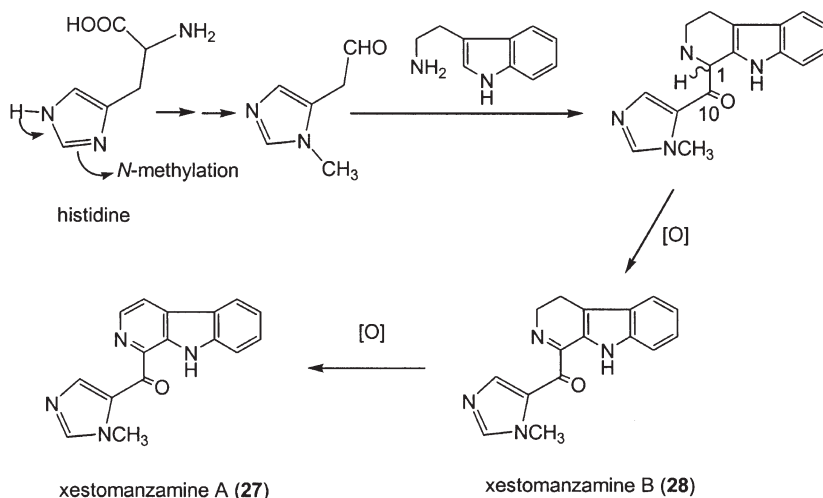


Scheme 12. Biomimetic Transformations among Manzamines A (**1**), X (**12**), and Y (**13**) (14).

(**39**) was optically active as mentioned previously (26,27). However, the crystal of **39** employed for X-ray analysis was revealed to be racemic. On the other hand, ingenamine, ingamine A, and ingenamine E were reported to be antipodal to the manzamines and ircinals. Both enantiomers of keramaphidin B (**39**) were separated by chiral HPLC [the ratio of (+)- and (–)-forms of the crystals was *ca.* 1 : 1], of which one maybe a biogenetic precursor of ircinals A (**35**) and B (**36**) and manzamines A (**1**) and B (**2**), while the other may be associated with the antipodes of the manzamine alkaloids, such as ircinols A (**37**) and B (**38**) (27). Synthetic strategies that utilized the likely biogenesis to varying degrees for the preparation of the manzamines are reported by a number of research groups (155–169).

## V. Pharmacology

In addition to being the first reported manzamine alkaloid, manzamine A (**1,1a**) has also been the subject of the greatest number of pharmacology studies revealing a portion of the biological activity for this complex alkaloid. Manzamine A hydrochloride (**1a**) showed an  $IC_{50}$  of 0.07  $\mu\text{g/mL}$  inhibiting the growth of P388 mouse leukemia cells (1). Keramamine-A (manzamine A) showed antimicrobial activity against *Staphylococcus aureus* with a minimum inhibitory concentration

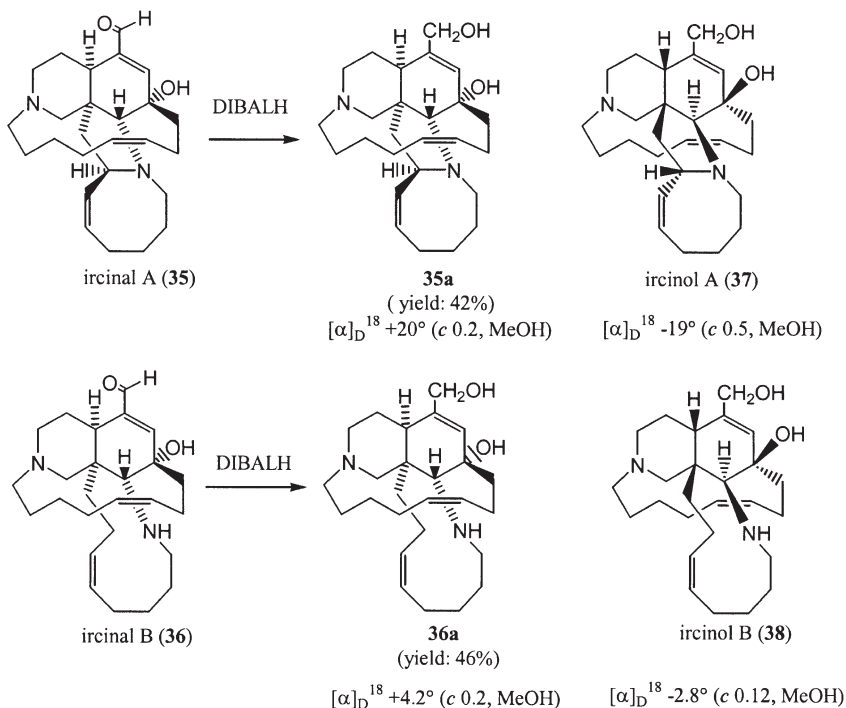


Scheme 13. Biogenetic Pathway of Xestomanzamines A (27) and B (28) (14)

(MIC) of 6.3  $\mu\text{g/mL}$  (6). Manzamine A (1) showed significant activity against KB ( $\text{IC}_{50}$  0.05  $\mu\text{g/mL}$ ), LoVo ( $\text{IC}_{50}$  0.15  $\mu\text{g/mL}$ ), and HSV-II (MIC 0.05  $\mu\text{g/mL}$ ) cells *in vitro* (11). Manzamine A can elicit an 80% growth inhibition of the insect *Spodoptera littoralis* larvae at 132 ppm (16). In addition, manzamine A exhibited insecticidal activity toward neonate larvae of the polyphagous pest insect *Spodoptera littoralis* with an  $\text{ED}_{50}$  of 35 ppm when incorporated into an artificial diet and offered to larvae in a chronic feeding bioassay.

Manzamine A was also active (antibacterial) against the Gram-positive bacteria *Bacillus subtilis* and *Staphylococcus aureus*. Manzamine A exhibited cytotoxicity against L1578y mouse lymphoma cells with an  $\text{ED}_{50}$  1.8  $\mu\text{g/mL}$ . Among the most promising activities of manzamine A is the fact that it inhibits the growth of the rodent malaria parasite *Plasmodium berghei* *in vivo*. More than 90% of the asexual erythrocytic stages of *P. berghei* were inhibited after a single intraperitoneal injection of manzamine A into infected mice. A remarkable aspect of manzamine A treatment is its ability to prolong the survival of highly parasitemic mice, with 40% recovery 60 days after a single injection. Oral administration of an oil suspension of manzamine A or (–)-8-hydroxymanzamine A ( $2 \times 100 \mu\text{M/kg}$ ) produced a significant reduction (90%) in parasitemia. The plasma manzamine A concentration peaked 4 h after injection and remained high even at 48 h. Morphological changes of *P. berghei* were observed 1 h after treatment of infected mice. Manzamine A also induced 98–99% inhibition of *Mycobacterium tuberculosis* (H37Rv) with an MIC < 12.5  $\mu\text{g/mL}$ , and it exhibits an MIC endpoint of 1.56  $\mu\text{g/mL}$  (18,170).

Initial *in vivo* studies of manzamine A against *P. berghei* provided a number of intriguing characteristics for this drug-lead as compared with either chloroquine or



Scheme 14. Conversion of Ircinals A (35) and B (36) into their Alcohol Forms (35a and 36a) (2,25).

artemisinin. At dosages of 50 and 100  $\mu\text{mol/kg}$  (i.p.) manzamine A (and 8 hydroxymanzamine A) showed significant improvements in survival times over mice treated with either chloroquine or artemisinin (170). In addition, it was observed that manzamine A possessed a rapid onset of action (1–2 hours) against malaria in mice and provided a continuous and sustained level of the drug in plasma when measured as long as 48 hours after administration. Manzamine A and chloroquine were both shown to be toxic to mice at an intraperitoneal (i.p.) dose of 500  $\mu\text{mol/kg}$ . However, the toxicity of manzamine A is slower acting than chloroquine suggesting that the *in vivo* toxicity of manzamine A may be associated with its cytotoxicity. The fact that mice treated with a single 100  $\mu\text{mol/kg}$  dose of manzamine A could survive longer carrying fulminating recurrent parasitemia and in some cases clear the parasite lead to speculation that manzamine A induced an immunostimulatory effect.

In order to further evaluate the effect that manzamine A may have on the immune system of *P. berghei* infected mice the serum concentrations of immunoglobulin G (IgG), interferon- $\gamma$  (IFN- $\gamma$ ), interleukin-10 (IL-10), and tumor necrosis factor- $\alpha$  (TNF- $\alpha$ ) were evaluated (18). Th1-mediated immunity was

found to be suppressed in mice infected with *P. berghei* and treated with manzamine while Th2-mediated immunity was found to be up-regulated. IL-10 and IgG concentrations did not increase with manzamine A alone suggesting that the immune-mediated clearance of malaria in mice maybe a product of the long half-life of manzamine A resulting in a delayed rise of the parasitemia. This delayed rise in parasitemia may provide the infected animal the time needed to up-regulate a Th2-mediated response. In addition, the possibility that manzamine A and the other active manzamines form a conjugate with a malaria protein may also help explain the Th2-mediated immune response.

Manzamine A was also selected for *in vivo* testing against *Toxoplasma gondii* because it was the most effective *in vitro* of the manzamines assayed. A daily i.p. dose of 8 mg/kg of manzamine A, for 8 consecutive days, beginning on day 1 following the infection prolonged the survival of Swiss Webster (SW) mice to 20 days, as compared with 16 days for the untreated control. These data indicate that the manzamines are valuable candidates for further investigations and development as leads against several serious infectious diseases, and in particular manzamine A is quite clearly a new and promising antimalarial agent (18,170). The effectiveness of manzamine A against malaria in laboratory mice, as well as tuberculosis *in vitro* suggests that they could have an extraordinary impact on infectious diseases in developing countries. The fact that manzamine A is found in a diversity of organisms and in reasonable high yields would facilitate the potential development of cost-effective antimalarial drugs in regions of the world that are saddled with the disease burden. In addition, the diversity of biological activity associated with this molecule further supports the growing possibility that these alkaloids are broad-spectrum antiparasitic-antibiotics generated ultimately by the sponge-associated microbial communities.

Manzamine B (2) with the C-11,12 epoxide group exhibited an  $IC_{50}$  of 6  $\mu\text{g/mL}$  against P388 leukemia cells *in vitro* (7). In the above assay, manzamines C (3) and D (4) exhibited  $IC_{50}$  values of 3 and 0.5  $\mu\text{g/mL}$  (7).

Manzamine E (5) showed an  $IC_{50}$  of 5  $\mu\text{g/mL}$  against P388 murine leukemia cells (9). Manzamine F (6, keramamine-B) showed antimicrobial activity against *Staphylococcus aureus* with a minimum inhibitory concentration (MIC) of 25  $\mu\text{g/mL}$  (6). Manzamine F (6) also showed an  $IC_{50}$  of 5  $\mu\text{g/mL}$  against P388 murine leukemia cells (9), 50.6% growth inhibition of the insect *S. littoralis* larvae (dose = 132 ppm), and cytotoxicity against L5178 mouse lymphoma cells of an  $ED_{50}$  of 2.3  $\mu\text{g/mL}$ . Manzamine F did not exhibit antimalarial activity. However, ent-manzamine F (6b) induced 98–99% inhibition of *Mycobacterium tuberculosis* (H37Rv) with a MIC of < 12.5  $\mu\text{g/mL}$  (18).

(+)-8-Hydroxymanzamine A (7, also known as manzamine G or manzamine K) was relatively active in the KB ( $IC_{50}$  0.30  $\mu\text{g/mL}$ ), LoVo ( $IC_{50}$  0.26  $\mu\text{g/mL}$ ), and HSV-II (MIC 0.1  $\mu\text{g/mL}$ ) assays (11). (–)-8-Hydroxymanzamine

A exhibits improved activity against P388 with an  $IC_{50}$  of 0.25  $\mu\text{g}/\text{mL}$ . This enantiomer displayed antimalarial activity *in vivo*, which was assayed against *P. berghei* with a single intraperitoneal (i.p.) dose of 100  $\mu\text{M}/\text{kg}$  and no apparent toxicity. It efficiently reduced parasitemia with an increase in the average survival days of *P. berghei*-infected mice (9–12 days), as compared with untreated controls (2–3 days). Three 50  $\mu\text{moles}/\text{kg}$  i.p. doses were found to be curative and totally cleared the parasite and two oral doses (100  $\mu\text{moles}/\text{kg}$ ) provided a notable reduction of parasitemia. (–)-8-Hydroxymanzamine A (**7a**) induced 98–99% inhibition of *Mycobacterium tuberculosis* (H37Rv) with MIC < 12.5  $\mu\text{g}/\text{mL}$ , and it exhibits a MIC endpoint of 3.13  $\mu\text{g}/\text{mL}$  (**18**).

Manzamines H (**8**) and J (**9**) exhibited cytotoxicity against L1210 murine leukemia cells with  $IC_{50}$  values of 1.3 and 2.6  $\mu\text{g}/\text{mL}$ , and KB human epidermoid carcinoma cells with  $IC_{50}$  values of 4.6 and > 10  $\mu\text{g}/\text{mL}$  *in vitro*, respectively (**10**). Manzamine L (**10**) exhibited cytotoxicity against murine lymphoma L1210 cells and human epidermoid carcinoma KB cells ( $IC_{50}$  3.7 and 11.8  $\mu\text{g}/\text{mL}$ , respectively) and antibacterial activity against: *Sarcina lutea*, *Staphylococcus aureus*, *Bacillus subtilis*, and *Mycobacterium* 607 (MIC 10, 10, 10, and 5  $\mu\text{g}/\text{mL}$ , respectively) (**27**).

Manzamine M (**11**) showed cytotoxicity against murine leukemia L1210 cells ( $IC_{50}$  1.4  $\mu\text{g}/\text{mL}$ ) (**17**). Manzamine X (**12**) exhibited weak cytotoxicity against KB cells with an  $IC_{50}$  of 7.9  $\mu\text{g}/\text{mL}$  (**14**). Manzamine Y (6-hydroxymanzamine A, **13**) and 3,4-dihydromanzamine A (**14**) showed antibacterial activity against the Gram-positive bacteria *Sarcina lutea* (MIC value, 1.25 and 4  $\mu\text{g}/\text{mL}$ , respectively). Alkaloids **13** and **14** were cytotoxic against L-1210 ( $IC_{50}$  values, 1.5 and 0.48  $\mu\text{g}/\text{mL}$ , respectively) and KB cells ( $IC_{50}$  2.5 and 0.61  $\mu\text{g}/\text{mL}$ , respectively) *in vitro* (**12**). 8-Hydroxy-2-*N*-methyl-1,2,3,4-tetrahydromanzamine A (**16**) was cytotoxic to P388 leukemia cells, and exhibited an  $ED_{50}$  of 0.8  $\mu\text{g}/\text{mL}$  (**13**). 3,4-Dihydro-6-hydroxymanzamine A (**17**) and 3,4-dihydromanzamine J (**18**) showed cytotoxicity against murine leukemia L1210 cells ( $IC_{50}$  3.1 and 12.5  $\mu\text{g}/\text{mL}$ , respectively) (**17**). The *N*-oxides (**19**, **21**) showed cytotoxicity *in vitro* against L1578y mouse lymphoma cells with an  $ED_{50}$  value of 1.6  $\mu\text{g}/\text{mL}$  (**16**).

Kauluamine (**25**) was inactive against tumor cell lines, but showed moderate immunosuppressive activity (MLR  $IC_{50}$  1.57  $\mu\text{g}/\text{mL}$ , LcV  $IC_{50}$  L > 25  $\mu\text{g}/\text{mL}$ , LcV/MLR > 16) in the mixed lymphoma reaction (**15**). *neo*-Kauluamine (**26**) possesses cytotoxicity with an  $IC_{50}$  of 1.0  $\mu\text{g}/\text{mL}$ , against human lung and colon carcinoma cells (**18**). It also displayed significant antimalarial activity *in vivo*, which was assayed against *Plasmodium berghei* with a single intraperitoneal (i.p.) dose of 100  $\mu\text{M}/\text{kg}$  and no apparent toxicity. It efficiently reduced parasitemia with an increase in the average survival time of *P. berghei*-infected mice (9–12 days), as compared with untreated controls (2–3 days).

Xestomanzamine B (**28**) exhibited weak cytotoxicity against KB cells with an  $IC_{50}$  14.0  $\mu\text{g}/\text{mL}$  (**14**). Ircinals A (**35**) and B (**36**) exhibited cytotoxicity against

L1210 murine leukemia cells with  $IC_{50}$  values of 1.4 and 1.9  $\mu\text{g/mL}$  and KB human epidermoid carcinoma cells with  $IC_{50}$  values of 4.8 and 3.5  $\mu\text{g/mL}$  *in vitro*, respectively (10). Ircinols A (37) and B (38) were cytotoxic against L1210 cells ( $IC_{50}$  values: 2.4 and 7.7  $\mu\text{g/mL}$ , respectively) and KB cells ( $IC_{50}$  values: 6.1 and 9.4  $\mu\text{g/mL}$ , respectively). Ircinol A (37) showed inhibitory activity against endothelin converting enzyme ( $IC_{50}$ : 55  $\mu\text{g/mL}$ ) (25).

Keramaphidin B (39) was cytotoxic against P388 murine leukemia and KB human epidermoid carcinoma cells with an  $IC_{50}$  of 0.28 and 0.3  $\mu\text{g/mL}$ , respectively (26). Xestocyclamine A (40) was moderately potent against PKC ( $IC_{50}$  4  $\mu\text{g/mL}$ ) and also exhibited activity in a whole cell IL-1 release assay with an  $IC_{50}$  of 1  $\mu\text{M}$ . This action appeared to be selective, as compound 40 was inactive against other cancer-relevant targets, including PTK and IMPDH. Finally, compound 40, at doses as high as 100  $\mu\text{M}$ , did not show *in vitro* growth inhibition effects against cancer cells in the NCI's disease oriented screening program (29). Ingamines A (42) and B (43) both showed *in vitro* cytotoxicity against murine leukemia P388 with an  $ED_{50}$  of 1.5  $\mu\text{g/mL}$  (30). Ingenamine (44) showed cytotoxicity against murine leukemia P388 ( $ED_{50}$  1  $\mu\text{g/mL}$ ) (31). Madangamine A (50) showed significant cytotoxic activity toward a number of tumor cell lines, including murine leukemia P388 ( $ED_{50}$  0.93  $\mu\text{g/mL}$ ) and human lung A549 ( $ED_{50}$  14  $\mu\text{g/mL}$ ), brain U373 ( $ED_{50}$  5.1  $\mu\text{g/mL}$ ), and breast MCF-7 ( $ED_{50}$  5.7  $\mu\text{g/mL}$ ) cancer cell lines (33). The saraines, such as saraine A (55c), generally display significant biological properties including, vasodilative, antineoplastic, and cytotoxic activities (53). Nakadomarin A (56) showed cytotoxicity against murine lymphoma L1210 cells ( $IC_{50}$  1.3  $\mu\text{g/mL}$ ) and inhibitory activity against cyclin dependent kinase 4 ( $IC_{50}$  9.9  $\mu\text{g/mL}$ ). Compound 56 exhibited antimicrobial activity against a fungus (*Trichophyton mentagrophytes*, MIC 23  $\mu\text{g/mL}$ ) and a Gram-positive bacterium (*Corynebacterium xerosis*, MIC 11  $\text{mg/mL}$ ) (57).

*ent*-12,34-Oxamanzamines E (57) and F (58), as well as 12,34-oxamanzamine A (59) were isolated from three Indo-Pacific sponges (58). The biocatalytic transformation of *ent*-8-hydroxymanzamine A (7a) to 58, using *Nocardia* sp. and *Fusarium oxysporium* ATCC 7601, has also been achieved (58). Eleven heterotrophic bacterial isolates, including actinomycetes and  $\alpha$ -proteobacteria, were isolated from one of these sponges in a preliminary investigation to identify a possible microbial origin for these alkaloids. The potent *in vitro* activity of the manzamines against malaria and the AIDS opportunistic infection (OI) pathogen, *Mycobacterium tuberculosis*, is also presented. The *in vitro* activity of manzamines against *Mycobacterium tuberculosis* (H37Rv) and the malaria parasite *Plasmodium falciparum* is reported with most manzamines showing activity against *M. tuberculosis* with MICs < 12.5  $\text{g/mL}$ . (+)-8-Hydroxymanzamine A had an MIC 0.91  $\mu\text{g/mL}$ , indicating improved activity for the (+) over the (−) enantiomer. The significant activity of ircinol A (1.93  $\mu\text{g/mL}$ ) indicates that the  $\beta$ -carboline moiety is not essential for activity against Mtb *in vitro*. This result suggests the candidacy of ircinol A as a possible antituberculosis lead for further development since it showed minimal toxicity and reduced structural complexity. The decreased activity of 57, 58,

and **59** against *M. tuberculosis* and *P. falciparum* is clearly associated with the changes in the molecule that result during the formation of the new C-12, C-34 oxygen bridge. This data provides significant improvements in the understanding of the SAR against malaria and Mtb (**58**).

A crude extract of an unidentified Palauan marine sponge showed initial inhibitory bioactivities in a yeast assay for inhibitors of methionine aminopeptidase-2 (Met AP-2). Bioassay-directed fractionation indicated that the activity was concentrated in the CH<sub>2</sub>Cl<sub>2</sub>-soluble fraction, and chromatography on silica gel led to the isolation of two new bioactive alkaloids *epi*-manzamine D (**60**) and *N*-methyl-*epi*-manzamine D (**61**) (**61**). The author's initial interest in the extract was due to its potential antiangiogenic activity, the differential activity observed between the  $\Delta$ map1 and  $\Delta$ map2 yeast strains was not significant for either compound **60** or **61**, and the authors thus conclude that neither compound has antiangiogenic activity. Both **60** and **61** did, however, show cytotoxic activity against HeLa and B16F10 cell lines. The greatest potency (IC<sub>50</sub> 0.1  $\mu$ g/mL) was observed for **61** against the B16F10 cell line (**61**).

The two novel manzamine-related alkaloids, manadomanzamines A (**62**) and B (**63**), were obtained from an Indonesian species of *Acanthostrongylophora* (**59**). The manadomanzamines **62** and **63** represent an unprecedented rearrangement of the manzamine skeleton and exhibit significant activities against Mtb and human immunodeficiency virus (HIV-1), with moderate cytotoxicity (**59**).

Both **62** and **63** exhibited strong activity against Mtb with MIC values of 1.86 and 1.53  $\mu$ g/mL, indicating that the manadomanzamines are a new class of antituberculosis leads. Manadomanzamines A and B exhibited modest cytotoxic activity against human tumor cells. Manadomanzamine A is active against human lung carcinoma A-549 and human colon carcinoma H-116 with IC<sub>50</sub> values of 2.5 and 5.0  $\mu$ g/mL while manadomanzamine B is only active against H-116 with an IC<sub>50</sub> value of 5.0  $\mu$ g/mL. Manadomanzamines A (**62**), B (**63**), and xestomanzamine A (**27**) are active against human immunodeficiency virus (HIV-1) with EC<sub>50</sub> values of 11.4, 62.7, and 42.7  $\mu$ M, respectively. Manadomanzamine B and xestomanzamine A are active against the fungus *Cryptococcus neoformans* with IC<sub>50</sub> values of 3.5 and 6.0  $\mu$ g/mL. Manadomanzamine A was active against the fungus *Candida albicans* with an IC<sub>50</sub> of 20  $\mu$ g/mL. It is worthy to note that manadomanzamines A, B, and xestomanzamine A, unlike manzamine A, 8-hydroxymanzamine A, and neo-kualuamine which are extraordinarily active antimalarial agents (**18,170**), only exhibited marginal activity against the malaria parasite indicating that the polycyclic ring system of the manzamine structure is important for antimalarial activity (**59**).

$\beta$ -Carboline containing manzamines 32,33-dihydro-31-hydroxymanzamine A (**64**), 32,33-dihydro-6,31-dihydroxymanzamine A (**65**), and 32,33-dihydro-6-hydroxymanzamine A-35-one (**66**) were isolated from an Indonesian sponge (**60**). Additional data regarding the *in vitro* activity of the manzamines against Mtb

(H37Rv), *P. falciparum*, and *Leishmania donovani*, the causative agent for visceral leishmaniasis, is reported. Most manzamines were active against *M. tuberculosis* with MICs < 12.5  $\mu\text{g/mL}$ . Although alkaloids **64** and **66** were inactive against malaria and leishmania, these results provide valuable information on the structural moieties required for activity against malaria and leishmania. This observation further supports the previous report (18), which indicates that reduction of the C32–C33 olefin and oxidation of C-31 also significantly reduces the antimalarial activity for the manzamine alkaloids *in vivo*. These combined data strongly suggest that the ability of the C-34 allylic carbon to form a stabilized carbocation after oxidation both in cell culture and in animals, followed by the inherent nucleophilic attack, may play a critical role in the biological activity of the manzamine alkaloids against the malaria parasite. The significant difference in biological activities of manzamine A, manzamine E, and their corresponding 12,34-*oxa*-derivatives indicate that the C-12 hydroxy, the C-34 methine, or the conformation of the lower aliphatic rings play a key role in the antimalarial and leishmanicidal activity and provides valuable insight into the structural moieties required for activity against malaria and leishmania parasites. The significant leishmanicidal activity of ircinol A (IC<sub>50</sub> 0.9  $\mu\text{g/mL}$  and IC<sub>90</sub> 1.7  $\mu\text{g/mL}$ ) indicates that the  $\beta$ -carboline moiety is not essential for activity against the leishmania parasite *in vitro*. The cytotoxic values of 6-deoxymanzamine X and manzamine X against A-548, HT-29, H-116, and MS-1 cell lines with IC<sub>50</sub> ( $\mu\text{g/mL}$ ), respectively, are as follows: 1, 5.1; 0.5, 0.5; 0.5, 5.1; 1, 5.1. The anti HIV (EC<sub>50</sub>) activity of manzamine A, 8-hydroxymanzamine A, and 6-deoxymanzamine X against human PBM cells acutely infected with HIV-1/LAI is 0.59, 4.2, and 1.6  $\mu\text{M}$ , respectively (60).

## VI. Conclusions

The manzamine alkaloids are unique and viable, leads to the treatment of malaria, as well as other infectious or tropical parasitic diseases, based on their significant activity in animal models. In addition, the relatively wide range of biological activity for the manzamines *in vitro* raises the question that perhaps these molecules maybe broad-spectrum antiparasitic antibiotics generated by a sponge-associated microbe. The ecological relationship between the microbial communities and the sponge in the case of the manzamines is particularly intriguing due to the structural complexity of these alkaloids.

In spite of the necessity of the  $\beta$ -carboline moiety for *in vitro* antimalarial activity, it has little effect on the antituberculosis activity *in vitro*, suggesting that several different possible mechanisms of action are likely to exist. Although further investigations are required to completely understand the SAR for this class of compounds, the absence of activity associated with the C-12, C-34 oxygen bridge system provides valuable insight into the structural moieties required for activity against Mtb and malaria. In addition, the formation of this new oxygen bridge and its reduced biological activity suggests that this alkaloid maybe a potential intermediate in the development of resistance to this class of bioactive alkaloids.



The significant reduction in biological activity observed against *P. falciparum* for the C-12, C-34 oxygen bridge system indicates that the C-12 hydroxy, C-34 methine, or the conformation of the lower aliphatic rings, plays a key role in the antimalarial activity. The reduction of the C32–C33 olefin and oxidation of C-31 also significantly reduces the antimalarial activity for the manzamine alkaloids *in vivo*. These data combined suggest that the ability of the C-34 allylic carbon to form a stabilized carbocation after oxidation both in cell culture and in animals, followed by the inherent nucleophilic attack, may play a critical role in the biological activity of the manzamine alkaloids.

Few classes of alkaloids are as unique and intriguing as the manzamine class. The biological activity of the manzamines against infectious diseases, cancer, and inflammatory diseases, combined with their unusual structure, strongly suggests that these alkaloids will ultimately yield useful clinical candidates. In addition, the manzamine alkaloids are clearly a key to understanding the sophisticated, but poorly understood, ecological and phylogenetic relationships between a diverse group of sponges and their associated microbial communities. Understanding the biosynthesis of this group of alkaloids, and the role that invertebrates and their microbial association play, will certainly provide a better understanding of the bioorganic evolution of these complex secondary metabolites and the evolutionary pressures required to ultimately produce them.

#### Acknowledgements

The preparation of this chapter was supported, in part, by NIH grants R01AI 36596 and KO2AI01502 from the National Institute of Allergy and Infectious Diseases. Microbiological studies were supported in part by NSF Microbial Observatories MCB-0238515 to RTH. MH thanks his research group for their assistance in the preparation of this chapter.

#### References

1. R. Sakai, T. Higa, C. W. Jefford, and G. Bernardinelli, *J. Am. Chem. Soc.* **108**, 6404–6405 (1986).
2. (a) M. Tsuda and J. Kobayashi, *Heterocycles* **46**, 765–794 (1997). (b) B. J. Baker, Beta-carboline and isoquinoline alkaloids from marine organisms, “Alkaloids: Chemical and Biological Perspectives” (W. Pelletier, ed.), vol. 10, pp. 357–407. Pergamon, Oxford, 1996. (c) M. Ihara and K. Fukumoto, *Nat. Prod. Rep.* **12**, 277–301 (1997).
3. R. Whitehead, *Annu. Rep. Prog. Chem. Sect. B* **95**, 183–205 (1999).
4. (a) S. Urban, S. J. H. Hickford, J. W. Blunt, M. H. G. Munro, *Curr. Chem. Org.* **4**, 765–807 (2000). (b) T. Higa, I. I. Ohtani, and J. Tanaka, *ACS Symposium Series*, Vol. 745 (Natural and Selected Synthetic Toxins), 12–21 (2000). (c) J. Rodríguez, *Studies in Natural Products Chemistry*, Vol. 24 [Bioactive Natural Products (Part E)], 573–681 (2000). (d) T. Higa, J. Tanaka, I. I. Ohtani, M. Musman, M. C. Roy, and I. Kuroda, *Pure Appl. Chem.* **73**, 589–593 (2000). (e) T. Higa, J. Tanaka, and L. T. Tan, Cytotoxic Macrocycles from Marine Sponges, New Trends Nat. Prod. Chem. (Int. Symp. Nat. Prod. Chem., 6th, Meeting Data 1996) (Atta-ur-Rahman and M. I. Choudhary, eds.),

- pp. 109–120. Harwood, Amsterdam, 1998. CA129: 185141. (f) L. Barriault, and L. A. Paquette, *Chemtracts* **12**, 76–281 (1999). CA131: 73818.
5. J. E. Baldwin and R. C. Whitehead, *Tetrahedron Lett.* **33**, 2059–2062 (1992).
  6. H. Nakamura, S. Deng, J. Kobayashi, Y. Ohizumi, Y. Tomotake, T. Matsuzaki, and Y. Hirata, *Tetrahedron Lett.* **28**, 621–624 (1987).
  7. T. Higa, R. Sakai, S. Kohmoto, and M. S. Lui, “Isolation of Antitumor Manzamines B, C, and D from *Haliclona*” Eur. Pat. Appl. EP 272,056 (Cl. C07D471/04), 22 Jun 1988, US Appl. 943,609, 18 Dec 1986; 14 pp.
  8. (a) R. Sakai, S. Kohmoto, T. Higa, C. W. Jefford, and G. Bernardinelli, *Tetrahedron Lett.* **28**, 5493–5496 (1987). (b) H. Seki, M. Nakagawa, A. Hashimoto, and T. Hino, *Chem. Pharm. Bull.* **41**, 1173–1176 (1987). (c) H. Seki, A. Hashimoto, and T. Hino, *Chem. Pharm. Bull.* **41**, 1169–1172 (1987).
  9. (a) T. Ichiba, R. Sakai, S. Kohmoto, G. Saucy, and T. Higa, *Tetrahedron Lett.* **29**, 3083–3086 (1988). (b) T. Higa, R. Sakai, and T. Ichiba, “Manzamine E and F from *Xestospongia* as Neoplasm Inhibitor” Patent CODEN: USXXAM US 4895852 A 19900123 (1990). (c) I. Kitagawa, and M. Kobayashi, *Yuki Gosei Kagaku Kyokaiishi* **49**, 1053–1061 (1991). CA116: 50671.
  10. (a) K. Kondo, H. Shigemori, Y. Kikuchi, M. Ishibashi, T. Sasaki, and J. Kobayashi, *J. Org. Chem.* **57**, 2480–2483 (1992) (b) K. Kondo, H. Shigemori, Y. Kikuchi, M. Ishibashi, J. Kobayashi, and T. Sasaki, *Tennen Yuki Kagobutsu Toronkai* **34**, 463–469 (1992). CA120: 86212.
  11. T. Ichiba, J. M. Corgiat, P. J. Scheuer, and M. Kelly-Borges, *J. Nat. Prod.* **57**, 168–170 (1994).
  12. J. Kobayashi, M. Tsuda, N. Kawasaki, T. Sasaki, and Y. Mikami, *J. Nat. Prod.* **57**, 1737–1740 (1994).
  13. P. Crews, X. C. Cheng, M. Adamczeski, J. Rodriguez, M. Jaspars, F. J. Schmitz, S. C. Traeger, and E. O. Pordesimo, *Tetrahedron* **50**, 13567–13574 (1994).
  14. M. Kobayashi, Y. J. Chen, S. Aoki, Y. In, T. Ishida, and I. Kitagawa, *Tetrahedron* **51**, 3727–3736 (1995).
  15. (a) I. I. Ohtani, T. Ichiba, M. Isobe, M. Kelly-Borges, and P. J. Scheuer, *J. Am. Chem. Soc.* **117**, 10743–10744 (1995), and Ohtani Supplemental Pages 1–16. (b) I. I. Ohtani, T. Ichiba, M. Isobe, M. Kelly-Borges, and P. J. Scheuer, *Tennen Yuki Kagobutsu Toronkai Koen Yoshishu* **37**, 236–241 (1995). CA124: 202710.
  16. R. A. Edrada, P. Proksch, V. Wray, L. Witte, W. E. G. Müeller, and R. W. M. Van Soest, *J. Nat. Prod.* **59**, 1056–1060 (1996).
  17. D. Watanabe, M. Tsuda, and J. Kobayashi, *J. Nat. Prod.* **61**, 689–692 (1998).
  18. (a) K. A. El Sayed, M. Kelly, U. A. K. Kara, K. K. H. Ang, I. Katsuyama, D. C. Dunbar, A. A. Khan, and M. T. Hamann, *J. Am. Chem. Soc.* **123**, 1804–1808 (2001). (b) M. T. Hamann, and K. A. El-Sayed, “Methods of Treating Drug-Resistant Infections through Administration of Pharmaceutical Compositions Containing Manzamine Alkaloids” *PCT Int. Appl.* CODEN: PIXXD2 WO 0217917 A1 200020307 (2002). (c) K. K. H. Ang, M. J. Holmes, and U. A. Kara, *Parasitology Research* **87**, 715–721 (2001). (d) A. U. Kara, T. Higa, M. Holmes, and K. H. Ang, “Antimalarial Activity of Beta-Carboline Alkaloids” *PCT Int. Appl.* CODEN: PIXXD2 WO 9959592 A1 19991125 (1999 US Patent 6,143,756. CA131: 346498.
  19. M. Tsuda, D. Watanabe, and J. Kobayashi, *Heterocycles* **50**, 485–488 (1999).
  20. (a) M. Tsuda, D. Watanabe, and J. Kobayashi, *Tetrahedron Lett.* **39**, 1207–1210 (1998). (b) J. Kobayashi, M. Tsuda, and M. Ishibashi, *Pure and Applied Chem.* **71**, 1123–1126 (1998).

21. M. L. Bourguet-Kondracki, M. T. Martin, and M. Guyot, *Tetrahedron Lett.* **37**, 3457–3460 (1996).
22. (a) M. Tsuda, N. Kawasaki, and J. Kobayashi, *Tetrahedron Lett.* **35**, 4387–4388 (1994). (b) M. Tsuda, N. Kawasaki, and J. Kobayashi, *Tennen Yuki Kagobutsu Toronkai Koen Yoshishu* **36**, 509–516 (1994). CA123: 193590.
23. G. Koren-Goldshlager, Y. Kashman, and M. Schleyer, *J. Nat. Prod.* **61**, 282–284 (1998).
24. D. E. Williams, P. Lassota, and R. J. Andersen, *J. Org. Chem.* **63**, 4838–4841 (1998).
25. M. Tsuda, N. Kawasaki, and J. Kobayashi, *Tetrahedron* **50**, 7957–7960 (1994).
26. (a) J. Kobayashi, M. Tsuda, N. Kawasaki, K. Matsumoto, and T. Adachi, *Tetrahedron Lett.* **35**, 4383–4386 (1994). (b) J. Kobayashi, N. Kawasaki, and M. Tsuda, *Tetrahedron Lett.* **37**, 8203–8204 (1994).
27. (a) M. Tsuda, K. Inaba, N. Kawasaki, K. Honma, and J. Kobayashi, *Tetrahedron* **52**, 2319–2324 (1996). (b) Y.-C. Shen, H.-R. Tai, and C.-Y. Duh, *Chin. Pharm. J. (Taipei)* **48**, 1–10 (1996).
28. J. Rodriguez and P. Crews, *Tetrahedron Lett.* **35**, 4719–4722 (1994).
29. J. Rodriguez, B. M. Peters, L. Kurz, R. C. Schatzman, D. McCarley, L. Lou, and P. Crews, *J. Am. Chem. Soc.* **115**, 10436–10437 (1993).
30. F. Kong, R. J. Andersen, and T. M. Allen, *Tetrahedron* **50**, 6137–6144 (1994).
31. F. Kong, R. J. Andersen, and T. M. Allen, *Tetrahedron Lett.* **35**, 1643–1646 (1994).
32. F. Kong and R. J. Andersen, *Tetrahedron* **51**, 2895–2906 (1995).
33. F. Kong, R. J. Andersen, and T. M. Allen, *J. Am. Chem. Soc.* **116**, 6007–6008 (1994).
34. N. Matzanke, R. J. Gregg, S. M. Weinreb, and M. Parvez, *J. Org. Chem.* **62**, 1920–1921 (1997).
35. F. Kong, E. I. Graziani, and R. J. Andersen, *J. Nat. Prod.* **61**, 267–271 (1998).
36. Y. Guo, E. Trivellone, G. Scognamiglio, and G. Cimino, *Tetrahedron* **54**, 541–550 (1998).
37. A. Kaiser, X. Billot, A. Gateau-Olesker, C. Marazano, and B. C. Das, *J. Am. Chem. Soc.* **120**, 8026–8034 (1998).
38. N. Fusetani, N. Asai, S. Matsunaga, K. Honda, and K. Yasumuro, *Tetrahedron Lett.* **35**, 3967–3970 (1994).
39. M. Kobayashi, K. Kawazoe, and I. Kitagawa, *Chem. Pharm. Bull.* **37**(6), 1676–1678 (1989).
40. G. Cimino, C. A. Mattia, L. Mazzarella, R. Puliti, G. Scognamiglio, A. Spinella, and E. Trivellone, *Tetrahedron* **45**, 3863–3872 (1989).
41. J. C. Braekman, D. Daloze, P. Macedo de Abreu, C. Piccinni-Leopardi, G. Germain, and M. Van Meerssche, *Tetrahedron Lett.* **23**, 4277–4280 (1982).
42. M. Nakagawa, M. Endo, N. Tanaka, and L. Gen-Pei, *Tetrahedron Lett.* **25**, 3227–3230 (1984).
43. N. Fusetani, K. Yasumuro, S. Matsunaga, and H. Hirota, *Tetrahedron Lett.* **30**, 6891–6894 (1989).
44. M. Kobayashi, K. Kawazoe, and I. Kitagawa, *Tetrahedron Lett.* **30**, 4149–4152 (1989).
45. G. Cimino, A. Spinella, and E. Trivellone, *Tetrahedron Lett.* **30**, 133–136 (1989).
46. Y. W. Guo, A. Madaio, E. Trivellone, G. Scognamiglio, and G. Cimino, *Tetrahedron* **52**, 8341–8348 (1996).
47. Y. W. Guo, A. Madaio, E. Trivellone, G. Scognamiglio, and G. Cimino, *Tetrahedron* **52**, 14961–14974 (1996).
48. R. D. Charan, M. J. Garson, I. M. Brereton, A. C. Willis, and J. N. A. Hooper, *Tetrahedron* **52**, 9111–9120 (1996).

49. J.-C. Quirion, T. Sevenet, H.-P. Husson, B. Weniger, and C. Debitus, *J. Nat. Prod.* **55**, 1505–1508 (1992).
50. B. J. Baker, P. J. Scheuer, and J. N. Shoolery, *J. Am. Chem. Soc.* **110**, 965–966 (1988).
51. M. Jaspars, V. Pasupathy, and P. Crews, *J. Org. Chem.* **59**, 3253–3255 (1994).
52. B. Harrison, S. Talapatra, E. Lobkovsky, J. Clardy, and P. Crews, *Tetrahedron Lett.* **37**, 9151–9154 (1996).
53. G. Cimino, G. Scognamiglio, A. Spinella, and E. Trivellone, *J. Nat. Prod.* **53**, 1519–1525 (1990).
54. K. Toshima, K. Ohta, A. Ohashi, T. Nakamura, M. Nakata, K. Tatsuta, and S. Matsumura, *J. Am. Chem. Soc.* **117**, 4822–4831 (1995).
55. A. M. S. Mayer, S. P. Gunasekera, S. A. Pomponi, and S. H. Sennett, “Anti-inflammatory Uses of Manzamines” *PCT Int. Appl.*, CODEN: PIXXD2 WO 0056304 A2 20000928 (2000).
56. (a) K. A. El Sayed, D. C. Dunbar, T. L. Perry, S. P. Wilkins, M. T. Hamann, J. T. Greenplate, and M. A. Wideman, *Agricultural and Food Chemistry* **45**, 2735–2739 (1997). (b) B. W. Nugroho, R. A. Edrada, F. Bohnenstengel, A. Supriyono, C. Eder, D. Handayani, and P. Proksch, “*Spodoptera littoralis* as a Test Model for Insecticidal Bioassays” *Natural Product Analysis: Chromatography, Spectroscopy, Biological Testing (Symposium)*, pp. 373–375. Wuerzburg, Germany, 1997.
57. (a) J. Kobayashi, D. Watanabe, N. Kawasaki, and M. Tsuda, *J. Org. Chem.* **62**, 9236–9239 (1997). (b) M. Tsuda, D. Watanabe, and J. Kobayashi, *Tennen Yuki Kagobutsu Toronkai Koen Yoshishu* **40**, 467–472 (1998). CA131: 142191.
58. (a) M. Yousaf, K. A. El Sayed, K. V. Rao, C. W. Lim, J.-F. Hu, M. Kelly, S. G. Franzblau, F. Zhang, O. Peraud, R. T. Hill, and M. T. Hamann, *Tetrahedron* **58**, 7397–7402 (2002). (b) N. Kasanah, K. V. Rao, M. Yousaf, D. E. Wedge, and M. T. Hamann, *Tetrahedron Lett.* **44**, 1291–1293 (2002).
59. J. Peng, J.-F. Hu, A. B. Kazi, S. G. Franzblau, F. Zhang, R. F. Schinazi, S. S. Wirtz, P. Tharnish, M. Kelly, and M. T. Hamann, *J. Am. Chem. Soc.* In press (2003).
60. K. V. Rao, B. D. Santarsiero, A. D. Mesecar, R. F. Schinazi, B. L. Tewani, and M. T. Hamann, *J. Nat. Prod.* **66**, 823–828 (2003).
61. B.-N. Zhou, C. Slebodnick, R. K. Johnson, M. R. Mattern, and D. G. I. Kingston, *Tetrahedron* **56**, 5781–5784 (2000).
62. J. Vacelet, P. Vasseur, and C. Lévi, *Mémoires du Muséum National D’Histoire Naturelle Serie A Zoologie XLIX*, 1–116 (1976).
63. R. Desqueyroux-Faúndez and C. Valentine, Family Petrosiidae Van Soest, 1980, in “Systema Porifera: A Guide to the Classification of Sponges” (J. N. A. Hooper and R. W. M. van Soest, eds.), pp. 906–917. Kluwer Academic/Plenum Publishers, New York, 2002.
64. M. Kelly-Borges and J. Vacelet, *Memoirs of the Queensland Museum* **38**, 477–503 (1995).
65. (a) O. Gillor, S. Carmeli, Y. Rahamim, Z. Fishelson, and M. Ilan, *Marine Biotechnology* **2**, 213–223 (2000). (b) N. S. Webster, and R. T. Hill, *Marine Biol.* **138**, 843–851 (2000). (c) N. S. Webster, K. J. Wilson, L. L. Blackall, and R. T. Hill, *Appl. Environ. Microbiol.* **67**, 434–444 (2000).
66. Y. Torisawa, A. Hashimoto, M. Nakagawa, and T. Hino, *Tetrahedron Lett.* **30**, 6549–6550 (1989).
67. Y. Torisawa, A. Hashimoto, M. Nakagawa, H. Seki, R. Hara, and T. Hino, *Tetrahedron* **47**, 8067–8078 (1991).
68. D. I. MaGee and E. J. Beck, *Can. J. Chem.* **78**, 1060–1066 (2000).

69. M. Arisawa, C. Kato, H. Kaneko, A. Nishida, and M. Nakagawa, *Perkin 1*, 1873–1876 (2000). CA133: 237976.
70. T. Vidal, E. Magnier, and Y. Langlois, *Tetrahedron* **54**, 5959–5966 (1998).
71. Y. Torisawa, A. Hashimoto, M. Okouchi, T. Iimori, M. Nagasawa, T. Hino, and M. Nakagawa, *Bioorg. & Med. Chem. Lett.* **6**, 2565–2570 (1996).
72. W. Nowak and H. Gerlach, *Liebigs Ann. Chem.*, 153–159 (1993).
73. M. Nakagawa, Y. Torisawa, T. Hosaka, K. Tanabe, F. Tavet, and T. Hino, *Tennen Yuki Kagobutsu Toronkai Toen Yoshishu* **34**, 408–415 (1992).
74. U. K. Pandit, B. C. Borer, and H. Bieraugel, *Pure & Appl. Chem.* **68**, 659–662 (1996).
75. M. Nakagawa, Y. Torisawa, T. Hosaka, K. Tanabe, T. Da-te, K. Okamura, and T. Hino, *Tetrahedron Lett.* **34**, 4543–4546 (1993).
76. J. D. Winkler and J. M. Axten, *J. Am. Chem. Soc.* **120**, 6425–6426 (1998).
77. L. Turet, I. E. Markó, B. Tinant, J.-P. Declercq, and R. Touillaux, *Tetrahedron Lett.* **43**, 6591–6595 (2002).
78. G. F. Solberghe, I. E. Marko, and L. Batiment, *Tetrahedron Lett.* **43**, 5061–5065 (2002).
79. J. M. Humphrey, Y. S. Liao, A. Ali, T. Rein, Y.-L. Wong, H.-J. Chen, A. K. Courtney, and S. F. Martin, *J. Am. Chem. Soc.* **124**, 8584–8592 (2002).
80. P. Magnus, M. R. Fielding, C. Wells, and V. Lynch, *Tetrahedron Lett.* **43**, 947–950 (2002).
81. M. Karle, and U. Koert, *Org. Syn. Highlights IV*, 91–96 (2000). CA136: 134290.
82. J.-M. Gomez, L. Gil, C. Ferroud, A. Gateau-Olesker, M.-T. Martin, and C. Marazano, *J. Org. Chem.* **66**, 4898–4903 (2001).
83. H. A. Lindsay, C. L. Salisbury, W. Cordes, and M. C. McIntosh, *Org. Lett.* **3**, 4007–4010 (2001).
84. D. Urban, E. Duval, and Y. Langlois, *Tetrahedron Lett.* **41**, 9251–9256 (2000).
85. M. Arisawa, M. Takahashi, E. Takezawa, T. Yamaguchi, Y. Torisawa, A. Nishida, and M. Nakagawa, *Chem. Pharm. Bull.* **48**, 1593–1596 (2000).
86. M. Nakagawa, *J. Heterocyclic Chem.* **37**, 567–581 (2000).
87. K. Kotsukibi and K. Gamou, *Chokoatsu Yuki Gosei*, 299–314 (1999).
88. M. Nakagawa, Y. Torisawa, H. Uchida, and A. Nishida, *Yuki Gosei Kagaku Kyokaishi (J. Synth. Org. Chem. Japan)*, **57**, 1004–1015 (1999). CA131: 351494.
89. I. Coldham, K. M. Crapnell, J.-C. Fernández, J. D. Moseley, and R. Rabot, *J. Org. Chem.* **67**, 6181–6187 (2002).
90. I. Coldham, J.-C. Fernandez, R. Rabot, and K. M. Crapnell, *Abstr. Pap.-Am. Chem. Soc.* 221st ORGN-027 (2001).
91. I. Coldham, K. M. Crapnell, J.-C. Fernandez, T. F. N. Haxell, A. B. Treacy, S. J. Coles, M. B. Hursthouse, and J. D. Moseley, *Chem. Commun.* 1757–1758 (1999).
92. D. Bland, G. Chambournier, V. Dragan, and D. J. Hart, *Tetrahedron* **55**, 8953–8966 (1999).
93. H. Uchida, Y. Kimura, M. Yamabe, A. Nishida, and M. Nakagawa, *Tennen Yuki Kagobutsu Toronkai Koen Yoshishu* **41**, 67–72 (1999). CA132: 279387.
94. H. Uchida, A. Nishida, and M. Nakagawa, *Tetrahedron Lett.* **40**, 113–116 (1999).
95. H. Uchida, E. Takezawa, T. Kawate, A. Nishida, and M. Nakagawa, *Tennen Yuki Kagobutsu Toronkai Koen Yoshishu* **40**, 601–606 (1998). CA131: 228862.
96. Y. Morimoto, C. Yokoe, H. Kurihara, and T. Kinoshita, *Tetrahedron* **54**, 12197–12214 (1998).
97. M. L. Lee, and D. I. MaGee, *216<sup>th</sup> ACS National Meeting* (Boston, August 23–27), ORGN-553 (1998).

98. W. P. D. Goldring, A. S. Hodder, and L. Weiler, *Tetrahedron Lett.* **39**, 4955–4958 (1998).
99. Y. Morimoto and C. Yokoe, *Tetrahedron Lett.* **38**, 8981–8984 (1997).
100. D. Bland, D. J. Hart, and S. Lacoutiere, *Tetrahedron* **53**, 8871–8880 (1997).
101. O. Sageot, D. Monteux, Y. Langlois, C. Riche, and A. Chiaroni, *Tetrahedron Lett.* **37**, 7019–7022 (1996).
102. Y. Torisawa, T. Soe, C. Katoh, Y. Motohashi, A. Nishida, T. Hino, and N. Nakagawa, *Heterocycles* **47**, 655–659 (1998).
103. Y. Torisawa, T. Hosaka, K. Tanabe, N. Suzuki, Y. Motohashi, T. Hino, and M. Nakagawa, *Tetrahedron* **52**, 10597–10608 (1996).
104. Y. Torisawa, M. A. Ali, F. Tavet, A. Kageyama, M. Aikawa, N. Fukui, T. Hino, and M. Nakagawa, *Heterocycles* **42**, 677–689 (1996).
105. Y. Torisawa, Y. Motohashi, and M. Nakagawa, *Tennen Yuki Kagobutsu Toronkai Koen Yoshishu* **37**, 451–456 (1995). CA124: 202699.
106. E. Magnier and Y. Langlois, *Tetrahedron* **54**, 6201–6258 (1998).
107. E. Magnier and Y. Langlois, *Tetrahedron Lett.* **39**, 837–840 (1998).
108. E. Magnier, Y. Langlois, and C. Mérienne, *Tetrahedron Lett.* **36**, 9475–9478 (1995).
109. H. Bieräugel, B. C. Borer, and U. K. Pandit, *Heterocyclic Commun.* **1**, 115–118. CA123: 56358 (1995).
110. J. S. Clark, P. B. Hodgson, M. D. Goldsmith, A. J. Blake, P. A. Cooke, and L. J. Street, *J. Chem. Soc., Perkin Trans. 1*, 3325–3337 (2001).
111. (a) J. S. Clark, R. J. Townsend, A. J. Blake, S. J. Teat, and A. Johns, *Tetrahedron Lett.* **42**, 3235–3238 (2001). (b) R. J. Townsend, and J. S. Clark, 216th ACS National Meeting (Boston, August 23–27), ORGN-551 (1998).
112. J. S. Clark and P. B. Hodgson, *Tetrahedron Lett.* **36**, 2519–2522 (1995).
113. S. M. Li and S. Yamamura, *Tetrahedron* **54**, 869–8710 (1998).
114. S. M. Li, S. Kosemura, and S. Yamamura, *Tetrahedron* **54**, 6661–6676 (1998).
115. S. M. Li, S. Yamamura, H. Hosomi, and S. Ohba, *Tetrahedron Lett.* **39**, 2601–2604 (1998).
116. S. M. Li and S. Yamamura, *Tetrahedron Lett.* **39**, 2597–2600 (1998).
117. S. M. Li, S. Ohba, S. Kosemura, and S. Yamamura, *Tetrahedron Lett.* **37**, 7365–7368 (1996).
118. S. M. Li, S. Kosemura, and S. Yamamura, *Tetrahedron Lett.* **35**, 8217–8220 (1994).
119. J. Leonard, S. P. Fearnley, M. R. Finlay, J. A. Knight, and G. Wong, *J. Chem. Soc., Perkin Trans. 1: Organic and Bio-Organic Chemistry* 2359–2361 (1994).
120. J. Ma, M. Nakagawa, Y. Torisawa, and T. Hino, *Heterocycles* **38**, 1609–1618 (1994).
121. T. M. Kamenecka and L. E. Overman, *Tetrahedron Lett.* **35**, 4279–4282 (1994).
122. B. C. Borer, S. Deerenberg, H. Bieräugel, and U. K. Pandit, *Tetrahedron Lett.* **35**, 3191–3194 (1994).
123. U. K. Pandit, H. S. Overkleeft, B. C. Borer, and H. Bieräugel, *Eur. J. Org. Chem.*, 959–968 (1999).
124. U. K. Pandit, Synthetic Studies on Anti-tumor Alkaloids. New Trends in Natural Product Chemistry, [International Symposium on Natural Product Chemistry], 15–22 (1998). CA129: 216790.
125. U. K. Pandit, *Farmaco* **50**, 749–754 (1995) CA124: 87434.
126. U. K. Pandit, B. C. Borer, H. Bieräugel, and S. Deerenberg, *Pure & Appl. Chem.* **66**, 2131–2134 (1994).
127. U. K. Pandit, *J. Heterocycl. Chem.* **31**, 615–624 (1994). CA121: 109360.
128. T. Hino and M. Nakagawa, *J. Heterocyclic. Chem.* **31**, 625–630 (1994).

129. S. F. Martin, J. M. Humphrey, A. Ali, and M. C. Hillier, *J. Am. Chem. Soc.* **121**, 866–867 (1999).
130. S. F. Martin, H.-J. Chen, A. K. Courtney, Y. S. Liao, M. Pätzelt, M. N. Ramser, and A. S. Wagman, *Tetrahedron* **52**, 7251–7264 (1996).
131. S. F. Martin, Y. Liao, Y. Wong, and T. Rein, *Tetrahedron Lett.* **35**, 691–694 (1994).
132. J. D. Winkler, J. E. Stelmach, M. G. Siegel, N. Haddad, J. Axten, and Dailey, W. P., III., *Isr. J. Chem.* **37**, 47–67 (1997).
133. (a) J. D. Winkler, J. Axten, A. H. Hammach, Y.-S. Kwak, U. Lengweiler, M. J. Lucero, and K. N. Houk, *Tetrahedron* **54**, 7045–7056 (1998). (b) J. M. Axten, and J. D. Winkler, 216th ACS National Meeting (Boston, August 23–27), ORGN-525 (1998).
134. J. D. Winkler, M. G. Siegel, and J. E. Stelmach, *Tetrahedron Lett.* **34**, 6509–6512 (1993).
135. M. Nakagawa, Y. Torisawa, T. Hosaka, K. Tanabe, T. Da-te, K. Okamura, and T. Hino, *Tetrahedron Lett.* **34**, 4543–4546 (1993).
136. R. E. Longley, O. J. McConnell, E. Essich, and D. Harmody, *J. Nat. Prod.* **56**, 915–920 (1993).
137. J. A. Campbell and D. J. Hart, *J. Org. Chem.* **58**, 2900–2903 (1993).
138. J. A. Campbell and D. J. Hart, *Tetrahedron Lett.* **33**, 6247–6250 (1992).
139. J. Leonard, S. P. Fearnley, and D.M. B Hickey, *Synlett*, 272–274 (1992).
140. V. M. Lynch, Y. S. Liao, S. F. Martin, and B. E. Davis, *Acta Cryst. Sect. C: Cryst. Struct. Commun.* **48**, 1703–1705 (1992).
141. Y. Torisawa, M. Nakagawa, T. Hosaka, K. Tanabe, Z. Lai, K. Ogata, T. Nakata, T. Oishi, and T. Hino, *J. Org. Chem.* **57**, 5741–5747 (1992).
142. I. E. Marko, J. M. Southern, and H. Adams, *Tetrahedron Lett.* **33**, 4657–4660 (1992).
143. I. E. Marko and A. Chesney, *Synlett*, 275–278 (1992).
144. K. M. J. Brands and L. M. DiMichele, *Tetrahedron Lett.* **39**, 1677–1680 (1998).
145. K. M. J. Brands, A. A. P. Meekel, and U. K. Pandit, *Tetrahedron* **47**, 2005–2026 (1991).
146. S. F. Martin, T. Rein, and Y. S. Liao, *Tetrahedron Lett.* **32**, 6481–6484 (1991).
147. D. D. O. Imbroisi and N. S. Simpkins, *J. Chem. Soc. Perkin Trans. 1*, 1815–1823 (1991).
148. K. M. J. Brands and U. K. Pandit, *Heterocycles* **30**, 257–261 (1990).
149. M. Nakagawa, Z. P. Lai, Y. Torisawa, and T. Hino, *Heterocycles* **31**, 999–1002 (1990).
150. A. Chesney and I. E. Marko, *Synth. Commun.* **20**, 3167–3180 (1990).
151. Y. Torisawa, M. Nakagawa, H. Arai, Z. P. Lai, T. Hino, T. Nakata, and T. Oishi, *Tetrahedron Lett.* **31**, 3195–3198 (1990).
152. K. M. J. Brands and U. K. Pandit, *Tetrahedron Lett.* **30**, 1423–1426 (1989).
153. D. J. Hart and J. A. McKinney, *Tetrahedron Lett.* **30**, 2611–2614 (1989).
154. R. Mohan, Y. L. Chou, and M. M. Morrissey, *Tetrahedron Lett.* **37**, 3963–3966 (1996).
155. M. Herdemann, A. Gateau-Olesker, A. Al Mourabit, and C. Marazano, Biomimetic Model of Manzamines: Cycloaddition of Aminopentadienes and Dihydropyridiniums. 2nd Euroconference on Marine Natural Products (Spain, Sept.) 168 (1999).
156. N. Matzanke, R. J. Gregg, and S. M. Weinreb, *Org. Prep. Proced. Int.* **30**, 1–51 (1998).

157. J. E. Baldwin, T. D. W. Claridge, A. J. Culshaw, F. A. Heupel, V. Lee, D. R. Spring, and R. C. Whitehead, *Chem. Eur. J.* **5**, 3154–3161 (1999).
158. J. E. Baldwin, T. D. W. Claridge, A. J. Culshaw, F. A. Heupel, V. Lee, D. R. Spring, R. C. Whitehead, R. J. Boughtflower, I. M. Mutton, R. J. Upton, *Angew. Chem. Int. Ed.* **37**, 2661–2663 (1998).
159. J. E. Baldwin, L. Bischoff, T. D. W. Claridge, F. A. Heupel, D. R. Spring, and R. C. Whitehead, *Tetrahedron* **53**, 2271–2290 (1997).
160. J. E. Baldwin, T. D. W. Claridge, A. J. Culshaw, F. A. Heupel, S. Smrcková, and R. C. Whitehead, *Tetrahedron Lett.* **37**, 6919–6922 (1996).
161. J. E. Baldwin, T. D. W. Claridge, F. A. Heupel, and R. C. Whitehead, *Tetrahedron Lett.* **35**, 7829–7832 (1994).
162. M. Herdemann, A. Al-Mourabit, M.-T. Martin, and C. Marazano, *J. Org. Chem.* **67**, 1890–1897 (2002).
163. K. Jakubowicz, K. Ben Abdeljelil, M. Herdemann, M.-T. Martin, A. Gateau-Olesker, A. Al Mourabit, C. Marazano, and B. C. Das, *J. Org. Chem.* **64**, 7381–7387 (1999).
164. J. Kobayashi and M. Tsuda, *Yuki Gosei Kagaku Kyokaiishi (J. Synth. Org. Chem. Japan)* **55**, 1114–1123 (1997). CA128: 61660.
165. J. Kobayashi, *Farumashia* **31**, 869–873 (1995). CA123: 139226.
166. J. Kobayashi, *Gendai Kagaku* **29**, 47–53 (1995). CA123: 79881.
167. L. Gil, X. Baucherel, M.-T. Martin, C. Marazano, and B. C. Das, *Tetrahedron Lett.* **36**, 6231–6234 (1995).
168. L. Gil, A. Gateau-Olesker, C. Marazano, and B. C. Das, *Tetrahedron Lett.* **36**, 707–710 (1995).
169. G. Q. Shen and B. J. Baker, *Tetrahedron Lett.* **35**, 1141–1144 (1994).
170. K. K. H. Ang, M. J. Holmes, T. Higa, M. T. Hamann, and U. A. K. Kara, *Antimicrobial Agents and Chemotherapy* **44**, 1645–1649 (2000).



## SESQUITERPENE PYRIDINE ALKALOIDS

LUCIANO M. LIÃO

*Instituto de Química, Universidade Federal de Goiás, Goiânia,  
GO, 74001-970, Brazil*

- I. Introduction
- II. Evoninate Sesquiterpene Pyridine Alkaloids and Derivatives
- III. Wilfordate Sesquiterpene Pyridine Alkaloids and Derivatives
- IV. Edulinate Sesquiterpene Pyridine Alkaloids
- V. Cassinate Sesquiterpene Pyridine Alkaloids
- VI. Lower Molecular Weight Sesquiterpene Pyridine Alkaloids
- VII. Non-Celastraceous Sesquiterpene Pyridine Alkaloids
- VIII. Biosynthesis and Biogenesis
- IX. Biological Activity
- X. Taxonomic Considerations
- XI. Synthesis

### References

### I. Introduction

Among the naturally occurring nitrogen-containing compounds the pyridine alkaloids constitute an important group, which are pharmacologically active constituents in a number of medicinal plants. Species from the Celastraceae and Hippocrateaceae families are rich sources of sesquiterpene pyridine alkaloids and are considered their chemotaxonomical markers. Their sesquiterpene backbones are polyesters of cyclic alcohols derived from dihydroagarofuran. This skeleton is comprised of A and B rings in the form of an axially dimethylated *trans*-decalin bicycle and a 1,3-diaxially fused  $(\text{CH}_3)_2\text{C}-\text{CO}$  bridge constituting the tetrahydrofuranlyl C-ring, as presented in structure A (Fig. 1). This core structure is found in nature in various oxygenated forms, bearing as many as nine hydroxyl groups, as in euonyminol and isoeuonyminol, as well as one carbonyl and eight hydroxyl groups, as in evoninol (Fig. 1). Stereochemical assignments for the sesquiterpene nucleus were determined by analysis of NOE correlations, and the correct absolute configuration is shown for those naturally occurring sesquiterpene pyridine alkaloid derivatives for which determinations have been made (1,2). Two

numbering systems have been employed for the sesquiterpene nucleus, and the most common, which is used throughout this text, is the one in line with the numbering system proposed for eudesman and its derivatives in the *Chemical Abstracts Index Guide* 75, 940 (1971), as illustrated in Fig. 1.

Aliphatic and aromatic acids esterify hydroxyl groups of the fundamental sesquiterpene (Fig. 2). The particular sesquiterpenoids differ from each other by the number of hydroxyl groups and by the composition of the ester substituents. Several of them have a *tert*-hydroxyl group attached exclusively to C-4. If the acid esterifying the hydroxyl group of sesquiterpenoids contains nitrogen, then the compounds are weakly basic alkaloids. Such an acid is nicotinic acid or its carboxylic acid derivatives (Fig. 3), substituted in positions 2,3 or 3,4 of the pyridine ring, which form macrolide bridges between C-3 and C-13.

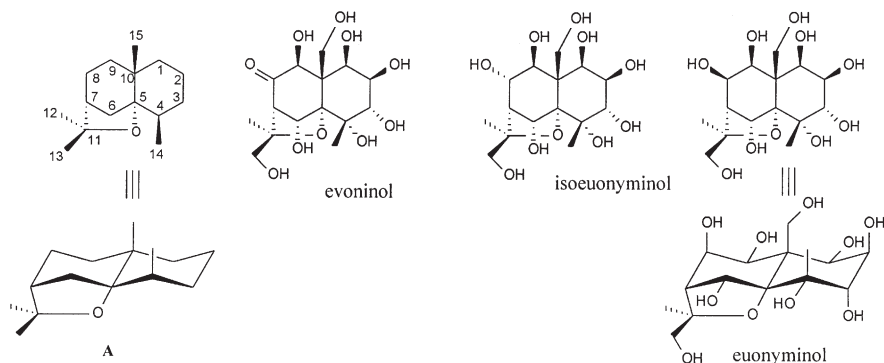


Figure 1. Classical dihydroagarofuran sesquiterpenes.

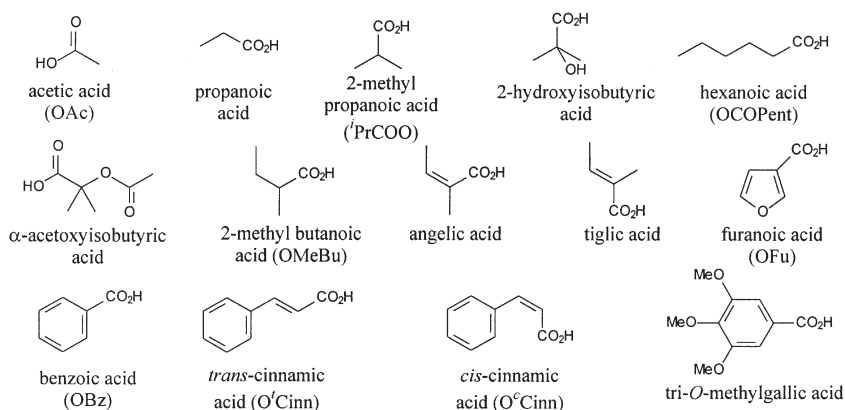


Figure 2. Esterifying acids of the sesquiterpene cores.

## II. Evoninate Sesquiterpene Pyridine Alkaloids and Derivatives

### A. EVONINATE ALKALOIDS

Evoninate sesquiterpene pyridine alkaloids, in which evoninic acid esterifies the sesquiterpene nucleus, represent the most extensive group of evoninate

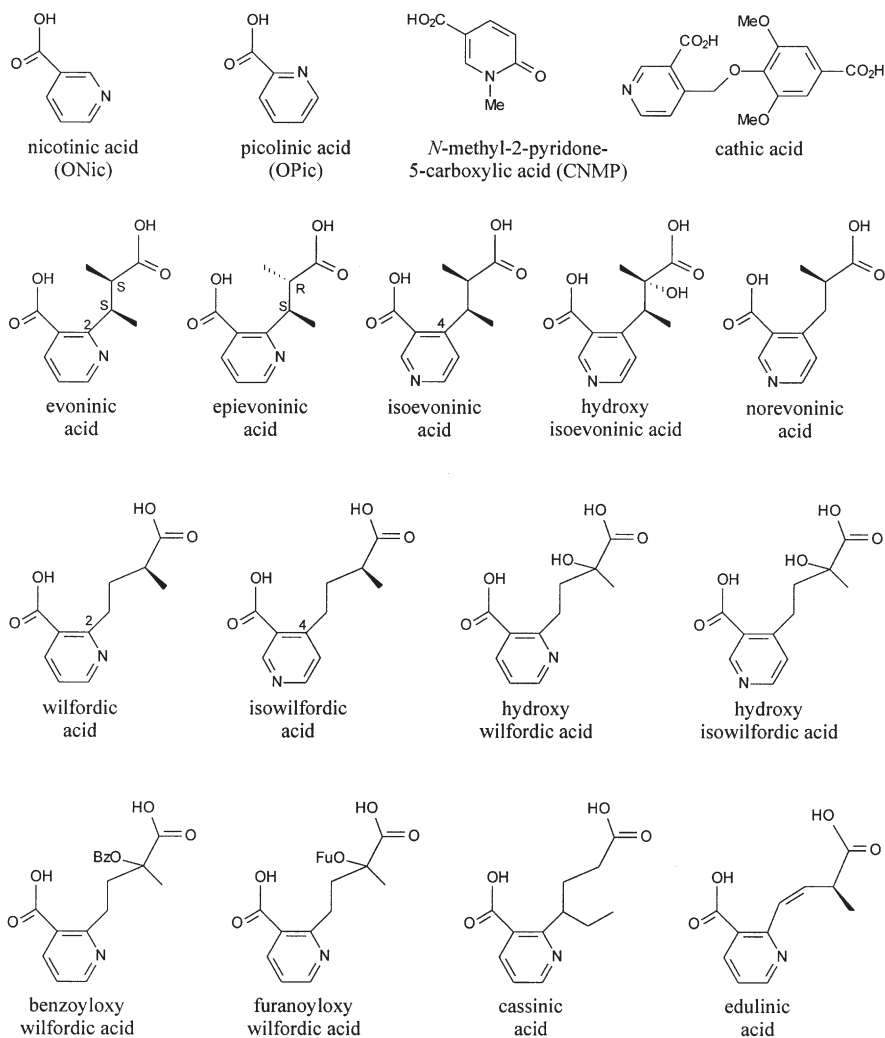


Figure 3. Nicotinic acid and its derivatives.

alkaloids. These alkaloids can be conveniently divided into evoninol, euonyminol, isoeuonyminol, 4-deoxyeuonyminol, and 4-deoxyisoeuonyminol groups based on the oxidation form of the sesquiterpene core (Fig. 1).

### 1. *Evoninol Derivatives*

In the evoninol group, evonine (**1**) has been frequently isolated from plants of the Celastraceae family. It was first obtained by Doebel and Reichstein (3) and later by Pailer and Libiseller (4). The latter group established the structure of evoninic acid (Fig. 3) as (2*S*,3*S*)-2-methyl-3-methyl-3-( $\beta$ -carboxy- $\alpha$ -pyridyl)-propionic acid by alkaline hydrolysis of evonine, and it was further revealed that evonine consisted of an evoninol sesquiterpene core esterified by acetic and evoninic acids (5,6). The 2*S*,3*S* configurations of the methyl groups in the evoninic acid side chain have also been determined by X-ray analysis (7), and confirmed by NOE analysis (8). The complete structure was elegantly deduced from the  $^1\text{H-NMR}$  and mass spectrometric data of evonine and its derivatives, and also by specific reactions approximately one decade later. Evoninol was separated as an octaacetate derivative prepared from the alkaloid by  $\text{LiAlH}_4$  reduction and subsequent acetylation of the product (5,9–11). At the same time, Pailer and Streicher independently deduced the structure of evonine (12).

The basic moiety of evonine constituted by evoninic acid is linked to C-3 and C-13 of the sesquiterpene backbone thus forming a fifteen-membered macrocyclic ring. Further evoninate sesquiterpene pyridine alkaloids that have been isolated from plants of the Celastraceae, containing evoninol as the sesquiterpene core, include the desacetyl derivative of evonine (Table I).

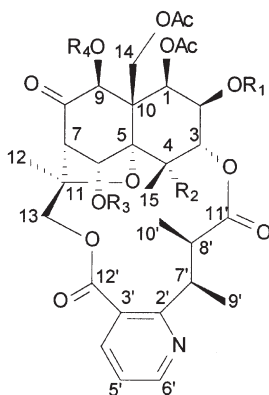
Evoninic acid is characterized in its  $^1\text{H-NMR}$  spectra by signals at  $\delta$  7.2 (dd,  $J=4.7, 7.8$  Hz), 7.9 (dd,  $J=1.5, 7.8$  Hz), and 8.6 (dd,  $J=1.5, 4.7$  Hz), for one 2,3-disubstituted pyridine unit, two secondary methyl groups at  $\delta$  1.2 (d,  $J=7.4$  Hz) and 1.4 (d,  $J=6.9$  Hz), and two methine protons at  $\delta$  2.8 (q,  $J=7.4$  Hz) and 4.2 (q,  $J=6.9$  Hz) which are coupled to each other.

### 2. *Euonyminol Derivatives*

Most of the macrocyclic sesquiterpene pyridine alkaloids found in the Celastraceae, including the Hippocrateaceae, contain euonyminol (Fig. 1) in their sesquiterpene nucleus. Esterifying acids may be observed as aliphatic, like acetic, 2-methylpropanoic, tiglic, or angelic acids, as aromatic, like benzoic and 3-furanoic acids, as well as nitrogen-containing acids, like nicotinic acid (Table II).

Another important group of euonyminol sesquiterpene pyridine alkaloid derivatives comprises the emarginatines, hippocrateines, and similar compounds (Table III). These alkaloids are characterized by a 5-carboxy-*N*-methyl-2-pyridone

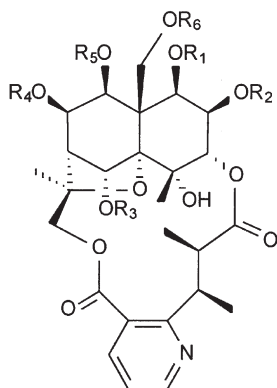
TABLE I.  
Evoninate Sesquiterpene Alkaloids – Evoninol Derivatives.



Alkaloid	R <sub>1</sub>	R <sub>2</sub>	R <sub>3</sub>	R <sub>4</sub>	Properties
1. Evonine	Ac	OH	Ac	Ac	C <sub>36</sub> H <sub>43</sub> NO <sub>17</sub> , mw: 761.25, mp: 183–188 °C, [α] <sub>D</sub> +21.1° (EtOH), IR, UV, MS, ORD (13), <sup>13</sup> C (14), mp: 184–190 °C, [α] <sub>D</sub> +8.4° (CHCl <sub>3</sub> ), UV, IR, <sup>1</sup> H (10)
2. Neoevonine or evorine	Ac	OH	H	Ac	C <sub>34</sub> H <sub>41</sub> NO <sub>16</sub> , mw: 719.24, mp: 264–265 °C, [α] <sub>D</sub> +24.9° (CHCl <sub>3</sub> ), UV, IR, <sup>1</sup> H (15)
3. Evozine	Ac	OH	H	H	C <sub>32</sub> H <sub>39</sub> NO <sub>15</sub> , mw: 677.23, mp: 288–289 °C, [α] <sub>D</sub> <sup>22</sup> +13° (CHCl <sub>3</sub> ), UV, IR, <sup>1</sup> H (16)
4. 2,6-Bisdesacetylevonine	H	OH	H	Ac	C <sub>32</sub> H <sub>39</sub> NO <sub>15</sub> , mw: 677.23, mp: 141 °C, UV, IR, <sup>1</sup> H (17)
5. 2-Desacetylevonine	H	OH	Ac	Ac	C <sub>34</sub> H <sub>41</sub> NO <sub>16</sub> , mw: 719.24, mp: 135 °C, UV, IR, <sup>1</sup> H (17)
6. Evonoline	Ac	H	Ac	Ac	C <sub>36</sub> H <sub>43</sub> NO <sub>16</sub> , mw: 745.26, [α] <sub>D</sub> +6.2° (EtOH), IR, UV, ORD (13); UV, IR, <sup>1</sup> H, <sup>13</sup> C (18)
7.	Ac	H	H	Ac	C <sub>34</sub> H <sub>41</sub> NO <sub>15</sub> , mw: 703.25, mp: 168–173 °C, UV, MS, <sup>1</sup> H (18)

(CNMP) ring attached to the sesquiterpene nucleus. The CNMP ring is characterized in its <sup>1</sup>H-NMR by signals at δ 6.6 (1H, d, *J* = 10.0 Hz), 7.9 (1H, dd, *J* = 10.0, 2.5 Hz), 8.4 (1H, d, *J* = 2.5 Hz), and 3.7 (3H, s, *N*-methyl). The hydroxyl groups of the euonyminol core can be esterified with acetic, benzoic, 2-methylpropanoic, 2-methylbutanoic, tiglic, or angelic acids.

TABLE II.  
Evoninate Sesquiterpene Alkaloids – Euonyminol Derivatives.



Alkaloid	R <sub>1</sub>	R <sub>2</sub>	R <sub>3</sub>	R <sub>4</sub>	R <sub>5</sub>	R <sub>6</sub>	Properties
8. Euonymine	Ac	Ac	Ac	Ac	Ac	Ac	C <sub>38</sub> H <sub>47</sub> NO <sub>18</sub> , mw: 805.28, mp: 140–146 °C (picrate), [α] <sub>D</sub> –20° (CHCl <sub>3</sub> ), UV, IR, <sup>1</sup> H (15); <sup>1</sup> H, <sup>13</sup> C (19)
9. Hyponine A	Ac	Ac	Fu	Ac	Ac	Ac	C <sub>41</sub> H <sub>47</sub> NO <sub>19</sub> , mw: 857.27, [α] <sub>D</sub> <sup>25</sup> –27.5° (CHCl <sub>3</sub> ), UV, IR, MS, <sup>1</sup> H, <sup>13</sup> C (14)
10. Hyponine B	Ac	Ac	Ac	Ac	Ac	Fu	C <sub>41</sub> H <sub>47</sub> NO <sub>19</sub> , mw: 857.27, [α] <sub>D</sub> <sup>25</sup> –19.5° (CHCl <sub>3</sub> ), UV, IR, MS, <sup>1</sup> H, <sup>13</sup> C (14)
11. Hyponine C	Ac	Ac	Ac	Ac	Ac	Bz	C <sub>43</sub> H <sub>49</sub> NO <sub>18</sub> , mw: 867.29, [α] <sub>D</sub> <sup>25</sup> –15.5° (CHCl <sub>3</sub> ), UV, IR, MS, <sup>1</sup> H, <sup>13</sup> C (14)
12. Hyponine D	Ac	Nic	Bz	Ac	Ac	Ac	C <sub>47</sub> H <sub>50</sub> N <sub>2</sub> O <sub>18</sub> , mw: 930.31, [α] <sub>D</sub> <sup>25</sup> +5.2° (MeOH), UV, IR, MS, <sup>1</sup> H, <sup>13</sup> C (20)
13. Hyponine E	Ac	Ac	Fu	Nic	Ac	Ac	C <sub>45</sub> H <sub>48</sub> N <sub>2</sub> O <sub>19</sub> , mw: 920.28, [α] <sub>D</sub> <sup>25</sup> –4.2° (MeOH), UV, IR, MS, <sup>1</sup> H, <sup>13</sup> C (20)
14. Hyponine F	Ac	Fu	Ac	Ac	Ac	Ac	C <sub>41</sub> H <sub>47</sub> NO <sub>19</sub> , mw: 857.27, [α] <sub>D</sub> <sup>25</sup> +7.0° (MeOH), UV, IR, MS, <sup>1</sup> H, <sup>13</sup> C (20)
15. Forrestine	Ac	Bz	Ac	Ac	Ac	Ac	C <sub>43</sub> H <sub>49</sub> NO <sub>18</sub> , mw: 867.29, mp: 113–115 °C, UV, IR, MS, <sup>1</sup> H, <sup>13</sup> C (21); <sup>1</sup> H (22)

(continued)

TABLE II.  
Continued.

Alkaloid	R <sub>1</sub>	R <sub>2</sub>	R <sub>3</sub>	R <sub>4</sub>	R <sub>5</sub>	R <sub>6</sub>	Properties
16. Cangorinine E-I	Ac	Ac	Bz	Ac	Ac	Ac	C <sub>43</sub> H <sub>49</sub> NO <sub>18</sub> , mw: 867.29, mp: 98–101 °C, [α] <sub>D</sub> –25.4° (CHCl <sub>3</sub> ), UV, IR, MS, <sup>1</sup> H, <sup>13</sup> C (8)
17. Neoeuonymine	Ac	Ac	H	Ac	Ac	Ac	C <sub>36</sub> H <sub>45</sub> NO <sub>17</sub> , mw: 763.27, mp: 259–262 °C, [α] <sub>D</sub> –11° (CHCl <sub>3</sub> ), UV, IR (15), <sup>1</sup> H (23)
18. 4-Hydroxy-7-epi-chuchuhuanine E-V	Ac	H	Ac	Ac	Ac	Ac	C <sub>36</sub> H <sub>45</sub> NO <sub>17</sub> , mw: 763.27, [α] <sub>D</sub> <sup>20</sup> –37.4° (CHCl <sub>3</sub> ), UV, IR, MS, <sup>1</sup> H, <sup>13</sup> C (24)
19. Angulatamine	Ac	Nic	Ac	CO <sup>i</sup> Pr	Ac	Ac	C <sub>44</sub> H <sub>52</sub> N <sub>2</sub> O <sub>18</sub> , mw: 896.32, [α] <sub>D</sub> <sup>25</sup> +13.67° (MeOH), IR, UV, MS, <sup>1</sup> H (22)
20. Putterine A or wilforinine G	Ac	Ac	Ac	Nic	Ac	Ac	C <sub>42</sub> H <sub>48</sub> N <sub>2</sub> O <sub>18</sub> , mw: 868.29, IR, <sup>1</sup> H (25); [α] <sub>D</sub> +11° (MeOH), UV, IR, MS, <sup>1</sup> H, <sup>13</sup> C (26)
21. Putterine B	Ac	CO <sup>i</sup> Pr	Ac	Nic	Ac	Ac	C <sub>44</sub> H <sub>52</sub> N <sub>2</sub> O <sub>18</sub> , mw: 896.32, IR, <sup>1</sup> H, <sup>13</sup> C (25)
22. Wilforinine F	Ac	H	Bz	Ac	Ac	Ac	C <sub>41</sub> H <sub>47</sub> NO <sub>17</sub> , mw: 825.28, [α] <sub>D</sub> +18.2° (MeOH), UV, IR, MS, <sup>1</sup> H, <sup>13</sup> C (26)
23. Celahinine A	Bz	Ac	Bz	Ac	Bz	Ac	C <sub>53</sub> H <sub>53</sub> NO <sub>18</sub> , mw: 991.33, mp: > 300 °C, IR, MS, <sup>1</sup> H, <sup>13</sup> C (27)
24. Ebenifoline E-I	Bz	H	Ac	Ac	Ac	Ac	C <sub>41</sub> H <sub>47</sub> NO <sub>17</sub> , mw: 825.28, mp: 183–185 °C, [α] <sub>D</sub> 0° (CHCl <sub>3</sub> ), UV, IR, MS, CD, <sup>1</sup> H, <sup>13</sup> C (19)
25. Ebenifoline E-II	Bz	Ac	Bz	Ac	Ac	Ac	C <sub>48</sub> H <sub>51</sub> NO <sub>18</sub> , mw: 929.31, mp: 174–177 °C, [α] <sub>D</sub> –13.2° (CHCl <sub>3</sub> ), UV, IR, MS, CD, <sup>1</sup> H, <sup>13</sup> C (19)
26. Ebenifoline E-III	Bz	Ac	Ac	Ac	Bz	Ac	C <sub>48</sub> H <sub>51</sub> NO <sub>18</sub> , mw: 929.31, mp: 174–177 °C, [α] <sub>D</sub> –25.8° (CHCl <sub>3</sub> ), UV, IR, MS, CD, <sup>1</sup> H, <sup>13</sup> C (19)
27. Ebenifoline E-V	Bz	Ac	H	Ac	Bz	Ac	C <sub>46</sub> H <sub>49</sub> NO <sub>17</sub> , mw: 887.30, mp: 165–169 °C, [α] <sub>D</sub> –27.5° (CHCl <sub>3</sub> ), UV, IR, MS, CD, <sup>1</sup> H, <sup>13</sup> C (19)

(continued)

TABLE II.  
Continued.

Alkaloid	R <sub>1</sub>	R <sub>2</sub>	R <sub>3</sub>	R <sub>4</sub>	R <sub>5</sub>	R <sub>6</sub>	Properties
28. Mayteine	Bz	Ac	Ac	Ac	Ac	Ac	C <sub>43</sub> H <sub>49</sub> NO <sub>18</sub> , mw: 867.29, mp: 168–170 °C, [α] <sub>D</sub> –22.4° (CHCl <sub>3</sub> ), UV, IR, MS, <sup>1</sup> H, <sup>13</sup> C (19); [α] <sub>D</sub> <sup>25</sup> –9.36° (CHCl <sub>3</sub> ) (28)
29. Euojaponine A	Bz	Ac	H	Ac	Ac	Ac	C <sub>41</sub> H <sub>47</sub> NO <sub>17</sub> , mw: 825.28, mp: 273–275 °C, [α] <sub>D</sub> <sup>25</sup> +24.67° (EtOH), UV, <sup>1</sup> H, <sup>13</sup> C (29)
30. Euojaponine C	Bz	H	Bz	Ac	Ac	Ac	C <sub>46</sub> H <sub>49</sub> N <sub>2</sub> O <sub>17</sub> , mw: 887.30, mp: 178–182 °C, [α] <sub>D</sub> –1.1° (CHCl <sub>3</sub> ), UV, IR, MS, <sup>1</sup> H, <sup>13</sup> C (19); mp: 172–175 °C, [α] <sub>D</sub> <sup>25</sup> +11.4° (EtOH), UV, <sup>1</sup> H, <sup>13</sup> C (29)
31. Euojaponine I	Nic	Ac	Ac	Ac	Ac	Ac	C <sub>42</sub> H <sub>48</sub> N <sub>2</sub> O <sub>18</sub> , mw: 868.29, mp: 168–171 °C, [α] <sub>D</sub> <sup>25</sup> +4.35° (EtOH), UV, <sup>1</sup> H, <sup>13</sup> C (29)
32. Euojaponine L	Nic	H	Bz	Ac	Ac	Ac	C <sub>45</sub> H <sub>48</sub> N <sub>2</sub> O <sub>17</sub> , mw: 888.30, mp: 195–197 °C, [α] <sub>D</sub> <sup>25</sup> +11.24° (EtOH), UV, <sup>1</sup> H, <sup>13</sup> C (29)
33. Euojaponine M	Nic	H	Ac	Ac	Ac	Ac	C <sub>40</sub> H <sub>46</sub> N <sub>2</sub> O <sub>17</sub> , mw: 826.28, mp: 188–190 °C, [α] <sub>D</sub> <sup>25</sup> +12.57° (EtOH), UV, <sup>1</sup> H, <sup>13</sup> C (29)
34. Laevisine A	Tig*	Ac	Ac	Ac	Ac	Ac	C <sub>41</sub> H <sub>51</sub> NO <sub>18</sub> , mw: 845.31, mp: 171–173 °C, [α] <sub>D</sub> <sup>25</sup> +97.3° (CHCl <sub>3</sub> ), UV, <sup>1</sup> H, <sup>13</sup> C (30)

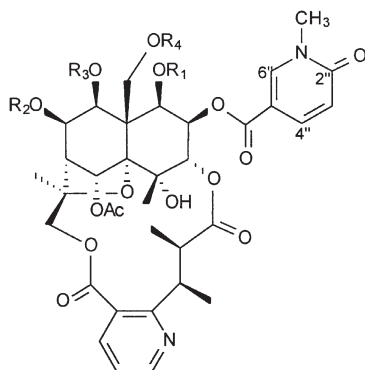
\*Tiglic or angelic acid, because double bond stereochemistry was not defined.

### 3. Isoeuonyminol Derivatives

Evoninate sesquiterpene alkaloids containing an isoeuonyminol core and a CNMP group have also been obtained from the Celastraceae family, although only three members of this class of alkaloids have been isolated, as shown in Table IV. Five isoeuonyminol derivatives not containing a CNMP group have also been isolated, as described in Table V. In its <sup>1</sup>H-NMR, isoeuonyminol differed from the euonyminol skeleton with respect to the <sup>1</sup>H coupling constants between the H-6, H-7, and H-8 methine protons. In the euonyminol skeleton, while their couplings are generally near 3.9 (*J*<sub>6,7</sub>) and 5.7 Hz (*J*<sub>7,8</sub>), in isoeuonyminol these couplings are near to 3.0 (*J*<sub>6,7</sub>) and 9.6 Hz (*J*<sub>7,8</sub>). Furthermore, H-7 and H-8 show NOE correlations with H-5 and H-14, respectively. The peripheral esterifying residues



TABLE III.  
Evoninate Alkaloids – CNMP Euonyminol Derivatives.

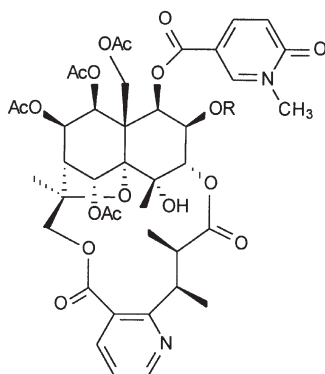


Alkaloid	R <sub>1</sub>	R <sub>2</sub>	R <sub>3</sub>	R <sub>4</sub>	Properties
35. Hippocrateine I	Bz	Ac	Ac	Ac	C <sub>48</sub> H <sub>52</sub> N <sub>2</sub> O <sub>19</sub> , mw: 960.31, mp: 300 °C, IR, UV, MS, <sup>1</sup> H, <sup>13</sup> C (31)
36. Hippocrateine II	Bz	Ac	Ac	MeBu	C <sub>51</sub> H <sub>58</sub> N <sub>2</sub> O <sub>19</sub> , mw: 1002.36, mp: 308 °C, IR, UV, MS, <sup>1</sup> H, <sup>13</sup> C (31)
37. Emarginatine A	Ac	Ac	Ac	Ac	C <sub>43</sub> H <sub>50</sub> N <sub>2</sub> O <sub>19</sub> , mw: 898.30, <sup>1</sup> H, <sup>13</sup> C (32); mp: 312–313 °C, [α] <sub>D</sub> <sup>22</sup> +70° (CHCl <sub>3</sub> ), UV, IR, <sup>1</sup> H, <sup>13</sup> C, X-ray (33)
38. Emarginatine C	Ac	Ac	H	Ac	C <sub>41</sub> H <sub>48</sub> N <sub>2</sub> O <sub>18</sub> , mw: 856.29, mp: 312–315 °C, [α] <sub>D</sub> +16.0° (CHCl <sub>3</sub> ), UV, IR, MS, <sup>1</sup> H, <sup>13</sup> C (34)
39. Emarginatine D	H	Ac	Ac	Ac	C <sub>41</sub> H <sub>48</sub> N <sub>2</sub> O <sub>18</sub> , mw: 856.29, mp: 192–202 °C, [α] <sub>D</sub> +51.0° (CHCl <sub>3</sub> ), UV, IR, MS, <sup>1</sup> H, <sup>13</sup> C (34)
40. Emarginatine G	Tig*	Ac	Ac	Ac	C <sub>46</sub> H <sub>54</sub> N <sub>2</sub> O <sub>19</sub> , mw: 938.33, mp: 315–318 °C, [α] <sub>D</sub> <sup>20</sup> +200° (CHCl <sub>3</sub> ), UV, IR, MS, <sup>1</sup> H, <sup>13</sup> C (35)
41. Emarginatine H	Ac	Ac	Ac	H	C <sub>41</sub> H <sub>48</sub> N <sub>2</sub> O <sub>18</sub> , mw: 856.29, mp: 313–316 °C, [α] <sub>D</sub> +35° (CHCl <sub>3</sub> ), IR, MS, <sup>1</sup> H, <sup>13</sup> C (32)
42	Ac	CO <sup>i</sup> Pr	Ac	Ac	C <sub>45</sub> H <sub>54</sub> N <sub>2</sub> O <sub>19</sub> , mw: 926.33, mp: 300–307 °C, [α] <sub>D</sub> +15.3° (CHCl <sub>3</sub> ), UV, <sup>1</sup> H, <sup>13</sup> C (36)
43	Ac	Ac	Ac	CO <sup>i</sup> Pr	C <sub>45</sub> H <sub>54</sub> N <sub>2</sub> O <sub>19</sub> , mw: 926.33, mp: 246–249 °C, [α] <sub>D</sub> +15.5° (CHCl <sub>3</sub> ), UV, <sup>1</sup> H, <sup>13</sup> C (36)

(continued)

TABLE III.  
Continued.

Alkaloid	R <sub>1</sub>	R <sub>2</sub>	R <sub>3</sub>	R <sub>4</sub>	Properties
44	H	Ac	CO <sup>i</sup> Pr	Ac	C <sub>43</sub> H <sub>52</sub> N <sub>2</sub> O <sub>18</sub> , mw: 884.32, mp: 194–198 °C, [α] <sub>D</sub> −4.3° (CHCl <sub>3</sub> ), UV, <sup>1</sup> H, <sup>13</sup> C (36)
45	CO <sup>i</sup> Pr	Ac	CO <sup>i</sup> Pr	Ac	C <sub>47</sub> H <sub>58</sub> N <sub>2</sub> O <sub>19</sub> , mw: 954.36, mp: 177–183 °C, [α] <sub>D</sub> −2.3° (CHCl <sub>3</sub> ), UV, <sup>1</sup> H, <sup>13</sup> C (36)



Alkaloid	R	Properties
46	Ac	C <sub>43</sub> H <sub>50</sub> N <sub>2</sub> O <sub>19</sub> , mw: 898.30, mp: 154–178 °C, [α] <sub>D</sub> −11.6° (CHCl <sub>3</sub> ), UV, <sup>1</sup> H, <sup>13</sup> C (36)
47	H	C <sub>41</sub> H <sub>48</sub> N <sub>2</sub> O <sub>18</sub> , mw: 856.29, mp: 192–199 °C, [α] <sub>D</sub> −22.8° (CHCl <sub>3</sub> ), UV, <sup>1</sup> H, <sup>13</sup> C (36)

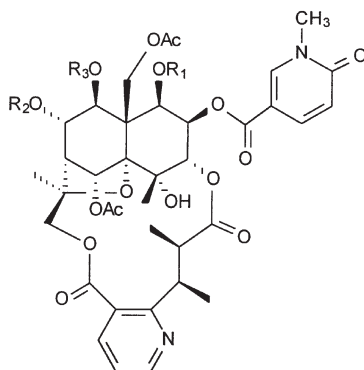
\*Tiglic or angelic acid, because double bond stereochemistry was not defined.

vary between acetic, benzoic, and nicotinic acids, and the relative positions of these residues distinguish each individual alkaloid.

#### 4. 4-Deoxy Sesquiterpene Cores

Chuchuhuanines are sesquiterpene pyridine alkaloids isolated from *Maytenus chuchuhuasca* (Celastraceae), a Brazilian medicinal plant used to treat skin cancer (41). These alkaloids are characterized by the absence of a 4-hydroxyl group on the isoeuonyminol dihydroagarofuran sesquiterpene core, forming a 4-deoxyisoeuonyminol backbone linked to evoninic or wilfordic acids. Evoninate type alkaloids are shown in Table VI, and wilfordate derivatives are discussed in the appropriate section. These alkaloids are characterized in their <sup>1</sup>H-NMR by one

TABLE IV.  
Evoninate Alkaloids – CNMP Isoeuonyminol Derivatives.



Alkaloid	R <sub>1</sub>	R <sub>2</sub>	R <sub>3</sub>	Properties
48. Emarginatine B	Ac	Ac	Bz	C <sub>48</sub> H <sub>52</sub> N <sub>2</sub> O <sub>19</sub> , mw: 960.32, mp: 191–194 °C, [α] <sub>D</sub> +26° (CHCl <sub>3</sub> ), UV, IR, MS, <sup>1</sup> H, <sup>13</sup> C (37)
49. Emarginatine E	H	Ac	H	C <sub>39</sub> H <sub>46</sub> N <sub>2</sub> O <sub>17</sub> , mw: 814.28, mp: 240–242 °C, [α] <sub>D</sub> –36.0° (CHCl <sub>3</sub> ), UV, IR, MS, <sup>1</sup> H, <sup>13</sup> C (34)
50. Emarginatine F	Bz	H	Ac	C <sub>46</sub> H <sub>50</sub> N <sub>2</sub> O <sub>18</sub> , mw: 918.31, mp: 221–223 °C, [α] <sub>D</sub> <sup>20</sup> +600° (CHCl <sub>3</sub> ), UV, IR, MS, <sup>1</sup> H, <sup>13</sup> C (35)

additional secondary methyl group and one methine proton at approximately  $\delta$  1.2 (d,  $J=7.9$  Hz) and 2.7 (q,  $J=7.9$  Hz), respectively.

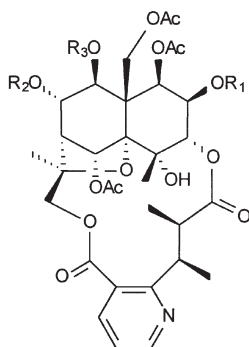
Three similar sesquiterpene alkaloids are 4-deoxyeuonymine (**61**), euojapnine N (**62**), and ebenifoline E-IV (**63**). These compounds also contain 4-deoxy sesquiterpene cores, although the esterifying groups attached at C-7 possess the  $\beta$ ax stereochemistry characteristic of the euonyminol nucleus. Their structures were elucidated by spectroscopic analyses.

### 5. Cathedulins Alkaloids

The narcotic drug khat, largely used in many countries of East Africa, consists of the fresh leaves and shoots of *Catha edulis*. The main physiological effects of khat are appetite suppression and stimulant action, which includes the ability to induce a feeling of elation and peacefulness. These effects have been attributed to the presence of cathine, also known as norpseudoephedrine, although cathedulins may also be implicated (43,44).

Cathedulin derivatives isolated to date are polyesters of two sesquiterpene cores, euonyminol and 3,4,6,13-tetradecoxy-9-epieuonyminol, and can be conveniently divided into three groups based on their molecular weights: lower

TABLE V.  
Evoninate Alkaloids – Isoeuonyminol Derivatives.



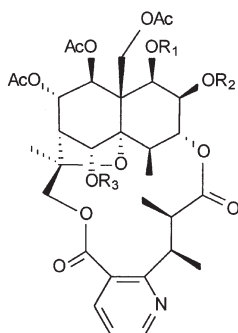
Alkaloid	R <sub>1</sub>	R <sub>2</sub>	R <sub>3</sub>	Properties
51. Horridina	Ac	Ac	Bz	C <sub>43</sub> H <sub>49</sub> NO <sub>18</sub> , mw: 867.29, <sup>1</sup> H, <sup>13</sup> C (38)
52. Aquifoliunine E-I	Ac	Bz	Ac	C <sub>43</sub> H <sub>49</sub> NO <sub>18</sub> , mw: 867.29, [α] <sub>D</sub> -3.1° (CHCl <sub>3</sub> ), IR, MS, <sup>1</sup> H, <sup>13</sup> C (39)
53. Aquifoliunine E-II	H	H	Ac	C <sub>34</sub> H <sub>43</sub> NO <sub>16</sub> , mw: 721.26, [α] <sub>D</sub> -17.2° (CHCl <sub>3</sub> ), IR, MS, <sup>1</sup> H, <sup>13</sup> C (39)
54. Aquifoliunine E-III	Ac	H	Ac	C <sub>36</sub> H <sub>45</sub> NO <sub>17</sub> , mw: 763.27, [α] <sub>D</sub> -20.8° (CHCl <sub>3</sub> ), IR, MS, <sup>1</sup> H, <sup>13</sup> C (40)
55. Aquifoliunine E-IV	Ac	Nic	Ac	C <sub>41</sub> H <sub>48</sub> N <sub>2</sub> O <sub>18</sub> , mw: 856.29, [α] <sub>D</sub> -15.2° (CHCl <sub>3</sub> ), IR, MS, <sup>1</sup> H, <sup>13</sup> C (40)

molecular weight (~600–700 D), medium molecular weight (~750–900 D), and high molecular weight (1100–1200 D) groups (45). The esterifying acids of the sesquiterpene cores of the khat alkaloids are acetic, 2-hydroxyisobutyric, 2-acetoxyisobutyric, benzoic, nicotinic, and tri-*O*-methylgallic acids. The lower molecular weight sesquiterpene pyridine alkaloids will be discussed in detail in the appropriate section.

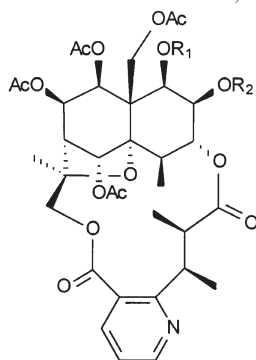
The cathedulin alkaloids of medium molecular weight comprise cathedulins K1, K2, K6, and K15 (Table VII), isolated from plant material collected in Kenya. The most abundant is cathedulin K2 and it was the most intensively studied. Mass and NMR spectroscopy, as well as ethanolsis of this alkaloid, showed an euonyminol sesquiterpene core, one evoninic acid, five acetic acid, and one 2-acetoxyisobutyric acid residues. Cathedulin K2 acted as a lead alkaloid in the formulation of the remaining three substances.

The high molecular weight group comprise cathedulins E3, E4, E5, and E6 isolated from plant material collected in Ethiopia, and K12, K17, K19, and K20 derived from khat of Kenyan origin (Table VIII). Alkaloids E3 and E4 are closely

TABLE VI.  
4-Deoxyisoeuonyminol and 4-Deoxyeuonyminol Alkaloids.



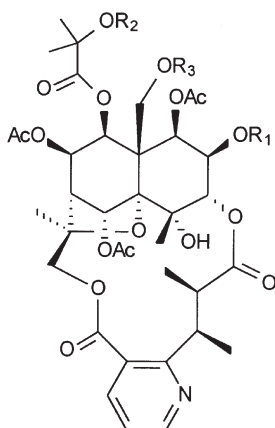
Alkaloid	R <sub>1</sub>	R <sub>2</sub>	R <sub>3</sub>	Properties
56. Chuchuhuanine E-I	Ac	Ac	Ac	C <sub>38</sub> H <sub>47</sub> NO <sub>17</sub> , mw: 789.28, mp: 247–250 °C, [α] <sub>D</sub> –23.3° (CHCl <sub>3</sub> ), UV, IR, MS, CD, <sup>1</sup> H, <sup>13</sup> C (41)
57. Chuchuhuanine E-II	Bz	Ac	Ac	C <sub>43</sub> H <sub>49</sub> NO <sub>17</sub> , mw: 851.30, mp: 158–160 °C, [α] <sub>D</sub> –8.5° (CHCl <sub>3</sub> ), UV, IR, MS, CD, <sup>1</sup> H, <sup>13</sup> C (41)
58. Chuchuhuanine E-III	Ac	Bz	Ac	C <sub>43</sub> H <sub>49</sub> NO <sub>17</sub> , mw: 851.30, mp: 156–160 °C, [α] <sub>D</sub> –412.5° (CHCl <sub>3</sub> ), UV, IR, MS, CD, <sup>1</sup> H, <sup>13</sup> C (41)
59. Chuchuhuanine E-IV	Ac	Ac	H	C <sub>36</sub> H <sub>45</sub> NO <sub>16</sub> , mw: 747.27, mp: 162–166 °C, [α] <sub>D</sub> –9.3° (CHCl <sub>3</sub> ), UV, IR, MS, CD, <sup>1</sup> H, <sup>13</sup> C (41)
60. Chuchuhuanine E-V	Ac	H	Ac	C <sub>36</sub> H <sub>45</sub> NO <sub>16</sub> , mw: 747.27, mp: 154–160 °C, [α] <sub>D</sub> –18.3° (CHCl <sub>3</sub> ), UV, IR, MS, CD, <sup>1</sup> H, <sup>13</sup> C (41)



(continued)

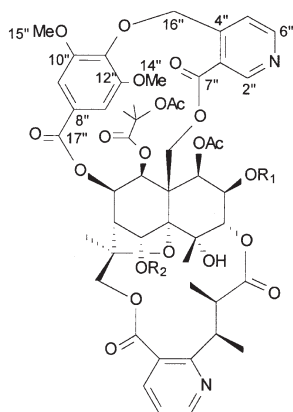
TABLE VI.  
Continued.

Alkaloid	R <sub>1</sub>	R <sub>2</sub>	Properties
61. 4-Deoxyeuonymine	Ac	Ac	C <sub>38</sub> H <sub>47</sub> NO <sub>17</sub> , mw: 789.28, mp: 138–142 °C, [α] <sub>D</sub> <sup>20</sup> –13.6° (CHCl <sub>3</sub> ), UV, IR, MS, CD, <sup>1</sup> H, <sup>13</sup> C (41)
62. Euojaponine N	Nic	Bz	C <sub>47</sub> H <sub>50</sub> N <sub>2</sub> O <sub>17</sub> , mw: 914.31, mp: 161–163 °C, [α] <sub>D</sub> <sup>28</sup> +31.6° (EtOH), <sup>1</sup> H, <sup>13</sup> C (42)
63. Ebenifoline E-IV	Bz	Ac	C <sub>43</sub> H <sub>49</sub> NO <sub>17</sub> , mw: 851.30, mp: 143–146 °C, [α] <sub>D</sub> <sup>20</sup> –7.8° (CHCl <sub>3</sub> ), UV, IR, MS, CD, <sup>1</sup> H, <sup>13</sup> C (19)

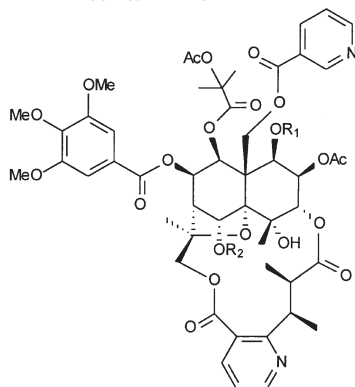
TABLE VII.  
Cathedulin Alkaloids of Medium Molecular Weight.

Alkaloid	R <sub>1</sub>	R <sub>2</sub>	R <sub>3</sub>	Properties
64. Cathedulin K1	Ac	Ac	Ac	C <sub>42</sub> H <sub>53</sub> NO <sub>20</sub> , mw: 891.32, IR, UV, MS, <sup>1</sup> H (46), mp: 165–168 °C; <sup>1</sup> H (47)
65. Cathedulin K2	H	Ac	Ac	C <sub>40</sub> H <sub>51</sub> NO <sub>18</sub> , mw: 849.31, mp: 181–184 °C, [α] <sub>D</sub> <sup>20</sup> –17.8° (CHCl <sub>3</sub> ), IR, UV, MS, <sup>1</sup> H, <sup>13</sup> C (46); <sup>1</sup> H (47)
66. Cathedulin K6	H	Ac	H	C <sub>38</sub> H <sub>49</sub> NO <sub>18</sub> , mw: 807.29, mp: 176–180 °C, IR, UV, MS, <sup>1</sup> H (46); <sup>1</sup> H (47)
67. Cathedulin K15	H	H	H	C <sub>36</sub> H <sub>47</sub> NO <sub>17</sub> , mw: 765.28, mp: 191–194 °C, IR, UV, MS, <sup>1</sup> H (46); <sup>1</sup> H (47)

TABLE VIII.  
Cathedulin Alkaloids of High Molecular Weight.



Alkaloid	R <sub>1</sub>	R <sub>2</sub>	Properties
68. Cathedulin E3	Ac	Ac	C <sub>53</sub> H <sub>57</sub> N <sub>2</sub> O <sub>23</sub> , mw: 1089.34, mp: 245–248 °C, [α] <sub>D</sub> <sup>20</sup> –44.8° (CHCl <sub>3</sub> ), IR, UV, <sup>1</sup> H, <sup>13</sup> C (46); <sup>1</sup> H, <sup>13</sup> C (48)
69. Cathedulin E4	Ac	H	C <sub>51</sub> H <sub>55</sub> N <sub>2</sub> O <sub>22</sub> , mw: 1047.32, [α] <sub>D</sub> <sup>27</sup> –37° (CHCl <sub>3</sub> ), IR, UV, <sup>1</sup> H (46); <sup>1</sup> H, <sup>13</sup> C (48)
70. Cathedulin K20	Bz	Ac	C <sub>58</sub> H <sub>59</sub> N <sub>2</sub> O <sub>23</sub> , mw: 1151.35, <sup>1</sup> H, <sup>13</sup> C (49)



Alkaloid	R <sub>1</sub>	R <sub>2</sub>	Properties
71. Cathedulin E5	Bz	Ac	C <sub>59</sub> H <sub>64</sub> N <sub>2</sub> O <sub>23</sub> , mw: 1168.39, <sup>1</sup> H, <sup>13</sup> C (48)
72. Cathedulin E6	Bz	H	C <sub>57</sub> H <sub>62</sub> N <sub>2</sub> O <sub>22</sub> , mw: 1126.38, IR, UV, <sup>1</sup> H, <sup>13</sup> C (46); <sup>1</sup> H, <sup>13</sup> C (48)
73. Cathedulin K12	Ac	Ac	C <sub>54</sub> H <sub>62</sub> N <sub>2</sub> O <sub>23</sub> , mw: 1106.37, mp: 268–272 °C, IR, UV, MS, <sup>1</sup> H (46); <sup>1</sup> H, <sup>13</sup> C (48)

related, since acetylation of E4 forms E3 exclusively, and partial methanolysis of E3 gave a reasonable yield of E4. In these alkaloids, a novel structural feature is the cathate bridge between the 8-axial oxygen and the 15-oxygen of the euonyminol core, forming a second macrocycle. Cathate acid (Fig. 3) was isolated as its dimethyl ester derivative after alcoholysis of cathedulin E3 and E4, together with 2-acetoxyisobutyric and acetic acids, which were also found as the peripheral esterifying residues on the euonyminol sesquiterpene core. Cathedulin K20 is also closely related to cathedulin E3, in which a benzoate residue replaced an acetate group located at C-2, according to the NMR spectra in which H-2 was at lower field than the corresponding proton in alkaloids containing an acetyl group attached to the C-2 position.

Three further alkaloids closely related to cathedulin E3 were isolated from plant material collected in Kenya and Ethiopia, although the cathate bridge was observed in the opened form. Thus, trimethylgallic and nicotinic acids are both esterifying agents of the euonyminol core. In cathedulin K12 the remaining ester positions are similar to those of E3. A benzoate group replacing acetate on C-1 characterizes cathedulin E5. The latter and E6 are also related, with the C-6 hydroxyl group esterified by an acetate residue.

TABLE IX.  
Evoninate and Hydroxyisoevoninate Triptonines.

74. Triptonine A	75. Triptonine B
Properties	Properties
$C_{45}H_{55}NO_{21}$ , mw: 945.33, mp: 284–285.5°C, $[\alpha]_D^{25}$ –24.1° (MeOH), UV, IR, MS, $^1H$ , $^{13}C$ , X-ray (50)	$C_{45}H_{55}NO_{22}$ , mw: 961.32, $[\alpha]_D^{25}$ +15.5° (MeOH), UV, IR, MS, $^1H$ , $^{13}C$ (51)



### 6. Dimacrocylic Sesquiterpene Pyridine Alkaloids

Triptonines A and B are sesquiterpene pyridine alkaloids that contain a second macrocycle in their structure, composed of a monoterpene unit forming a macrolactone bridge between C-8 and C-14. These alkaloids represent the first examples of sesquiterpene pyridine alkaloids in which two terpenoid units are present (Table IX). This ester linkage was corroborated in their HMBC spectrum in which the proton signals of H-7 and H-14 were correlated with the carbonyl signals of the monoterpene unit. In order to confirm the structure of triptonine A (74), X-ray analysis was undertaken (50). In triptonine B (75) a novel structural feature is the isomeric form of evoninic acid, called isoevoninic acid, where the acyl substituents on the pyridine ring are located at positions 3 and 4. Isoevoninic acid has also been obtained in the hydroxylated form, as in triptonine B. Isoevoninate sesquiterpene pyridine alkaloid derivatives are discussed in the next section.

Triptonines have been isolated from *Tripterygium hypoglaucum*, a plant of the Celastraceae family (51). However, two other reported sesquiterpene alkaloids isolated from *Tripterygium wilfordii* were also named as triptonine A (140) and B (141) (72). Their structures are presented in Table XIX.

### B. ISOEVONINATE ALKALOIDS

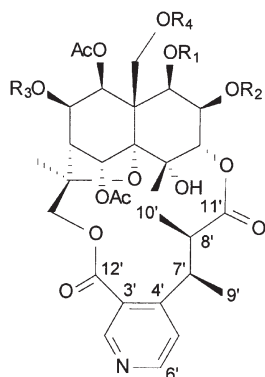
Evoninate type alkaloids are the most predominant sesquiterpene pyridine alkaloids isolated from the Celastraceae, although the isomeric evoninic acid has also been reported in the literature (Table X). The dibasic isoevoninic acid contains a 3,4-substituted nicotinic acid grouping rather than a 2,3-substituted one, as in the case of evoninic acid. This isomeric form is characterized in the <sup>1</sup>H-NMR spectra by resonances at  $\delta$  9.0 (s, H-2'), 8.7 (d,  $J=5.7$  Hz, H-6'), and 7.5 (d,  $J=5.7$  Hz, H-5'), along with two methyl doublets at  $\delta$  1.1 ( $J=7.1$  Hz, H-10') and 1.4 ( $J=6.8$  Hz, H-9'). On the other hand, the signals of H-4', H-5', and H-6' in evoninic acid are observed as double doublets. Furthermore, in their HMBC spectrum correlations between H-2' and carbons C-3', C-12', and C-6', as well as proton H-5' with carbons C-3', C-4', and C-7' were observed.

Isoevoninate sesquiterpene alkaloids containing a CNMP ring have also been isolated from Celastraceae (Table XI). Species from this family can synthesize two classes of CNMP sesquiterpene pyridine alkaloids. The first class of alkaloid possessing evoninic acid as the alkaloid portion, like the emarginatines and the hippocrateines (*vide infra*), and the second represented by hippocrateine III (82), characterized by isoevoninic acid as the diester moiety.

### C. HYDROXYISOEVONINATE ALKALOIDS

A small group of sesquiterpene pyridine alkaloids contain a dibasic hydroxyisoevoninic acid as their alkaloid diester portion (Table XII). This oxidized residue is characterized in the <sup>1</sup>H-NMR by the resonances at  $\delta$  9.0 (s, H-2'), 8.7

TABLE X.  
Isoevoninate Sesquiterpene Pyridine Alkaloids.

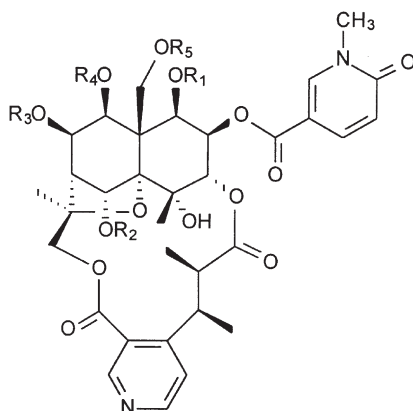


Alkaloid	R <sub>1</sub>	R <sub>2</sub>	R <sub>3</sub>	R <sub>4</sub>	Properties
76. Wilfordinine A	Ac	H	Ac	Ac	C <sub>36</sub> H <sub>45</sub> NO <sub>17</sub> , mw: 763.27, [α] <sub>D</sub> <sup>25</sup> -11° (MeOH), UV, IR, MS, <sup>1</sup> H, <sup>13</sup> C (51)
77. Wilfordinine J	H	Ac	Ac	Ac	C <sub>36</sub> H <sub>45</sub> NO <sub>17</sub> , mw: 763.27, [α] <sub>D</sub> -8.1° (MeOH), UV, IR, MS, <sup>1</sup> H, <sup>13</sup> C (26)
78. Peritassine A	Ac	Ac	Ac	Ac	C <sub>38</sub> H <sub>47</sub> NO <sub>18</sub> , mw: 805.28, mp: 116–117°C, IR, <sup>1</sup> H, <sup>13</sup> C (52)
79. Peritassine B	Ac	Ac	Bz	Ac	C <sub>43</sub> H <sub>49</sub> NO <sub>18</sub> , mw: 867.29, mp: 148–150°C, IR, <sup>1</sup> H, <sup>13</sup> C (52)
80	Ac	Ac	CO <sup>t</sup> Pr	Ac	C <sub>40</sub> H <sub>51</sub> NO <sub>18</sub> , mw: 833.31, mp: 162–164°C, [α] <sub>D</sub> -36.8° (CHCl <sub>3</sub> ), UV, <sup>1</sup> H, <sup>13</sup> C (36)
81. Hypoglaunine D	Ac	Ac	Ac	Fu	C <sub>41</sub> H <sub>47</sub> NO <sub>19</sub> , mw: 857.27, [α] <sub>D</sub> <sup>25</sup> -15.3° (MeOH), UV, IR, MS, <sup>1</sup> H, <sup>13</sup> C (53)

(d,  $J = 5.3$  Hz, H-6'), and 7.8 (d,  $J = 5.3$  Hz, H-5'), along with two methyl signals at  $\delta$  1.2 (d,  $J = 7.1$  Hz, H-9') and 1.4 (s, H-10'). These signals are very similar to those of the isoevoninate type, differing only by the multiplicity of H-10', that was observed as a doublet in the isoevoninate alkaloids. Thus, a 2-hydroxy-2,3-dimethyl-3-(3'-carboxy-4'-pyridyl)-propanoic acid, could be characterized.

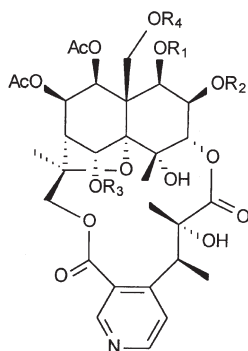
Wilfordinines and hypoglaunines are hydroxyisoevoninate sesquiterpene pyridine alkaloids isolated from *T. wilfordii* and *T. hypoglaucum*, respectively. These plants of the Celastraceae family have been used to treat several diseases in traditional Chinese medicine.

TABLE XI.  
CNMP Isoevoninate Sesquiterpene Pyridine Alkaloids.



Alkaloid	R <sub>1</sub>	R <sub>2</sub>	R <sub>3</sub>	R <sub>4</sub>	R <sub>5</sub>	Properties
<b>82.</b> Hippocrateine III	Ac	Ac	Ac	Ac	MeBu	C <sub>46</sub> H <sub>56</sub> N <sub>2</sub> O <sub>19</sub> , mw: 940.35, UV, IR, <sup>1</sup> H, <sup>13</sup> C (54)
<b>83</b>	Ac	Ac	CO <sup>i</sup> Pr	Ac	Ac	C <sub>45</sub> H <sub>54</sub> N <sub>2</sub> O <sub>19</sub> , mw: 926.33, mp: 189–196 °C, [α] <sub>D</sub> +2.3° (CHCl <sub>3</sub> ), UV, <sup>1</sup> H, <sup>13</sup> C (36)
<b>84</b>	Ac	Ac	CO <sup>i</sup> Pr	Ac	CO <sup>i</sup> Pr	C <sub>47</sub> H <sub>58</sub> N <sub>2</sub> O <sub>19</sub> , mw: 954.36, mp: 179–187 °C, [α] <sub>D</sub> +6.3° (CHCl <sub>3</sub> ), UV, <sup>1</sup> H, <sup>13</sup> C (36)
<b>85</b>	Ac	Ac	CO <sup>i</sup> Pr	CO <sup>i</sup> Pr	CO <sup>i</sup> Pr	C <sub>49</sub> H <sub>62</sub> N <sub>2</sub> O <sub>19</sub> , mw: 982.39, mp: 186–190 °C, [α] <sub>D</sub> –18.6° (CHCl <sub>3</sub> ), UV, <sup>1</sup> H, <sup>13</sup> C (36)
<b>86</b>	Ac	H	CO <sup>i</sup> Pr	Ac	CO <sup>i</sup> Pr	C <sub>45</sub> H <sub>56</sub> N <sub>2</sub> O <sub>18</sub> , mw: 912.35, mp: 171–176 °C, [α] <sub>D</sub> +12.5° (CHCl <sub>3</sub> ), UV, <sup>1</sup> H, <sup>13</sup> C (36)
<b>87</b>	H	Ac	CO <sup>i</sup> Pr	CO <sup>i</sup> Pr	CO <sup>i</sup> Pr	C <sub>47</sub> H <sub>60</sub> N <sub>2</sub> O <sub>18</sub> , mw: 940.38, mp: 189–194 °C, [α] <sub>D</sub> –21.7° (CHCl <sub>3</sub> ), UV, <sup>1</sup> H, <sup>13</sup> C (36)
<b>88</b>	CO <sup>i</sup> Pr	Ac	Ac	CO <sup>i</sup> Pr	CO <sup>i</sup> Pr	C <sub>49</sub> H <sub>62</sub> N <sub>2</sub> O <sub>19</sub> , mw: 982.39, mp: 206–210 °C, [α] <sub>D</sub> –16° (CHCl <sub>3</sub> ), UV, <sup>1</sup> H, <sup>13</sup> C (36)

TABLE XII.  
Hydroxyisoevонinate Sesquiterpene Pyridine Alkaloids.

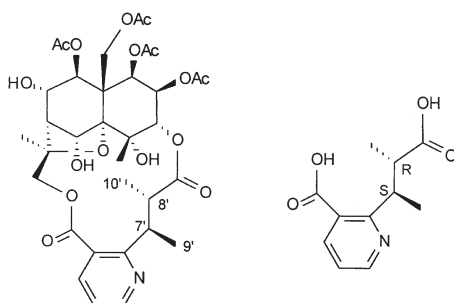


Alkaloid	R <sub>1</sub>	R <sub>2</sub>	R <sub>3</sub>	R <sub>4</sub>	Properties
89. Wilfordinine B	Ac	Ac	Ac	Ac	C <sub>38</sub> H <sub>47</sub> NO <sub>19</sub> , mw: 821.27, [α] <sub>D</sub> <sup>25</sup> +43.5° (MeOH), UV, IR, MS, <sup>1</sup> H, <sup>13</sup> C (51)
90. Wilfordinine C	Bz	Ac	Ac	Ac	C <sub>43</sub> H <sub>49</sub> NO <sub>19</sub> , mw: 883.29, [α] <sub>D</sub> <sup>25</sup> +39.1° (MeOH), UV, IR, MS, <sup>1</sup> H, <sup>13</sup> C (51)
91. Wilfordinine I	Ac	Bz	Bz	Ac	C <sub>48</sub> H <sub>51</sub> NO <sub>19</sub> , mw: 945.31, [α] <sub>D</sub> +63° (MeOH), UV, IR, MS, <sup>1</sup> H, <sup>13</sup> C (26)
92. Hypoglaunine A	Ac	Ac	Ac	Fu	C <sub>41</sub> H <sub>47</sub> NO <sub>20</sub> , mw: 873.27, [α] <sub>D</sub> <sup>25</sup> +42.8° (MeOH), UV, IR, MS, <sup>1</sup> H, <sup>13</sup> C (53)
93. Hypoglaunine B	Ac	Fu	Ac	Ac	C <sub>41</sub> H <sub>47</sub> NO <sub>20</sub> , mw: 873.27, [α] <sub>D</sub> <sup>25</sup> +46.2° (MeOH), UV, IR, MS, <sup>1</sup> H, <sup>13</sup> C (53)
94. Hypoglaunine C	Ac	Bz	Ac	Ac	C <sub>43</sub> H <sub>49</sub> NO <sub>19</sub> , mw: 883.29, [α] <sub>D</sub> <sup>25</sup> +56.7° (MeOH), UV, IR, MS, <sup>1</sup> H, <sup>13</sup> C (53)

#### D. EPIMERIC EVONINATE ALKALOIDS

Epimeric evoninate sesquiterpene pyridine alkaloids are a restricted group of alkaloids, characterized by the presence of *epi*-evoninic acid (Table XIII). This epimeric form was established as (2*R*,3*S*)-2-methyl-3-methyl-(β-carboxy-α-pyridyl)-propionic acid, forming a fifteen-membered macrocyclic ring containing two ester linkages with the isoeuonyminol sesquiterpene core. Its stereochemistry was confirmed by X-ray diffraction analysis of a single crystal (56). For evoninic acid the configuration of the methyl groups are 2*S* (C-8') and 3*S* (C-7'). The epimeric relationship of the evoninic acid side chain was also characterized in the <sup>1</sup>H-NMR in which the secondary methyl groups and the methine protons of epimeric acanthothamine (95) are observed at δ 0.95 (d, *J* = 7.0 Hz, H-10'), 1.37 (d, *J* = 7.0 Hz, H-9'), 2.35 (m, H-8'), and 4.37 (m, H-7'). On the other hand, in euonymine (8) these signals are observed at δ 1.19 (d, *J* = 7.1 Hz, H-10'), 1.39 (d, *J* = 7.0 Hz, H-9'),

TABLE XIII.  
Epimeric Evoninate Sesquiterpene Pyridine Alkaloids.



Acanthothamine (95)

Properties

$C_{34}H_{43}NO_{16}$ , mw: 721.26, mp: 287–290 °C, IR,  $^1H$ ,  $^{13}C$  (55)

2.57 (q,  $J=7.1$  Hz, H-8'), and 4.64 (q,  $J=7.0$  Hz, H-7') (19). Acanthothamine represents a new epievoninate sesquiterpene pyridine alkaloid-type.

E. NOREVONINATE ALKALOIDS

Norevoninic acid is another evoninic acid derivative that comprises the alkaloid moiety of the sesquiterpene pyridine alkaloids found in the Celastraceae (Table XIV). In their mass spectra, the molecular ions were 14 Da smaller than their analogs, suggesting that hydrogen replaces a methyl group. In the  $^1H$ -NMR spectrum the norevoninic residue was characterized by the presence of signals due to a methylene group at  $\delta$  2.8 (1H, dd,  $J=13.0, 8.5$  Hz) and at  $\delta$  4.4 (1H, d,  $J=13.0$  Hz), and by the loss of a doublet methyl signal (H-9'). This evidence indicated that the secondary methyl group at C-7' was replaced by a proton. Thus, the dibasic acid which composes the alkaloid moiety was 2-methyl-3-(3-carboxy-2-pyridyl)-propanoic acid.

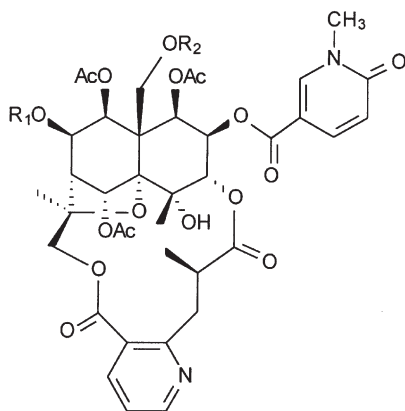
Sesquiterpene pyridine alkaloids containing the norevoninic residue have been isolated only from *Hippocratea excelsa*.

III. Wilfordate Sesquiterpene Pyridine Alkaloids and Derivatives

A. WILFORDATE ALKALOIDS

Wilfordate sesquiterpene pyridine alkaloids are dihydroagarofuran sesquiterpenes esterified by wilfordic acid, and they form a sixteen-membered macrocyclic

TABLE XIV.  
Norevoninate Sesquiterpene Pyridine Alkaloids.



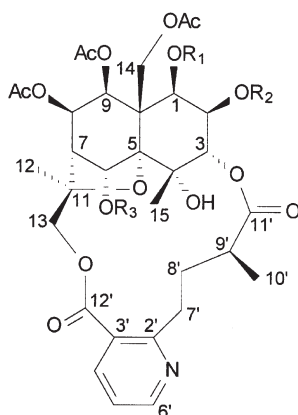
Alkaloid	R <sub>1</sub>	R <sub>2</sub>	Properties
96	Ac	Ac	C <sub>42</sub> H <sub>48</sub> N <sub>2</sub> O <sub>19</sub> , mw: 884.28, mp: 177–184 °C, [α] <sub>D</sub> +1.8° (CHCl <sub>3</sub> ), UV, <sup>1</sup> H, <sup>13</sup> C (36)
97	Ac	CO <sup>i</sup> Pr	C <sub>44</sub> H <sub>52</sub> N <sub>2</sub> O <sub>19</sub> , mw: 912.32, mp: 178–192 °C, [α] <sub>D</sub> +4.2° (CHCl <sub>3</sub> ), UV, <sup>1</sup> H, <sup>13</sup> C (36)
98	CO <sup>i</sup> Pr	CO <sup>i</sup> Pr	C <sub>46</sub> H <sub>56</sub> N <sub>2</sub> O <sub>19</sub> , mw: 940.35, mp: 161–164 °C, [α] <sub>D</sub> +2.6° (CHCl <sub>3</sub> ), UV, <sup>1</sup> H, <sup>13</sup> C (36)

ring, which contains two intramolecular ester linkages between C-3 and C-13. Wilfordic acid is an evoninic acid isomer where 2-methylbutanoic acid is linked at carbon 2 of nicotinic acid. The *S* configuration of the stereocenter in the 2-methylbutanoic acid side chain of wilfordate type alkaloids was determined by <sup>1</sup>H-NMR, mainly using coupling constants and nuclear Overhauser enhancement (19), and it was reinforced by an X-ray analysis of wilforine (100) (57).

Evoninol, euonyminol, 4-deoxyeuonyminol, and 4-deoxyisoeuonyminol cores characterize the sesquiterpene nucleus of the wilfordate type alkaloids. The particular sesquiterpene alkaloids differ from each other by the esterifying acids, which include aliphatics such as acetic acid, aromatics such as benzoic and 3-furanoic acids, as well as nitrogen-containing acids such as nicotinic and CNMP (Table XV).

4-Deoxy sesquiterpene pyridine alkaloids have also been found in the wilfordate group. These alkaloids are predominantly euonyminol derivatives, although sesquiterpene cores composed of isoeuonyminol have also been isolated. These alkaloids are presented in Table XVI.

TABLE XV.  
Wilfordate Sesquiterpene Pyridine Alkaloids.

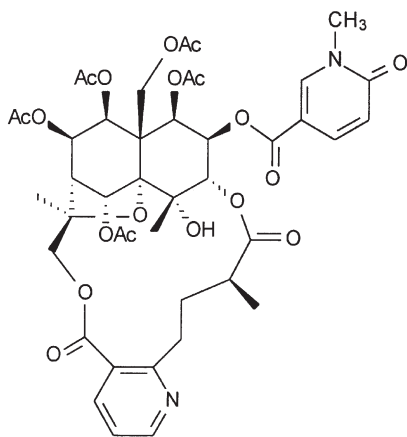


Alkaloid	R <sub>1</sub>	R <sub>2</sub>	R <sub>3</sub>	Properties
99. Euonine	Ac	Ac	Ac	C <sub>38</sub> H <sub>47</sub> NO <sub>18</sub> , mw: 805.28, mp: 150 °C, [α] <sub>D</sub> <sup>25</sup> -2.5° (CHCl <sub>3</sub> ), UV, MS, <sup>1</sup> H, <sup>13</sup> C (58)
100. Wilforine	Ac	Bz	Ac	C <sub>43</sub> H <sub>49</sub> NO <sub>18</sub> , mw: 867.29, mp: 169–170 °C, [α] <sub>D</sub> <sup>25</sup> +30° (Me <sub>2</sub> CO), UV, IR (59); <sup>1</sup> H (21)
101. Wilforgine	Ac	Fu	Ac	C <sub>41</sub> H <sub>47</sub> NO <sub>19</sub> , mw: 857.27, mp: 211 °C, [α] <sub>D</sub> <sup>25</sup> +25° (Me <sub>2</sub> CO) (60)
102. Wilforjine	Ac	H	Ac	C <sub>36</sub> H <sub>45</sub> NO <sub>17</sub> , mw: 763.27, mp: 156–158 °C, IR, MS, <sup>1</sup> H, <sup>13</sup> C (61)
103. Wilforzine	Ac	Bz	H	C <sub>41</sub> H <sub>47</sub> NO <sub>17</sub> , mw: 825.28, mp: 177–178 °C, [α] <sub>D</sub> <sup>25</sup> +6° (Me <sub>2</sub> CO) (60)
104. Euojaponine D	Bz	Ac	H	C <sub>41</sub> H <sub>47</sub> NO <sub>17</sub> , mw: 825.28, mp: 253 °C, [α] <sub>D</sub> <sup>25</sup> +28.6° (CHCl <sub>3</sub> ), UV, MS, <sup>1</sup> H, <sup>13</sup> C (58)
105. Euojaponine F	Bz	Ac	Ac	C <sub>43</sub> H <sub>49</sub> NO <sub>18</sub> , mw: 867.29, mp: 142 °C, [α] <sub>D</sub> <sup>25</sup> +9.0° (CHCl <sub>3</sub> ), UV, MS, <sup>1</sup> H, <sup>13</sup> C (58)
106. Euojaponine K	Bz	H	Ac	C <sub>41</sub> H <sub>47</sub> NO <sub>17</sub> , mw: 825.28, mp: 188 °C, [α] <sub>D</sub> <sup>25</sup> +26.2° (CHCl <sub>3</sub> ), UV, MS, <sup>1</sup> H, <sup>13</sup> C (58)
107. Cangorinine W-I	Ac	Bz	Bz	C <sub>48</sub> H <sub>51</sub> NO <sub>18</sub> , mw: 929.31, mp: 149–151 °C, [α] <sub>D</sub> <sup>25</sup> +14.4° (CHCl <sub>3</sub> ), UV, IR, MS, <sup>1</sup> H, <sup>13</sup> C (8)

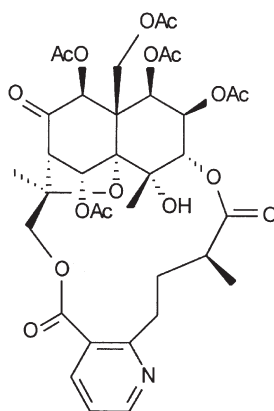
(continued)

TABLE XV.  
Continued.

Alkaloid	R <sub>1</sub>	R <sub>2</sub>	R <sub>3</sub>	Properties
108. Cangorinine W-II	Ac	Bz	Nic	C <sub>47</sub> H <sub>50</sub> N <sub>2</sub> O <sub>18</sub> , mw: 930.31, mp: 153–158 °C, [α] <sub>D</sub> +7.9° (CHCl <sub>3</sub> ), UV, IR, MS, <sup>1</sup> H, <sup>13</sup> C (8)
109. Wilformine	Ac	Nic	Ac	C <sub>42</sub> H <sub>48</sub> N <sub>2</sub> O <sub>18</sub> , mw: 868.29, mp: 177–178 °C, IR, MS, <sup>1</sup> H, <sup>13</sup> C (62)
110. Laevisine B	Nic	Ac	Ac	C <sub>42</sub> H <sub>48</sub> N <sub>2</sub> O <sub>18</sub> , mw: 868.29, mp: 148–150 °C, [α] <sub>D</sub> <sup>25</sup> +31.2° (CHCl <sub>3</sub> ), UV, <sup>1</sup> H, <sup>13</sup> C (30)
111. Ebenifoline W-I	Bz	Bz	Ac	C <sub>48</sub> H <sub>51</sub> NO <sub>18</sub> , mw: 929.31, mp: 222–224 °C, [α] <sub>D</sub> +47.1° (CHCl <sub>3</sub> ), UV, IR, MS, CD, <sup>1</sup> H, <sup>13</sup> C, X-ray (19)
112. Ebenifoline W-II	Bz	Bz	H	C <sub>46</sub> H <sub>49</sub> NO <sub>17</sub> , mw: 887.30, mp: 118–122 °C, [α] <sub>D</sub> +61.1° (CHCl <sub>3</sub> ), UV, IR, MS, CD, <sup>1</sup> H, <sup>13</sup> C (19)



113

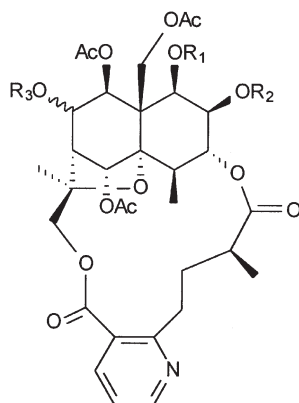


114. Isevonine or evonimine

Properties	Properties
C <sub>43</sub> H <sub>50</sub> N <sub>2</sub> O <sub>19</sub> , mw: 898.30, mp: 178–182 °C, [α] <sub>D</sub> +23.6° (CHCl <sub>3</sub> ), UV, <sup>1</sup> H, <sup>13</sup> C (36)	C <sub>36</sub> H <sub>43</sub> NO <sub>17</sub> , mw: 761.25, [α] <sub>D</sub> +30.5° (EtOH), IR, UV, ORD, <sup>1</sup> H (13); [α] <sub>D</sub> +21° (CHCl <sub>3</sub> ) (63); <sup>13</sup> C (64)



TABLE XVI.  
4-Deoxywilfordate Sesquiterpene Pyridine Alkaloids.

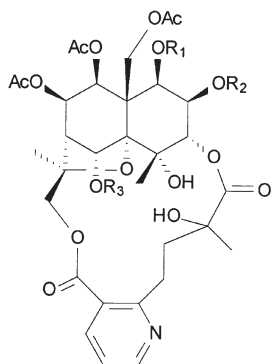


Alkaloid	R <sub>1</sub>	R <sub>2</sub>	R <sub>3</sub>	Properties
115. Chuchuhuanine W-I	Ac	Bz	Ac ( $\alpha$ )	C <sub>43</sub> H <sub>49</sub> NO <sub>17</sub> , mw: 851.30, mp: 149–154 °C, $[\alpha]_D^{25} +14.8^\circ$ (CHCl <sub>3</sub> ), UV, IR, MS, CD, <sup>1</sup> H, <sup>13</sup> C (41)
116. Eujaponine J	Bz	H	Ac ( $\beta$ )	C <sub>36</sub> H <sub>45</sub> NO <sub>16</sub> , mw: 747.27, mp: 243 °C, $[\alpha]_D^{25} +26.2^\circ$ (CHCl <sub>3</sub> ), UV, MS, <sup>1</sup> H, <sup>13</sup> C (58)
117. Neowilforine	Ac	Bz	Ac ( $\beta$ )	C <sub>43</sub> H <sub>49</sub> NO <sub>17</sub> , mw: 851.30, mp: 156.5–157.5 °C, $[\alpha]_D^{26} +15.53^\circ$ (Me <sub>2</sub> CO), UV, IR, MS, <sup>1</sup> H (65)
118. Alatusamine	Ac	Ac	Ac ( $\beta$ )	C <sub>38</sub> H <sub>47</sub> NO <sub>17</sub> , mw: 789.28, mp: 138–144 °C (picrate), $[\alpha]_D^{22} -11^\circ$ (CHCl <sub>3</sub> ), UV, IR, <sup>1</sup> H (66)

## B. HYDROXYWILFORDATE ALKALOIDS

Hydroxywilfordate alkaloids are a group of sesquiterpene pyridine alkaloids that contain the dibasic hydroxywilfordic acid as their alkaloid diester portion, and are characterized by a hydroxyl group replacing H-9', as presented in Table XVII. The <sup>1</sup>H-NMR resonances are very similar to those of the wilfordate type, differing mainly in the H-10' multiplicity that was observed as a singlet at  $\delta$  1.5. In the wilfordate type this proton signal was a doublet observed near  $\delta$  1.2 ( $J = 6.0$  Hz).

TABLE XVII.  
Hydroxywilfordate Sesquiterpene Alkaloids.



Alkaloid	R <sub>1</sub>	R <sub>2</sub>	R <sub>3</sub>	Properties
119. Wilfordine	Ac	Bz	Ac	C <sub>43</sub> H <sub>49</sub> NO <sub>19</sub> , mw: 883.29, mp: 170–176 °C, [α] <sub>D</sub> <sup>22</sup> +5° (CHCl <sub>3</sub> ), UV, IR, <sup>1</sup> H (67); <sup>1</sup> H, <sup>13</sup> C (62)
120. Wilfortrine	Ac	Fu	Ac	C <sub>41</sub> H <sub>47</sub> NO <sub>20</sub> , mw: 873.27, mp: 233–234 °C, [α] <sub>D</sub> <sup>27</sup> +12.21° (Me <sub>2</sub> CO), UV, IR, MS, <sup>1</sup> H (65)
121. Wilfordine	Ac	H	Ac	C <sub>36</sub> H <sub>45</sub> NO <sub>18</sub> , mw: 779.26 (68)
122. 1-Desacetylwilfordine	H	Bz	Ac	C <sub>41</sub> H <sub>47</sub> NO <sub>18</sub> , mw: 841.28, mp: 182–184 °C, IR, MS, <sup>1</sup> H, <sup>13</sup> C (62)
123. 1-Desacetylwilfortrine	H	Fu	Ac	C <sub>39</sub> H <sub>45</sub> NO <sub>19</sub> , mw: 831.26, mp: 179–182 °C, IR, MS, <sup>1</sup> H, <sup>13</sup> C (62)
124. 5-Benzoyl-5-desacetylwilfordine	Ac	H	Bz	C <sub>41</sub> H <sub>47</sub> NO <sub>18</sub> , mw: 841.28, mp: 187–189 °C, IR, MS, <sup>1</sup> H, <sup>13</sup> C (69)
125. Alatusinine	Ac	Ac	Ac	C <sub>38</sub> H <sub>47</sub> NO <sub>19</sub> , mw: 821.27, [α] <sub>D</sub> <sup>26</sup> –16° (CHCl <sub>3</sub> ), UV, IR, <sup>1</sup> H (66)
126. Emarginatinine	Ac	CNMP	Ac	C <sub>43</sub> H <sub>50</sub> N <sub>2</sub> O <sub>20</sub> , mw: 914.30, mp: 238–241 °C, [α] <sub>D</sub> –130° (CHCl <sub>3</sub> ), UV, IR, MS, <sup>1</sup> H, <sup>13</sup> C (34)

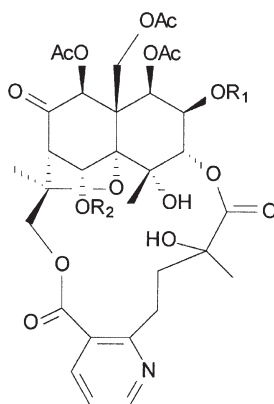
(continued)

### C. ISOWILFORDATE ALKALOIDS

The isomeric wilfordic acid alkaloid moiety in the sesquiterpene pyridine alkaloids has also been reported (Table XVIII). The dibasic isowilfordic acid contains a 3,4-substituted nicotinic acid group rather than a 2,3-substituted one, as in the case of the wilfordate-derived. This isomeric form is characterized in the

TABLE XVII.

Continued.



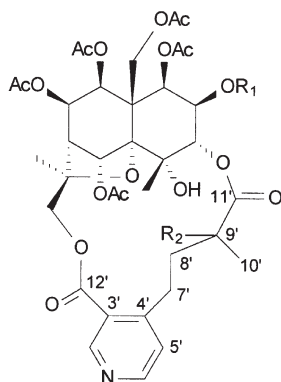
Alkaloid	R <sub>1</sub>	R <sub>2</sub>	Properties
127. Alatamine	Bz	Ac	C <sub>41</sub> H <sub>45</sub> NO <sub>18</sub> , mw: 839.26, mp: 185–193 °C, [α] <sub>D</sub> <sup>22</sup> +44° (CHCl <sub>3</sub> ), UV, IR, <sup>1</sup> H (67)
128. Wilforfine E	Ac	Ac	C <sub>36</sub> H <sub>43</sub> NO <sub>18</sub> , mw: 777.25, [α] <sub>D</sub> +1.1° (MeOH), UV, IR, MS, <sup>1</sup> H, <sup>13</sup> C (26)
129. Neoalatamine	Bz	H	C <sub>39</sub> H <sub>43</sub> NO <sub>17</sub> , mw: 797.25, [α] <sub>D</sub> <sup>26</sup> +42° (CHCl <sub>3</sub> ), UV, IR, <sup>1</sup> H (66)

<sup>1</sup>H-NMR by resonances near δ 9.2 (s, H-2'), 8.7 (d,  $J = 5.1$  Hz, H-6'), and 7.3 (d,  $J = 5.1$  Hz, H-5'), along with one methyl doublet at about δ 1.2 (6.4 Hz, H-10') and five multiplets between δ 1.6 and 3.9, referring to H<sub>2</sub>-7', H<sub>2</sub>-8', and H-9'. <sup>1</sup>H-NMR spectral data of hydroxyisowilfordic acid derivatives were similar to those of isowilfordic derivatives differing significantly only in the H-10' multiplicity. In addition, the proton H<sub>2</sub>-7' showed long-range correlation with the pyridinyl carbon C-3'; the proton H-5' correlated to carbons C-6', C-4', C-3', and C-7', and the proton resonance H<sub>3</sub>-10' correlated with the carbonyl carbon C-11' in the HMBC spectrum (70).

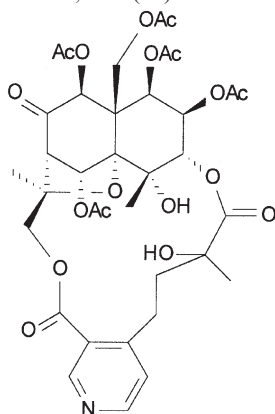
#### D. BENZOYLOXY AND FURANOYLOXYWILFORDATE ALKALOIDS

Wilforfines and triptonines are sesquiterpene pyridine alkaloids isolated from *T. wilfordii* in which the hydroxyl group in the hydroxywilfordic acid is replaced by benzoyl or furanoyl groups (Table XIX). Furthermore, benzoyloxywilfordic and furanoyloxywilfordic acids represent two new derivative classes of nicotinic acids. These alkaloids are characterized in the NMR by the presence of seven ester groups and a pyridine ring.

TABLE XVIII.  
Isowilfordate and Hydroxyisowilfordate Alkaloids.



Alkaloid	R <sub>1</sub>	R <sub>2</sub>	Properties
130. Wilfordinine D	Fu	H	C <sub>41</sub> H <sub>47</sub> NO <sub>19</sub> , mw: 857.27, [α] <sub>D</sub> <sup>25</sup> +14.6° (MeOH), IR, UV, MS, <sup>1</sup> H, <sup>13</sup> C (70)
131. Wilfordinine E	Ac	H	C <sub>38</sub> H <sub>47</sub> NO <sub>18</sub> , mw: 805.28, [α] <sub>D</sub> <sup>25</sup> -0.6° (MeOH), IR, UV, MS, <sup>1</sup> H, <sup>13</sup> C (70)
132. Wilfordinine F	Bz	H	C <sub>43</sub> H <sub>49</sub> NO <sub>18</sub> , mw: 867.29, [α] <sub>D</sub> <sup>25</sup> +16.2° (MeOH), IR, UV, MS, <sup>1</sup> H, <sup>13</sup> C (70)
133. Wilfordinine H	Fu	OH	C <sub>41</sub> H <sub>47</sub> NO <sub>20</sub> , mw: 873.27, [α] <sub>D</sub> <sup>25</sup> +1.4° (MeOH), IR, UV, MS, <sup>1</sup> H, <sup>13</sup> C (70)
134. Isowilfordine	Bz	OH	C <sub>43</sub> H <sub>49</sub> NO <sub>19</sub> , mw: 883.29, mp: 165–167°C, IR, MS, <sup>1</sup> H, <sup>13</sup> C (71)

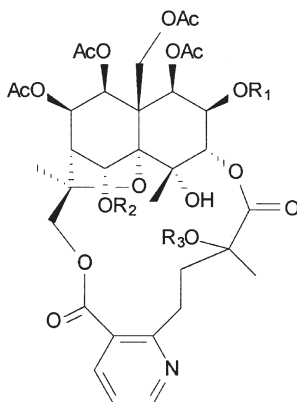


135. Wilfordinine G

Properties

C<sub>36</sub>H<sub>43</sub>NO<sub>18</sub>, mw: 777.25, [α]<sub>D</sub><sup>25</sup> +4.3° (MeOH), IR, UV, MS, <sup>1</sup>H, <sup>13</sup>C (70)

TABLE XIX.  
Benzoyloxy and Furanoyloxywilfordate Alkaloids.



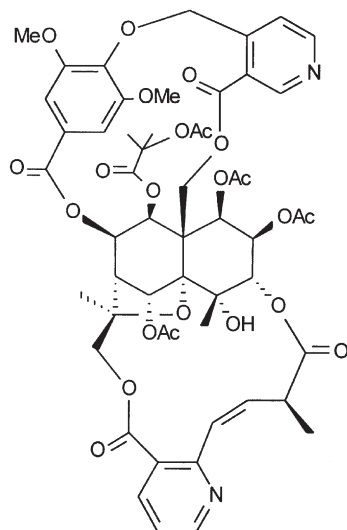
Alkaloid	R <sub>1</sub>	R <sub>2</sub>	R <sub>3</sub>	Properties
136. Wilfornine A	Ac	Ac	Bz	C <sub>45</sub> H <sub>51</sub> NO <sub>20</sub> , mw: 925.30, [α] <sub>D</sub> -41.9° (MeOH), UV, IR, <sup>1</sup> H, <sup>13</sup> C (26)
137. Wilfornine B	Ac	H	Bz	C <sub>43</sub> H <sub>49</sub> NO <sub>19</sub> , mw: 883.29, [α] <sub>D</sub> -17.8° (MeOH), UV, IR, MS, <sup>1</sup> H, <sup>13</sup> C (26)
138. Wilfornine C	Ac	Bz	Bz	C <sub>50</sub> H <sub>53</sub> NO <sub>20</sub> , mw: 987.32, [α] <sub>D</sub> -50° (MeOH), UV, IR, MS, <sup>1</sup> H, <sup>13</sup> C (26)
139. Wilfornine D	Ac	Ac	Fu	C <sub>43</sub> H <sub>49</sub> NO <sub>21</sub> , mw: 915.28, [α] <sub>D</sub> -21.1° (MeOH), UV, IR, <sup>1</sup> H, <sup>13</sup> C (26)
140. Triptonine A	Fu	Ac	Bz	C <sub>48</sub> H <sub>51</sub> NO <sub>21</sub> , mw: 977.30, mp: 163–164°C, [α] <sub>D</sub> <sup>27</sup> -36° (Me <sub>2</sub> CO), IR, MS, <sup>1</sup> H, <sup>13</sup> C (72)
141. Triptonine B	Fu	Ac	Fu	C <sub>46</sub> H <sub>49</sub> NO <sub>22</sub> , mw: 967.27, mp: 160–161°C, [α] <sub>D</sub> <sup>30</sup> -13° (Me <sub>2</sub> CO), IR, MS, <sup>1</sup> H, <sup>13</sup> C (72)

Triptonines A and B represented the first report of 9'-*O*-esterified sesquiterpene pyridine alkaloids. In a previous section, two other sesquiterpene alkaloids were named as triptonine A and B, although their structures contain a monoterpene unit comprising a macrodilactone bridge between C-8 and C-14 of the sesquiterpene moiety (Table IX). They were isolated from *T. hypoglaucum* (50).

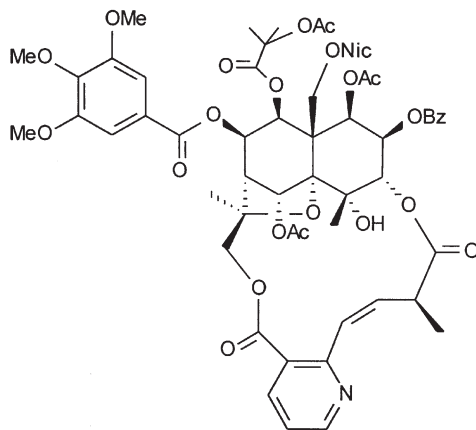
#### IV. Edulinate Sesquiterpene Pyridine Alkaloids

Edulinate sesquiterpene pyridine alkaloids are dihydroagarofuran sesquiterpenes esterified by edulnic acid (Fig. 3), a dihydro wilfordic acid derivative that

TABLE XX.  
Edulinate Sesquiterpene Pyridine Alkaloids.



142. Cathedulin K17



143. Cathedulin K19

Properties

$C_{54}H_{58}N_2O_{23}$ , mw: 1102.34,  $^1H$  (49)

Properties

$C_{59}H_{62}N_2O_{23}$ , mw: 1166.37, mp: 249–251 °C,  $^1H$ ,  $^{13}C$  (49)

forms a sixteen-membered macrocyclic ring, and contains two intramolecular ester linkages between C-3 and C-13 (Table XX). In the NMR spectrum, the proton connectivity pattern of edulinic acid was established by decoupling, and the *Z* configuration of the double bond was observed by NOE difference spectroscopy and by a coupling constant of 11 Hz (49). The *S* configuration of the C-9' was attributed by comparison with its synthetic analog (*S*)-edulindiol. This compound containing an *S* configuration was obtained on reduction of cathedulin K-19, which contains an edulinic acid residue esterifying a sesquiterpene core (44).

Cathedulins K17 and K19 isolated from khat of Kenyan origin and classified as cathedulin alkaloids of high molecular weight, contain a novel diester bridge derived from edulinic acid. The sesquiterpene core of these compounds is again euonyminol, and the esterifying acids detected by the NMR spectrum are cathic, acetic, and acetoxyisobutyric acids. In K17, trimethylgallate and nicotinate residues replace the cathate bridge.

TABLE XXI.  
Cassinate Sesquiterpene Pyridine Alkaloids.

144. Orthosphenine	145. Cassinine
Properties	Properties
$C_{37}H_{45}NO_{17}$ , mw: 775.27, IR, UV, MS, $^1H$ , $^{13}C$ (73)	$C_{44}H_{51}NO_{18}$ , mw: 881.31, mp: 295–298 °C (60)

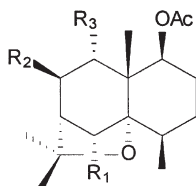
### V. Cassinate Sesquiterpene Pyridine Alkaloids

Cassinate sesquiterpene pyridine alkaloids are dihydroagarofuran sesquiterpenes esterified by cassinic acid (Fig. 3) forming a sixteen-membered macrocyclic ring, and containing two intramolecular ester linkages between C-3 and C-13. Only two alkaloids have been isolated to date in this class of alkaloid sesquiterpene ester, orthosphenine (144) and cassinine (145) (Table XXI). The former has evoninol in the sesquiterpene core, and was obtained from *Orthosphenia mexicana*, a plant in the Celastraceae family. The latter sesquiterpene core is comprised of euonyminol, and was isolated from *Cassine matabelicum*, another Celastraceae species.

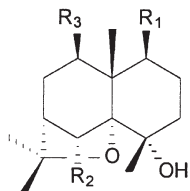
### VI. Lower Molecular Weight Sesquiterpene Pyridine Alkaloids

Lower molecular weight sesquiterpene pyridine alkaloids containing a dihydroagarofuran sesquiterpene core are exclusively isolated from plants belonging to the Celastraceae family, and they have been considered as its chemotaxonomical markers (Tables XXII, XXIII, XXIV and XXV). They are characterized by the absence of a macrocyclic ring, and despite their sesquiterpene core, these alkaloids are nitrogenous bases through esterification. Thus, they are legitimately described as alkaloids and have been reviewed as such (103). These

TABLE XXII.  
Triesterified Lower Molecular Weight Alkaloids.



Alkaloid	R <sub>1</sub>	R <sub>2</sub>	R <sub>3</sub>	Properties
146. Triptogelin F-1	ONic	H	OBz	C <sub>30</sub> H <sub>35</sub> NO <sub>7</sub> , mw: 521.24, mp: 193–195 °C, [α] <sub>D</sub> <sup>23</sup> +67.7° (MeOH), IR, MS, <sup>1</sup> H, <sup>13</sup> C (74)
147. Celapagin	OBz	OH	ONic	C <sub>30</sub> H <sub>35</sub> NO <sub>8</sub> , mw: 537.24, mp: 275–283 °C, MS, <sup>1</sup> H (75)



Alkaloid	R <sub>1</sub>	R <sub>2</sub>	R <sub>3</sub>	Properties
148	ONic	OBz	ONic	C <sub>34</sub> H <sub>36</sub> N <sub>2</sub> O <sub>8</sub> , mw: 600.25, [α] <sub>D</sub> <sup>25</sup> +67.7° (MeOH), UV, IR, MS, CD, <sup>1</sup> H, <sup>13</sup> C (76)
149	OAc	ONic	OBz	C <sub>30</sub> H <sub>35</sub> NO <sub>8</sub> , mw: 537.24, IR, MS, <sup>1</sup> H, <sup>13</sup> C (14)
150. Regelidine	OBz	ONic	OBz	C <sub>35</sub> H <sub>37</sub> NO <sub>8</sub> , mw: 599.25, mp: 292–294 °C, [α] <sub>D</sub> <sup>26</sup> +50° (CHCl <sub>3</sub> ), UV, IR, MS, <sup>1</sup> H, <sup>13</sup> C, X-ray (77); [α] <sub>D</sub> +92.7° (CHCl <sub>3</sub> ), <sup>1</sup> H, <sup>13</sup> C (78)
151. Wilforcidine	ONic	ONic	O'Cinn	C <sub>36</sub> H <sub>38</sub> N <sub>2</sub> O <sub>8</sub> , mw: 626.26, mp: 189 °C, [α] <sub>D</sub> <sup>25</sup> +17.4° (CHCl <sub>3</sub> ), UV, IR, MS, <sup>1</sup> H, <sup>13</sup> C (79)

(continued)

alkaloids are also known as nicotinoyl sesquiterpene alkaloids. Esterifying groups include aliphatic and aromatic acids, as well as nitrogen-containing aromatic acids.

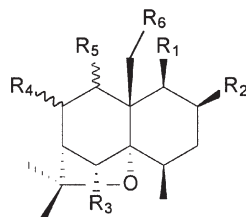
### VII. Non-Celastraceous Sesquiterpene Pyridine Alkaloids

Most of the sesquiterpene pyridine alkaloids isolated from higher plants possess a dihydroagarofuran backbone at the terpene moiety, and are obtained

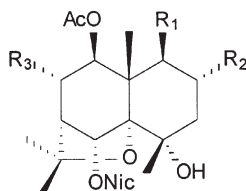


TABLE XXII.

Continued.



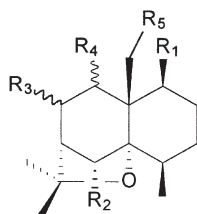
Alkaloid	R <sub>1</sub>	R <sub>2</sub>	R <sub>3</sub>	R <sub>4</sub>	R <sub>5</sub>	R <sub>6</sub>	Properties
152. Triptogelin C-4	OAc	OH	ONic	H	$\alpha$ -OBz	H	C <sub>30</sub> H <sub>35</sub> NO <sub>8</sub> , mw: 537.24, $[\alpha]_D^{23} +193^\circ$ (MeOH), IR, MS, <sup>1</sup> H (80)
153	OAc	H	H	$\alpha$ -OH	$\beta$ -OBz	ONic	C <sub>30</sub> H <sub>35</sub> NO <sub>8</sub> , mw: 537.24, $[\alpha]_D^{23} +47.6^\circ$ (CHCl <sub>3</sub> ), UV, IR, MS, <sup>1</sup> H, <sup>13</sup> C (81)
154. Triptogelin A-7	OH	OH	OAc	$\beta$ -ONic	$\beta$ -OBz	H	C <sub>30</sub> H <sub>35</sub> NO <sub>9</sub> , mw: 553.23, $[\alpha]_D^{25} +63.1^\circ$ (MeOH), IR, MS, <sup>1</sup> H, <sup>13</sup> C (82)



Alkaloid	R <sub>1</sub>	R <sub>2</sub>	R <sub>3</sub>	Properties
155	O <sup>i</sup> Cinn	OH	H	C <sub>32</sub> H <sub>37</sub> NO <sub>9</sub> , mw: 579.25, IR, MS, <sup>1</sup> H (83)
156	OBz	H	OH	C <sub>30</sub> H <sub>35</sub> NO <sub>9</sub> , mw: 553.23, mp: 184–186 °C, IR, MS, <sup>1</sup> H (83)

from the Celastraceae, including the Hippocrateaceae. On the other hand, sesquiterpene pyridine alkaloids isolated from non-Celastraceous plants, represent a small number of these alkaloids (Table XXVI). Rotundines, for example, are sesquiterpene pyridine alkaloids that have been isolated from *Cyperus rotundus* (Cyperaceae), which have an unprecedented sesquiterpene skeleton containing a cyclopentane ring attached to the pyridine ring (104). Rotundine B is an epimer of rotundine C at the C-6 position, although the C-6 stereochemistry has not yet been determined. Thus, their structures could be interchangeable. Other examples of

TABLE XXIII.  
Tetraesterified Lower Molecular Weight Alkaloids.



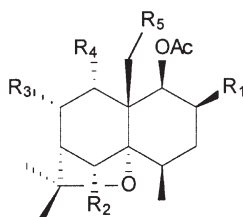
Alkaloid	R <sub>1</sub>	R <sub>2</sub>	R <sub>3</sub>	R <sub>4</sub>	R <sub>5</sub>	Properties
157. Ejap-7	OAc	OAc	H	$\alpha$ -ONic	OAc	C <sub>27</sub> H <sub>35</sub> NO <sub>9</sub> , mw: 517.23, IR, MS, <sup>1</sup> H (84)
158. Angulatueoid D	OAc	H	$\alpha$ -OAc	$\beta$ -OBz	OPic	C <sub>32</sub> H <sub>37</sub> NO <sub>9</sub> , mw: 579.25, mp: 184–185 °C, IR, UV, MS, <sup>1</sup> H, <sup>13</sup> C (85)
159. Angulatueoid E	OCO <sup>i</sup> Pr	H	$\alpha$ -OAc	$\beta$ -OBz	ONic	C <sub>34</sub> H <sub>41</sub> NO <sub>9</sub> , mw: 607.28, mp: 175.5–177.5 °C, IR, UV, MS, <sup>1</sup> H, <sup>13</sup> C (86)
160. Angulatueoid F	OCOEt	H	$\alpha$ -OAc	$\beta$ -OBz	ONic	C <sub>33</sub> H <sub>39</sub> NO <sub>9</sub> , mw: 593.26, mp: 178.5–180.5 °C, IR, UV, MS, <sup>1</sup> H, <sup>13</sup> C (86)
161	OAc	H	$\alpha$ -OAc	$\alpha$ -ONic	OBz	C <sub>32</sub> H <sub>37</sub> NO <sub>9</sub> , mw: 579.25, mp: 168–170 °C, [ $\alpha$ ] <sub>D</sub> +25.4° (MeOH), UV, IR, MS, <sup>1</sup> H, <sup>13</sup> C (87)
162	OAc	H	$\alpha$ -OCO <sup>i</sup> Pr	$\beta$ -OBz	ONic	C <sub>34</sub> H <sub>41</sub> NO <sub>9</sub> , mw: 607.28, [ $\alpha$ ] <sub>D</sub> <sup>23</sup> +49.9° (CHCl <sub>3</sub> ), UV, IR, MS, <sup>1</sup> H, <sup>13</sup> C (81)
163	OAc	H	$\alpha$ -OMeBu	$\beta$ -OBz	ONic	C <sub>35</sub> H <sub>43</sub> NO <sub>9</sub> , mw: 621.29, [ $\alpha$ ] <sub>D</sub> <sup>23</sup> +44.4° (CHCl <sub>3</sub> ), UV, IR, MS, <sup>1</sup> H, <sup>13</sup> C (81)
164	OAc	H	$\beta$ -OBz	$\beta$ -OBz	ONic	C <sub>37</sub> H <sub>39</sub> NO <sub>9</sub> , mw: 641.26, [ $\alpha$ ] <sub>D</sub> <sup>23</sup> -102° (CHCl <sub>3</sub> ), UV, IR, MS, <sup>1</sup> H, <sup>13</sup> C (81)
165	OAc	H	$\alpha$ -OAc	$\beta$ -OBz	ONic	C <sub>32</sub> H <sub>37</sub> NO <sub>9</sub> , mw: 579.25, [ $\alpha$ ] <sub>D</sub> +48.6° (MeOH), UV, IR, MS, <sup>1</sup> H, <sup>13</sup> C (87)
166. Triptogelin B-2	ONic	OAc	$\beta$ -OBz	$\beta$ -OBz	H	C <sub>37</sub> H <sub>39</sub> NO <sub>9</sub> , mw: 641.26, [ $\alpha$ ] <sub>D</sub> <sup>23</sup> +52.3° (MeOH), UV, IR, MS, <sup>1</sup> H, <sup>13</sup> C (88)

(continued)

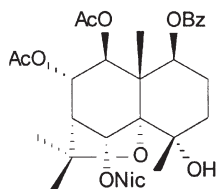
TABLE XXIII.

Continued.

Alkaloid	R <sub>1</sub>	R <sub>2</sub>	R <sub>3</sub>	R <sub>4</sub>	R <sub>5</sub>	Properties
167. Celapanin	OAc	OFu	$\beta$ -OAc	$\alpha$ -ONic	H	C <sub>30</sub> H <sub>35</sub> NO <sub>10</sub> , mw: 569.23, mp: 245–249 °C, $[\alpha]_D^{26}$ –64.7° (CHCl <sub>3</sub> ), IR, UV, MS, <sup>1</sup> H (75)
168. Celapanigin	OAc	OBz	$\beta$ -OAc	$\alpha$ -ONic	H	C <sub>32</sub> H <sub>37</sub> NO <sub>9</sub> , mw: 579.25, mp: 184–185 °C, IR, UV, MS, <sup>1</sup> H (75); mp: 284–285 °C (89)



Alkaloid	R <sub>1</sub>	R <sub>2</sub>	R <sub>3</sub>	R <sub>4</sub>	R <sub>5</sub>	Properties
169. Triptogelin C-2	OAc	ONic	H	OBz	H	C <sub>32</sub> H <sub>37</sub> NO <sub>9</sub> , mw: 579.25, mp: 191–194 °C, $[\alpha]_D^{23}$ +43.2° (CHCl <sub>3</sub> ), UV, IR, MS, <sup>1</sup> H, <sup>13</sup> C (88)
170. Heterophylline	ONic	ONic	H	OBz	H	C <sub>36</sub> H <sub>38</sub> N <sub>2</sub> O <sub>9</sub> , mw: 642.26, mp: 132–135 °C, $[\alpha]_D$ +63.2° (CHCl <sub>3</sub> ), UV, IR, <sup>1</sup> H, <sup>13</sup> C (90)
171. Cathedulin E8	OAc	H	OH	OBz	ONic	C <sub>32</sub> H <sub>37</sub> NO <sub>10</sub> , mw: 595.24, IR, UV, MS, <sup>1</sup> H (46); <sup>1</sup> H (91)
172. Maymyrsine	OBz	OAc	H	ONic	OH	C <sub>32</sub> H <sub>37</sub> NO <sub>10</sub> , mw: 595.24, mp: 185–187 °C, $[\alpha]_D$ +93° (CHCl <sub>3</sub> ), UV, IR, MS, <sup>1</sup> H, X-ray (92)



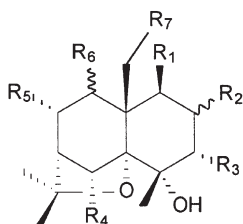
173

C<sub>32</sub>H<sub>37</sub>NO<sub>10</sub>, mw: 595.24, mp: 114–116 °C, IR, MS, <sup>1</sup>H (83)

(continued.)

TABLE XXIII.

Continued.



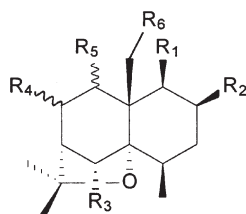
Alkaloid	R <sub>1</sub>	R <sub>2</sub>	R <sub>3</sub>	R <sub>4</sub>	R <sub>5</sub>	R <sub>6</sub>	R <sub>7</sub>	Properties
174. Cathidin D	OAc	$\beta$ -OBz	OH	H	H	$\alpha$ -ONic	OAc	C <sub>32</sub> H <sub>37</sub> NO <sub>11</sub> , mw: 611.24, mp: 219.5–222 °C, $[\alpha]_D$ +74° (CHCl <sub>3</sub> ) (60)
175	ONic	$\alpha$ -OAc	OAc	OH	H	$\alpha$ -O'Cinn	H	C <sub>34</sub> H <sub>39</sub> NO <sub>11</sub> , mw: 637.25, $[\alpha]_D^{25}$ +10° (CHCl <sub>3</sub> ), UV, IR, MS, <sup>1</sup> H, <sup>13</sup> C (93)
176	OH	$\beta$ -ONic	H	OH	OAc	$\beta$ -OBz	OMeBu	C <sub>35</sub> H <sub>43</sub> NO <sub>12</sub> , mw: 669.28, $[\alpha]_D^{27}$ +42.1° (CHCl <sub>3</sub> ), UV, IR, MS, CD, <sup>1</sup> H, <sup>13</sup> C (94)

non-Celastraceous lower molecular weight sesquiterpene alkaloids are patchouli-pyridine, guaipyridine, and cananodine (105–108). The latter was isolated from *Cananga odorata* (Annonaceae), and the others were isolated from the essential oil of *Pogostemon patchouli* (Lamiaceae).

### VIII. Biosynthesis and Biogenesis

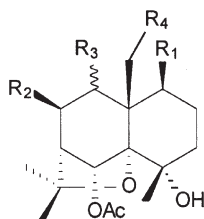
Sesquiterpene pyridine alkaloid formation in nature involves a mixed biosynthetic route. Whilst the sesquiterpene moiety originates from acetate metabolism by way of mevalonic acid, the alkaloid portion has a pathway employing glyceraldehyde 3-phosphate and amino acid precursors. Coupling between nicotinic acid and (3*S*)-isoleucine forms evoninic acid. This configuration is the same as at C-8' of the evoninate sesquiterpene pyridine alkaloids. Wilfordic and edulinic acids have a similar pathway, although the coupling involves another

TABLE XXIV.  
Pentaesterified Lower Molecular Weight Alkaloids.

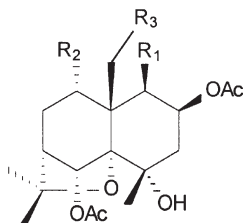


Alkaloid	R <sub>1</sub>	R <sub>2</sub>	R <sub>3</sub>	R <sub>4</sub>	R <sub>5</sub>	R <sub>6</sub>	Properties
177. Ejap-14	OAc	H	OAc	$\beta$ -OAc	$\alpha$ -ONic	OAc	C <sub>29</sub> H <sub>37</sub> NO <sub>11</sub> , mw: 575.24, IR, MS, <sup>1</sup> H (84)
178	OAc	OAc	H	$\alpha$ -OAc	$\beta$ -ONic	ONic	C <sub>33</sub> H <sub>38</sub> N <sub>2</sub> O <sub>11</sub> , mw: 638.25, mp: 183–184 °C, [ $\alpha$ ] <sub>D</sub> <sup>25</sup> +64.8° (CHCl <sub>3</sub> ), MS, <sup>1</sup> H, <sup>13</sup> C (95)
179. Angulatueoid A	OAc	OAc	H	$\alpha$ -OAc	$\beta$ -OBz	OPic	C <sub>34</sub> H <sub>39</sub> NO <sub>11</sub> , mw: 637.25, mp: 227–230 °C, IR, UV, MS, <sup>1</sup> H, <sup>13</sup> C, X-ray (85)
180. Catheduln E2	OAc	OAc	H	$\beta$ -ONic	$\alpha$ -OBz	ONic	C <sub>38</sub> H <sub>40</sub> N <sub>2</sub> O <sub>11</sub> , mw: 700.26, mp: 149–151 °C, [ $\alpha$ ] <sub>D</sub> <sup>31</sup> –74° (CHCl <sub>3</sub> ), IR, UV, MS, <sup>1</sup> H, <sup>13</sup> C (46)
181. Acetylmaymysine	OAc	OBz	OAc	H	$\alpha$ -ONic	OAc	C <sub>34</sub> H <sub>39</sub> NO <sub>11</sub> , mw: 637.25, [ $\alpha$ ] <sub>D</sub> +92° (CHCl <sub>3</sub> ), UV, IR, <sup>1</sup> H (92)
182. Ever-1	OMeBu	OAc	OAc	H	$\alpha$ -ONic	OAc	C <sub>32</sub> H <sub>43</sub> NO <sub>11</sub> , mw: 617.28, mp: 188–192 °C, <sup>1</sup> H, X-ray (96)
183	OAc	OAc	OAc	H	$\alpha$ -ONic	OAc	C <sub>29</sub> H <sub>37</sub> NO <sub>11</sub> , mw: 575.24, UV, IR, MS, <sup>1</sup> H (64)
184. Triptogelin A-5	ONic	OBz	OAc	$\beta$ -OMeBu	$\beta$ -OBz	H	C <sub>42</sub> H <sub>47</sub> NO <sub>11</sub> , mw: 741.31, [ $\alpha$ ] <sub>D</sub> <sup>25</sup> +200.1° (CHCl <sub>3</sub> ), UV, IR, MS, <sup>1</sup> H, <sup>13</sup> C (82)
185. Triptogelin A-6	OBz	OBz	OAc	$\beta$ -ONic	$\beta$ -OBz	H	C <sub>44</sub> H <sub>43</sub> NO <sub>11</sub> , mw: 761.28, [ $\alpha$ ] <sub>D</sub> <sup>25</sup> +31.5° (CHCl <sub>3</sub> ), UV, IR, MS, <sup>1</sup> H, <sup>13</sup> C (82)
186. Triptogelin A-9	OBz	OCOPent	OAc	$\beta$ -ONic	$\beta$ -OBz	H	C <sub>43</sub> H <sub>49</sub> NO <sub>11</sub> , mw: 755.33, [ $\alpha$ ] <sub>D</sub> <sup>25</sup> +12.1° (MeOH), UV, IR, MS, <sup>1</sup> H, <sup>13</sup> C (82)
187. Triptogelin A-10	ONic	OBz	OAc	$\beta$ -OBz	$\beta$ -OBz	H	C <sub>44</sub> H <sub>43</sub> NO <sub>11</sub> , mw: 761.28, [ $\alpha$ ] <sub>D</sub> <sup>23</sup> +77.6° (MeOH), UV, IR, MS, <sup>1</sup> H, <sup>13</sup> C (88)

(continued)

TABLE XXIV.  
Continued.

Alkaloid	R <sub>1</sub>	R <sub>2</sub>	R <sub>3</sub>	R <sub>4</sub>	Properties
<b>188</b>	OAc	OBz	$\beta$ -ONic	OAc	C <sub>34</sub> H <sub>39</sub> NO <sub>12</sub> , mw: 653.25, $[\alpha]_D^{25}$ -52.4° (MeOH), UV, IR, MS, <sup>1</sup> H, <sup>13</sup> C (76)
<b>189.</b> Triptofordinine A-1	O <sup>c</sup> Cinn	ONic	$\beta$ -OBz	OAc	C <sub>41</sub> H <sub>43</sub> NO <sub>12</sub> , mw: 741.28, mp: 193–194 °C, $[\alpha]_D$ -81.4° (MeOH), UV, MS, <sup>1</sup> H, <sup>13</sup> C (97)
<b>190.</b> Triptofordinine A-2	O <sup>c</sup> Cinn	ONic	$\beta$ -OBz	OAc	C <sub>41</sub> H <sub>43</sub> NO <sub>12</sub> , mw: 741.28, mp: 94–95 °C, $[\alpha]_D$ -101° (MeOH), <sup>1</sup> H, <sup>13</sup> C (97)
<b>191</b>	Oac	ONic	$\alpha$ -OBz	OMeBu	C <sub>37</sub> H <sub>45</sub> NO <sub>12</sub> , mw: 695.29, $[\alpha]_D^{27}$ -31.3° (CHCl <sub>3</sub> ), UV, IR, MS, <sup>1</sup> H, <sup>13</sup> C (94)



Alkaloid	R <sub>1</sub>	R <sub>2</sub>	R <sub>3</sub>	Properties
<b>192.</b> Maytine	OAc	ONic	OAc	C <sub>29</sub> H <sub>37</sub> NO <sub>12</sub> , mw: 591.23, UV, IR, <sup>1</sup> H (98)
<b>193</b>	ONic	OFu	OCO <sup>i</sup> Pr	C <sub>34</sub> H <sub>41</sub> NO <sub>13</sub> , mw: 671.26, mp: 127–128 °C, $[\alpha]_D^{20}$ +34.5° (MeOH), IR, UV, MS, <sup>1</sup> H, <sup>13</sup> C (99)
<b>194</b>	ONic	OFu	OMeBu	C <sub>35</sub> H <sub>43</sub> NO <sub>13</sub> , mw: 685.27, $[\alpha]_D^{20}$ +30.1° (MeOH), IR, UV, MS, <sup>1</sup> H, <sup>13</sup> C (99)
<b>195</b>	ONic	OFu	OAc	C <sub>32</sub> H <sub>37</sub> NO <sub>13</sub> , mw: 643.23, $[\alpha]_D^{20}$ +23.9° (MeOH), IR, UV, MS, <sup>1</sup> H, <sup>13</sup> C (99)

(continued)

TABLE XXIV.

Continued.

Alkaloid	R <sub>1</sub>	R <sub>2</sub>	R <sub>3</sub>	Properties		
<b>196</b>	ONic	OBz	OAc	C <sub>34</sub> H <sub>39</sub> NO <sub>12</sub> , mw: 653.25, [α] <sub>D</sub> <sup>20</sup> +43.9° (MeOH), IR, UV, MS, <sup>1</sup> H, <sup>13</sup> C (99)		
Alkaloid	R <sub>1</sub>	R <sub>2</sub>	R <sub>3</sub>	R <sub>4</sub>	R <sub>5</sub>	Properties
<b>197</b>	OCO <sup>t</sup> Pr	H	OH	ONic	β-OBz	C <sub>36</sub> H <sub>43</sub> NO <sub>13</sub> , mw: 697.27, [α] <sub>D</sub> <sup>20</sup> +43.4° (MeOH), IR, UV, MS, <sup>1</sup> H, <sup>13</sup> C (100)
<b>198. Maytoline</b>	OAc	OH	OAc	H	α-ONic	C <sub>29</sub> H <sub>37</sub> NO <sub>13</sub> , mw: 607.27, UV, IR, <sup>1</sup> H (98)

TABLE XXV.

Hexaesterified Lower Molecular Weight Alkaloids.

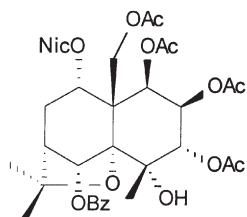
Alkaloid	R <sub>1</sub>	R <sub>2</sub>	R <sub>3</sub>	R <sub>4</sub>	R <sub>5</sub>	R <sub>6</sub>	Properties
<b>199. Cangorin A</b>	OAc	ONic	ONic	ONic	OBz	OAc	C <sub>44</sub> H <sub>43</sub> N <sub>3</sub> O <sub>14</sub> , mw: 837.27, mp: 136–140 °C, [α] <sub>D</sub> +45.7° (CHCl <sub>3</sub> ), UV, IR, MS, <sup>1</sup> H, <sup>13</sup> C (101)
<b>200. Cangorin B</b>	ONic	ONic	OBz	ONic	OBz	OAc	C <sub>49</sub> H <sub>45</sub> N <sub>3</sub> O <sub>14</sub> , mw: 899.29, mp: 137–141 °C, [α] <sub>D</sub> +77.3° (CHCl <sub>3</sub> ), UV, IR, MS, <sup>1</sup> H, <sup>13</sup> C (101)
<b>201. Cangorin C</b>	OAc	ONic	OBz	ONic	OBz	OAc	C <sub>45</sub> H <sub>44</sub> N <sub>2</sub> O <sub>14</sub> , mw: 836.28, mp: 122–126 °C, [α] <sub>D</sub> +45° (CHCl <sub>3</sub> ), UV, IR, MS, <sup>1</sup> H, <sup>13</sup> C (101)

(continued)

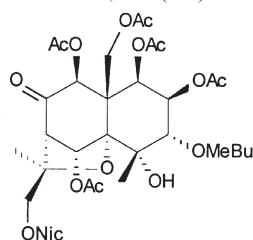
TABLE XXV.

Continued.

Alkaloid	R <sub>1</sub>	R <sub>2</sub>	R <sub>3</sub>	R <sub>4</sub>	R <sub>5</sub>	R <sub>6</sub>	Properties
202. Cangorin D	OAc	ONic	OAc	ONic	OBz	OAc	C <sub>40</sub> H <sub>42</sub> N <sub>2</sub> O <sub>14</sub> , mw: 774.26, mp: 123–128 °C, [α] <sub>D</sub> +11.2° (CHCl <sub>3</sub> ), UV, IR, MS, <sup>1</sup> H, <sup>13</sup> C (101)
203. Cangorin E	ONic	ONic	OAc	OBz	OBz	OAc	C <sub>45</sub> H <sub>44</sub> N <sub>2</sub> O <sub>14</sub> , mw: 836.28, mp: 103–108 °C, [α] <sub>D</sub> +26.3° (CHCl <sub>3</sub> ), UV, IR, MS, <sup>1</sup> H, <sup>13</sup> C (101)
204. Cangorin F	OAc	ONic	OH	ONic	OBz	OAc	C <sub>38</sub> H <sub>40</sub> N <sub>2</sub> O <sub>13</sub> , mw: 732.25, mp: 214–217 °C, [α] <sub>D</sub> +6.6° (CHCl <sub>3</sub> ), UV, IR, MS, CD, <sup>1</sup> H, <sup>13</sup> C, X-ray (102)
205. Cangorin G	ONic	ONic	OH	ONic	OBz	OAc	C <sub>42</sub> H <sub>41</sub> N <sub>3</sub> O <sub>13</sub> , mw: 795.26, mp: 124–128 °C, [α] <sub>D</sub> +29.4° (CHCl <sub>3</sub> ), UV, IR, MS, CD, <sup>1</sup> H, <sup>13</sup> C (102)
206. Cangorin H	ONic	ONic	OAc	ONic	OBz	OAc	C <sub>44</sub> H <sub>43</sub> N <sub>3</sub> O <sub>14</sub> , mw: 837.27, mp: 125–130 °C, [α] <sub>D</sub> +43.4° (CHCl <sub>3</sub> ), UV, IR, MS, CD, <sup>1</sup> H, <sup>13</sup> C (102)
207. Cangorin I	ONic	OAc	OBz	ONic	OBz	OAc	C <sub>45</sub> H <sub>44</sub> N <sub>2</sub> O <sub>14</sub> , mw: 836.28, mp: 111–115 °C, [α] <sub>D</sub> +14.8° (CHCl <sub>3</sub> ), UV, IR, MS, CD, <sup>1</sup> H, <sup>13</sup> C (102)
208. Cangorin J	OAc	ONic	OAc	ONic	OBz	OAc	C <sub>40</sub> H <sub>42</sub> N <sub>2</sub> O <sub>14</sub> , mw: 774.26, mp: 115–120 °C, [α] <sub>D</sub> +20° (CHCl <sub>3</sub> ), UV, IR, MS, CD, <sup>1</sup> H, <sup>13</sup> C (102)
209	OAc	OAc	OAc	ONic	OBz	OMeBu	C <sub>39</sub> H <sub>47</sub> NO <sub>14</sub> , mw: 753.30, [α] <sub>D</sub> <sup>27</sup> –33.1° (CHCl <sub>3</sub> ), UV, IR, MS, <sup>1</sup> H, <sup>13</sup> C (94)
210	OAc	OAc	OAc	ONic	OBz	OAc	C <sub>36</sub> H <sub>41</sub> NO <sub>14</sub> , mw: 711.25, [α] <sub>D</sub> <sup>25</sup> –38.4° (MeOH), UV, IR, MS, <sup>1</sup> H, <sup>13</sup> C (76)
211	OAc	OFu	OAc	OCO <sup>i</sup> Pr	ONic	OCO <sup>i</sup> Pr	C <sub>38</sub> H <sub>47</sub> NO <sub>15</sub> , mw: 757.29, [α] <sub>D</sub> <sup>20</sup> +45.8° (MeOH), IR, UV, MS, <sup>1</sup> H, <sup>13</sup> C (100)



212. Maytolidine



213

Properties

C<sub>36</sub>H<sub>41</sub>NO<sub>14</sub>, mw: 711.25,  
mp: 128–132 °C, UV, IR, MS (98)

Properties

C<sub>36</sub>H<sub>45</sub>NO<sub>17</sub>, mw: 763.27, [α]<sub>D</sub><sup>25</sup> +14.1°  
(MeOH), UV, IR, <sup>1</sup>H, <sup>13</sup>C (76)

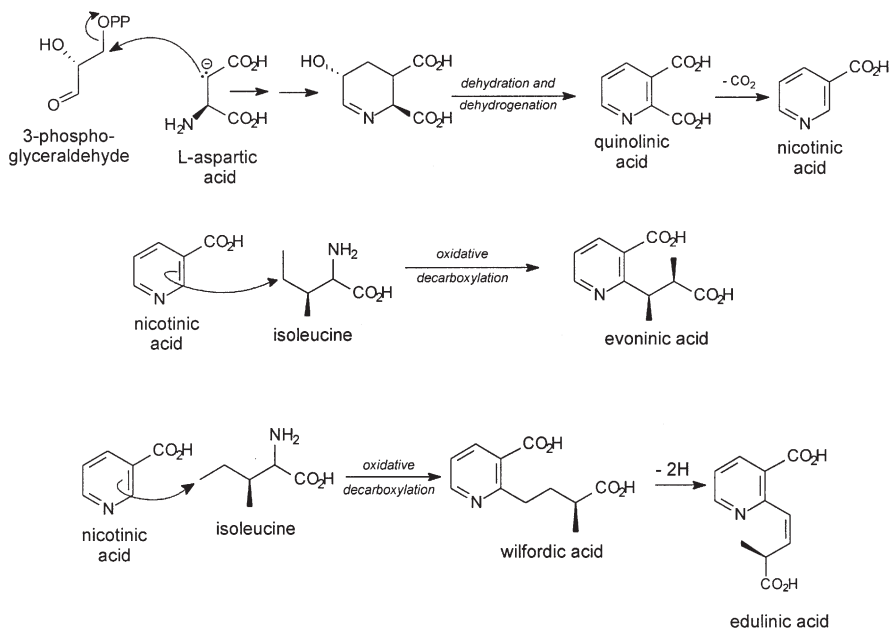


TABLE XXVI.  
Non-Celastraceous Sesquiterpene Pyridine Alkaloids.

<b>214. Rotundine A</b>	<b>215. Rotundine B</b>	<b>216. Rotundine C</b>
$C_{15}H_{21}NO$ , mw: 231.16, $[\alpha]_D^{27} -12.3^\circ$ ( $CHCl_3$ ), UV, IR, MS, $^1H$ , $^{13}C$ (104)	$C_{15}H_{23}NO$ , mw: 233.18, $[\alpha]_D^{25} -14.7^\circ$ ( $CHCl_3$ ), UV, IR, MS, $^1H$ , $^{13}C$ (104)	$C_{15}H_{23}NO$ , mw: 233.18, $[\alpha]_D^{25} -10.2^\circ$ ( $CHCl_3$ ), UV, IR, MS, $^1H$ , $^{13}C$ (104)
<b>217. Patchoulipyridine</b>	<b>218. Guaipyridine</b>	
$C_{15}H_{21}N$ , mw: 215.17, $[\alpha]_D^{28} -31.3^\circ$ (MeOH), IR, $^1H$ , $^{13}C$ (105)	$C_{15}H_{21}N$ , mw: 215.17, $^1H$ (106); IR, $^1H$ (107)	
<b>219. Epiguaipyridine</b>	<b>220. Cananodine</b>	
$C_{15}H_{21}N$ , mw: 215.17, IR, $^1H$ (107)	$C_{15}H_{23}NO$ , mw: 233.18, $[\alpha]_D^{25} -76.2^\circ$ ( $CHCl_3$ ), UV, IR, MS, $^1H$ , $^{13}C$ (108)	

carbon of isoleucine, as shown in Scheme 1 (49). To corroborate nicotinic acid as precursor of the pyridinium moiety of the sesquiterpene pyridine alkaloids, an experiment involving nicotinic acid-6- $^{14}C$  was developed. Labeled nicotinic acid was efficiently incorporated into wilfordic and hydroxywilfordic acids, the pyridinium moieties of these terpene alkaloids (109).

In the sesquiterpene pathway, farnesyl pyrophosphate, the fundamental sesquiterpene precursor, can adopt both the *E* and *Z* configuration at the double



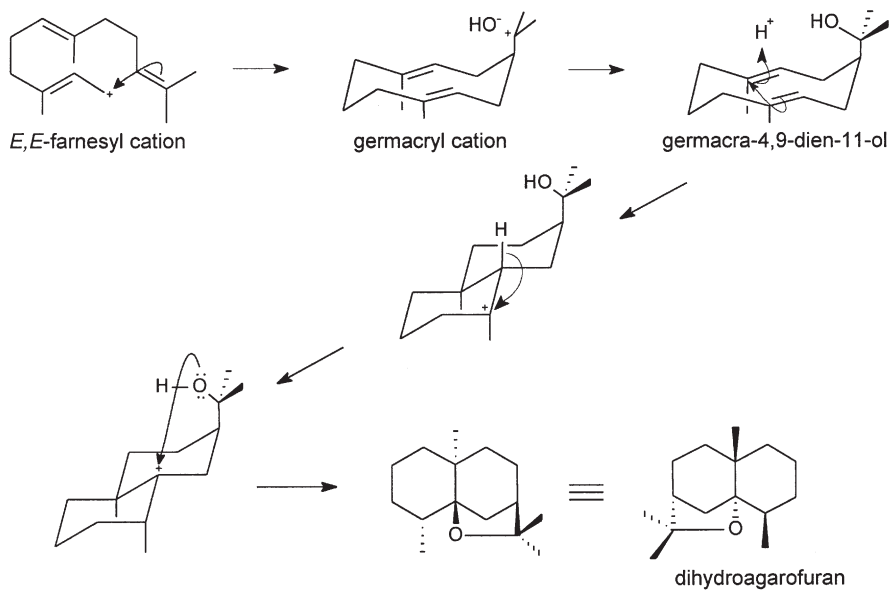
Scheme 1. Biogenesis of the pyridinium moiety.

bond nearest the pyrophosphate group. Its *E,E* cation after cyclization by electrophilic attack to an appropriate double bond leads to the germacryl cation, a precursor of the dihydroagarofuran sesquiterpenes, according to Brüning and Wagner as depicted in [Scheme 2 \(60\)](#).

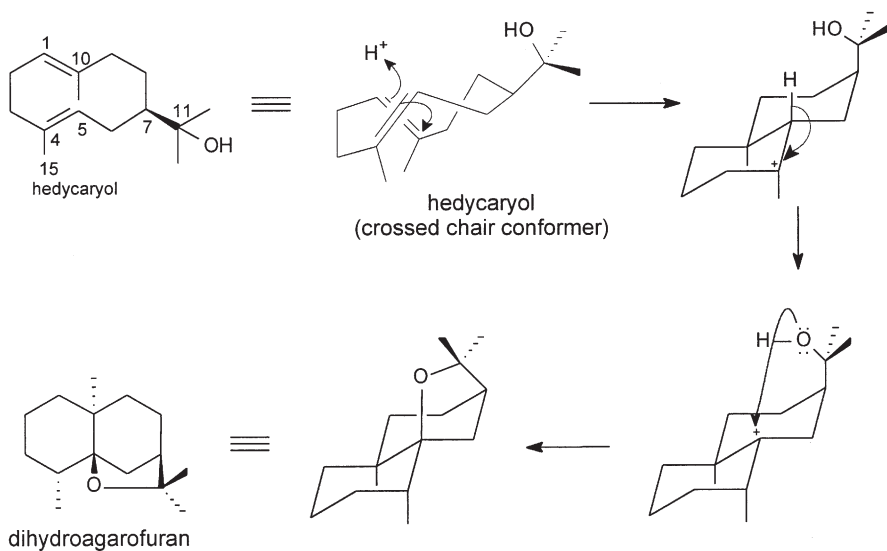
In the Swell and Tucker proposal, hedycaryol, also formed via a germacryl cation, can theoretically adopt eight different conformations, although only three have experimental substance ([110,111](#)). Of these, the crossed chair conformer could cyclize in the reverse direction leading to a *trans* decalin cation and hence dihydroagarofuran ([Scheme 3](#)).

The controversy between the two proposals involves the isomeric forms of hedycaryol. Whilst germacra-4,9-dien-11-ol is employed as an intermediate in the dihydroagarofuran route in the former pathway, *E,E*-hedycaryol [1(10),4-diene] is involved in the latter.

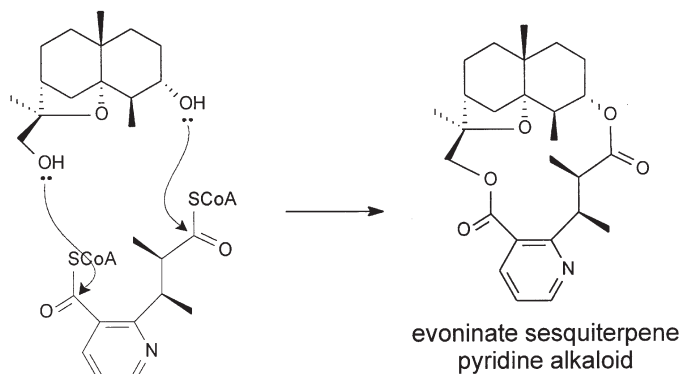
The last step in the biogenetic process involves the formation of a macrocyclic ring. The dicarboxylic bridges are formed from the corresponding pyridine alkaloid derivative and an appropriate dihydroagarofuran sesquiterpene, as shown in [Scheme 4](#).



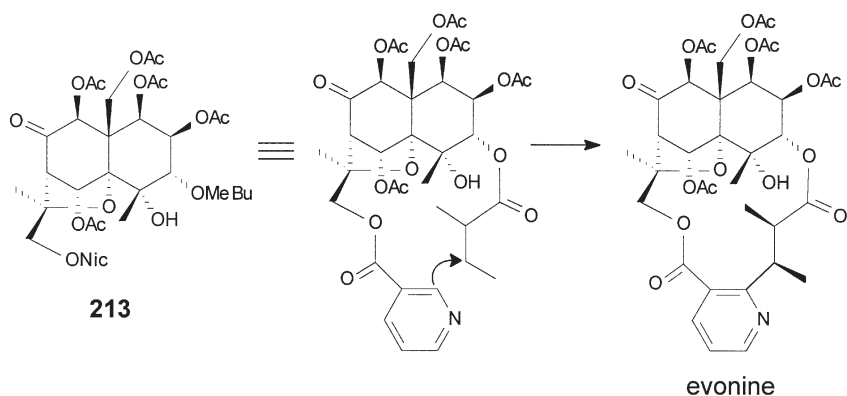
Scheme 2. Biogenesis of the sesquiterpene moiety – Wagner and Brünning proposal (60).



Scheme 3. Biogenesis of the sesquiterpene moiety – Southwell and Tucker proposal (110).



Scheme 4. Macrocyclic ring formation.



Scheme 5. Alternative pathway for evonine biosynthesis.

An alternative pathway for the biosynthesis of the sesquiterpene pyridine alkaloids may also be proposed. This route involves the lower molecular weight sesquiterpene alkaloid **213**, isolated from *T. wilfordii*, which is esterified with nicotinic and 2-methylbutanoic acids in appropriate positions, and whose structure is very close to those of the macrocyclic evonines (76). Its CoA derivative may be viewed as an intermediate involved in the evoninate biogenetic pathway, as depicted in [Scheme 5](#).

## IX. Biological Activity

### A. INSECT ANTIFEEDANT AND INSECTICIDAL ACTIVITY

The family Celastraceae contains several species that have been used as natural insecticides for a long time in traditional Chinese agriculture.

Dihydroagarofuran sesquiterpene esters and alkaloids are the main compounds having insect antifeedant and insecticidal activities that have already been isolated from species of Celastraceae. Insecticidal properties of *T. wilfordii* roots have been cited in the literature since 1931 (112), and the sesquiterpene pyridine alkaloids wilforine (100) and wilfordine (119) were identified as its active components (59). These alkaloids exhibited potent larvicidal activity against the European corn bore *Pyrausta nubilalis* at concentrations of 60 ppm, inducing 100% mortality after 3 days (113). Extracts of the roots have also produced the alkaloids wilforgine (101), wilfortrine (120), and wilforzine (103) (114,115), and biological assay results have shown that the individual bases exert a similar insecticidal effect (116). An exception is the alkaloid 103, which displayed a lower activity than wilforine (100) when tested toward the larvae of *Crotalus adamanteus*. Evaluation of structure–activity relationships has suggested that the esterifying pattern modulates the insecticidal property (115). Additionally, wilforine was assayed toward the third instar larvae of the diamondback moth, and was shown to be more effective than dimilin used as positive control (117). This alkaloid has also shown effective antifeedant activity toward the grasshopper *Locusta migratoria* and the caterpillar *Pieris rapae* at  $5 \times 10^{-5}\%$  and  $1 \times 10^{-5}\%$  dry weight, respectively. This makes wilforine more potent against these pests than azadirachtin, which is one of the strongest, naturally occurring, insect growth inhibitors known. The latter is a limonoid isolated from *Azadiracta indica* (Meliaceae), and has been shown to be active at  $1 \times 10^{-2}\%$  dry weight against *L. migratoria* (118). An interesting point is that the sesquiterpene alkaloids from the roots of *T. wilfordii* are not toxic for mammals (13). Three cathedulins alkaloids have also shown insecticidal activity comparable to azadirachtin in an artificial diet-feeding assay using a lepidopterous pest insect, the pink bollworm (*Pectinophora gossypiella*). Cathedulins E3 (68), E4 (69), and E5 (71) exhibited potent growth inhibitory activity at approximately 1 ppm (119).

The insecticidal properties of the bark and fruits of some *Euonymus* species are also noteworthy. Many sesquiterpene esters and alkaloids exhibiting this property have been isolated from *Euonymus* species (67,120). The fresh fruit extracts of *E. nanus* yielded the alkaloid evonine (1), which was found to display larvicidal activity against the large white cabbage butterfly, *Pieris brassicae* L. (Lepidoptera), inducing 74% mortality at the dosage of 200  $\mu\text{g}$  per specimen, topically applied (64).

Traditionally, the powdered root bark of *Celastrus angulatus* Max. (Celastraceae), has been used in China to protect plants from insect damage (121). Non-alkaloidal and alkaloidal sesquiterpenes were found to be responsible for this insecticidal property (99,122). Four lower molecular weight sesquiterpene alkaloids (193–196) from this species exhibited strong antifeedant activity when tested against *P. rapae* L., *Ostrina furnacalis*, and *Tribolium castaneum* at 222 ppm, in preliminary screening experiments. Small doses of these substances paralyzed the tested insects for many hours. After recovering, the insects fed again, but gradually starved to death (99). In another study, three sesquiterpene alkaloids (149, 156, and

**173**) were assayed against the Egyptian cotton leafworm *Spodoptera littoralis*, using the leaf disk method. The results showed the highest activity for the sesquiterpene alkaloid **173**, which was active at  $0.1 \mu\text{g cm}^{-2}$ . It was ten-fold more active than the antifeedant agent triphenyl tin acetate, used as a positive control. The comparable results suggested that the compact tricyclic system is very important for antifeedant or insecticidal activity in this type of sesquiterpene (**123**).

## B. ANTI-HIV ACTIVITY

There has been an ever-increasing interest on different plant species to investigate their potential therapeutic applications. In this context, researchers interested in AIDS treatment, a disease that has affected millions of people around the world, detected some sesquiterpene pyridine alkaloids, isolated from *T. hypoglaucum* and a clinically used extract of *T. wilfordii*, which showed anti-HIV activity (**51**). Nineteen compounds were evaluated, and the best results were obtained for triptonine B (**75**), hypoglaunine B (**93**), hyponine B (**10**), and wilfortrine (**120**), which displayed potent inhibition of HIV virus replication in human lymphocyte cells. The  $\text{IC}_{50}$  and  $\text{EC}_{50}$  values were similar, with the  $\text{EC}_{50}$  values of the first and last alkaloids, as  $< 0.10 \mu\text{g ml}^{-1}$ . However, the most significant results obtained involved the *in vitro* therapeutic indexes that presented values of  $> 1000 \mu\text{g ml}^{-1}$ . The therapeutic index ( $\text{IC}_{50}/\text{EC}_{50}$ ) represents the selectivity for diseased cells over healthy cells, and in general values greater than 5.0 are considered to be significant.

## C. CYTOTOXIC ACTIVITY

Herbal therapies have been characterized as the most popular in cancer treatment. In this context, species of the Celastraceae have a long history in traditional medicine, including in cancer therapy (**124**). In a search for antitumor agents in higher plants, extracts of stems and branches of *Maytenus emarginata* were evaluated, and sesquiterpene pyridine alkaloids bearing a 5-carboxy-*N*-methylpyridonyl substituent, known as emarginatines and emarginatinine, were isolated. Emarginatines A–B, E–G, and emarginatinine (**126**) were shown to have inhibitory activity *in vitro* against cells derived from a human epidermoid carcinoma of the nasopharynx (KB cells), while emarginatines C (**38**) and D (**39**) were inactive. These results suggested that the nature of the groups at C-1 and C-9 positions might affect the cytotoxicity. Emarginatine B (**48**) and F (**50**), which are esterified by acetic and benzoic acids at these positions, were the most active with  $\text{ED}_{50}$  values of 0.4 and  $0.5 \mu\text{g ml}^{-1}$ , respectively. On the other hand, emarginatine E (**49**), with hydroxyl groups at both positions, was approximately six-fold less active. Emarginatine G (**40**), which contains an alkene group at C-1, was also inactive. The C-8 configuration was also suggested as an additional structural feature involved in cytotoxic activity, since emarginatines B and E, which possess the isoeuonyminol sesquiterpene core were more active than emarginatines A (**37**), C, and D that contain the euonyminol sesquiterpene core. The hydroxywilfordate-type emarginatinine (**126**) was slightly more active than its evoninate-type analog

emarginatine A ( $ED_{50} = 2.1$  vs.  $4.0 \mu\text{g ml}^{-1}$ ). Emarginatines F (**50**) and G (**40**) were also evaluated against other tumor cells. The best cytotoxicities of emarginatine F were against the human melanoma cell line RPMI-7951 ( $ED_{50} < 0.1 \mu\text{g ml}^{-1}$ ), and against the medulloblastoma cell line TE-671 ( $ED_{50} = 0.21 \mu\text{g ml}^{-1}$ ). Alkaloid **50** also showed interesting results against the murine leukemia cell line P-388 ( $ED_{50} = 0.69 \mu\text{g ml}^{-1}$ ) and against the human colon adenocarcinoma cell line HCT-8 ( $ED_{50} = 1.29 \mu\text{g ml}^{-1}$ ). However, an ambiguous result was obtained for cytotoxicity against the human lung carcinoma cell line A-549 ( $ED_{50} = 5.5 \mu\text{g ml}^{-1}$ ). The alkaloid **40** was inactive in these five cell lines (34,35).

Recently, the chemopreventive ability of euonymine (**8**) was evaluated, using the Epstein-Barr virus early antigen (EBV-EA) method, and marginal inhibitory activity was observed (73.6% at 1000 mol ratio/TPA). Structure-activity considerations, also involving non-alkaloidal dihydroagarofuran sesquiterpenes, suggested that enlargement of the molecule leads to a decrease in its inhibitory activities (125).

The fruit extracts of *C. odorata*, a non-Celastraceae plant, have also yielded a cytotoxic sesquiterpene pyridine alkaloid (108). Cananodine (**220**) was evaluated for cytotoxicity against two hepatocarcinoma cancer cell lines (Hep G<sub>2</sub> and 2,2,15), and showed strong cytotoxicity against the former cancer cell line ( $IC_{50} = 0.22 \mu\text{g ml}^{-1}$ ).

#### D. IMMUNOSUPPRESSIVE ACTIVITY

Recently, another important biological activity that has been reported for sesquiterpene pyridine alkaloids is their immunosuppressive action, an essential factor in organ transplant therapy (26). A series of sesquiterpene alkaloids, isolated from the clinically used T<sub>II</sub> extract of *T. wilfordii*, was evaluated in a screen for immunosuppressive agents on cytokine production, and fifteen of them showed an inhibitory effect. Ebenifoline E-II (**25**) and cangorinine E-I (**16**) displayed the most significant results, inhibiting 100% of two human cytokines (IL-2 $\beta$  and IL-4 $\beta$ ) at  $10 \mu\text{g ml}^{-1}$ , when compared to prednisolone, used as the reference compound, which showed 65 and 76% of inhibition at  $0.3 \mu\text{g ml}^{-1}$ .

#### E. REVERSAL OF MULTIDRUG RESISTANCE

Multidrug resistance (MDR) is a great problem in several disease treatments. A primary mechanism of MDR is attributed to the over-expression of P-glycoprotein (Pgp) in the plasma membrane of resistant cells. The MDR phenotype due to Pgp has been extensively documented as a very efficient mechanism to reduce intracellular drug accumulation in parasitic protozoans including *Plasmodium* and *Leishmania* (126,127). Three lower molecular weight sesquiterpene pyridine alkaloids, isolated from *Crossopetalum tonduzii*, have exhibited reversal of resistance from the parasitic protozoan *Leishmania tropica* to growth inhibition by daunomycin. The alkaloid **191** was the most active producing

more than 90% growth inhibition at 15  $\mu\text{M}$  as compared to control growth. The other alkaloids (**176** and **209**), tested in the same conditions, produced 21% and 32% inhibition of growth, respectively. The size of the group at C-2 was suggested to be important for MDR activity. The most active compounds, including non-alkaloidal sesquiterpenes, have hydrogen or hydroxyl groups in this position, in contrast with the acetate or nicotinoyl groups in the less active compounds. The presence of a 2-methyl butanoate group attached to C-15 is another essential factor for MDR activity (94).

### X. Taxonomic Considerations

As noted throughout this chapter, sesquiterpene pyridine alkaloids have been encountered mainly in plants belonging to the Celastraceae and Hippocrateaceae families of the angiosperm Celastrales order. These families contain several species that are reported to be useful in folk medicine, and several research laboratories are intensively researching this family, inspired by the different types of pharmacological actions displayed by its constituents.

The Celastraceae, known as the bittersweet family, consists of about 50 genera and 800 species distributed in both the tropical and subtropical regions. The chief genera are *Maytenus* (225 tropical species) and *Euonymus* (176 species mostly from the Himalayas, China, and Japan). The family Hippocrateaceae consists of about 25 genera and more than 300 species which are widespread in tropical regions (128), and mainly distributed in the genera *Hippocratea* (100) and *Salacia* (200). In another botanical view these genera are subdivided (as many as 12 for *Hippocratea* alone) with *Hippocratea* sens. strict. becoming a monotype (129).

The taxonomic position of the family Hippocrateaceae has been debated. Some taxonomists combine this family with the Celastraceae, while others maintain that it should be considered as a family distinct from the Celastraceae. According to Robson, the Hippocrateaceae genera are not a natural group, being derived in two separate lines from the Celastraceae (130). The connection between these families has been reinforced by the presence of some common chemotaxonomic markers such as the quinonemethide triterpenoids, and dulcitol (60). In this context, sesquiterpene pyridine alkaloids that have also been considered Celastraceae chemotaxonomic markers have been recently obtained from Hippocrateaceae. This gives support for the botanical classification in which the two families are grouped as only one family, as shown in Table XXVII. This table also shows the natural source of all of the sesquiterpene alkaloids described in this chapter. If the family Hippocrateaceae is united with Celastraceae, the name Hippocrateaceae is rejected in favor of Celastraceae.

### XI. Synthesis

Very recently Spivey *et al.* have published a comprehensive review of Celastraceae sesquiterpenoids in which the synthetic approaches to the



TABLE XXVII.  
Natural Sources of Sesquiterpene Pyridine Alkaloids.

Plant*	Sesquiterpene alkaloid ( <i>ref.</i> )
Celastraceae	
<i>Acanthoamnus aphyllus</i> (Schltdl.) Standl.	95 (55)
<i>Cassine matabelicum</i> (Loes.) Steedman	145 (60)
<i>Catha edulis</i> (Vahl) Forssk. ex Endl.	64–67 (47); 68–69, 71–73 (48); 70, 142–143 (49); 171, 180 (91)
<i>Celastrus angulatus</i> Maxim.	19 (22); 153, 162–164 (81); 158, 179 (85); 159–160 (86); 161, 165 (87); 178 (95); 193–196 (99); 197, 211 (100)
<i>Celastrus hindsii</i> Benth.	23, 37 (27)
<i>Celastrus paniculata</i> Willd.	147, 167–168 (75)
<i>Crossopetalum tonduzii</i> (Loes.) Lundell	176, 191, 209 (94)
<i>Euonymus alatus</i> Forma <i>Striatus</i> (Thunb.) Makino	1–2, 8, 119, 127 (67); 118, 125, 129 (66)
<i>Euonymus europaeus</i> L.	2–6, 114 (60)
<i>Euonymus japonicus</i> Thunb.	28–33 (29); 62 (42); 99, 104–106, 116 (58), 157, 177 (84)
<i>Euonymus nanus</i> M. Bieb.	1, 114, 183 (64)
<i>Euonymus sachalinensis</i> (F. Schmidt) Maxim.	6 (18), 183 (64)
<i>Euonymus sieboldianus</i> Blume	1–2, 8, 17 (15); 6, 99, 114 (60)
<i>Euonymus verrucosus</i> Scop.	182 (96)
<i>Maytenus aquifolium</i> Mart.	52–53 (39); 54–55 (40)
<i>Maytenus blepharodes</i> Lundell	175 (93)
<i>Maytenus buchananii</i> (Loes.) R. Wilczek	124 (69)
<i>Maytenus chuchuhuasca</i> Raymond-Hamet and Colas	8, 24–28, 56–60, 115 (41)
<i>Maytenus cuzcoina</i> Loes.	8 (125)
<i>Maytenus diversifolia</i> (Maxim.) Ding Hou	41 (32)
<i>Maytenus ebenifolia</i> Reissek	1, 8, 24–28, 30, 63, 105, 111–112 (19)
<i>Maytenus emarginata</i> (Willd.) Ding Hou	35, 40, 50 (35); 37 (33); 38–39, 49, 126 (34); 48 (37)
<i>Maytenus guianensis</i> Klotzsch	1, 8, 28, 119 (28)
<i>Maytenus heterophylla</i> (Eckl. and Zeyh.) N. Robson	170 (90)
<i>Maytenus horrida</i> Reissek	51 (38)
<i>Maytenus ilicifolia</i> Mart. ex Reissek	16, 107–108 (8); 199–203 (101); 204–208 (102)
<i>Maytenus laevis</i> Reissek	1, 8, 24, 28, 31, 34, 100, 105, 110 (30)
<i>Maytenus myrsinoides</i> Reissek	172, 181 (92)

(continued.)

TABLE XXVII.

Continued.

Plant*	Sesquiterpene alkaloid ( <i>ref.</i> )
<i>Maytenus putterlickioides</i> (Loes.) Exell and Mendonca	20–21, 28 (25)
<i>Maytenus senegalensis</i> (Lam.) Exell	100 (13)
<i>Maytenus serrata</i> (Hochst. ex A. Rich.) Wilczek	192, 198, 212 (98)
<i>Orthosphenia mexicana</i> Standl.	144 (73); 149 (14); 155–156 (83)
<i>Rzedowskia tolantonguensis</i> Medrano	149 (14); 173 (83)
<i>Tripterygium forrestii</i> Loes.	15, 100, 119 (21)
<i>Tripterygium hypoglaucum</i> (H. Lévé.) Hutch.	1, 9–11, 16, 150 (14); 12–15, 17 (20); 74–75 (51); 8, 81, 92–94, 100–101, 119–120 (53)
<i>Tripterygium wilfordii</i> Hook. f.	1, 100, 119, 125, 130–133, 135 (20); 8, 12, 16, 20, 22, 25, 28, 74, 77, 91, 128, 136–139 (26); 76, 78, 89–90, 94 (51); 101, 120, 140–141 (72); 102 (61); 99, 103, 109, 121–123 (62); 117 (65); 134 (71); 148, 188, 210, 213 (76); 151 (79)
<i>Tripterygium wilfordii</i> (Hook) var. <i>regelii</i> (Makino)	146 (74); 152 (80); 154, 184–186 (82); 166, 169, 187 (88); 150 (78); 189–190 (97)
Hippocrateaceae	
<i>Hippocratea excelsa</i> Kunth	28, 82 (54); 35–37 (31); 42–47, 80, 83–88, 96–98, 113 (36)
<i>Peritassa campestris</i> (Cambess.) A. C. Smith.	8, 15, 18, 24, 99–100, 102–103, 105, 117 (24)
<i>Peritassa compta</i> Miers	78–79, 99, 100, 105, 111 (52)
Annonaceae	
<i>Cananga odorata</i> (Lam.) Hook. f. and Thomson	220 (108)
Cyperaceae	
<i>Cyperus rotundus</i> Linn.	214–216 (104)
Lamiaceae	
<i>Pogostemon patchouly</i> Pellet.	217, 219 (105); 218 (106)

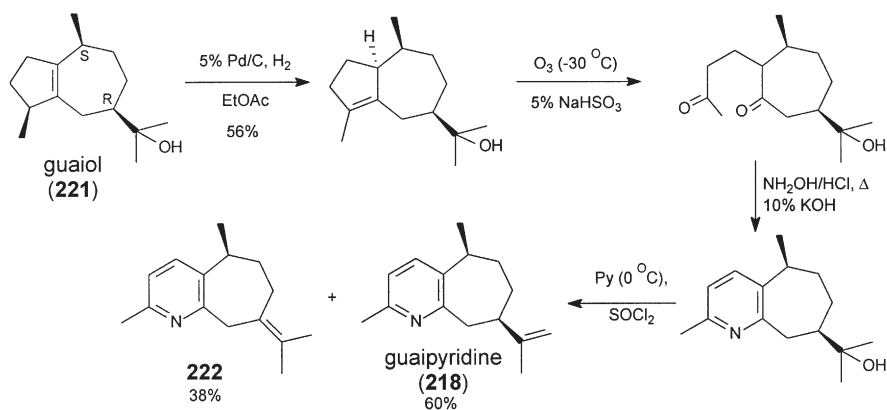
\*Names according Missouri Botanical Garden (<http://www.mobot.org>) and The International Plant Names Index (<http://www.ipni.org>).

dihydroagarofuran sesquiterpene core have been well discussed (131). Their work emphasizes developments on strategies for synthesis of the dihydroagarofuran nucleus, and the synthetic approaches involved in forming the highly oxygenated agarofuran derivatives. The synthetic complexity of the macrocyclic sesquiterpene pyridine alkaloids was also discussed, and a unique study relating to macrolactone synthesis was presented. Thus, we are going to focus only on the synthesis of non-Celastraceous sesquiterpene alkaloids.

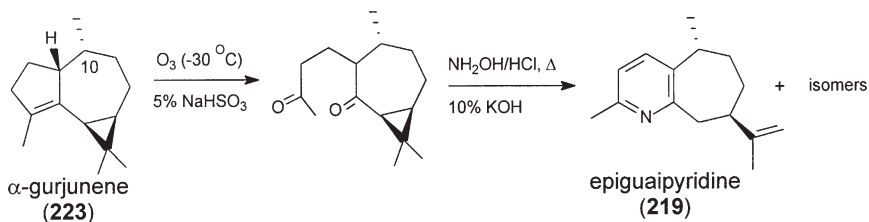
The first guaipyridine (218) asymmetric synthesis, which is an alkaloid of patchouli oil, was reported by Van Der Gen *et al.* using guaiol (221), one of the major components of patchouli oil, as starting material (Scheme 6) (107). Guaipyridine was obtained in a mixture with its double bond isomer (222), and the total yield of guaipyridines, based on guaiol, was 22%. Pure components were isolated by preparative gas chromatography.

Gen and coworkers have also provided a synthesis of epiguaipyridine (219), a C(10)-epimer of guaipyridine (Scheme 7). In this synthesis, the sesquiterpene  $\alpha$ -gurjunene (223) was used as starting material, and the first step was an oxidative ring opening of 223 by ozonolysis. In this synthetic approach epiguaipyridine was produced in a mixture with four pyridine derivatives, including the C(10)-epimers. Epiguaipyridine was purified by preparative gas chromatography, and obtained in low yield. The overall efficiency of this synthesis was compromised by the composition of the starting natural  $\alpha$ -gurjunene (223), which by GC analysis was shown to be a mixture with 10-epi- $\alpha$ -gurjunene in a ratio of 4 to 1 (107).

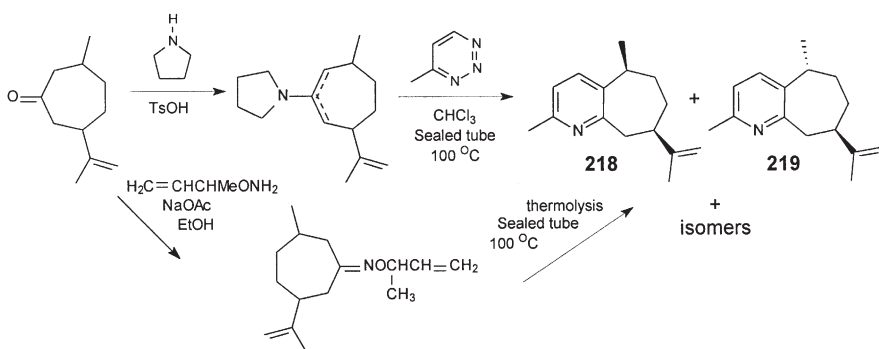
More recently, Okatani and coworkers have described two new syntheses of guaipyridine and epiguaipyridine (106,132). The first of the two syntheses employed Diels-Alder reaction of 1,2,3-triazine with a mixture of enamines, where the cycloaddition selectively occurred at N-3/C-6 of the 1,2,3-triazine nucleus, and at



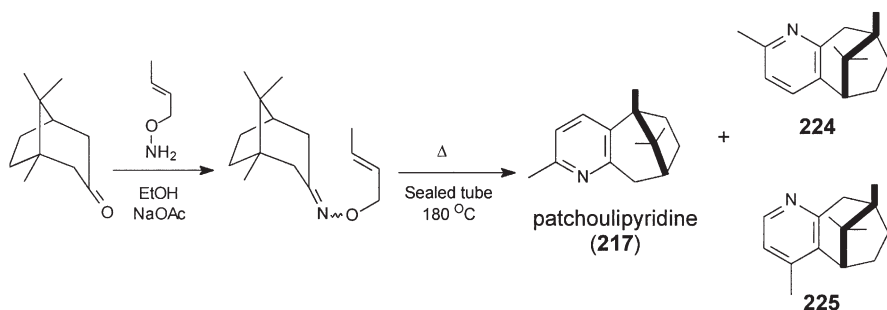
Scheme 6. The Gen guaipyridine synthesis (107).



Scheme 7. The Gen epiguaipyrindine synthesis (107).



Scheme 8. The two Okatani guaipyrindine and epiguaipyrindine syntheses (106,131).



Scheme 9. The Okatani patchoulypyridine synthesis (105).

the nucleophilic carbon of the enamine (Scheme 8). This process resulted in two mixtures of isomers. One was the mixture of diastereoisomers **218** and **219** in a ratio 1:2, and in a yield of 11.6%, later separated by HPLC. The other mixture was the isomers of **218** and **219** alkaloids. In the other synthetic approach, the method for constructing cycloalkenopyridines by the thermal rearrangement of an oxime *O*-allyl ether was employed, and the resulting isomeric mixture was the same as the one resulting from the other synthesis.

The Okatani group has also synthesized the optically active patchouli-pyridine alkaloid (**217**) as depicted in [Scheme 9](#) using the same thermal rearrangement (*vide infra*) ([105](#)). The process results in a mixture of cycloalkenopyridines, which were purified by preparative thin layer chromatography. The overall yield of alkaloid **217** was 7.8%.

### References

1. H. Wada, Y. Shizuri, K. Sugiura, K. Yamada, and Y. Hirata, *Tetrahedron Lett.* **33**, 3131 (1971).
2. B. H. Han, M. K. Park, J. H. Ryu, J. H. Park, and H. Naoki, *Phytochemistry* **29**, 2303 (1990).
3. K. Doebel and T. Reichstein, *Helv. Chim. Acta* **32**, 592 (1949).
4. M. Pailer and R. Libiseller, *Monatsh. Chem.* **93**, 403 (1962).
5. M. Pailer and R. Libiseller, *Monatsh. Chem.* **93**, 511 (1962).
6. R. Libiseller and A. Presinger, *Monatsh. Chem.* **93**, 417 (1962).
7. K. Sasaki and Y. Hirata, *J. Chem. Soc., Perkin Trans. II* **9**, 1268 (1972).
8. O. Shirota, H. Morita, K. Takeya, and H. Itokawa, *Heterocycles* **38**, 383 (1994).
9. Y. Shizuri, H. Wada, K. Yamada, and Y. Hirata, *Tetrahedron* **29**, 1795 (1973).
10. Y. Shizuri, H. Wada, K. Sugiura, K. Yamada, and Y. Hirata, *Tetrahedron* **29**, 1773 (1973).
11. Y. Shizuri, H. Wada, K. Sugiura, K. Yamada, and Y. Hirata, *Tetrahedron Lett.* **28**, 2659 (1971).
12. M. Pailer and R. Streicher, *Monatsh. Chem.* **102**, 1873 (1971).
13. L. Dúbravková, Z. Votický, and J. Tomko, in "Acta Facultatis Pharmaceuticae", Tomo XLII, p. 141, 1988.
14. H.-Q. Duan, K. Kawazoe, and Y. Takaishi, *Phytochemistry* **45**, 617 (1997).
15. K. Sugiura, Y. Shizuri, H. Wada, K. Yamada, and Y. Hirata, *Tetrahedron Lett.* **29**, 2733 (1971).
16. A. Klasek, Z. Samek, and F. Santavy, *Tetrahedron Lett.* **13**, 941 (1972).
17. L. Crombie, P. J. Ham, and D. A. Whiting, *Phytochemistry* **12**, 703 (1973).
18. J. Hohmann, G. Nagy, G. Günther, and L. Varjas, *Phytochemistry* **34**, 879 (1993).
19. H. Itokawa, O. Shirota, H. Morita, K. Takeya, and Y. Litaka, *J. Chem. Soc., Perkin Trans. I* **11**, 1247 (1993).
20. H.-Q. Duan and Y. Takaishi, *Phytochemistry* **52**, 1735 (1999).
21. C. Chunquan, L. Jikai, and W. Dagang, *Phytochemistry* **31**, 4391 (1992).
22. L. Jikai, W. Dagang, and J. Zhongjian, *Phytochemistry* **32**, 487 (1993).
23. K. Yamada, K. Sugiura, Y. Shizuri, H. Wada, and Y. Hirata, *Tetrahedron* **33**, 1725 (1977).
24. L. M. Lião, P. C. Vieira, E. Rodrigues-Filho, J. B. Fernandes, and M.F.G.F. Silva, *Phytochemistry* **58**, 1205 (2001).
25. B. T. Schaneberg, D. K. Green, and A. T. Sneden, *J. Nat. Prod.* **64**, 624 (2001).
26. H.-Q. Duan, Y. Takaishi, H. Momota, Y. Ohmoto, T. Taki, Y. Jia, and D. Li, *J. Nat. Prod.* **64**, 582 (2001).
27. Y.-H. Kuo, C.-F. Chen, L.-M.Y. Kuo, M.-L. King, C.-F. Chen, and K.-H. Lee, *J. Nat. Prod.* **58**, 1735 (1995).
28. J. R. Sousa, J. A. Pinheiro, E. F. Ribeiro, E. Souza, and J. G. S. Maia, *Phytochemistry* **25**, 1776 (1986).

29. B.-H. Han, M. K. Park, J.-H. Ryu, J. H. Park, and H. Naoki, *Phytochemistry* **29**, 2303 (1990).
30. S. Piacente, N. Tommasi, and C. Pizza, *J. Nat. Prod.* **62**, 161 (1999).
31. R. Mata, F. Calzada, E. Díaz, and R. A. Toscano, *J. Nat. Prod.* **53**, 1212 (1990).
32. Y.-H. Kuo, J.-C. Ou, K.-H. Lee, and C.-F. Chen, *J. Nat. Prod.* **58**, 1103 (1995).
33. Y.-H. Kuo, C.-H. Chen, L.-M.Y. Kuo, M.-L. King, T.-S. Wu, S.-T. Lu, I.-S. Chen, D. R. McPhail, A. T. McPhail, K.-H. Lee, *Heterocycles* **29**, 1465 (1989).
34. Y.-H. Kuo, C.-H. Chen, M.-L. King, T.-S. Wu, and K.-H. Lee, *Phytochemistry* **35**, 803 (1994).
35. Y.-H. Kuo, M.-L. King, C.-F. Chen, H.-Y. Chen, C.-H. Chen, K. Chen, and K.-H. Lee, *J. Nat. Prod.* **57**, 263 (1994).
36. M. Furukawa, M. Makino, T. Uchiyama, K. Ishimi, Y. Ichinohe, and Y. Fujimoto, *Phytochemistry* **59**, 767 (2002).
37. Y.-H. Kuo, C.-H. Chen, L.-M.Y. Kuo, M.-L. King, T.-S. Wu, M. Haruna, and K.-H. Lee, *J. Nat. Prod.* **53**, 422 (1990).
38. A. G. González and A. Gutierrez, in "Revista de la Real Academia de Ciencias Exactas y Naturales de Madrid", Tomo LXXXIV, p. 237, 1990.
39. J. Corsino, V. S. Bolzani, A. M. S. Pereira, S. C. França, and M. Furlan, *Phytochemistry* **48**, 137 (1998).
40. J. Corsino, V. S. Bolzani, A. M. S. Pereira, S. C. França, and M. Furlan, *Phytochemistry* **49**, 2181 (1998).
41. O. Shiota, A. Otsuka, H. Morita, K. Takeya, and H. Itokawa, *Heterocycles* **38**, 2219 (1994).
42. J.-H. Ryu, J.-H. Eun, S.-Y. Lee, J.-S. Chang, M. K. Park, J. H. Park, Y.-N. Han, and B.-H. Han, *Yakhak Hoeji* **41**, 554 (1997).
43. O. Wolfes, *Arch. Pharm.* **268**, 81 (1930).
44. T.-S. Kim and J. D. White, *Tetrahedron Lett.* **34**, 5535 (1993).
45. L. Crombie, W. M. L. Crombie, and D. A. Whiting, in "The Alkaloids" vol. 39, pp. 139. Academic Press, San Diego, 1990.
46. R. L. Baxter, L. Crombie, D. J. Simmonds, D. A. Whiting, O. J. Braenden, and K. Szendrei, *J. Chem. Soc., Perkin Trans. I* **12**, 2965 (1979).
47. L. Crombie, W. M. L. Crombie, and D. A. Whiting, *J. Chem. Soc., Perkin Trans. I* **12**, 2976 (1979).
48. R. L. Baxter, W. M. L. Crombie, L. Crombie, D. J. Simmonds, D. A. Whiting, and K. Szendrei, *J. Chem. Soc., Perkin Trans. I* **12**, 2989 (1979).
49. L. Crombie, D. Toplis, and D. A. Whiting, *J. Chem. Soc., Perkin Trans. I* **3**, 531 (1986).
50. H.-Q. Duan, Y. Takaishi, M. Bando, M. Kido, Y. Imakura, and K.-H. Lee, *Tetrahedron Lett.* **40**, 2969 (1999).
51. H.-Q. Duan, Y. Takaishi, Y. Imakura, Y. Jia, D. Li, L. M. Cosentino, and K.-H. Lee, *J. Nat. Prod.* **63**, 357 (2000).
52. J. Klass, W. F. Tinto, W. F. Reynolds, and S. McLean, *J. Nat. Prod.* **56**, 946 (1993).
53. H.-Q. Duan and Y. Takaishi, *Phytochemistry* **49**, 2185 (1998).
54. F. Calzada and R. Mata, *Phytochemistry* **40**, 583 (1995).
55. A. A. Sánchez, J. Cárdenas, M. Soriano-García, R. Toscano, and L. Rodríguez-Hahn, *Phytochemistry* **25**, 2647 (1986).
56. M. Soriano-García, R. A. Tosano, A. A. Sánchez, and L. Rodríguez-Hahn, *J. Cryst. Spectrosc. Res.* **16**, 567 (1986).
57. L. M. Lião, I. Caracelli, J. Zukerman-Schpector, M.F.G.F. Silva, E. Rodrigues-Filho, J. B. Fernandes, and P. C. Vieira, *Anais Assoc. Bras. Quím.* **46**, 184 (1996).

58. B.-H. Han, J.-H. Ryu, Y.-N. Han, M. K. Park, J. H. Park, and H. Naoki, *J. Nat. Prod.* **53**, 909 (1990).
59. M. Beroza, *J. Am. Chem. Soc.* **73**, 3656 (1951).
60. R. Brüning and H. Wagner, *Phytochemistry* **17**, 1821 (1978).
61. F. Deng, Z. Xia, R. Xu, and J. Chen, *Zhiwu Xuebao* **34**, 618 (1992).
62. L. Ya, G. M. Strunz, and L. A. Calhoun, *Can. J. Chem.* **68**, 371 (1990).
63. K. Sugiura, K. Yamada, and Y. Hirata, *Tetrahedron Lett.* **2**, 113 (1973).
64. J. Hohmann, G. Nagy, Z. Dini, G. Günther, I. Pelczer, G. Jerkovich, and L. Varjas, *J. Nat. Prod.* **58**, 1192 (1995).
65. Z.-S. He, Y. Li, S.-D. Fang, and S.-H. Hong, *Acta Chim. Sin.* **47**, 178 (1989).
66. H. Ishiwata, Y. Shizuri, and K. Yamada, *Phytochemistry* **22**, 2839 (1983).
67. K. Yamada, Y. Shizuri, and Y. Hirata, *Tetrahedron* **34**, 1915 (1978).
68. Z.-S. He, S.-H. Hong, Y. Li, S.-H. Hong, and X.-G. Yu, *Acta Chim. Sin.* **43**, 593 (1985).
69. K. V. S. Sekar, J. M. Campagne, and A. T. Sneden, *Planta Med.* **62**, 368 (1996).
70. H.-Q. Duan, Y. Takaishi, Y. Jia, and D. Li, *Chem. Pharm. Bull.* **47**, 1664 (1999).
71. L. Ya, G. M. Strunz, and L. A. Calhoun, *Phytochemistry* **30**, 719 (1991).
72. T. Morota, C.-X. Yang, Y. Ikeya, W.-Z. Qin, H. Nishimura, L.-H. Xu, M. Ando, K.-L. Miao, M. Maruno, B.-H. Yang, *Phytochemistry* **39**, 1219 (1995).
73. A. G. González, L. S. Andrés, A. G. Ravelo, J. G. Luis, I. A. Jiménez, and X. A. Domínguez, *J. Nat. Prod.* **52**, 1338 (1989).
74. Y. Takaishi, F. Aihara, S. Tamai, K. Nakano, and T. Tomimatsu, *Phytochemistry* **31**, 3943 (1992).
75. H. Wagner, E. Heckel, and J. Sonnebichler, *Tetrahedron* **31**, 1949 (1975).
76. H.-Q. Duan, Y. Takaishi, Y.-F. Jia, and D. Li, *Phytochemistry* **56**, 341 (2001).
77. H. Hori, G. M. Pang, K. Harimaya, Y. Iitaka, and S. Inayama, *Chem. Pharm. Bull.* **35**, 4683 (1987).
78. K. Nakano, C. Yoshida, W. Furukawa, Y. Takaishi, and K. Shishido, *Phytochemistry* **49**, 1821 (1998).
79. Z.-S. He, H.-M. Wu, M. Niwa, and Y. Hirata, *J. Nat. Prod.* **57**, 305 (1994).
80. Y. Takaishi, S. Tamai, K. Nakano, K. Murakami, and T. Tomimatsu, *Phytochemistry* **30**, 3027 (1991).
81. Y.-Q. Tu and Y.-X. Ma, *Phytochemistry* **32**, 1339 (1993).
82. Y. Takaishi, K. Tokura, H. Noguchi, K. Nakano, K. Murakami, and T. Tomimatsu, *Phytochemistry* **30**, 1561 (1991).
83. A. G. González, C. M. González, I. L. Bazzocchi, A. G. Ravelo, J. G. Luiz, and X. A. Domínguez, *Phytochemistry* **26**, 2133 (1987).
84. Z. Rózsa, A. Perjési, I. Pelczer, G. Argay, and A. Kálmán, *J. Chem. Soc., Perkin Trans. I* **6**, 1079 (1989).
85. C. Chunquan, W. Dagang, and L. Jikai, *Phytochemistry* **31**, 2777 (1992).
86. L. Jikai, C. Chunquan, and W. Dagang, *Phytochemistry* **32**, 379 (1993).
87. Y. Wang, L. Yang, Y. Tu, K. Zhang, Y. Chen, and J. Fan, *J. Nat. Prod.* **61**, 942 (1998).
88. Y. Takaishi, K. Tokura, S. Tamai, K. Ujita, K. Nakano, and T. Tomimatsu, *Phytochemistry* **30**, 1567 (1991).
89. H. Wagner, E. Heckel, and J. Sonnenbichler, *Tetrahedron Lett.* **15**, 213 (1974).
90. K. Y. Orabi, S. I. Al-Qasoumi, M. M. El-Olemy, J. S. Mossa, and I. Muhammad, *Phytochemistry* **58**, 475 (2001).
91. R. L. Baxter, L. Crombie, D. J. Simmonds, and D. A. Whiting, *J. Chem. Soc., Chem. Commun.* **12**, 465 (1976).

92. G. Baudouin, F. Tillequin, M. Koch, M.E.T.H. Dau, J. Guilhem, and H. Jacquemim, *Heterocycles* **22**, 2221 (1984).
93. A. G. González, F. M. Rodriguez, I. L. Bazzocchi, and A. G. Ravelo, *J. Nat. Prod.* **63**, 48 (2000).
94. J. M. Pérez-Victoria, B. M. Tincusi, I. A. Jiménez, I. L. Bazzocchi, M. P. Gupta, S. Castanys, F. Gamarro, and A. G. Ravelo, *J. Med. Chem.* **42**, 4388 (1999).
95. Y.-Q. Tu, G.-S. Huang, and Y.-X. Ma, *Phytochemistry* **32**, 458 (1993).
96. M. J. Begley, L. Crombie, R. A. Fleming, and D. A. Whiting, *J. Chem. Soc., Perkin Trans. I* **3**, 535 (1986).
97. Y. Takaishi, K. Ujita, H. Noguchi, K. Nakano, T. Tomimatsu, S. Kadota, K. Tsubono, and T. Kikuchi, *Chem. Pharm. Bull.* **35**, 3534 (1987).
98. S. M. Kupchan and R. M. Smith, *J. Org. Chem.* **42**, 115 (1977).
99. J.-K. Liu, Z.-J. Jia, D.-G. Wu, J. Zhou, and Q.-G. Wang, *Phytochemistry* **29**, 2503 (1990).
100. L.-J. Kai, H.-X. Wen, J.-Z. Jian, J. Yong, and W.-H. Qin, *Phytochemistry* **30**, 3437 (1991).
101. H. Itokawa, O. Shirota, K. Ichitsuka, H. Morita, and K. Takeya, *J. Nat. Prod.* **56**, 1479 (1993).
102. H. Itokawa, O. Shirota, H. Morita, K. Takeya, and Y. Iitaka, *J. Nat. Prod.* **57**, 460 (1994).
103. R. M. Smith, in "The Alkaloids" (R. H. F. Manske, ed.), vol. 16, pp. 213. Academic Press, London, 1977.
104. S.-J. Jeong, T. Miyamoto, M. Inagaki, Y.-C. Kim, and R. Higuchi, *J. Nat. Prod.* **63**, 673 (2000).
105. J. Koyama, T. Okatani, T. Ogura, K. Tagahara, and H. Irie, *Chem. Pharm. Bull.* **39**, 481 (1991).
106. T. Okatani, J. Koyama, K. Tagahara, and Y. Suzuta, *Heterocycles* **26**, 595 (1987).
107. A. Van Der Gen, L. M. Van Der Linde, and J. G. Witteveen, *Recl. Trav. Chim. Pays-Bas.* **91**, 1433 (1972).
108. T.-J. Hsieh, F.-R. Chang, Y.-C. Chia, C.-Y. Chen, H.-F. Chiu, and Y.-C. Wu, *J. Nat. Prod.* **64**, 616 (2001).
109. H.-J. Lee and G. R. Waller, *Phytochemistry* **11**, 2233 (1972).
110. I. A. Southwell and D. J. Tucker, *Phytochemistry* **33**, 857 (1993).
111. P. S. Wharton, Y. C. Poon, and H. C. Kluender, *J. Org. Chem.* **38**, 735 (1973).
112. W. T. Swingle, H. L. Haller, E. H. Siegler, and M. C. Swingle, *Science* **93**, 60 (1941).
113. M. Beroza and G. T. Bottger, *J. Econom. Entomol.* **47**, 188 (1954).
114. M. Beroza, *J. Am. Chem. Soc.* **75**, 44 (1953).
115. M. Beroza, *J. Am. Chem. Soc.* **75**, 2136 (1953).
116. M. Beroza, *J. Am. Chem. Soc.* **74**, 1585 (1952).
117. S.-F. Chiu and Y.-T. Qiu, *J. Appl. Entomol.* **116**, 479 (1993).
118. F. Delle-Monache, G. B. M. Bettolo, and E. A. Bernays, *Z. Angew. Entomol.* **97**, 406 (1984).
119. I. Kubo and J. A. Klocke, in "ACS Sympos. Ser." vol. 296, pp. 206. American Chemical Society, Washington, 1986.
120. K. Ujita, Y. Takaishi, A. Iida, and T. Fujita, *Phytochemistry* **31**, 1289 (1992).
121. M. Jacobson, in "Insecticides from Plants. A Review of the Literature, 1941-1953", Agricultural Handbook No 154, USDA, p. 44, U.S. Government Printing Office, Washington, DC, 1958.
122. N. Wakabayashi, W. J. Wu, R. M. Waters, R. E. Redfern, G. D. Mills Jr., A. B. DeMilo, W. R. Lusby, and D. Andrzejewski, *J. Nat. Prod.* **51**, 537 (1988).



123. A. G. Gonzalez, I. A. Jimenez, A. G. Ravelo, J. Coll, J. A. Gonzalez, and J. Lloria, *Biochem. Syst. Ecol.* **25**, 513 (1997).
124. O. Muñoz, A. Peñaloza, A. G. González, A. G. Ravelo, A. Crespo, I. L. Bazzochi, N. L. Alvarenga, in "Series Studies in Natural Products" (A. Atta-Ur-Rahman, ed.), vol. 18, p. 739, Elsevier Science, Amsterdam, 1996.
125. A. G. González, B. M. Tincusi, I. L. Bazzocchi, H. Tokuda, H. Nishino, T. Konoshima, I. A. Jiménez, and A. G. Ravelo, *Bioorg. Med. Chem.* **8**, 1773 (2000).
126. S. J. Foote, J. K. Thompson, A. F. Cowman, and D. J. Kemp, *Cell* **57**, 921 (1989).
127. M. J. Chiquero, J. M. Pérez-Victoria, F. O'Valle, J. M. Gonzalez-Ros, R. del Moral, J. A. Ferragut, S. Castanys, and F. Gamarro, *Biochem. Pharmacol.* **55**, 131 (1998).
128. R. F. Thorne, *Bot. Rev.* **58**, 225 (1992).
129. A. Cronquist, in "An Integrated System of Classification of Flowering Plants", pp. 713. Columbia University Press, New York, 1981.
130. N. Robson, *Bot. Soc. Brot.* **39**, 5 (1965).
131. A. C. Spivey, M. Weston, and S. Woodhead, *Chem. Soc. Rev.* **31**, 43 (2002).
132. T. Okatani, J. Koyama, K. Tagahara, Y. Suzuta, and H. Irie, *Heterocycles* **26**, 925 (1987).

## CHEMICAL AND BIOLOGICAL ASPECTS OF MELANIN\*

D.P. CHAKRABORTY AND SHYAMALI ROY

*Institute of Natural Products, Calcutta 700 036, India*

- I. Introduction
  - II. Biogenesis of Melanin
  - III. Natural Melanins
  - IV. Investigations of Melanins by Physical Methods
  - V. Synthetic Melanins
  - VI. Physicochemical Properties and Biological Functions of Melanins
- References

### I. Introduction

Melanins, the natural cosmetics of skin, hair, and feathers, represent broadly a group of natural and synthetic pigments of diverse origin and chemical functions. In nature, they usually occur in the form of insoluble fine granules accumulated in certain parts of animal and plant tissues. The term melanin ( $\mu\epsilon\lambda\alpha S$  = black) is, however, misleading and confusing since not all pigments of biological origin are black. For example, the pheomelanins, which vary from red to brown, or even yellow, are biologically related to the black eumelanins.

Some related synthetic melanins are also known. These are named after the compounds from which they were prepared via chemical and enzymatic oxidation, such as tyrosine-melanin, dopa-melanin, catechol-melanin, etc.

---

\*This chapter is dedicated to the Late Professor D. P. Chakraborty, deceased July 24, 2000.

Melanins have been a subject of interest for a long time. The fact that skin pigmentation was a natural phenomenon, led researchers to be involved in finding the nature and origin of these natural cosmetics. Earlier, it was believed that the color of black skin was due to insoluble granular pigments derived from bile (1). LeCat (2) compared the black pigment obtained from a black Ethiopian cadaver with that of the choroid of the eye and the ink of the squid and found that they were similar to each other and had similar general features. It was a stimulating result obtained in the early part of melanin research. Later, similar pigments were also found from hair, melanomas, and other mammalian tissues, including *substantia nigra* of the brain. However, these comparative studies were confined to animals, since the studies of plant melanins were either neglected or overlooked (3). On the other hand, the high degree of insolubility of melanins in almost all solvents, as well as lack of experimental methods, led the workers to converge on biological and physiological studies of skin pigmentation. One major development in melanin research, as a result of these studies, was the recognition and demonstration that melanin formation takes place in highly specialized cells, named melanocytes (4) subsequently.

The term melanin, according to Thomson (5), appears to have been used first with some precision in 1902 by Fürth and Schneider (6) with respect to the black precipitate they obtained *in vitro*, by the action of insect tyrosinase on tyrosine. The fact that the general properties and the carbon, hydrogen, and nitrogen analyses of these materials were in approximate agreement with those reported for natural pigments obtained from hair, melanomas, *sepia* black, etc. implied that these natural pigments were also formed by tyrosinase oxidation of tyrosine and related compounds. This is now generally accepted, and the term melanin is here restricted to those pigments which are described as highly complex nitrogenous polymers of high molecular weight and which are produced by a series of oxidation reactions involving tyrosinase, oxygen, and an organic substrate, either tyrosine or a related compound. The naturally occurring melanins are often conjugated with protein, and their resistance to either chemical or enzymatic digestion provides an image of inert materials (7).

The pigmentation of human skin has substantial protective, social, and cosmetic significance. Although melanins lack well-defined physical and spectral characteristics, they possess some effective chemical properties by acting as redox polymers, ion exchangers, and radical scavengers. The extensive studies of these chemical reactivities of melanin and putative melanin precursors have led researchers to infiltrate into many areas of scientific research, including the molecular biology of pigment-related genes (8–10). International meetings, conferences, and seminars have been held to bring together physicists, chemists, biochemists, geneticists, cytologists, anthropologists, and clinicians for discussion on melanin pigmentation and its chemical, biological, and applied significance, to control epidermal melanogenesis, and its application to human diseases like melanoma (tumor in melanin-producing melanocytes), vitiligo, albinism, etc.

A number of reviews covering the many aspects of melanin are available (5,11–16). Nicolaus in his voluminous classic book has given an excellent, comprehensive, and detailed account of these pigments (17). In the present article, an attempt has been made to give an account of the chemical and biological aspects of melanin in condensed form.

## II. Biogenesis of Melanin

### A. MELANOCYTES

Epidermal melanin synthesis is a multistage process involving fast or slow reactions, some enzyme catalyzed, others requiring only oxygen. The process is controlled by the pH, temperature, redox potential, and activity of enzyme, and the presence of inhibitors. The overall reaction occurs in a genetically controlled, biochemical environment in specialized cells, called melanocytes. These are complex structures, mainly made up of protein and various oxidase systems, including tyrosinase (18). Melanocytes contain unique organelles, called premelanosomes, and melanosomes in which the biosynthesis of melanin occurs (19,20).

In “premelanosome,” the enzyme molecules (i.e., protyrosinases) are arranged in an ordered pattern. The biosynthesis begins when the protyrosinases become active (i.e., tyrosinases); then the unit is called “melanosome.” As melanin accumulates in the cytoplasm, melanosome gradually transforms into uniformly dense and structureless particles, “the melanin granule,” in which no tyrosinase activity is detectable (19). In fact, a reciprocal relationship exists between the melanization process and tyrosinase activity in melanosomes, i.e., melanin granules. Electron microscope studies support this melanosome theory and, using various modern techniques, studies on melanin, melanin granules, and melanoma, revealing informative results, have been reported. Thus, according to some authors melanin granules or melanosomes have a composite structure made up of a colorless protein matrix on which melanin is deposited (21–24), while others support the mitochondrial origin of melanin granules, as appears from mixed particle studies and a common affinity for Janus green (25,26).

Morphologically, melanocytes and melanin granules from various sources, are very similar. It has been observed that premelanin granules originate in the Golgi area from the concentration of minute particles (50–100 Å) producing a nidus for the formation of a melanin granules (27). The electron micrographs of melanin granules from various human and animal sources have revealed that these particles exist as elongated rods ( $0.1 \times 0.4 \mu$  to  $0.18 \times 0.6 \mu$ ) or as spheres (0.2–2  $\mu$  in diameter) (28). According to Hu *et al.* (29), a definite correlation exists between the size and morphology of the melanocytes of human skin and their pigment-forming activities. Biologically active membrane structures exist in melanocytes which differ biochemically and morphologically from tumor microsomes and which may participate in the biosynthesis of specialized cell proteins (30,31).

Pituitary hormones have an important role in melanin biosynthesis. It has been observed that an appropriate hormone stimulates the stem cells (i.e., melanoblasts), which then divide giving rise to melanocytes (32,33). According to Tchen *et al.* (34) the primary effect of these hormones is not at the genetic level, but at the cytoplasmic level.  $\alpha$ MSH (intermedin) possesses the greatest ability in this respect (35). The hormone prolactin can stimulate tyrosinase activity and is able to supply available substrate for *in vivo* melanin synthesis (36).

Melatonin, on the other hand, reverses the darkening action of MSH, ACTH, and caffeine on frog skin (37,38). The synthetic peptide histidylphenyl-alanylarginyl-5-methoxy-tryptamine also possesses this activity to some extent (39). Colchicine, a well-known inhibitor of mitosis, does not inhibit the action of tyrosinase, but has some effect on ACTH-induced melanocyte formation (40).

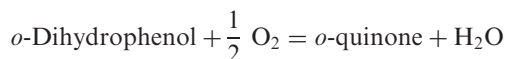
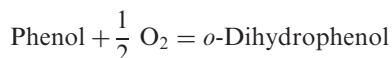
The chemical composition of melanosoma and mitochondria have been determined and compared by Seiji *et al.* (41), using differential and density-gradient techniques. The data show that melanosomal fractions contain a high percentage of zinc and a low content of RNA and phospholipid-P, as compared with mitochondrial fractions. The high percentage of zinc exhibits its important role in the decarboxylative rearrangement of dopachrome (42,43). The low content of RNA indicates the occurrence of very limited protein biosynthesis in melanosoma. The lack of succinoxidase and glutamate oxidase activities supports the evidence that melanosomes are subcellular particles, different from mitochondria and contain a particular specialized metabolic pathway through which tyrosine or dopa is converted into melanin (44).

## B. THE CHARACTERISTICS OF THE ENZYME

The enzymes which catalyze the oxidation of polyphenols are known as polyphenol oxidases and are widespread in the animal kingdom (45). They are also abundant in some species of mushrooms. Animal melanomas are rich in tyrosinase, an enzyme capable of transforming tyrosine into dopa, and then dopa into dopaquinone at the initial stages of melanin synthesis. Studies on *in vitro* melanogenesis using mushroom polyphenol oxidase have been considered as valid for mammalian melanogenesis, although the enzymes isolated from different sources show qualitative differences, e.g., the mammalian tyrosinase is more specific for L-dopa and L-tyrosine and does not significantly oxidize catechol (46,47). The methods of extraction and purification of the enzyme from mushrooms (48), *Neurospora crassa* (49), and hamster melanoma (50) have been reported.

Tyrosinase is a copper-protein complex (45,51), and copper is essential for normal pigmentation in mammals (3). Moreover, the similarity of the absorption spectrum of holoenzyme with that of apoenzyme reveals the univalent state of the metal, as found in other copper-protein complexes (52,53). The oxidation of monohydroxy phenols to *o*-quinones by molecular oxygen in the presence of a copper-secondary amine complex is known (53,54). The "cresolase activity" (i.e.,

hydroxylation of monohydroxy phenol) and the “catecholase activity” (i.e., oxidation of an *o*-diphenol) by the enzyme tyrosinase can be represented by the following equations.



Both reactions require oxygen. According to Mason, during the *o*-hydroxylation process an intermediate complex is formed involving one molecule of oxygen and two neighboring cuprous atoms attached to a protein chain. The formation of such a structure depends on the relative position of the copper atoms, hence the “cresolase activity” would be sensitive to any variation in the configuration of the protein chain (55). The *o*-quinones formed by “catecholase activity” from the substrate tyrosine are extremely reactive, and undergo intermolecular reactions to form indole derivatives, which subsequently polymerize to melanin.

An induction period is often marked in the tyrosine–tyrosinase reaction before oxidation initiation (3,56). This time lag can be shortened by the addition of a catalytic amount of dopa or related compounds (57,58), and there is no time lag when the substrate is dopa (59). This occurs because tyrosinase is only active toward tyrosine in the reduced (i.e., cuprous) state. When the enzyme is in the oxidized form (i.e., cupric), it immediately effects the oxidation of dopa, but remains inert toward tyrosine until activated by a catalyst (i.e., dopa, catechol, etc.) (52,60). In mammalian melanogenesis, the induction period is prolonged due to the low concentration of tyrosinase in epidermal melanocytes. On incubation of sections of human skin in separate solutions containing dopa, tyrosine, and related *o*-dihydroxy phenyl compounds, Bloch (61) observed that only dopa was oxidized to melanin. He concluded that melanoblasts in human skin contained a specific enzyme which he named “dopa oxidase.” Later, Fitzpatrick *et al.* (62) in 1950, established the presence of tyrosinase in human epidermis.

Many substances inhibit tyrosinase activity (3,63); notably, thiol compounds found in human epidermis, which combine with copper, are mainly responsible for the inactivation of tyrosinase in normal unpigmented skin (64,65). Flesh (65) and other workers (66) have shown that the concentration of thiol groups in the human epidermis can be reduced on exposure to ultraviolet radiation when thiol groups oxidize, releasing copper, and thus formation of dopa catalyzes the tyrosine–tyrosinase reaction. Tyrosine can be converted into dopa under similar conditions e.g., the formation of melanin during sun tanning. The tyrosinase system in human epidermal melanocytes is normally inhibited unless activated by radiation, whereas in the melanocytes of pigmented human hair it is active (67); this accounts for the coexistence of black hair and white skin.

Dopa at high concentrations inhibits the hydroxylation reaction and ascorbate increases this inhibition. Tyrosine acts as substrate inhibitor at above  $8 \times 10^{-4}$  M, which can be reversed by increasing the concentration of dopa from a catalytic amount to  $8 \times 10^{-4}$  M (57,68). Copper-chelating agents (69), and cyanide and benzoic acid (70) inhibit tyrosinase activity. The pH optimum for the enzyme is 6–7.

### C. MELANOGENESIS AND MELANIN FORMATION FROM TYROSINE

The enzymatic nature of the melanin-producing reaction was first observed by Bourquelot and Bertrand (71,72) in 1895, when they recognized an enzyme in certain fungi capable of transforming tyrosine into a black product. It was named tyrosinase. Later, a similar enzyme was also found in other plants and from tissues of various invertebrates and vertebrates, including mammals (73). Since then, melanin and melanogenesis are of obvious interest and consequently have been subjected to intensive study with substantial progress made by different laboratories.

The pioneering work of Raper (74) on the *in vitro* enzymatic oxidation of tyrosine revealed that melanin formation occurs in three stages:

- (a) oxidation of tyrosine to give a red pigment
- (b) decolorization of the red pigment
- (c) oxidation of the colorless substance to give melanin

Raper used an enzyme obtained from meal worms. He concluded that the enzyme was essential only for the first stage, i.e., the conversion of tyrosine to dopa and then dopa to dopaquinone. The latter stages occurred spontaneously without enzyme (75,76). The importance of temperature and pH control, the purity of the enzyme and hence its activity, the amount of substrate present, and the influence of certain heavy metals in the reaction rate were also recognized by Raper (77). The percentage of nitrogen (8.4%) in the melanin formed was found to be slightly higher than in tyrosine, indicating that no deamination occurs during this enzymatic reaction (78).

Using dilute acid, Raper precipitated the enzyme from the reaction mixture and removed it by filtration. The resulting red solution at pH 6 was allowed to decolorize by standing in vacuum or simply by adding a small amount of sulfurous acid. Raper identified the following compounds in the solution: some unchanged tyrosine (1), 3, 4-dihydroxy-phenylalanine or dopa (2), 5,6-dihydroxyindole (7), and 5,6-dihydroxyindole-2-carboxylic acid (6). The compounds 6 and 7 were isolated as dimethyl ethers. Later, Pittelle *et al.* (79) isolated 7 by extracting with ether a solution of pH 6.8, obtained by enzymatic oxidation of dopa.

On exposure to air, especially in alkaline solution, the compound 7 rapidly darkened and deposited a black precipitate. The identification of these indole derivatives led Raper to formulate the red compound (dopachrome) as 2,3-dihydroindole-5,6-quinone-2-carboxylic acid (5), and the preceding steps as shown in Fig. 1.

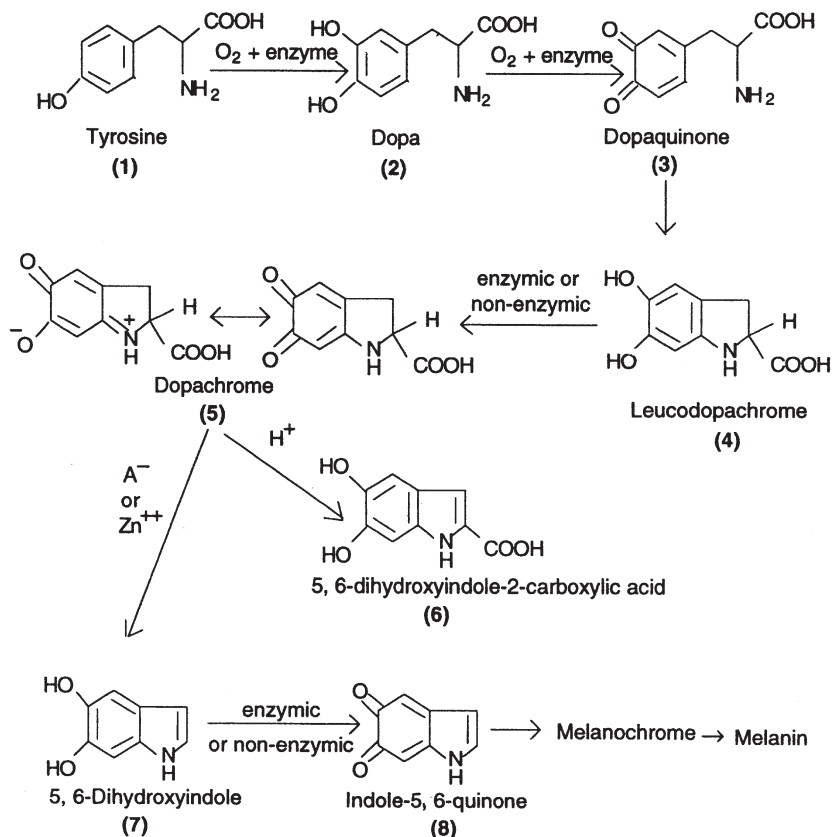


Figure 1. The Raper–Mason scheme of melanogenesis.

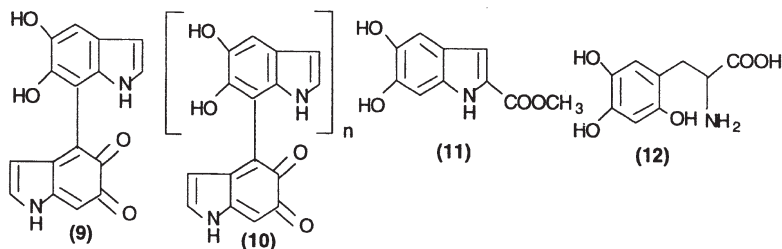
The formation of dopachrome (5) from dopaquinone (3) is normally a quinone–amine addition reaction, but the next base-catalyzed rearrangement of dopachrome (5), which is accompanied by decarboxylation except under acid conditions (80), is an important step in melanin synthesis. Zn ions catalyze this decarboxylative rearrangement, the base catalysis of which is a special feature of such *o*-quinoid structures (42,43). The corresponding *p*-quinones are stable to base (81). It is noteworthy that the choroid of the vertebrate eye, which is heavily melanized, contains a remarkably high concentration of zinc (82).

Mason studied the (80) enzymatic oxidation of dopa spectrophotometrically and characterized three chromophoric phases:

- (a) with absorption maxima at 305 and 475 m $\mu$
- (b) with absorption maxima at 300 and 540 m $\mu$
- (c) general absorption



The first phase (a) was considered to correspond to Raper's dopachrome (red) and the third phase was considered to correspond to black melanin. Oxidizing 5,6-dihydroxyindole with mushroom polyphenol oxidase at pH 6.8, Mason obtained a purple colored pigment having a broad absorption maxima at 540 m $\mu$ , which he considered was due to the compound **8**. However, Beer *et al.* (83) pointed out that this light absorption of the purple pigment was not due to indole-5,6-diquinone (**8**), but to a small polymer, similar to that of indolylbenzoquinone derived from **8**. Later Bu'Lock *et al.* (84) confirmed that during oxidation of 5,6-dihydroxyindole, an intermediate (purple color) representing a dimeric stage similar to **9** was first formed having an absorption maxima at 530 m $\mu$ . The following stages have broad absorption maxima around 540 m $\mu$  and were believed to be oligomers **10** occurring between the dimer and the melanin polymer.



Nicolaus *et al.* (85) have shown that the polymeric fractions which have a strong absorption at 522 m $\mu$  are formed by the chemical oxidation of **11** and that the properties of these fractions agree with those of oligomers **10**.

Another unknown compound, not easily reducible, giving a positive ninhydrin test was detected by Lissitzky *et al.* (86) in the oxidation reaction of tyrosine and mushroom oxidase. The tentative structure **12** was assigned. The formation of such compound by the hydroxylation of *o*-quinone at position 6 is not uncommon in biological metabolism (87,88).

Paper chromatography has been used to detect the probable intermediates during oxidation of L-dopa by polyphenol oxidase, and three compounds **5**, **6**, and **7** have been identified. An unidentified product which exhibits a weak yellow fluorescence (385 m $\mu$ ) is also observed (89).

Dulière and Raper (90) measured the oxygen uptake during the enzymatic oxidation of tyrosine and dopa to melanin. Mason and Wright (91) observed that in the conversion of dopa into dopachrome the oxygen uptake was too fast and that there was no evolution of CO<sub>2</sub> in this phase, while in the subsequent phases oxygen uptake diminished and CO<sub>2</sub> was evolved. On the basis of Raper's work and the spectrophotometric analysis of different phases of melanogenesis, Mason (92) concluded that melanins are homopolymers arising by the oxidation of tyrosine with the consumption of five atoms of oxygen and the evolution of one molecule of

carbon dioxide from the carboxyl group of tyrosine. Later, Nicolaus *et al.* (93) suggested that melanins are rather a "poikilopolymer" derived by the random coupling of various intermediary metabolites in the Raper pathway.

Swan *et al.* and other authors (94,95) suggested that the evolution of  $\text{CO}_2$  could result from ring-fission caused by  $\text{H}_2\text{O}_2$ . Fattorusso *et al.* (96) concluded from their experiments that in the process of melanogenesis, 5,6-dihydroxyindole is oxidized with  $\text{H}_2\text{O}_2$  formation.

Evidence for  $\text{H}_2\text{O}_2$  formation also comes from chemical studies on the synthetic and natural pigments (93). Figure 2 shows the oxidation process of 5,6-dihydroxyindole (5) in which a free-radical mechanism cannot be ruled out.

Although, according to Raper (97), tyrosinase and polyphenol oxidase act only on tyrosine and dopa and not on other amino acids, incorporation of different

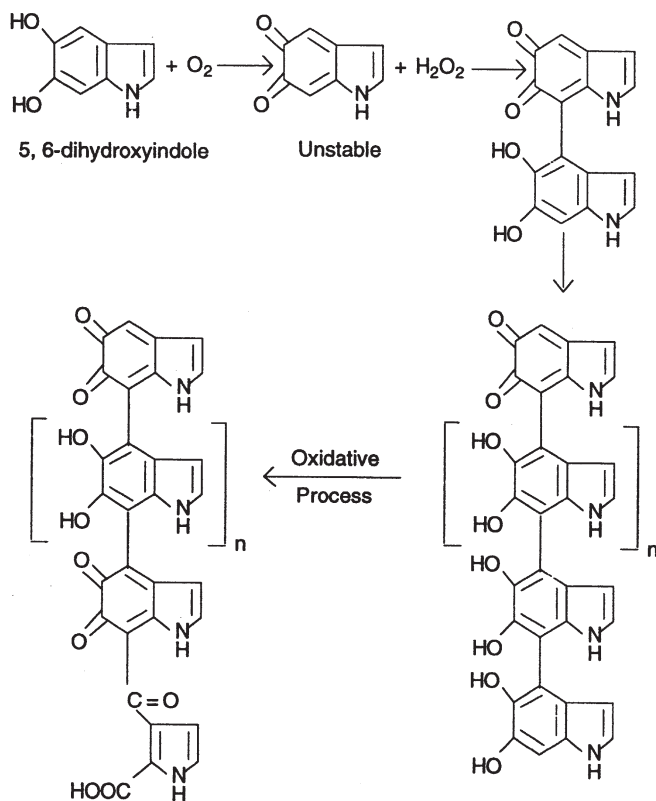


Figure 2. Polymerization of 5,6-dihydroxyindole.

precursors into melanin has been established using labeled compounds during *in vitro* melanin synthesis. Thus, it has been found that in one sample of dopa-melanin, 23.5% of the melanin units are of the dopachrome and uncyclized units (98), while another sample contains 13% of uncyclized dopa or dopaquinone (99). According to Chen *et al.* (100), copolymerization of intermediates (including tyrosine and dopa without decarboxylation) during the melanization process may be due to the different degrees of attraction between the intermediates resulting from their structural similarity and polarity.

Copolymerization can also occur in *in vivo* melanin synthesis. Melanoma-melanin has been found to contain dopaquinone, 5,6-indolequinone, and 5,6-indolequinone-2-carboxylic acid in the ratio of 3:2:1 (101).

### III. Natural Melanins

At the end of the nineteenth century, with the isolation of the enzyme tyrosinase from *Russula nigricans* (71,72), it became apparent that most of the pigment found in animals originates in processes catalyzed by this enzyme (102). It was also noticed that some pigment granules possess optical properties such as diffraction, light absorption, scattering, and interference, by which they can enhance further the beauty of the natural colors, e.g., blue eyes in animals, the fascinating color in the feather of birds, etc. (103).

Presently, melanin pigmentation is mainly determined by two, chemically distinct, but biologically related, types of pigments. One of them is the dark insoluble eumelanins, produced from the tyrosinase-catalyzed oxidation of tyrosine, and the other is the alkali soluble phaeomelanins, originating from the eumelanin pathway through the intervention of cysteine. There exist, however, certain hybrid pigments in the epidermal tissues that possess structural features, as well as chemical and physical properties, of both the eu- and phaeomelanins (8,104).

Although melanins are widespread in the animal kingdom (17), only a few have been isolated and chemically characterized. A short discussion on the chemical and biosynthetic studies of some natural melanins is given here in two parts: (A) eumelanins and (B) phaeomelanins.

#### A. EUMELANINS

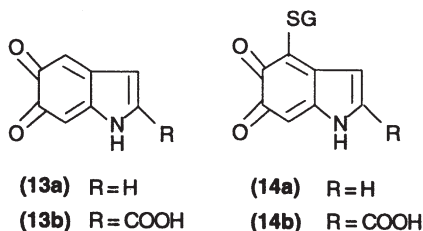
Eumelanins, obtained from hair, skin, and malignant tumors have been intensively studied by geneticists and cytologists, while the chemistry of eumelanins present in the ink sac of the cuttlefish *Sepia officinalis* has been investigated to a greater extent due to the ease of isolation and collection of the pigment. A commercial preparation of this pigment is now available (8).

### 1. Sepiomelanin

*a. Tracer Studies on Melanin Synthesis.* Nicolaus and his collaborators, using labeled precursors, studied melanin formation in cuttlefish (105). The slow incorporation of radioactive precursors indicated that the relatively large amount of the pigment formation in cuttlefish was the result of a long period of storage. The amount of radioactivity incorporated after the injection of L-tyrosine-carboxyl- $^{14}\text{C}$  was about one-tenth of that incorporated when L-tyrosine- $^{14}\text{C}$  (U) was injected. Thus a considerable part of the tyrosine carboxylic group is eliminated during the melanization process. Tracer experiments were also carried out with labeled tyramine, L-phenylalanine, histidine, etc. Tryptophan was tested both in the presence and absence of enzyme and a very low level of radioactivity [about 1/40 of that obtained when L-tyrosine- $^{14}\text{C}$  (U) was injected] was found in the pigment of the ink sac gland. These results imply that, besides the main units derived from tyrosine, other units, especially aromatic amino acids, if present in the cell during melanogenesis, can be incorporated into sepiomelanin.

*b. Protein Content.* Epidermal eumelanins are often associated with a protein forming sepiomelanoprotein complex which is homogeneous on electrophoresis. From the amount of amino acids (18 in number) removed by hydrolysis (boiling native melanin with 30% HCl), it has been calculated that the protein constitutes about 10% of the weight of melanoprotein (106). After hydrolysis, sepiomelanin contains about 0.2% sulfur. This sulfur forms part of a cysteine residue, as can be shown by oxidizing sepiomelanin with peracetic acid; cysteic acid and taurine are formed (106). However, the same result would also be in keeping with the incorporation of glutathione (GSH) into the growing pigment polymer (107). Thus, conjugation of protein could occur by addition of a cysteine residue to the pigment polymer forming the sulfur-linked melanoprotein.

The position of the sulfur bond is not known. Model studies have shown that GSH reacts with enzymatically generated 5,6-indolequinone **13a** and its 2-carboxy analog **13b** to give the C-4-linked adducts **14a** and **14b**, respectively (108).



An alternative mode of conjugation of the protein residue could be through a peptide linkage. Using the model peptide tyrosylglycine and mushroom oxidase, Bu'Lock *et al.* (109) found a red solution having an absorption spectrum identical

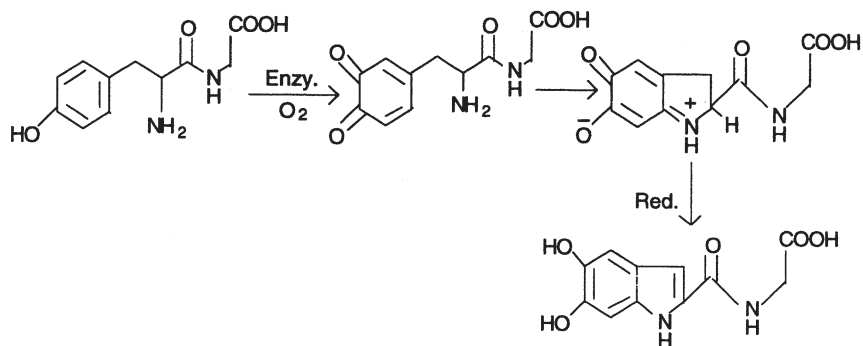


Figure 3. Tyrosinase-catalyzed oxidation of tyrosinylglycine.

to that of the dopachrome-like chromophore. On keeping in nitrogen, the red solution decolorized forming apparently, a dihydroxyindole peptide (Fig. 3), which could presumably be oxidized to the quinone, followed by copolymerization with 5,6-indolequinone derived from free tyrosine.

*c. Isolation and Analysis.* According to M. Thomas (110) "no melanin, whether a naturally occurring pigment or produced *in vitro* by the action of tyrosinase or by chemical means, has yet been isolated as a single chemical compound of definite composition." The main difficulty, apart from the generally intractable nature of the material, lies in separating the pigment from concomitant protein and other impurities, such as metal ions, and the hydrated state of the sample. Thus variations have been noticed in the analytical values of eumelanins from different sources.

The procedure for the extraction of eumelanins from natural sources involves destruction or removal of all components of the tissue by prolonged digestion with conc. HCl at room temperature or by boiling with 6 M HCl (12,17), the latter being more drastic. In 1980, Benathan and Wyler (111) developed a mild process comprising the mechanical separation of the pigment granules, followed by a short treatment with 0.5 N HCl at room temperature and extensive sonication in deionized water. Likewise, melanosomes from melanoma tissues have been purified by sucrose density gradient ultracentrifugation after digestion with detergents or proteolytic enzymes at neutral pH (8). Whether these mild processes can remove the associated proteins and other impurities from pigment granules is not clear, but this is undoubtedly a minor drawback compared with the alternative drastic acid treatment.

Nicolaus *et al.* (112) using the drastic method, prepared a highly purified sepiomelanin containing C, 64.08; H, 3.0; N, 8.52; and S, 0.2%. However, repeated analyses of the same pigment are often significantly divergent. Considering all these limitations, the use of the molar ratio of carbon to nitrogen (C/N) of the pigment is preferred for characterization purposes (113). As a rule, C/N ratios lower than 8.1 (corresponding to that of a 5,6-dihydroxyindole) are indicative of acid

degradation of the pigment backbone with loss of  $\text{CO}_2$ , while higher values suggest the presence of associated protein, and/or of C-9 units, such as 5,6-dihydroxyindole-2-carboxylic acid.

*d. Carboxylic and Phenolic Functions.* Sepiomelanin contains less carbon and nitrogen, but more hydrogen and oxygen, than does the theoretical 5,6-indolequinone polymer. This discrepancy can partly be explained by the presence of carboxyl groups in melanin which have been determined by titration, by decarboxylation, and by esterification (114). The difference between the methoxyl values from sepiomelanin treated with methanolic HCl (60%) and that treated with diazomethane (18.8%) clearly gave a content of phenolic hydroxyl groups of 13.1%. Similar results have been obtained with other pigments investigated (114a).

The ratio of carboxylic and phenolic groups in native melanin has been found to be 1.1, which was reduced to 0.8 after the removal of the protein content with acid (111,115). Significant differences are also noticed between enzymatic (0.5) and autooxidative (1.7) dopamelanin, the latter possessing the highest proportion of carboxylic groups. This result is in accordance with the isotopic and degradative studies by Swan *et al.* (114a). According to them, during *in vitro* melanogenesis,  $\text{H}_2\text{O}_2$  is generated, which attacks the 5,6-indolequinone moieties giving rise to carboxylate pyrrolic units (Fig. 4). The same mechanism also seems to be operative *in vivo* (106).

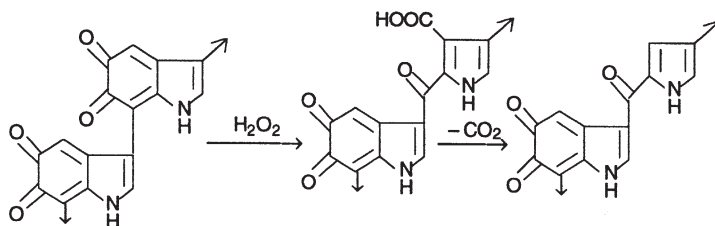
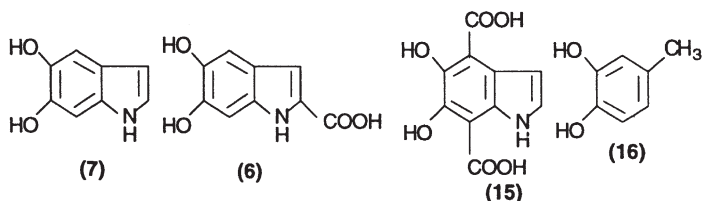


Figure 4. Proposed model of peroxidative cleavage of 5,6-dihydroxyindole units in the eumelanin polymer.

Recently, it was found that the carboxyl content increases with oxygenation time from 4.8 (4 h) to 8.9% (24 h) when dopamelanin is synthesized by autooxidation at neutral pH (116).

*e. Chemical Degradation.* The chemical degradation of sepiomelanins was extensively studied by Nicolaus and coworkers (106,117). Although the yields of the products obtained in most experiments were very low and identified only by paper chromatography, they appear to have some structural meaning. Thus the four compounds **7**, **6**, **15**, and **16** identified among the series of products obtained by the alkali fusion of sepiomelanin, suggests the presence of an indole

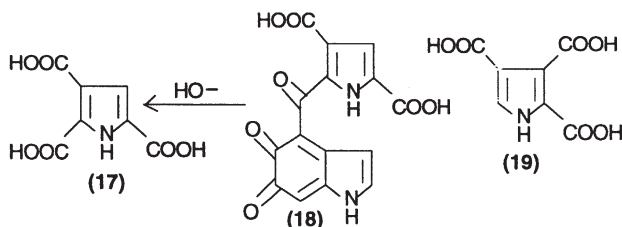
“moiety” in the pigment, and that some of the units are linked through the positions 4 and 7 as indicated by the formation of 5,6-dihydroxyindole-4,7-dicarboxylic acid (**15**).



The carboxyl group of **6** is present as such in the pigment polymer, while 4-methyl catechol (**16**), which does not arise by alkali fusion of synthetic 5,6-dihydroxyindolemelanin, is ascribed to the presence of dopachrome unit in the natural pigment (*117*).

When sepiomelanin was boiled with 4% aqueous NaOH solution, pyrrole-2,3,5-tricarboxylic acid (**17**) (1%) was obtained, presumably arising from hydrolysis of the terminal carboxylated pyrrole units **18** linked through a carbonyl to positions 4 or 7 of the 5,6-indolequinone units (*118*).

The compound **17**, along with other minor products, such as pyrrole-2,3,4-tricarboxylic acid (**19**), 2,3-pyrroledicarboxylic acid (**20**), and pyrrole 2,3,4,5-tetracarboxylic acid (**21**), were obtained when sepiomelanin was oxidized with  $\text{KMnO}_4$  (*119*). Quite interestingly, the yield of the dicarboxylic acid increased, and that of tricarboxylic acid decreased, when decarboxylated sepiomelanin was oxidized with  $\text{KMnO}_4$ . Moreover, two further acids 2,4-pyrroledicarboxylic acid (**22**) and 2,5-pyrroledicarboxylic acid (**23**) were also obtained in the degradation products (*117*) (Fig. 5). Formation of these acids can be explained by the presence of carboxylated pyrrole units in the pigment polymer.



The interpretation of these results was confirmed by the data obtained from the chromatographic separation of the degradation products of sepiomelanin ether (*106*).

Benathan and Wyler (*111*) found that oxidation of eumelanins with periodate in the presence of a catalytic amount of  $\text{KMnO}_4$ , results in oxalic and oxamic acids and, trace amounts of some pyrrolic acids. Five of them were

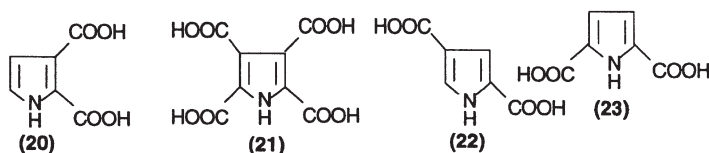
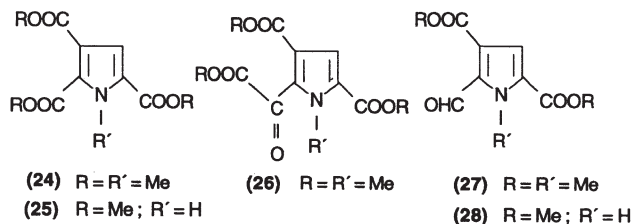


Figure 5.  $\text{KMnO}_4$ -oxidation products of sepiomelanin.

identified by GC-MS as the methylated derivatives **24**, **25**, **26**, **27**, and **28** after treatment with diazomethane.



*f. Biosynthetic Studies.* The previous discussions on eumelanins, reveal that these natural pigments are highly complex macromolecules, or a mixture of macromolecules composed of heterogeneous units. Their intractable nature has rendered their isolation in a pure state difficult, leading to uncertainty in their chemical composition. Conventional methods used to determine the chemical and physical properties of a complex polymer are not applicable to these pigments. On the other hand, since the biosynthetic precursors are known, the extensive studies of biomimetic reactions under biologically relevant conditions can successfully be used to understand the chemistry of melanin involving the chemical reactivity of the putative pigment precursors, identification of the intermediates, the formation of melanins, and their properties. This biomimetic approach was first exploited with remarkable success by Raper (74). Later, with more advanced techniques, biosynthetic studies of eumelanin polymers revealed many aspects of the diversity of pigment origin, the heterogeneity of its structure, and its unique properties.

In the Raper scheme of melanin biosynthesis (74,78), tyrosine via dopa is enzymatically converted to dopaquinone. The next subsequent oxidation steps leading to melanin formation depend on the biochemical environment of the reaction site. However, in the melanization process *in vivo* or *in vitro*, there are two crucial turning points: (i) the rearrangement of dopachrome and regulatory factors, and (ii) the oxidative polymerization of 5,6-dihydroxyindoles – which have been discussed here.

(i) Two possible mechanisms were suggested for the oxidative conversion of dopachrome (**5**) to 5,6-dihydroxyindole (DHI) (**7**) (Fig. 6) (120). The first (path-a) involves, decarboxylation giving indolenine **29a**, followed by tautomerization to **7**. Alternatively, (path-b), a hydrogen shift from position 3 could give



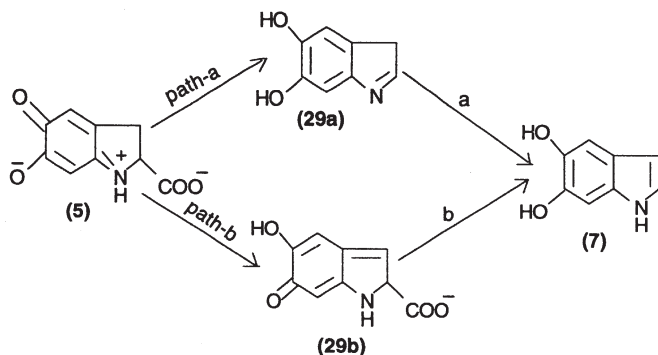


Figure 6. Alternative mechanisms for the rearrangement of dopachrome (5) to DHI (7).

a quinone-methide **29b**, which would then undergo decarboxylation to **7**. The latter mechanism was supported by different authors (*121,122*).

In a confirmatory study (*123*), the rate constants for the rearrangement of [2-<sup>2</sup>H<sub>2</sub>]- and [3,3-<sup>2</sup>H<sub>2</sub>]-dopachrome were measured and found to be 0.055 and 0.0073 min<sup>-1</sup>, respectively. The primary isotope effect ( $k_H/k_D = 8.2$ ) observed for [3,3-<sup>2</sup>H<sub>2</sub>]-dopachrome, indicates the base-catalyzed removal of H-3 is the first step of the reaction. Further analysis of the analytical data from various laboratories (*58,123,124*) has shown that the yield of DHI versus DHICA (5,6-dihydroxyindole-2-carboxylic acid) is about 95 to 5, at a pH range from 3 to 8.5. This finding indicates that tyrosinase-catalyzed synthetic dopamelanin is made up mainly of DHI-derived units, as held by Mason (*14*). Hence, the carboxyl content of dopamelanins must be due to peroxidative cleavage of indole units rather than to a random incorporation of carboxylated biosynthetic intermediates.

Evidence suggests that some steps in the melanization process are directed by regulatory factors, and certain metal ions, especially copper, zinc, iron, cobalt, etc. have long been known to participate in melanin biosynthesis (*8,125*). Bu'Lock and Harley-Mason (*126*) first reported that in the presence of zinc acetate, dopachrome rearranges very rapidly to give DHI. This reaction has been ascribed (*127*) to the ability of the metal ion to catalyze two sequential reactions, i.e., the rearrangement of dopachrome and the subsequent oxidation of the resulting indole(s). However, the zinc acetate used in these experiments was far from being biomimetic. In fact, under rigorously anaerobic conditions, the zinc-catalyzed reaction gives mainly DHICA rather than DHI (Fig. 7). Copper and iron were found to be more effective than zinc, in catalyzing the non-decarboxylating rearrangement of dopachrome (*128*).

Recent studies (*129*) have revealed the presence in melanocytes of a melanosomal protein different from tyrosinase, which has the ability to catalyze the rearrangement of dopachrome to DHICA. This enzymatic reaction is highly

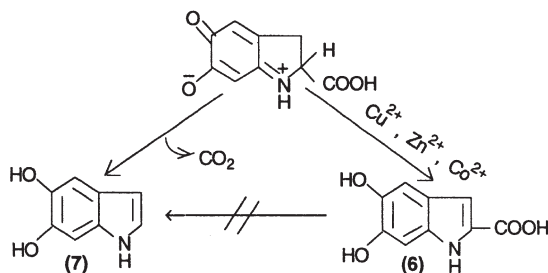


Figure 7. Effect of metal ions on the rearrangement of dopachrome.

stereospecific for normal L-dopachrome, unaffected by metal chelators and has an optimal pH of about 6.8. Different names have been proposed for this enzyme, i.e., dopachrome conversion factor (129), dopachrome oxido reductase (130), dopachrome isomerase (131), and dopachrome tautomerase (132). It is of interest that another enzyme, named dopaquinoneimine conversion factor, has the remarkable ability to catalyze the decarboxylative rearrangement of dopachrome to DHI rather than DHICA (122).

According to Pawelek *et al.* (133), the biosynthesis of melanin in Cloudman melanoma cells is a complex process and is regulated by three factors: (a) a dopamine conversion factor which converts dopamine to 5,6-dihydroxyindole (7), (b) a 5,6-dihydroxyindole conversion factor which catalyzes the conversion of 5,6-dihydroxyindole to melanin, and is active when the cells are exposed to melanotropin (MSH), and (c) a 5,6-dihydroxyindole blocking factor which restricts melanogenesis at the 5,6-dihydroxyindole stage. They have also shown that at least three steps in the Raper–Mason hypothesis of melanin formation from tyrosine are catalyzed by tyrosinase.

Using the Udenfriend system ( $\text{Fe}^{2+}$ /ascorbic acid/EDTA/ $\text{O}_2$ ), a biomimetic study on tryptophan participation in melanogenesis by Chakraborty *et al.* (134) revealed that *in vitro* melanin formation is a complex process requiring the regulation of various participating reactions (monooxygenases/dioxygenases/deamination). Their results may have relevance to Pawelek's regulating factors for *in vivo* melanin formation.

(ii) (a) Polymerization of 5,6-dihydroxyindole (DHI): During the enzymatic oxidation of DHI, Mason (80) in 1948, observed the appearance of a transient purple pigment with a broad absorption maxima at 540–560 nm, known as melanochrome. Bu'Lock and Harley-Mason (109) through model experiments with simple quinones and indoles (Fig. 8), obtained blue indolylquinones (30), indicating the involvement of the 3-position of the indole ring.

In further studies, by Cromartic *et al.* (135), as well as Beer *et al.* (83), found that 1-, 2-, 4-, and 7-methyl-5,6-dihydroxyindoles on oxidation gave melanin

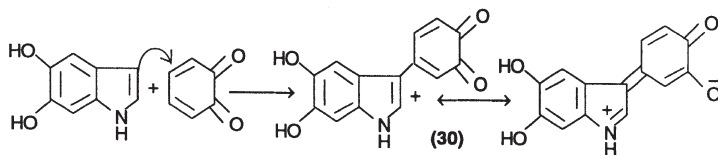
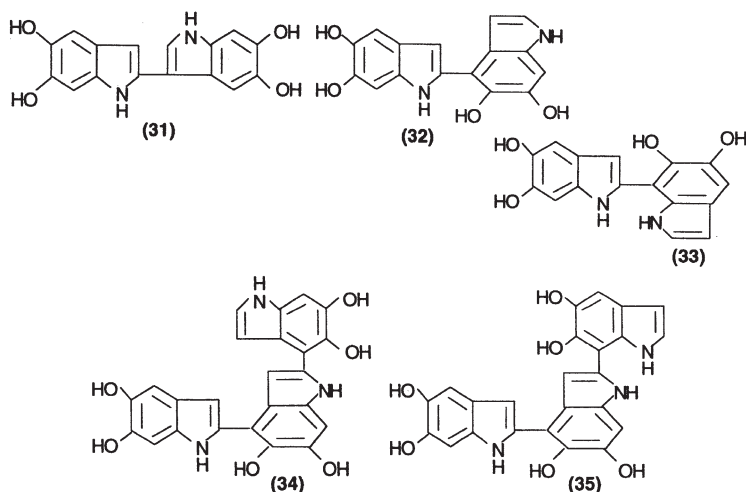


Figure 8. Michael addition of 5,6-dihydroxyindole to 1,2-benzoquinone.

polymers insoluble in the common organic solvents, but slightly soluble in pyridine. On the other hand, 3-methyl- and 4,7-dimethyl-5,6-dihydroxyindole gave a polymer soluble in ethanol. These results demonstrated that for the formation of melanin, it was essential to have a free 3-position.

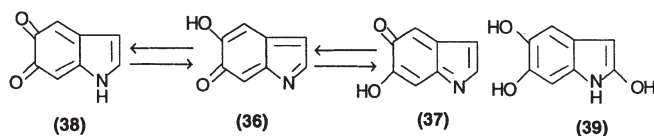
In a reexamination of the problem, Napolitano *et al.* (136) prepared melanochrome by autooxidation of DHI in presence of Zn ions acting as a catalyst. On reduction and subsequent acetylation, the blue melanochrome thus formed afforded a mixture of oligomers of DHI in which a symmetrical dimer **31**, formed by the coupling of DHI at the 2-position predominated.

In further studies (137), the oxidation of DHI was done under the usual enzymatic conditions of melanogenesis *in vitro*, and another dimer identified as a 2,4-biindolyl (**32**) was obtained from the oxidation mixture. Using oxidative enzyme peroxidase, which is far more effective than tyrosinase, in the polymerization of DHI (138), three more new oligomers were isolated, besides **32** by preparative HPLC. They were identified as the 2,7-dimer **33** and the related trimers **34** and **35**.

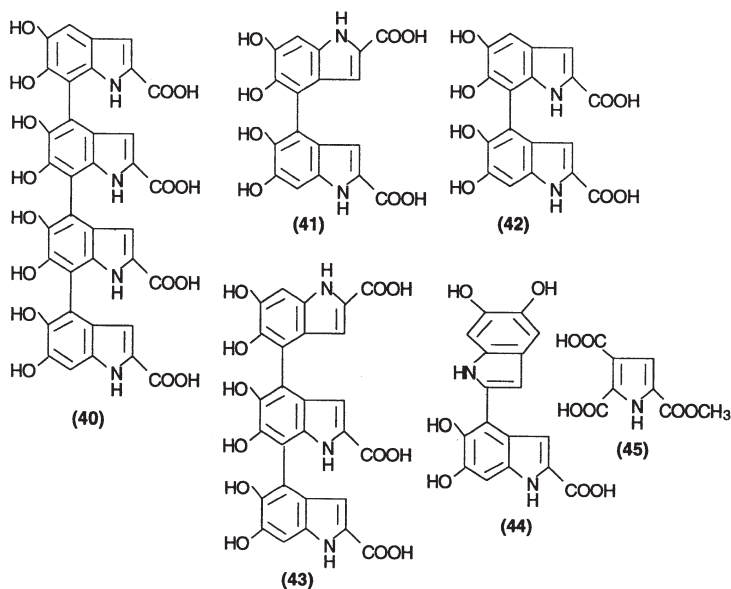


Overall consideration of the structure of the oligomers, identified so far, reveals that the dominant mode of coupling of DHI is via the 2- and 4-positions of the indole ring, with a minor contribution from the 7-position.

The mechanism of the polymerization reaction has not yet been characterized; the reaction is too fast to identify the reactive intermediates. Using fast reaction techniques to study short-lived reactive intermediates, Al-kazwini *et al.* (139) compared the kinetics and spectral data of the 430 nm species with those of the oxidation products of the model compounds, 6-hydroxy-5-methoxyindole and 5-hydroxy-6-methoxyindole. It was inferred that the dominant species in DHI oxidation is the quinone methide **36** which is in equilibrium with the quinoneimine **37** and the corresponding quinone **38**. Lambert *et al.* (140) found that the decay of the 430 nm species was halved when the oxidation was performed in D<sub>2</sub>O rather than in H<sub>2</sub>O. This suggested the intermediacy of a trihydroxy-indole **39** arising by the nucleophilic addition of water to **36**.



(b) Polymerization of 5,6-dihydroxyindole-2-carboxylic acid (DHICA): Cromartic and Harley-Mason (135) first suggested that the polymerization of DHICA must involve both the 4- and 7-positions of indole ring. Ito and Nicol (141) obtained a tetramer **40** from the *Tapetum lucidum* of the catfish that was considered to arise biogenetically via tyrosinase-catalyzed oxidation of DHICA. When this reaction was performed *in vitro*, three oligomers were isolated (142) as the acetyl methylester derivatives, and identified as the symmetrical dimer **41**, the 4,7-dimer **42**, and the trimer **43**. As in the case of DHI, the kinetics of the reaction was slow.



The peroxidase-catalyzed oxidation of DHICA in the presence of DHI was also studied (143) in order to understand whether, and to what extent, copolymerization of the two melanogenic precursors can occur under biologically relevant conditions. Analysis of the oxidation mixture revealed that it consisted mainly of DHI and DHICA oligomers, but one mixed dimer **44**, arising presumably by the trapping of 5,6-indolequinone-2-carboxylic acid by the nucleophilic 2-position of DHI, was isolated in 5% yield. Isolation of **44** provides the first evidence of the cross-coupling of DHI and DHICA, and supports the concept of eumelanin as being a mixture of macromolecules composed of homopolymers of DHI and DHICA and copolymers of two different indole units. The relative proportion of the homo- and copolymers depends on the ratio of formation of DHI and DHICA from the rearrangement of dopachrome.

## 2. Melanoma-Melanin

Nicolaus and coworkers (144) studied chemically treated rat melanoma-melanin similarly as they investigated sepiomelanin chemically. Different experimental results reveal that the melanins differ in the chromophoric system of their structures, though it is believed that they may have the same precursors, i.e., dopa.

Purification of rat melanoma-melanin involved treatment with 6N hydrochloric acid. Permanganate oxidation of the pigment yielded pyrrole-2,3-dicarboxylic acid (**20**), 2,3,5-pyrrole-tricarboxylic acid (**17**), 2,3,4,5-pyrrole tetracarboxylic acid (**21**), and pyrrole-2,4 (**22**) and pyrrole-2,5-dicarboxylic acids (**23**). The latter two carboxylic acids were obtainable from sepiomelanin only after the pigment was decarboxylated. Alkali fusion of melanoma-melanin gave 5,6-dihydroxyindole (**7**) and 5,6-dihydroxyindole-2-carboxylic acid (**6**).

Melanoma-melanin, after treatment with diazomethane followed by oxidation with  $\text{KMnO}_4$ , yielded 5-carbomethoxy pyrrole-2,3-dicarboxylic acid (**45**) (see earlier), as in the case of sepiomelanin (119). The formation of **45** indicates the presence of some indole units with carboxyl groups at position 2 in the structure of melanoma-melanin. In addition, the trimethyl amine found among the oxidation products, reveals the existence of an uncyclized amino acid side chain in the chromophoric system. Methylated sepiomelanin does not give trimethylamine on oxidation.

Hampel (101) in his experiments injected mice, bearing Harding-Passey melanomas, with dopa labeled in various positions. He observed that all of the positions in dopa were involved to a greater or lesser extent in the polymerization process, thus supporting the work of Nicolaus (117,118) that melanins are heterogeneous polymers with heterogeneous bonds. Hampel concluded that melanoma-melanin is a copolymer of dopaquinone, 5,6-indolequinone, and 5,6-indolequinone-2-carboxylic acid in a ratio of 3:2:1. This formula of melanin as a pure 5,6-indolequinone polymer contradicts the Raper-Mason hypothesis and

needs more confirmation. Moreover, the amino group of some melanins was determined by Bloch and Schaaf (145), and only one-tenth of the nitrogen of melanoma-melanin was found to be in the amino group, while sepiomelanin has no amino group in its chromophore.

Dopa has been identified as a tyrosinase cofactor in melanoma (146). Blois *et al.* (147) found that the administration of DL-3,4-dihydroxy phenylalanine-2-<sup>14</sup>C to mice with melanomas results in an appreciable uptake of radioactivity into the tumor. Hampel (101), by injecting mice with tritiated dopa, concluded that dopa is the specific precursor of the tumor melanin. According to Greenstein *et al.* (148) in the melanoprotein of mouse melanoma, the protein is conjugated to the pigment through sulfur bonds.

### 3. Hair-Melanin

The hair bulb can produce both eu- and phaeomelanins. Melanin from human hair, obtained in the form of a black powder by treatment with boiling 6 N HCl, when subjected to KMnO<sub>4</sub> oxidation or alkali fusion yielded the same products as rat melanoma-melanin produced on similar treatment (144). The behavior of methylated hair-melanin, on oxidation, was also similar to that of melanoma-melanin. The disease phenylketonuria, in which the patient has light-colored hair due to an incapacity of conversion of phenylalanine to tyrosine, provides evidence that tyrosine is essential in the pigmentation process (144).

### 4. Choroid-Melanin

Melanin from the eye was first studied by Berzelius (149) in 1840 and it was found to be insoluble in acids, but slightly soluble in alkali. The color of human eyes and those of animals is produced by the scattering of white light by melanin granules, the size of which control the color (17). Melanin can form complexes with heavy metals which change the shade and intensity of the color (82,150). Nicolaus *et al.* (144) found that ox-choroid melanin when oxidized, yielded pyrrole-2,3-dicarboxylic acid (20), 2,3,5-pyrroleticarboxylic acid (17), and 2,3,4,5-pyrroletetracarboxylic acid (21). On alkali fusion it gave 5,6-dihydroxyindole (7) and 5,6-dihydroxyindole-2-carboxylic acid (6).

### 5. Feather-Melanin

The black feathers of many birds are due to the presence of eumelanins, while phaeomelanins give the red color in feathers. On the other hand, the combination of eumelanins and phaeomelanins, in the presence or absence of accessory pigments acting as a screen, can produce all of the spectacular color patterns in feathers (103).

Some genes inhibit the formation of melanin in the skin without influencing the pigmentation of the plumage. Thus the white silky fowl, with a pure white plumage and a purplish-black skin, is an example of the genetic control of

melanogenesis (9,10). Oxidation or fusion with alkali of bird eumelanins yielded the same products as did melanin from hair or melanoma (144).

#### 6. *Melano-sclerotins*

Sclerotins are peculiar proteins responsible for hardening of the insect cuticle. It has been suggested that the cuticular darkening due to sclerotization involves cross-linking copolymerization of proteins and enzyme-generated quinones, probably derived from tyrosine during melanogenesis (151). Diphenols related to tyrosine, e.g., dopa, etc. have been found in the cuticle of insects. However, it is not clear if the hardening process and melanin formation are due to the same quinones (152). On the other hand, pigments of certain insects are "indole" in nature and yield on  $\text{KMnO}_4$  oxidation, 2,3,5-pyrroletri-carboxylic acid (17) as one of the degradation products, while 5,6-dihydroxyindole (7) and 5,6-dihydroxyindole-2-carboxylic acid (6) are obtained on alkali fusion (153).

### B. PHAEOMELANINS

Phaeomelanins are responsible for the brown, red, and yellow color pigmentation of mammalian hair and bird feathers. Unlike the eumelanins, which are widely distributed throughout various tissues in the animal kingdom, true phaeomelanins are restricted to the epidermal tissues, such as skin and hair and are often associated with biologically related trichochromes (104). Phaeomelanins also differ from eumelanins in their solubility in dilute alkali. Fox and Uppdegraff (154) first isolated the pigment in crude form and a tentative formula  $\text{C}_{41}\text{H}_{72}\text{N}_{12}\text{O}_{25}\text{S}_2$  was given. Later the pigment was found to be a mixture of peptides derived from glycine and three novel amino acids, adeno-chromine-A, -B, and -C which form chelates with Fe (III) (155).

The chemistry of the phaeomelanins, as known so far, has come from studies of the pigments obtained from the feathers of New Hampshire chickens (*Gallus gallus*). Earlier, acid treatment was used for the isolation of the pigments from red hair and feathers, and only minor products such as trichochromes were obtained. Later, Nicolaus and coworkers (156) developed an alkaline extraction procedure. The feathers of New Hampshire hens were treated with 0.1 N NaOH at room temperature. The extract was acidified and a red-brown, amorphous precipitate was isolated from the yellow-orange supernatant. The precipitate was dialyzed, subjected to chromatography on Sephadex or Biogel P columns, when four gallophaeomelanin fractions 1-4 were isolated. The yellow-orange supernatant was subjected to ion-exchange chromatography, followed by chromatography on Sephadex, yielding a number of pigments. It was found that the acid-soluble pigment fractions contained trichochromes.

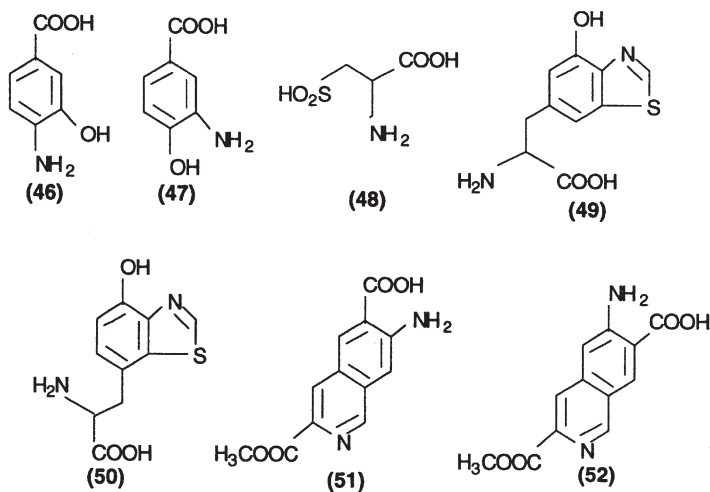
More recently, Deibel *et al.* (157) have developed another method for isolation which involves preparative isoelectric focusing on a granulated bed.

However, the gallophaeomelanins thus obtained are inhomogeneous from molecular viewpoint, each fraction consists of a mixture of polymers with similar physical and chemical characteristics.

### 1. Gallophaeomelanins

Among the four gallophaeomelanin fractions, the most abundant pigment is the protein-free gallophaeomelanin-1, with an average molecular weight of ca. 2000 and a N/S ratio of 2.1. Biogenetically, it is related to trichochromes (156–158) and is zwitterionic in character. It contains carboxyl, primary amino, and phenolic groups, though UV, IR, and NMR spectral analysis do not indicate a distinctive chromophoric system.

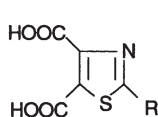
On alkali fusion, the pigment gave a mixture of simple catechols and *o*-aminophenols e.g., **46** and **47**, while H<sub>2</sub>O<sub>2</sub> oxidation gave cysteic acid (**48**) in 10% yield (156). When heated in HCl or HI, it yielded 4-amino-3-hydroxy phenylalanine (**69**), benzothiazole (**49**), and the corresponding isomers **71** and **50** (156,157). From the HI reaction products, the benzothiazole amino acid **70** and isoquinolines **51** and **52** were isolated as dimethylethers (159).



On KMnO<sub>4</sub> oxidation, the pigment gave, in addition to various thiazolic and pyridine acids e.g., **53**, **54**, **55**, **56**, **57**, and **58**, a larger fragment, identified as the polyacid **59** (160–162). Isolation of **59** suggested the presence of a chromophoric system like **60** in the pigment polymer, containing tetrahydroisoquinoline, benzothiazole, and possibly 1,4-benzothiazine units substituted at the 3-position. Other phaeomelanin fractions (2–4) studied (163) gave a similar pattern of degradation products, indicating that they have the same general



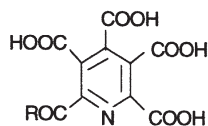
structure, but differ in molecular size and sequence of various structural units in the polymer chain.



(53) R = H

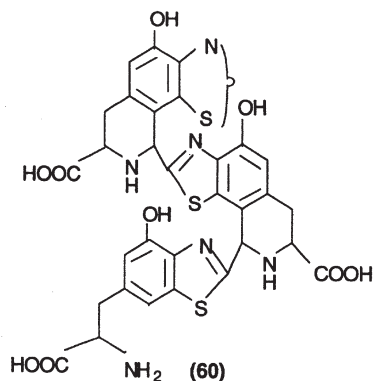
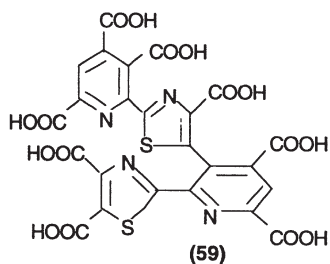
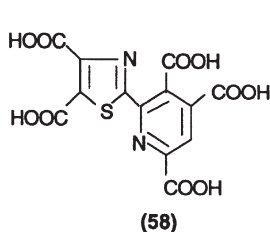
(54) R = COOH

(55) R = CONH<sub>2</sub>



(56) R = OH

(57) R = NH<sub>2</sub>



Although the presence of 1,4-benzothiazine units in the gallophaeomelanins is generally accepted and is supported by biomimetic studies, the concepts of other units in the pigment polymers are questionable and require more investigation (104). The characterization of protein-containing gallophaeomelanin fractions (2-4) by isoelectric focusing and amino acid analysis, etc. have yet to reveal definite answers (164).

## 2. Trichochromes

Trichochromes are derivatives of  $\Delta^{2,2'}$ -bi-(2H-1,4-benzothiazine), which contains a double conjugated system  $-S-C=C-N-$ , not previously known in

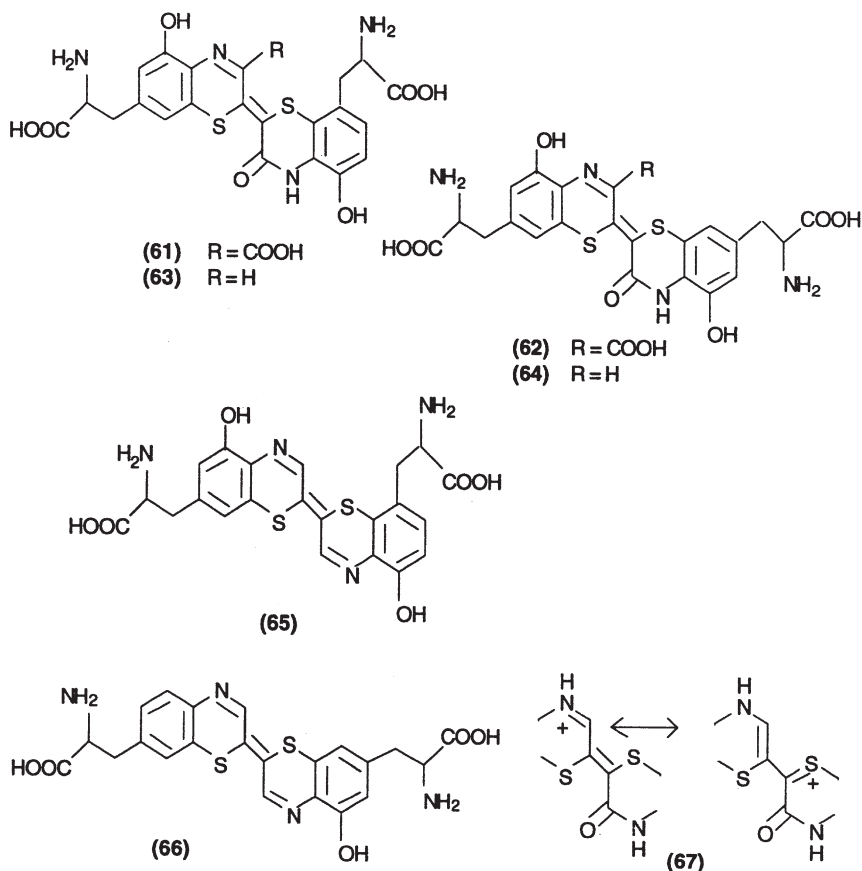
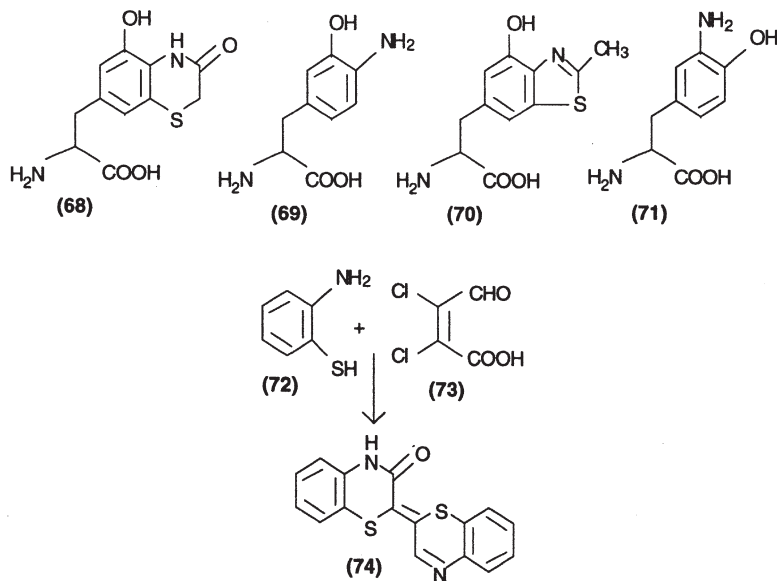


Figure 9. Structures of selected trichochromes.

natural products. The pigments so far identified from natural sources are trichochromes B (61), C (62), E (65), and F (66), shown in Fig. 9. A number of useful reviews on the trichochromes are available (104,165,166). In acid solution, trichochromes E and F produce the mesomeric cation 67.

Trichochrome C, on treatment with HI and red phosphorus, undergoes reductive cleavage of the chromophore resulting mainly in the benzothiazinone amino acid 68 and 4-amino-3-hydroxy phenylalanine (69), along with smaller amounts of the benzothiazole amino acid 70 (167). Under similar conditions, degradation of trichochrome B with HI and red phosphorus gives an isomeric mixture of 69 and 71. Thus, trichochromes B and C differ only in the position of

one alanine side chain on the  $\Delta^{2,2'}$ -benzothiazine ring system, which is fully consistent with the biosynthetic studies (168).



Kaul (169) synthesized the basic chromophore of trichochromes B and C, i.e., 74, by condensing *o*-aminothiophenol (72) with mucochloric acid (73). However, the stereochemistry of the  $\Delta^{2,2'}$ -benzothiazine skeleton in the trichochromes has not been defined.

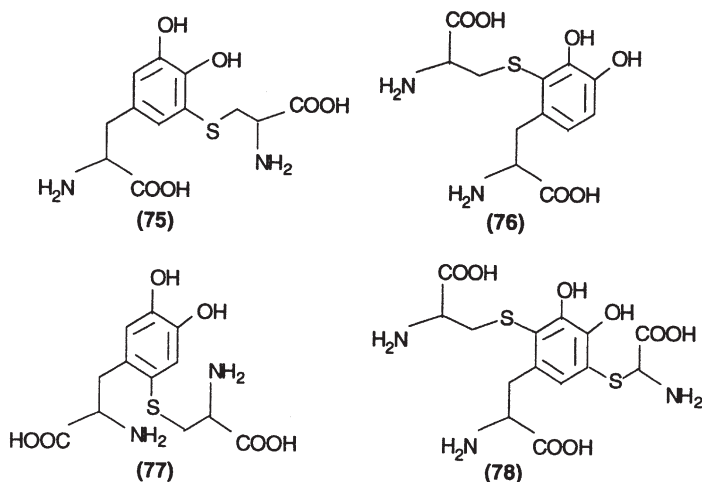
### 3. Biosynthesis of Phaeomelanins

From the discussion stated so far, it appears that the eu- and phaeomelanins and the trichochromes are biogenetically related, originating from a common precursor, i.e., tyrosine (74,78,170). The amount and type of products in the overall reaction pathways depend on the reactivity of the nascent dopaquinone as affected by the genetically controlled biochemical environment of the melanocytes (9,10). Thus, the biosynthesis of eumelanin *in vivo* or *in vitro*, involves a sequence of oxidation steps, cyclization of dopaquinone, rearrangement of dopachrome, and polymerization of 5,6-dihydroxyindole.

On the other hand, the presence of available sulfhydryl compounds, such as cysteine (171), in melanocytes involves the rapid interaction between nascent dopaquinone and these sulfur compounds, which twists the normal course of melanogenesis toward the formation of sulfur-containing pigments. In support of this mechanism is the classical observation by Cleffman (172) that in tissue culture, phaeomelanin-forming melanocytes produce only a black pigment, but revert to

phaemelanin production when sufficient GSH or cysteine is added to the nutrient medium. The reddish-brown pigment obtained in the *in vitro* experiment, on analysis showed close similarity with gallophaemelanins. When the oxidation was stopped after a short time by acidification, the pale yellow solution turned violet in a few minutes, and a small, but significant, amount of trichochromes E and F were obtained (173).

In another experiment, the formation of cystdopa was studied under biomimetic conditions (174). The reaction mixture, after chromatographic separation, gave, in addition to 2- and 5-cysdopa (75) and (76), a small amount of the 6-isomer 77, and a diadduct identified as 2,5-dicystein-*S,S*-yldopa (78) in the ratio 14:74:1:5, which is consistent with their relative contribution in the biosynthesis of the natural pigments. The identification of these intermediates also supports the intractable and heterogeneous nature of the pigment polymer.



An alternative pathway that has also been considered, involves the reaction of dopaquinone with glutathione a (GSH) followed by enzymatic hydrolysis of the corresponding adducts (Fig. 10), i.e., glutathionyldopas (GSH dopas) to cystdopas (175,176). The enzymes necessary for this transformation, i.e.,  $\gamma$ -glutamyltransferase and peptidase, are widespread in biological systems and have been detected in malignant melanoma (175,177). Moreover, both 5-cysdopas and 5-GSH dopas have been found in melanoma tissue (178).

Which of the two possible pathways is operative *in vivo* has not yet been assessed. GSH is by far the most abundant sulfhydryl compound in cells, which points to an important role of GSH dopa in the biosynthesis of cystdopas (179). According to Ito *et al.* (180), tyrosinase-catalyzed cooxidation of dopa and GSH proceeds in a similar fashion as with cysteine. On the other hand, the presence of

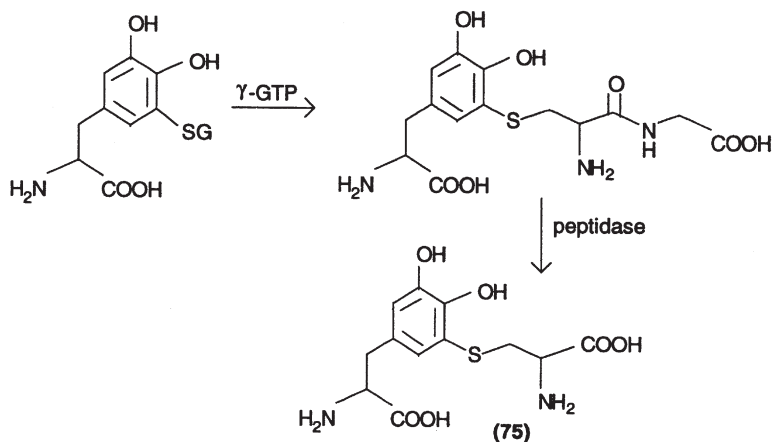


Figure 10. Enzymatic conversion of 5-glutathionyl-dopa to 5-cysdopa (75).

cysdopa and not GSH dopa in the pigmented tissues accounts for the direct addition of cysteine to dopaquinone.

Homogeneous synthetic phaeomelanins are accessible through oxidation of a single isomer, such as 5-cysdopa, under biologically relevant conditions (181). It has been suggested that the corresponding *o*-quinone **79** undergoes intramolecular cyclization of the amino group onto the carbonyl carbon to form an unstable quinoneimine **80** intermediate; this can either give rise to the dihydrobenzothiazine (**81**) by redox exchange with the starting material, or undergo rearrangement, with or without decarboxylation, to give the corresponding 1,4-2*H*-benzothiazines **82**, and **83** (Fig. 11). Which of the products predominates depends on number of parameters such as pH, oxygen tension, and the presence of metal ions (182).

After the formation of the 1,4-benzothiazines, very little is known about the fate of this intermediate in the later stages of the *in vitro* biosynthesis of phaeomelanin. Radiotracer studies (183) and model experiments (184) suggest that the reaction probably proceeds via an enamine-imine type condensation of the 1,4-benzothiazine-ring system.

Prota and coworkers (185) reexamined the enzymatic oxidation of 5-cysdopa in phosphate buffer at pH 6.8 and found rapid and almost quantitative conversion to the dihydrobenzothiazine (**81**), after which the reaction proceeded smoothly giving a discrete number of oligomeric products. Two of these were isolated and identified as two diastereoisomers with the gross structure **84**. Compound **84** is the first product obtained beyond the benzothiazine stage in the biomimetic synthesis of phaeomelanins, though its exact role in the formation of

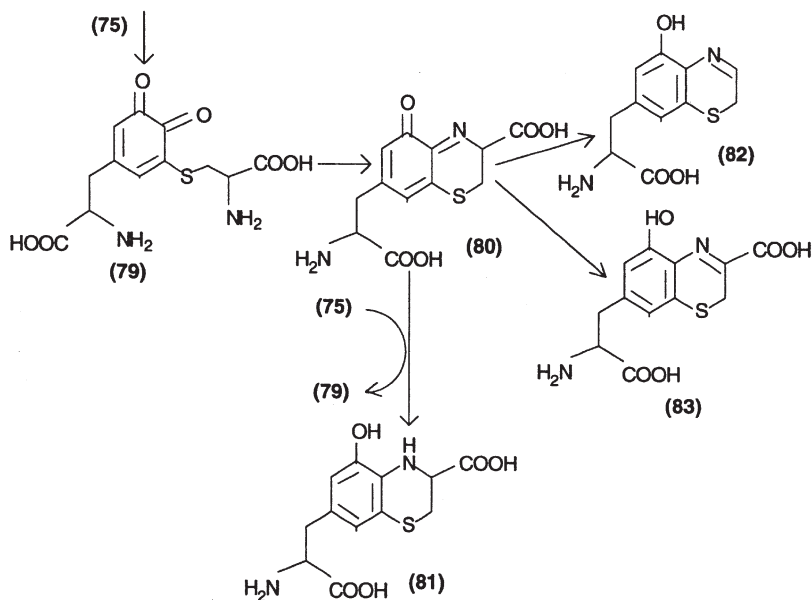
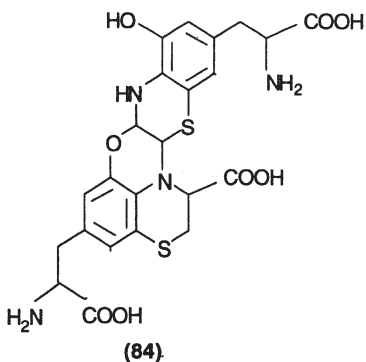


Figure 11. Oxidative conversion of 5-cysdopa to 1,4-benzothiazinylalanines.

pigment polymer is still not known. It is noteworthy, however, that **84** is unstable in acid solution and rapidly gives rise to the violet trichochrome F (**66**).



#### IV. Investigations of Melanins by Physical Methods

##### A. ULTRAVIOLET AND INFRARED SPECTROSCOPY

Melanins have been studied by UV and IR spectroscopic methods, but no significant results have been obtained in elucidating the structure of the pigment

polymer. The high insolubility of natural melanins and the scarce solubility of the synthetic one produce problems of scattered light which prevent the normal course of light absorption. In the visible range, the spectrum of melanin shows high absorption, but no definite bands. The absorption increases toward shorter wavelengths in the UV. Solid films of eumelanins show spectra even less resolved (186). According to Wolbarsht *et al.* (187), the absorbing and scattering properties of melanin particles have a light-trap role *in vitro* and their hypothesis provides a model of the overall optical properties. The proposed absorption mechanism of melanin as an amorphous semiconductor (188), with phonon coupling to an excited electronic state, helps to explain the efficient absorption of internally scattered light.

The IR spectra of melanins show absorption bands as expected in aromatic substances, but line-broadening and overlapping prevents a detailed interpretation. However, using very dilute KBr pellets, Bridelli *et al.* (189) obtained fairly good results in the fingerprint region. The protonation and deprotonation of titrable groups at different pH, thus monitoring the binding of iron to various chelating groups has been studied by this method. Moreover, a comparative study of the natural and synthetic melanins has been possible by this method (189–191).

#### B. NUCLEAR MAGNETIC RESONANCE SPECTROSCOPY

$^{13}\text{C}$ -NMR has been widely used to study the structural features of both the synthetic and natural melanins. Chedekel *et al.* (192) used this technique to investigate the conversion of labeled L-dopa and 5,6-dihydroxyindole (DHI) to melanin. The  $^{13}\text{C}$ -NMR of enzymatically produced melanin, has shown the benzylic carbon of L-dopa as the C-3 carbon in the DHI (or its carboxyl derivative) repeating unit. In the melanin produced by autooxidation, the C-3 carbon appears both as pyrrole-like and a carbonyl carbon. Eumelanins produced in a similar way from DHI show no carbonyl carrying structural units. These results suggest that the positions 4 and 7 of the indole moiety are involved in the polymerization process leading to melanin. Aime and Crippa (193) showed that the spectral features can differentiate samples according to their various sources and that different functionalities present in eumelanins can be identified.

#### C. X-RAY DIFFRACTION STUDIES

Previous X-ray diffraction studies on melanins have revealed evidence of only a short-range order in the arrangement of indole units, which are stacked upon one another to form a  $\pi$ -complex, with an average interlayer spacing of about 3.4 Å. It has been assumed that these units are members of different polymer chains or distant members of the same chain (194). Albanese and coworkers (195) reinvestigated this subject using a new diffraction technique which has an extremely high energy resolution ( $\Delta E/E \cdot 10^{13}$ ) and provides both detailed structural and dynamic information. The spectra show a broad-structured peak arising mainly from interlayer distances and a second peak due to intermolecular distances. The hydrated state of the pigment polymer affects the X-ray diffraction

curve and is responsible for the inelastic part of the spectrum. The net radical distribution function deduced from the elastic part shows the atomic distribution of the melanin structure, a typical layered structure with large anisotropics in the bonding forces. The X-ray diffraction curve for lyophilized melanosomes appears similar to that obtained for a synthetic melanin (196). A recent study with synthetic DHI-melanin indicates the presence of a pentameric structure with DHI units being linked at the 4- and 7-positions, and twisted in a helix with a  $180^\circ$  repeat at each end (197).

#### D. MOSSBAUER SPECTROSCOPY

The ion-exchange capability of various melanins allows binding of the  $^{57}\text{Fe}$  isotope, the most common probe used in Mossbauer spectroscopy. Natural sepia and bovine eye melanins, as well as synthetic D,L-dopa melanin, have been studied by this method (190,198). From the results, it has been suggested that all melanins occur in the form of very small paracrystalline particles with a broad-size range and showing a superparamagnetic behavior.

#### E. ELECTRON SPIN RESONANCE SPECTROSCOPY

Eumelanins were the first biological molecules studied by ESR spectroscopy. Commoner and coworkers (199) detected ESR signals in melanin and concluded that the paramagnetism was due to free radicals trapped in the pigment. Considerable attempts were made to correlate the free-radical properties with some alleged functions of melanins in the physiology of vision and in photoprotection (200).

##### 1. Characteristics of the ESR Spectra

Both natural and synthetic eumelanins exhibit a similar type of ESR spectrum, including a single, slightly asymmetrical signal with a linewidth of about 4–6 G and a  $g$ -value close to 2.004. The spin concentration is within the range of  $4\text{--}10 \times 10^{17}$  spins/g, and no hyperfine coupling is detected. The presence of residual protein in natural melanin does not influence the ESR lineshape or intensity. However, the effect of temperature on paramagnetism (201) influences the spin concentration and linewidth in the spectra, indicating temperature-dependent equilibria between diamagnetic groups (quinone, hydroquinone, etc.) and their paramagnetic counterparts (biradicals, semiquinone radicals, etc.).

Semiconductor models and charge-transfer complexes through the stacked monomer units of the eumelanin polymer have been proposed for these organic radicals by some authors (202,203), while most workers support Blois's interpretation that the paramagnetism is due to a small fraction of semiquinonoid units deeply trapped into the polymer (204). The concentration of melanin radicals



can be varied reversibly with experimental conditions, e.g., alkaline pH, metal complexation.

The ESR spectra of phaeomelanins are quite different, exhibiting a triplet with  $g = 2.0052$ , a value typical of immobilized radicals with hyperfine splitting due to nitrogen. Experiments were carried out with cysdopa-melanins (205) at various pH values in  $D_2O$  and in the presence of metal ions, and a comparative study of natural melanins and synthetic melanins was made. The ESR spectral analysis supports the view that natural phaeomelanins are copolymers of dopa- and cysteinyl-dopa-derived monomers (176).

## 2. Effect of Light on Free Radicals

When melanins are irradiated with UV and visible light, an increased population of free radicals is generated, which has been detected by ESR spectroscopy. A more complex ESR spectrum with a shorter  $T_1$ , a higher  $g$ -value, and a broader linewidth is produced. The transient free radicals consist of two components, one characterized by a low yield (ca. 1–2%) and a decay time of a few seconds, and the other with a decay time of a few milliseconds, that accounts for about 50% of the signal (206). Under continuous irradiation, the yield of the latter component is 50–100 times that of the former, and the photoexcitation process shows the characteristics of a singlet–triplet intersystem crossing mechanism. The presence of reducing agents, e.g., NADH, enhances the production of free radicals. Photooxidation of the pigment polymer induces the formation of superoxide anion and  $H_2O_2$  (207). During photolysis of phaeomelanins, biologically active OH and  $O_2H$  are produced in concentrations about 100 times higher than in the eumelanins (208).

## V. Synthetic Melanins

Synthetic melanins are obtained by a biomimetic-oxidation reaction using known precursors. They are named after the compounds from which they are prepared, e.g., dopa-melanin, DHI-melanin, cysdopa-melanin, etc. There are four different methods of melanin synthesis: *in vitro* enzymatic, autooxidative, electrochemical, and photochemical. Of these, the first two methods have been used, in general, for the large-scale preparation of melanins, while the latter two, i.e., electrochemical and photochemical synthesis, have most effectively been used to study the melanization process.

The exact conditions under which the oxidation occurs are extremely important, and a minor variation can change the reaction sequence and hence the structure and properties of the final product. Unfortunately, no standardized procedure for melanin preparation by any of these methods has been developed so far. Thus, the melanins obtained by these methods, although they look superficially alike, are by no means similar, as evidenced by analytical, degradative, ESCA, and NMR data (12,192,209,210).

### A. ENZYMATIC SYNTHESIS

Catecholamines and related compounds are used as starting materials for the synthesis of eumelanins and pheomelanins (112,211). The oxidation reaction is carried out at optimum pH 6–7 in the presence of mushroom tyrosinase, a metalloenzyme that carries a coupled, binuclear copper active site (73). The enzyme activity is assayed by the oxidation of tyrosine to dopaquinone at 280 nm or at 475 nm (212).

Dopa, dopamine, and tyrosine are the most common substrates used in the preparation of synthetic eumelanins. In a typical experiment, a mixture of 15 ml solution of enzyme (30 mg enzyme in 100 ml Sorensen's buffer, pH 7) and 150 mg of L-dopa (in 500 ml pH 7 buffer) is kept in air at 38 °C. Air is bubbled through the solution mixture. The melanin formed is separated by filtration, fractional sedimentation, or more efficiently, by centrifuging (500 to 100,000 g), especially after acidification (pH < 3.5) (213). The sample is further purified by repeated resuspension and centrifugation or dialysis (214).

The syntheses of pheomelanins are similarly performed by enzymatic oxidation of L-dopa or L-tyrosine in the presence of excess L-cysteine at pH 6.8. The chromatographic separation of the acid-soluble fraction on a Sephadex column yields four major reddish-brown fractions that are similar to the pheomelanins obtained from hair and feathers. 5-S-Cysteinyl-dopa has been used as a substrate in some procedures, with a catalytic amount of L-dopa in the reaction mixture. Enzymatic copolymerization of dopa and 5-S-cysteinyl-dopa (in various ratios) led to products with both eu- and pheomelanin properties (211).

### B. AUTOOXIDATIVE SYNTHESIS

In this method, melanins are obtained by air oxidation of dopa and other related substrates in alkaline medium (pH > 8). They are named after the bases used in these syntheses, such as NaOH-melanin, NH<sub>3</sub>-melanin, etc. (215,216). In a typical experiment (217), air is bubbled for 3 days through a solution of D,L-dopa (10 g) in 2 liters of deionized water adjusted with concentrated ammonia to pH 8. Melanin separates after acidification (pH 2), and is washed with 10 mM HCl and deionized water. Heavy metal ions such as Cu(II), Zn(II), or Fe(III), which are commonly found in pigmented tissues, can accelerate the formation of melanins by this method (218). Palumbo *et al.* (142) observed that autooxidation of 5,6-dihydroxyindole-2-carboxylic acid in the presence of Co(III) at slightly alkaline pH proceeds rapidly yielding a dark-brown melanin.

### C. ELECTROCHEMICAL SYNTHESIS

Electrochemical synthesis of melanin is a major outcome of melanin research since 1980. Different authors have studied this method using various

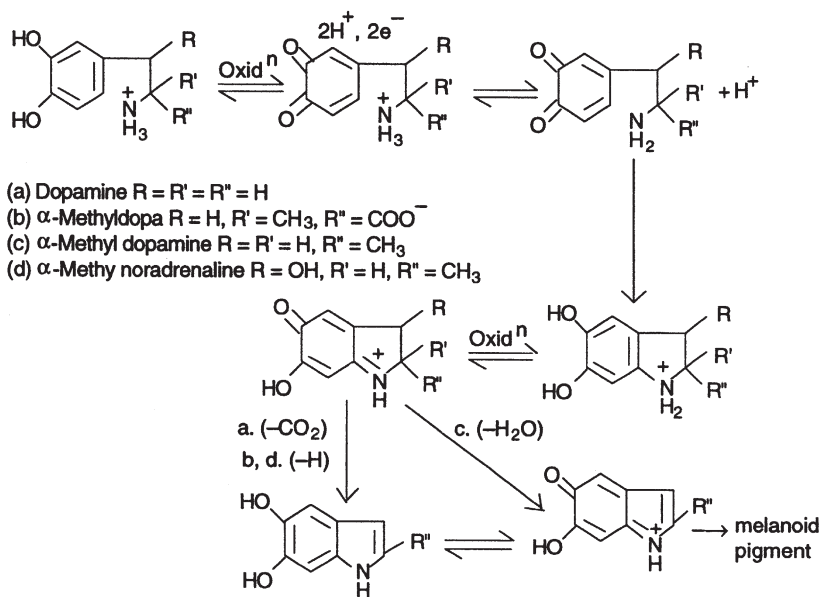


Figure 12. Electrochemical oxidation of catecholamines to melanoid pigments.

catecholamines and related compounds as substrates (219,220). These studies (219) have confirmed the validity of the Raper–Mason's scheme of melanogenesis, and also provided information regarding the mechanism of the chemical steps that occur in the early stages of the melanization process, identification of each electron-transfer process, and determination of the rate constants of the nonoxidative reactions. The oxidation reactions involved in a typical electrochemical synthesis of catecholamines are shown in Fig. 12.

Using a selective amperometric detector in combination with liquid chromatography, the pH effect on the sequence of events that occur during electrooxidation and the quantitative estimation of catecholamines, have been studied (221). Thus, the cyclic voltammogram in 1 M HClO<sub>4</sub> showed only peaks corresponding to the catechol–quinone redox couple at pH 6, since the protonation of the amino group prevents the cyclization steps. At pH 6.36, appearance of new redox couple indicates the formation of cyclic products, i.e., the respective dihydroindole derivative, in the reaction mixture. At an even higher pH (>7.68), the absence of a cathodic peak suggests the half-life of the corresponding quinone to be of the order of tens of milliseconds (219) and simultaneous darkening around the anode is considered evidence for melanin formation by electrooxidation. The overall reaction sequence in the electrochemical process, however, is very slow, involving only a few monolayers.

#### D. PHOTOCHEMICAL SYNTHESIS

Catecholamines are thermodynamically and photochemically unstable compounds. This phenomenon has been utilized in the synthesis of melanin photochemically (222,223). Thus, an oxygen-saturated dilute solution of adrenaline, isoprenaline, and noradrenaline on irradiation (254 nm) gives the corresponding aminochromes in 65, 56, and 35% yield, respectively (223). Longer irradiation produces melanins (223). Studies of the action spectrum confirmed the excited state of the catecholamine as the primary factor in the transformation processes. *N*-Substituted catecholamines have been found to react more rapidly than the corresponding *N*-unsubstituted ones (223).

Using radiolysis, Thompson *et al.* (224) found that in the presence of azide radicals, dopa and cysteinyl dopa yield the unstable semiquinones that disproportionate into a quinone–quinol complex. The quinones rapidly decay to more stable products, i.e., dopaquinones produce dopachromes, and cysteinyl-dopaquinones rearrange to benzothiazine isomers.

Photooxidation of various melanin precursors, e.g., dihydroxyindole, has been studied to understand the mechanism of the immediate pigment darkening, i.e., natural skin tanning (225). The experiments are performed both under physiological conditions (phosphate buffer, pH 7) and in organic solvents, e.g., methanol, but no definite conclusions can be drawn from the results obtained.

### VI. Physicochemical Properties and Biological Functions of Melanins

Natural melanins, although they hold an image of inert material due to their high insolubility, structural heterogeneity, and unusual spectral characteristics, possess some distinctive physicochemical properties of biological significance. For example, in biological systems, melanin can act as an electron-exchange polymer capable of protecting a tissue against redox reactions and trapping the free radicals which could disrupt the metabolism of living cells (200). Melanins thus protect the skin against the harmful UV radiations (226). Longuet-Higgins described melanin as a one-dimensional semiconductor with the protons acting as electron traps (227). In eyes, melanin acts as light screen and strongly resists light adaptation. Interestingly, unlike other alkaloids, reactions of insoluble melanins are heterogeneous in character and involve both the surface and the interior of the melanin particles. Moreover, in living systems, alkaloid molecules diffuse to receptor sites, while owing to their immobility, melanosomes are targets for molecules that diffuse toward them (12). In this section, some of the physicochemical properties and biological functions of melanin are discussed.

#### A. USE OF MELANIN FOR DEFENSE

The melanin of sepia is found in the ink sac of the cuttlefish. Aristotle, in his book “*Historia Animalia*” mentioned this pigment. According to him (Aristotle,

315 BC), "instead of intestines molluscs have an organ known as the *mytin* where a black is found which is especially abundant in cuttlefish; they put forth this black when frightened, particularly the cuttlefish" (17). The ink has considerable staining power, and is alkaline and odorless. When fresh it disperses readily in water and is partly soluble in alkali, but insoluble in acid. This biological function of melanin appears to be defensive, but the mechanism is uncertain (228).

#### B. MELANIN AS A LIGHT SCREEN IN THE EYES

The melanin granules of the eye generate a free radical when irradiated with visible light. According to Sever *et al.* the rapid generation of a free radical in light and its decay in the dark, coupled with the proximity of the melanin granules in the rods and cones of the eye, suggests that melanin plays a more important role in the visual process than the mere absorption of stray light (229).

The stimulation of a visual receptor in a vertebrate eye by an intense flash of light generates a fast electrical response, the early receptor potential (RP). A similar response in the pigment epithelium-choroid complex (PE-CC) of the eye was observed by Brown (230), which, unlike the early RP, is photostable and resistant to light adaptation. The PE-CC consists of the cell layers immediately behind the retina which are densely pigmented with melanin. Brown concluded from his experimental results that the photopigment involved in the PE-CC response was related to the visual pigments contained in myeloid bodies, which are somewhat similar to the outer segments of the visual receptors found in the PE-CC cells.

Ebrey and Cone (231) reexamined the phenomenon using isolated PE-CC layers and found that the amplitude of the major peak of the PE-CC response is proportional to the energy of the stimulus flash. They also studied the action spectrum of PE-CC response using whole-eye preparations and found that the early RP which is photolabile to continuous light, dominates the entire response recorded in the spectrum, and that the resulting action spectrum corresponds to the appropriate visual pigments. At the far end of the spectrum, the whole-eye response changes shape, and its action spectrum levels out and remains unaltered when the eye is exposed to steady light that fully bleaches the visual pigments. After bleaching, a new response is observed with a flat action spectrum which is similar to that obtained from isolated PE-CC. The authors concluded that the photopigments for these responses absorb all the wavelengths of light equally well and melanins, present in the PE-CC cells, are primarily responsible for generating at least part of the PE-CC response. This new electrical response of the PE-CC is, however, fundamentally different from the early RP which depends on visual pigments.

#### C. MELANIN AND ITS REDOX FUNCTIONS

One of the most characteristic features of melanins is their ability to exchange electrons with reducing and oxidizing agents. The processes merely involve the reversible exchange of two electrons and two protons. Thus, eumelanins

can act either as electron acceptors or electron donors revealing their existence in both the oxidized quinone and reduced quinol forms (232).

To examine the changes in the oxidation state of melanins, the ESR technique has been used extensively, while to determine the concentration changes of the reagents (oxidants, reductants), spectrophotometric or electrochemical methods were used. Owing to the presence of carboxyl and phenolic groups (acidic groups) in melanins, positively charged reagents are found to react much faster than anions or neutral species, especially in basic media. Thus the slow reaction with Nitro Blue Tetrazolium is dramatically accelerated in the presence of a cationic detergent (233). Generally, reduction of both natural and synthetic melanins results in a lighter color and changes in the ESR spectra (235). The populations and the role of semiquinone states assumed to be responsible for the characteristic ESR signal have been evaluated (234,235).

Both reduction and oxidation processes have been found to be biphasic. Thus, in kinetic studies of the reduction of synthetic D,L-dopa melanin with  $Ti^{3+}$  and oxidation with  $Fe^{3+}$ , respectively, a fast electron-exchange step was followed by a slow second step (236). The biphasic character of the electron-exchange processes was interpreted as the difference in the reaction mechanisms involving the surface and the core of the melanin granules (237).

The electron-exchange properties of melanins have been studied with a number of reagents in order to understand the electron-exchange mechanism, as well as the role of the melanin redox properties in biological systems. The processes have been found to be strongly irradiation dependent (both by visible and UV light). Thus nitroxide radicals are reversibly reduced by melanins in the dark (238), and the redox equilibria are altered on irradiation. Similarly, other processes in living systems (involving NADH, NADPH, and cytochrome) have been found to be directly linked to the redox properties of melanins (239).

Of particular significance to biological systems is the reaction of melanins with oxygen, and the effect of external factors on this reaction, e.g., pH, illumination with visible light, temperature, and catalase, has been studied in detail (240). Melanins were studied in their native, reduced, oxidized, and methylated forms, and the reaction was monitored via ESR. The rates of oxygen uptake were, generally, higher with illumination and over the pH range 5.5–11.9.

#### D. MELANIN IN THE PHOTOPROTECTION OF SKIN

Melanin can absorb electrons, as has been observed for some cation-exchange polymers, and its ion-exchange activity plays an important role in the biological system when skin is exposed to sunlight or ionizing radiation (241). Studies on this characteristic property of melanin by different authors revealed the mechanism of photoprotection and broadened our knowledge regarding melanin color.

The absorption spectra of both the eu- and phaeomelanins throughout the UV and visible range, show a monotonic increase of the absorbance with decreasing wavelength without any distinct absorption peak related to the extended conjugation of a macromolecular  $\pi$ -electron system (242). To explain this phenomenon, McGinness and Proctor (188) propose an amorphous semiconductor theory which states that melanin is black because the absorbed light is not reradiated, but is instead captured and converted to rotational and vibrational energy (photon–photon coupling). The relatively structureless spectrum of melanin means that such photon capture is available for any energy level from the UV through the visible and into the IR region. Hence melanin can be considered “black” not just in the visible region.

On the other hand, Wolbarsht *et al.* (187) suggest that melanin acts as a light trap because it is an efficient light scatterer (multiple scattering of the Rayleigh type). However, solutions of melanin, which show no evidence of scattering, exhibit a very similar absorption spectrum (243,244), and this experimental observation contradicts Wolbarsht’s suggestion. An expression for optical density (OD) derived from the amorphous semiconductor theory can be stated as follows:

$$OD_z^{1.2} = KE_0^{1.2}(Z - 1)$$

where  $Z$  equals  $1.242/\lambda E_0$  (dimensionless),  $E_0$  is the optical bandgap in eV,  $\lambda$  the vacuum wavelength in  $\mu\text{m}$ ,  $z$  a dimensionless independent variable, and  $K$  a constant. This relationship appears to hold for both eu- and phaeomelanin and can explain both the above theories.

Photoprotection is believed to be one of the major functions of melanin pigments (245), but both the localization of the pigment and its mode of action with light, seem somewhat inconsistent with the conventional suncreening functions. However, melanin can effectively protect skin from sunlight and UV radiation by a photoinduced chemical reaction, resulting in the consumption of molecular oxygen (246) or by scavenging active oxygen species (247) such as superoxide anion and  $\text{H}_2\text{O}_2$ .

In biological systems, superoxide and  $\text{H}_2\text{O}_2$  are formed in small quantities during normal processes and both species produce harmful effects in tissues. While the cell-defense mechanisms are adequate to remove these active oxygen species under normal conditions, with exposure to UV light, their concentration increases (247) and thus the function of melanin as an *in situ* quencher is important for the protection of skin. However, with continuous exposure to UV radiation, melanin itself may become energetically overloaded into a toxic state (248) augmenting the radiative damage to cells (12). There exists evidence of phaeomelanin’s role in sunlight-induced skin cancer (249).

The process of photoinduced interaction of melanin with molecular oxygen is accompanied by photobleaching (243,244,246). Using ESR measurements, the rates

of photooxidation of eu- and phaeomelanins have been studied and phaeomelanin has been found to be more resistant toward photobleaching than eumelanin (250).

#### E. BINDING, COMPLEXATION, AND MEDICINAL ASPECTS OF MELANIN

Metal cations and organic species carrying positive charge(s), possess a strong affinity to melanins, and binding occurs through an ion-exchange mechanism. This characteristic phenomenon has been studied by different authors to explain the medicinal aspects which may involve affinity and binding of various molecules to melanins in substantia nigra, in malignant melanoma cells, and in the toxicity of drugs. For example, a pathological pigmentation often occurs in the skin of the patients taking large doses of chlorpromazine (251). It has been suggested that chlorpromazine acts on the autonomic nervous system by blocking the production of pigment-lightening factors such as melatonin (252). According to some authors, white light produces free radicals from chlorpromazine and the formation of a stable charge-transfer complex with melanin is the mechanism of action for this chemical hyperpigmentation (253,254).

Studies of metal binding by both native and synthetic melanins have provided data that confirm the ion-exchange properties of melanins and reveal relative affinities of metals to melanins (255). Thus, similar to other ion exchangers, affinity for melanin increases with valency of the cation and atomic number of the element (i.e.,  $\text{Cs}^+ \gg \text{Li}^+$ ;  $\text{Ba}^{2+} \gg \text{Mg}^{2+}$ ). However, the exceedingly high affinity found for  $\text{Pb}^{2+}$  when compared with similar divalent ions suggests the possible involvement of other factors, though the proteins present in native melanins play a minor role in the binding of metals (255).

Binding studies, combined with ESR spectroscopy, have revealed the mechanism of interaction of metal ions with melanins, indicating the formation of a chelate complex between di- and trivalent diamagnetic metal ions and *o*-semiquinone radical centers (217). This interaction often results in an increase of total free-radical concentration. Further, for melanins of different origin, the binding capacity varies with the number of reactive sites (256).

The cation-exchange mechanism has also been observed in the binding of organic molecules (mostly bases and often positively charged) with melanins (257). A systematic structure–affinity study was reported for a series of heterocyclic compounds and synthetic D,L-melanin (258). Relative affinities measured from absorption in pH 7 phosphate buffer, showed that the  $\pi$ -electron system, basicity, and steric factors are the main determining factors for the affinity toward melanin. These results are consistent with the stability of the charge-transfer complexes between an organic molecule (as donor) and melanin (as acceptor). This structure–affinity relationship can be used in the application of drugs which may selectively target melanocytes (e.g., melanoma cells) or drugs with low toxicity that are not accumulated in melanin-containing tissues, such as the eyes.



## References

1. W. Montagna, G. Prota, and J. Kenney, "Black Skin", Academic Press, New York, 1993.
2. C. N. LeCat, *Traité de la Couleur de la Peau Humaine en general, decellules Negres en particulier, en de la Metamorphose d'une de ces Couleurs en Pautre, soit de Naissance, Soit accidentellement*, M.M. Rey, Amsterdam, 1765.
3. A. B. Lerner and T. B. Fitzpatrick, *Physiol. Rev.* **30**, 91 (1950).
4. R. E. Billingham and W. K. Silvers, *Q. Rev. Biol.* **35**, 1 (1960).
5. R. H. Thomson, in "Comparative Biochemistry" (M. Florkin and H. S. Mason, eds.), vol. III, Part A, pp. 727. Academic Press, New York, 1962.
6. O. V. Fürth and H. Schneider, *Beitr. Chem. Physiol. Pathol.* **1**, 229 (1902).
7. G. A. Swan, in "Pigment Cell" (V. J. McGovern and P. Russell, eds.), vol. I, pp. 151. Karger, Basel, Switzerland, 1973.
8. G. Prota, "Melanins and Melanogenesis", Academic Press, San Diego, CA, 1992.
9. V. J. Hearing and K. Tsukamoto, *FASEB J.* **5**, 2902 (1991).
10. T. Takeuchi, in "The Pigment Cell" (Y. Mishima, ed.), Munksgaard, Copenhagen, 1992.
11. G. Prota, *Fortschr., Chem. Organ. Naturst.* **64**, 93 (1995).
12. R. Crippa, V. Horak, G. Prota, P. Svornos, and L. Wolfram, in "The Alkaloids" (A. Brossi, ed.), vol. 36, pp. 253. Academic Press, San Diego, CA, 1989.
13. G. A. Swan, *Fortschr. Chem. Organ. Naturst.* **31**, 521 (1974).
14. H. S. Mason, in "Advances in Biology of Skin" (W. Montagna and F. Hu, eds.), vol. VIII, pp. 293. Pergamon Press, Oxford, 1967.
15. V. Riley, in "Pigment Cell Biology" (M. Gordon, ed.), pp. 389. Academic Press, New York, 1959.
16. I. W. Sizer, *Adv. Enzymol.* **14**, 129 (1953).
17. R. A. Nicolaus, "Melanins", Hermann, Paris, 1968.
18. H. S. Mason, *Adv. Enzymol.* **16**, 105 (1955).
19. M. Seiji, K. Shima, M. S. C. Birbeck, and T. B. Fitzpatrick, *Ann. N. Y. Acad. Sci.* **100**, 497 (1963).
20. R. R. Cardell, F. Hu, and R. S. Knighton, *Henry Ford Hosp. Med. Bull.* **12**, 273 (1964).
21. G. Laxer, J. Sikorski, C. S. Whell, and H. J. Woods, *Biochim. Biophys. Acta* **15**, 174 (1954).
22. F. H. Moyer, *Ann. N. Y. Acad. Sci.* **100**, 584 (1963).
23. Y. Mishima and A. V. Laud, *Ann. N. Y. Acad. Sci.* **100**, 607 (1963).
24. J. R. Whittaker, *Dev. Biol.* **14**, 1 (1966).
25. H. G. DuBuy, J. L. Showacre, and M. L. Hesselbach, *Ann. N. Y. Acad. Sci.* **100**, 569 (1963).
26. M. Woods, D. Burk, and J. Hunter, *Ann. N. Y. Acad. Sci.* **100**, 534 (1963).
27. S. R. Wellings and B. W. Siegel, *Ann. N. Y. Acad. Sci.* **100**, 548 (1963).
28. H. S. Mason, H. Kahler, R. C. MacCardle, and A. J. Dalton, *Proc. Soc. Exp. Biol. Med.* **66**, 421 (1947).
29. F. Hu and P. F. Lesney, *Henry Ford Hosp. Med. Bull.* **8**, 52 (1960).
30. M. Karasek and T. Hultin, *Nature* **194**, 87 (1962).
31. S. R. Wellings and B. W. Siegel, *J. Ultrastructure Res.* **3**, 147 (1959).
32. W. Chavin, K. Kim, and T. T. Tchen, *Ann. N. Y. Acad. Sci.* **100**, 678 (1963).
33. K. Kim, T. T. Tchen, and F. Hu, *Ann. N. Y. Acad. Sci.* **100**, 708 (1963).

34. T. T. Tchen, R. N. Ammeraal, K. Kim, C. M. Wilson, W. Chavin, and F. Hu, National Cancer Institute, Monograph No. **13**, 67 (1964).
35. H. B. F. Dixon, *Biochem. J.* **62**, 25 (1956).
36. B. Kosto, G. E. Pickford, and M. Foster, *Endocrinology* **65**, 869 (1959).
37. A. B. Lerner, J. D. Case, and Y. Takahashi, *J. Biol. Chem.* **235**, 1992 (1960).
38. M. R. Wright and A. B. Lerner, *Endocrinology* **66**, 599 (1960).
39. H. Yajma, K. Kawasaki, Y. Okoda, and S. Lande, *Biochim. Biophys. Acta* **107**, 141 (1965).
40. K. Kim, T. T. Tchen, and F. Hu, *Exp. Cell Res.* **25**, 454 (1961).
41. M. Seiji, T. B. Fitzpatrick, R. T. Simpson, and M. S. C. Birbeck, *Nature* **197**, 1082 (1963).
42. J. Harley-Mason and J. D. Bu'Lock, *Nature* **166**, 1036 (1950).
43. R. A. Heacock, in "Advances in Heterocyclic Chemistry" (A. R. Katritzky, ed.), vol. V, pp. 205. Academic Press, New York, 1965.
44. M. Seiji, T. B. Fitzpatrick, and M. S. C. Birbeck, *J. Invest. Dermatol.* **36**, 243 (1961).
45. D. Kertész and R. Zito, in "Oxygenases" (O. Hayaishi, ed.), pp. 307. Academic Press, New York, 1962.
46. M. Okun, L. Edelstein, N. Or, G. Hamada, and B. Donnellan, *Life Sci.* **9**, 491 (1970) Part-II.
47. D. Kertész, *J. Natl. Cancer Inst.* **14**, 1093 (1954).
48. R. M. Nelson and H. S. Mason, in "Methods in Enzymology" (H. Tabor and C. W. Tabor, eds.), vol. XVII A, pp. 626. Academic Press, New York, 1970.
49. N. H. Horowitz, M. Fling, and G. Horn, in "Methods in Enzymology" (H. Tabor and C. W. Tabor, eds.), vol. XVII, pp. 615. Academic Press, New York, 1970.
50. S. H. Pomerantz and J. P. C. Li, in "Methods in Enzymology" (H. Tabor and C. W. Tabor, eds.), vol. XVII, pp. 620. Academic Press, New York, 1970.
51. H. J. Bright, B. J. B. Wood, and L. I. Ingraham, *Ann. N. Y. Acad. Sci.* **100**, 965 (1963).
52. A. B. Lerner, *Am. J. Med.* **51**, 141 (1971) and references therein.
53. W. Brackman and E. Havinga, *Rec. Trav. Chim. Pays-Bas* **74**, 1107 (1955).
54. R. Vercauteren and I. Massart, in "Oxygenases" (O. Hayaishi, ed.), pp. 355. Academic Press, New York, 1962.
55. H. S. Mason, *Nature* **177**, 79 (1956).
56. A. B. Lerner, T. B. Fitzpatrick, E. Calkins, and W. H. Summerson, *J. Biol. Chem.* **178**, 185 (1949).
57. S. H. Pomerantz, *J. Biol. Chem.* **241**, 161 (1966).
58. V. J. Hearing, Jr., T. M. Ekel, P. M. Montague, and J. M. Nicholson, *Biochim. Biophys. Acta* **611**, 251 (1980).
59. A. Palumbo, G. Misuraca, M. d'Ischia, and G. Prota, *Biochem. J.* **228**, 647 (1985).
60. D. Kertész and R. Zito, *Biochim. Biophys. Acta* **96**, 447 (1965).
61. B. Bloch, *Zeit Physiol. Chem.* **98**, 226 (1917).
62. T. B. Fitzpatrick, S. W. Becker, A. B. Lerner, and H. Montgomery, *Science* **112**, 223 (1950).
63. Y. M. Chen and W. Chavin, in "Pigmentation, its Genesis and Biological Control" (V. Riley, ed.), pp. 593. Appleton-Century-Crofts, New York, 1972.
64. S. Rothman, H. F. Krysa, and A. M. Smiljanic, *Proc. Soc. Exp. Biol. Med.* **62**, 208 (1946).
65. P. Flesch, *Proc. Soc. Exp. Biol. Med.* **70**, 136 (1949).
66. T. B. Fitzpatrick, A. B. Lerner, E. Calkins, and W. H. Summerson, *Arch. Dermatol. Syphilis* **59**, 620 (1949).

67. A. Kukita and T. B. Fitzpatrick, *Science* **121**, 893 (1955).
68. S. H. Pomerantz, *J. Biol. Chem.* **238**, 2351 (1963).
69. G. Agrup, C. Hansson, H. Rorsman, and E. Rosengren, *Arch. Dermatol. Res.* **272**, 103 (1982).
70. H. W. Duckworth and J. E. Coleman, *J. Biol. Chem.* **245**, 1613 (1970).
71. E. Bourquelet and G. Bertrand, *Comp. Rend. Soc. Biol.* **47**, 582 (1895).
72. G. Bertrand, *C. R. Acad. Sci.* **122**, 1215 (1896).
73. D. A. Robb, in "Copper Proteins" (R. Loutie, ed.), vol. II, pp. 207. CRC Press, Boca Raton, 1984.
74. H. S. Raper, *Physiol. Rev.* **8**, 245 (1928).
75. W. C. Evans and H. S. Raper, *Biochem. J.* **31**, 2162 (1937).
76. L. Califano and D. Kertész, *Enzymology* **6**, 233 (1939).
77. D. Kertész, *Biochim. Biophys. Acta* **9**, 170 (1952).
78. H. S. Raper, *J. Chem. Soc.*, 125 (1938).
79. M. Piattelli, E. Fattorusso, and S. Magno, *Rend. Acad. Sci. Fis. Mat. (Napoli)* [4] **28**, 168 (1961).
80. H. S. Mason, *J. Biol. Chem.* **172**, 83 (1948).
81. S. Senoh and B. Witkop, *J. Am. Chem. Soc.* **81**, 6231 (1959).
82. J. M. Bowness and R. A. Morton, *Biochem. J.* **53**, 620 (1953).
83. R. J. S. Beer, T. Broadhurst, and A. Robertson, *J. Chem. Soc.*, 1937 (1954).
84. J. D. Bu'Lock, *Arch. Biochem. Biophys.* **91**, 189 (1960).
85. R. A. Nicolaus, K. Hempel, and H. S. Mason, in "Advances in Biology of Skin" (W. Montagna and F. Hu, eds.), vol. VIII, pp. 313. Pergamon Press, Oxford, 1967.
86. S. Lissitzky and M. Rolland, *Nature* **193**, 881 (1962).
87. S. Senoh, C. R. Creveling, S. Udenfriend, and B. Witkop, *J. Am. Chem. Soc.* **81**, 6236 (1959).
88. J. W. Ralls, *Chem. Rev.* **59**, 329 (1959) and references therein.
89. S. Bouchilloux and A. Kodja, *C. R. Acad. Sci.* **247**, 2484 (1958).
90. W. L. Dulière and H. S. Raper, *Biochem. J.* **24**, 239 (1930).
91. H. S. Mason and C. I. Wright, *J. Biol. Chem.* **180**, 235 (1949).
92. H. S. Mason, in "Pigment Cell Growth" (M. Gordon, ed.), pp. 281. Academic Press, New York, 1953.
93. R. A. Nicolaus and M. Piattelli, *Rend. Acc. Sci. Fis. Mat. (Napoli)* **XXXII**, 82 (1965).
94. G. R. Clemo, F. K. Duxbury, and G. A. Swan, *J. Chem. Soc.*, 3464 (1952).
95. G. A. Swan and D. Wright, *J. Chem. Soc.*, 381 (1954).
96. E. Fattorusso, R. A. Nicolaus, H. Sussmann, and D. Kertész, *Rend. Acc. Sci. Fis. Mat. (Napoli)* **XXVIII** (1966).
97. F. C. Happold and H. S. Raper, *Biochem. J.* **19**, 92 (1925).
98. G. A. Swan, private communication, 1966.
99. G. W. Kirby and L. Ogunkoya, *Chem. Commun.* **21**, 546 (1965).
100. Y. M. Chen and W. Chavin, *Anal. Biochem.* **13**, 234 (1965).
101. K. Hempel, in "Structure and Control of the Melanocyte" (G. Della Prota and O. Mühlbock, eds.), pp. 162. Springer-Verlag, Berlin, 1966.
102. G. Prota, in "Advances in Pigment Cell Research" (H. Bagnata, ed.), pp. 101. Academic Press, New York, 1988.
103. D. L. Fox, "Animal Biochromes and Structural Colour", 2nd ed., Univ. of California Press, Berkeley, 1976.
104. G. Prota, *Med. Res. Rev.* **8**, 525 (1988).

105. V. Scardi, M. Iaccarino, and R. A. Nicolaus, unpublished results, Dept. of Organic Chemistry, University of Naples, 1962. [Ref. (17), p. 69].
106. M. Piattelli, E. Fattorusso, S. Magno, and R. A. Nicolaus, *Tetrahedron* **19**, 2061 (1963).
107. S. Ito, Y. Imai, K. Jimbow, and K. Fujita, *Biochim. Biophys. Acta* **964**, 1 (1988).
108. M. d'Ischia, A. Napolitano, and G. Prota, *Tetrahedron* **43**, 5351–5357 (1987).
109. J. D. Bu'Lock and J. Harley-Mason, *J. Chem. Soc.*, 703 (1951).
110. M. Thomas, in "Modern Methods of Plant Analysis" (K. Peach and M. V. Tracey, eds.), vol. IV, pp. 662. Springer, Berlin-Göttingen-Heidelberg, 1955.
111. M. Benathan and H. Wyler, *Yale J. Biol. Med.* **53**, 389 (1980).
112. R. A. Nicolaus, M. Piattelli, and G. Narni, *Tetrahedron Lett.* **21**, 14 (1959).
113. S. Ito, *Biochim. Biophys. Acta* **883**, 155 (1986).
114. M. Piattelli and R. A. Nicolaus, *Tetrahedron* **15**, 66 (1961).
- 114a. G. A. Swan and A. Waggott, *J. Chem. Soc. (C)*, 1409 (1970).
115. L. Zeise and M. R. Chedekel, *Pigment Cell Res.* **5**, 230 (1992).
116. O. Crescenzi, M. d'Ischia, and G. Prota, *Gazz. Chim. Ital.* **125** (1995).
117. M. Piattelli, E. Fattorusso, G. S. Mano, and R. A. Nicolaus, *Tetrahedron* **18**, 941 (1962).
118. R. A. Nicolaus and M. Piattelli, *Rend. Acc. Sci. Fis. Mat. (Napoli)* [4] **32**, 1 (1965).
119. M. Piattelli, E. Fattorusso, and S. Magno, *Tetrahedron Lett.*, 718 (1961).
120. W. A. Remers, in "Indoles" (W. I. Haulihan, ed.), Part I, pp. 152. J. Wiley, New York, 1972.
121. O. Crescenzi, C. Costantini, and G. Prota, *Tetrahedron Lett.* **30**, 6095 (1990).
122. M. Sugumaran and V. Semensi, *Bioorg. Chem.* **18**, 144 (1990).
123. C. Costantini, O. Crescenzi, and G. Prota, *Tetrahedron Lett.* **31**, 3849 (1991).
124. J. M. Pawelek, *Pigment Cell Res.* **4**, 53 (1991).
125. T. Sibata, G. Prota, and Y. Mishima, *J. Invest. Dermatol.*, 274S (1993).
126. J. D. Bu'Lock and J. Harley-Mason, *J. Chem. Soc.*, 2248 (1951).
127. A. Napolitano, F. Chioccare, and G. Prota, *Gazz. Chim. Ital.* **115**, 357 (1985).
128. A. Palumbo, M. d'Ischia, G. Misuraca, and G. Prota, *Biochim. Biophys. Acta* **925**, 203 (1987).
129. A. Korner and J. Pawelek, *J. Invest. Dermatol.* **75**, 192 (1980).
130. L. Lionard, J. D. Townsend, and R. A. King, *Biochemistry* **27**, 1656 (1988).
131. J. M. Pawelek, *Biochem. Biophys. Res. Commun.* **166**, 1328 (1990).
132. P. Aroca, J. C. Gracia-Borrón, F. Solano, and J. A. Lozano, *Biochim. Biophys. Acta* **1035**, 266 (1990).
133. J. Pawelek, A. Korner, A. Bergstram, and J. Bologna, *Nature* **286**, 617 (1980).
134. D. P. Chakraborty, S. Roy, A. K. Chakraborty, and R. Rakshit, *IRCS Med. Sci.* **14**, 940 (1986).
135. R. I. T. Cromartie and J. Harley-Mason, *Biochem. J.* **66**, 713 (1957).
136. A. Napolitano, M. G. Corradini, and G. Prota, *Tetrahedron Lett.* **26**, 2805 (1985).
137. M. G. Corradini, A. Napolitano, and G. Prota, *Tetrahedron* **42**, 2083 (1986).
138. M. d'Ischia, A. Napolitano, and G. Prota, *Biochim. Biophys. Acta* **1073**, 423 (1991).
139. A. T. Al-Kazwini, P. O'Neal, R. B. Cundall, G. I. Adams, A. Junino, and J. Maignant, *Tetrahedron Lett.* **33**, 3045 (1992) and references therein.
140. C. Lambert, J. N. Chacon, M. R. Chedekel, E. J. Land, P. A. Riley, A. Thompson, and G. Truscott, *Biochim. Biophys. Acta* **993**, 12 (1989).
141. S. Ito and J. A. C. Nicol, *Biochem. J.* **143**, 207 (1974).
142. P. Palumbo, M. d'Ischia, and G. Prota, *Tetrahedron* **43**, 4203 (1987).
143. A. Napolitano, O. Crescenzi, and G. Prota, *Tetrahedron Lett.* **34**, 885 (1993).

144. R. A. Nicolaus, M. Piattelli, and E. Fattorusso, *Tetrahedron* **20**, 1163 (1964).
145. B. Bloch and F. Schaaf, *Biochim. Z.* **162**, 181 (1926).
146. S. H. Pomerantz and M. C. Warner, *Biochim. Biophys. Res. Commun.* **24**, 32 (1966).
147. M. S. Blois and R. F. Kallman, *Cancer Res.* **24**, 863 (1964).
148. J. P. Greenstein, F. C. Turner, and W. V. Jenrette, *J. Natl. Cancer Inst.* **1**, 377 (1940).
149. J. J. Berzelius, *Lehrb. Chemie* **9**, 522 (1940).
150. S. Lukiewicz, *Folia Histochem. Cytochem.* **10**, 93 (1972).
151. M. G. M. Pryor, in "Comparative Biochemistry" (M. Florin and H. S. Mason, eds.), vol. IV, pp. 371. Academic Press, New York, 1962 and references therein.
152. R. Dennell, *Biol. Rev.* **33**, 178 (1958).
153. E. Fattorusso, M. Piattelli, and R. A. Nicolaus, *Rend. Acc. Sci. Fis. Mat. (Napoli)* **32**, 200 (1965).
154. D. L. Fox and D. M. Uppdegraff, *Arch. Biochem.* **1**, 339 (1943).
155. G. Prota, in "Marine Natural Products" (J. P. Scheuer, ed.), vol. 3, pp. 141. Academic Press, New York, 1980.
156. L. Minale, E. Fattorusso, G. Cimino, S. deStefano, and R. A. Nicolaus, *Gazz. Chim. Ital.* **97**, 1636 (1967).
157. R. B. Diebel and M. R. Chedel, *J. Am. Chem. Soc.* **104**, 7306 (1982).
158. E. Fattorusso, L. Minale, S. deStefano, G. Cimino, and R. A. Nicolaus, *Gazz. Chim. Ital.* **98**, 1443 (1968).
159. E. Fattorusso, L. Minale, G. Cimino, S. deStefano, and R. A. Nicolaus, *Gazz. Chim. Ital.* **99**, 29 (1969).
160. E. Fattorusso, L. Minale, G. Cimino, S. deStefano, and R. A. Nicolaus, *Gazz. Chim. Ital.* **100**, 880 (1970).
161. L. Minale, E. Fattorusso, G. Cimino, S. deStefano, and R. A. Nicolaus, *Gazz. Chim. Ital.* **99**, 431 (1969).
162. L. Minale, E. Fattorusso, S. deStefano, and R. A. Nicolaus, *Gazz. Chim. Ital.* **100**, 461 (1970).
163. E. Fattorusso, L. Minale, and G. Sodano, *Gazz. Chim. Ital.* **100**, 452 (1970).
164. R. B. Deibel, "Biosynthetic and structural studies on phaeomelanin." Ph.D. Thesis, The Johns Hopkins University, Baltimore, MD, 1983.
165. R. H. Thomson, *Angew. Chem., Int. Ed. Engl.* **13**, 305 (1974).
166. C. Brown and R. M. Davidson, in "Advances in Heterocyclic Chemistry" (A. R. Katritzky, ed.), vol. 38, pp. 135. Academic Press, New York, 1985.
167. R. A. Nicolaus, G. Prota, C. Santacroce, G. Scherillo, and D. Sica, *Gazz. Chim. Ital.* **99**, 323 (1969).
168. G. Prota, A. Suarato, and R. A. Nicolaus, *Experientia* **27**, 1381 (1971).
169. B. L. Kaul, *Helv. Chim. Acta* **57**, 2664 (1974).
170. M. Pasenkiewicz-Gietula, W. Korytowski, and J. Gietula, *Z. Nauk. Univ. Adviellon. Pr. Biol. Mol.* **II**, III (1985).
171. G. Prota and R. A. Nicolaus, *Adv. Biol. Skin* **8**, 323 (1967).
172. G. Cleffmann, *Exp. Cell Res.* **35**, 590 (1964).
173. G. Prota and R. A. Nicolaus, *Gazz. Chim. Ital.* **97**, 666 (1967).
174. S. Ito and G. Prota, *Experientia* **33**, 1118 (1977).
175. H. Rorsman, G. Agrup, C. Hansson, and E. Rosengren, in "Pigment Cell" (R. M. Mackie, ed.), vol. 6, pp. 93. Karger, Basel, Switzerland, 1983.
176. G. Prota, *J. Invest. Dermatol.* **75**, 122 (1980).
177. A. Meister and M. E. Anderson, *Ann. Rev. Biochem.* **52**, 711 (1983).

178. G. Agrup, C. Hansson, B. M. Kennedy, K. Persson, H. Rorsman, A. M. Rosengren, and E. Rosengren, *Acta Derm. Venereol.* **56**, 491 (1976).
179. G. Prota, M. d'Ischia, and A. Napolitano, *Pigment Cell Res.* **1S**, 48 (1988).
180. S. Ito, A. Palumbo, and G. Prota, *Experientia* **41**, 960 (1985).
181. S. Crescenzi, G. Misuraca, E. Novellino, and G. Prota, *Chim. Ind. (Milan)* **57**, 392 (1975) and references therein.
182. A. Palumbo, G. Nardi, M. d'Ischia, G. Misuraca, and G. Prota, *Gen. Pharmacol.* **14**, 253 (1983).
183. M. R. Chedekel, K. V. Subbarao, P. Bhan, and T. M. Schultz, *Biochim. Biophys. Acta* **912**, 239 (1987).
184. S. Ito and G. Prota, *J. Chem. Soc. Chem. Commun.*, 251 (1977).
185. C. Constantini, O. Crescenzi, G. Prota, and A. Palumbo, *Tetrahedron* **46**, 6831 (1990).
186. P. R. Crippa, V. Cristofolletti, and N. Romeo, *Biochim. Biophys. Acta* **538**, 164 (1978).
187. M. L. Wolbarsht, A. W. Walsh, and G. George, *Appl. Opt.* **20**, 2184 (1981).
188. J. McGinness and P. Proctor, *J. Theor. Biol.* **39**, 677 (1973).
189. M. G. Bridelli, R. Capelletti, and P. R. Crippa, *Physiol. Chem. Phys.* **12**, 233 (1981).
190. L. Baradani, M. G. Bridelli, M. Catbucicchio, and P. R. Crippa, *Biochem. Biophys. Acta* **716**, 8 (1982).
191. M. G. Bridelli, M. DeMattei, and A. C. Levi, *Ital. J. Biochem.* **31**, 315 (1982).
192. M. R. Chedekel, D. G. Patil, B. P. Murphy, M. Clark, J. Gardella, and T. Schultz, *Pigment Cell Res.* **1**, 282 (1988).
193. S. Aime and P. R. Crippa, *Pigment Cell Res.* **1**, 355 (1988).
194. Y. T. Thathachari and M. S. Blois, *Biophys. J.* **9**, 77 (1969).
195. G. Albanese, M. G. Bridelli, and A. Deriu, *Biopolymers* **23**, 1481 (1984).
196. M. G. Bridelli, A. Deriu, and S. Ito, *Hyperfine Interact.* **29**, 1395 (1980).
197. T. M. Schulz, J. Wolfram, S. Kurtz, M. Clark, and J. Gardella, *Commun. Pigment Cell. Meet.* (1988).
198. M. Carbuicchio and P. R. Crippa, *Physiol. Chem. Phys.* **14**, 111 (1982).
199. B. Commoner, J. Townsend, and G. E. Pake, *Nature* **174**, 689 (1954).
200. H. S. Mason, D. J. E. Ingram, and B. Allen, *Arch. Biochem. Biophys.* **86**, 225 (1960).
201. S. S. Chio, J. S. Hyde, and R. C. Sealy, *Arch. Biochem. Biophys.* **199**, 133 (1980).
202. D. S. Galvao and M. J. Caldas, *J. Chem. Phys.* **93**, 2848 (1990).
203. J. E. McGinness, P. Corry, and P. Proctor, *Science* **183**, 853 (1974).
204. M. S. Blois, A. B. Zahlan, and J. E. Maling, *Biophys. J.*, 471 (1964).
205. R. C. Sealy, J. S. Hyde, C. C. Felix, I. A. Menon, G. Prota, H. M. Swartz, S. Persad, and H. F. Haberman, *Proc. Natl. Acad. Sci. USA* **79**, 2885 (1982).
206. P. R. Crippa, M. Mazzini, and D. Salmelli, *Physiol. Chem. Phys.* **11**, 491 (1979).
207. W. Korytowsky, B. Blois, T. Sarna, and B. Kalyanaraman, *Photochem. Photobiol.* **45**, 185 (1987).
208. M. R. Chedekel, E. J. Land, R. S. Sinclair, D. Tait, and T. G. Truscott, *J. Am. Chem. Soc.* **102**, 6587 (1980).
209. S. Aime, M. Fasano, and C. Croombridge, *Gazz. Chim. Ital.* **120**, 663 (1990).
210. M. B. Clark, J. A. J. Gardella, T. M. Schultz, D. G. Patil, and L. J. Salvati, *Anal. Chem.* **62**, 949 (1990).
211. S. Ito, E. Novellino, F. Chioccaro, G. Misuraca, and G. Porta, *Experientia* **36**, 822 (1980).
212. Y. Tomita, A. Hariu, C. Kato, and M. Seiji, *J. Invest. Dermatol.* **82**, 573 (1984).

213. E. V. Gan, H. F. Haberman, and I. A. Menon, *Biochim. Biophys. Acta* **370**, 62 (1974).
214. C. C. Felix, J. S. Hyde, and R. C. Sealy, *Biochim. Biophys. Res. Commun.* **88**, 456 (1979).
215. B. Kalyanaraman, C. C. Felix, and R. C. Sealy, *J. Am. Chem. Soc.* **106**, 7327 (1984).
216. T. Wilezok, B. Bilinska, E. Buszman, and M. Kopera, *Arch. Biochem. Biophys.* **231**, 257 (1984).
217. C. C. Felix, J. S. Hyde, T. Sarna, and R. C. Sealy, *J. Am. Chem. Soc.* **100**, 3922 (1978).
218. T. M. Schultz, M. d'Ischia, and G. Prota, *Pigment Cell Res.* **1**, 265 (1988).
219. T. E. Young and B. W. Babbitt, *J. Org. Chem.* **48**, 562 (1983) and references therein.
220. M. D. Howley, S. V. Tatawawadi, S. Piekarski, and R. N. Adams, *J. Am. Chem. Soc.* **89**, 447 (1967).
221. P. T. Kissinger and W. R. Hinman, in "Laboratory Techniques in Electroanalytical Chemistry", pp. 611. Merceel Dekker, New York, 1984.
222. E. Walaas, *Photochem. Photobiol.* **2**, 9 (1963).
223. N. J. de Mol, G. M. J. Beijersbergen van Henegouwen, and K. W. Gerritsma, *Photochem. Photobiol.* **29**, 479 (1979) and references therein.
224. A. Thompson, E. J. Land, M. R. Chedelkel, K. V. Subbarao, and T. G. Truscott, *Biochim. Biophys. Acta* **843**, 49 (1985).
225. M. d'Ischia and G. Prota, *Tetrahedron* **43**, 431 (1987).
226. F. Daniels, *J. Invest. Dermatol.* **32**, 147 (1959).
227. H. C. Longuet-Higgins, *Arch. Biochem. Biophys.* **86**, 231 (1960).
228. D. Tompsett, "Memoirs on Typical British Marine Plants and Animals" Vol. XXXII. University Press, Liverpool, 1939.
229. R. J. Sever, F. W. Cope, and B. D. Polis, *Science* **137**, 128 (1962).
230. K. T. Brown, *Nature* **207**, 1249 (1965).
231. T. G. Ebrey and R. A. Cone, *Nature* **213**, 360 (1967).
232. H. G. Cassidy and K. A. Kun, "Oxidation-Reduction Polymers: Redox Polymers", Wiley Interscience, New York, NY, 1965.
233. V. A. Lapina, A. E. Dontsov, and M. A. Ostrovskii, *Biokhimiya (Moskow)* **49**, 1712 (1984); *Chem. Abs.* **102**, 2110j (1985).
234. R. C. Sealy, C. C. Felix, J. S. Hyde, and H. M. Swartz, in "Free Radicals in Biology" (W. A. Pryor, ed.), vol. 4, pp. 209. Academic Press, New York, NY, 1980 and references therein.
235. L. Chauffe, J. J. Windle, and M. Friedman, *Biophys. J.* **15**, 565 (1975).
236. V. Horak and J. R. Gillette, *Mol. Pharmacol.* **7**, 429 (1971).
237. M. Manimala and V. Horok, *J. Electrochem. Soc.* **133**, 1987 (1986).
238. T. Sarna, W. Korytowski, and R. C. Sealy, *Arch. Biochem. Biophys.* **239**, 226 (1985).
239. E. V. Gan, H. F. Haberman, and I. A. Menon, *Arch. Biochem. Biophys.* **173**, 666 (1976).
240. T. Sarna, A. Duleba, W. Korytowski, and H. Swartz, *Arch. Biochem. Biophys.* **200**, 140 (1980).
241. L. P. White, *Nature* **182**, 1427 (1958).
242. M. S. Blois, *Photochem. Photobiol. Rev.* **3**, 115 (1978).
243. A. Oikawa and M. Nakayasu, *Anal. Biochem.* **63**, 634 (1975).
244. Y. Miyake and Y. Izumi, *Struct. Funct. Melanin* **1**, 3 (1984).
245. M. A. Pathak, K. Junbow, G. Szabo, and T. B. Fitzpatrick, *Photochem. Photobiol. Rev.* **1**, 211 (1977).
246. T. Sarna, I. A. Menon, and R. C. Sealy, *Photochem. Photobiol.* **39**, 805 (1984).

247. N. S. Ranadive and I. A. Menon, *Pathol. Immunopathol. Res.* **5**, 118 (1986).
248. P. Proctor, J. McGinness, and P. Corry, *J. Theor. Biol.* **48**, 19 (1974).
249. M. R. Chedekel, P. W. Post, R. M. Deibel, and M. Kalus, *Photochem. Photobiol.* **26**, 651 (1977).
250. L. Albrecht, D. Patil, and L. J. Wolfram, *J. Invest. Dermatol.* **87**, 396 (1986).
251. A. S. Zelickson and H. C. Zeller, *J. Am. Med. Assoc.* **188**, 394 (1964).
252. A. C. Greiner and G. A. Nicolson, *Can. Phys. Assoc. J.* **10**, 109 (1965) and references therein.
253. M. S. Blois, *J. Invest. Dermatol.* **45**, 475 (1965).
254. A. G. Bolt and I. S. Forrest, *Proc. West. Pharm. Soc.* **9**, 21 (1966).
255. B. Larsson and H. Tjalve, *Acta Physiol. Scand.* **104**, 479 (1978).
256. T. Sarna, W. Froncisz, and J. S. Hyde, *Arch. Biochem. Biophys.* **202**, 304 (1980) and references therein.
257. B. Larsson, A. Oskarsson, and H. Tjalve, *Exp. Eye Res.* **25**, 353 (1977).
258. B. Larsson, A. Oskarsson, and H. Tjalve, *Biochem. Pharmacol.* **27**, 1721 (1978).



# INDEX

Note: Page numbers followed by f or t refer to the figure or table on that page, respectively.

- Acanthostrongylophora* sp., 215, 216t, 219, 222, 259, 260, 261, 263, 264, 276  
Acanthothamine, 307t  
*Acanthothamnus aphyllus*, 335t  
26-*epi*-10-*O*-Acetyllolitrem N  
  isolation, 107–108  
  properties, 61  
Acetylmaymysine, 323  
27-*O*-Acetylpaxilline  
  isolation, 67  
  properties, 56  
10-*O*-Acetylpenitrem A, 88  
*Acremonium lolii*, 65, 68  
*Acremonium* sp., 52, 104, 149  
Adenocarcinoma, 333  
Adverse effects. *see* Side effects  
*Aedes aegypti*, 121  
 $\beta$ -Aflatrem  
  isolation, 79  
 $\beta$ -Aflatrem  
  properties, 58  
  spectral assignments, 80  
Aflatrem  
  isolation, 77–79  
  tremorgenicity, 156  
Aflatremanes  
  aflatrem, 77–79  
   $\beta$ -aflatrem, 79  
  paspalitrem A, 79, 81  
  properties, 58–59  
  structure, 52  
AIDS, 276  
Alatamine, 313  
Alatusamine, 311t  
Alatusinine, 312  
*Albophoma yamanashiensis*, 53, 70  
9-Aminocamptothecin, 29–30  
*Amphimedon* sp., 215, 216t, 218, 219, 221, 222, 258, 261  
Angiogenesis, 276  
Angulatamine, 293  
Angulatueoid A, 323  
Angulatueoid E, 320t  
Angulatueoid F, 320t  
Annonaceae, 336t  
Antiangiogenesis activity, 276  
Antifungal activity, 276–277  
Antimicrobial activity, 271–277  
Antitumor activity  
  CPT analogs, 12  
  irinotecan, 14–18  
  sesquiterpene pyridine alkaloids, 332–333  
  topotecan, 25–27  
Apoptosis, mechanism of camptothecins, 7  
Aquifoliunines, 298t  
*Aspergillus* sp., 149  
*Aspergillus alliaceus*, 53  
*Aspergillus flavus*, 53, 64, 78  
*Aspergillus nomius*, 70  
*Aspergillus parasiticus*, 78  
*Aspergillus sulphureus*, 82, 83, 88, 93  
*Azadiracta indica*, 331  
5-Benzoyl-5-desacetylwilfordine, 312  
Benzoyloxywilfordic acid, 289f  
Benzoyloxywilfordate alkaloids, 313, 315t  
2,6-Bisdesacetylevonine, 291t  
*Bontia daphnoides*, 108  
Brain cancer, 275  
Breast cancer  
  and 9-aminocamptothecin, 29  
  and irinotecan, 16t  
  and lurtotecan, 33  
  and madangamine, 275  
Bukittinggine  
  structure, 168, 172  
  synthesis, 200, 202  
Calycinine A, 167  
Calyxinine, 171

- Camptotheca acuminata*, 1  
 Camptothecins. *see also* Irinotecan;  
 Topotecan  
 9-substituted derivatives, 29–30  
 biotransformation, 34  
 diflomotecan, 31–32  
 discovery, 1  
 dosage time vs. efficacy, 7  
 exatecan mesylate, 30–31  
 homocamptothecins, 31  
 lurtotecan, 32–33  
 mechanisms of action, 3–7  
 mutagenicity, 7–9  
 route of administration, 27–29  
 structure, 1–2  
*Canaga odorata*, 333, 336t  
 Cananodine, 322, 327f, 333  
 Cancer. *see* Antitumor activity; Secondary  
 cancer  
 Cangorin A–J, 325–326  
 Cangorinine E–I, 293, 333  
 Cangorinine W–I, 309  
 Cangorinine W–II, 310  
 $\beta$ -Carboline-containing manzamine alkaloids,  
 215, 218–222, 224f, 277  
 recently isolated, 222–223  
 Cassinate alkaloids, 317  
*Cassine matabelicum*, 317, 335t  
 Cassinic acid, 289f  
*Catha edulis*, 296, 335t  
 Cathedulin alkaloids, 296–298  
 high molecular weight, 301  
 medium molecular weight, 300  
 Cathedulin E2, 323  
 Cathedulin E8, 321  
 Cathedulin K17, 316  
 Cathedulin K19, 316  
 Cathic acid, 289f  
 Cathidin D, 322  
 Celahinine A, 293  
 Celapagin, 318  
 Celapanigin, 321  
 Celapanin, 321  
 Celastraceae, 289, 294, 319, 330  
 bittersweet, 334  
*Celastrus angulatus*, 331, 335t  
*Celastrus hindsii*, 335t  
*Celastrus paniculata*, 335t  
 Cell death. *see* Apoptosis  
 Cervical cancer, 16t  
 Chemotherapy  
 combination with topotecan, 26–27  
 combinations with irinotecan, 18–19  
 Choroid melanin, 365  
 Chronic myelomonocytic leukemia.  
*see* CMML  
 Chuchuhuanine W–I, 311t  
 Chuchuhuanines, 299  
*Cimex lectularius*, 108, 121  
*Claviceps* sp., 149  
*Claviceps paspali*, 52, 54  
 Clinical trials. *see also* Phase I clinical trials;  
 Phase II clinical trials; Phase III clinical  
 trials  
 irinotecan, 16t  
 irinotecan and NSCLC, 9  
 Cloudman melanoma cells, 361  
 CMML  
 and combination chemotherapy, 27  
 and topotecan, 25  
 CNMP isoevoniinate sesquiterpene pyridine  
 alkaloids, 305t  
 Codaphniphylline  
 structure, 166, 171  
 synthesis, 199–200, 201  
 Colon cancer, 333  
 Colorectal cancer  
 and 9-aminocamptothecin, 29  
 irinotecan, 15–16  
 and kauluamine, 275  
 and lurtotecan, 33  
 Combination chemotherapy  
 irinotecan, 18–19  
 topotecan, 26–27  
 CPT. *see* Camptothecins  
 Creatine, 21  
*Cribochalina* sp., 216t, 220, 259, 260, 270  
 Crigler-Najjar syndrome, 10  
*Crossopetalum tonduzii*, 333, 335t  
*Crotalus adamanteus*, 331  
*Ctenocephalides felis*, 121  
 CYP3A, 19  
 CYP3A4, 12  
 Cyperaceae, 336t  
*Cyperus rotundus*, 319, 336  
 Cytotoxicity. *see* Antitumor activity  
 Dahlsgrass poisoning, 64  
 Daphgraciline, 168, 172  
 Daphgracine, 168, 172

- Daphmacrine, 166, 171
- Daphmacropodine, 166, 171
- Daphmanidin alkaloids  
biogenesis, 191–192  
NOESY correlations, 184f  
structure, 170
- Daphmanidins  
structure, 183–184
- Daphnane-type alkaloids  
biogenesis, 185–187  
structure, 170–171  
transformation of unsaturated amine, 193
- Daphnezomine alkaloids  
biogenesis, 187–189  
daphnezomine B CD spectra, 174f  
daphnezomine B molecular structure, 175f  
stereochemistry, 175  
structure, 169, 172–177
- Daphnicyclidin A  
molecular structure, 178f  
NOESY correlations, 179f
- Daphnicyclidin alkaloids  
biogenesis, 190–191  
structure, 170, 177–183
- Daphnigraciline, 168, 172
- Daphnigracine, 168, 172
- Daphnijsmine, 167, 171
- Daphnilactone A-type alkaloids  
structure, 171  
synthesis, 197
- Daphnilactone alkaloids  
structure, 168
- Daphnilactone B-type alkaloids, 172
- Daphnimacrine, 170
- Daphnimacropine, 166, 171
- Daphniphyllidine, 166, 171
- Daphniphylline, 166, 170
- Daphniphyllum* alkaloids  
biogenetic pathway, 166  
biomimetic chemical transformations,  
193–194  
biomimetic total synthesis, 194–202  
biosynthesis, 184–185  
daphmanidin biogenesis, 191–192  
daphmanidin skeletal types, 170  
daphmanidins, 183–184  
daphnane-type structures, 170–171  
daphnezomine skeletal types, 169  
daphnicyclidins, 190–191  
daphnicyclidin skeletal types, 170  
daphnilactone A and N structures, 168  
daphnilactone A structures, 171  
daphnilactone B-type alkaloids, 172  
polycyclization cascade, 200, 202  
secodaphnane-type structure, 167, 171  
skeletal types, 166  
yuzurimine skeletal types, 167, 171  
*Daphniphyllum gracile*, 172  
*Daphniphyllum humile*, 165, 172, 177  
*Daphniphyllum macropodum*, 165, 171, 172  
*Daphniphyllum teijsmanni*, 165, 172, 177  
Daphnitejsmanine, 167, 171  
Daphnitejsmine, 167  
Deacetyl daphnijsmine  
isolation, 171  
structure, 167, 171  
Deacetyl yuzurimine, 171  
4-Deoxyeuonymine, 300  
4-Deoxyeuonyminol alkaloids, 299  
4-Deoxyisoeuonyminol alkaloids, 299  
4-Deoxywilfordate alkaloids, 311  
Deoxyyuzurimine, 167  
structure, 171  
2-Desacetyllevonine, 291t  
1-Desacetylwilfortrine, 312  
13-Desoxypaxilline  
isolation, 66–67  
properties, 56  
Diflomotecan, 31–32  
32,33-Dihydro-31-hydroxymanzamine A,  
223, 277  
32,33-Dihydro-31-hydroxymanzamine  
A-35-one, 223  
32,33-Dihydro-6-hydroxymanzamine  
A-35-one, 277  
32,33-Dihydro-6,31-dihydromanzamine A,  
223, 277  
Dihydroagarofuran sesquiterpenes,  
288f, 328  
insect antifeedant and insecticidal activity,  
331  
2,3-Dihydroindole-5,6-quinone-2-carboxylic  
acid, 350  
Dihydroprotodaphniphylline, 196  
2,18-Dioxo-2,18-seco-paxilline  
properties, 56  
14-(*N,N*-Dimethyl-L-valyloxy)paspalinine  
isolation, 70  
properties, 57  
DNA topoisomerases, 3–5, 6t, 7

- Dosage  
  irinotecan, 10, 12–14  
  topotecan, 20, 22–25
- Dose-limiting toxicity  
  9-Aminocamptothecin, 29  
  irinotecan, 13  
  topotecan, 24
- Drug interaction, irinotecan, 11–12
- DX-8951f, 30–31
- Ebenifoline E-I, 293
- Ebenifoline E-III, 293
- Ebenifoline E-V, 293
- Ebenifoline E-II, 293, 333
- Ebenifoline E-IV, 300
- Ebenifoline W-I, 310
- Ebenifoline W-II, 310
- Echinopogan* sp., 65
- Edulinate alkaloids, 315–317
- Edulinic acid, 289f  
  biosynthetic pathway, 322–323
- Ejap-14, 323
- Ejap-7, 320t
- Emarginatines, 295, 297t, 332, 333
- Emarginatinine, 312, 332
- Emericella* sp., 65, 146
- Emericella desertorum*, 65
- Emericella foveolata*, 65
- Emericella striata*, 53, 65, 66
- Emindole SB  
  isolation, 64  
  properties, 55
- Emindoles, 147
- ent*-12,34-Oxamanzamines E and F, 275
- ent*-8-hydroxymanzamine, 275
- epi*-Manzamine D, 223, 276
- Epidermoid carcinoma, 274, 275
- Epievonic acid, 289f
- Epiguaipyridine, 327f  
  synthesis, 337–338
- Epimeric evoninate alkaloids, 304–307, 307t
- Epioxodaphnigracilline, 168, 172
- Etoposide, 8
- Eumelanin  
  ESR spectra, 375  
  photoprotection of skin, 382  
  pigmentation, 354  
  redox functions, 380–381  
  sepiomelanin, 355–364
- Eunonymine, 292t
- Euojaponine D, 309
- Euojaponine F, 309
- Euojaponine J, 311t
- Euojaponine K, 309
- Euojaponine N, 300
- Euojaponines, 294
- Euonine, 309
- Euonymine, 306
- Euonyminol derivatives, 290, 292–294t
- Euonymus, 334
- Euonymus alatus*, 335t
- Euonymus europaeus*, 335t
- Euonymus japonicus*, 335t
- Euonymus nanus*, 335t
- Euonymus sachalinensis*, 335t
- Euonymus sieboldianus*, 335t
- Euonymus verrucosus*, 335t
- Eupenicillium shearii*, 64, 65, 67, 98, 99
- Ever-1, 323
- Evonimine, 310
- Evoninate alkaloids  
  cathedulin alkaloids, 296–298  
  CNMP euonyminol derivatives, 295–296t  
  CNMP isoeuonyminol derivatives, 297t  
  4-deoxy sesquiterpene cores, 294, 296  
  4-deoxyeuonyminol alkaloids, 299–300t  
  4-deoxyisoeuonyminol alkaloids,  
    299–300t  
  euonyminol derivatives, 290, 292t  
  evoninol derivatives, 289–290, 291t  
  isoeuonyminol derivatives, 290–291, 298t  
  macrocylic ring formation, 330  
  triptonines, 302–303  
  types, 288
- Evonine, 291t  
  biosynthesis, 330
- Evoninic acid, 289f
- Evoninol, 287
- Evonoline, 291t
- Evorine, 291t
- Exatecan mesylate, 30–31
- Feather melanin, 365
- Flea control, 108, 122, 124t
- Forrestine, 292t
- 5-FU, 16–17
- Furanoyloxy wilfordate alkaloids,  
  313, 315t
- Furanoyloxy wilfordic acid, 289f
- Fusarium oxysporium*, 223, 275

- Gallophaeomelanins, 367–368  
*Gallus gallus*, 366  
Gastric cancer, 16t  
GG211, 32–33  
GI147211, 32–33  
Gilbert's disease, 10  
Glioblastoma, 29  
Glioma, 11–12  
Guaipyridine, 322, 327f  
    synthesis, 337–338
- Haliclona* sp., 218, 258, 259, 261  
*Haliclona tulearensis*, 216t  
Head and neck cancer  
    and 9-aminocamptothecin, 29  
    and irinotecan, 16t  
    and topotecan, 25–26  
*Helicorperla zea*, 70  
*Heliothis zea*, 86, 98  
Hepatic function and topotecan, 20  
Heterophylline, 321  
*Hippocratea* sp., 334  
*Hippocratea excelsa*, 307, 336t  
Hippocrateaceae, 319, 334, 336t  
Hippocrateine I and II, 295  
Hippocrateine III, 305t  
Homocamptothecins, 31  
Horridina, 298t  
Human immunodeficiency virus  
    (HIV), 276  
    and sesquiterpene pyridine alkaloids, 332  
8-Hydroxy-1,2,3,4-tetrahydromanzamine A  
    isolation, 220  
10 $\beta$ -Hydroxy-13-desoxypaxilline  
    isolation, 68  
    properties, 56  
    structure, 67  
7 $\alpha$ -Hydroxy-13-desoxypaxilline  
    isolation, 67  
    properties, 56  
8-Hydroxy-2-*N*-methyl-1,2,3,4-  
    tetrahydromanzamine A, 220  
4-Hydroxy-7-*epi*-chuchuhuanine, 293  
Hydroxyisowilfordic acid, 289f  
Hydroxywilfordic acid, 289f  
Hydroxydaphgracilline  
    structure, 168, 172  
Hydroxyisoevonninate alkaloids, 303–304,  
    306t  
Hydroxyisoevonninic acid, 289f  
8-Hydroxymanzamine A, 276, 277  
    isolation, 219  
    pharmacology, 274  
14-Hydroxypaspalinine  
    isolation, 70  
    properties, 57  
7 $\alpha$ -Hydroxypaxilline, 68  
Hydroxywilfordate alkaloids, 311–313, 314t,  
    332–333  
Hydroxywilfordic acid, 327  
Hypoglaunine, 304t  
Hypoglaunine A, B, C, 306t  
Hyponines A-F, 292t  
*Hyrtios* sp., 261  
*Hyrtios erecta*, 217t, 218, 261
- Immune system  
    manzamine effect on, 273  
    and sesquiterpene pyridine alkaloids, 333  
Indole diterpenoids  
    biogenetic pathway, 149  
    biological origin, 52  
    structure, 52  
    structure and tremorgenicity, 155–158  
Infusion. *see also* dosage  
    camptothecins, 27–29  
    irinotecan, 12–14  
Ingamine A, 269  
Ingenamine, 256, 269, 275  
Ingenamine E, 269  
Insecticide activity  
    manzamines, 271–277  
    nodulisporanes, 108, 121–122  
    sesquiterpene pyridine alkaloids,  
        330–332  
Ircinal A, 256  
    biogenetic pathway, 266–267  
    configurations, 269  
    conversion to alcohol forms, 272  
    isolation, 219  
    total synthesis, 268  
Ircinal B, 272  
    biogenetic pathway, 266–267  
    configurations, 269  
    isolation, 219  
*Ircinia* sp., 217t, 219, 261, 266  
Ircinol A, 222  
    cytotoxicity, 275  
    and Mtb, 276  
    total synthesis, 268

- Ircinol B, 222  
  cytotoxicity, 275
- Irinotecan  
  antitumor activity, 14–18  
  clinical pharmacology, 9–12  
  clinical trials, 16t  
  combination chemotherapy trials, 18–19  
  combined with 5-FU/leucovorin, 16–17  
  dosage, 10  
  and NSCLC, 9  
  oncological use, 3  
  safety guidelines, 14t
- Isodaphnilactone B, 168, 172
- Isoeunoyminol derivatives, 298t
- Isoeunoyminol derivatives, 290–291
- Isoevoninate alkaloids, 303, 304t
- Isoevonine, 310
- Isoevoninic acid, 289f
- 21-Isopentenylpaxilline, 84
- Isowilfordate alkaloids, 312–313, 314t
- Isowilfordic acid, 289f
- Isowilfordine, 314t
- Janthitrem B, 157
- Janthitrem E  
  isolation, 96  
  spectral assignments, 97–98
- Janthitremanes  
  janthitremes, 94–98  
  properties, 59–60  
  shearinines, 98–100  
  structure, 52, 94
- Janthitremes A–D, 94–98
- Kauluamine, 221, 275
- Keramamine C, 255
- Keramaphidin B, 269, 275
- Keramaphidin C, 255
- Keramaphidins, 222
- Khat, 296
- Laevisine A, 294
- Laevisine B, 310
- Lamaiaceae, 336t
- Leishmania tropica*, 333
- Leishmanicidal activity, 277
- Leukemia  
  and camptothecins, 8  
  and exatecan mesylate, 31  
  and irinols A and B, 275  
  and irinotecan, 16t  
  and manzamine B, 273  
  and manzamines H and J, 274  
  and sesquiterpene pyridine alkaloids, 333  
  and topotecan, 25–26
- Locusta migratoria*, 331
- Lolicine  
  isolation, 106  
  properties, 61
- Lolicines  
  biogenetic pathway, 152  
  biosynthesis, 150
- Lolillene, 61
- Lolilline, 105–106, 150
- Lolitrem A  
  isolation, 101  
  tremorgenicity, 157
- Lolitrem B  
  isolation, 101–104  
  spectral assignments, 102  
  structure, 100  
  tremorgenicity, 157
- Lolitrem C, 104
- Lolitrem D, 105
- Lolitrem E, 105
- Lolitrem F, 105
- 26-*epi*-Lolitrem N, 61
- Lolitrem N, 61
- Lolitremanes  
  26-*epi*-10-*O*-acetyllohitrem N, 107–108  
  isolation, 100  
  lolicine, 106  
  lolilline, 105–106  
  lolitremes, 100–105  
  properties, 60–62  
  11-*O*-propionyllohitrem A, 106–107  
  11-*O*-propionyllohitrem B, 107  
  10-*O*-propionyllohitrem N, 107  
  structure, 52, 100
- Lolitremes  
  A/B ring system stereospecificity, 150  
  biogenetic pathway, 151  
  properties, 60–61
- Loliritriol, 60
- Lolium perenne*, 53, 74, 100, 103, 105, 106, 107, 150
- Lucilia sericata*, 108, 121
- Lung cancer, 275, 276, 333
- Lurtotecan, 32–33

- Lymphoma  
 and 9-aminocamptothecin, 29  
 and irinotecan, 16t
- Macrodaphnine, 167, 171
- Macrodaphniphyllamine, 167, 171
- Macrodaphniphyllidine, 167, 171
- Madangamine A, 222, 275
- Malaria, 213, 272, 274, 276
- Manadomanzamines, 276
- Mandomanzamine A, 257
- Mandomanzamine B, 257
- Manzamine A  
 biogenetic pathway, 209  
 biomimetic methods, 267  
 isolation, 218–219  
 pharmacology, 271  
 synthesis, 266  
 total synthesis, 268  
 toxicity, 273
- Manzamine B  
 biogenetic pathway, 209  
 isolation, 218  
 and leukemia, 273
- Manzamine C  
 biogenetic pathway, 255  
 synthesis, 265
- Manzamine D, 268
- Manzamine E, 219
- Manzamine F, 219
- Manzamine G, 218
- Manzamine H, 219, 221, 223
- Manzamine J, 219
- Manzamine L, 221
- Manzamine M, 219
- Manzamine-related marine alkaloids, 213f, 222
- Manzamine X  
 biomimetic methods, 267  
 isolation, 220
- Manzamines  
<sup>13</sup>C-NMR data, 234–243  
<sup>1</sup>H-NMR data, 244–255  
 bioactivities, 210, 213, 214  
 biogenetic pathway, 223  
 biological activity, 208  
 biomimetic methods, 267–271  
 biosynthetic intermediates, 255–258  
 configuration similarities, 269  
 containing  $\beta$ -carboline, 210, 211, 212, 215,  
 218–223, 224f, 277  
 isolation, 208–209, 214–223  
 marine sponge sources, 216–217  
 marine sponge taxonomy, 258–261  
 pharmacology, 271–277  
 physical properties, 223, 225–233  
 ring structure, 207  
 semisynthesis, 266–267, 269  
 total synthesis, 265–266
- Marine sponges, 216–217, 258–261
- Maymysine, 321
- Mayteine, 294
- Maytenus aquifolium*, 335t
- Maytenus blepharodes*, 335t
- Maytenus buchananii*, 335t
- Maytenus chuchuhuasca*, 294, 335t
- Maytenus cuzcoina*, 335t
- Maytenus diversifolia*, 335t
- Maytenus ebenifolia*, 335t
- Maytenus emarginata*, 332, 335t
- Maytenus guianensis*, 335t
- Maytenus heterophylla*, 335t
- Maytenus horrida*, 335t
- Maytenus ilicifolia*, 335t
- Maytenus laevis*, 335t
- Maytenus myrsinoides*, 335t
- Maytenus putterlickioides*, 336t
- Maytenus senegalensis*, 336t
- Maytenus serrata*, 336t
- Maytine, 324
- Maytolidine, 326
- Maytoline, 325
- Meduloblastoma, 333
- Melanin  
<sup>13</sup>C-NMR data, 374  
 about, 346  
 autooxidative synthesis, 377  
 binding capacity, 383  
 biogenesis, 347–354  
 complexation, 383  
 as defense mechanism, 379–380  
 electrochemical synthesis, 377–378  
 electron spin resonance spectroscopy,  
 375–376  
 enzymatic synthesis, 377  
 from eye, 365  
 from feathers, 365–366  
 formation from tyrosine, 350–354  
 in hair, 365  
 as light screen for eyes, 380  
 medicinal aspects, 383

- Mossbauer spectroscopy, 375  
natural and synthetic, 345, 354  
photochemical synthesis, 379  
photoprotection of skin, 381–383  
pigmentation, 354  
redox functions, 380–381  
synthetic, 376–379  
UV and IR spectroscopy, 373–374  
X-ray diffraction studies, 374–375
- Melano-sclerotins, 365
- Melanocytes, 347–348  
action in hair and skin, 349
- Melanogenesis, 350–354  
Raper-Mason scheme, 351f
- Melanoma, 333, 361, 364–365
- Melatonin, 348
- 8-Methoxymanzamine A, 267
- N*-Methyl-2-pyridone-5-carboxylic acid (CNMP), 289f
- N*-Methyl-*epi*-manzamine D, 223, 276
- Methyl homodaphniphyllate  
structure, 166, 171  
synthesis, 197, 198, 199
- Methyl homosecodaphniphyllate  
biomimetic total synthesis, 194  
structure, 167, 171
- Misenine, 259
- Mtb, 213, 276
- Multidrug resistance, 333–334
- Multiple myeloma, 27
- Myelodysplastic syndrome (MDS)  
and combination chemotherapy, 27  
and topotecan, 25–26
- Nakadomarin A, 256  
cytotoxicity, 275
- Neosalatamine, 313
- Neoeuonymine, 293
- Neotyphodium lolii*, 53, 67, 74, 100, 106, 107, 150
- Neotyphodium* sp., 52, 65
- Neoevonine, 291t
- Neowilforine, 311t
- Neurospora crassa*, 348
- Nicotinic acid, 289f  
and derivatives, 289f
- 9-Nitrocampthotecin (9-NC), 30
- Nocardia* sp., 223, 275
- Nodulisporamides, 120–121
- Nodulisporanes  
biological activity, 121–122  
flea control, 124t  
nodulisporamides, 120–121  
nodulisporic acid A, 109, 139–143  
nodulisporic acid A<sub>1</sub>, 111  
nodulisporic acid A<sub>2</sub>, 112  
nodulisporic acid B, 112–114  
nodulisporic acid C, 115–117  
2''-oxazole derivatives, 119–120  
structure, 52, 108  
2''-thiazole derivatives, 119–120
- Nodulisporic acid A  
biosynthesis, 153–155  
chemistry, 117–118  
cleavage of side chain, 118–119  
isolation, 109  
medicinal chemistry, 122–125  
spectral assignments, 110–111  
synthesis, 139–143
- Nodulisporic acid A<sub>1</sub>, 111
- Nodulisporic acid A<sub>2</sub>, 112
- Nodulisporic acid B, 112–114
- Nodulisporic acid C, 115–117
- Nodulisporium* sp., 108, 109, 112, 114, 115
- Non-celastraceous sesquiterpene pyridine alkaloids, 322
- Non-small cell lung cancer. *see* NSCLC
- Norevoninate alkaloids, 307, 308t
- Norevoninic acid, 289f
- NSCLC  
and 9-aminocampthotecin, 29  
and irinotecan, 9, 16t  
and irinotecan with other chemotherapies, 18–19  
and lurtotecan, 33  
and topotecan, 25–26
- Orthosphenia mexicana*, 317, 336t
- Ostrina furnacalis*, 331
- Ovarian cancer  
and 9-nitrocampthotecin, 30  
and irinotecan, 16t  
and topotecan, 3, 22, 25–26
- 12,34-Oxamanzamines, 222–223, 275
- 2''-Oxazole derivatives, 119–120
- Oxodaphnigraciline, 168, 172
- Oxodaphnigracine, 168, 172
- PachyPELLINA* sp., 217t, 259
- Pancreatic cancer  
and irinotecan, 16t



- and 9-nitrocamptothecin, 30
- Paspalanes
  - 27-*O*-acetylpaxilline, 67
  - biosynthesis, 144–147
  - 13-desoxypaxilline, 66–67
  - 14-(*N,N*-dimethyl-L-valyloxy)paspalinine, 70
  - emindole SB, 64
  - 10 $\beta$ -hydroxy-13-desoxypaxilline, 68
  - 7 $\alpha$ -hydroxy-13-desoxypaxilline, 67
  - 14-hydroxypaspalinine, 70
  - 7 $\alpha$ -hydroxypaxilline, 68
  - 21-isopentenylpaxilline, 84
  - paspalicine, 54, 130–134
  - paspaline, 53, 125–129
  - paspaline B, 64
  - paspalinine, 54, 130–134
  - paspalitrem B, 81
  - paspalitrem C, 81–82
  - paxilline, 65–66
  - paxinorol, 69
  - PC-M5', 68
  - PC-M6, 69
  - properties, 55–58
  - structure, 52
  - sulpinines, 82–83
  - terpendole L, 84
  - terpendoles, 70–76
  - thiersinines, 76–77
- Paspalicine
  - isolation, 54
  - properties, 55
  - structure, 54
  - synthesis, 130–134
- Paspaline
  - biosynthesis, 144
  - and indole diterpenoid synthesis, 149
  - isolation, 53
  - properties, 55
  - spectral assignments, 63
  - structure, 54
  - synthesis, 125–129
- Paspaline B
  - isolation, 64
  - properties, 55
  - structure, 54
- Paspalinine
  - isolation, 54
  - properties, 55
  - structure, 54
- synthesis, 130–134
- tremorgenicity, 155
- Paspalitrem A, 79, 81
  - tremorgenicity, 156
- Paspalitrem B
  - isolation, 81
  - tremorgenicity, 156
- Paspalitrem C, 81–82
- Paspalitrem, 58
- Paspalum* sp., 64
- Patchoulipyridine, 322, 327f, 338
- Paxilline
  - as biosynthetic intermediate, 147–150
  - isolation, 65–66
  - properties, 55
  - semi-synthetic derivatives, 66
  - spectral assignments, 63
  - tremorgenicity, 156
- Paxinorol
  - isolation, 69
  - properties, 57
- PC-M5'
  - isolation, 68
  - properties, 56
- PC-M6
  - isolation, 69
  - properties, 56
- Pectinophora gossypiella*, 331
- Pellina* sp., 217t, 219
- Penetremanes, 59
- Penicillium crustosum*, 68, 69, 145, 146
- Penicillium janczewski*, 148
- Penicillium janthinellum*, 53, 94, 95, 96, 148
- Penicillium nigricans*, 92
- Penicillium palitans*, 85
- Penicillium paxilli*, 67, 68, 69, 150–153
- Penicillium* sp., 93, 149
- Penicillium theirsii*, 76
- Penitrem A
  - isolation, 85–86
  - labeling pattern, 145
  - spectral assignments, 87
  - structure, 88
  - tremorgenicity, 156
- Penitrem B
  - isolation, 88–89
  - structure, 88

- Penitrem C, 89
- Penitrem D  
isolation, 89  
synthesis, 134–139
- Penitrem E  
isolation, 89–90  
structure, 90
- Penitrem F  
isolation, 90  
structure, 90
- Penitremanes  
biosynthesis, 144–147  
penitrem A-F, 85–90  
penitrem D synthesis, 134–139  
penitremones, 93–94  
pennigritrem, 92  
secopenitrem B, 90–91  
structure, 52, 85  
thomitrem A, 91  
thomitrem E, 91  
tremogenicity, 156
- Penitremones  
biological activity, 94  
isolation, 93–94  
properties, 59
- Penitrems, 59
- Pennigritrem  
isolation, 92  
properties, 59
- Peritassa campestris*, 336t
- Peritassa compta*, 336t
- Peritassine A, 304t
- Peritassine B, 304t
- Petrosaspongia mycofijiensis*, 261
- Petrosia* sp., 260, 261
- Petrosia contignata*, 217t, 220, 261
- Phaeomelanins  
biosynthesis, 370–373  
ESR spectra, 376  
gallophaeomelanins, 367–368  
photoprotection of skin, 382  
pigmentation, 354  
and skin cancer, 382  
synthesis, 377  
trichochromes, 368–370
- Pharmacology  
8-hydroxymanzamine A, 274  
irinotecan, 9–12, 9–12  
manzamines, 271–277  
topotecan, 19–22
- Phase I clinical trials  
9-nitrocampptothecin, 30  
campptothecins, 3  
irinotecan, 11–14  
irinotecan and other chemotherapies, 18  
topotecan, 20–21
- Phase II clinical trials  
9-Aminocampptothecin, 29  
irinotecan, 14–18  
irinotecan and other chemotherapies, 18–19  
lurtotecan, 33  
ovarian cancer and topotecan, 22
- Phase III clinical trials  
irinotecan, 15–16  
topotecan, 26
- Phomopsis* sp., 81
- Picolinic acid, 289f
- Pieris brassicae*, 331
- Plasmodium* sp., 333
- Pogostemon patchouly*, 337t
- Premelanosome, 347
- Prianos*, 221, 258, 259
- 11-*O*-Propionyllolicine A  
isolation, 106–107  
properties, 61
- 11-*O*-Propionyllolicine B  
isolation, 107  
properties, 61
- 10-*O*-Propionyllolitrem N  
isolation, 107  
properties, 61
- Proto-daphniphylline, 187  
biomimetic total synthesis, 194
- Putterine A, 293
- Putterine B, 293
- Pyrausta nubilalis*, 331
- Regelidine, 318
- Renal function, 20
- Reneira sarai*, 259
- Reniera*, 216t, 222, 258, 261
- Rotundines, 319, 327f
- Rzedowskia tolantonguensis*, 336t
- Salacia* sp., 334
- Saraine A, 259
- Saraines, 275
- SCLC  
and combination chemotherapy, 26  
and irinotecan, 16t

- and lurtotecan, 33
- and topotecan, 3, 22, 25–26
- Secodaphnane-type alkaloids
  - biogenesis, 185–187
  - structure, 167, 171
- Secodaphniphylline
  - structure, 167, 171
  - synthesis, 196–197
- Secopenitrem B
  - isolation, 90–91
  - properties, 59
- Sepia officinalis*, 354
- Sepiomelanin
  - biosynthetic studies, 359–364
  - carboxylic and phenolic functions, 357
  - chemical degradation, 357–359
  - isolation and analysis, 356–357
  - and melanin synthesis, 355
  - and melanoma-melanin, 364–365
  - protein content, 355–356
- Sesquiterpene pyridine alkaloids
  - anti-HIV activity, 332
  - benzoyloxywilfordate alkaloids, 313, 315t
  - biogenesis of sesquiterpene moiety, 329
  - biosynthesis, 322–323, 326–330
  - cassinate alkaloids, 317
  - CNMP isoevoinate alkaloids, 305t
  - 4-deoxywilfordate alkaloids, 311t
  - dimacrocyclic, 302–303
  - edulinate alkaloids, 315–317
  - epimeric evoninate alkaloids, 304–307, 307t
  - esterifying acids of sesquiterpene cores, 288f
  - furanoyloxywilfordate alkaloids, 313, 315t
  - hydroxyisoevoinate alkaloids, 303–304
  - hydroxywilfordate alkaloids, 311–313
  - immunosuppressive activity, 333
  - insect antifeedant and insecticidal activity, 330–332
  - isoevoinate alkaloids, 303, 304t
  - isowilfordate alkaloids, 312–313
  - and multidrug resistance, 333–334
  - natural sources, 335–336t
  - non-Celastraceous, 318–319, 322
  - norevoinate alkaloids, 307
  - structure, 287
  - synthesis, 334, 337–339
  - taxonomic considerations, 334
  - transesterified lower molecular weight, 320–322
  - wilfordate alkaloids, 307–311
- Shearinines, 98–100
  - properties, 59–60
- Side effects
  - camptothecins, 3
  - irinotecan, 10–11, 13
  - topotecan, 25
- Skin cancer, 382
- Small cell lung cancer. *see* SCLC
- SN-38, 9, 12
- Spodoptera frugiperda*, 77
- St. John's wort, 12
- Sulpinines
  - isolation, 82–83
  - properties, 58
- Tapetum lucidum*, 363
- Terpendole L, 59, 84
- Terpendoles
  - biological activity, 76
  - isolation, 70–76
  - properties, 57–58
  - spectral assignments, 72–73
  - structure, 71
- 33,35,25,39-Tetrahydropenitrem A
  - structure, 88
- 2''-Thiazole derivatives, 119–120
- Thiersinines
  - isolation, 76–77
  - properties, 58
- Thomitrem, 59
- Thomitrem A
  - isolation, 91
  - structure, 92
- Thomitrem E
  - isolation, 91
  - structure, 92
- Tick control, 108
- Topoisomerase I inhibitors, 3
  - mechanisms of action, 33
  - mutagenicity, 7–9
  - oral administration, 34
  - route of administration, 27–29
- Topotecan
  - antitumor activity, 25–27
  - bioavailability, 21
  - clinical pharmacology, 19–22
  - dosage, 22–25
  - mutagenicity, 8
  - safety guidelines, 23
  - toxicity, 24

- Toxicity. *see also* Dose-limiting toxicity  
  camptothecins, 3  
  irinotecan, 15t  
  SN-38, 12  
  topotecan, 24
- Tribolium castaneum*, 331
- Trichochromes, 368–370
- Tripterygium forrestii*, 336t
- Tripterygium hypoglaucum*, 303, 304, 315, 336t
- Tripterygium wilfordii*, 303, 304, 313, 330, 331, 332, 333, 336t
- Triptofordinine A-1, 324
- Triptofordinine A-2, 324
- Triptogelin A-7, 319
- Triptogelin B-2, 320t
- Triptogelin C-2, 321
- Triptogelin C-4, 319
- Triptogelin F-1, 318
- Triptogelins, 323
- Triptonines, 302–303
- Tuberculosis, 273, 276
- Tyrosinase inhibitors, 348–350
- Wilfordicine, 318
- Wilfordate alkaloids, 307–311
- Wilfordic acid, 289f, 327  
  biosynthetic pathway, 322–323
- Wilfordine, 312
- Wilfordine D-H, 314t
- Wilfordinine A, 304t
- Wilfordinine B, 306t
- Wilfordinine C, 306t
- Wilfordinine I, 306t
- Wilfordinine J, 304t
- Wilforgine, 309, 331
- Wilfordine, 312
- Wilforine, 309
- Wilforjine, 309
- Wilforine, 310
- Wilforinine A-D, 315t
- Wilforinine E, 313
- Wilforinine F, 293
- Wilforinine G, 293
- Wilfortrine, 312, 331
- Wilforzine, 309, 331
- Xestocyclamine A, 222, 275
- Xestomanzamine A, 220, 268, 271, 276
- Xestomanzamine B, 275
- Xestospongia ashmorica*, 216t, 218, 219, 220
- Xestospongia exigua*, 217t, 222
- Xestospongia ingens*, 217t, 222
- Xestospongia* sp., 216t, 218, 219, 220, 222, 259, 260, 270
- Yuzuriha, 165
- Yuzurimine alkaloids  
  skeletal types, 167  
  structure, 171
- Yuzurine-type alkaloids  
  structure, 168, 172
- Zwitterionic alkaloid  
  isolation, 171, 172  
  structure, 168